

Guidance for Performing Probabilistic Seismic Hazard Analysis for a Nuclear Plant Site: Example Application to the Southeastern United States

Lawrence Livermore National Laboratory

**U.S. Nuclear Regulatory Commission
Office of Nuclear Regulatory Research
Washington, DC 20555-0001**



Guidance for Performing Probabilistic Seismic Hazard Analysis for a Nuclear Plant Site: Example Application to the Southeastern United States

Manuscript Completed: September 2002
Date Published: October 2002

Prepared by
J. B. Savy, W. Foxall,
N. Abrahamson, D. Bernreuter

Lawrence Livermore National Laboratory
Livermore, CA 94550

E. Zurflueh, S. Pullani, NRC Project Managers

Prepared for
Division of Engineering Technology
Office of Nuclear Regulatory Research
U.S. Nuclear Regulatory Commission
Washington, DC 20555-0001
NRC Job Codes W6496 and Y6245



Guidance for Performing Probabilistic Seismic Hazard Analysis for a Nuclear Plant Site: Example Application to the Southeastern United States

Manuscript Completed: September 2002
Date Published: October 2002

Prepared by
J. B. Savy, W. Foxall, N. Abrahamson, D. Bernreuter

Lawrence Livermore National Laboratory
Livermore, CA 94550

E. Zurflueh, S. Pullani, NRC Project Managers

**Prepared for
Division of Engineering Technology
Office of Nuclear Regulatory Research
U.S. Nuclear Regulatory Commission
Washington, DC 20555-0001
NRC Job Codes W6496 and Y6245**

Disclaimer

This document was prepared as an account of work sponsored by an agency of the United States Government. Neither the United States Government nor the University of California, nor any of their employees, makes any warranty, express or implied, or assumes any legal liability or responsibility for the accuracy, completeness, or usefulness of any information, apparatus, product, or process disclosed, or represents that its use would not infringe privately owned rights. Reference herein to any specific commercial product, process, or service by trade name, trademark, manufacturer, or otherwise, does not necessarily constitute or imply its endorsement, recommendation, or favoring by the United States Government or the University of California. The views and opinions of authors expressed herein do not necessarily state or reflect those of the United States Government or the University of California and shall not be used for advertising or product endorsement purposes.

This work was supported by the United States Nuclear Regulatory Commission under a Memorandum of Understanding with the United States Department of Energy, and was performed under the auspices of the U.S. Department of Energy by University of California Lawrence Livermore National Laboratory under NRC Contract Job Code 6496.

ABSTRACT

From 1981 to 1989, Lawrence Livermore National Laboratory (LLNL) developed a Probabilistic Seismic Hazard Analysis (PSHA) method for the eastern United States (NUREG/CR-5250), followed in 1993 by improvements in the handling of the uncertainties (NUREG-1488). Differences between these results and those of a utilities-sponsored study (Electric Power Research Institute, 1989) led to the formation of the Senior Seismic Hazard Analysis Committee (SSHAC) to identify the sources of differences and give guidance on how to perform a state-of-the-art PSHA (NUREG/CR-6372, 1997).

The present study is a trial implementation of the SSHAC guidance. As part of the project, additional guidance was developed and proposed for performing a PSHA. The trial implementation project tested the issue of development of the seismic zonation and seismicity models for two sites: Watts Bar and Vogtle. It was found that the uncertainty generated by disagreements among experts could be considerably reduced through interaction and discussion of the data, and by concentrating on the elements common to all experts' interpretations. The present study includes analyses of the differences between its results and the NUREG-1488 results (Appendix G).

CONTENTS

Abstract	iii
Executive Summary.....	xi
Acknowledgments.....	xiii
Abbreviations.....	xv
1. Introduction	1
1.1 Background	1
1.2 Purpose of the Study, Scope.....	1
1.3 Organization of the Report.....	2
1.4 Use of This Document	2
2. General Requirements of a PSHA	3
2.1 Fundamental SSHAC Guiding Principle.....	3
2.2 Procedural Recommendations.....	3
2.3 Implementation for Ground Motion Attenuation and Seismic Source Characterization.....	5
3. Guidance For a Practical Approach.....	7
3.1 General Road Map	7
3.2 Data Requirements.....	8
3.3 Elicitation and Integration Process.....	9
3.3.1 Selection of TFI.....	9
3.3.2 Selection of Experts.....	10
3.3.3 Conduct of the Workshops.....	11
3.3.4 Conduct of the Interviews.....	12
3.3.5 Final Integration	12
3.4 Peer Review.....	13
3.5 Documentation	13
4. Case Study: Detailed Implementations for Two Sites in Southeastern U.S.	15
4.1 Expert Selection.....	15
4.2 Seismic Source Characterization	16
4.2.1 Introduction	16
4.2.2 Road Map for the Seismic Source Characterization.....	17
4.2.3 Review of Technical Issues, Workshop 1.....	17
4.2.4 Proponents Models, Workshop 2.....	21
4.2.5 One-on-one Elicitation Interviews	24
4.2.6 Integration and Feedback, Workshop 3.....	25
4.2.7 Feedback Comments.....	28
4.3 Ground Motion Attenuation in Eastern North America	30
4.3.1 Introduction	30
4.3.2 Structure of Elicitation Process	32
4.3.3 Ground Motion Characterization.....	34
4.3.4 Attenuation Relations.....	38
4.4 Analysis.....	40
4.4.1 General Scope of Calculations	40
4.4.2 Input Used in the Analyses.....	40

4.4.3	Comparison of the Hazard for an Individual Expert and for the Composite Seismicity Rates	41
4.4.4	Comparison of the Hazard Estimates for an Individual Expert and the Composite Zonation Maps	41
4.4.5	Comments on the Use of Composite Models	42
4.4.6	Comparison with the 1993 Eastern US Update for Watts Bar.....	42
References.....		137

Appendices

A	White Papers Developed as a Result of Issues Raised in Workshop #1.....	A-1
B	White Papers Assigned to Experts in Preparation of Workshop #3	B-1
C	Preliminary Source Geometries Developed by the Experts in Preparation of the Seismic Source Exercise of Workshop #2.....	C-1
D	Ground Motion Uncertainty in Probabilistic Hazard Analyses.....	D-1
E	Documentation of Excel 5.0 Spreadsheets and Fortran Codes for Developing Hybrid Empirical Ground-Motion Estimates for the Midcontinent of the Eastern United States.....	E-1
F	Trial Implementation Project—Plots of Maximum Magnitude and Recurrence Rate Estimates for Each Expert, and Composite Probability Distribution Function.....	F-1
G	Comparison of the Proabilistic Seismic Hazard Analysis Results of 1993 Eastern U.S. Update and 1998 Trial Implementation Project Studies for Watts Bar.....	G-1

Figures

4.2.6-1	Zonation Maps That Define the Various Alternative Interpretations.....	43
4.2.6-2A	Logic Tree Representation of Experts' Interpretations for Module 1: Charleston Issue.	57
4.2.6-2B	Logic Tree Representation of Experts' Interpretations for Module 2: Vogtle Local Region.....	58
4.2.6-2C(a)	Logic Tree Representation of Experts' Interpretations for Module 3: South Carolina–Georgia Issue.....	59
4.2.6-2C(b)	Logic Tree Representation of Experts' Interpretations for Module 4: Eastern Tennessee Seismic Zone Issue.....	60
4.2.6-2D	Logic Tree Representation of Experts' Interpretations for Module 5: Seismicity Rate Estimation Methodology.....	62
4.2.6-3	Example of Rates of Probability Distribution for One Zone, and Integration Into a Composite Probability Distribution.	63
4.3.3-1	Definition of Observation Points for Ground Motion Estimates.	64
4.3.3-2	Crustal Structure Regionalization for the EUS.....	64
4.3.3-3	Example of Material Given to the Experts for the Seismic Rate Estimates.	65
4.3.3-4a	Examples of Proponents Models Median Estimates of the Peak Ground Acceleration for Mw5.	66
4.3.3-4b	Examples of Proponents Models Median Estimates of the Peak Ground Acceleration for Mw7.	67
4.3.3-5a	Examples of Proponents Models Median Estimates of the 1-Second Period Spectral Acceleration for Mw5.....	68

4.3.3-5b	Example of Proponents Model Median Estimates of the 1-Second Period Spectral Acceleration for Mw7.....	69
4.3.3.6a	Examples of Proponents Estimates of the Aleatory Variability for the Peak Ground Acceleration Estimates.	70
4.3.3.6b	Examples of Proponents Estimates of the Aleatory Variability for the Peak Ground Acceleration Estimates.	71
4.3.4-1	Comparison of Regression Model Fits for the 5 Experts of the Study and the Composite Model, for the Horizontal Component Median Peak Ground Acceleration for Magnitude Mw7.....	72
4.3.4-2	Comparison of Regression Model Fits for the 5 Experts of the Study and the Composite Model, for the Horizontal Component Median Peak Ground Acceleration for Magnitude Mw5.	73
4.3.4-3	Comparison of Regression Model Fits for the 5 Experts and for the Composite Model, for the Horizontal Component Median 1-Second Period Spectral Acceleration for Magnitude Mw7.....	74
4.3.4-4	Comparison of Regression Model Fits for the 5 Experts and for the Composite Model, for the Horizontal Component Median 1-Second Period Spectral Acceleration for Magnitude Mw5.....	75
4.3.4.-5	Comparison of the Models of Aleatory Variability for the Horizontal Component of the Peak Acceleration.....	76
4.3.4.-6	Comparison of the Models of Aleatory Variability for the Horizontal Component of the 1-Second Period Spectral Acceleration.....	76
4.3.4.-7	Comparison of the Models of the Epistemic Variability for the Median Estimates of the Horizontal Component of the Peak Ground Acceleration for Magnitude Mw5.....	77
4.3.4.-8	Comparison of the Models of the Epistemic Variability for Median Estimates of the Horizontal Component for the 1-Second Period Spectral Acceleration for Magnitude Mw5.	77
4.3.4.-9	Comparison of the Models of the Epistemic Variability for the Median Estimates of the Horizontal Component of the Peak Ground Acceleration for Magnitude Mw7.....	78
4.3.4.-10	Comparison of the Models of the Epistemic Variability for Median Estimates of the Horizontal Component for the 1-Second Period Spectral Acceleration for Magnitude Mw7.....	78
4.3.4.-11	Comparison of the Models for the Epistemic Variability for the Median Estimates of Peak Ground Acceleration.....	79
4.3.4.-12	Comparison of the Models for the Epistemic Variability for the Median Estimates of the 1-Second Period Spectral Acceleration.....	79
4.4-1	Probabilistic Hazard Estimates for Vogtle. PGA for Bollinger’s Zonation Maps and Seismicity Rates, and Composite Ground Motion Model.....	80
4.4-2	Probabilistic Hazard Estimates for Vogtle. Uniform Hazard Spectra for Bollinger’s Zonation Maps and Seismicity Rates, and Composite Ground Motion Model.	80
4.4-3	Probabilistic Hazard Estimates for Vogtle. PGA for Bollinger’s Zonation Maps, Composite Seismicity Rates, and Composite Ground Motion Model.....	81
4.4-4	Probabilistic Hazard Estimates for Vogtle. Uniform Hazard Spectra for Bollinger’s Zonation Maps and Composite Seismicity Rates, and Composite Ground Motion Model.	81
4.4-5	Probabilistic Hazard Estimates for Watts Bar. PGA for Bollinger’s Zonation Maps and Seismicity Rates, and Composite Ground Motion Model.	82

4.4-6	Probabilistic Hazard Estimates for Watts Bar. Bollinger’s Zonation Maps and Seismicity Rates, and Composite Ground Motion Model.....	82
4.4-7	Probabilistic Hazard Estimates for Watts Bar. PGA for Bollinger’s Zonation Maps, Composite Seismicity Rates, and Composite Ground Motion Model.....	83
4.4-8	Probabilistic Hazard Estimates for Vogtle. Uniform Hazard Spectra for Bollinger’s Zonation Maps, Composite Seismicity Rates, and Composite Ground Motion Model.....	83
4.4-9	Probabilistic Hazard Estimates for Vogtle. PGA for Composite Models of Zonation Maps, Seismicity Rates, and Ground Motion Attenuation.....	84
4.4-10	Probabilistic Hazard Estimates for Vogtle. Uniform Hazard Spectra for Composite Models of Zonation Maps, Seismicity Rates, and Ground Motion Attenuation.....	84
4.4-11	Probabilistic Hazard Estimates for Watts Bar. PGA for Composite Models of Zonation Maps, Seismicity Rates, and Ground Motion Attenuation.....	85
4.4-12	Probabilistic Hazard Estimates for Watts Bar. Uniform Hazard Spectra for Composite Models of Zonation Maps, Seismicity Rates, and Ground Motion Attenuation.....	85

Tables

4.1-1	Expert Evaluators Selection Criteria.....	86
4.1-2	Weights Assigned to Each of the Criteria of Table 4.1-1	87
4.1-3	Pool of Experts Considered	87
4.1-4	Final Selection of Expert Evaluators for the Seismic Source Characterization.....	88
4.2-2-1	Detailed Road Map for the Performance of the TIP Project.....	89
4.2.3-1	List of Participants at Workshop 1	93
4.2.6-1	List of Participants to the PSHA Source Characterization Trial Implementation Project Workshop III.....	94
4.2.6-2	Description of the Minimum Set Zones.....	95
4.3.1-1	Point Estimates Considered in the 1994 Trial Application	97
4.3.2-1	List of Candidates for Ground Motion Experts Considered for the TIP Project	98
4.3.3-1	Proponent Models	98
4.3.3-2	Point Estimate Matrix.....	99
4.3.3-3	ENA Velocity Profile.....	99
4.3.3-4	Q Model.....	99
4.3.3-5	132 Case Definitions for Point Estimates	100
4.3.3-6	D. L. Bernreuter: General Model Weighting Scheme.....	105
4.3.3-7	D. M. BOORE: Model Weighting Scheme	105
4.3.3-8	K. W. CAMPBELL: General Model Weighting Scheme	106
4.3.3-9	K. JACOB: Model Weighting Scheme, μ Estimates (Unnormalized Values)	107
4.3.3-10	P. G. SOMERVILLE: Model Weighting Scheme.....	109
4.3.4-1A	D. L. Bernreuter: Regression Coefficients Median Model.....	110
4.3.4-1B	D. L. Bernreuter: Regression Coefficients Sigma Model	110
4.3.4-1C	D. L. Bernreuter: Regression Coefficients Sigma-Mu Model.....	111
4.3.4-1D	D. L. Bernreuter: Regression Coefficients Sigma-Sigma Model.....	111
4.3.4-2A	D. M. Boore: Regression Coefficients Median Model.....	112

4.3.4-2B	D. M. Boore: regression Coefficients Sigma Model.....	112
4.3.4-2C	D. M. Boore: Regression Coefficients Sigma-Mu Model.....	113
4.3.4-2D	D. M. Boore: Regression Coefficients Sigma-Sigma Model.....	113
4.3.4-3A	K. W. Campbell: Regression Coefficients Median Model.....	114
4.3.4-3B	K. W. Campbell: Regression Coefficients Sigma Model.....	114
4.3.4-3C	K. W. Campbell: Regression Coefficients Sigma-Mu Model.....	115
4.3.4-3D	K. W. Campbell: Regression Coefficients Sigma-Sigma Model.....	115
4.3.4-4A	K. Jacob: Regression Coefficients Median Model.....	116
4.3.4-4B	K. Jacob: Regression Coefficients Sigma Model.....	116
4.3.4-4C	K. Jacob: Regression Coefficients Sigma-Mu Model.....	117
4.3.4-4D	K. Jacob: Regression Coefficients Sigma-Sigma Model.....	117
4.3.4.5A	P. G. Somerville: Regression Coefficients Median Model.....	118
4.3.4.5B	P. G. Somerville: Regression Coefficients Sigma Model.....	118
4.3.4.5C	P. G. Somerville: Regression Coefficients Sigma-Mu Model.....	119
4.3.4.5D	P. G. Somerville: Regression Coefficients Sigma-Sigma Model.....	119
4.3.4-6A	Expert Composite: Regression Coefficients Median Model.....	120
4.3.4-6B	Expert Composite: Regression Coefficients Sigma Model.....	120
4.3.4-6C	Expert Composite: Regression Coefficients Sigma-Mu Model.....	121
4.3.4-6D	Expert Composite: Regression Coefficients Sigma-Sigma Model.....	121
4.4-1	Probability Distributions of the Upper Magnitude Cutoff Mu for Bollinger.....	122
4.4-2	Probability Distributions of the Upper Magnitude Cutoff Mu for Chapman.....	123
4.4-3	Probability Distributions of the Upper Magnitude Cutoff Mu for Coppersmith.....	124
4.4-4	Probability Distributions of the Upper Magnitude Cutoff Mu for Jacob.....	125
4.4-5	Probability Distributions of the Upper Magnitude Cutoff Mu for Talwani.....	126
4.4-6	Probability Distributions of the Seismicity Rates $f(4)$ for Bollinger.....	127
4.4-7	Probability Distributions of the Seismicity Rates $f(4)$ for Chapman.....	128
4.4-8	Probability Distributions of the Seismicity Rates $f(4)$ for Coppersmith.....	129
4.4-9	Probability Distributions of the Seismicity Rates $f(4)$ for Jacob.....	130
4.4-10	Probability Distributions of the Seismicity Rates $f(4)$ for Talwani.....	131
4.4-11	Probability Distributions of the Seismicity Rates $f(m1)$ for Bollinger.....	132
4.4-12	Probability Distributions of the Seismicity Rates $f(m1)$ for Chapman.....	133
4.4-13	Probability Distributions of the Seismicity Rates $f(m1)$ for Coppersmith.....	134
4.4-14	Probability Distributions of the Seismicity Rates $f(m1)$ for Jacob.....	135
4.4-15	Probability Distributions of the Seismicity Rates $f(m1)$ for Talwani.....	136

EXECUTIVE SUMMARY

During a previous project under the sponsorship of the Nuclear Regulatory Commission, the Department of Energy (DOE), and with contribution by the Electric Power Research Institute (EPRI), a panel of scientists was convened to perform a study of probabilistic seismic hazard assessment (PSHA) methodologies. The panel, named the Senior Seismic Hazard Analysis Committee (SSHAC), developed a set of guidelines which were published as NUREG/CR-6372 and referred to as the SSHAC report.

The SSHAC was tasked with developing an improved methodology that would be useable for regulatory applications for about the next decade for both regional and site-specific analyses. In evaluating existing methodologies and general principles, they found that most of the problems in past PSHA applications were caused by flawed expert elicitation and procedural guidance for PSHA and rigorous treatment of uncertainties. Where necessary, the SSHAC also provided guidance for the subjects of seismic source characterization and ground motion estimation.

Their overall conclusion is that there are important pitfalls in using experts effectively, and that the key task is technical integration. Depending on technical complexities and regulatory significance, the study is led by either a Technical Integrator (TI) or a Technical Facilitator/ Integrator (TFI) who is responsible for the results of the PSHA. The TI is commonly used for less complex tasks, such as a site-specific study for a bridge or other project. The TFI is employed for more complex regional studies or for investigations related to a critical facility, such as a nuclear power plant. The TFI would commonly consist of two or three individuals with the requisite range of experience in earth sciences and expert elicitation. The TFI evaluates a range of hypotheses and models presented by the experts, and arrives at a representation of the knowledge of the group and of the scientific community at large. The expert elicitation depends heavily on

group interaction and structured workshops where available facts are presented. The aim of the TFI process is to develop as much of a consensus as possible; however, where that goal is not reached and where there may be “outlier” opinions, it is up to the TFI to formulate the most consistent result, including behavioral aggregation involving qualitative judgment.

With respect to uncertainties in seismic hazard assessment, the SSHAC adopted a rigorous treatment based on a distinction between epistemic and aleatory uncertainties. Epistemic uncertainties are based on a lack of scientific understanding that may be reduced in the future. Aleatory or “random” uncertainties cannot be reduced for all practical purposes. These terms were chosen to avoid multiple meanings associated with words such as “uncertainty” for epistemic. Further characteristics of the SSHAC methodology involve careful documentation of the PSHA process and of the data and models used. Also required is adequate peer review in both the TI and TFI processes, including technical and process peer review. In the course of their work, the SSHAC held several workshops that served to refine the guidelines and prove their efficiency.

Two of the most significant aspects of the new guidelines provided by SSHAC are the TFI concept and a departure from relying on inflexible aggregation schemes, such as a priori equal weights. The guidelines were reviewed by a committee of the National Academy of Sciences (NAS) and given generally positive comments. The review committee, in particular, agreed with and further emphasized the principle of not relying on mechanical aggregation schemes.

The efforts of the SSHAC concentrated on defining the overall procedure for eliciting expert interpretations and integrating them. The procedure was tested partially on the problem of developing ground motion attenuation models. The seismic source characterization is a more difficult problem which was not tackled by the SSHAC, and thus became the starting point for a

new project described in this report and called the Trial Implementation Project (TIP). The scope of TIP was to test the recommendation of the SSHAC on the characterization of the seismic sources, and to finalize the development of ground motion attenuation models for eastern North America started by SSHAC. The study had the goal of testing and implementing the SSHAC guidelines for the specific case of the southeastern United States and of two nuclear plant sites in that region, namely Vogtle and Watts Bar. Workshops and expert elicitations were held in accordance with SSHAC principles, with emphasis on seismic source characterization. This project has shown that the TFI procedures can lead to an unusual degree of agreement among experts through thorough discussion of the available data, and through interaction between the experts. Together with the focusing effect of the TFI, this leads to narrower margins of variation without any coercion. For the southeastern U.S. this led to an integrated map of source zones that incorporated the opinions of all the experts involved, even though they began with fairly different source zone maps. This is in stark contrast to the previous situation, where each expert produced a series of map interpretations, leading to a large number of source zone maps, most of which were totally different from each other.

The process used for the southeastern U.S. source map eliminated several variations in source zones, because different experts were able to agree on a compromise solution that was consistent with their interpretation and would not significantly change the final hazard. In some cases, such as near the Watts Bar plant, where a change in zone boundaries can change the site hazard substantially, differing opinions were incorporated by using three versions of a source zone boundary. Each zone boundary variant was assigned a probability relating to the level to which each expert believes it is supported by the observed data and general physical concepts, thus incorporating the range of expert opinions. We found that by concentrating on extracting from the experts' interpretations what was common to all or to the majority, we were able to identify a set of

common seismic source zones that all experts could use to formulate their own interpretations in the form of different zonation maps.

However, we were careful to identify enough common zones to be able to represent all the diversity in the experts' interpretations. The main purpose of this process was to minimize the unnecessary, or artificial, diversity by making sure that those interpretations which appeared different, were indeed different. Those which were not were folded into a common interpretation, with some uncertainty. These minimum set zones which we refer to as the common building blocks allow us to have a limited number of seismic sources to express all the possible alternatives of all the experts. Then we consider each seismic source separately and obtain its seismicity rate, upper magnitude cutoff characterization (a probability distribution function) by eliciting all of the experts, to model both the aleatory and epistemic uncertainty.

In addition to keeping all of the experts' zonation maps separate (but still using the minimum set zones) we tested the effect of developing a set of composite seismic zonation maps developed by the TFI. We found that to perform that task we needed to include in the set of alternatives all of the experts' alternatives to preserve the dependencies between the seismic sources. This, however, was a relatively easy task, done by putting together the various combinations of seismic sources in the minimum set to build all the needed maps. Our test cases show that the use of composite ground motion models, composite seismic zonation maps, and composite seismicity rates constitutes an estimate of the seismic hazard, the main reasons being that (1) it uses the same building block seismic sources as those defined by the experts and (2) the elicitation process emphasized the effect of the dominant sources on the hazard and consequently experts' diversity is minimized for these seismic sources. The only difficulty that has remained in this and other projects using the SSHAC guidelines is the treatment of uncertainties. Many of the experts still have problems following a rigorous distinction between various epistemic and aleatory uncertainties.

ACKNOWLEDGMENTS

This project has been sponsored by the U.S. Nuclear Regulatory Commission (NRC). The project manager for the NRC was Ernst Zurflueh, and Jean Savy led the project for Lawrence Livermore National Laboratory. We would like to thank all the persons who contributed to the realization of this project: the expert evaluators for the source characterization G. Bollinger, M. Chapman, K. Coppersmith, K. Jacob, and P. Talwani, and for the ground motion characterization D. Bernreuter, D. Boore, K. Campbell, K. Jacob, and P. Somerville. We extend our thanks to all the other participants, for without their presence and knowledge, this project would not have been possible. These included D. Amick, B. Gelinas, A. Johnston,

R. Lee, R. Marple, J. Martin, C. Mueller, M. Petersen, C. Powell, D. Stephenson, A. Stievi, and G. Vlahovic, as well as the observers from the Department of Energy, Jeff Kimball, and from the NRC, C. Munson and B. Ibrahim.

We want to give special thanks to A. Cornell, who can always keep his cool and humor and yet keep us in line and pushes us to always try our best.

Pulling all this material together and writing this report has tested the patience, and the strong desire to complete this study, of the two main authors N. Abrahamson and J. Savy, and has shown invaluable support from R. Yamamoto.

ABBREVIATIONS

DOE	Department of Energy
EPRI	Electric Power Research Institute
ETSZ	Eastern Tennessee Seismic Zone
EVA	Expert Evaluator
NPR	New Production Reactor
NRC	Nuclear Regulatory Commission
PSHA	Probabilistic Seismic Hazard Analysis
SRS	Savannah River Site
SSHAC	Senior Seismic Hazard Analysis Committee
TFI	Technical Facilitator Integrator
TI	Technical Integrator
TIP	Trial Implementation Project

1. INTRODUCTION

1.1 Background

Probabilistic Seismic Hazard Analysis (PSHA) is a methodology that estimates the likelihood that various levels of earthquake-caused ground motion will be exceeded at a given location in a given future time period. Due to large uncertainties in all the geosciences data and in their modeling, multiple model interpretations are often possible. This leads to disagreement among experts, which in the past has led to disagreement on the selection of ground motion for design at a given site.

In 1994, in order to review the present state-of-the-art and improve on all the overall stability of the PSHA process, the U.S. Nuclear Regulatory Commission (NRC), the U.S. Department of Energy (DOE), and the Electric Power Research Institute (EPRI) co-sponsored a project to provide methodological guidance on how to perform a PSHA.

The project has been carried out by a seven-member Senior Seismic Hazard Analysis Committee (SSHAC) supported by a large number of other experts.

The SSHAC reviewed past studies, including the Lawrence Livermore National Laboratory and the EPRI landmark PSHA studies of the 1980's and examined ways to improve on the present state-of-the-art.

The Committee's most important conclusion was that differences in PSHA results are due to procedural rather than technical differences. Thus, in addition to providing a detailed documentation on state-of-the-art elements of PSHA, the SSHAC report (NRC 1997), provides a series of procedural recommendations. As part of the SSHAC effort, the recommendations of the SSHAC were partially tested in the development of a ground motion attenuation model for North America. That test had been selected because of the relative simplicity of formulation of the ground motion attenuation models. The issues to be discussed and the input to be generated is limited to the characterization of a few, well defined single parameters. In

contrast to the case of the development of ground motion attenuation models, the development of seismic zonation maps involves the evaluation of multi dimensional data sets. The description of future seismicity through the use of seismic zonation maps and occurrence models are multiparameters models with very complex formulation and correlation structure.

Although the SSHAC did not test its recommendations on the development of zonation and seismicity models it was understood that the recommendations provided were general enough to apply to any problems in which it is important to characterize the epistemic uncertainty through the use of multiple experts inputs including for the case of seismic source zonation modeling.

1.2 Purpose of the Study, Scope

The purpose of this project, under Job Code W6496, titled "Trial Implementation of SSHAC Guidelines", is to test and implement the guidelines developed by the Senior Seismic Hazard Analysis Committee (SSHAC) developed under FIN L2503 (NRC 1997). Like the SSHAC project, the TIP (Trial Implementation Project) has the purpose of improving our ability to quantify and reduce uncertainties in seismic hazard estimation. The objectives of this study are to exercise the process improvement recommended in the SSHAC report specifically for seismic source characterization and to implement the methodology in a manner designed to achieve optimum stability in the PSHA results.

The scope of this project also includes an update of the ground motion models developed in the test by SSHAC. The test had been limited by the number of pairs of magnitudes and distances sampled by the experts. This project revisits the work done by SSHAC and extends it to a much bigger set of pairs of magnitudes and distances.

As a more substantial effort than the development of ground motion models, the seismic source characterization effort includes investigating the motion of composite seismic

zonation maps, and minimum set zones. This part of the scope includes a demonstration of the development of a set of seismic zonation maps which are meant to sample the interpretation of the seismicity experts selected for the project. At each step in this implementation of the SSHAC guidelines, new procedural steps are identified consistent with the guidelines, but specific to the task of seismic source characterization.

1.3 Organization of the Report

After summarizing the general requirements and the guiding principles of SSHAC in Section 2, Section 3 provides some practical guidance on performing a PSHA. The guidance is based on the actual implementation of the SSHAC guidelines documented in Section 4.

Section 4 contains a detailed account of the procedure implemented. It includes the selection

of the experts, the process of elicitation of the experts interpretations, the formulation of the alternative maps, the reduction of the set of zones to the minimum set by the Technical Facilitator Integrator (TFI). Section 4.3 gives a detailed account of the process applied to the ground motion attenuation models, and Section 4.4 gives some hazard results for two sites.

1.4 Use of This Document

This document is not intended to provide a compulsory method of performing PSHA. It gives guidance on ways to approach the issue of uncertainty in the characterization of seismic sources and in the development of ground motion models. The guidance will help the analyst in providing a checklist of tested methods for ensuring that all criteria which define a quality PSHA, as set by the SSHAC (NRC 1997) are met.

2. GENERAL REQUIREMENTS OF A PSHA

2.1 Fundamental SSHAC Guiding Principle

PSHA inputs involve multiple issues, e.g., ground motion models, ground motion uncertainty, seismic source identification, seismicity parameters, etc. The complexity, importance and diversity of judgments within the appropriate scientific community regarding any one of these issues vary between study location (east vs. west U.S.), range of the study (site-specific vs. regional), and other factors.

SSHAC (NRC 1997) clearly sets the driving principle for the basis of the inputs in a PSHA as follows:

“A basic principle defined by the Committee is that the underlying basis for the inputs related to any of these issues must be the composite distribution of views represented in the appropriate scientific community. Expert judgment is used to represent the informed scientific community’s state of knowledge. Of course, it is impractical—and unnecessary—to engage an entire scientific community in any meaningful interactive process. Decision makers must always rely on a smaller, but representative, set of experts. Thus, we view an expert panel as a sample of the overall expert community and the individual Technical Integrator (defined later) as the expert “pollster” of that community, the one responsible for capturing efficiently and quantitatively the community’s degree of consensus or diversity.

“Regardless of the scale of the PSHA study, the goal remains the same: to represent the center, the body, and the range of technical interpretations that the larger informed technical community would have if they were to conduct the study.”

2.2 Procedural Recommendations

Following the fundamental principle, restated above, SSHAC’s investigation of the issues led to a set of nine recommendations which are felt

to summarize the procedural guidance to achieve the goals of the fundamental principle. These recommendations are reproduced below and constitute the basis for the performance of a state-of-the-art PSHA. (Taken from NRC 1997):

- 1) SSHAC identifies and describes several different roles for experts based on its conclusion that confusion about the various roles is a common source of difficulty in executing the aspect of PSHA involving the use of experts. The roles for which SSHAC provides the most extensive guidance include the expert as proponent of a specific technical position, as an evaluator of the various positions in the technical community, and a technical integrator (see the next paragraph).
- 2) SSHAC identifies four different types of consensus, and then concludes that one key source of difficulty is failure to recognize that 1) there is not likely to be “consensus” (as the word is commonly understood) among the various experts and 2) no single interpretation concerning a complex earth sciences issue is the “correct” one. Rather, SSHAC believes that the following should be sought in a properly executed PSHA project for a given difficult technical issue: (1) a representation of the legitimate range of technically supportable interpretations among the entire informed technical community, and (2) the relative importance or credibility that should be given to the differing hypotheses across that range. As SSHAC has framed the methodology, this information is what the PSHA practitioner is charged to seek out, and seeking it out and evaluating it is what SSHAC defines as technical integration.
- 3) SSHAC identifies a hierarchy of complexity for technical issues, consisting of four levels (representing increasing levels of participation by technical experts in the development of the desired results), and then concentrates much of its guidance on the most complex level (level 4) in which a

panel of experts is formally constituted and the panel's interpretations of the technical information relevant to the issues are formally elicited. To deal with such complex issues, SSHAC defines an entity that it calls the Technical Facilitator/Integrator (TFI), which is differentiated from a similar entity for dealing with issues at the other three less-complex levels, which SSHAC calls the Technical Integrator (TI). Much of SSHAC's procedural guidance involves how the TI and TFI function should be structured and implemented. (Both the TI and TFI are envisioned as roles that may be filled by one person or, in the TFI case, perhaps by a small team).

- 4) The role of technical integration is common to the TI and TFI roles. What is special about the TFI roles, in SSHAC's formulation, is the facilitation aspect, when an issue is judged to be complex enough that the views of a panel of several experts must be elicited. SSHAC's guidance swells on that aspect extensively, in part because SSHAC believes that this is where some of the most difficult procedural pitfalls are encountered. In fact, the main report identifies a number of problems that have arisen in past PSHAs and discussed how the TFI function explicitly overcomes each of them.
- 5) For most technical issues that arise in a typical PSHA, the issue's complexity does not warrant a panel of experts and hence the establishment of a TFI role. Technical integration for these issues can be accomplished—indeed, is usually best accomplished—by a TI. In fact, SSHAC has structured its recommended methodology so that even the most complex issues can be dealt with using the less expensive TI mode, although with some sacrifice in the confidence obtained in the results on both the technical and the procedural sides.
- 6) One special element of the TFI process is SSHAC's guidance on sequentially using the panel of experts in different roles. Heavy

emphasis is placed on assuring constructive give-and-take interactions among the panelists thought the process. Each expert is first asked, based on his/her own knowledge (yet cognizant of the views of other as explored through the information-exchange process), to act as an evaluator, that is, to evaluate the range of technically legitimate viewpoints concerning the issue at hand. Then, each expert is asked to play the role of technical integrator, providing advice to the TFI on the appropriate representation of the composite position of the community as a whole.

Contrasting the classical role of experts on a panel acting as individuals and providing inputs to a separate aggregation process, the TFI approach views the panel as a team, with the TFI as the team leader, working together to arrive at (i) a composite representation of the knowledge of the group, and then (ii) a composite representation of the knowledge of the technical community at large. (Neither of these representations necessarily reflects panel consensus—they may or may not and their validity does not depend on whether a panel consensus is reached.)

The SSHAC guidance to the TFI emphasizes that a variety of techniques are available for achieving this composite representation. SSHAC recommends a blending of behavioral or judgmental methods with mathematical methods, and in the body of the report several techniques along these lines are described in detail. Key objective for the TFI is to develop an aggregate result that can be endorsed by the expert panel both technically and in terms of the process used.

- 7) The TFI's integrator role should be viewed not as that of a "super-expert" who has the final say on the weighting of the relative merits of either specific technical interpretations or the various experts' interpretations of them; rather, the TFI role should be seen as charged with characterizing both the commonality and the

diversity in a set of panel estimates, each representing a weighted combination of different expert positions. SSHAC thus sees the TFI as performing an integration assisted by a group of experts who provide integration advice.

- 8) Thus, the TFI as facilitator structures interaction among the experts to create conditions under which the TFI's job as integrator will be simplified (e.g., either a consensus representation is formed or it is appropriate to weight equally the experts' evaluations of the knowledge of the technical community at large). In the rare case in which such simple integration is not appropriate, additional guidance is provided. In the main report, guidance is presented on two possible approaches involving (i) explicit quantitative but unequal weights (when it becomes obvious that using equal weighting misrepresents the community-as-a-whole); and (ii) "weighing" rather than "weighting", in cases when the experts themselves, acting as evaluators and integrators, find fixed numerical weights to be artificial, and when it is appropriate to represent the community's overall distribution in a less rigid way.
- 9) The SSHAC guidance gives special emphasis to the importance of an independent peer review. We distinguish between a participatory peer review and a late-stage peer review, and we also distinguish between a peer review of the process aspects and of the technical aspects for the more complex issues. We strongly recommend a participatory peer review, especially or the process aspects for the more complex issues. This paper details the pitfalls of an inadequate peer review.

2.3 Implementation for Ground Motion Attenuation and Seismic Source Characterization

SSHAC had already demonstrated the applicability of its general principle and procedures to the case of development of ground motion attenuation models. In this area, the

study reported here does not add substantially to the overall methodology described in the SSHAC report (NRC 1997). Rather, our effort was concentrated on re-sampling the ground motion experts to provide a higher resolution in the definition of the inputs to defining the composite ground motion attenuation models, and incorporate the latest scientific developments in the area of ground motion estimation.

The implementation for the seismic source characterization is more complex because different experts will typically offer alternative models of seismic sources, and of recurrence of earthquakes which seem to have no commonalities. This makes impossible the task of providing composite distribution of views about well identified parameters.

Therefore, the basic driving concept in developing the inputs for seismic source characterization consisted of:

- Identifying the commonalities between the alternative models of seismic sources formulated by all the experts.
- Developing a core seismic sources model that all the experts agree upon, (although each expert might assign different degree of credibility on the models).
- Characterizing each seismic zone by simple parameters which can be the object of discussion by all the experts and lead to a composite distribution of views.
- Developing the remaining set of seismic sources to represent the views of all experts for those alternatives not included in the core seismic sources.

The main challenge in this exercise is sorting out between different experts what constitutes real scientific disagreement and what is merely misunderstanding or nuances of interpretation of the same idea. For example it is not uncommon to have two experts formulate two different seismic zone shape and/or size for a particular area. In this case, the role of the TFI is just to determine whether the two different models

come in two different interpretations of the data, through the use of different, say equally valid, physical models. If this is the case, it is not possible to reduce the two different models to a single, simpler one. However, if it is found, after full interaction of the experts, TFI, and possibly other experts, that the scientific bases for formulating the model are common, it is then possible to narrow the differences and formulate a simpler single model, with uncertainty to express the various nuances of interpretation.

This study demonstrates that it is possible to express the entire distribution of views of all the experts in seismic source characterization with a limited number of individual seismic sources. This we call the minimum zone set. Each seismic source and its uncertainty is the results of interaction between all the experts in the project and each of the identifiable parameters characterizing a source are defined by these distributions of views of the experts. It is at the level of these distributions of views (which for single parameters translate into probability distribution functions) that we talk about a consensus of the experts.

3. GUIDANCE FOR A PRACTICAL APPROACH

3.1 General Road Map

The level of effort that will be allocated for a project will determine the level of detail and size of each portion of the project tasks. However, following the set of principles established by the SSHAC and summarized in Section 2, it is important to recognize that the overall process of a PSHA which relies on the use of experts inputs needs to contain all of the following twelve steps:

1. Selection of participants
 - Technical Facilitator Integrator (TFI) either single or team
 - Experts, (Technical Experts and Expert Evaluators EVA) either individuals or teams
2. Knowledge dissemination for the seismic source definitions, and ground motion modeling
 - general data
 - proponent interpretations
 - issues relevant to the particular project
 - training of the participants (hazards, uncertainty)
3. EVAs evaluate individually and formulate draft interpretation of sources, or of ground motion estimates or model selections prior to extensive interaction.
4. EVA's individual interpretations are discussed, explained, clarified in group interactive session organized and facilitated by the TFI.
 - clarification of EVA's interpretation
 - Formulation by the TFI of the Minimum Zone Set
 - Formulation of acceptable ground motion attenuation models
5. EVA finalize their individual set of alternative interpretations
6. Detailed documentation is generated by the EVA for the geometrical description of the source zones for the derivation of ground motion estimates.
7. Knowledge dissemination for the sources seismicity characterization
 - review data bases
 - analysis tools
 - analysis support
 - review technical issues relevant to the particular project
8. EVAs evaluate individually and formulate draft interpretations of seismicity characteristics.
9. EVAs individual interpretations are discussed explained and clarified in group interactive sessions and facilitated by the TFI.
10. EVAs finalize their individual interpretations.
11. Detailed documentation is generated by EVA for the models of seismicity characterization.
12. Peer Review of the implementation of the actual PSHA process.

This general road map applies for both the seismic source characterization and ground motion attenuation modeling.

The twelve elements can be implemented in a variety of ways. The case study in Chapter 4 describes one of the ways which can be viewed as intermediary between a simple minimum type of analysis and a full fledged analysis.

The selection of the TFI and of the experts is the first step and a very delicate one. To avoid bias or other problems likely to shed negative lights on a study, it is recommended, as much as

possible to adopt a well structured, well documented process at least of the type described in the case study Section 4.1.

The knowledge dissemination, formulation of draft interpretations and finalization constitute the “experts” elicitation process. It can be achieved by a combination of interactive workshops, extensive one-on-one interaction between the TFI and the EVAs, generation of white papers to discuss specific issues, written questionnaires, one-on-one (elicitation) interviews, and (TFI) facilitated group interaction sessions.

Figure 3-1 shows a typical example of the general structure of a PSHA.

Not shown on Figure 3-1 are numerous possible improvements. Implementation of the improvements is dependent on the overall level of analysis, for a specific project. They include, but are not limited to the possibility of providing interaction between the ground motion attenuation experts and the seismic source characterization experts. This is always desirable as it helps both sets of experts understand the practical issues. It helps them identify the important elements of their modeling, so they can concentrate on those rather than effects less important to the hazard. For example, an expert might consider different types of attenuation models if the most important seismic sources are faults close to the site for which the hazard is to be estimated, as opposed to the case where the dominant hazard would be contributed by a distant source. The type of faulting, hanging wall, foot wall etc., are also considerations that would influence a ground motion expert in the selection of appropriate models of attenuation.

White papers are very useful tools to help the experts interact by pushing them to develop position sometimes in opposition to their own beliefs and scientific persuasions. They discover some ways of interpreting data, that are new to them, and help them formulate ranges of possible interpretations that they would not see otherwise.

Sensitivity analyses are important to show the experts, in a generic fashion, the effects of various hypotheses on the estimation of the seismic hazard. It is crucial that these sensitivity studies be generic so that the owner of the results cannot be accused of influencing the experts by presenting “undesirable” results.

There is a need however to present the final results to all the experts and ask for their comments. In the case of disagreement among experts, there is no absolute need to make additional changes, but all forms of disagreement need to be documented as well as all forms of consensus developed by the experts.

3.2 Data Requirements

All of the available data that could have an influence in forming the bases for models of where, when and what types of earthquakes occur as well as the ground motion they might generate at the site of the nuclear power plant, must be collected reviewed and evaluated. A detailed description of the type of data, their use and how to evaluate them is given in NUREG/CR-6372.

At each step of the way in the study, the need for additional data might become an issue. In particular, site specific geotechnical data are essential for performing educated soil amplification studies. What and how much data is enough cannot be determined in the absolute. It depends on many factors, including, technical need and economics.

At the minimum, before embarking in a costly field investigation campaign, a simple cost benefit analysis should be performed. In most cases, additional field investigations, such as “geologic” trenches, help in confirming a hypothesis (or informing) regarding the existence of a fault or some of its characteristics. As mentioned above, soil sampling and laboratory testing can be essential in developing input for models of the soil amplification at a site.

3.3 Elicitation and Integration Process

One of the goals of the TIP was to determine whether it is possible to develop a composite model of the seismic source zonations by integrating the models formulated by a set of individual experts (or separate teams of experts), into a single set of alternative zonation maps. This would be obviously possible by stacking all the experts' maps but very impractical. Instead it is possible, at the cost of losing some aspects of the correlation between the source zones, to develop a simplified integrated set of maps that we call the composite seismic source zonation model. All other things being equal, the composite model should lead to the same mean hazard but possibly only slightly different estimates of the uncertainty.

The TFI will develop the composite SSC. In doing so, the features of the models of all the EVA which are important to the hazard at the site, and important to the quantification of the uncertainty on the hazard, will be included in the composite model.

Thus, deciding whether one wants to perform an analysis including all the experts interpretation kept separate or by using a composite model will depend on the amount of resources and time available. The development of a composite model should follow all the same principles of Section 3.1, and for which guidance is given in the following subsections, but for which each step can be simplified.

For example, a simplified approach could be based on small team of analysts including a TFI. In this case, the SSHAC (NUREG/CR-6372, p. 22) makes a distinction between Technical Integrator (TI) and the Technical Facilitator Integrator (TFI). The case where there is a need for full extensive interaction with a well identified group of experts who are an integral part of the project, and "a component distribution of the informed technical community" is sought, is referred to the role of the TFI. The role of the TI is also to develop "a composite distribution of the informed technical community" but without the expensive trappings

attached to the TFI approach. In this guidance document, we do not differentiate between the TI or TFI, they are seen as the same entity, implementing different levels of the same process. C'est tout! Experts will be consulted, formally, but not necessarily within the context of workshops. The TFI gathers all the information, proceeds with interaction with the experts, following all the basic steps, on step 1 through 12 described above, but without formally eliciting the experts. The experts interpretations are inferred by the TFI and discussed with the experts. The peer review can be a simple review of the process by an independent reviewer who understands the SSHAC process and seismic hazard analysis.

3.3.1 Selection of TFI

The primary role of the TFI is to facilitate the interaction between the technical experts and help them evaluate the data and the proposed models of data interpretation. The TFI does not evaluate the data but rather evaluates the extent to which each of the EVA's interpretations are supported by the data and have threads of commonality so that an integrated version, the composite model, can be developed which represent a distribution of the informed technical community. In consequence, the attributes sought for in a TFI (or TFI Team) are as follows:

- Knowledgeable in the PSHA process as defined in this guidance document and in NUREG/CR-6372.
- Be Technically independent, (not being the proponent of any specific model),
- Knowledgeable in the generic aspects of the related scientific areas to understand the technical issues and be able to facilitate the experts discussion.
- Have general knowledge of the statistical, geological and geophysical analysis tools used in PSHA and by the experts.
- Have demonstrated the ability to socially interact positively with a group of engineers and scientists with different views.

- Be able and willing to devote all the needed level of effort to carry out the implementation of the project within the bounds of time required by the sponsor.

The above attributes, augmented by considerations specific to a particular project will be used to identify a pool of candidates for the TI/TFI team from which to select one in a manner similar to the process described in Section 3.3.2 for the selection of the experts. However, in practice the choice is limited between a few candidates or teams in general already associated with the sponsoring organization. Nevertheless, the same general attributes have to be used for the final selection. A lack of the right pedigree on the part of the TI/TFI Team could jeopardize the overall credibility and value of the final results, especially in controversial licensing cases, such as those of Nuclear Power Plants siting or other critical facilities siting.

3.3.2 Selection of Experts

Experts can be asked to play several different roles in the course of a PSHA. The Senior Seismic Hazard Analysis Committee (NRC 1997) defines the expert roles of proponent, evaluator, and integrator, roles that were understood and employed by the experts. A proponent advocates a particular technical hypotheses or interpretation, an evaluator considers the support for alternative hypotheses and interpretations in the available data and evaluates the uncertainties associated with the assessments, and an integrator combines the evaluators' alternative interpretations into a composite distribution that includes uncertainties. The experts are informed of their roles as evaluator experts and of the need to forsake the role of proponent in making their interpretations and evaluating uncertainties. Proponents of specific hypotheses or interpretations are engaged as resources and present their hypotheses or interpretations in workshops. Alternative proponent views are presented to the experts and open scientific debates of alternative views are facilitated among them at the workshops. Some expert evaluators also can be engaged temporarily as

proponents to describe a particular hypothesis or interpretation in a workshop.

Expert interactions are deemed vital in the SSHAC process and must be properly facilitated. Experience from numerous seismic hazard studies has shown that experts interact frequently in their professional activities, and that workshops serve to provide information and interaction that facilitate their consideration of hypotheses and data and, ultimately, their evaluations and interpretations. Expert interactions are encouraged and must be facilitated through multiple workshops and, for seismic source characterization, a field trip if possible.

Finally, the SSHAC (1997) process emphasizes the need to consider at the outset the strategy for integration or aggregation of the experts' evaluations, so that the analyses are structured in a way that is conducive to aggregation. This project at the outset defined a strategy to combine the evaluations of the experts using equal weights. The key procedural components of the project (ranging from the selection of experts to the dissemination of data sets) were designed to allow the equal-weights strategy to be implemented in a defensible manner.

The selection process must therefore be tailored to fulfill these requirements. The final selected individuals/teams should as best as possible represent a uniform sampling of the community of experts. No particular school of thoughts or specific interests should be more represented than others.

All the experts/teams selected should be among the best available technically and be among the most knowledgeable of the issues of interest, including knowledge of the data, the current interpretations of the data, the methods and tools of analysis and above all show the willingness to devote the necessary time and effort to the elicitation process. In this regard, experience shows that volunteer individuals do not perform as well as individuals on paid assignments to the project. Costly delays can develop as a result of lack of availability or commitment of an expert.

The case study gives a typical example of how to select individual experts. (See Section 4.1.)

3.3.3 Conduct of the Workshops

There is no general rule for setting up, organizing and conducting the workshops since their purpose and goals can be very different. In general, there will be the need for a workshop or working meeting each time an issue or series of issues need to be discussed interactively with all the “appropriate” experts associated with a particular project. The word “appropriate” is used here to signify that the type of issue, the area of study, will be the main considerations to determine who should be part of these workshops. Depending on the level of funding and the level of effort allocated to a project the participants to these workshops can be either the members of the analysis team, including a TFI, or can also include outside technical experts for the purpose of discussing single particular issues. To maximize the usefulness of the workshops several conditions must be met which will also help in generating a positive atmosphere and facilitate the interaction between participants.

- There must be a clear agenda for the workshop, with purpose and goals clearly explained to all the participants sufficiently in advance of the meetings.
- The role of each of the experts must be clearly explained and understood prior to the meetings.
- All the technical material necessary in support of presentation and technical discussions must be made available to the experts sufficiently in advance of the meeting that they can review the material and come prepared to the meetings.
- A detailed summary of the meetings, with account of resolutions, identification of issues must be part of the overall documentation.

Essentially there are three types of workshops:

1. Workshops on data dissemination.

All the data available relevant to the issues of interest are brought together for evaluation and to ensure that all the experts are uniformly cognizant of the entire body of information available. The general conduct of such a workshop is very much free flow. After the project analyst or project manager provides general introductory information the project and the agenda, purpose and goals, with presentation and discussion of the overall methodology of the project all the information available is reviewed.

Since the presentation of the data and all information is principally intended to provide a uniform basis of knowledge and to ensure that no important piece of information is being overlooked, the participants are not required to make any specific preparation, other than that associated with their own presentation if requested.

2. Workshop on formulation of models. The data and all relevant information have been collected and reviewed, the group of expert evaluators (EVA), are required to formulate their own independent models. In the case of the seismic source characterization they are asked to formulate seismic source maps which reflect their interpretation of the data as to where they believe earthquakes are likely to occur in the future. In the case of the ground motion attenuation they are requested to develop estimates of ground motion parameter values for a selected set of magnitudes and distances and possibly for a variety of source mechanisms and regions.

The expert evaluators will come to the workshop with their initial formulations ready.

The purpose of the workshop will be to review each individual expert’s formulation, evaluate, and for the TFI and the experts to

interactively construct the composite model, or distribution of views of the EVAs.

For this task, it is important to conduct the workshop in such a way as to ensure that each expert formulation is first clearly presented and fully understood by all before any real challenging, critique and/or endorsements are expressed in order to avoid any biasing or misunderstanding by the experts. One way of achieving this is to: (1) have each expert present his/her own interpretation of the data formulation and only allow questions related to understanding the details of what is proposed; (2) open the floor for detailed discussions including friendly challenges, critique, comparisons etc., where the TFI has the double duty of opening, steering without introducing his/her own personal opinions and biases, and also very importantly facilitating the discussion to keep it within the margins of civility, courtesy and professionalism.

3. Feedback Workshops.

The purpose of these workshops is to review the result of the integration process and evaluate it in the light of the existing data and information. It is an important step in verifying that the experts' inputs have been used as intended, clear up misunderstandings and gross errors. It is also a necessary step to allow the experts to update their formulations if they deem it necessary once they have been able to compare them with the rest of the group of experts who also have provided input. Therefore, a feedback workshop will generally consist of at least three parts. The first part intended to review and evaluate the result of the integration by the TFI and a second part to update individual expert's inputs and finally a third part for the TFI to finalize the integration.

3.3.4 Conduct of the Interviews

The elicitation process is not limited to the act of responding to a request for information. It is the

combination of all those tasks which enable the expert evaluators to formulate their opinion, express it and finally document it. The elicitation process comprises workshops, writing individual papers or formulation of models in interpretation of data, by the experts, open interaction with other experts and the TFI. It can also include answering questions to a series of questionnaires. Another way of securing and documenting the inputs from the experts is through one-on-one interviews.

The purpose of these one-on-one interviews is to ensure that the input provided comes entirely from the individual expert, to make sure that the original true diversity is preserved, and that it will appear at the time of the integration in the form of uncertainty.

The interviewing team must be composed of at least one person specialized in the elicitation of experts with an emphasis on expressing ranges of views on specific issues and must be able to help the expert express his/her uncertainty in a way that can lead to a quantification. In addition to this normative elicitor, another person, the technical elicitor must be fully cognizant of the technical issues pertaining to the elicitation. It is possible in some cases to use experienced individuals who can cumulate both functions.

It is recommended however to have one separate individual entirely devoted to the documentation of the interview, so that all notes remarks and important results can be passed on to the expert later for review. All data sets and information developed in the project must be available at the interview, and the conduct of the interview must follow a logical flow, predictable by the interviewees, with an interview preparation at the beginning to repeat the purpose goals, roles and modus operandi.

3.3.5 Final Integration

The concept of integration envisioned by SSHAC (NRC 1997) is the process of developing a composite model, as a range of views or a distribution of alternatives which represent the full range of views of the expert evaluators. The final composite model is the

result of a careful weighting, in the view of the data and all the information, and level of support for each of all the alternative models, done interactively by the TFI in “complete symbiosis” with the group of experts. For the simple case of the characterization of a single numerical parameter, this translates into the development of a probability distribution function, where the input from each expert is fully represented. The integration process ends up being a consensus process in which the consensus is on the procedure that led to the composite model. Implicitly it is a consensus on the property of the distribution functions (or ranges of views), but it is not a consensus on any particular value of the model parameter since the experts may still retain different individual views.

3.4 Peer Review

The purpose of the Peer Review is to provide assurance that the study incorporates the diversity of views prevailing within the technical community, that uncertainties have been properly considered and incorporated into the analysis and the documentation of the study is clear and complete.

SSHAC (NRC 1997) identifies two types of peer reviews:

- Technical peer review
- Process peer review

and two modes of performing the review:

- Participatory
- Late-stage

It is important that both the technical and process peer reviews be performed to provide credibility to a PSHA study. On the other hand, participatory or late-stage is a matter of practicality and depends on the circumstances. A late-stage review can have the disadvantage of creating “surprises”, participatory will provide a continuous feedback to the analyst, but it also

can be an important additional burden and introduce biases added by the reviewers.

In any case, an internal peer-review should be seen as integral part of the study itself even before the results of the study are released. In this instance the word “internal” is meant to signify that the peer-review is internal to the project itself, although to satisfy the recommendations of SSHAC (NRC 1997), the actual reviewers must be outside of the project team to ensure independence.

3.5 Documentation

SSHAC (NRC 1997) has extensively described the attributes of the documentation necessary to ensure that:

- Others in the technical community can understand or review the analysis and the results
- A later analysis team with new information or improved model can utilize a PSHA to update it, revise it, or validate that it does not need an update or revision.
- the sponsoring organization can retain an adequate record of the process it supported.

The reader is referred to the SSHAC document for details on the documentation process. We only reproduce here the list of the various elements of the PSHA process for which documentation is required.

- Roles and Responsibilities of the Project Participants and Consultants
- Comparisons with other PSHA Studies
- Internal Quality Control and Review
- PSHA Methodology
- PSHA Results
- External Peer Review
- Documenting Citations

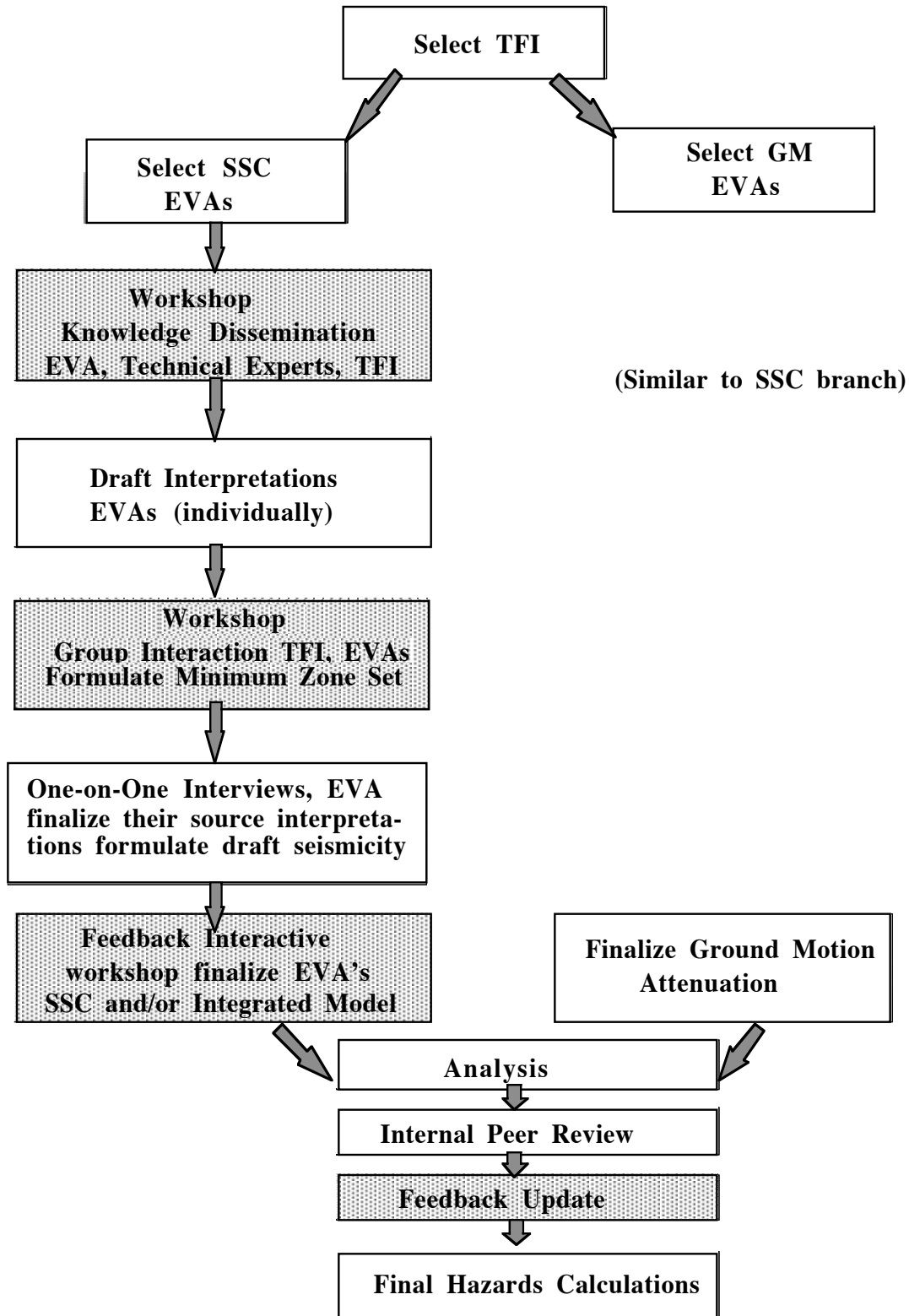


Figure 3-1 Typical PSHA Road Map.

4. CASE STUDY: DETAILED IMPLEMENTATIONS FOR TWO SITES IN SOUTHEASTERN U.S.

4.1 Expert Selection

The selection of the expert evaluators consists of a relative ranking of the experts in the pool performed by an analysis team according to a weighted average of the grades assigned to the experts for a series of criteria which express the requisite attributes needed of an expert evaluator. The value given to a grade is intended to express the degree to which an expert satisfies the criterion. The importance of each of the criteria with respect to the project at hand is specifically evaluated and is reflected in the weight assigned, relative to the other criteria.

The attribution of the weights which define the importance of each criterion, and of the grades that each of the experts in the pool are given for each of the criteria, is performed by the analysis team. It is a subjective process which is based on the knowledge that the team has of each of the experts in the pool. In performing this operation, the members of the team made a concerted effort to gain the maximum possible information on each of the experts in the pool, and exchange all known information between themselves before actually assigning grades. Each member of the team, then, assigned his own grades, the weighted grades were calculated for each expert in the pool and finally averaged over the members of the analysis team. The individuals were then ranked according to this averaged weighted grade, the highest grade leading to the highest rank.

The task of selecting the expert evaluators is probably one of the most important tasks in a PSHA with multiple experts. It has to be conducted very carefully and in full possession of all the necessary information on the experts in the pool. However it is only a small portion of such a project and must be organized in such a way as to maximize the resources of the project. It is not the project itself and is generally supported by limited funds. Thus the analysis team is not always in the position of being able to develop complete information on each of the experts in the pool and is constrained to assign

grades sometimes with little information. For the purpose of this project, after a reasonable effort to gain knowledge on a particular expert, it was assumed that if the information was still not sufficient, the grade assigned to this particular expert would be some arbitrary low value, to reflect the lack of general notoriety.

For the purpose of this project, a set of criteria selected by the analysis team and arranged in five classes is given in Table 4.1-1.

The criteria for the purpose of ranking the experts in the pool are sorted into three classes:

1. Knowledge
2. Lack of bias, credibility
3. Interaction abilities

In addition, a fourth class of criteria was used to evaluate the availability of the individuals and finally a fifth class of criteria was used for achieving a balance in the composition of the panel of evaluators:

4. Availability
5. Balance of the panel

Table 4.1-1 gives the criteria used in implementing the procedure described above for the TIP project. Table 4.2-2 gives the weight assigned to each criterion. The list of experts in the pool is given in Table 4.1-3. The first column of the table gives the names of individuals identified and the weights assigned to each of the criteria appears in the line labeled "Normalized weights". Note that for this project, the analysis team selected a total weight of 0.5 for knowledge. Lack of bias and credibility was given 0.3 and Interaction abilities was given 0.2.

The last column of criteria in Table 4.1-2, dealing with availability, was given a weight of zero to perform the pre-selection of the experts. It was to be used in case there would be a choice to make between several selected candidates.

Following that procedure, the final selection of expert evaluators (EVA) is given in Table 4.1-4.

4.2 Seismic Source Characterization

4.2.1 Introduction

4.2.1.1 Background

In 1989, the results of a multi-year study supported by the Nuclear Regulatory Commission and performed by LLNL provided probabilistic estimates of the seismic hazard for 69 sites in the eastern United States (Bernreuter et al. 1989). The study used individual experts to develop the seismic source characterization and the ground motion attenuation models. During the same period the Electric Power Research Institute (EPRI 1989) published the results of a similar industry-sponsored study. The EPRI study was also based on input from experts, but those were grouped in teams.

Both studies used various techniques of elicitation to develop the inputs to their analysis. These included written questionnaires, workshops, elicitation interviews and peer reviews.

From the experience of these two studies and others later on, the SSHAC developed the recommendation published in 1997 (NRC 1997), based on a critical evaluation of the various procedures of elicitation and overall approach to performing PSHA.

The emphasis of these recommendations is on using procedures of elicitation that ensure the highest quality possible of inputs from the experts. This is achieved by insisting on reviewing, evaluating, challenging and critiquing the work of the experts so that no misunderstandings or errors are likely to be introduced in their work.

The newer and more important aspect of the SSHAC recommendations is in advocating the concept of integration and composite models.

It is this aspect of integration, especially integration of the epistemic uncertainty that this Trial Implementation Project is testing. Studies

prior to the SSHAC study (NRC 1997), [except for a study for the Department of Energy, for the seismic site characterization of the New Production Reactor (NPR) (Savy 1992), and the development of ground motion for the update of the 1989 NRC study (Savy 1993).] did not use the same concept of integration.

4.2.1.2 Objectives

The objective of the seismic source characterization task was to develop an integrated set of seismic sources, with their seismicity rates, using the elicitation procedure recommended by SSHAC (NRC 1997). Just like the concept of a composite model was used in the development of ground motion attenuation models in the NRC Seismic Update study (Savy 1993), and recommended by SSHAC, we tested the same concept on the development of seismic source maps.

The seismic source models were developed for each of the experts and a set of common elements, common sources, are identified as basic building blocks for all the sources and alternative sources proposed by the experts. These building blocks, which we named the minimum zone set, were then used to create the composite model of seismic sources.

4.2.1.3 Products of the Expert Elicitation

Using the information and data described in section 4.2 below, the seismic source experts each developed a set of initial seismic source models. They provided all the elements necessary to express their uncertainty, in the form of alternate sources, alternative full maps, with an assessment of their level of support for each map or portions of map. Following the objective set for this project, the experts' input was received and analyzed. The final set of maps based on the experts' personal maps was developed using the building blocks of the minimum zone set.

Since all the seismic sources in the final experts' models are common as being parts of the minimum zone set, the recurrence properties of each one were developed by all the experts.

For every single seismic source in the minimum zone set, the probability distribution function of the recurrence parameters was elicited from all the experts. These included the upper magnitude cutoff, estimation of the frequency of events for two different magnitude values and the nature of the recurrence process, i.e., whether the occurrence rate followed a truncated exponential model or a characteristic model. In the case of characteristic model, additional information was necessary, including the range of magnitude of recurrence of the characteristic event, its frequency of occurrence, and separately if necessary, the description of the non-characteristic part.

An important aspect of the elicitation was to quantify the uncertainties. For the single independent parameters, which describe the activity rates of each of the seismic sources in the minimum zone set, the uncertainties were simply included in the final composite probability distribution functions.

For the seismic source maps, the experts were asked to construct a set of alternative maps and assign weight to each of them. These sets of alternative maps each constitute the composite models of seismic source zonation. One composite set for each expert.

4.2.2 Road Map for the Seismic Source Characterization

In following the recommendations of the SSHAC, we developed a project plan in which the flow went from acquisition and confirmation of the experts and TFI knowledge to identification of the range of interpretations, clarification, then formulation of alternative models, feedback, review and document control. This was implemented through a series of workshops, one-on-one interviews, white papers and otherwise any other type of communication systems as shown in Table 4.2.2-1.

The first workshop was intended to ensure that all the experts contributing to the project had a similar level of knowledge of the scientific data available and of the issues associated with the

development of probabilistic seismic hazard estimates for the two sites considered.

The objectives of the second workshop were to evaluate the experts interpretations, discuss an integration of their inputs into a minimum set of possible alternative source maps and to discuss methods of estimating the seismicity models, including the uncertainty.

The third workshop had the goal of finalizing the experts' models of seismic source maps and the integrated model.

A detailed summary of each of the workshops is given in the following sections as the first workshop dealt in the review of technical issues, the second workshop dealt in the review of proponent models and review of the data, and the third dealt in finalizing the models of the experts after their interpretations had been developed through interviews and intensive interaction at the previous workshops.

4.2.3 Review of Technical Issues, Workshop 1

The first phase in defining the technical issues was to review previous studies and design the first workshop so that the knowledge dissemination would be in large part directed towards identifying and discussing these issues. In summary, the most important technical issues were:

- Seismic source definition methodology.
- The Charleston Earthquake source zone.
- The Eastern Tennessee Seismic Zone.
- The local seismic source zone for the Vogtle site.

The first workshop took place in Augusta , Georgia on June 17-18, 1996. Participants in the Augusta workshop (see List of Participants in Table 4.2.3-1) included the panel of five expert evaluators, the Technical Facilitator/Integrator (TFI) team, expert proponents and presenters, and Allin Cornell, consultant to the TFI team.

The objectives of the workshop were: (1) To ensure that the evaluators are up to date on the

seismotectonics of the southeastern US and of specific earthquakes, and techniques for defining seismic sources and estimating maximum magnitudes in the eastern US; (2) to initiate interaction and feedback among the panel, presenters and TFI team in order to narrow unintentional disagreements among the panel members arising from misunderstandings, to define important unresolved issues, and to ensure maximum transfer of knowledge; and (3) to begin to utilize this knowledge in seismic source characterization by having each evaluator prepare individual first-cut source maps.

The first objective was achieved by presentations of recent research and interpretations by the presenters. In order to avoid covering well-trodden ground, the evaluators were expected to be familiar with the state of knowledge as it existed at the end of 1992, the time of the Savannah River Site (SRS) New Production Reactor (NPR) summary report. To this end, the evaluators were furnished with copies of relevant material, including the NPR report and supporting material before the workshop.

The format of the workshop was designed to maximize interaction and feedback. Participants were encouraged to ask questions during and after presentations to ensure understanding of data and interpretations. Each of the technical sessions was followed by a discussion moderated by the TFI team in which key outstanding technical issues were defined. These key issues were then assigned to evaluators as the topics of "white papers" to be written after the workshop. The objective of these papers is to clarify the arguments for and against key interpretations having direct bearing on seismic source characterization in a way that will stimulate interaction among the evaluators.

4.2.3.1 Technical Background

The technical background session introduced the study region and test sites and summarized existing site-centered source characterization for the region. The main rationale for choosing the Vogtle and Watts Bar nuclear plants as test sites is that the technical issues in defining the

sources that make the main contribution to the hazard differ at each site. The hazard at Vogtle is characterized by relatively little near-by seismicity but is potentially influenced by the distant Charleston source zone. The nearby, comparatively active Eastern Tennessee Seismic Zone is the major potential contributor to the hazard at Watts Bar. Nuclear sites were also chosen because of the availability of existing data on potential local sources.

4.2.3.2 Seismic Source Definition Methodology

The first technical session dealt with recent developments in defining source zones based on smoothed seismicity catalogs. These techniques are currently gaining favor as a means of mapping seismicity rates and can be utilized at the same time to help define source zones. The panel concurred that these techniques are potentially valuable and the evaluators expressed their desire to have them available. The TFI agreed to develop this capability. This entailed evaluating the relative utility of the techniques that have been proposed and the sensitivity of the resulting maps to the functional form of the smoothing kernel and to parameterization. The most critical parameters were identified as the smoothing (correlation) length and cut-off distance. Another aspect to be investigated was the use of anisotropic smoothing, based, for example, on moment tensors (Kagan and Jackson) or lineations defined in the seismicity maps. There is still a question as to the validity of using the distribution of low magnitude seismicity to predict the occurrence of large earthquakes.

4.2.3.3 Charleston Earthquakes

The second technical session dealt with recent work on the Charleston earthquake source zone. (Dave Amick had coordinated with Pradeep Talwani, who was able to merge Dave's paleoseismicity presentations with his own. Dave attended the second day of the workshop so was able to participate in the discussion of paleoseismic issues.) The issues dealt with in this session were: (1) whether the Charleston earthquakes should be characterized by a discrete source or by a broader source zone; and

(2) the size of the 1886 and other Charleston-type earthquakes.

Charleston Source Zone

Integrated interpretation of seismicity, geophysical (aeromagnetic, gravity, seismic reflection), morphological, and geodetic data presented by Pradeep Talwani and Ron Marple strengthens the case for a discreet source, the Woodstock fault, within the 1886 Somerville-Middleton Place epicentral area. The existence of this NNE-striking buried fault had originally been inferred from sparse seismicity data and is now tentatively identified as the possible source of a 200 km-long "zone of river anomalies" trending NNE through the epicentral area. If this hypothesis is correct, then it implies that the minimum length of the Woodstock fault is about 200 km. However, the evidence is still inconclusive and, at the other extreme, it remains possible that the 1886 earthquake is characteristic of the zone between the fall line and continental slope break along the entire eastern seaboard. The consensus was, therefore, that this remains a key issue to be addressed by evaluator white papers.

The hazard at the Vogtle plant will be sensitive to the northwestern and western extents of the Charleston source zone. There appears to be no compelling reason to extend the source to the northwest from the 1886 epicentral area by connecting the Somerville-Middleton Place and Bowman zones of microseismicity. Dave Amick has found no paleoliquefaction evidence for strong ground shaking in the Bowman area, and the microseismicity there is much shallower than in the epicentral area.

Ongoing work on paleoliquefaction features in the zone of seismicity in the southeastern US, along the SC Coastal Plain provides strong evidence for recurring earthquakes in the Charleston area. The main outstanding question being addressed by this work is whether clustered paleoliquefaction features near Georgetown and Bluffton, SC, northeast and southwest of Charleston, respectively, were all caused by Charleston earthquakes (perhaps by focusing), or whether they imply three separate

sources. Preliminary analysis of existing data allows most but not all of the Georgetown and Bluffton paleoliquefaction events to be associated with Charleston events, but present results remain equivocal. It was agreed that this issue has only a secondary effect in defining source geometries because all three of the possible source zones are at similar distances from the Vogtle site. However, this question has an influence on determining recurrence for Charleston and possible similar earthquakes. A major source of uncertainty in recurrence is the effect of sea level fluctuations on liquefaction susceptibility along the Coastal Plain.

Charleston Earthquake Magnitude

The best estimate of $M_W 7.3 \pm 0.26$ for the 1886 Charleston earthquake resulting from Arch Johnston's latest analysis based on M_W vs. intensity regressions for the eastern US, is somewhat lower than previous estimates (Arch's previous estimate was $M_W 7.5$). This estimate is generally consistent with the range of 7.0-7.5 estimated by Jimmy Martin based on near-field liquefaction. Jimmy favors $M_W \approx 7$, but suggests that this near-field estimate is consistent with Arch's estimate based on far-field intensity when the potential attenuating effect of the Coastal Plain sedimentary wedge is considered.

Assuming reasonable source parameters, Arch's best estimate for the length of the $M_W 7.3$ Charleston source is 50 km, approximately consistent with the maximum dimension of the 1886 meizoseismal area. One important issue that remains unresolved is whether there is evidence for events larger than the 1886 earthquake in the paleoliquefaction data.

4.2.3.4 Eastern Tennessee Seismic Zone

The Watts Bar site is situated close to the northwestern boundary of the 300 km long northeast-trending Eastern Tennessee Seismic Zone (ETSZ). Because it is the most extensive and most active, the ETSZ will make the major contribution to the hazard at Watts Bar. The level of the estimated hazard will depend critically upon the way in which the ETSZ is characterized. Martin Chapman presented evidence suggesting that activity within the

ETSZ may be associated with a conjugate system of west- and northeast-striking faults. The features defined by Martin's analysis of the seismicity range from several tens to over 100 km long. Chris Powell demonstrated the striking correlation of the northwestern boundary of the ET SZ — now sharply defined by hypocenters relocated in the UNC group's 3-D velocity model — with the New York-Alabama magnetic lineament, the regional-scale, long-wavelength gravity anomaly, and the steep northwest-southeast transition from high to low crustal velocities. This leads to the hypothesis that the ET SZ (and perhaps the Appalachian zone as a whole) represents a northeast-striking, left-stepping, right-lateral fault system several hundreds of km long. The overall capability of this hypothesized fault system would depend upon its origin and stage of evolution; for example, if it is forming by reactivation of Iapetan normal faults or is actually a pre-existing right-lateral system.

The question as to whether these new results are sufficient to allow the ET SZ to be characterized as a system of discrete faults rather than, as in the past, an areal source zone based purely on the seismicity was identified as the second key unresolved issue to be addressed by evaluator white papers.

4.2.3.5 Vogtle Local Sources

Dale Stephenson and Alice Stieve presented results of the very extensive studies in the vicinity of SRS since 1987. Dale concluded that there is no evidence for direct association of seismicity in the vicinity of SRS with major tectonic structures, such as basin-bounding faults imaged by deep seismic reflection. The South Carolina-Georgia seismic zone looks similar to the Central Virginia zone in that the seismicity appears to be occurring by reactivation of numerous splays off a major detachment at about 10 km depth. Alice presented detailed evidence, including high-resolution reflection, Quaternary geology and drilling results, that the Pen Branch fault is the northwest bounding fault of the Triassic Dumbarton basin that was reactivated in compression during the Cretaceous and early Tertiary. However, the

most recent displacement that is presently well defined occurred about 50 Ma ago. It is doubtful that more recent movement could be seen in the geology, and much better near-surface velocity control is needed to correlate reflections with dateable horizons. Recent small earthquakes at SRS apparently were not associated with the Pen Branch fault. A USGS reflection profile shows that the fault continues across the Savannah River.

The question arising from this session is whether the available data require that characterization of local sources for Vogtle should include specific faults, specifically the Pen Branch fault, or whether local sources are adequately accounted for by including the Vogtle area in a broad Coastal Plain-Piedmont zone based on seismicity. Given that the Pen Branch fault passes within 1.5 km of the Vogtle site, it appears to be a classic case of a reactivated Mesozoic boundary fault, and would be assigned a length of ~50 km (the apparent length of the Dumbarton Basin), the consensus was that this is a key issue affecting the hazard at Vogtle that will be addressed by evaluator white papers. These white papers will also specifically address the intersecting fault model put forward by Richard Holt, one of the expert evaluators for the NPR study.

4.2.3.6 Watts Bar Local Sources

There is very little site-specific information in the Watts Bar FSAR. Geomatrix's recent study for the Haysi dam project, located close to the ET SZ further to the northwest, indicate that the ET SZ is the controlling source for sites within the Appalachian Highland.

4.2.3.7 White Papers

In all three different issues were deemed to warrant additional discussion and interaction through the use of white paper writing. In this situation the experts were asked to act as proponents of a certain scientific position and since the issues selected involved dichotomous positions they sometimes had to argue for a position that they do not necessarily defend. This has the advantage of forcing the experts,

and all the participants, into discovering the positive aspects of scientific concepts other than their own. The assigned subjects of white papers were as follows:

Discrete Charleston earthquake source.

Pro: Pradeep Talwani

Con: Gill Bollinger

Discrete fault sources within the ETSZ.

Pro: Martin Chapman

Con: Klaus Jacob

Discrete local fault sources for Vogtle

Pro: Kevin Coppersmith

Con: Pradeep Talwani

A copy of each of the above white papers is given in Appendix A.

4.2.3.8 Preliminary Source Maps

As the conclusion to the workshop the five evaluators spent about 30 minutes preparing first-cut source maps, which they then presented. The purpose of this final exercise was to capture the evaluators' initial thoughts and ideas in a very preliminary set of maps, to get an initial feel for how closely they agreed (or otherwise). The range of the sources in these maps reflects the key outstanding issues. Evaluators who had previously been involved in source characterization for the region modified their source maps, in some cases significantly, in light of the recent work presented at the workshop. Most encouraging to the goal of arriving at a small set of maps that spans the existing different interpretations of the data was that all of the evaluators included alternative characterizations (some weighted) for some of their sources.

4.2.4 Proponents Models, Workshop 2

After the first workshop, the expert evaluators studied the positions defended in the white papers resulting from the workshop discussions and developed their own interpretations for possible scenarios of specific seismic source

zones. These interpretations would later be taken in workshop 2 as the proponents' models. Then, still prior to workshop 2, the experts developed a first draft of their set of models of seismic source zonations. These preliminary maps provided by the experts are shown in Appendix B. They were not intended to be detailed and final positions of the experts. Some were actually drawn by hand without recourse to sophisticated tools or plotting software.

All the above work was performed in preparation of the second workshop on Source Characterization, which was held in Boulder, Colorado on September 5 and 6, 1996.

Participation in this workshop was limited to the five-member expert evaluator panel, the technical facilitator-integrator (TFI) team, Ernst Zurflueh, TIP project manager for NRC, and Allin Cornell, consultant to the TFI.

The first source characterization workshop (June 17-18, 1996) had focused on knowledge dissemination. At the conclusion of the first workshop the five expert evaluators prepared preliminary source maps for each of the two test sites, the Vogtle and Watts Bar nuclear plants in Georgia and Tennessee, respectively, based upon their previous knowledge and upon the new information presented at the workshop. In the interval between the first and second workshops each evaluator finalized his source map(s) (some of the evaluators had alternative maps), based upon careful consideration of all the available information, and documented his results. As an important part of this process, each evaluator wrote a "white paper" on a significant issue identified during the first workshop (see Workshop I summary). The white papers were circulated among the evaluators during the inter-workshop period to facilitate elucidation of these issues and to promote interaction among the evaluators and between the evaluator panel and the TFI. During the inter-workshop period the TFI carried out hazard sensitivity analyses based upon the alternative source definitions contained in the evaluator's draft source maps. The TFI also performed spatial smoothing of the VPI/EPRI seismicity catalog using a variety of smoothing kernels and

their associated parameters (see discussion below).

4.2.4.1 Objectives of the Second Workshop

The objectives of the second workshop were to :

Examine and discuss in detail the individual evaluators' final source maps.

Integrate the evaluators' source maps into the smallest possible set of maps that spans the opinions of the panel.

Elicit the evaluators' weights for each of the sources and/or each complete map in the integrated set of maps.

Determine methods for estimating distributions of recurrence rates and maximum magnitudes for the sources in the integrated set of maps, including assignment of white papers dealing with significant issues in rate and maximum magnitude estimation.

4.2.4.2 Conduct of the Workshop

Before the meeting, the TFI decided that presentation and discussion of the "strawman" integrated maps would not be particularly useful, and may in fact be detrimental to the process of map integration. The time allocated for this purpose was therefore used for extended discussion of the individual evaluator maps.

4.2.4.3 Presentations of Evaluator Maps

Each evaluator made a detailed presentation of his preliminary source map(s) (Appendix C), and provided the rationale underlying his preliminary source characterization and the data and interpretations upon which it is based. The TFI encouraged maximum interaction during these presentations, which provoked in-depth discussion among the participants about the alternative characterizations and their underlying bases. This interaction was effective in maximizing the evaluators' understanding of all of the alternatives. The discussion also helped some evaluators to clarify their thinking about their own maps, for example, in defining dependencies among certain source zones. Most importantly, the discussions proved to be a good

preparation for the map integration process. The evaluators' final maps and documentation are contained in Appendix C. At the conclusion of the presentations, the TFI summarized the significant differences among the maps.

4.2.4.4 Source Sensitivity

The purpose of the sensitivity studies carried out by the TFI before the workshop was to give the evaluators an idea of how much influence differences among their source characterizations have on hazard estimates at the test sites. This is of value in the map integration process; for example, demonstrating that relatively minor differences in alternative definitions of a given source have only a small impact on hazard would enable the evaluators to reach an appropriate compromise with which they are all comfortable, thus helping to achieve the objective of a small set of integrated source maps. The sensitivity analyses concentrated on the sources having the greatest potential impact on hazard variability. These were identified as Charleston in the case of the Vogtle site and the eastern Tennessee seismic zone for Watts Bar. The example analyses were carried out using the VPI/EPRI catalog to estimate seismicity rates. The main conclusions from the sensitivity results, presented by Don Bernreuter, were: (1) The Charleston source is significant to the long period ground motion hazard at Vogtle, but the detailed nature of the source characterization is not critical; (2) the short period ground motion hazard at Vogtle is sensitive to the geometry of the "host" source zone and the location of its SW boundary; (3) Because Watts Bar is located very close to the NW boundary of the ETSZ, the hazard there is sensitive to the exact location and characterization of that boundary.

4.2.4.5 Seismicity Smoothing

At the first workshop, the evaluator panel expressed their wish to evaluate the use of smoothed seismicity maps to define source zones and in mapping seismicity rates. Two evaluators, Martin Chapman and Klaus Jacob, include regional smoothed seismicity as one alternative source map. Later in the second workshop, all but one of the evaluators gave a

moderate to high weight to determining seismicity rates within the ETSZ by smoothing.

Bill Foxall presented smoothed seismicity maps both for the study region as a whole and for the ETSZ alone, using Gaussian, Epanechnikov, and $1/R^a$ smoothing kernels. (Gaussian and $1/R^a$ kernels are being used to construct hazard maps by USGS and by SCEC and CDMG, respectively.) Trials with Gaussian and Epanechnikov kernels utilized a range of smoothing widths. As is generally observed, only minor differences were found between the results obtained with the Gaussian and Epanechnikov kernels; essentially the same maps result when the Epanechnikov smoothing width is 1.5-2.5 times the Gaussian width. Fairly good definition of the major regional seismicity zones, including the ETSZ, Charleston meizoseismal zone, central Virginia and Giles county, and the NW-trending South Carolina-Georgia zone, is obtained using Gaussian widths in the range of 25-50 km. Further work is needed to determine the optimal smoothing length for seismicity rate mapping. The $1/R^a$ kernel does not appear to smooth the seismicity enough, but picks out small concentrations of seismicity such as Somerville and Bowman. Gaussian smoothing lengths in the range of 15-20 km appear to provide good definition of the ETSZ. In applying smoothing to the ETSZ, the evaluators favor finding the smoothing length that produces a definition of the zone that most closely matches the shape and size determined visually from the seismicity in conjunction with geophysical and geological information. The seismicity rates within the ETSZ obtained using that smoothing length will then be used for hazard calculation. Application of the $1/R^a$ kernel to the ETSZ merits further investigation.

4.2.4.6 Map Integration

Final integration of the evaluator maps was accomplished during a 5-hour session led by the TFI. Following the evaluators' presentations, the TFI had finalized the list of significant differences among the maps, which provided the starting point of the formal integration process.

The following source zones have significantly different alternative definitions:

Charleston

Vogtle local zone

South Carolina-Georgia Piedmont and coastal plain.

ETSZ

Based upon the evaluators' definitions of each of these source zones, the TFI, interactively with the rest of the participants, developed the smallest set of zone geometries that incorporates all of the evaluators' zone definitions. Thus, for example, five alternative zones are required to represent what the evaluators consider to be the range of feasible sources for Charleston. In this particular case, the integrated set contains all of the alternatives originally proposed by the evaluators. This is because all of the evaluators wish to include two or more alternative characterizations of the Charleston source, rather than strongly supporting only one model. The five alternative geometries for the ETSZ similarly reflect consensus on the configurations most of the evaluators want to see represented, rather than disagreement among the panel. In contrast, all but one of the evaluators' geometries for the South Carolina-Georgia seismic zone are similar, so the integrated set contains only three alternatives; in fact, the one evaluator zone that is significantly different from the rest forms a background zone to the other two alternatives.

Integration of the maps progressed smoothly. Most probably, this was possible largely due to the previous detailed discussion of the evaluator maps, which meant that all of the participants had developed a good understanding of the significant issues in integrating the maps before the formal process began. Integration was also made easier by the fact, noted above, that, in most cases, evaluators wanted to see alternative source definitions in the integrated product, rather than strongly favoring single interpretations. This, on the other hand, results in a rather larger set of integrated maps than might have been anticipated. The final

geometries of all of the zones are shown in Figures 4.2.6-1 and 4.2.6-2 and Table 4.2.6-2.

4.2.4.7 Source Weighting

The source weighting session also evolved into an interactive process. The need for this approach became obvious when the participants began to consider the rather intricate dependencies among some of the source zones, particularly among the Charleston zones and between Charleston and the SC-GA host zones for Vogtle. These dependencies necessitated further careful thought about the implications of each zone during the weighting process. Therefore, weighting was approached through interactive development of an event tree composed of branches that correspond to the alternative source definitions and that expresses the source dependencies. Having developed the tree, each evaluator, after deliberation, independently assigned weights to the branches. The TFI provided some coaching on the method of assigning the weights. (Kevin Coppersmith had to leave the workshop in the early afternoon, so his weights were elicited in San Francisco at a later date.)

4.2.4.8 Preparation to the Elicitation Process

We had intended to hold a mock elicitation to show the experts the type of procedure and interaction. Instead, Kevin Coppersmith talked about the extensive experience in expert elicitation gained by the Geomatrix team during the Yucca Mountain probabilistic volcanic hazards study. The purpose this talk was to familiarize the evaluators with the individual elicitation process in preparation for the elicitation of their seismicity rate estimates.

4.2.4.9 Rate Methodologies

The two interactive sessions, on map integration and source weighting, were successful in generating the desired product - a small set of source maps together with source weights. In the next phase of the hazard analysis the evaluators will assign their distributions of recurrence rates and maximum magnitudes to each source. At the end of the second day of the workshop there was a general discussion of the requirements for the

next phase of the project and the approaches that will be adopted for estimating rate and magnitude distributions. This involves the TFI supplying the evaluator panel with alternative sets of rate and magnitude estimates. Feedback from the panel about data bases, methodology, etc. will largely drive this effort.

4.2.4.10 White Papers

We also discussed more general issues, including estimation of maximum magnitude, in general and for specific sources such as Charleston, extrapolating rates from small magnitudes to large, estimating magnitude from intensity in the eastern US, and catalog completeness and de-clustering. Based upon this discussion, white paper topics were assigned for the next phase of the project. The assignments agreed upon at the workshop were:

extrapolating rates for small magnitudes to large magnitudes:

pro: Klaus

con: Martin

estimating maximum magnitude:

strong position on using fault plane area/length for ETSZ Gil

strong position on using global data Kevin

Pradeep subsequently agreed to tackle the problem of estimating magnitude from paleoliquefaction data, but lacking a volunteer for the "con" position, he actually looked at both sides.

A copy of actual completed assignments is given in Appendix B.

4.2.5 One-on-one Elicitation Interviews

A formal elicitation interview between the elicitation team and each expert was held after the second workshop, in preparation for the finalization of the experts' seismic source models and for the characterization of the seismic source activity rates.

The elicitation team included Bill Foxall and Jean Savy. Each of the interviews started with a

general discussion on the purpose, objective and goals of the elicitation interview. The experts were given an opportunity to clarify the description of models proposed at the workshops and in the white papers. We reviewed in detail all the seismic source models and reviewed briefly the procedures for characterizing uncertainty. We re-emphasized the fact that the interview on seismic activity rates was for the purpose of developing preliminary probability distributions of the occurrence models and that the process of integration into a composite model, for each seismic source would be performed during workshop 3.

The parameters to be elicited during these one-on-one interviews were:

the upper magnitude cutoff M_{max} , for each seismic source, all in the $M_{bl.g}$ scale.

$F_{(mo)}$, the number of events, per year, equal or greater than a maximum $M_{bl.g}$ magnitude $M_o = 4.0$

$F_{(m1)}$, the number of events, per year, greater or equal to a $M_{bl.g}$ magnitude, arbitrarily equal to 1/2 unit less than M_{max}

For each seismic source, the experts were asked to characterize the shape of the probability distribution (uniform, triangular, trapezoidal with left taper, trapezoidal with right taper, or beta).

Then the experts were asked to provide a lower bound (interpreted as a 5% percentile) the upper bound (95% percentile) and the mode, median or most likely value of the parameter value.

All the material available to the elicitation team was brought to the interviews. This included all the seismic source descriptions, all the results of the preliminary rate calculations, made with several different approaches as requested by the experts, including various approaches corrections for completeness of the catalogs, and area smoothing. That information, had also been sent to the experts prior to the interview. The experts were requested to review the material and prepare their interpretation. They were asked to perform analyses if necessary and

generally get ready to provide their estimates of the seismic sources seismicity rates parameter probability distribution.

The interviews were given a full day of available time, but most of them were actually completed in half a day. The experts were in general well prepared. In two cases, the experts reserved their estimation for one or a few seismic sources until after they had gone back to their offices and been allowed to perform additional analyses of their own. In these cases, the experts provided their additional input before or at Workshop 3.

4.2.6 Integration and Feedback, Workshop 3

4.2.6.1 Introduction

The third workshop on source characterization for the Test Implementation Project was held at the LLNL offices in Germantown, MD on January 15-17, 1997. Participation in this workshop was limited to the five-member expert evaluator panel, the technical facilitator-integrator (TFI) team, Ernst Zurflueh, TIP project manager for NRC, Allin Cornell, consultant to the TFI, and observers from the Department of Energy (Jeff Kimball) and the NRC/NRR (Cliff Munson) and NRC/NMSS (Bakr Ibrahim) (see list of participants—Table 4.2.6-1).

The first source characterization workshop (June 17-18, 1996) had focused on knowledge dissemination. At the conclusion of the first workshop the five expert evaluators prepared preliminary source maps for each of the two test sites, the Vogtle and Watts Bar nuclear plants in Georgia and Tennessee, respectively. In the interval between the first and second workshops each evaluator finalized his source maps (some of the evaluators had alternative maps), based upon careful consideration of all the available information, and documented his results.

The second source characterization workshop (September 5-6, 1996) focused on development of the smallest set of source zone geometries that incorporates all of the zone definitions contained in the maps of the individual evaluators. The final set of zone geometries is

shown in the maps contained in Fig. 4.2.6-1. The zones in this set comprise the basic building blocks which are variously combined by the evaluators to construct the final versions of their source maps, or "scenarios". Therefore, although the source scenarios differ among the evaluators, the evaluators and TFI are able to concentrate on determining magnitude recurrence parameters for a *common* set of zones. Combining the zones into source scenarios was accomplished by constructing logic trees for five source "modules" (see Figure 4.2.6-2) during an interactive TFI-led session. Each scenario is represented by one complete path along a set of connected branches (i.e. source zones). The evaluators built their scenarios by assigning preliminary weights to each of the branches.

As a result of discussion of maximum magnitudes, in general and for specific sources, several "white papers" were assigned to help the evaluators in assigning maximum magnitudes. The justification for extrapolating rates from small magnitudes to large magnitudes was debated by Klaus Jacob and Martin Chapman, and methods of estimating maximum magnitude from fault length and from global data were discussed by Gil Bollinger and Kevin Coppersmith, respectively. Pradeep Talwani evaluated the use of paleoliquefaction data in estimating maximum magnitudes for Charleston and other paleoliquefaction sites along the coastal plain. The white papers were passed to all the evaluators to aid in their preparation for Workshop 3.

In the interval between Workshops 2 and 3, the TFI digitized the set of source zone geometries finalized during Workshop 2, and, following the general directions given by the evaluators during and subsequent to Workshop 2, computed magnitude-frequency distributions for the zones using two alternative approaches (see below). The evaluators were provided with this material as a basis for their recurrence rate estimates. The TFI elicited maximum magnitude and recurrence rate estimates from individual evaluators on December 18, 19, 20, 1996 and January 7, 1997. This provided the preliminary magnitude

recurrence parameter estimates that were the starting point for discussion at Workshop 3.

4.2.6.2 Objectives of the Third Workshop

The objectives of the third workshop were to:

Review and confirm all source zone geometries.

Integrate the evaluators' source scenarios for each source module into a composite set (i.e. a composite logic tree for that module).

Integrate the evaluators' preliminary maximum magnitude and seismicity rate estimates and their uncertainties into a set of composite probability distribution functions.

Elicit the evaluators opinions on the overall process employed in the project (feedback).

4.2.6.3 Conduct of Workshop 3

Source Zone Maps and Logic Trees

The workshop started promptly with the development of a set of composite logic trees, which were intended to represent the full range of the evaluators' source scenarios. The underlying assumption in adopting this approach was that, among all the possible scenarios, there is a small set of dominant ones on which the community of experts (here the panel of evaluators) would agree. To complete the composite logic trees, the uncertainty, or rather the full range of interpretations, was to be expressed with a small set of additional scenarios.

It quickly became clear that even though the EVAs may agree on the choice of a dominant (preferred) topology for some parts of the logic trees, their opinions on the correlations and dependencies between the different portions of the trees could be drastically different, meaning that the weights assigned to each branch vary widely. This makes it impossible to develop simple composite logic trees in which all the dependencies are faithfully represented for all the evaluator opinions. It was concluded that the only way that the latter objective could be achieved was by developing all of the logic trees implied by all of the evaluators' interpretations.

Therefore, it was decided to realign the workshop to this new realization by focusing on the formulation of the simplest set of trees for each expert, rather than on composite trees. It was agreed by all participants that the TFI team would still develop composite trees after the workshop and that the results of both approaches would be compared and evaluated, including at the level of the hazard.

Presentation of the Evaluators' Maps and Logic Trees

Each of the logic trees corresponding to the 5 source zonation modules was reviewed together with the source zone maps. The experts had the opportunity to revise, modify and update the branches and weights of their logic trees. The revised trees are shown as Fig. 2.2.6-2a to 2.2.6-2e (see also Table 4.2.6-2 for explanations of seismic sources). The weights assigned by the evaluators to the branches of each tree are shown in the table below the tree.

The approach used in developing preliminary weights for the composite trees was discussed at length, leading to following simple rules:

Take the average weight across the experts for those branches where the spread of weights is small.

When the range of weights is large and there is a strong dominant value, use that value for the composite.

When the distribution of the weights is clearly bi-modal create two separate alternative origin nodes.

Maximum Magnitudes and Rates of Occurrence at M_0 and M_1

Most of the second day of the workshop was spent in reviewing, comparing and revising the maximum magnitude and M_0 (= magnitude 4) and M_1 occurrence rate estimates given by the evaluators in their individual elicitations. The evaluators had estimated the maximum magnitude for each of the zones based upon a variety of data, including the seismicity catalog, recent work by Arch Johnston on the Charleston

earthquake, geological considerations, and the EPRI global study. They had based their rate estimates upon cumulative frequency-magnitude plots supplied by the TFI before the elicitations, paleoseismic data for the Charleston earthquakes, and upon the evaluators' own analyses of the seismicity data. The TFI had derived cumulative frequency curves for relevant zones using both the LLNL Probability of Detection Model and Stepp's method for estimating completeness intervals together with maximum likelihood fitting. The results of both analyses had been supplied to the evaluators. Gil Bollinger had independently analyzed the data using Stepp's method, and the resulting maximum likelihood cumulative frequency curves had also been supplied to the evaluators. Subsequent to elicitation, some of the evaluators had been able to supply revised estimates for presentation at the workshop.

The purpose of this session was to enable the evaluators to confirm their preliminary estimates or revise them based either upon prior reevaluation or as a result of debate during the session, and to develop composite distributions. Since the seismic source zones are common to all the experts, the concept of composite maximum magnitude and seismicity rate distributions remains valid. M_U and rate estimates were presented by the TFI in the form of comparative summary plots, which show the evaluators' modal, lower bound, and upper bound estimates for each of the magnitude recurrence parameters. These proved to be an effective means of critically comparing the individual estimates and discussing differences arising from alternative interpretations of the data or differing recurrence analysis methods. The evaluators had given rate estimates at M_0 and at $M_U-0.5$ ($=M_1$). To enable comparison, the individual M_1 rate estimates were interpolated to the rate at a common upper magnitude, taken as the arithmetic mean of the evaluators' M_1 s, using the b-slopes implied by the M_0 and M_1 rates given by each evaluator. These b-values were presented so that the evaluators could check that their estimates were consistent and reasonable. Composite distributions were shown only for M_U , as rate estimates had not been

available from all of the evaluators before the workshop.

We worked through the zones in turn, considering M_U and the occurrence rates at the same time. When necessary, evaluators summarized the rationale and justification for particular estimates. Revised summary plots that include changes made by the evaluators during and subsequent to this workshop session and that show the actual shapes of the distributions and all of the composites are contained in Fig. 4.2.6-3.

The main results of this session are as follows.

The maximum magnitude estimates for most of the zones can be adequately described by a single composite distribution, formed by summing the normalized individual distributions (Fig. 4.2.6-3). The estimates for some zones, notably 1D, 1E, and Zone 3, are clearly bi-modal. Bi-modal distributions for M_U represent differing interpretations of the fundamental tectonic processes responsible for earthquakes in these zones, and so should be reflected in the weighting of the logic trees. The rate estimates for almost all the zones can be well characterized by a single composite distribution. In all but one of the few cases of bi-modal composite distributions, the bi-modal shapes appear to stem from differences in assignment of maximum magnitude and perhaps interpretation of the rate data, rather than differences in interpretation of tectonic processes. Even though it was concluded that composite distributions appear to be adequate representations of the ranges of magnitude recurrence parameters, it was also decided that we would verify this by comparing hazard results computed using individual estimates with those based upon composite distributions.

Significant systematic differences were evident in many of the rate estimates, and in particular between those based upon the completeness intervals estimated by Gil Bollinger and those based upon the TFI's recurrence analyses. The chief cause of these differences appears to be differing interpretations of catalog completeness, which are subsequently being further

investigated by Gil Bollinger and Don Bernreuter. In addition, the uncertainty on Gil Bollinger's rate estimates are formal estimates of 5 and 95% confidence bounds, and are systematically narrower than those of the other evaluators.

4.2.7 Feedback Comments

At the end of the second day of workshop 3, the EVAs were asked to prepare notes summarizing their comments on the process. Recalling that the purpose of this project is to produce a guidance document for performing a PSHA, the role of this feedback was to get some insights on the aspects of the process with which the EVAs felt comfortable and those with which they did not, and to understand what worked and what did not. On the strength of this information we can develop a guidance document that is more focused and more in tune with the needs of the experts. The EVAs brought these comments in writing the next day for discussion in an interactive session between the EVAs, the TFI team and the other participants. The discussion was moderated by a member of the TFI team. First we reproduce the comments of each expert verbatim (in italics), and then add clarification and additional comments generated during the discussions.

4.2.7.1 Gil Bollinger:

Feedback on Implementation Process

Zone: Very good overall, but confusion on zone nomenclature and definition. Logic trees not available soon enough after meeting.

Recommend meeting minutes distributed promptly after each meeting.

M_{max} — Estimates surprisingly similar - real disagreement minimal - Procedures by EVAs seem well-developed and stable. Ditto for uncertainty estimates.

Rates — Need for considerable improvements:

Documentation for recurrence curves and their genesis much more extensive and complete.

Labeling of curves more carefully and completely done.

Prior to submittal, find out what the EVAs want/require and tell them what you'll be submitting and why. Tailor your submittal of recurrence curves to the EVAs needs rather than a "shotgun approach" of multiple scenarios - many of which raise more questions than they provide insights - why produce and mail material that will not be used or found helpful? Rather, check with the EVAs first. A portion of the first meeting should be devoted to this topic - advise EVAs prior to coming with their requirements in mind.

Uncertainties — Some early group discussion of these procedures/techniques by the entire group would be helpful to make certain everyone is on the same page even if they're using very different process.

Additional comments expressed during the feedback interaction.

Conduct of the workshop should focus quickly on content.

White papers are a must. They are very useful to the EVAs and should be an integral part of the process.

Ask the EVAs to participate by presenting their interpretations of the methodologies and describe their tools specifically for the estimation of the uncertainties.

Should have a dedicated person only to take notes at the workshops and elicitation.

Minutes should contain a log of all decisions made during the workshop.

Workshop #2 could have had 1 more day to explore in more details the needs of the experts for estimating the seismicity rates and uncertainty.

4.2.7.2 Martin Chapman:

Probability — Logic trees need to be diagrammed and branches needs to be defined in detail, with the results distributed to all workshop participants as soon as possible following the workshop.

Seismicity rates/per unit area somehow need to be considered simultaneously with development of same process.

Sensitivity — Testing of contentious options at an early stage might be helpful.

Additional comments expressed during the feedback interaction.

Use maps of smoothed seismicity (contours) for a few smoothing parameters to help in defining zones boundaries.

Capability for doing all types of seismicity and hazard, and ground motion calculation "on-the-fly" during the workshops and during elicitation would be very useful to EVAs, to explore different zone configurations.

4.2.7.3 Kevin Coppersmith:

Not present

4.2.7.4 Klaus Jacob:

Dissemination of information (Workshop #1) can be less extensive if it results in spending additional time and resources on Workshop #2, elicitation, and Workshop #3.

After each Workshop or elicitation meeting it is essential that the resulting data, documents (logic trees, etc.) be available to the EVAs for review and feedback to assure quality control and avoidance of misunderstandings.

Make sure that all members of the TFI and EVAs teams use consistent and unique identifiers. If this principle is not followed rigorously confusion is inevitable in projects of complexity.

In my judgment it is insufficient to only solicit seismicity input from EVAs without feeding back to the EVAs the results (in form of hazard curves) of their input [even if only a single attenuation law is used]. Without each EVA knowing what the effect of his/her input on the resulting hazard is the EVA cannot take full responsibility (and therefore responsible ownership) of his/her input. This feed-back loop must be closed in future projects. !!!

I strongly recommend that the inter expert variation (all branches of proposed models) be preserved in parallel with composite models. As pointed out by some EVA (K. Coppersmith) and TFI consultants (Allin Cornell), in real projects, this will be the only way to allocate “ownership” and hence responsibility for input/output.

White papers were very helpful.

Additional comments expressed during the feedback interaction.

Feedback loop must be devised so that EVAs understand and see clearly the impact of their choices, in particular by making comparison with data.

4.2.7.5 Pradeep Talwani:

Label recurrence curves so that they are user friendly.

Perhaps explain methodology in some detail (short write up).

Provide some feedback as to the consequence of our choices on the resultant estimation of seismic hazard values.

I was not too clear on how the recurrence curves were attained specially when the resulting b and a values were unrealistic (see 2 above). In other works, it would be useful to end up with physically realistic values. Or is something that the EVAs should do.

I also want to give some kudos! I appreciated the very helpful attitude of Bill, Jean, and Rosa in trying to ensure that I had all I needed to do my job!!!

4.3 Ground Motion Attenuation in Eastern North America

4.3.1 Introduction

4.3.1.1 Background

In 1994, there was a trial application of the SSHAC methodology to the problem of estimation of ground motions for Eastern North

America. The results of this trial application were summarized by Boore et al. (1996).

The 1994 trial application demonstrated several important aspects of this type of study. The preliminary estimates were made independently by each expert. In the feedback workshop, the interaction between the experts lead to a reduction in the expert-to-expert uncertainty.

One significant source of uncertainty that remained was the conversion from mb to moment magnitude (Mw). In the 1994 study, the cases were defined in terms of mb, but most of the ground motion models are defined in terms of Mw. Therefore, the experts were required to first convert from mb to Mw before applying the proponent models. This lead up to a 0.5 magnitude unit difference between the experts when the models were applied. This uncertainty in the magnitude conversion tended to obscure the underlying uncertainty in the ground motion attenuation.

The 1994 study had several limitations that prevented the results from being used to develop attenuation relations. First, there were some misunderstandings about the distance definition. The distance was defined to be the closest distance to the rupture plane (rupture distance), however, several of proponent model estimates were run for hypocentral distance or shortest horizontal distance to the surface projection of the rupture (Joyner-Boore distance). As a result, the short distance estimates (5 km rupture distance) could not be used. This limited the useable point estimates to distances greater than 20 km.

A second limitation of the 1994 study was that a limited number of distances and magnitudes were evaluated (Table 4.3.1-1). The 1994 study considered just two magnitudes (mb = 5.5 and mb = 7.0). Additional magnitudes are needed to define the magnitude scaling, particularly for the long periods. Without the 5 km distance (due to the misinterpretation of the distance definition discussed above), there were only 1-3 distances for the various spectral periods. Estimation of the ground motion at additional distances are also needed to adequately define the attenuation.

Input to a PSHA for vibratory ground motion includes the characterization of all significant earthquake sources and the ground motions they may generate at a site. Characterizing the latter requires describing motions developed by the various types of potential seismogenic sources - whether planar features such as faults or more general areal sources. Motions resulting from the different styles of faulting (strike-slip or dip-slip, and if the latter then normal or reverse faulting) should also be incorporated into the ground motion characterization. Thus the seismogenic sources to a degree define the technical issues which the ground motion characterization must address. Further, the seismic hazard is calculated using a computer code which incorporates both inputs. Therefore, the ground motion characterization was also formulated in a manner consistent with the input format to the computer codes which perform the hazard computation.

4.3.1.2 Project Objectives

The objective of this study is to develop response spectral attenuation relations for hard rock conditions in Eastern North America using the SSHAC expert elicitation methodology. This study builds on the 1994 SSHAC exercise, by addressing the shortcomings of the 1994 study and expanding the number of point estimates (magnitude-distance-frequency triplets) considered.

The resulting point estimates are then used to estimate attenuation relations based on regression analyses. The attenuation relations are developed for the individual experts and for a composite model which represents all of the experts estimates.

4.3.1.3 Products of the Expert Elicitation

Using the various information and data discussed below, the ground motion experts each developed a series of estimates of ground motions for a defined suite of earthquake magnitudes and distances, fault geometries, and faulting styles. The estimates included the median ground motion and its aleatory variability, and the epistemic (scientific

knowledge) uncertainty on both. To clarify the meaning and the classification of the various types of uncertainty which are used in this study, the reader is referred to a detailed discussion in Appendix D.

These point estimates were fitted to yield attenuation equations for all four quantities. The independent variables used in the regression were selected by the expert and the analyses were performed by the TFI team.

Each expert formed his/her interpretations using the information and data presented in two Workshops. Additionally, the elicitation process included a formal interview, in which each expert presented and defended his preliminary point estimates. The TFI challenged each expert to defend and, as necessary, clarify his or her thought process to ensure that all relevant data and information were evaluated. As a computational aid, the TFI provided the experts with estimates of the ground motions from the proponent models that the experts selected for the study.

Following this Introduction, Section 4.3.2 details the process by which the ground motion experts' interpretations were developed. Section 4.3.3 presents the resulting ground motions estimates from the experts. Section 4.3.4 presents the attenuation relations developed from each expert's estimates.

Input to a PSHA for vibratory ground motion includes the characterization of all significant earthquake sources and the ground motions they may generate at a site. Characterizing the latter requires describing motions developed by the various types of potential seismogenic sources - whether linear features such as faults or more general areal sources. Motions resulting from the different styles of faulting (strike-slip or dip-slip, and if the latter then normal or reverse faulting) should also be incorporated into the ground motion characterization. Thus the seismogenic sources to a degree define the technical issues which the ground motion characterization must address. Further, the seismic hazard is calculated using a computer code which incorporates both inputs. Therefore, the ground motion

characterization was also formulated in a manner consistent with the input format to the computer codes which perform the computation.

4.3.2 Structure of Elicitation Process

4.3.2.1 Expert Elicitation Guidance

The assessments of ground motion attenuation in ENA require a degree of data interpretation. Expert elicitation is an ideal approach to integrating the range of data interpretations inherent in the assessments. The National Research Council and DOE have both sponsored examinations of the expert judgment elicitation process resulting in three key guideline documents utilized in the ground motion characterization (Savy *et al.* 1993; NRC, 1996; NRC, 1997; National Research Council 1997).

The expert elicitation process as it applies to ground motion interpretations originated over a decade ago in a Lawrence Livermore National Laboratory (LLNL) study to develop a methodology for characterizing seismic hazards in the Eastern U. S. (EUS). In the LLNL project, each member of a panel of experts was required to independently evaluate various data and each assigned weights to existing ground motion models. A parallel study was performed by the Electric Power Research Institute (EPRI) relying instead on three models with weights assigned by a single Technical Integrator after a meeting of the experts. Differences in the hazard results prompted a close comparison of the two studies, which identified differences in attenuation and its associated variability as a major cause of numerical differences. In turn, examinations of the elicitation process itself have led to further development and refinement of elicitation techniques (Savy *et al.* 1993; NRC 1997).

In recognition of an anticipated reliance on expert elicitation within the nuclear industry, the NRC prepared a Branch Technical Position (Kotra *et al.* 1996) on the use of the technique which was consistent with the approach followed in the PSHA. LLNL refined its elicitation procedures using the experience of the 1982 study (Savy *et al.* 1993) and prepared a set of recommendations directly relevant to

eliciting interpretations on ground motion and its distribution. Boore *et al.* (NRC 1997) applied the SSHAC methodology in a demonstration project for EUS ground motion. The lessons from these previous studies were considered in the current study.

4.3.2.2 Elicitation Methodology

4.3.2.2.1 Project Plan

The Project Plan consisted of an elicitation and a feedback workshop. This format was developed to insure that the experts interacted, explained their own interpretations and questioned the interpretations of other experts. The key purpose of the workshop was to provide a common information base for the interpretations and a forum for interaction among the experts to achieve a common understanding of the data and existing ground motion models. A thorough understanding by all the experts of the technical limitations and advantages of the data was needed to ensure that differences in the final interpretations were based on differences in expert judgment and not incomplete knowledge.

As a direct result of lessons learned in the LLNL study (Savy *et al.* 1993), ground motion experts in the TIP PSHA were required to provide estimates of median ground motion, its variability, and the uncertainties associated with each for each of a selected set of magnitudes and distances. This was intended to focus the experts on the ground motions and uncertainties themselves, and not on evaluating weights to apply to known attenuation models (as ground motion elicitation was first practiced). Attenuation relations were to be developed using these values.

4.3.2.2.2 Roles of Participants

The TFI Team aided the experts in all phases of developing their ground motion interpretations. The TFI Team Leader role required an individual with recognized technical expertise. Responsibilities of the TFI leader included planning and conducting the technical workshop. The workshops were intended to be coordinated to respond to requests from the experts for technical information and also to further the process by which the experts reached

their final interpretations. Most importantly, he facilitated the interaction between the experts during the workshop. He also led the formal elicitation interviews and provided feedback to the experts. The Facilitation Team Leader was to specifically avoid guiding the experts towards a personally preferred view of ground motion characterization.

The ground motion experts were required to function in two distinct roles, namely proponents and evaluators. Ultimately and most importantly, each was required to impartially view and evaluate all proponent models based on the information presented in the workshops. However, many of the models assessed were developed by members of the panel so these experts were also asked to act at specified times as proponents of their own models. As proponent experts, their role was to explain and argue for a particular model. The Technical Facilitation Team Leader provided specific instructions at the outset of the project to clearly define the roles of evaluators and proponents. Not all of the ground motion experts acted as proponents; experts selected for this role either developed the model or were widely identified professionally with the modeling technique. After acting as proponents, experts resumed their primary roles as evaluators.

As evaluator experts, each panel member was expected to assess all models and data presented and integrate them into an individual best estimate of the ground motion distribution and its uncertainty. The experts were to evaluate all models in light of their own technical judgment separate from cognitive bias towards classes of models.

4.3.2.3 Selection of Experts

Experts must represent the range of scientific disciplines required to perform the required evaluations and interpretations. Thus their professional expertise must cover the range of issues and technical foundation regarding the tectonic and seismic environment of ENA as well as ground motion estimation.

Since this study was building on the previous 1994 study, most of the experts were selected from those involved in the previous study. The 1994 study used seven expert evaluators: Abrahamson, Atkinson, Bernreuter, Campbell, Joyner, Silva, and Somerville. The TFI team consisted of Boore, Toro, Morris, and Cornell.

In the current study, Abrahamson and Savy made up the TFI team. We also considered others outside of the 1994 study who had been working recently on ground motion attenuation in ENA (Table 4.3.2-1)

For this trial implementation project, the budget allowed for five expert evaluators. We selected the evaluators with varying background and areas of expertise that would provide a good test of the methodology.

From the original seven experts, we selected Bernreuter, Campbell, and Somerville. We added Boore as an expert evaluator due to his expertise in the stochastic model (both single corner and double corner sources). We added Jacob as an expert evaluator since he has been involved in many engineering projects in the eastern U.S. and his estimates had been much larger than previous estimates which should challenge the methodology. The resulting five expert evaluators are:

Bernreuter
Boore
Campbell
Jacob
Somerville

4.3.2.4 Compilation and Discussion of Data and Information

The experts were familiar with the proponent model that had been considered in the 1994 study so a separate data dissemination workshop was not held. There were some new models and revisions to previous models that were discussed at the feedback workshop. The new models were Frankel (1996) and Horton (1997). The Campbell model had been revised since the 1994

study. These new models were reviewed at the start of the Feedback workshop.

4.3.2.5 Elicitation Interviews

An initial workshop was held in December, 1996 to review the proponents models used in the 1994 study, identify additional proponent models that the experts wished to consider, and define the range of point estimates (magnitudes and distance pairs), for which the experts would estimate ground motion. A formal elicitation interview between the elicitation team and each expert was held before the feedback Workshop. The interviews were conducted in accordance with guidelines developed by the U. S. Nuclear Regulatory Commission (1997). The elicitation team consisted of N. Abrahamson and J. Savy. N. Abrahamson was present at all of the interviews. J. Savy was present at all but the Jacob and Bernreuter interviews.

The interviews were private and uninterrupted. In the interview, each expert was asked to explain the procedures he adopted to obtain median estimates, aleatory uncertainties, and the epistemic uncertainties on both. Each defended his selection of 'relevant' proponent models and also explained on what basis other models were rejected.

The elicitation interview was an important source of feedback for the experts. Inconsistencies in the treatment of uncertainty were identified and corrected by the experts.

The TFI calculated the preliminary ground motion estimates for each expert using weights supplied by the expert. A single computer program was developed by the TFI for use by all experts in weighting proponent models as a step towards forming their point estimates. This computer program (WT_AVE) was used to compute weighted model values (used as preliminary point estimates) for each of the experts. This allowed the experts to simply develop weights for the models freeing them to concentrate on evaluating the resulting point estimates. The weighted values were used solely for preliminary computations: the experts were

charged to evaluate the preliminary estimates to form their final point estimates.

4.3.2.6 Feedback and Revision

Feedback for the experts occurred at two different times. As mentioned above, the elicitation interviews resulted in significant feedback in terms of identifying inconsistencies by the experts. The main source of feedback was the feedback workshop.

Following the feedback workshop, the experts revised their estimates. The TFI developed revised attenuation models based the experts' revised estimates.

4.3.2.7 Documentation

In this application of the SSHAC methodology, the experts' estimates were documented by the TFI in terms of the weights given to each model (and the magnitude, distance and frequency dependence of those weights). In a full application of the SSHAC methodology, each expert would document the reasoning behind his development of the point estimates.

4.3.3 Ground Motion Characterization

4.3.3.1 Review of Technical Issues

There are very few strong motion data available in eastern North America (ENA). The sparse strong motion data set is summarized in EPRI (1993). As a result of the sparse set, most ground motion models for ENA are based on numerical simulations or by correcting the more plentiful western North America (WNA) strong motion data for differences in the source, path, and site differences between the two regions.

4.3.3.2 Proponent Model and Data Needs Workshop

A workshop was held in December 20, 1996 to review the various proponent models and to define the point estimates to be developed by the experts.

At this workshop, Abrahamson reviewed the proponent models used in the 1994 study: EPRI (1993), Atkinson and Boore (1995), Somerville (1994). Revisions to the hybrid empirical model

developed by Campbell were presented by Campbell. At the workshop, requests were made by the experts to include the Horton (1997) numerical simulation model which was used extensively in New York, and the Frankel (1996) point source stochastic model which was used in the development of the national seismic hazard maps. The complete set of proponent models is listed in Table 4.3.3-1. The proponent models considered in this study are described in Section 4.3.3.3.

As noted previously, there were several shortcomings of the 1994 study that made it difficult to develop ground motion attenuation relations from the expert estimates. These shortcomings were addressed in the initial workshop resulting in the changes described below.

First, the seismic source was defined in terms of moment magnitude rather than m_b . This eliminated the uncertainty in the magnitude conversion in terms of ground motion estimation. Because the earthquake catalogs for ENA tend to be given in terms of m_b , this magnitude conversion must be addressed in hazard calculations.

Second, specific fault rupture geometries were defined for the point estimates rather than just a distance (Figure 4.3.3-1). This reduced the misunderstanding in the distance definition although some confusion remained in the Horton proponent model.

Third, additional magnitude-distance pairs were included to allow determining the magnitude and distance scaling at each of the five response spectral periods, in the regression analysis. In particular, an additional distance was added at 120 km to identify possible flattening of the attenuation relation due to post-critical reflections from the Moho ("Moho bounce"). Additional magnitudes were also added to allow a quadratic magnitude scaling term to be estimated for longer periods. In all, four magnitudes were considered: $M_w=5.0, 6.0, 7.0$ and 7.5 . All five response spectral periods are evaluated for the full matrix of cases. Three

depths were also considered for the short distances (Table 4.3.3-2).

For the TIP project, the main contributors to the hazard will be in EPRI regions 3 and 5 (Figure 4.3.3-2) which have similar attenuation to the Mid-continent model developed in the EPRI (1993) study. Therefore, the Mid-continent model was selected as the reference velocity model in this study (Tables 4.3.3-3 and 4.3.3-4).

The site condition was defined as ENA hard rock: 2800 m/s average shear wave velocity over the top 30 m; median kappa = 0.006 sec. This is consistent with the 1994 study.

It was also decided to include both strike-slip and reverse slip faulting in defining the cases. The final exercises are listed in Table 4.3.3-5.

4.3.3.3 Proponent Models

Brief descriptions of the ground motion models are given below. All models provide estimates for hard rock conditions (or were converted to hard rock conditions) as defined in Section 4.3.3.2.

4.3.3.3.1 Campbell Hybrid Empirical

The Campbell hybrid empirical model uses the point source stochastic model to adjust empirical attenuation models developed for WNA to be applicable to ENA. The point source stochastic model is used to account for differences between typical Q and kappa values in WNA and ENA. Details of this model are given in Appendix E.

4.3.3.3.2 Somerville Numerical Simulations

The Somerville model is a finite source numerical simulation based on empirical source functions with region specific path effects incorporated using ray theory (Somerville et al. 1990). The "empirical source functions" include scattering and kappa effects. The empirical source functions used in the Somerville proponent model are from a 1979 Imperial Valley aftershock ($M=5, 11/15/79$). Therefore, the source functions have scattering effects representative of WNA which are implicitly assumed to be applicable to ENA. The site effect (parameterized by kappa) is corrected from WNA to ENA by imposing a flat Fourier

amplitude spectrum on the empirical source functions at high frequencies ($f > 15$ Hz) and then applying a kappa correction to the spectrum.

4.3.3.3.3 Horton Numerical Simulations

The Horton model is a simplified finite source model with three subevents. Each subevent is a single-corner w2 point source. The wave propagation is computed using wavenumber integration. Scattering is introduced using empirical scattering functions derived from the Saguenay earthquake. Therefore, this model has ENA-specific scattering.

4.3.3.3.4 Frankel Numerical Simulations (1996)

The Frankel model is based on the point source stochastic model with a single-corner w2 spectrum and $1/R$ attenuation (Boore 1983). The median stress drop is 150 bars. The point source distance, R , is hypocentral distance. For distances less than 10 km, Frankel uses a constant ground motion defined at $R = 10$ km.

4.3.3.3.5 EPRI (1993)

The EPRI (1993) model is based on the point source stochastic model with a single-corner w2 spectrum and ray theory wave propagation. The median stress drop is 120 bars. The point source distance, R , is the "Joyner-Boore" distance measure, which allows the model to include effects of source distance.

4.3.3.3.6 Atkinson and Boore (1994)

The Atkinson and Boore (1994) model uses the stochastic model with an empirical two-corner source model and empirical attenuation. The median stress drop is 180 bars. The point source distance corresponds to hypocentral distance.

4.3.3.4 Elicitation Interviews

In the formal elicitation interviews, each expert explained the procedures he used to obtain estimates of the median motion (m), aleatory uncertainty (s), and the epistemic uncertainties on both (sm , ss). Each expert developed weighting schemes for the proponent models and explained the reasoning for the weights given to each model. In most cases, the weights were not the same for all magnitudes, distances, and frequencies but varied according to the

experts evaluation of the strengths and weaknesses of each model.

The elicitations all revealed that sm and ss were not well-understood by the experts. In particular, there was confusion how these epistemic uncertainties should vary as the number of proponent models considered increased. One result of the elicitations was that each expert assumed that the distribution of uncertainty on m and s was symmetric since they did not have significant evidence to the contrary. Ultimately, each expert developed weighting schemes only for m and s from which the 5th and 95th percentile values were computed. Given these limits and symmetric distributions, sm and ss could be computed.

4.3.3.5 Feedback Workshop

To facilitate comparisons between the individual experts' point estimates, a series of plots of these estimates and the proponent model estimates on which they were based was shown. An example is shown in Figure 4.3.3-3. A full set of plots (one for each case and each frequency) was given to the experts.

The feedback workshop considered three of the 132 cases. These three cases included magnitude moderate and large magnitude events at short distances and a large magnitude event a large distances. These three events were used to focus the discussion of the important differences in the proponent models. The strengths and weaknesses of the proponent models were discussed in the context of these three cases.

Much of the discussion focused on the 1 second spectral value. This value is particularly sensitive to the one-corner frequency vs. two-corner frequency model assumption: the two-corner model of Atkinson and Boore gives much lower median values than the one-corner assumption used in the other models. Additional recent results were provided to the experts that supported the two-corner model. In considering the one- and two corner models, some of the experts favored the one-corner model because it is more conservative in the 1-second range. This

sort of conservatism is not the intent of the study, but it is difficult to avoid.

4.3.3.6 Experts' Weights and Point Estimates

The experts estimated median ground motion, aleatory uncertainty, and associated epistemic uncertainties for a matrix of event magnitudes, distances, and faulting styles and at five spectral frequencies. The matrix of point estimates, 132 cases in all (Table 4.3.3-5), covers a magnitude range of 5.0 to 7.5, distances from 0 km to 200 km, strike-slip and reverse dip-slip faulting, and both hanging wall and footwall for the latter style. The matrix of magnitude-distance pairs was selected to provide adequate constraints on the attenuation without overburdening the experts. The same five frequencies that were used in the 1994 study were used in this work.

Most experts developed a general set of weights applicable for all magnitudes, distances, periods, and mechanisms and applicable for both m and s . The experts did not explicitly provide weights to derive s_s and s_m . Rather, because each expert chose a symmetric distribution around m and s , the 5th and 95th percentile values were simply computed from the m and s estimates and, thence, the s_s and s_m values. The experts modified their general rules as they deemed appropriate, to emphasize or de-emphasize certain models. Each expert's rules are discussed below.

Bernreuter (Table 4.3.3-6): Weights for m estimates are independent of period, distance, and mechanism but are dependent on magnitude. No weights are applied to the Frankel stochastic model as it is approximately duplicated by the EPRI model. No weight is assigned to the Horton simulation model as it is not judged to be as well validated as other models. At low magnitude (M 5), the two remaining stochastic models (Atkinson and Boore and EPRI) receive 60% of the total weight (0.3 weight each) and the Campbell hybrid model receives 40% of the total weight (0.4 weight); no simulation results are available for the Somerville model at M 5. At M 6, weights on the stochastic models are unchanged at 60% of the total; the hybrid model and Somerville simulation models combined

total 40% (weights of 0.2 each) and. At large magnitudes, all four models are equally weighted (0.25 each); thus weight is effectively decreased on the stochastic models to 50% of the total. Bernreuter judged that the EPRI model provides the best single estimate of s values and used these values alone.

Boore (Table 4.3.3-7): Weights are assigned independent of magnitude, distance, period, or mechanism; different schemes were used for m and s . For m , Atkinson and Boore is preferred overall insofar as it is a two-corner model (weighted 0.5). The single-corner EPRI model is given lower weight (weighted 0.3). The balance of the weight is equally distributed between the two simulation models (Somerville and Horton, weighted 0.1 each). No weight is assigned the hybrid or Frankel models. For the former, use of equivalent point source distances accounts for finite fault effects thus there is no need to use the hybrid model. Regarding the latter, the selection of stress drop is arbitrary and the model is not significantly different from the EPRI model. In computing s , weight was equally distributed between the Atkinson and Boore stochastic, the EPRI stochastic, and the Campbell hybrid models (weighted 0.33, 0.34, 0.33 respectively).

Campbell (Table 4.3.3-8): Weights on m are assigned independent of period or mechanism. In general, weight is equally distributed between the hybrid empirical, the stochastic, and simulation models (total weights of 0.33, 0.33, and 0.34). Preference is given to the Atkinson and Boore model over the EPRI and Frankel stochastic models (weights 0.17, 0.08, and 0.08 respectively) and the Somerville and Horton simulation models are equally weighted (0.17 each). The Campbell hybrid model is (in general) gradually downweighted at distances of 70 km and greater due to a lack of data constraining empirical WUS relations. At M 5 and 6 the weight is halved at 70 km (0.17), halved again at 120 km (0.08), and set to zero at 200 km. At M 7 and 7.5, the downweighting is not as severe: it is halved at 120 km (0.17), and halved again at 200 km (0.08). Campbell adopted s values independent of those predicted

by the models; values selected are from the empirical western US attenuation relations considered in the hybrid model.

Jacob (Table 4.3.3-9): Weights are independent of period and distance; they are dependent on magnitude and mechanism. Jacob developed a weighting system in which each model was assigned a 'moderate' weight (value of 2), 'high' weight (value of 3), 'low' weight (value of 1), or was not weighted (not applicable or not available; value of 0). The weights were subsequently normalized by the sum of the weights for all models at each magnitude level for a specific mechanism. All weights are summarized in Table 4.3.3-9. Divergences from moderate weights for estimates of m include (typically):

Atkinson and Boore model upweighted at M 5, downweighted at M 7 and 7.5 for all mechanisms

Frankel model downweighted at M 7 and 7.5

Horton model upweighted for strike-slip, zero-weighted for footwall

Somerville model low or zero-weighted for most mechanisms and magnitudes

Divergences from moderate weights for estimates of s include (typically):

Atkinson and Boore model downweighted for strike-slip at all magnitudes

Campbell model upweighted for strike-slip at all magnitudes

Frankel model upweighted for all mechanisms at all magnitudes

Horton model downweighted or zero-weighted for all mechanisms and magnitudes

Somerville model downweighted or zero-weighted for all mechanisms and magnitudes

Somerville (Table 4.3.3-10): Weights are independent of period or mechanism and dependent on distance and magnitude. Weight is distributed primarily between the stochastic, hybrid, and Somerville simulation models. No

weight is assigned to the Horton model. At low magnitude (M 5), 60% of the total weight is distributed between the stochastic models (Atkinson and Boore, EPRI, and Frankel) and 40% to the Campbell hybrid model. Simulations using the Somerville model were not computed at M 5. There is no distance dependence at M 5. At M 6 and distances greater than 20 km, 30% of the total weight is assigned to the stochastic models, 40% to the hybrid model, and 30% to the Somerville simulation model. At closer distances, the stochastic models are downweighted slightly to 20% of the total and the Somerville model is upweighted to 40% of the total. The same weights are applied at M 7 and 7.5 as at M 6, excepting the distance cutoff is changed to 70 km.

Examples of the proponent model median estimates for peak acceleration are shown in Figures 4.3.3-4a and b for magnitude 5 and 7, respectively. Similar comparisons for 1 second period spectral acceleration are shown in Figures 4.3.3-5a and b. The aleatory variability for the proponent models for peak acceleration and 1 second spectral acceleration are shown in Figures 3-6a and b.

4.3.4 Attenuation Relations

4.3.4.1 Introduction

To facilitate the use of the ground motion models in the hazard calculation, the experts' point estimates were parameterized by attenuation relations. The regression analysis to develop the attenuation relations was performed by the TFI team.

4.3.4.2 Regression Model Form

Based on an examination of the experts' point estimates general functional forms were selected. Different functional forms were used for the median estimates, the aleatory variability, and the epistemic uncertainties.

The independent variables used in all regressions correspond to:

- M Moment magnitude
- R Rupture Distance (in km)

The predicted values for m are in natural logarithm of g for spectral acceleration and natural logarithm of cm/s for peak velocity. The sal , sm , and ss are all in natural log units. “Rupture distance”, defined as the closest distance from the site to the fault rupture was selected as the distance metric.

The adopted general forms for the regression model are given below in equation 4.1 to 4.4. As noted above, in some instances the experts added constraints to these general forms. These constraints are summarized in Table 4.3.4-1.

Median (m):

For $M < m_1$,

$$\mu = a_1 + a_2(M - m_1) + a_6(8.5 - M)^2 + [a_3 + a_5(M - m_1)] \cdot \ln \sqrt{R^2 + a_8^2} + a_7F \quad (4.1a)$$

For $M \geq m_1$,

$$\mu = a_1 + a_4(M - m_1) + a_6(8.5 - M)^2 + [a_3 + a_5(M - m_1)] \cdot \ln \sqrt{R^2 + a_8^2} + a_7F \quad (4.1b)$$

Aleatory Variability (s_{al}):

For $M < b_4$,

$$\sigma_{al} = b_1 + b_2(M - b_4) \quad (4.2a)$$

For $M \geq b_4$,

$$\sigma_{al} = b_1 \quad (4.2b)$$

Epistemic Uncertainty in the Median (s_m):

$$\sigma_\mu = c_1 + c_2(M - c_6) + c_3 \ln(R + 1) + c_4 [\ln(R + 1)]^2 + c_5F \quad (4.3)$$

Epistemic Uncertainty in the Aleatory Variability (s_s):

For $M < d_4$,

$$\sigma_\sigma = d_1 + d_2(M - d_4)$$

For $M \geq d_4$,

$$\sigma_\sigma = d_1 \quad (4.4b)$$

Minimum values of 0.3 for σ_{al} , 0.15 for σ_μ and 0.05 for σ_{σ_μ} are recommended on the models to keep the models reasonable.

4.3.4.3 Regression Results

Attenuation relations were developed for each expert’s point estimates individually and for a composite model that combines all of expert’s point estimates. In all cases the m_1 coefficient was constrained to:

$$m_1 = 6.25.$$

4.3.4.3.1 Individual Expert Attenuation Relations

The regression analysis was evaluated by comparing each expert’s point estimates to the regression model fits. These comparisons (not shown) indicate that the regression analysis adequately models the experts’ point estimates.

Coefficients a_i , b_i , c_i , and d_i are listed in Table 4.3.4-2. The process of fitting the experts' point estimates with a smooth equation leads to additional aleatory variability due to the misfit between the equation and the point estimates. To account for this additional variability, the total aleatory variability is given by the combination of the experts' estimate of the aleatory variability (parameterized by the regression equation as S_{al}) and the standard deviation of the fit to the median ground motion (listed as Sigma Fit in the Table 4.3.4-2). The total aleatory variability is given by

$$\sigma_{total} = \sqrt{\sigma_{fit}^2 + \sigma_{al}^2} \quad (4-5)$$

Comparison of the regression model fits and the experts' point estimates are shown in Figures 4.3.4-1 to 4.3.4-4. These figures show that the range in the median ground motions from these models is generally less than a factor of 1.5. Examples of the resulting attenuation relations for the seven experts are compared for peak ground acceleration and for 1 Hz spectral acceleration for two magnitudes: 5.0 and 7.0. The models for the horizontal component median ground motions are compared in Figures 4.3.4-1 and 4.3.4-4. These figures show that the range in the median ground motions from these models is generally less than a factor of 1.5. The models for the horizontal component aleatory variability are compared in Figures 4.3.4-5 and 4.3.4-6 for peak acceleration and spectral acceleration at a period of 1 second. The range in the aleatory variability in the models is generally less than 0.1 natural log units. The epistemic variability in the median horizontal ground motion is compared in Figures 4.3.4-7 to 4.3.4-10. The range of the models is generally less than 0.1 natural log units except for Anderson's model which has much larger values due to his estimates of the epistemic uncertainty in the proponent model median estimates. Finally, the epistemic uncertainty in the aleatory variability is shown in Figure 4.3.4-11 and 4.3.4-12. The range of these models is generally less than 0.1 natural log units.

4.3.4.3.2 Composite Model

A single composite model is developed for the combined point estimates from all five experts. These composite models are also shown in Figure 4.3.4-1 to 4.3.4-12. For the composite model, the variability of the μ and σ_{al} between experts is added to the average of the epistemic uncertainty (σ_{μ} and σ_{σ}) given by the five experts.

4.4 Analysis

4.4.1 General Scope of Calculations

A preliminary set of analyses showed that the differences between the ground motion experts' models were not significant in terms of effect on the hazard at the two sites selected, i.e., Watts Bar and Vogtle. Consequently we used the composite ground motion models (See Section 4.3) for all calculations.

An analysis of the effect of using the composite zonation model rather than the individual expert's model, (Savy 1993) had shown that only small differences could be expected, and only in some extreme cases.

To show this difference, we selected one zonation expert's input (i.e., Bollinger) for which we calculated the hazard with his own seismicity rates and secondly with the composite seismicity rates. In another comparison, we performed a calculation with a composite seismic source set of models. The estimates are all for a minimum magnitude of $M_{bl.g}$ 5.0 and for rock conditions. A site specific estimate will require adding a correction to account for the geotechnical site specificity at Watts Bar and at Vogtle.

4.4.2 Input Used in the Analyses

A summary of all the seismic source characteristics is given in Tables 4.4-1 to 4.4-15. Tables 4.4-1 to 4.4-5 give the final estimates of the probability distributions of the upper magnitude cutoffs M_u ($M_{bl.g}$), for Bollinger, Chapman, Coppersmith, Jacob and Talwani, respectively. Tables 4.4-6 to 4.4-10 give the final estimates of the probability distributions of the number of events, per year, f ($m = 4$), for

each expert's seismic source and for magnitude $M_{bl,g}$ 4.0. Additional information is also given to permit comparison between the various zones. It includes the activity rate per square kilometer of the seismic sources and the return period of the events greater or equal to $M_{bl,g}$ magnitude 4.0.

Tables 4.4-11 to 4.4-15 give the rate $f(m_1)$ estimates for a magnitude m_1 equal to 0.5 unit less than the upper magnitude cutoff, for each seismic source.

Figures in Appendix F show the rates for each expert and the composite distribution.

The Appendix F shows for each expert, the probability distributions of the upper magnitude cutoff M_u , the estimate $f(4.0)$ and $f(m_1)$. In addition a plot of the combined probability distribution is given. Here, the combined input is obtained by superimposing all the individuals' input and normalizing.

The seismic source maps used for each expert are given in Section 4.2.6 (Tables 4.2.6-1 to 4.2.6-5) and in Figures 4.4.1 to 4.4-14.

Each of the maps shown in Figures 4.4-1 to 4.4-14 shows one alternative map representing the range of experts interpretation using the common building block sources, as shown in Tables 4.2.6-1 to 4.2.6-5.

4.4.3 Comparison of the Hazard for an Individual Expert and for the Composite Seismicity Rates

The seismic hazard was calculated using an individual expert's input seismic rates and using the composite rates; no special method was used to define the composite rates but rather, we used the combined probabilities as shown in Appendix F.

Figures 4.4-1 and 4.4-3 show the two sets of calculation, for the expert's rates and composite rates, respectively, for the case of the PGA, for the Vogtle site. The mean hazard is higher for the composite rates, with a slightly greater total uncertainty on the hazard estimate in the .2 g range of acceleration. The same observation can be made with the spectral acceleration, (see Figure 4.4-2 and 4.4-4.). The conclusion is

reversed, for the case of the Watts-Bar site, where the expert's mean and hazard estimate total uncertainty is greater with the expert's seismic rates. It appears that the dominant sources to the hazard for the Vogtle site are several large zones around the site, and their seismicity rates are more sharply defined by each one of the experts than in the combined estimates. Furthermore, Bollinger's rate estimates are lower than the group of experts estimates, and consequently lower than the composite estimates.

For the Watts Bar site, the dominant sources are the portion of the ETSZ close to the site (Zone 4B2) and the large background [zone (5-1) and (5-2)] around it. Most of the experts gave higher emphasis to these zones than Bollinger did. As a result, the composite seismicity rates are on the average lower than for Bollinger for the dominant zones. Most of the experts had much smaller uncertainties than for Bollinger for the dominant zones. This also leads the uncertainty for the composite rates case to be smaller than Bollinger case. These observations apply to both PGA and uniform hazard spectra cases (see: Figures 4.4-5, 4.4-7 and 4.4-6, 4.4-8, for PGA and UHS respectively).

The differences that can be observed between the two cases: Individual expert's seismicity rates versus composite seismicity rates are in the order of 15 to 25% of the ground motion value for a given hazard level in the 10^{-4} to 10^{-5} hazard range, more for higher hazard (lower ground motion values).

4.4.4 Comparison of the Hazard Estimates for an Individual Expert and the Composite Zonation Maps

The composite maps are very similar to the maps of all the experts, since they use all the same building blocks as those used for the experts maps. As a result, the composite maps are essentially the same as the experts maps but with different weights. In this test, we have limited the number of alternative maps from all experts to those which could have an impact on the hazard, i.e., those including the dominant source zones. The weights assigned to the

composite maps were calculated using the TFI weights shown in the Tables 4.2.6-2A to 4.2.6-2D.

The final results show little difference between the individual expert's maps and composite maps when using the composite seismicity rates. Compare results in Figures 4.4-3 with 4.4-9 and 4.4-4 with 4.4-10 for Vogtle and Figures 4.4-7 with 4.4-11 and 4.4-8 with 4.4-12 for Watts Bar.

4.4.5 Comments on the Use of Composite Models

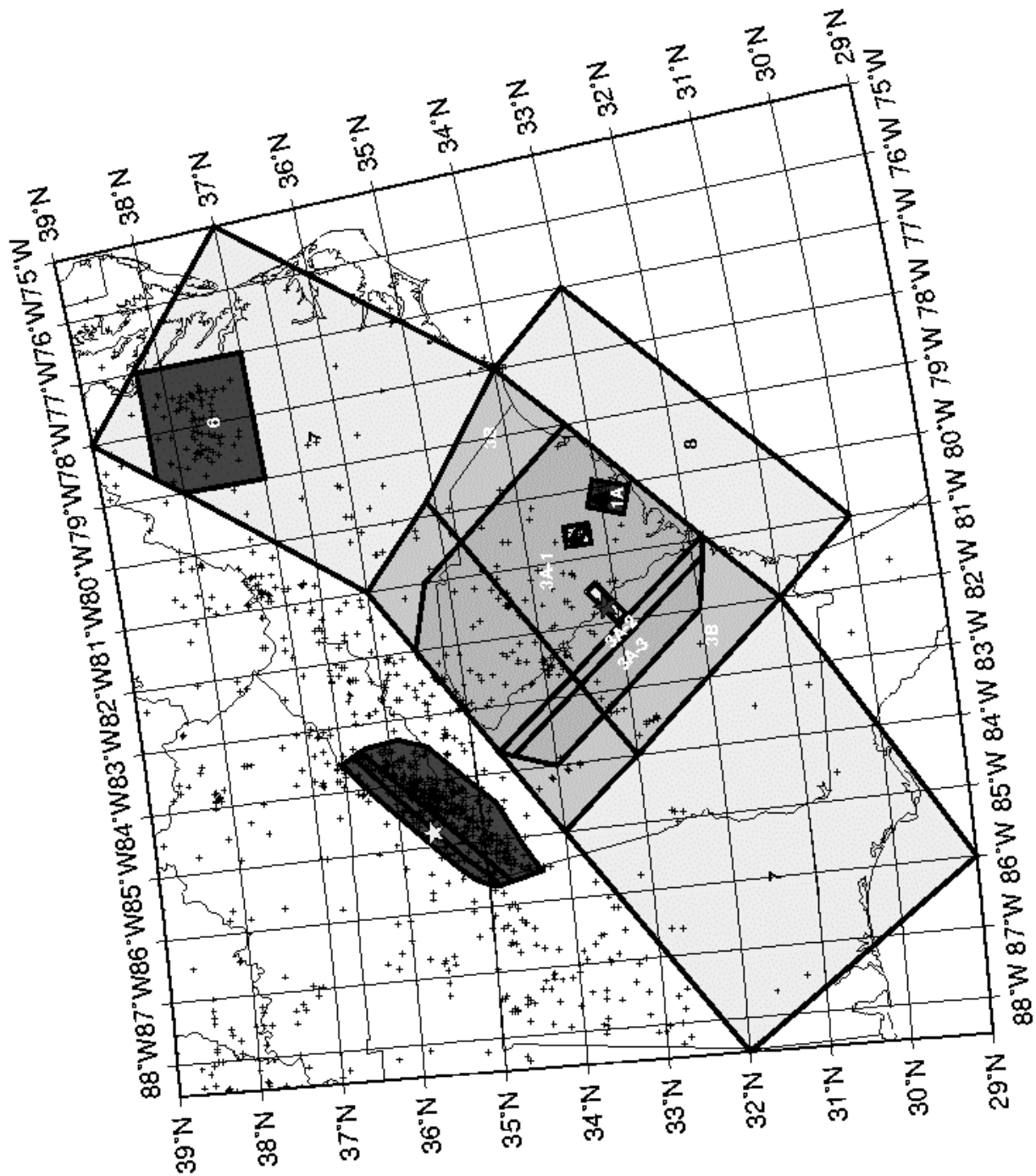
The use of composite models is appealing since it would allow us to incorporate the alternative range of alternatives and possible interpretation into a single model for the seismicity rates. For the zonation maps, we learned that by necessity, to be able to encompass the entire range of interpretation, the set of composite maps essentially had to contain all the maps which contain the dominant source zones, otherwise some classes of interpretations could be under-represented, and important dependencies between source zones would be lost. However,

because we concentrated on the elements which were common between all the experts' interpretations, and because we formulated a set of common building (source zones) blocks, this had the effect of creating convergence in the modeling of the dominant source zones among experts.

As a result, the final results using both composite maps and composite rates appear to be very robust in the sense that even with an expert's individual set of maps, the results would not be greatly different. Not to jump to hasty conclusion, it is important to emphasize that the individual maps are, in fact, already aggregated since they are formed with the minimum set zones, the building block source zones which are the results of the full integration of all the experts' inputs.

4.4.6 Comparison with the 1993 Eastern US Update for Watts Bar

A study conducted subsequent to this one compared PSHA results for the Watts Bar Site; the report is presented in Appendix G.



GMT Feb 3 15:28 VOGTLE MAP 1

Figure 4.2.6-1 Vogtle Map 1 — Zonation Maps That Define the Various Alternative Interpretations.

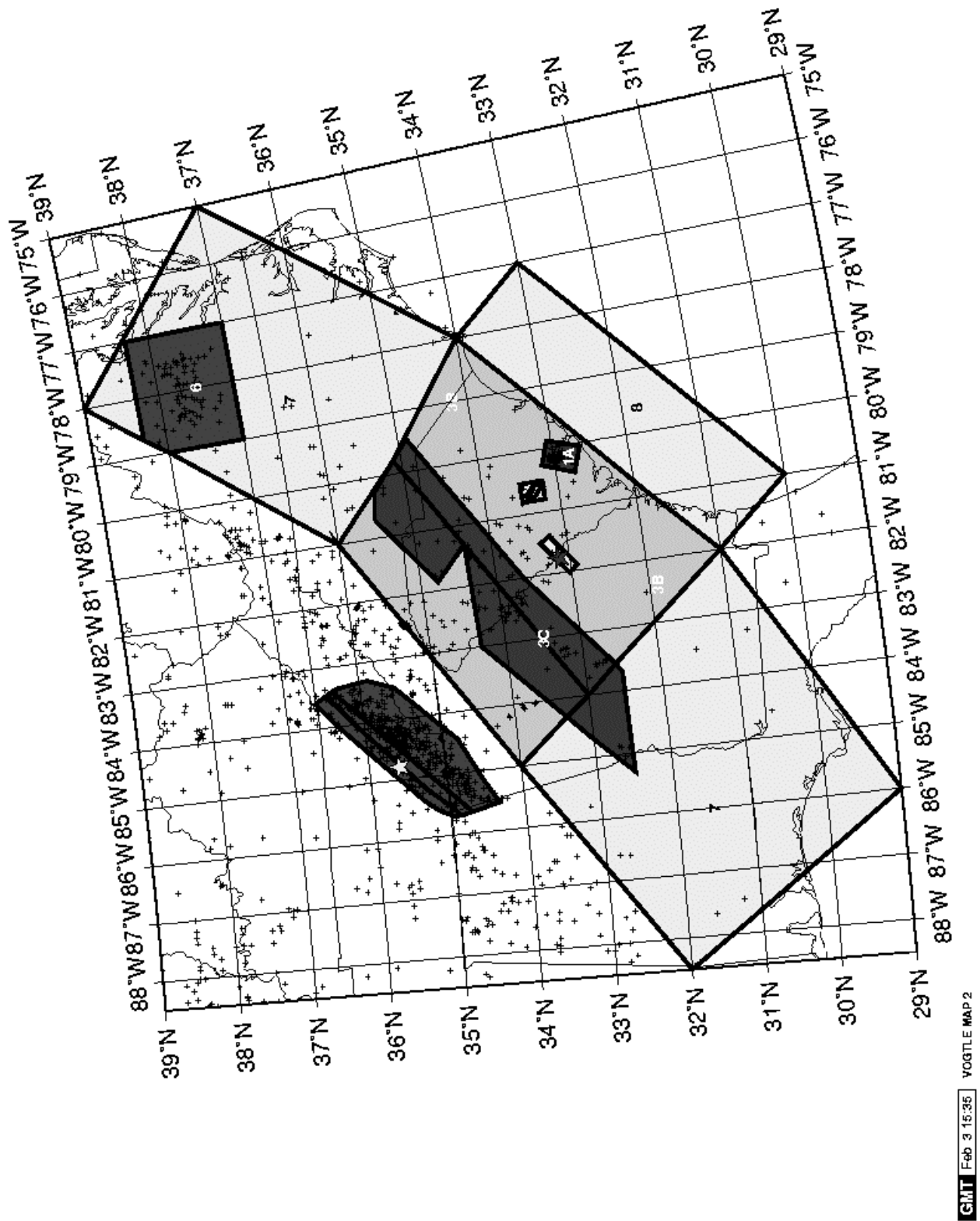
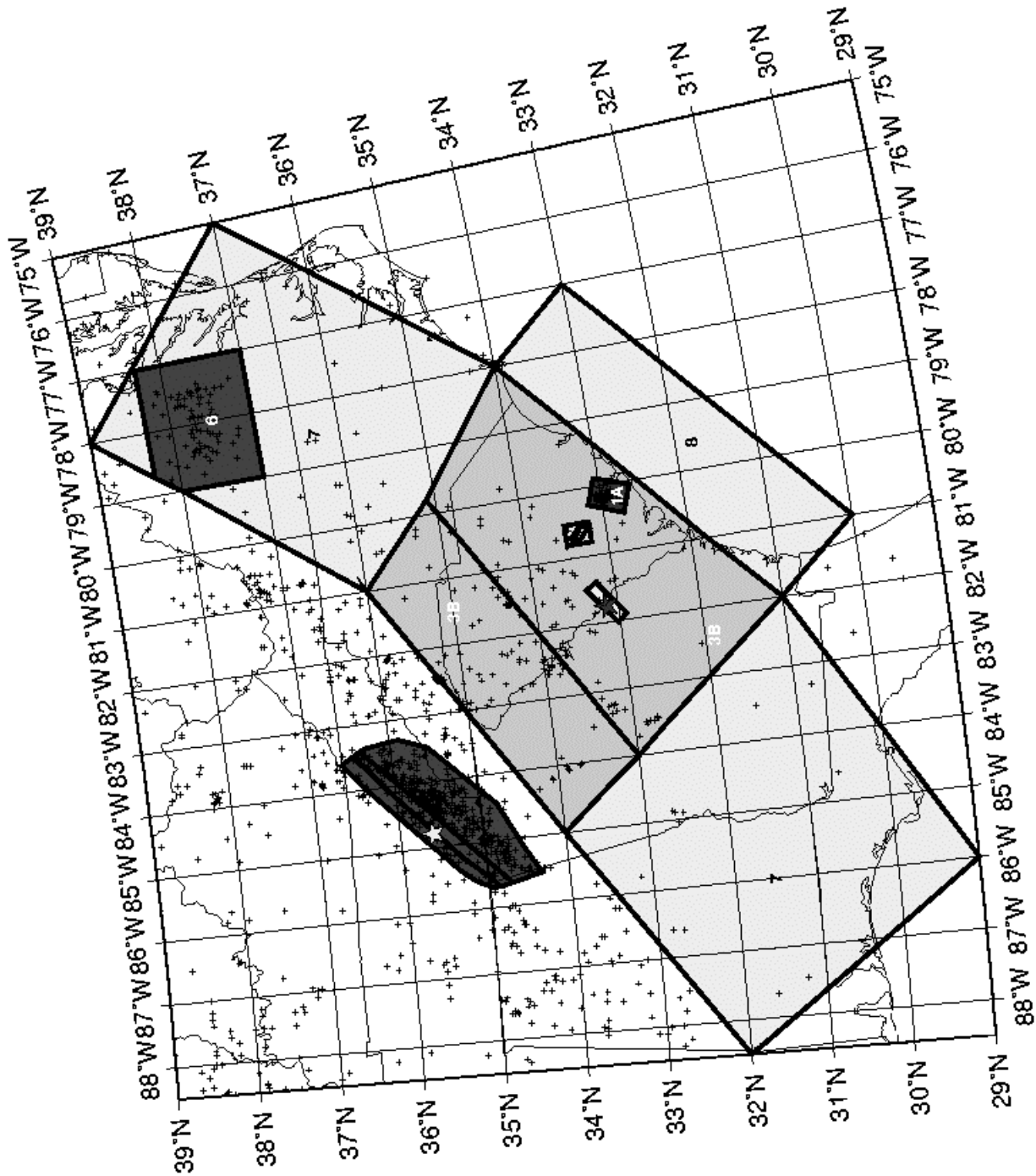


Figure 4.2.6-1 (cont'd) Vogtle Map 2 — Zonation Maps That Define the Various Alternative Interpretations.



GMT Feb 3 15:35 VOGTLE MAP 3

Figure 4.2.6-1 (cont'd) Vogtle Map 3 — Zonation Maps That Define the Various Alternative Interpretations.

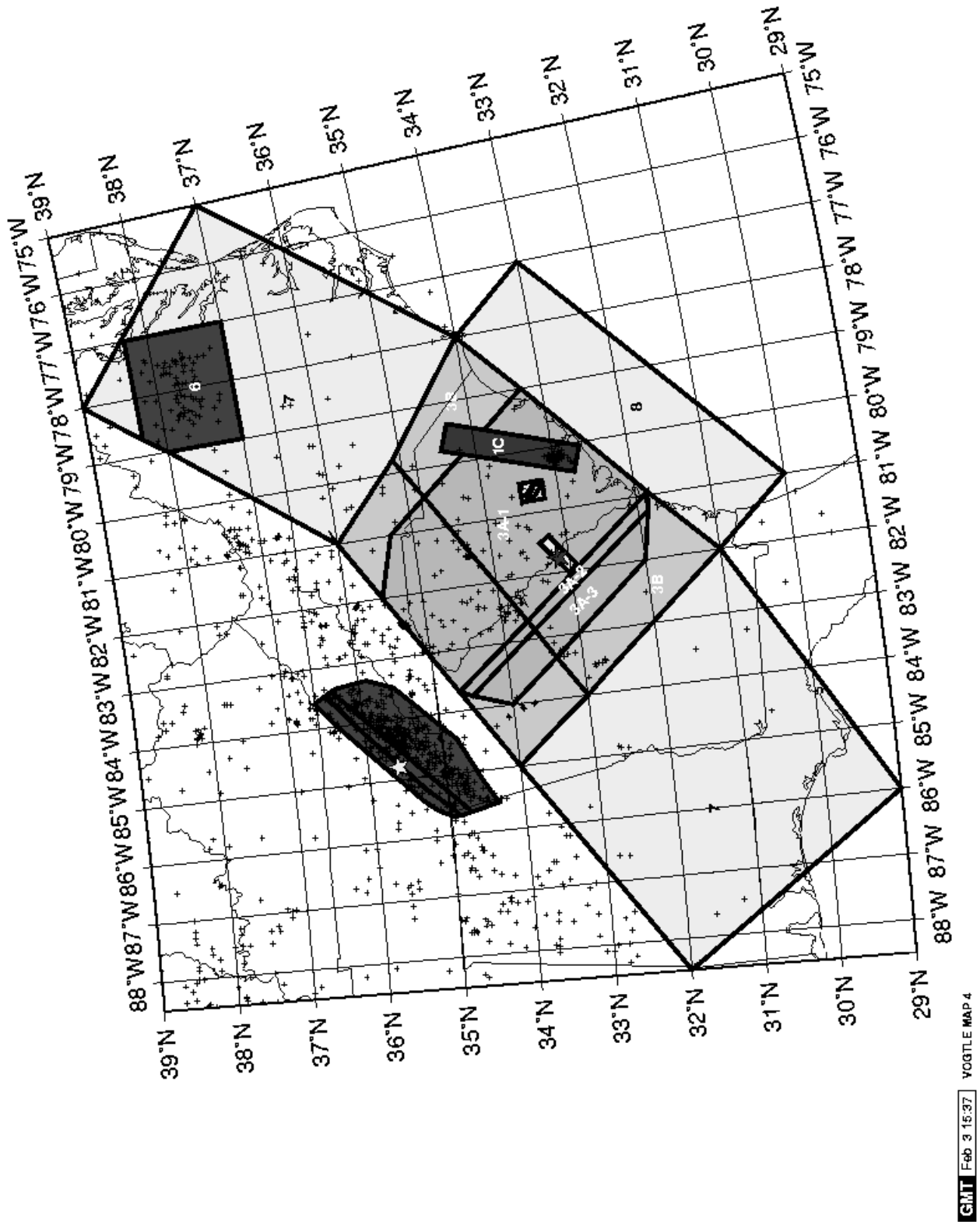
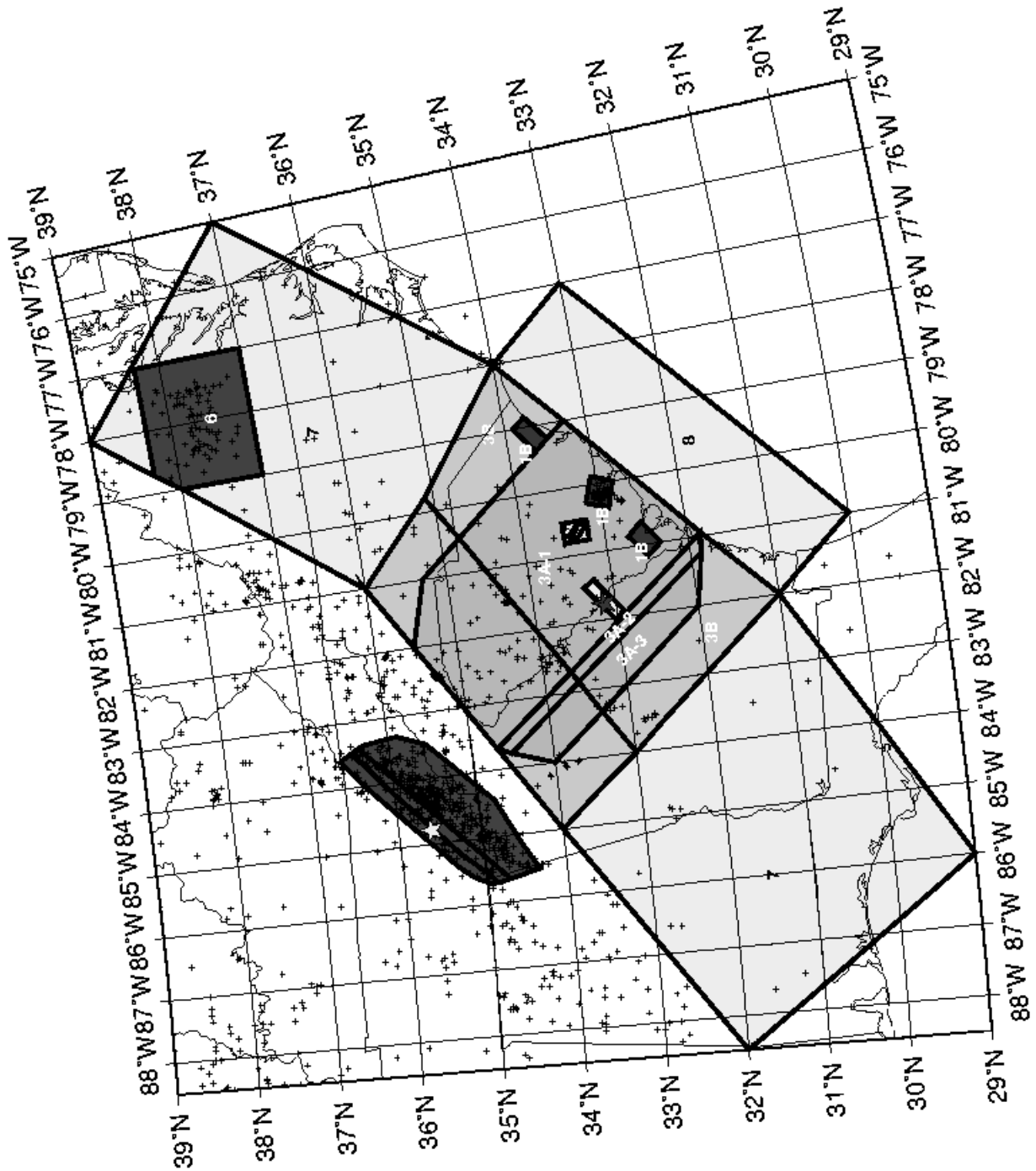


Figure 4.2.6-1 (cont'd) Vogtle Map 4 — Zonation Maps That Define the Various Alternative Interpretations.



GMT Feb 3 15:38 VOGTLE MAP 5

Figure 4.2.6-1 (cont'd) Vogtle Map 5 — Zonation Maps That Define the Various Alternative Interpretations.

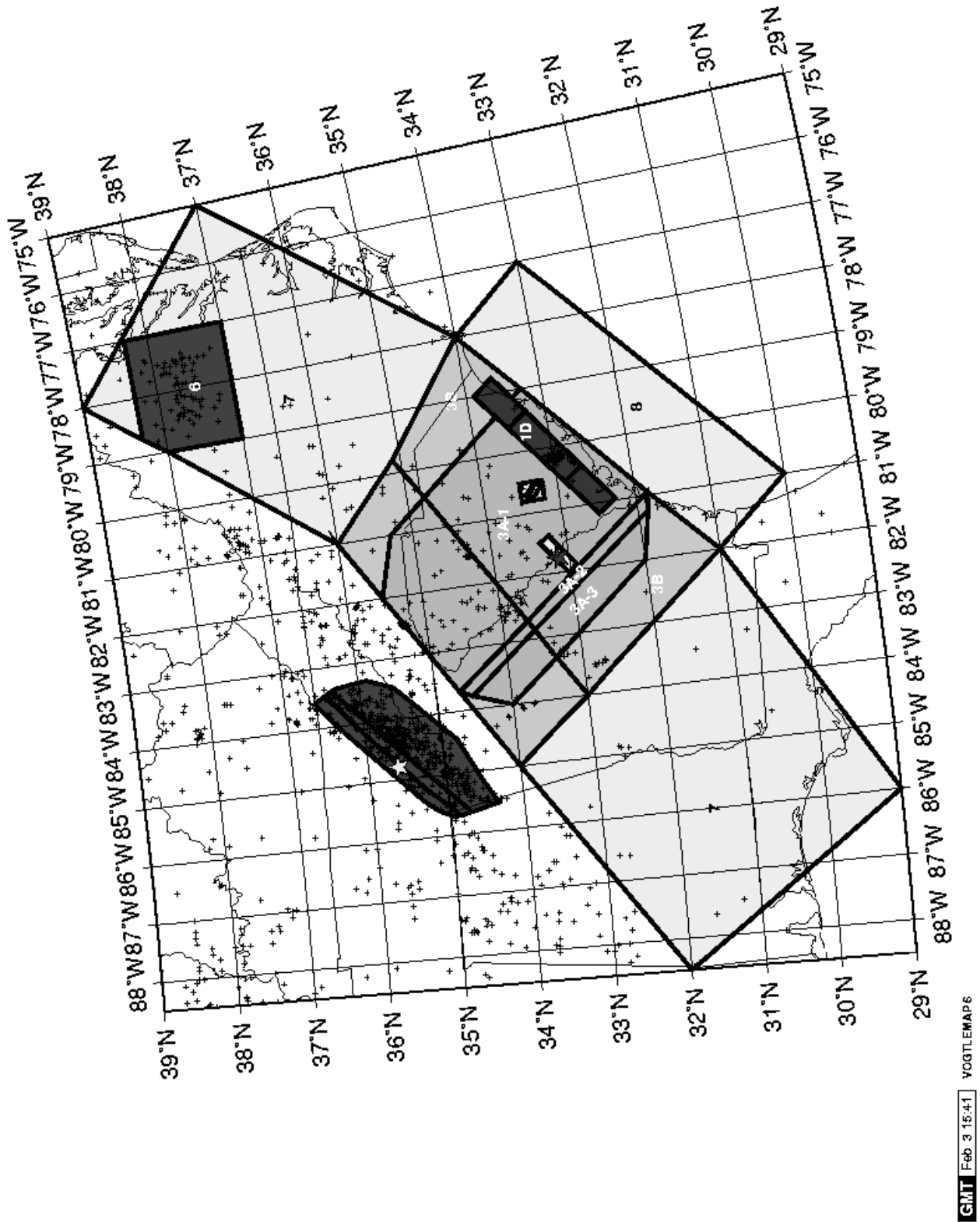


Figure 4.2.6-1 (cont'd) Vogtle Map 6 — Zonation Maps That Define the Various Alternative Interpretations.

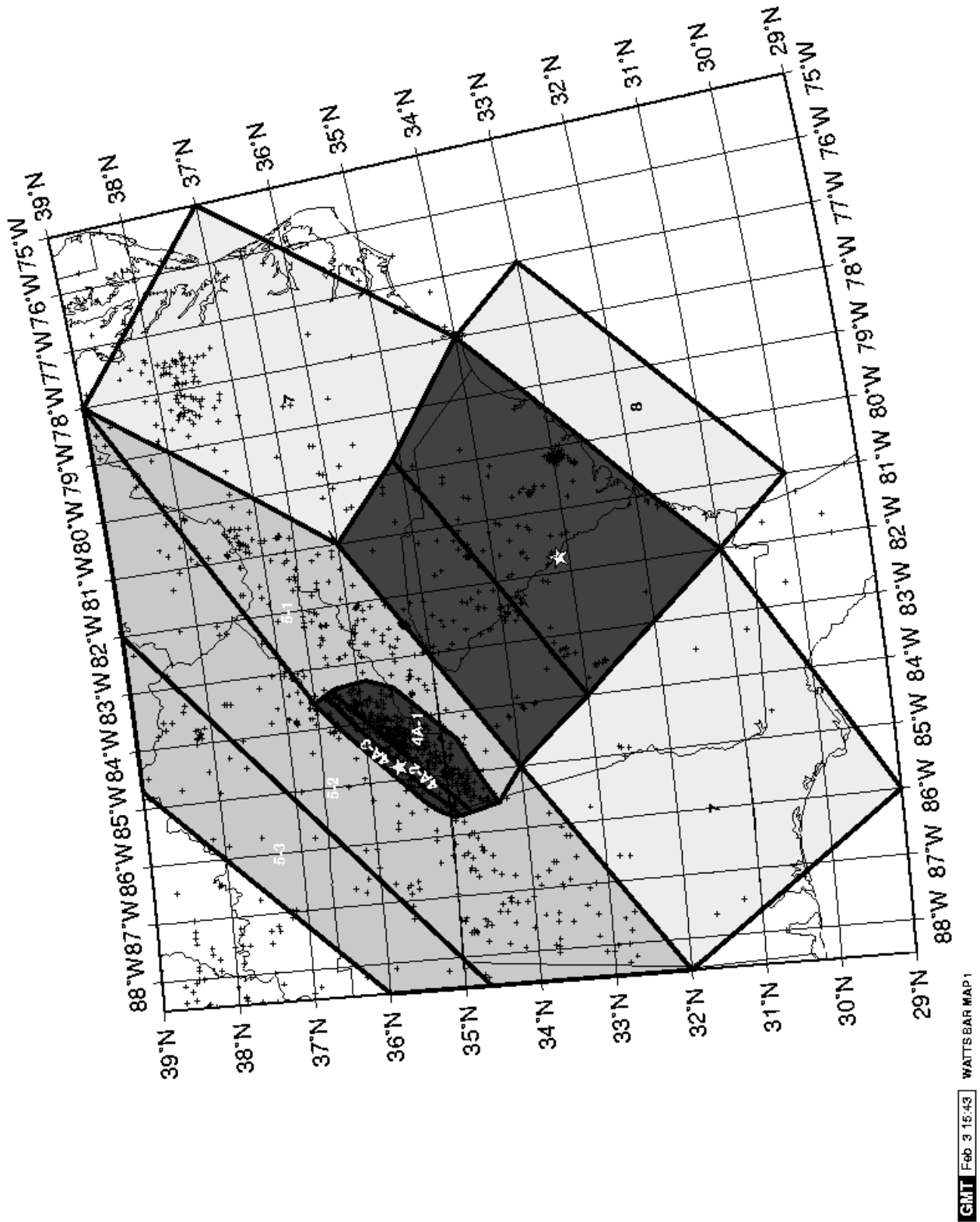


Figure 4.2.6-1 (cont'd) Watts Bar Map 1 — Zonation Maps That Define the Various Alternative Interpretations.

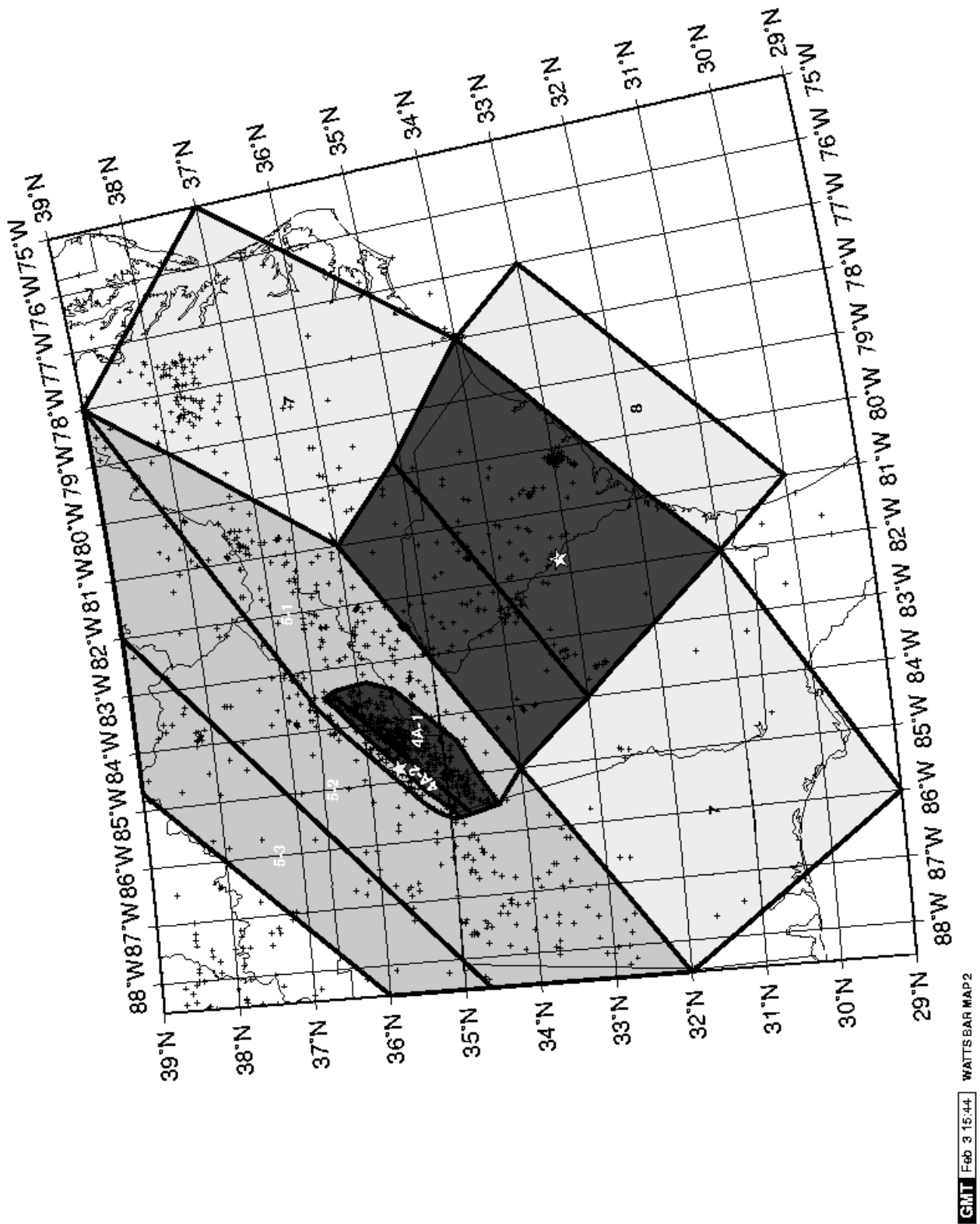


Figure 4.2.6-1 (cont'd) Watts Bar Map 2 — Zonation Maps That Define the Various Alternative Interpretations.

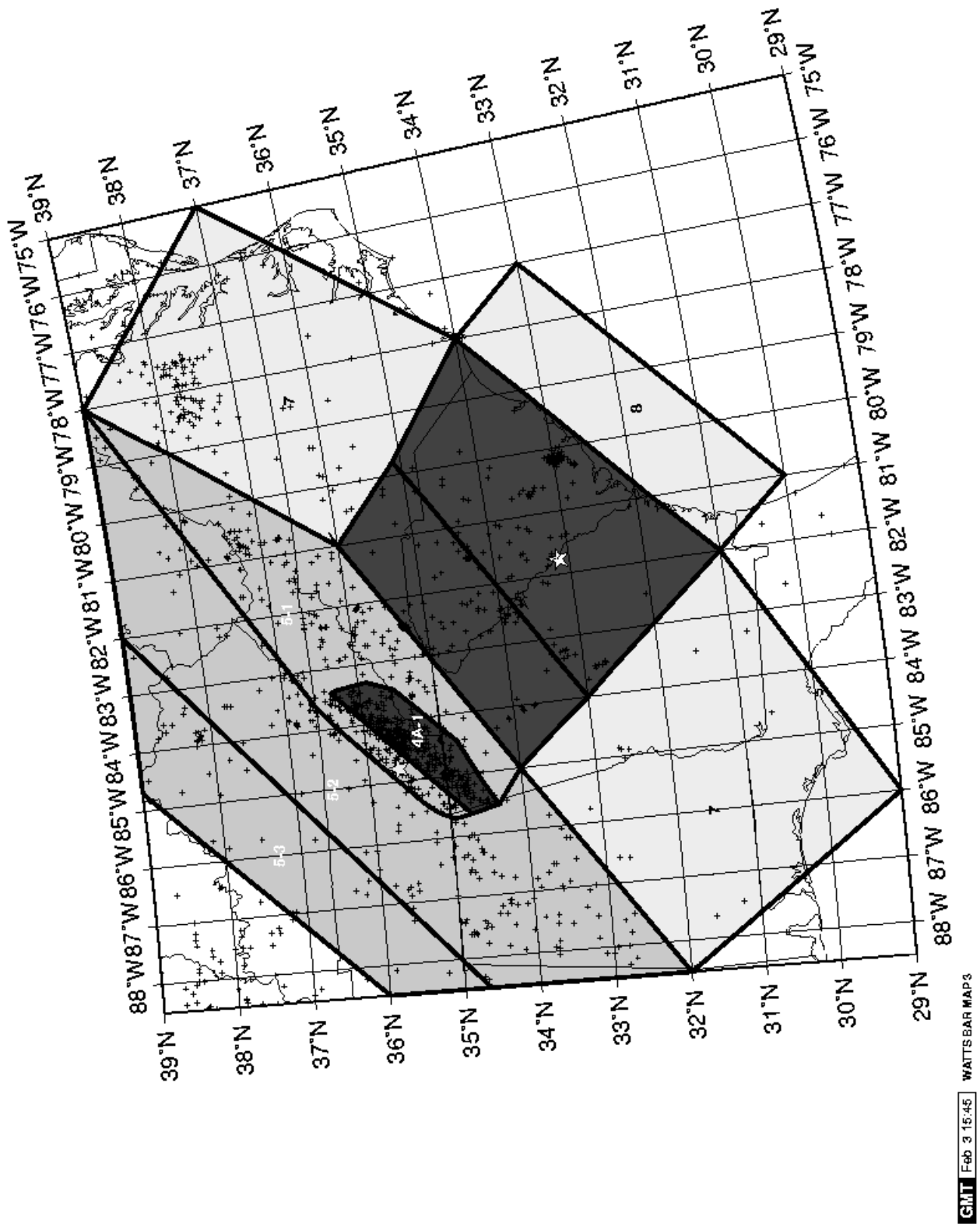


Figure 4.2.6-1 (cont'd) Watts Bar Map 3 — Zonation Maps That Define the Various Alternative Interpretations.

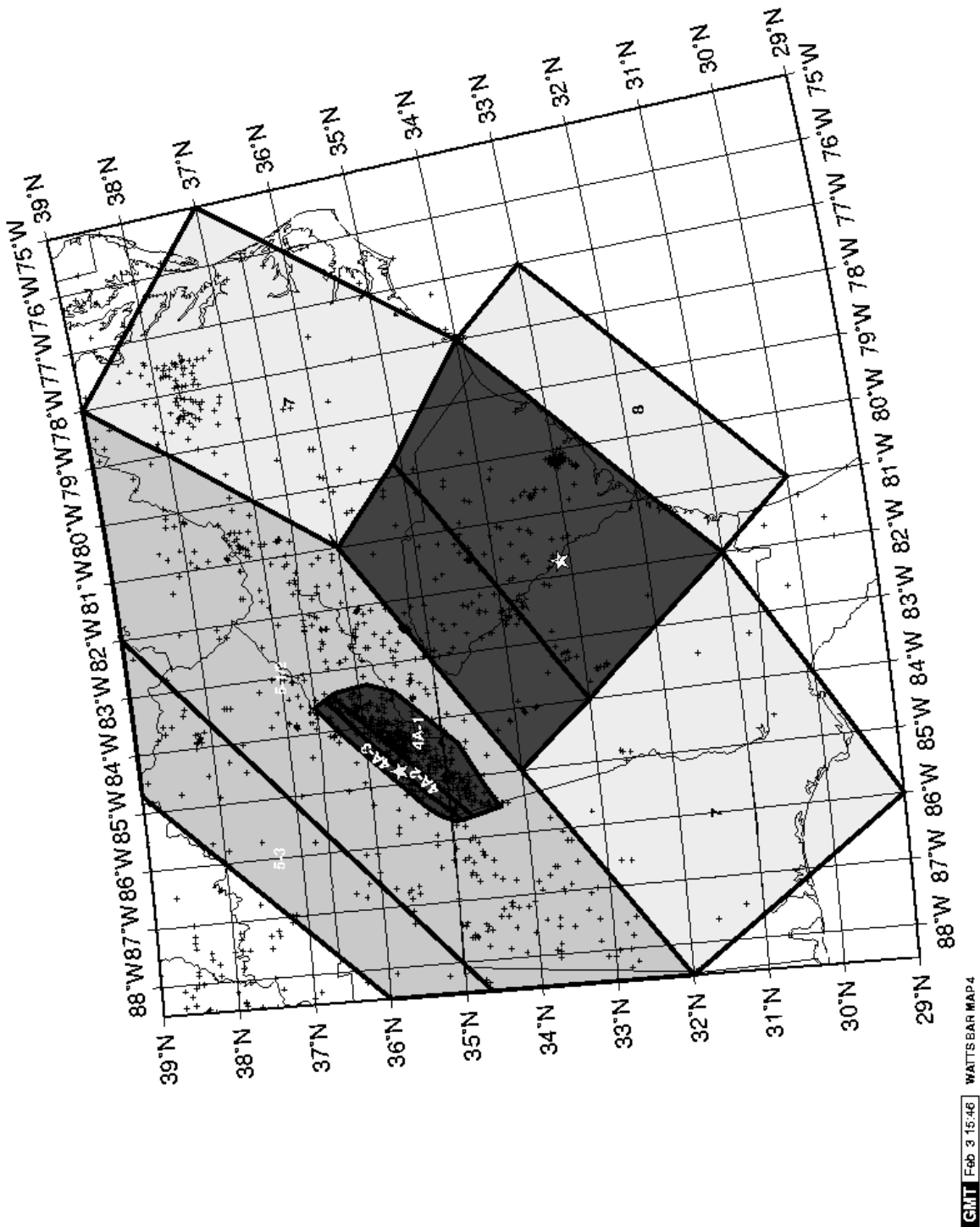


Figure 4.2.6-1 Watts Bar Map 4 — Zonation Maps That Define the Various Alternative Interpretations.

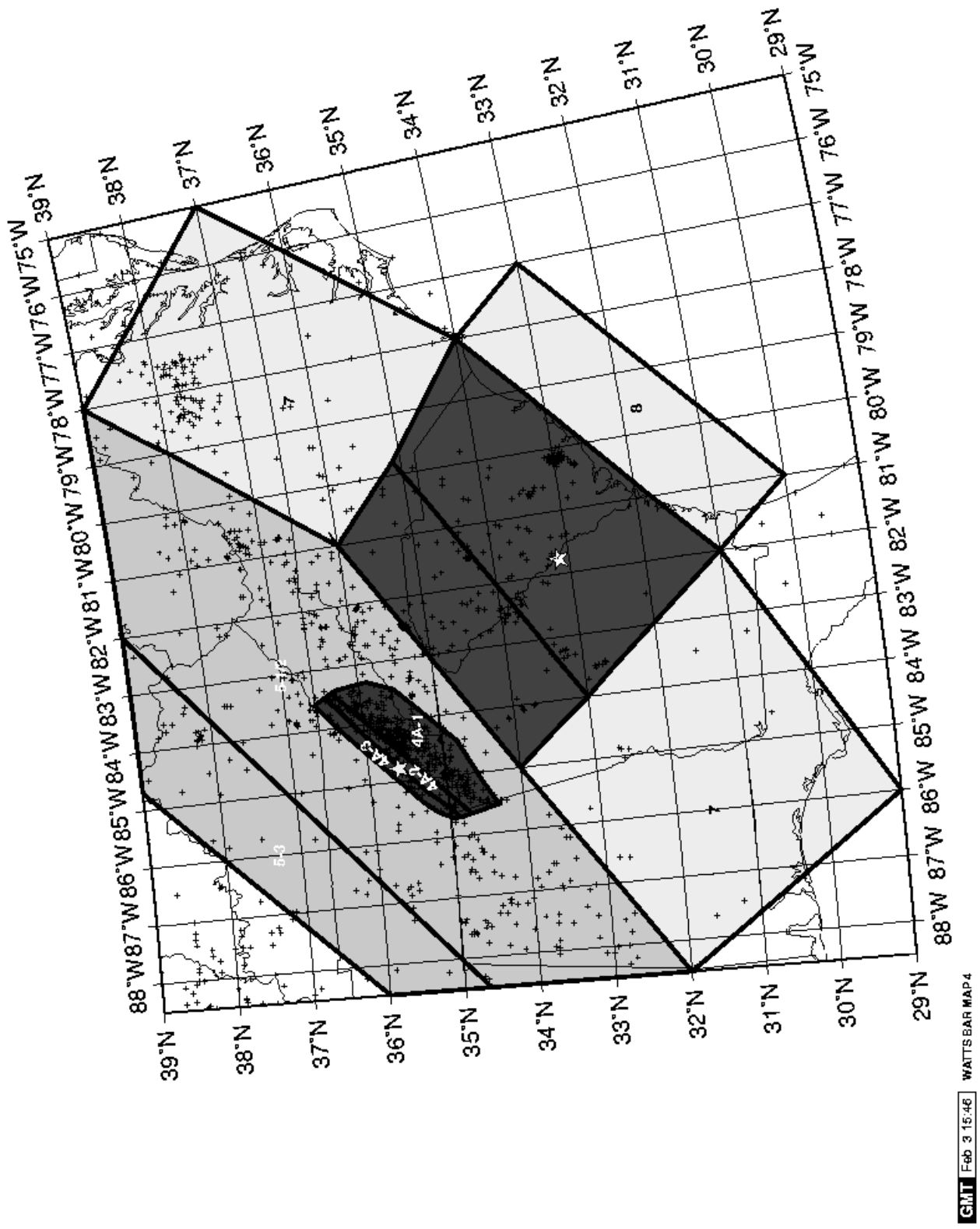


Figure 4.2.6-1 (cont'd) Watts Bar Map 5 — Zonation Maps That Define the Various Alternative Interpretations.

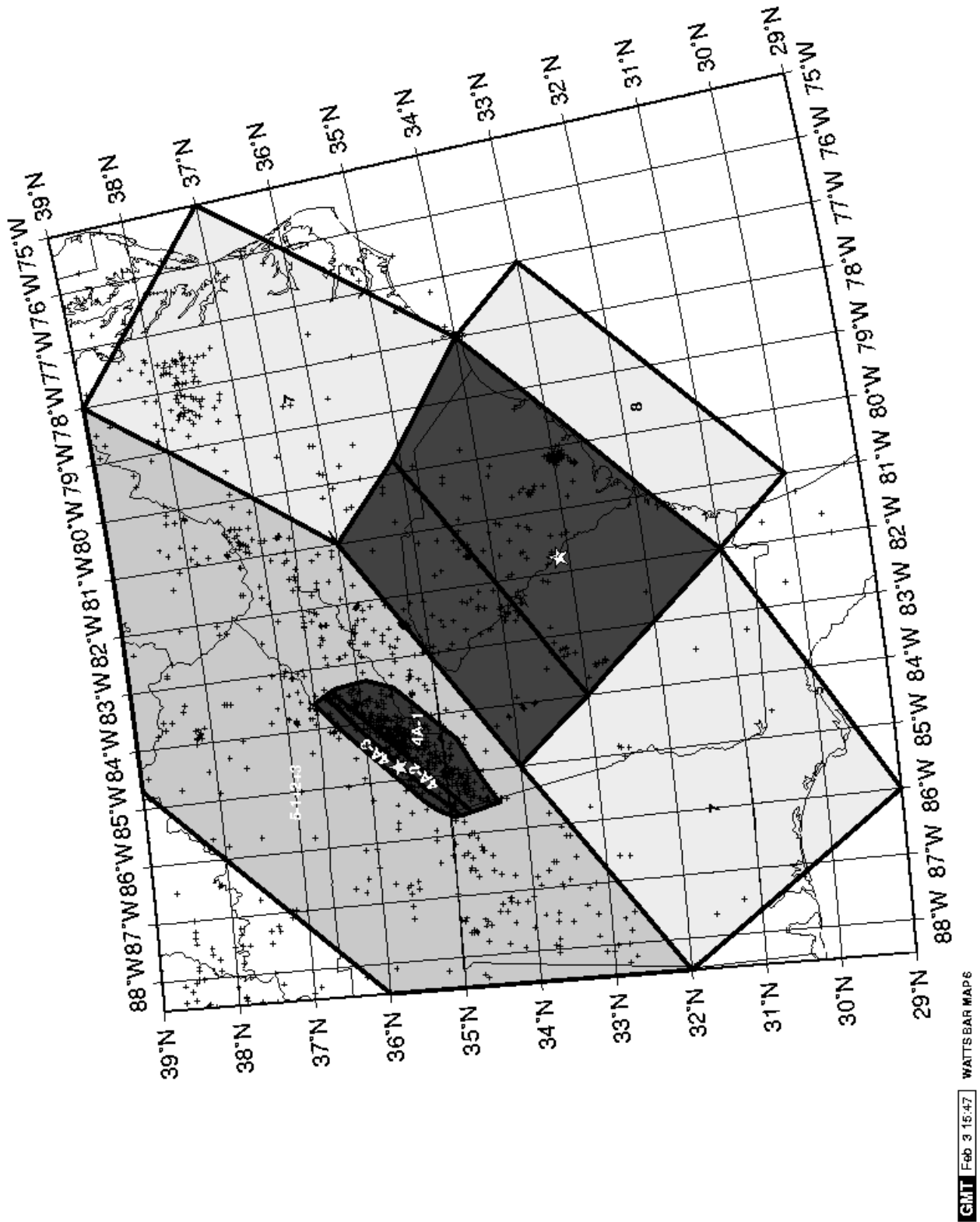


Figure 4.2.6-1 (cont'd) Watts Bar Map 6 — Zonation Maps That Define the Various Alternative Interpretations.

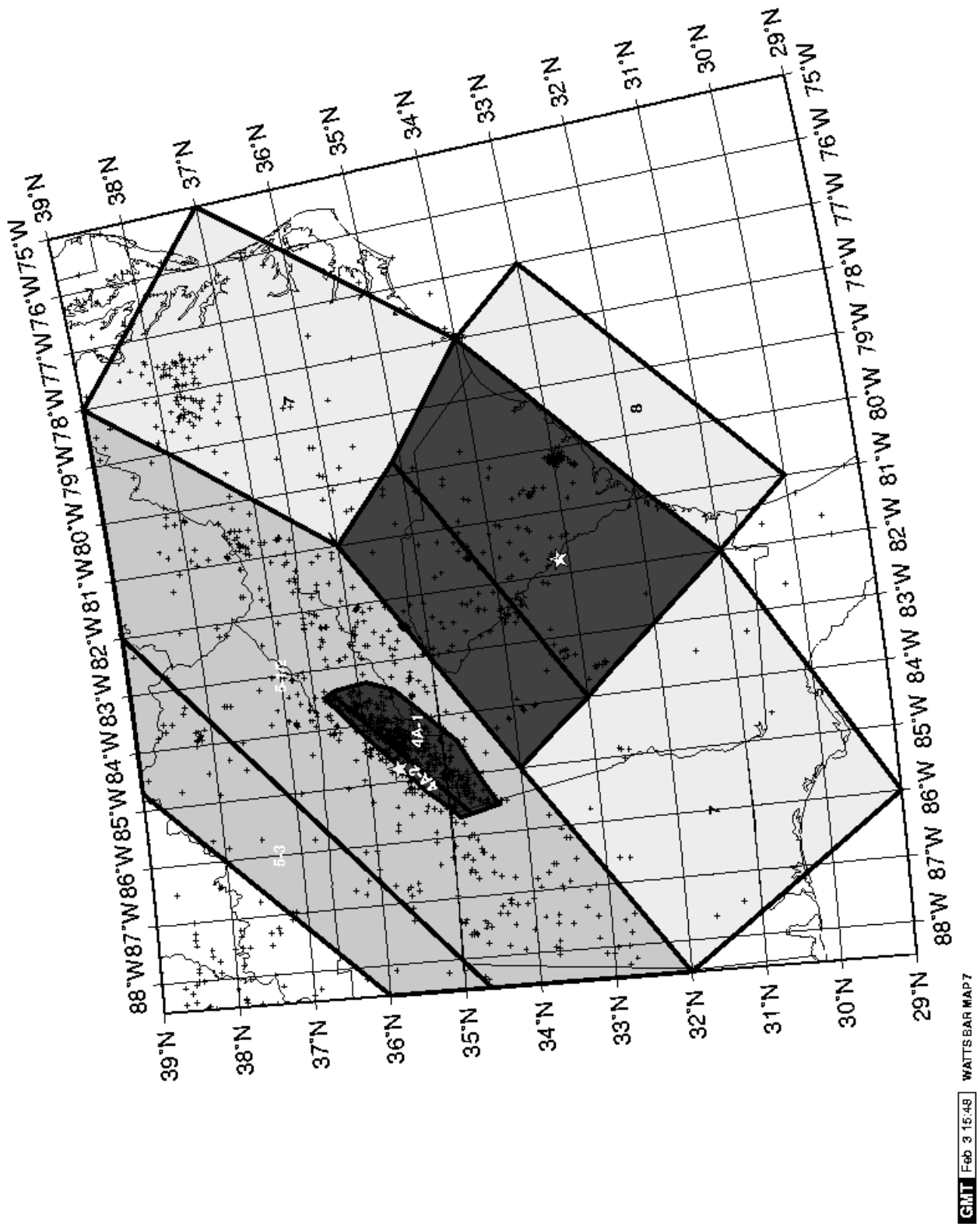


Figure 4.2.6-1 (cont'd) Watts Bar Map 7 — Zonation Maps That Define the Various Alternative Interpretations.

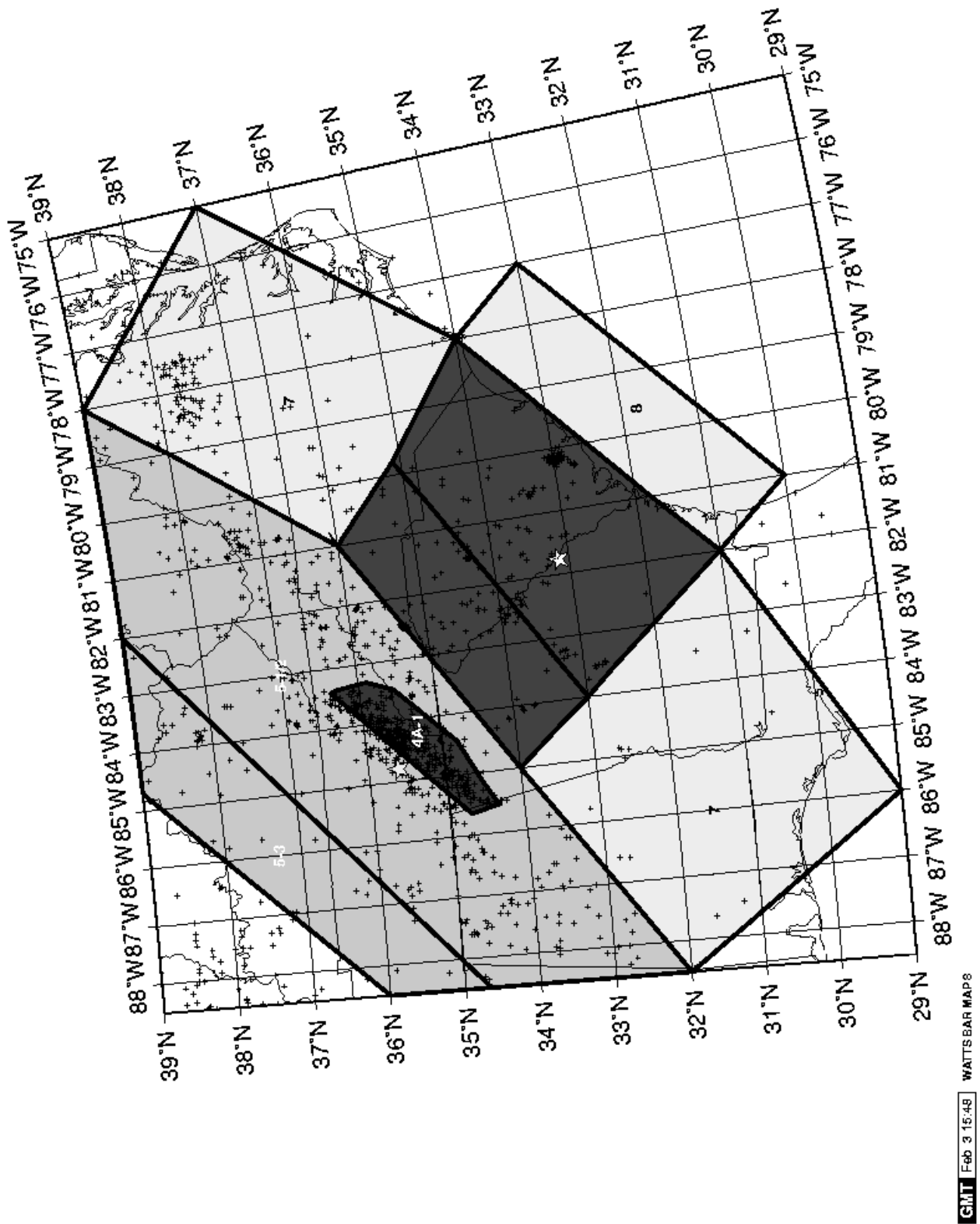


Figure 4.2.6-1 (cont'd) Watts Bar Map 8 — Zonation Maps That Define the Various Alternative Interpretations.

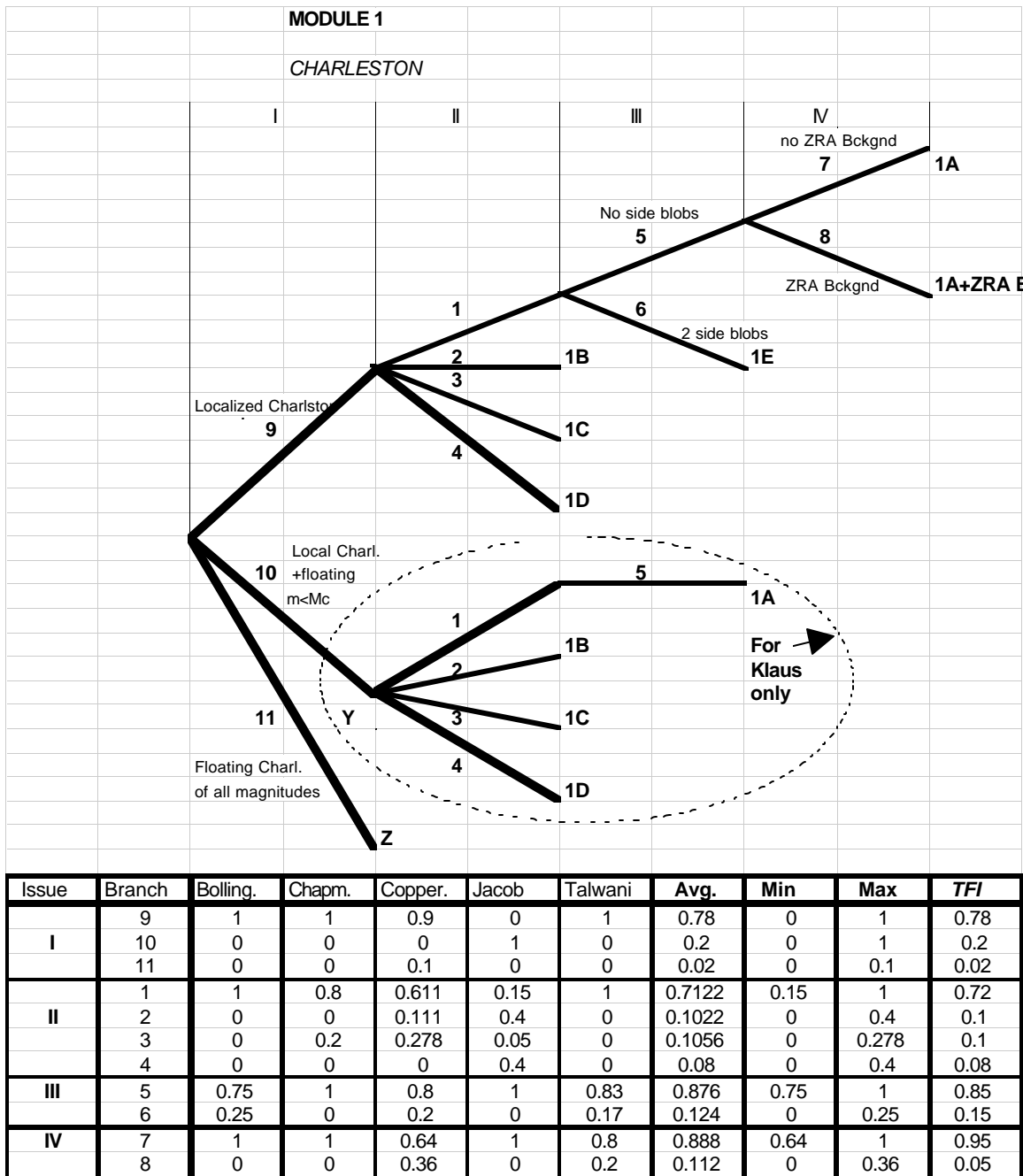


Figure 4.2.6-2A Logic Tree Representation of Experts' Interpretations for Module 1: Charleston Issue.

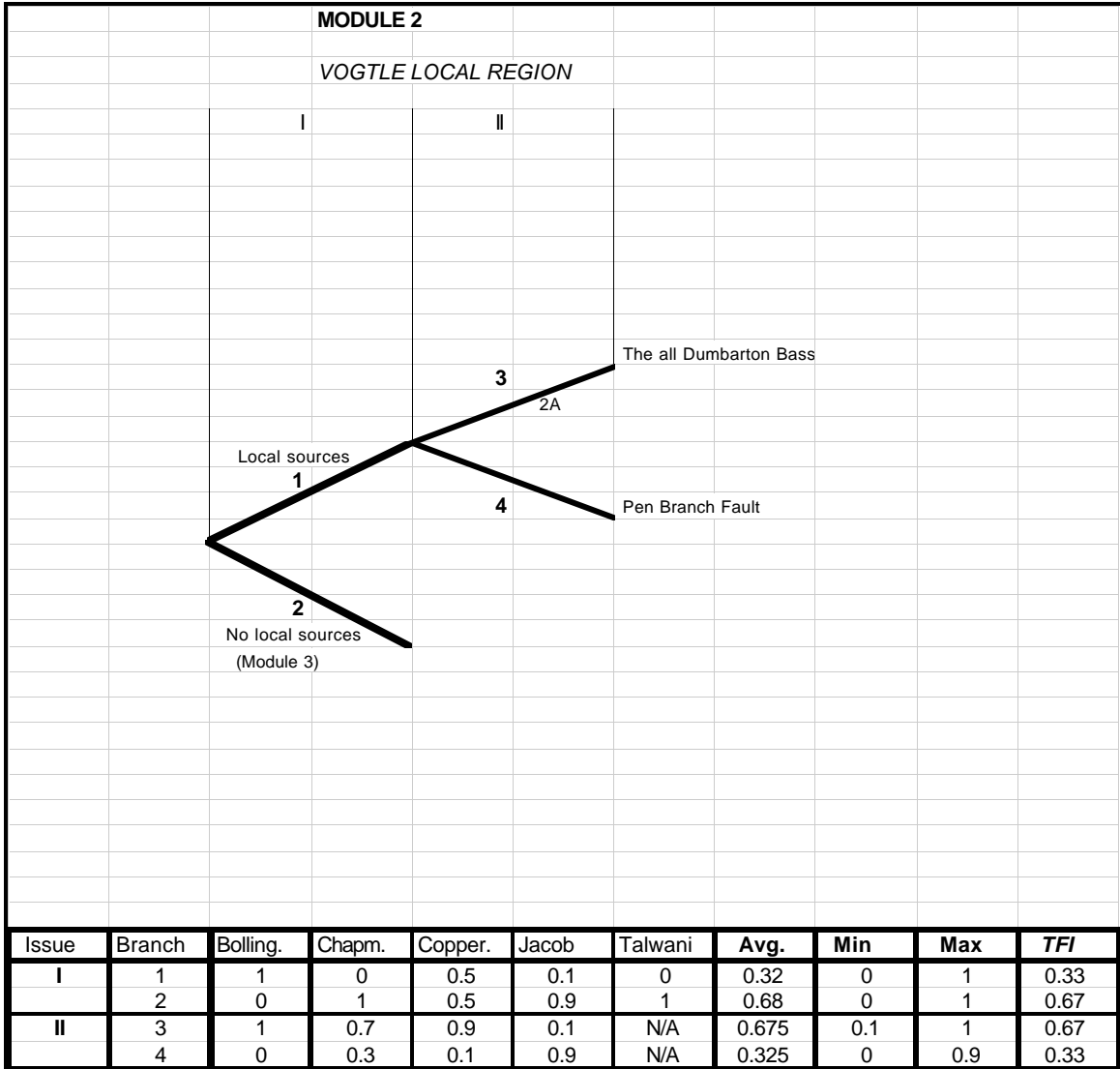


Figure 4.2.6-2B Logic Tree Representation of Experts' Interpretations for Module 2: Vogtle Local Region.

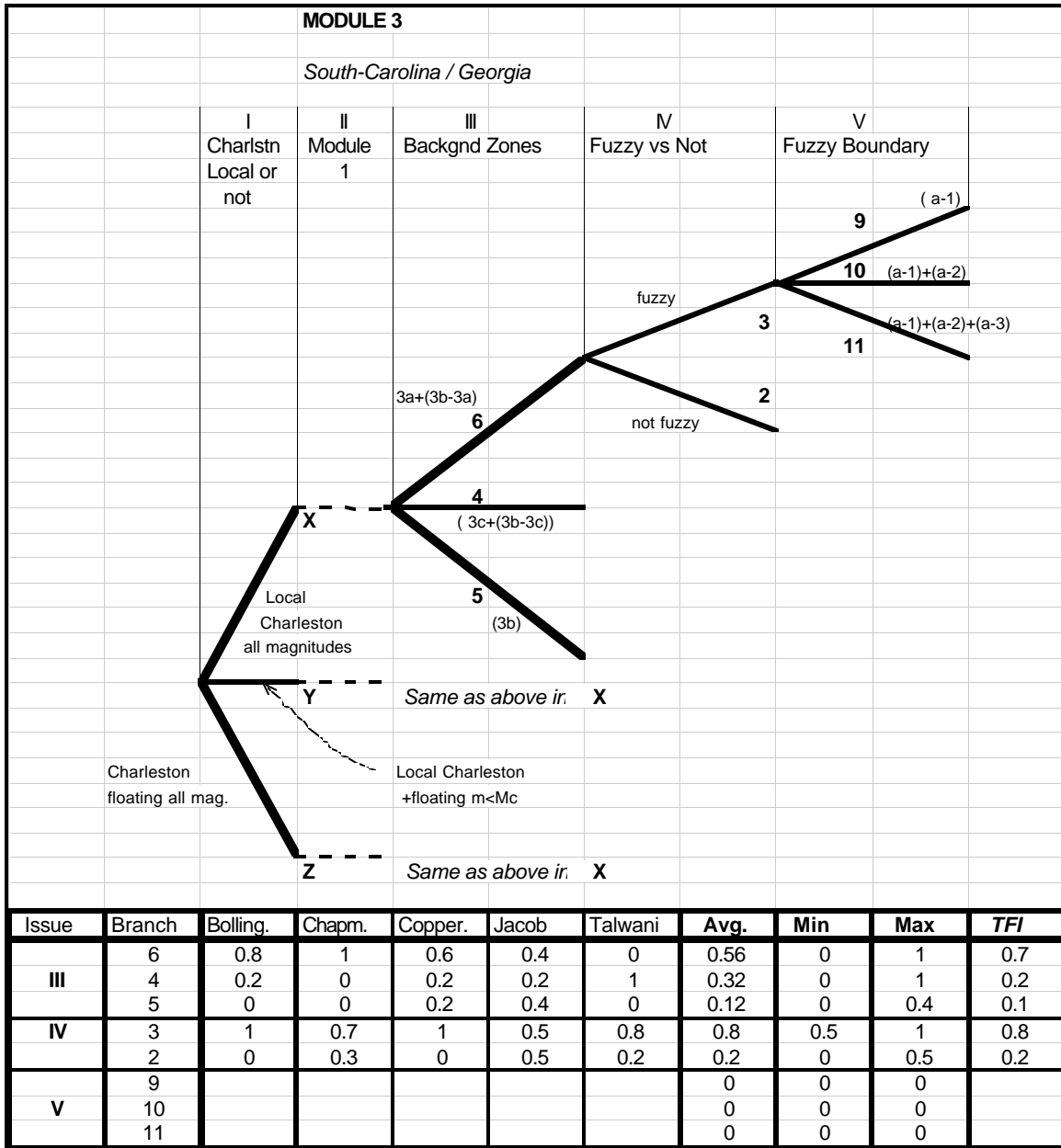


Figure 4.2.6-2C(a) Logic Tree Representation of Experts' Interpretations for Module 3: South Carolina-Georgia Issue.

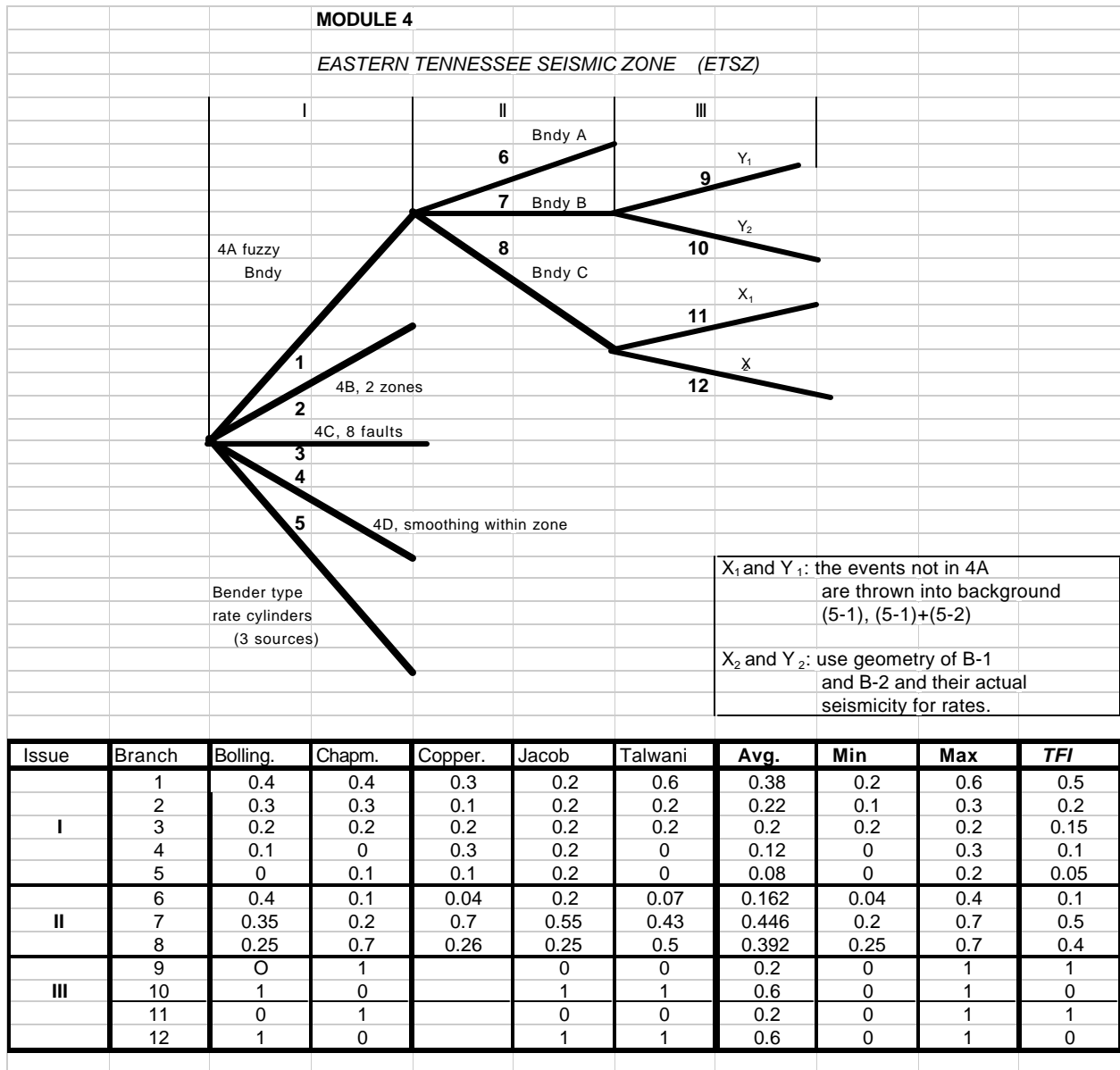


Figure 4.2.6-2C(b) Logic Tree Representation of Experts' Interpretations for Module 4: Eastern Tennessee Seismic Zone Issue.

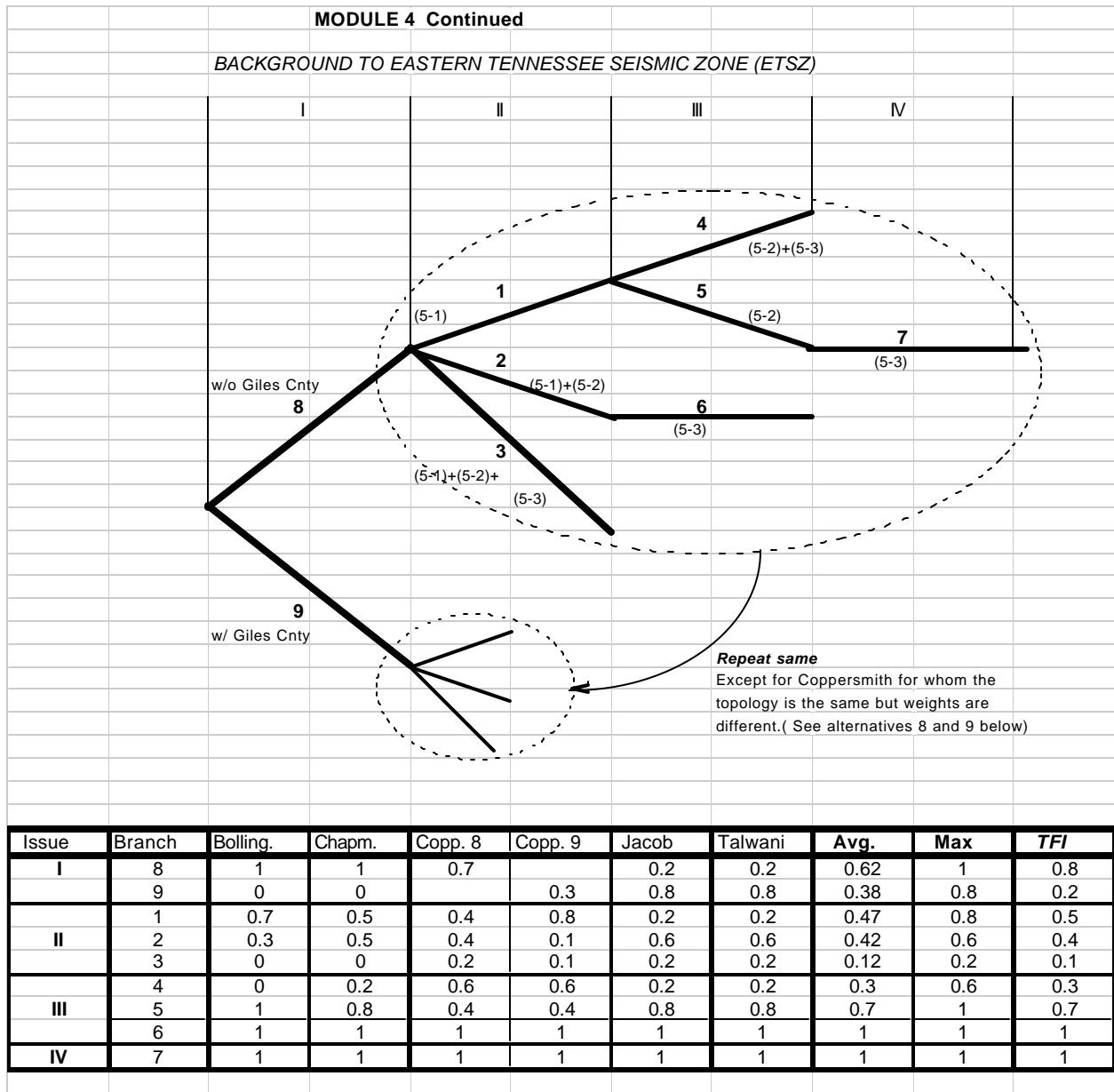
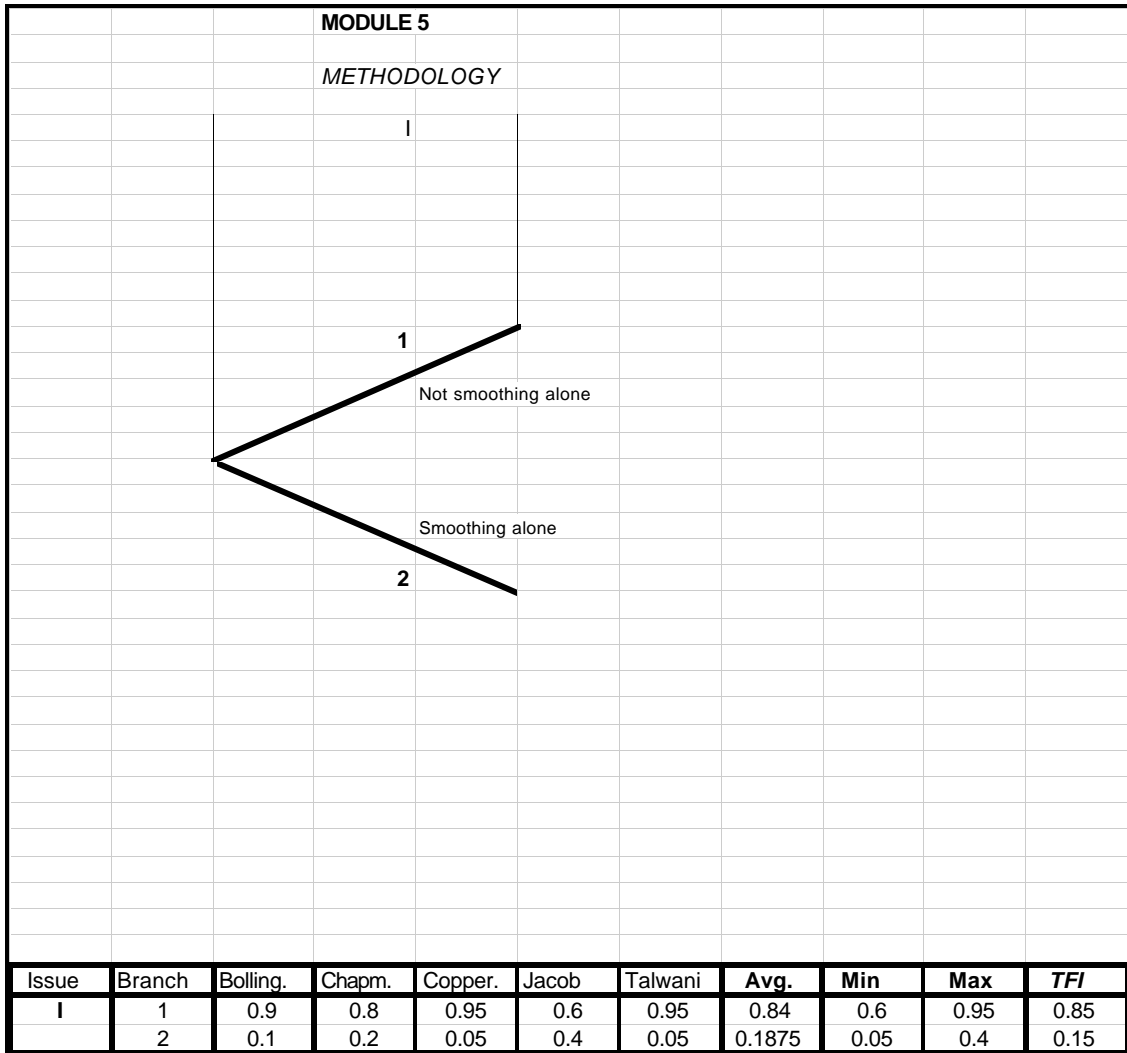


Figure 4.2.6-2C(b) (cont'd) Logic Tree Representation of Experts' Interpretations for Module 4: Eastern Tennessee Seismic Zone Issue.



**Figure 4.2.6-2D Logic Tree Representation of Experts' Interpretations for
Module 5: Seismicity Rate Estimation Methodology.**

F at M1; ZONE 3a

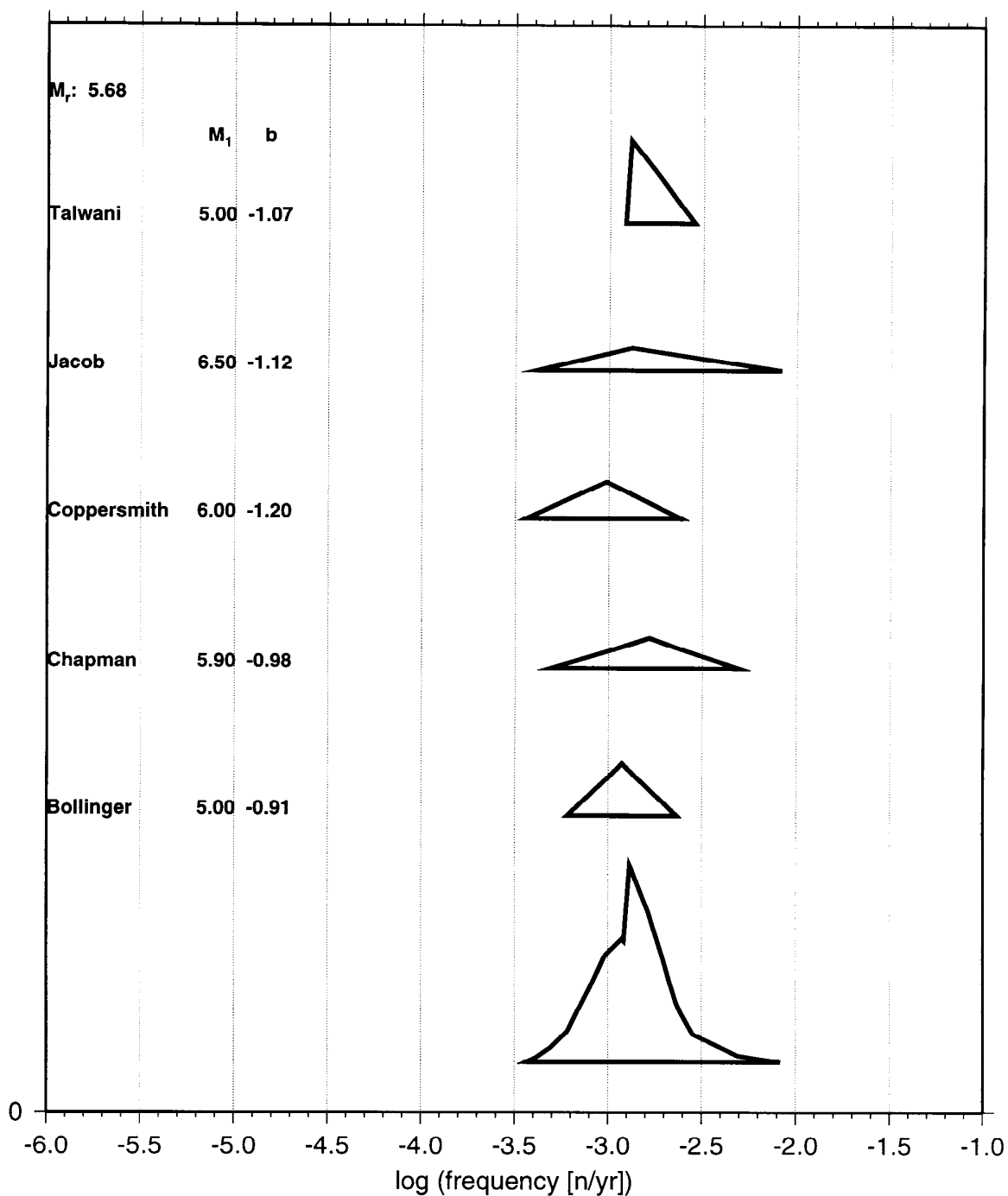


Figure 4.2.6-3 Example of Rates of Probability Distribution for One Zone, and Integration Into a Composite Probability Distribution.

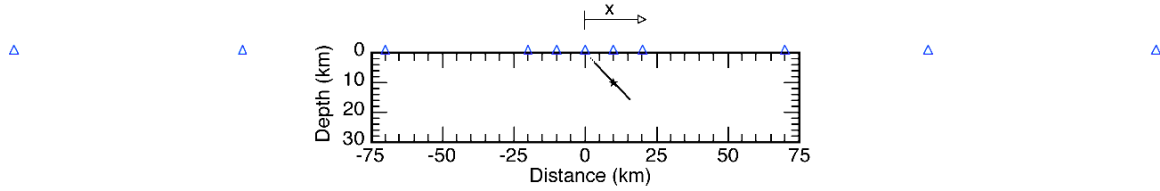
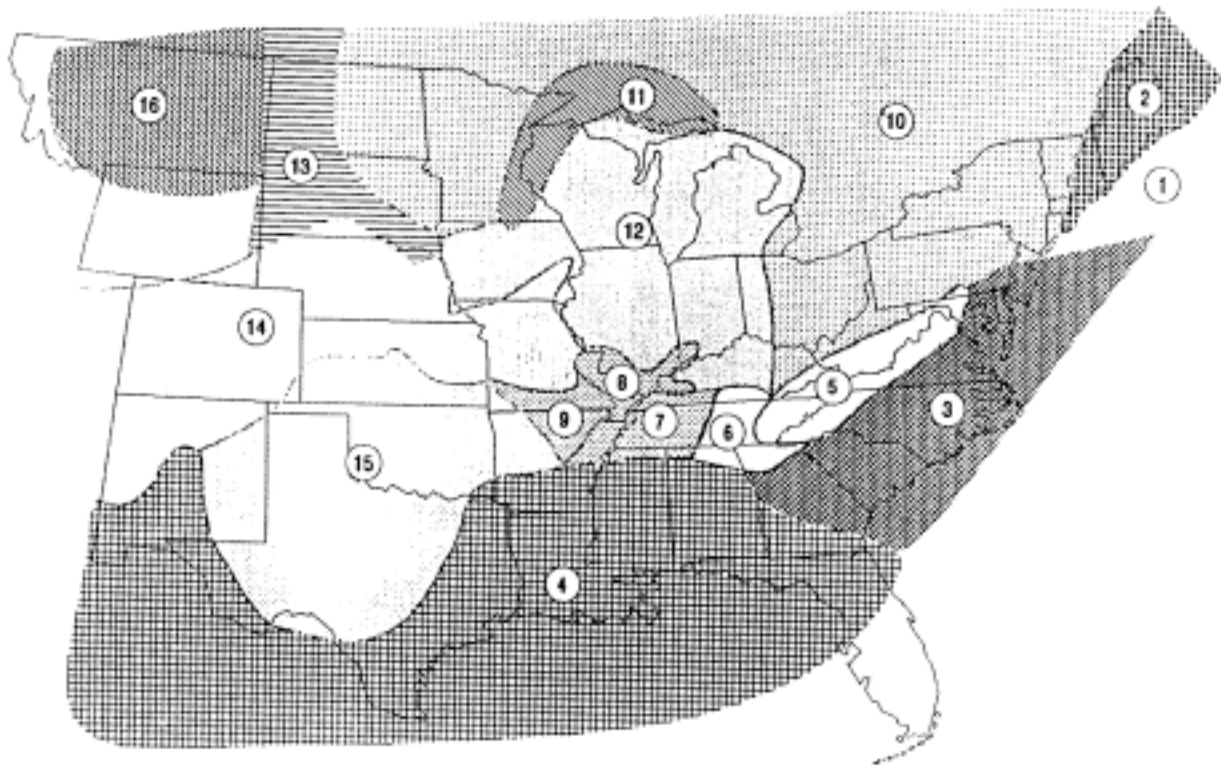


Figure 4.3.3-1 Definition of Observation Points for Ground Motion Estimates.



Legend: 1. Offshore New England, 2. Northern Appalachians, 3. Atlantic Coastal Plain, 4. Gulf Coast Plain, 5. Southern Appalachians, 6. Central Tennessee, 7. Western Tennessee, 8. New Madrid Rift, 9. Ozarks, 10. Northern Grenville-Superior, 11. Lake Superior Basin, 12. Mid-continent, 13. Northern Great Plains, 14. Central Plains, 15. Southern Great Plains, 16. Williston Basin

Figure 4.3.3-2 Crustal Structure Regionalization for the EUS.

(Woodward-Clyde 1991)

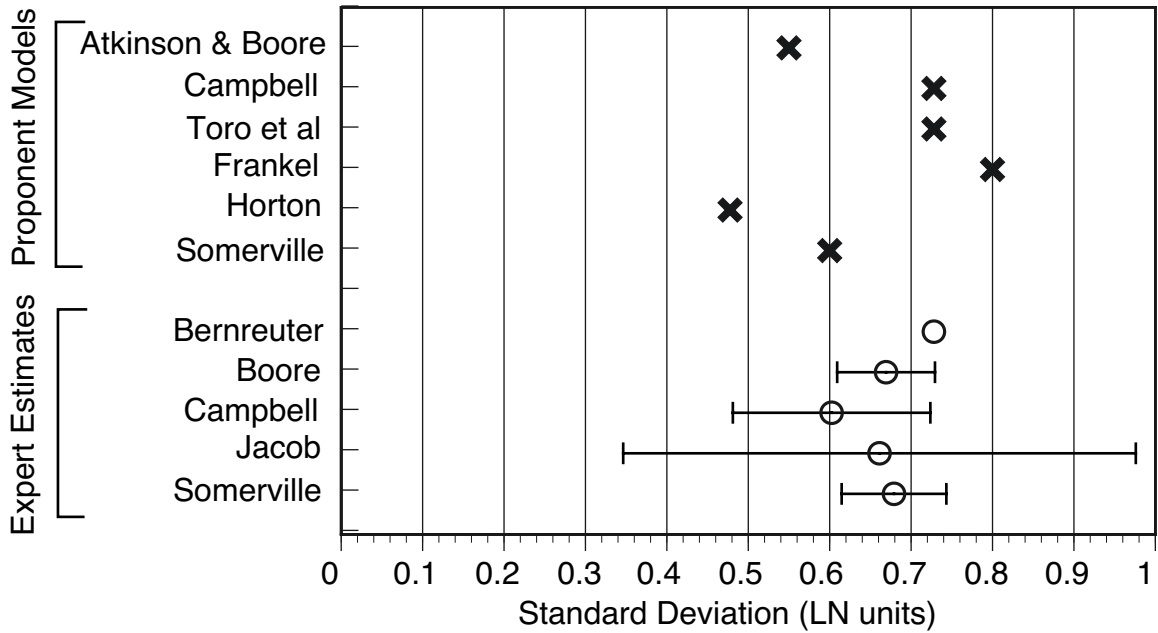
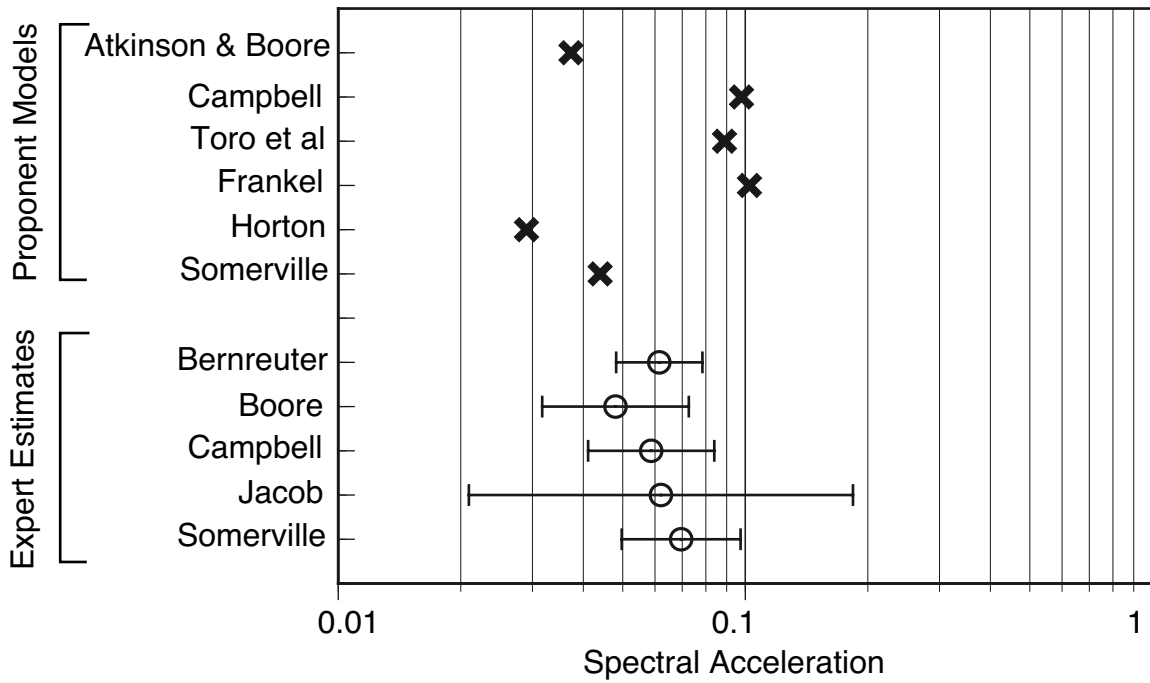


Figure 4.3.3-3 Example of Material Given to the Experts for the Seismic Rate Estimates.

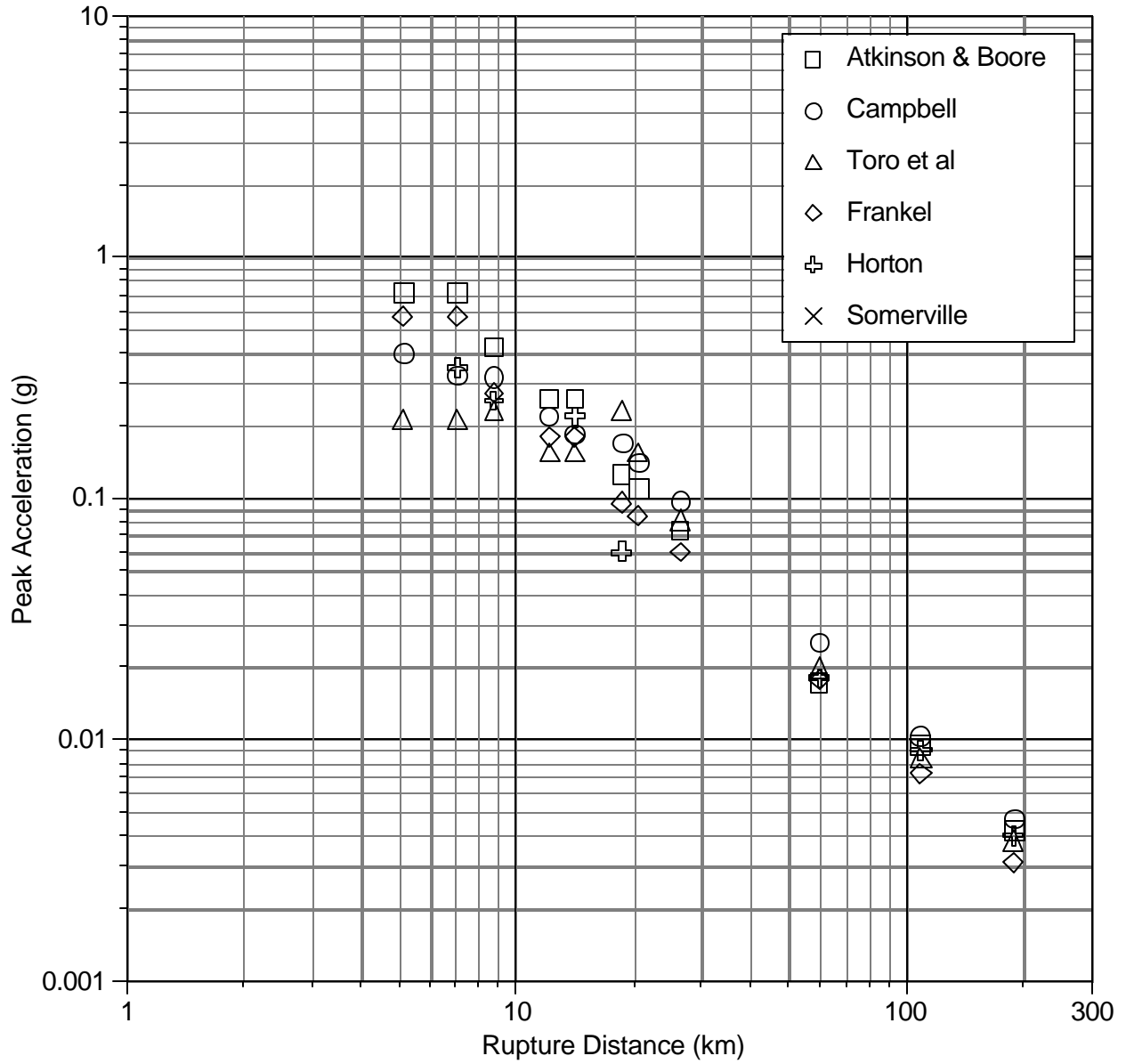


Figure 4.3.3-4a Examples of Proponents Models Median Estimates of the Peak Ground Acceleration for $M_w 5$.

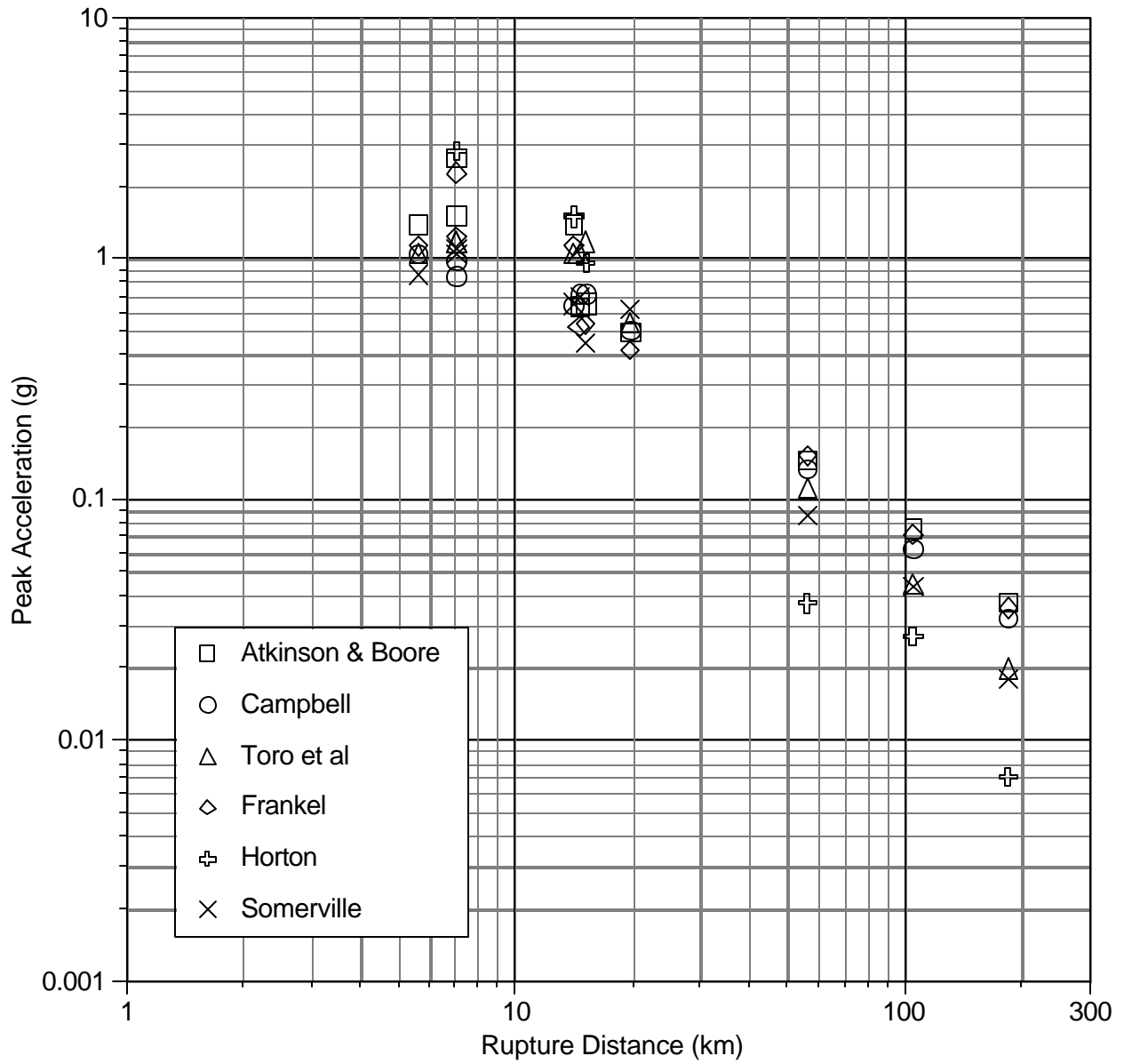


Figure 4.3.3-4b Examples of Proponents Models Median Estimates of the Peak Ground Acceleration for $M_w 7$.

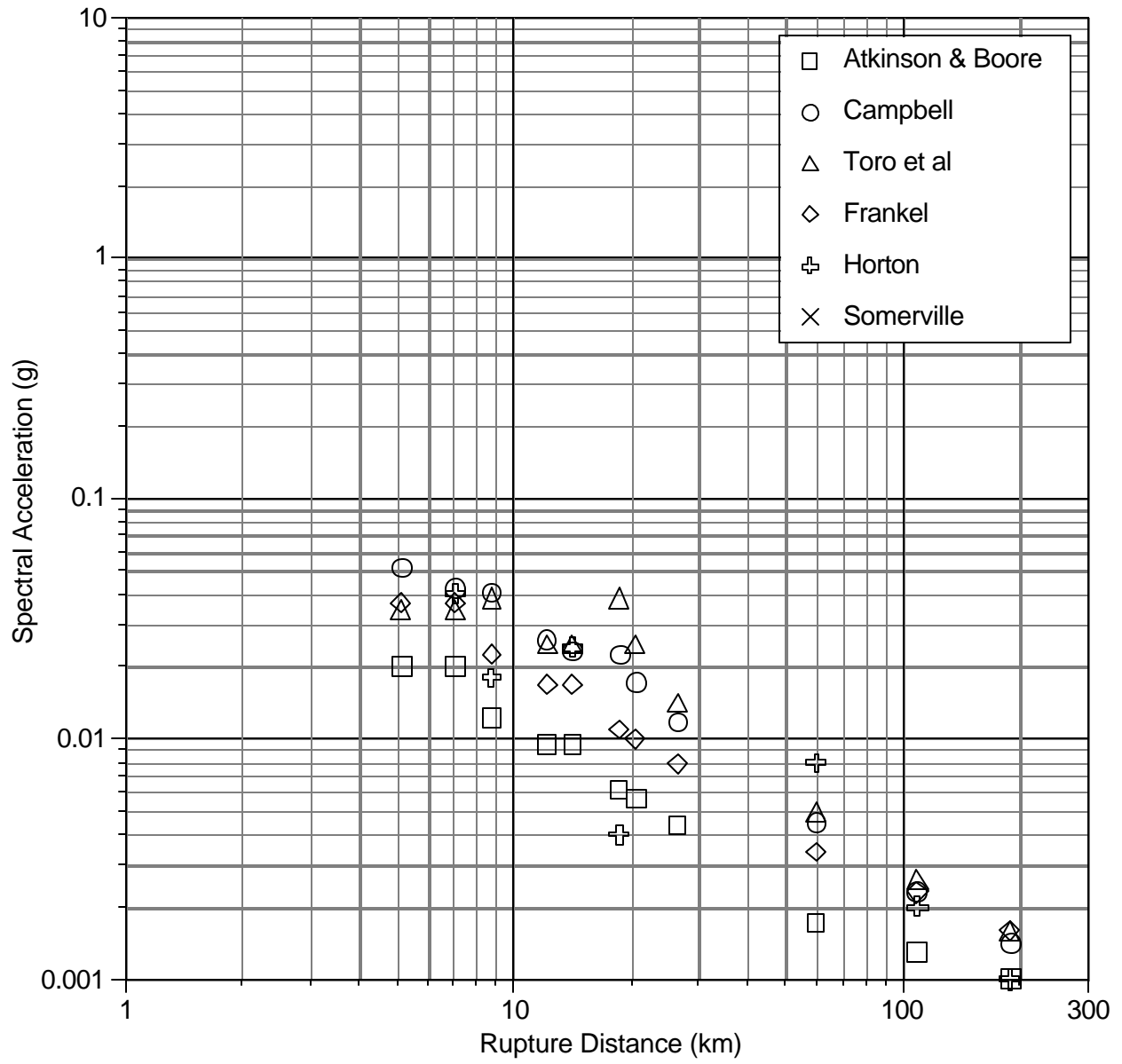


Figure 4.3.3-5a Examples of Proponents Models Median Estimates of the 1-Second Period Spectral Acceleration for $M_w 5$.

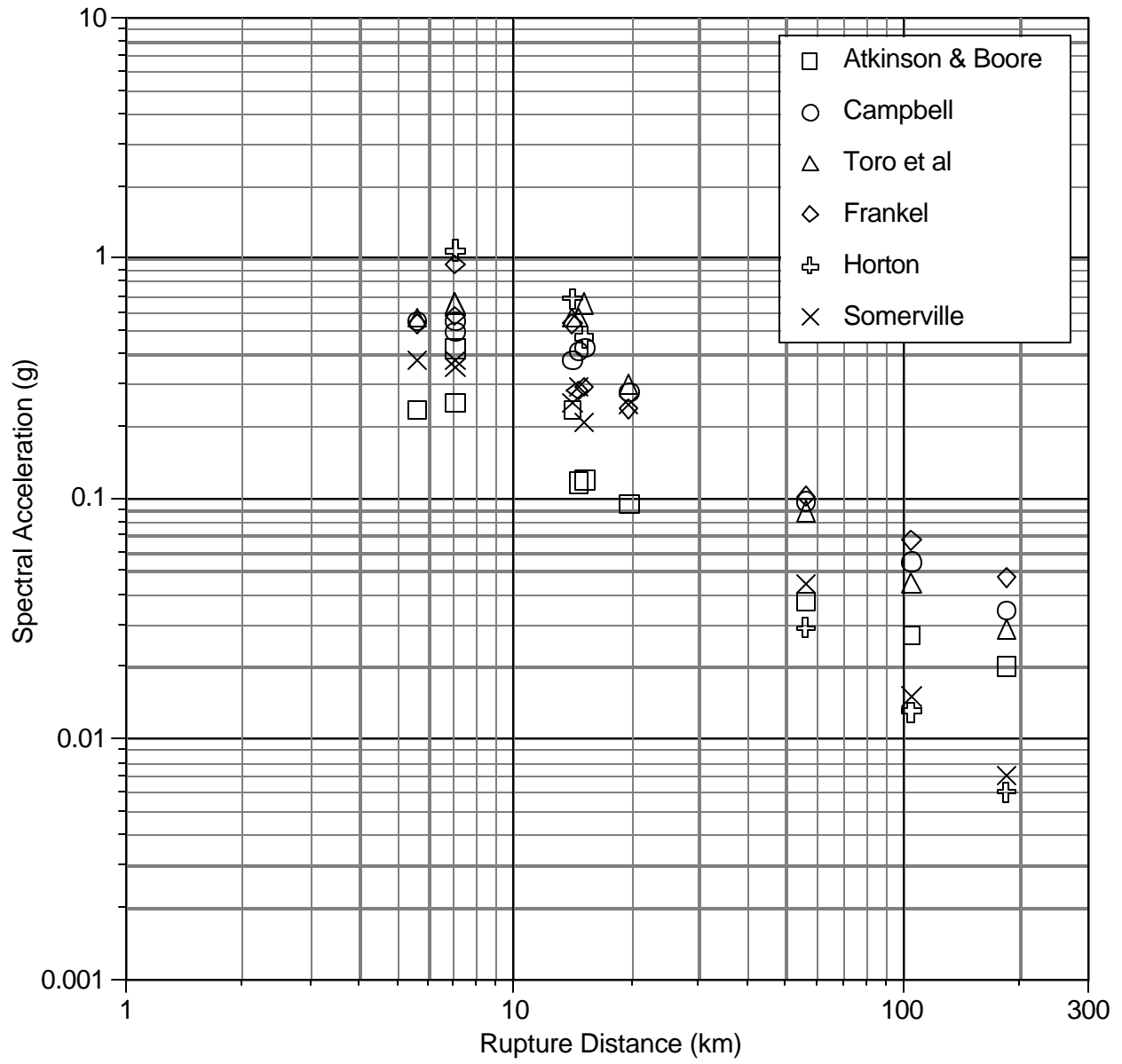


Figure 4.3.3-5b Example of Proponents Model Median Estimates of the 1-Second Period Spectral Acceleration for $M_w 7$.

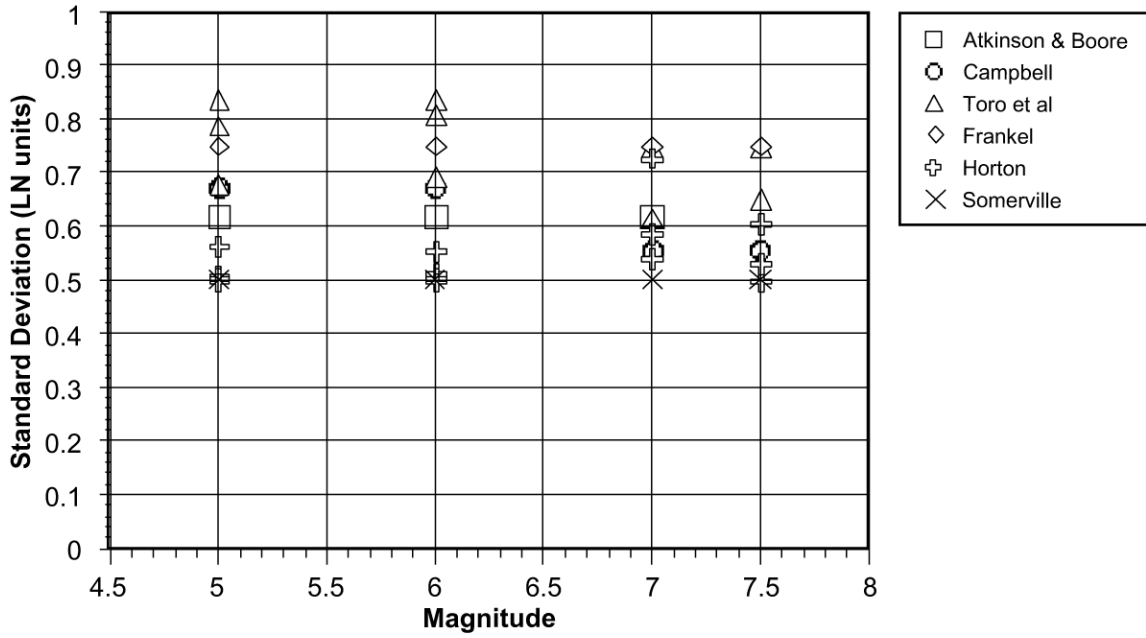


Figure 4.3.3-6a Examples of Proponents Estimates of the Aleatory Variability for the Peak Ground Acceleration Estimates.

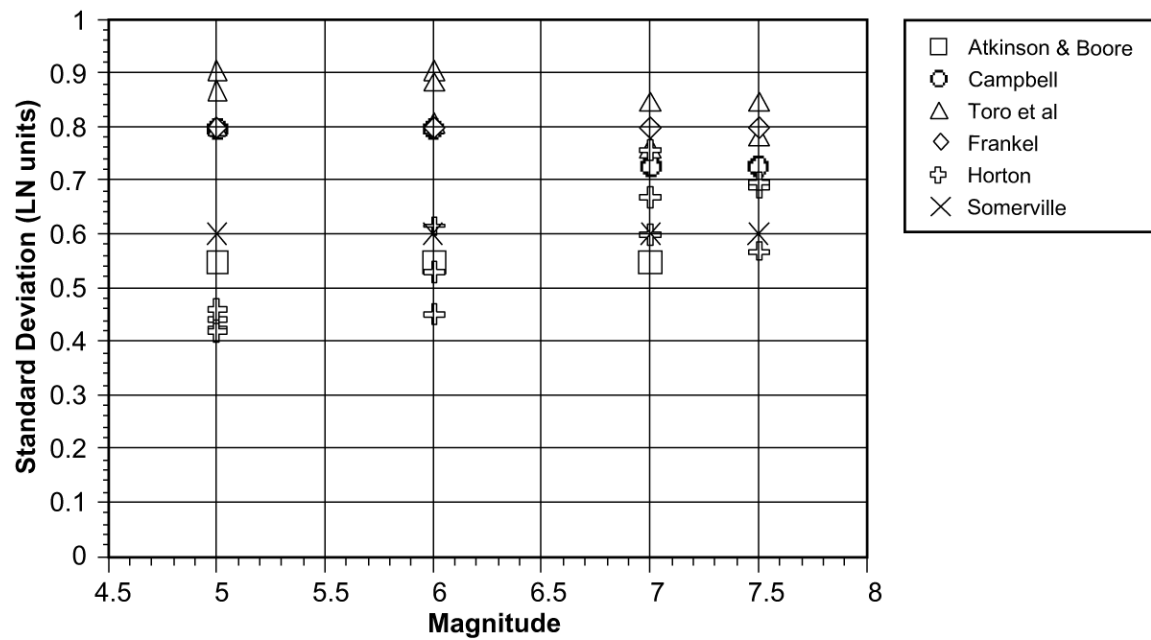


Figure 4.3.3-6b Examples of Proponents Estimates of the Aleatory Variability for the Peak Ground Acceleration Estimates.

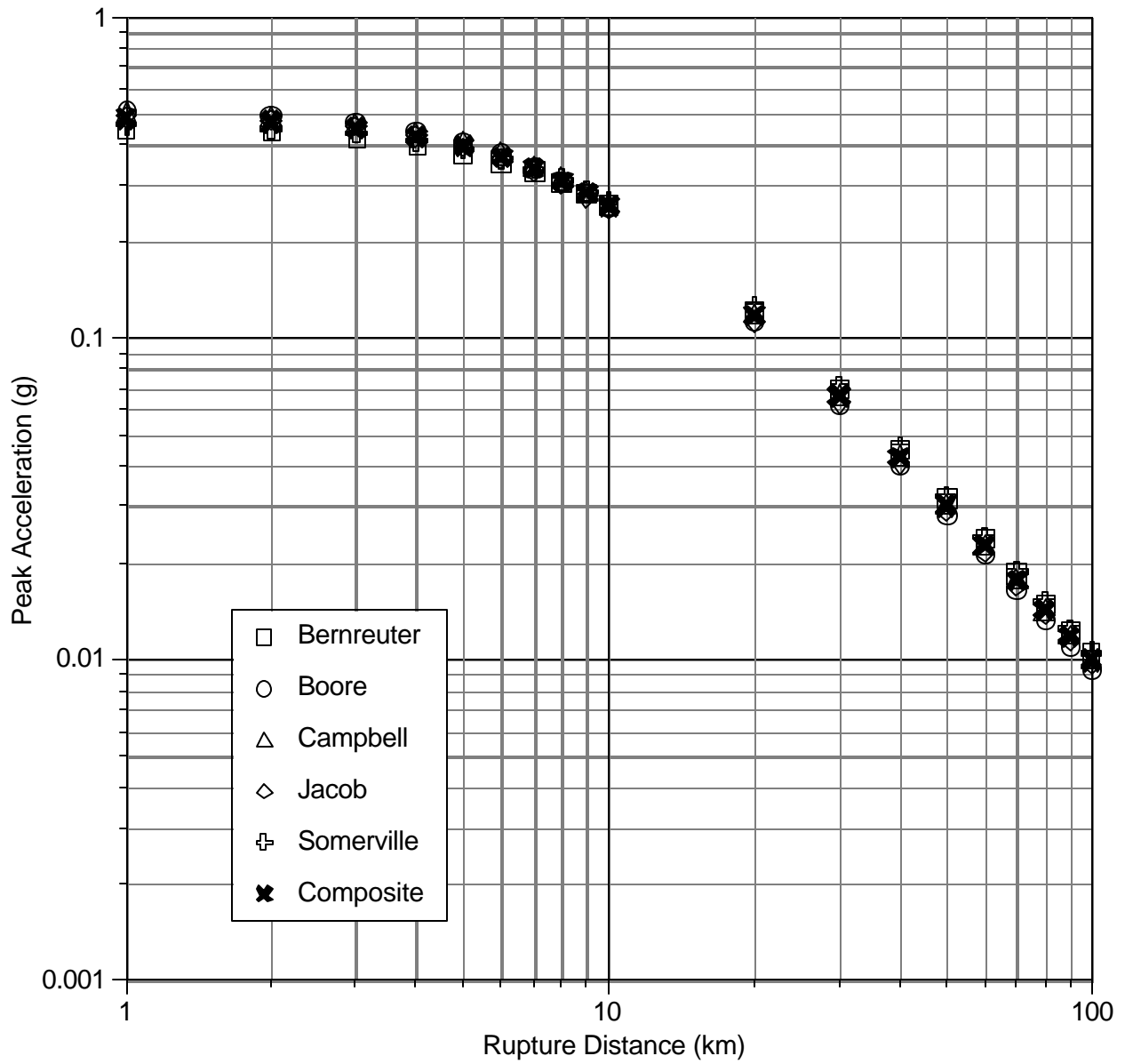


Figure 4.3.4-1 Comparison of Regression Model Fits for the 5 Experts of the Study and the Composite Model, for the Horizontal Component Median Peak Ground Acceleration for Magnitude M_w 7.

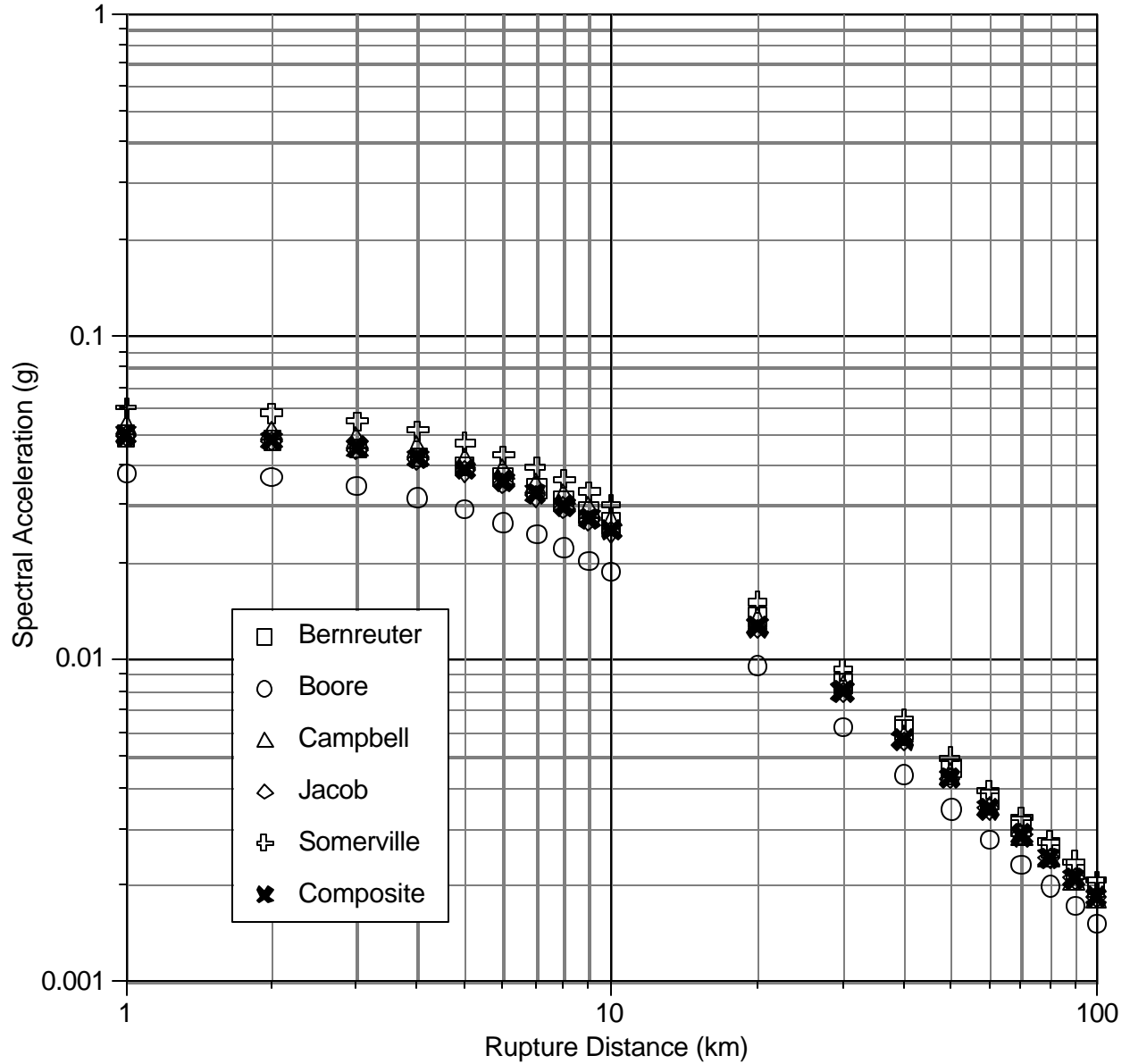


Figure 4.3.4-2 Comparison of Regression Model Fits for the 5 Experts of the Study and the Composite Model, for the Horizontal Component Median Peak Ground Acceleration for Magnitude M_w 5.

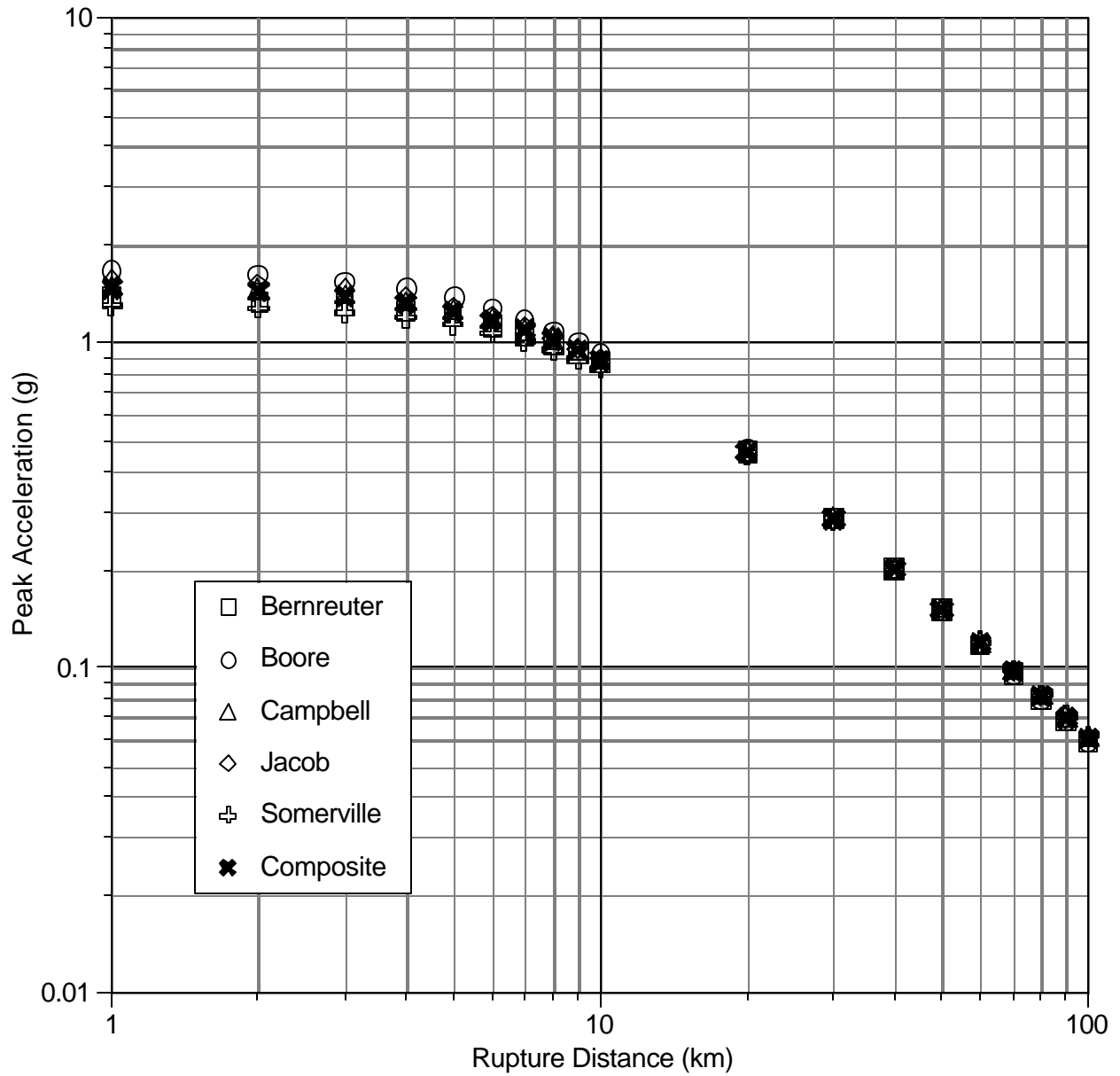


Figure 4.3.4-3 Comparison of Regression Model Fits for the 5 Experts and for the Composite Model, for the Horizontal Component Median 1-Second Period Spectral Acceleration for Magnitude M_w 7.

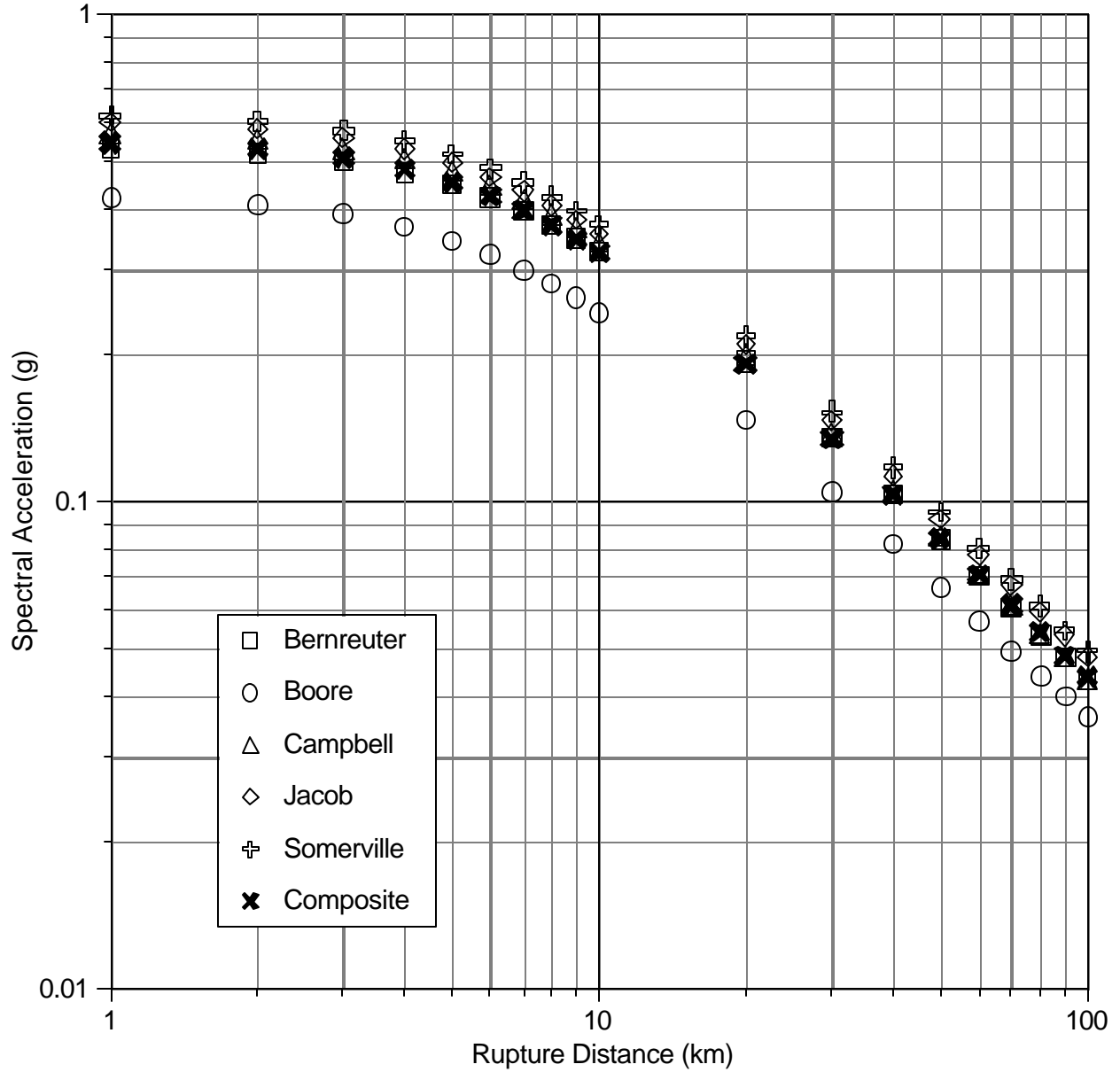


Figure 4.3.4-4 Comparison of Regression Model Fits for the 5 Experts and for the Composite Model, for the Horizontal Component Median 1-Second Period Spectral Acceleration for Magnitude $M_w 5$.

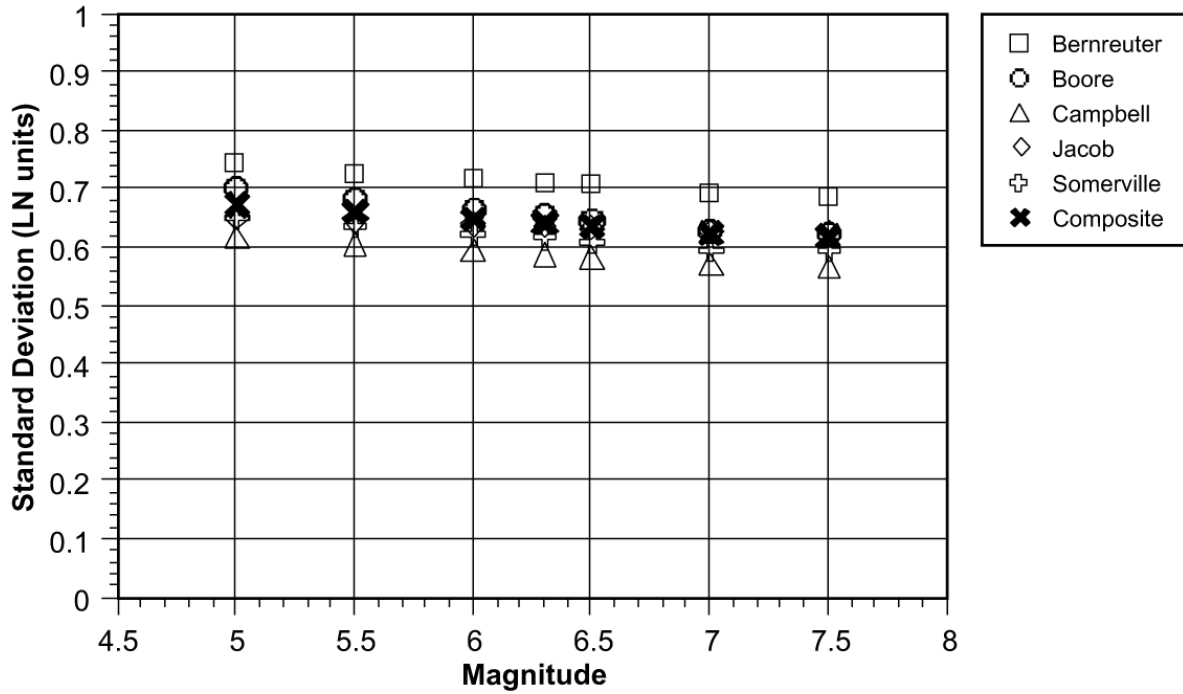


Figure 4.3.4-5 Comparison of the Models of Aleatory Variability for the Horizontal Component of the Peak Acceleration.

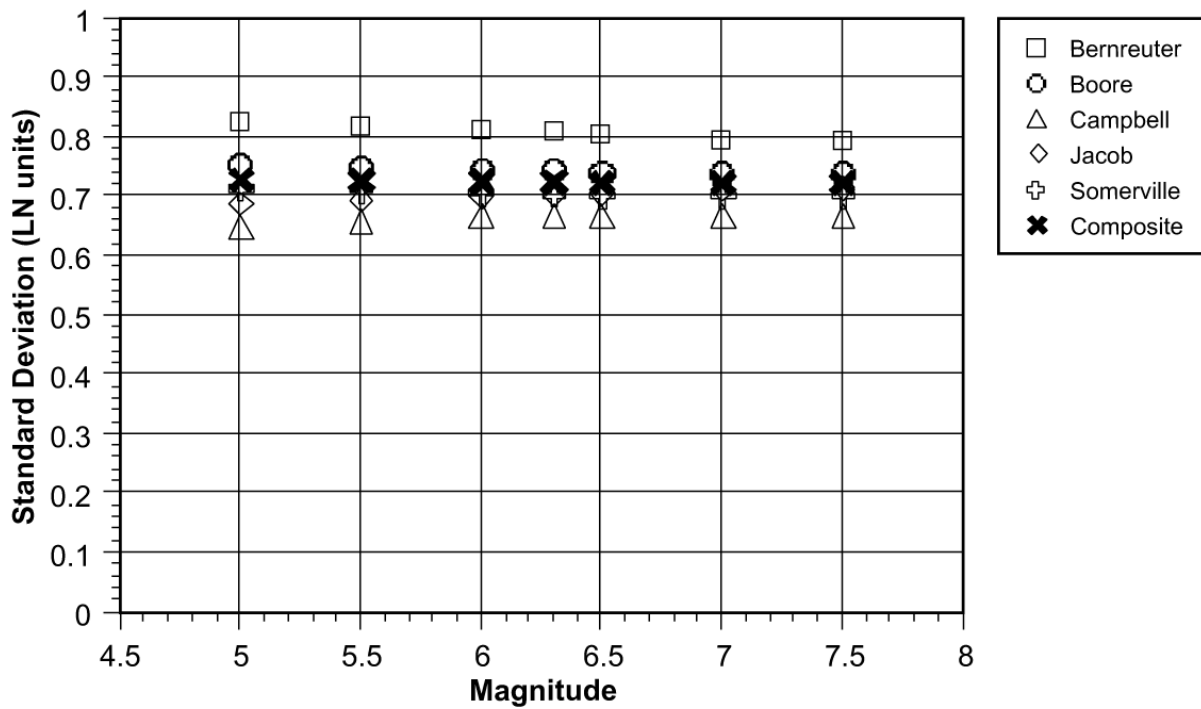


Figure 4.3.4-6 Comparison of the Models of Aleatory Variability for the Horizontal Component of the 1-Second Period Spectral Acceleration.

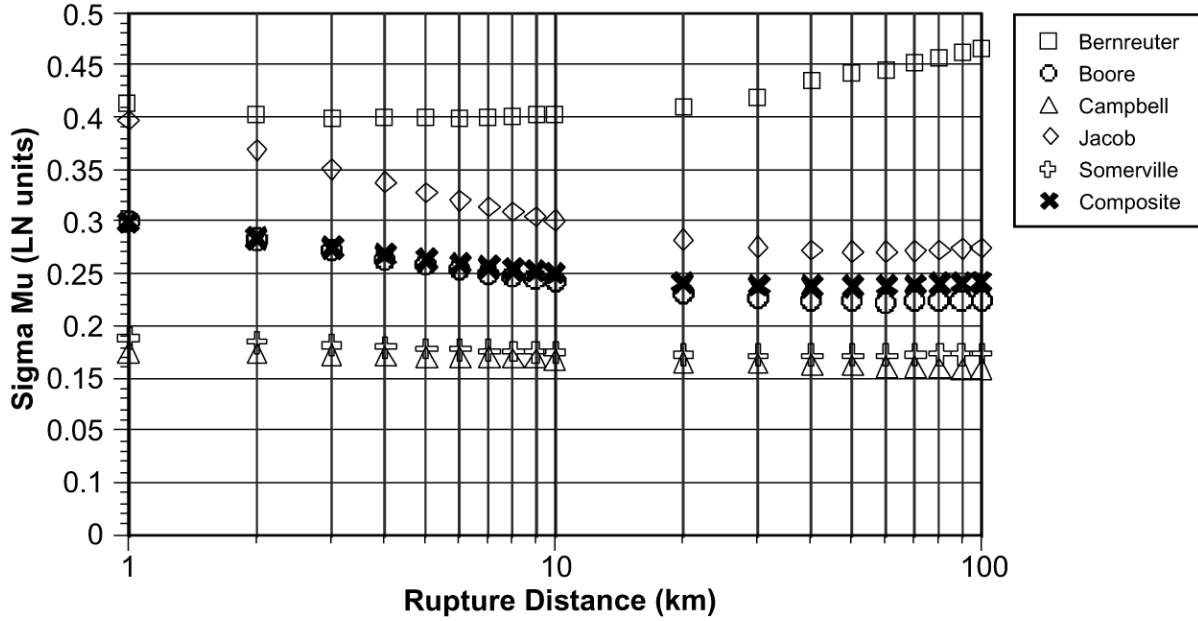


Figure 4.3.4-7 Comparison of the Models of the Epistemic Variability for the Median Estimates of the Horizontal Component of the Peak Ground Acceleration for Magnitude M_w5 .

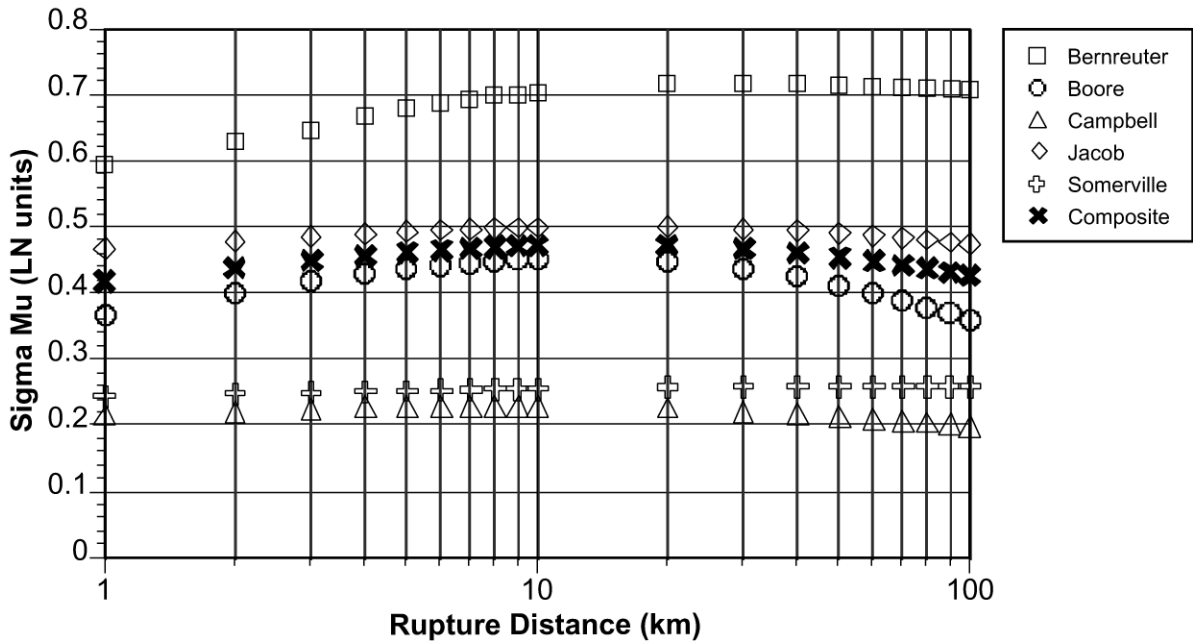


Figure 4.3.4-8 Comparison of the Models of the Epistemic Variability for Median Estimates of the Horizontal Component for the 1-Second Period Spectral Acceleration for Magnitude M_w5 .

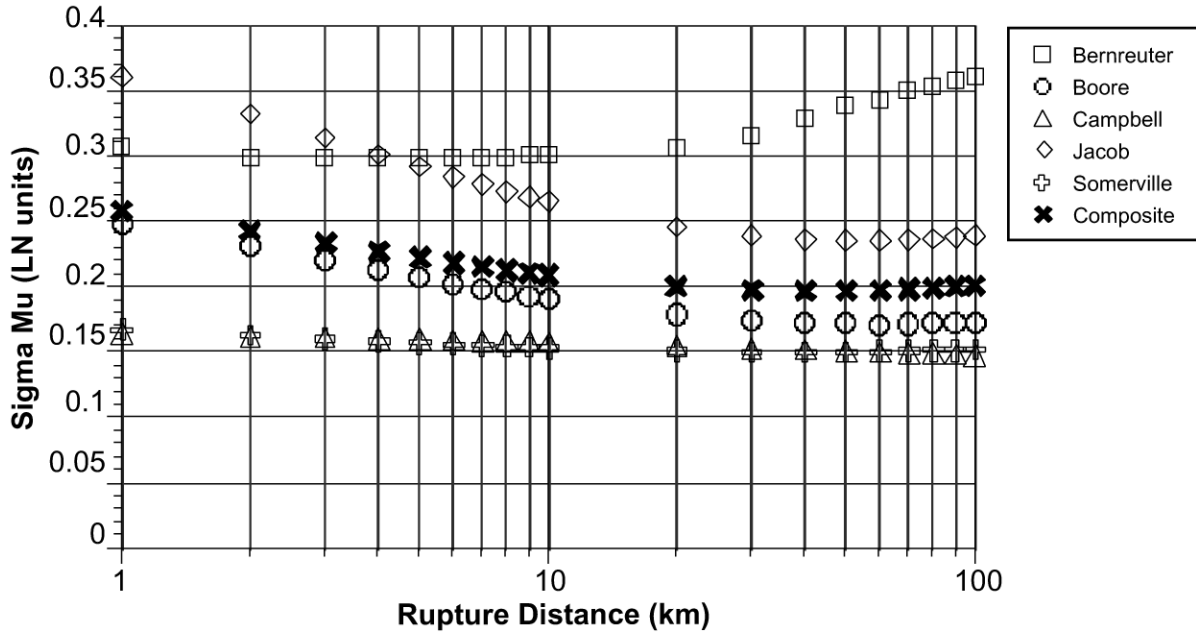


Figure 4.3.4-9 Comparison of the Models of the Epistemic Variability for the Median Estimates of the Horizontal Component of the Peak Ground Acceleration for Magnitude M_w7 .

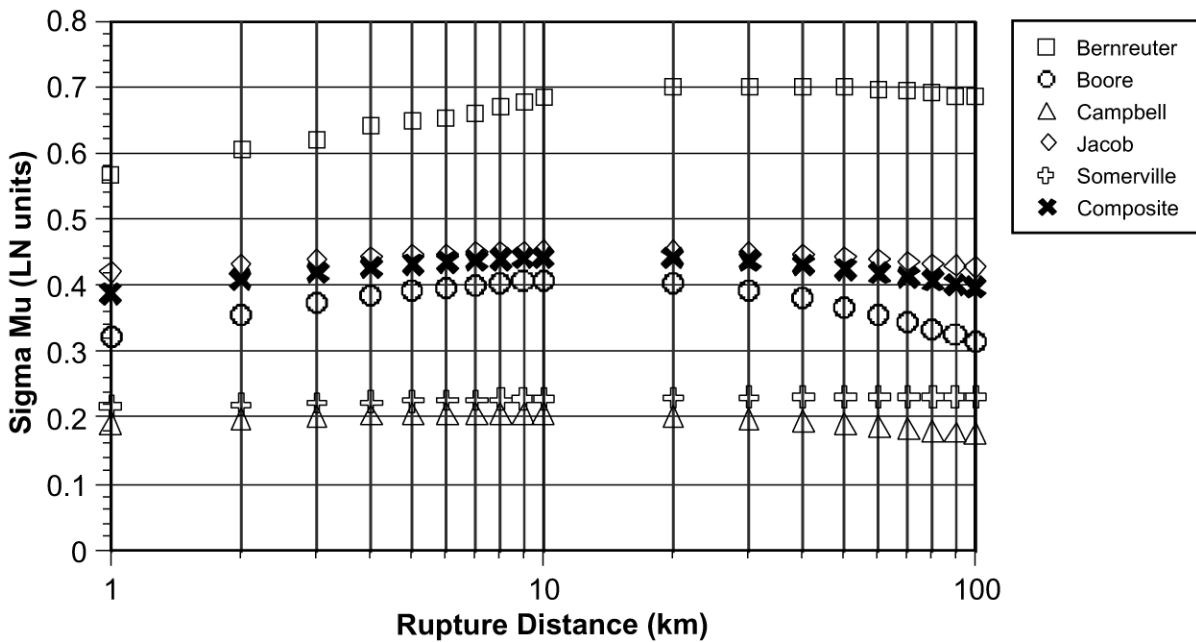


Figure 4.3.4-10 Comparison of the Models of the Epistemic Variability for Median Estimates of the Horizontal Component for the 1-Second Period Spectral Acceleration for Magnitude M_w7 .

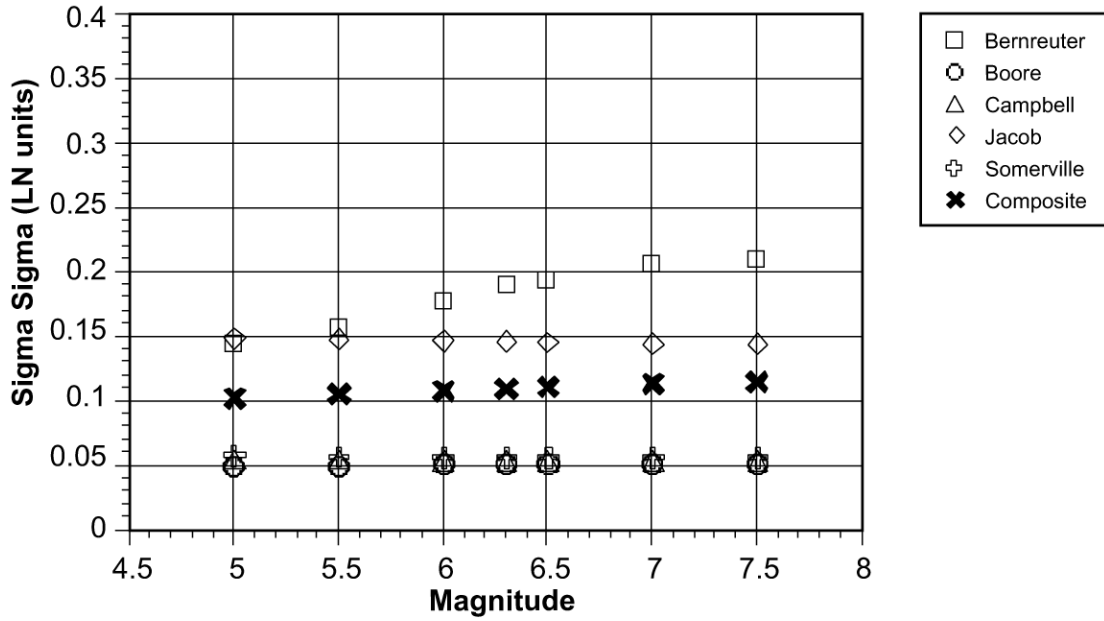


Figure 4.3.4-11 Comparison of the Models for the Epistemic Variability for the Median Estimates of Peak Ground Acceleration.

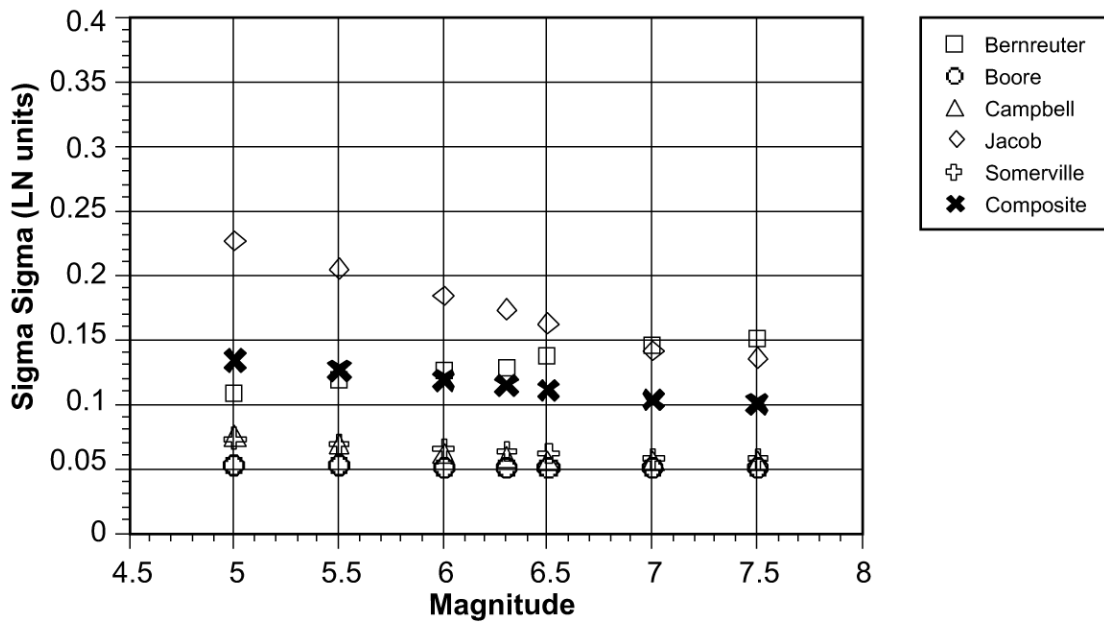


Figure 4.3.4-12 Comparison of the Models for the Epistemic Variability for the Median Estimates of the 1-Second Period Spectral Acceleration.

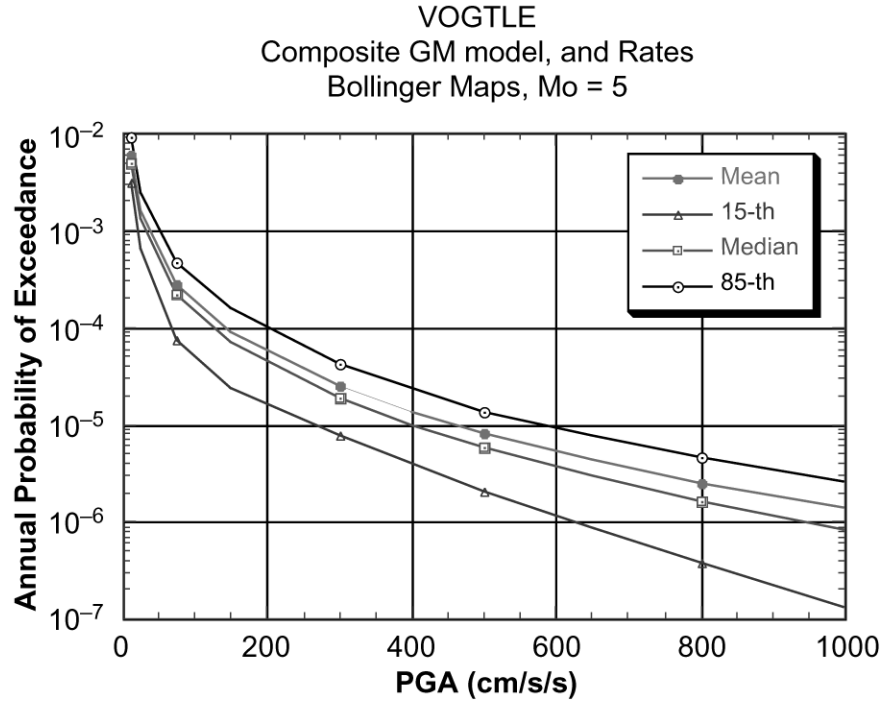


Figure 4.4-1 Probabilistic Hazard Estimates for Vogtle. PGA for Bollinger’s Zonation Maps and Seismicity Rates, and Composite Ground Motion Model.

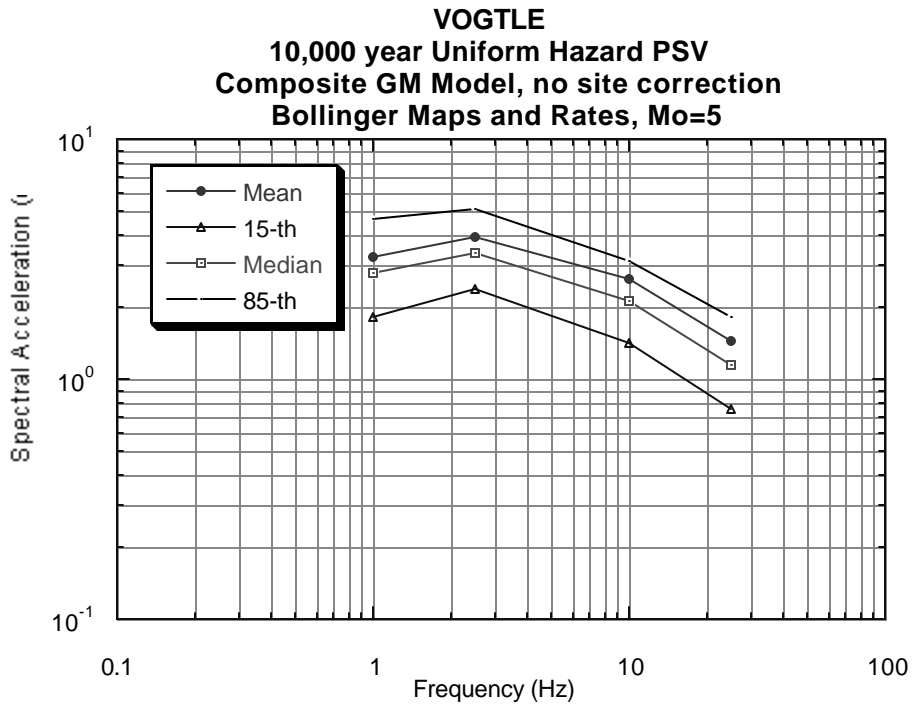


Figure 4.4-2 Probabilistic Hazard Estimates for Vogtle. Uniform Hazard Spectra for Bollinger’s Zonation Maps and Seismicity Rates, and Composite Ground Motion Model.

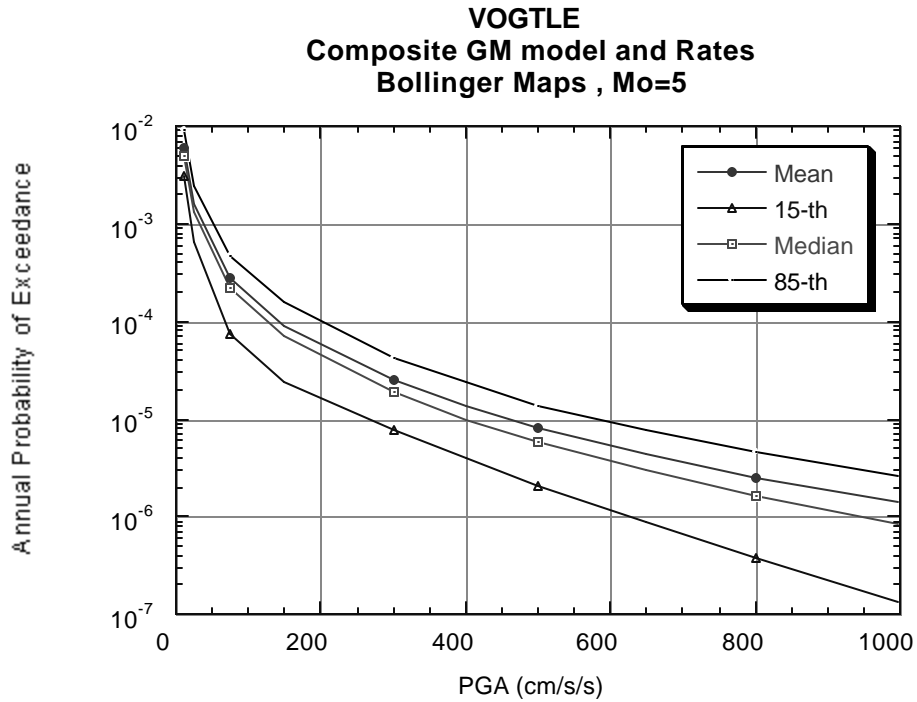


Figure 4.4-3 Probabilistic Hazard Estimates for Vogtle. PGA for Bollinger’s Zonation Maps, Composite Seismicity Rates, and Composite Ground Motion Model.

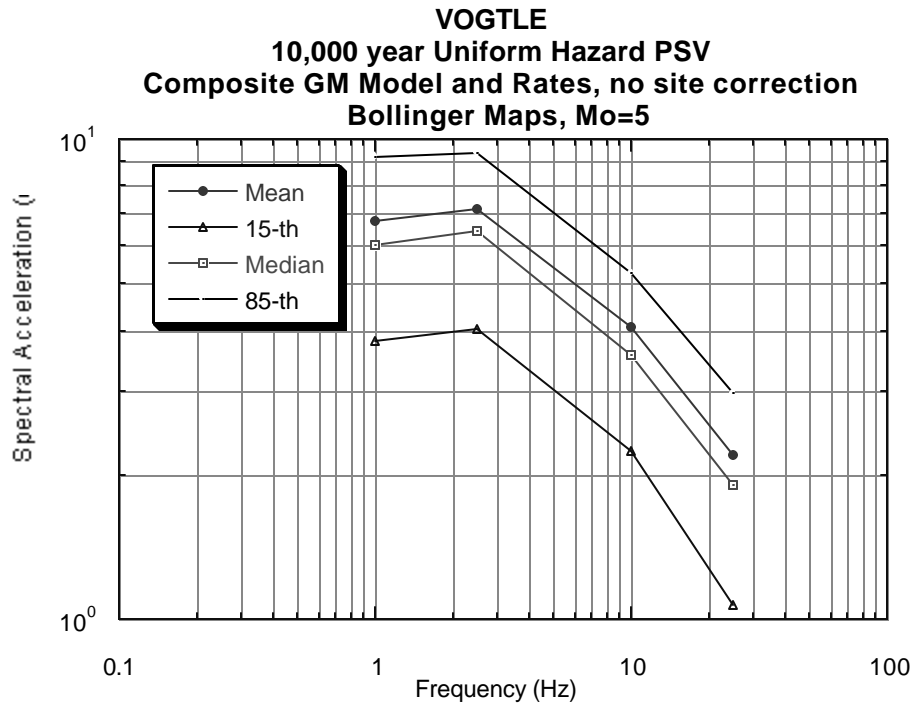


Figure 4.4-4 Probabilistic Hazard Estimates for Vogtle. Uniform Hazard Spectra for Bollinger’s Zonation Maps and Composite Seismicity Rates, and Composite Ground Motion Model.

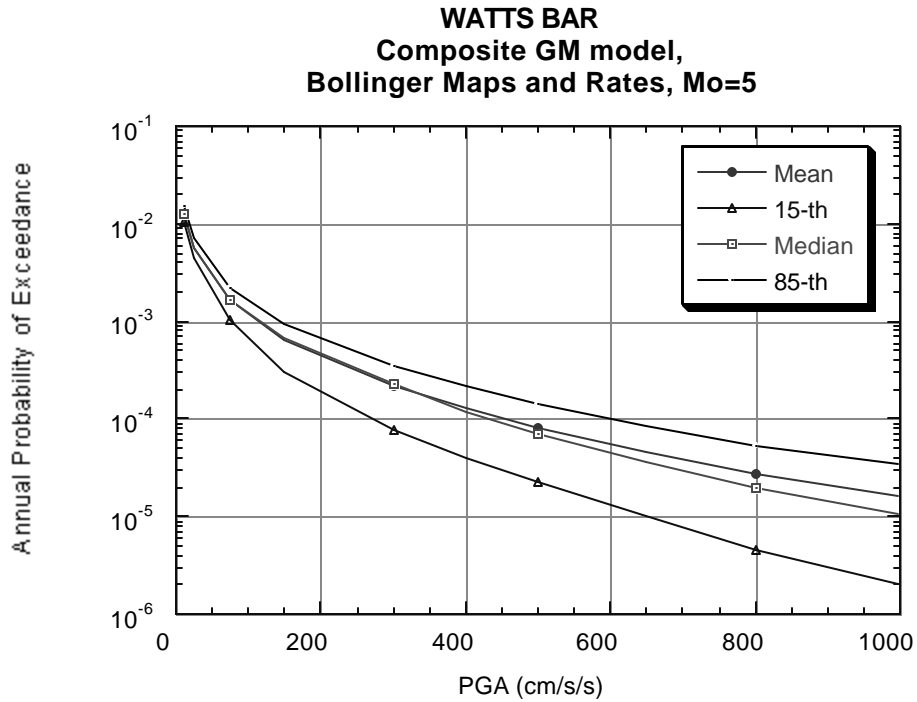


Figure 4.4-5 Probabilistic Hazard Estimates for Watts Bar. PGA for Bollinger’s Zonation Maps and Seismicity Rates, and Composite Ground Motion Model.

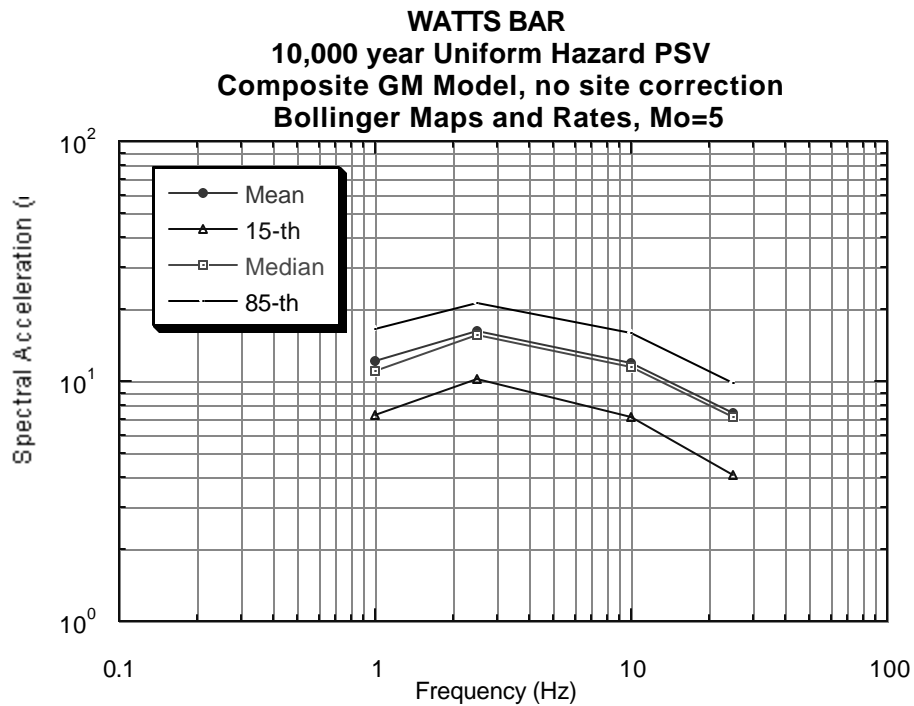


Figure 4.4-6 Probabilistic Hazard Estimates for Watts Bar. Bollinger’s Zonation Maps and Seismicity Rates, and Composite Ground Motion Model.

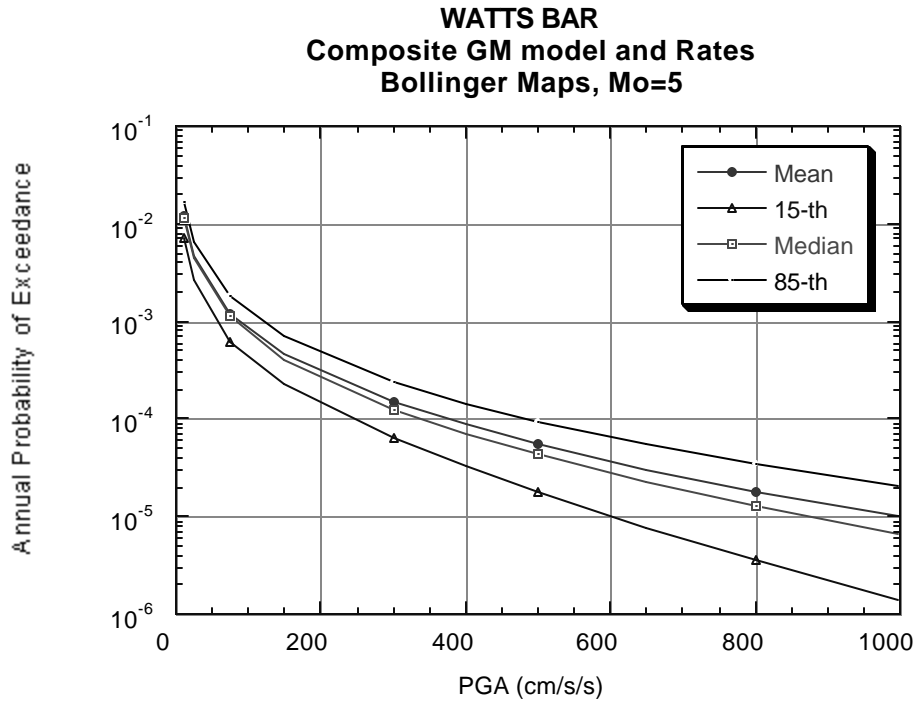


Figure 4.4-7 Probabilistic Hazard Estimates for Watts Bar. PGA for Bollinger’s Zonation Maps, Composite Seismicity Rates, and Composite Ground Motion Model.

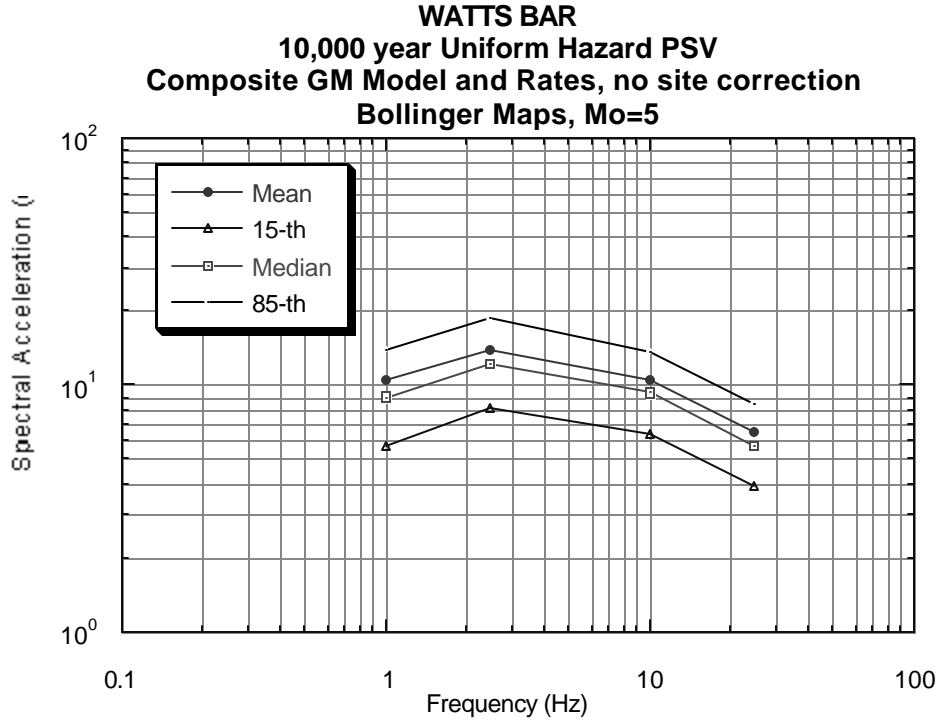


Figure 4.4-8 Probabilistic Hazard Estimates for Vogtle. Uniform Hazard Spectra for Bollinger’s Zonation Maps, Composite Seismicity Rates, and Composite Ground Motion Model.

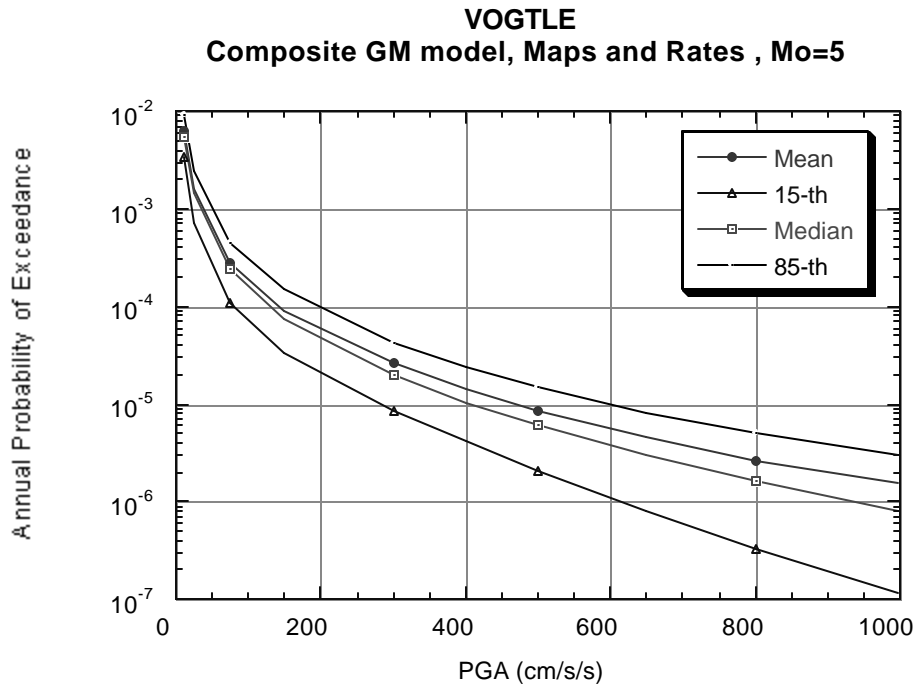


Figure 4.4-9 Probabilistic Hazard Estimates for Vogtle. PGA for Composite Models of Zonation Maps, Seismicity Rates, and Ground Motion Attenuation.

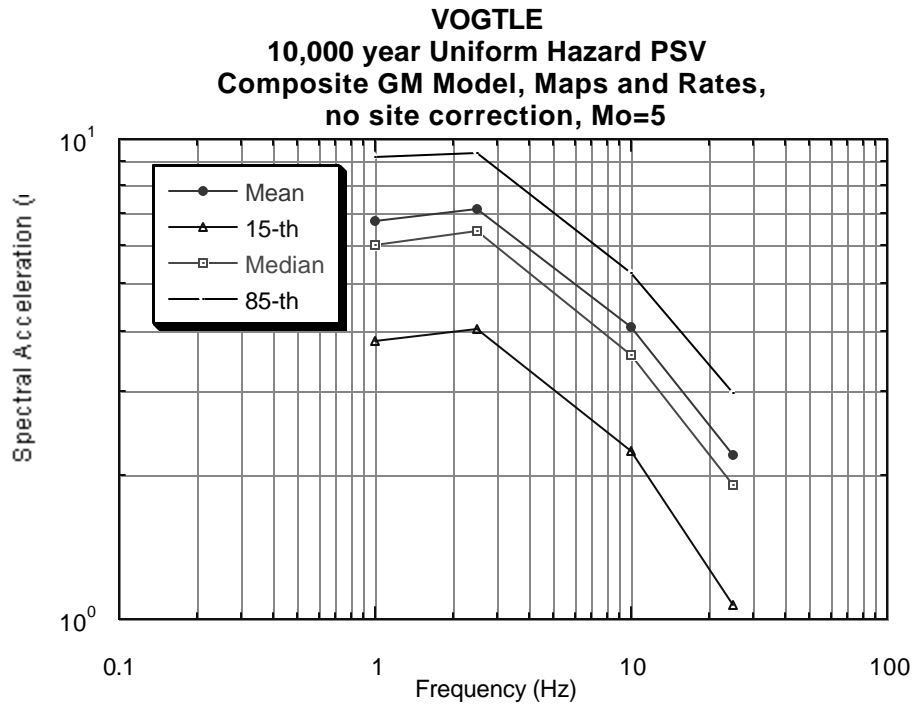


Figure 4.4-10 Probabilistic Hazard Estimates for Vogtle. Uniform Hazard Spectra for Composite Models of Zonation Maps, Seismicity Rates, and Ground Motion Attenuation.

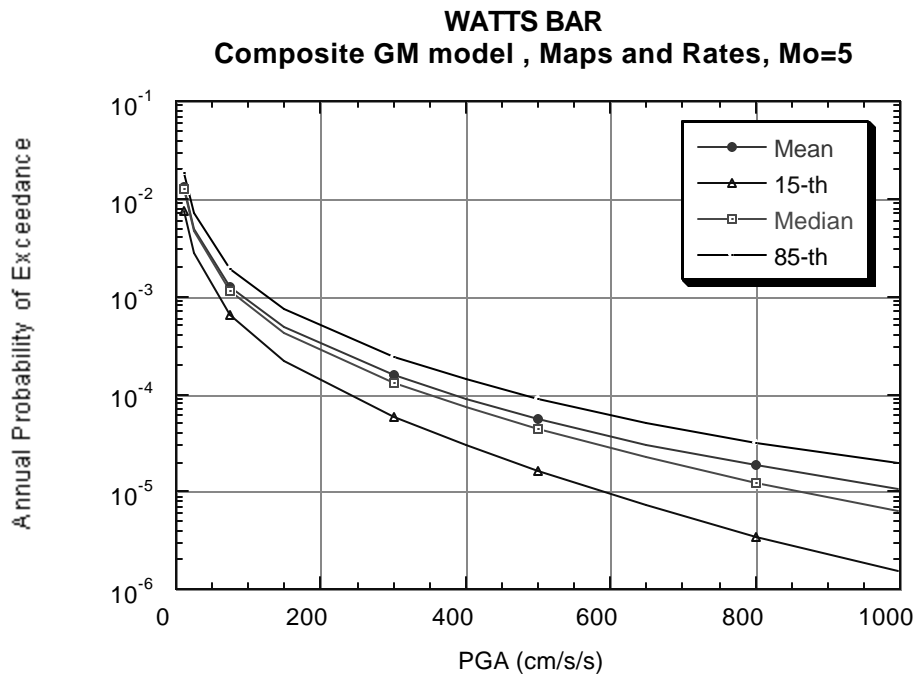


Figure 4.4-11 Probabilistic Hazard Estimates for Watts Bar. PGA for Composite Models of Zonation Maps, Seismicity Rates, and Ground Motion Attenuation.

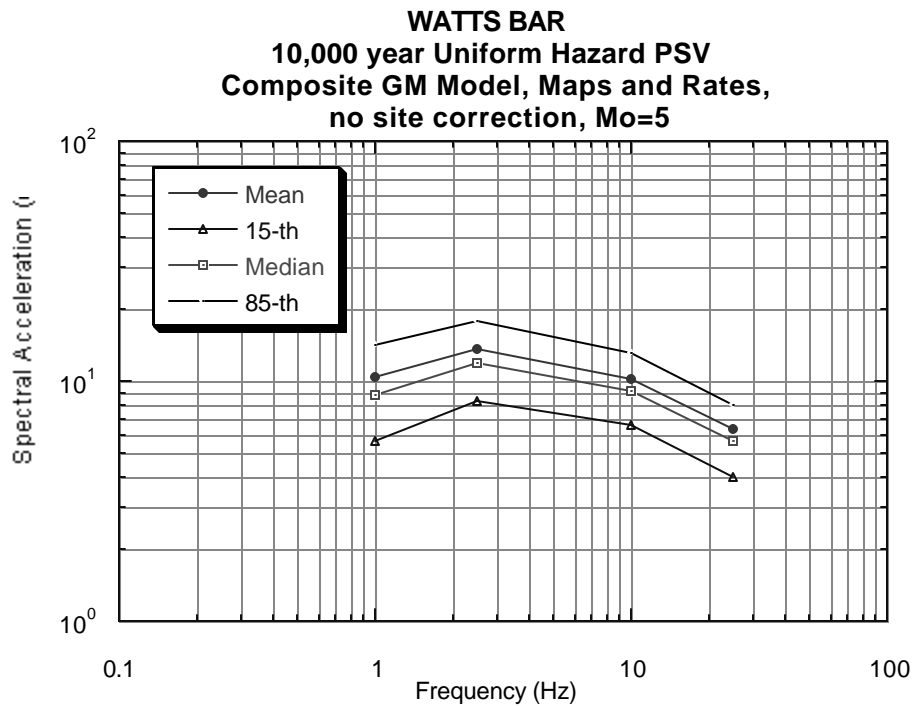


Figure 4.4-12 Probabilistic Hazard Estimates for Watts Bar. Uniform Hazard Spectra for Composite Models of Zonation Maps, Seismicity Rates, and Ground Motion Attenuation.

Table 4.1-1 Expert Evaluators Selection Criteria

1. Knowledge		
I	1.	Experience in tectonic modeling of the EUS.
II	2.	Specialized knowledge of the local geology, seismicity and tectonics of the site.
III	3.	Expertise in probabilistic seismic hazard in the South east US.
IV	4.	Qualified by training and experience.
V	5.	Knowledge of the spectrum of the relevant technical issues and alternative viewpoints.
VI	6.	Familiar with, or willing to learn, broad aims and requirements of PSHA.
VII	7.	Specialized unique knowledge concerning specific scientific issues of relevance.
VIII	8.	Participated in NRC/LLNL/EPRI characterization of the Savannah River site.
IX	9.	Current peer-reviewed publications on relevant topics, such as South East US tectonics, fault mechanics, paleogeology, etc.
2. Lack of bias, credibility		
X	1.	Willing and able to forego proponent role and adopt role as impartial evaluator of data driven hypotheses. Main attributes are impartiality and flexibility.
XI	2.	Level of comfort with probability concepts
XII	3.	Professionally well respected by peers.
3. Interaction abilities		
XIII	1.	Communication and interpersonal skills.
4. Availability		
XIV	1.	Willing and motivated to serve on the panel.
XV	2.	Willing to invest time in panel meetings, and adequate preparation
5. Balance of the Panel		
XVI	1.	Represents the entire community of experts for the relevant issues. Full spectrum of scientific issues.
XVII	2.	“New blood”. Balance in panel between experience in PSHA and fresh approaches brought by new individuals.
XVIII	3.	Panel balance with respect to technical expertise: geology, seismology and tectonics of the site.
XIX	4.	Balance of controversial and non-controversial views(proponents).
XX	5.	Panel balance with respect to specific project goals and aims. (i.e. demonstration, finalization and writing up of a guidance document for the methodology).

Table 4.1-2 Weights Assigned to Each of the Criteria of Table 4.1-1

CRITERIA INDICES	INDEX OF THE CRITERIA FOR THE SELECTION OF THE EVALUATING EXPERTS										Weighted grade	Relative ranking							
	KNOWLEDGE	CRITERIA	BIAS, CREDIBILITY	INTER-ACTION	AVAILABILITY														
	I	II	III	IV	V	VI	VII	VIII	IX	X	XI	XII	XIII	XIV	XV				
RELATIVE IMPORTANCE	10	8	7	8	7	8	5	3	2	10	6	4	10	10	6				
NORMALIZED WEIGHT	0.09	0.07	0.06	0.07	0.06	0.07	0.04	0.03	0.02	0.1	0.06	0.04	0.2	0.06	0.04	1			
TOTAL WEIGHT PER CLASS	0.5															0.2	0.2	0.1	1

Table 4.1-3 Pool of Experts Considered

Alexander	Chapman	Furlong	Jacobs	Lee	Perkins	Seeber	Stephenson	Toksoz
Algermissen	Cluff	Goen	Johnston	Lettis	Phinney	Shandra	Stepp	Van Price
Amick	Coppersmith	Gomberg	Kafka	Litehiser	Pomeroy	Shedlock	Street	Wentworth
Armbruster	Costain	Hanson	Kagan	Long	Powell	Sholz	Swan	Wheeler
Bodin	Dewey	Hatcher	Kimball	McWhorter	Quittmayer	Sibol	Sykes	Youngs
Bollinger	Ebel	Herrmann	Klimkiewicz	Mitchel	Rial	Simpson	Talwani	Zoback, Marilu
Braile	Ellis	Holt	Krinitzsky	Newell	Rice	Smith	Thenhaus	Zoback, Marc
Calhoun	Frankel	Jackson	Lawson	Obermeier	Schwartz	Statton	Thompson	

Table 4.1-4 Final Selection of Expert Evaluators for the Seismic Source Characterization

GIL BOLLINGER,	Consultant, formerly professor of seismology Virginia Polytechnic Institute, Blacksburg, Virginia.
MARTIN CHAPMAN	Professor of geophysics, Virginia Polytechnic Institute. Blacksburg, Virginia.
KEVIN COPPERSMITH	Geologist, GEOMATRIX Consultants, San Francisco. California.
KLAUS JACOB	Geophysicist, Lamont Doherty Earth Observatory of Columbia University, Palisades, New York.
PRADEEP TALWANI	Professor of geophysics, University of South Carolina, Columbia, South Carolina.

Table 4.2.2-1 Detailed Road Map for the Performance of the TIP Project

1. Select Expert Evaluators (EVAs)

Define selection criteria for pool

Build pool of experts

Define selection criteria for evaluators

Rank and select according to criteria

Set contracts

2. Workshop #1

Augusta Ga, June 17-18

Scope

- First set the stage for the characterization of the general regional seismic environment
- Second, concentrate on specific sites:
 - Vogtle and Watts Bar (influenced by Charleston and E. Tennessee seismic zones, respectively).
 - Concentrate on defining the geometry of seismic sources

Communicate that the goal is to formulate a consensus set of geometry models simple enough to allow an interactive, group treatment of the occurrence rate information.

Preparation

- Review existing information.
- Draft issues. TFI identify issues and proponents
- Interact with evaluators and other potential workshop presenters
- Workshop participants to better define issues.
- Assign tasks for presentations and preparation of material

Conduct of Workshop 1

- Information exchange
- Discuss proponents' models
- Discuss issues and data interpretations

Table 4.2.2-1 Detailed Road Map for the Performance of the TIP Project (cont'd)

Assign tasks to experts and analysts for writing white papers on special issues and data Interpretations (Including processing of catalogues, smoothing, etc...). Select a small set of issues and separate individuals develop the pros and cons.

- Debrief experts to get input on what worked and what did not.

3. Exchange And Review Of White Papers By All Participants

Specific, focused on one side of the issues

Exchanges take place by phone, small meetings, E-mail, etc.

4. Expert Evaluators Formulate Ranges Of Models (Geometry Only)

Each expert evaluator formulates own range of zonation models, including formulation of alternative models for the expression of the uncertainty.

The evaluators prepare a simple but complete documentation of their interpretations, to be available to all the participants prior to the workshop # 2.

Generic simple calculations, sensitivity.

TFI will visit the experts to help make sure that level of effort is fairly uniform.

5. Workshop #2. Source Geometry Models (Denver, CO, Sept. 5-6)

Scope

- Finalize the consensus range of geometry models for the region and specific sites
- Develop regional rates information for the consensus sources
- Prepare for site specific characterization

Preparation

See steps 3 and 4 above

Conduct of Workshop # 2

- Expert Evaluators present their range of regional models
 - Presentation, documentation
 - Interaction
 - Challenge, clarifications, update
- TFI develops ranges of consensus regional models, interactively with EVAs 'are asked to weigh (weight?) the various maps and/or set probabilities of existence, probabilities of activity for the sources in each consensus map.

Table 4.2.2-1 Detailed Road Map for the Performance of the TIP Project (cont'd)

5. Start writing guidance document

Site specific information exchange

- review existing information
- identify issues relative to site specific case
- proponents views, presentations

TFI develops a consensus “near-site” geometry to permit concentrating on only a few simple rate parameters (a, b, or rate(m1), rate(m2), and max magnitude distributions)

Conduct a mock-up, yet realistic,(i.e. On a single simple parameter) elicitation.

Assign tasks for discussion of selected issues: white papers, pros and cons

Example: seismicity parameters, completeness of the catalogues, uncertainty in the rate estimates, (all types of uncertainties), smoothing, algorithms for estimation etc.

De-briefing the EVAs, collect comments, evaluations, recommendations.

Get directions from experts on follow-up calculations.

6. Analysts And Selected Experts Prepare Seismicity Rate Information

The purpose is to develop necessary information for the Eva to formulate their estimates with all the uncertainties, possibly through the use of alternative models

Standard analyses of catalogues for zones

Sensitivity on catalogues for zones

Sensitivity on other parameters. (smoothing)

Preliminary Hazard analysis with consensus map and analyst's seismicity rates, sensitivity analysis de-aggregation. (Distances close, boundaries etc.,

Focus on site specific estimates

7. Expert Evaluators Review Seismicity Rate Information

Eva's get to review the information generated in 6 above

8. Workshop #3, Local Rates of Seismicity

Analysts/TFI presents regional seismicity rate models.

Interaction, discussion and finalize with experts.

Analyst presents a sensitivity analysis, based on agreed upon models so far, to determine which are the most important rate parameters for the sites considered.

Table 4.2.2-1 Detailed Road Map for the Performance of the TIP Project (cont'd)

Expert evaluators, present models for site specific estimates. For a few selected common source zones (say Giles County, Charleston...). This is analogous to concentrating on estimating the ground motion for one pair of M-R at a time.

TFI develops consensus model ranges for regional seismicity rates.

Experts present their site specific models

TFI develops site specific consensus rate characterization:

- zonation (background, zones boundaries)
- seismicity rates.

Debrief the Evas. Collect comments, evaluation, recommendations.

9. Analysts Finalize. Perform Update Calculations

Update calculations

Brief documentation

Send to evaluators for review and comments

Obtain evaluation of the process from the Evas. What worked and what did not. Recommendations

Table 4.2.3-1 List of Participants at Workshop 1

**PSHA SOURCE CHARACTERIZATION TRIAL IMPLEMENTATION:
KNOWLEDGE DISSEMINATION WORKSHOP**

June 17-19, 1996

Augusta, Georgia

Technical Facilitator/Integrator (TFI) Team

Don Bernreuter	Lawrence Livermore National Laboratory
Bill Foxall	Lawrence Livermore National Laboratory
Jean Savy	Lawrence Livermore National Laboratory
Allin Cornell	Consultant, CAC Corp., California

Expert Evaluators (EVAs)

Gill Bollinger	Consultant, Buffalo, Wyoming
Martin Chapman	Virginia Polytechnic Institute
Kevin Coppersmith	Geomatrix Consultants
Klaus Jacob	Lamont Doherty Earth Observatory
Pradeep Talwani	University of South Carolina

Nuclear Regulatory Commission

Ernst Zurflueh	Nuclear Regulatory Commission/Office of Nuclear Regulatory Research
----------------	---

Other Presenters and Participants

Dave Amick	Science Applications International Corp., Augusta
Bob Gelinis	Science Applications International Corp., Augusta
Arch Johnston	Center for Earthquake Research and Information
Richard Lee	Savannah River Site, Westinghouse
Ron Marple	University of South Carolina
Jimmy Martin	Virginia Polytechnic Institute
Chuck Mueller	United State Geological Survey, Denver
Mark Petersen	California Department of Mines & Geology
Chris Powell	University of North Carolina
Dale Stephenson	Savannah River Site, Westinghouse
Alice Stievi	Savannah River Site, Westinghouse
Gordana Vlahovic	University of North Carolina

**Table 4.2.6-1 List of Participants to the PSHA Source Characterization
Trial Implementation Project Workshop III**

**Germantown, MD
January 15-17, 1997**

Don Bernreuter Lawrence Livermore National Laboratory P.O. Box 808, L-203 Livermore, CA 94550	Jeff Kimball Department of Energy Facilities Eng. Division - DP-31 19901 Germantown Road Germantown, MD 20875
Gil Bollinger P.O. Box 806 - 39 Shady Lane Buffalo, WY 82834	Klaus Jacob LDEO of Columbia University Route 9W Palisades, NY 10964
Martin Chapman VPI - Dept. Geol Science 4044 Derring Hall, VPI Blacksburg, VA 24061	Cliff Munson U.S. NRC - Office of NRR Washington, DC 20555
Kevin Coppersmith Geomatrix 100 Pine Street, 10th Floor San Francisco, CA 94111	Jean Savy LLNL P.O. Box 808, L-203 Livermore, CA 94550
Allin Cornell CAC/Stanford 110 Coquito Avenue Portola Valley, CA 94025	Pradeep Talwani University of S. Carolina Geological Sciences Columbia, SC 29208
Bill Foxall Lawrence Livermore National Lab. P.O. Box 808 - L202 Livermore, CA 94550	E. Zurflueh U. S. NRC - Office of RES Mail Stop T-10L1 Washington, DC 20555
Bakr Ibrahim U.S. NRC - Office of NMSS Washington, DC 20555	

Table 4.2.6-2 Description of the Minimum Set Zones

EARTHQUAKE SOURCE ZONE MAPS

Explanatory Notes on Zone Maps

1. General

There are six maps showing the source zones significant to Vogtle and eight showing the source zones for Watts Bar. The maps shown in Figure 4.2.6-1a through m are intended to show the individual zone geometries and the spatial relationships among the zones. The maps are not intended to represent any particular source model scenarios (i.e. particular combinations of the zones); the scenarios are summarized in the logic trees shown in Figure 4.2.-2a through e.

2. Charleston

- Zone 1E is not shown. It *coexists* with 1A and comprises 2 areas, which are coincident with the NE and SW areas of 1B (Vogtle Map 5)

3. SC-GA Piedmont/Coastal Plain

- 3A and 3C are exclusive alternatives
- 3A-1 and 3A-2 represent fuzzy boundary of 3A. Possible combinations are:

(3A-1)

(3A-1) + (3A-2)

(3A-1) + (3A-2) + (3A-3)

- 3B (Vogtle Map 3) can exist without 3A or 3C
- 3B forms the background to 3A and 3C (Vogtle Maps 1 and 2), so the following combinations are possible:

3B

3A, (3B-3A)

3C, (3B-3C)

- Zone 7 forms the background to all Zone 3 alternatives and to Zone 6

Table 4.2.6-2 Description of the Minimum Set Zones (*cont'd*)

4. ETSZ

There are 5 basic alternative zone definitions for the ETSZ, 4A, 4B, 4C, 4D, and 4E (see Attachment 4), all of which have the same overall bounding geometry as Zone 4A, which is shown on the Watts Bar maps.

- 4A-2 and 4A-3 represent a fuzzy boundary. Possible combinations are:

(4A-1) + (4A-2) + (4A-3) (Watts Bar Map 1)

(4A-1) + (4A-2) (Watts Bar Map 2)

(4A-1) (Watts Bar Map 3)

- Zone 4B is made up of two areas:

the geometry of 4B-1 is identical to 4A-1

the geometry of 4B-2 is identical to (4A-2) + (4A-3)

- possible combinations are:

(4B-1)

(4B-1) + (4B-2)

- The geometry of Zone 4C is identical to (4A-1) + (4A-2) + (4A-3), within which the sources are defined as eight discrete faults

- The geometry of Zone 4D is identical to (4A-1) + (4A-2) + (4A-3), within which the recurrence rate is inhomogeneous (rate spatial distribution determined by smoothing the seismicity map), rather than homogeneous as in each part of 4A, 4B, and 4E.

- The bounding geometry of Zone 4E is identical to (4A-1) + (4A-2) + (4A-3), but has a graded boundary defined by three cylindrical sources (Bender).

5. Appalachian/Central US

- Zone 5 forms the background to the ETSZ, and comprises three areas. The alternative combinations are:

(5-1), (5-2), (5-3)

(5-1) + (5-2), (5-3)

(5-1), (5-2) + (5-3)

(5-1) + (5-2) + (5-3)

- For all 4A alternative definitions for the ETSZ other than (4A-1) + (4A-2) + (4A-3) and for definition (4B-1), seismicity in the remaining Zone 4 areas [(4A-2) or (4A-2) + (4A-3), (4B-2)] is included in Zone 5 (e.g., Watts Bar Maps 2, 3, 7, 8)

- the Zone 5 alternatives can exist with or without a small, separate Giles County zone (not shown).

Table 4.3.1-1 Point Estimates Considered in the 1994 Trial Application

$m_b=5.5$

Period	5 km	20 km	70 km	200 km
1.0 Hz	-	x	x	x
2.5 Hz	-	x	-	-
10 Hz	-	x	x	-
25 Hz	-	x	-	-
PGA	-	-	x	-

$m_b=7.0$

Period	5 km	20 km	70 km	200 km
1.0 Hz	-	x	x	x
2.5 Hz	-	x	-	-
10 Hz	-	x	x	-
25 Hz	-	x	-	-
PGA	-	-	x	-

Table 4.3.2-1 List of Candidates for Ground Motion Experts Considered for the TIP Project

Name	Affiliation	Involvement in 1994 Study
Gail Atkinson	Carlton Univ.	Evaluator
Don Bernreuter	Lawrence Livermore National Laboratory	Evaluator
David Boore	US Geological Survey	TF Team
Ken Campbell	EQE	Evaluator
Art Frankel	US Geological Survey	None
Klaus Jacob	NCEER	None
Bill Joyner	US Geological Survey	Evaluator
Walt Silva	Pacific Engineering and Analysis	Evaluator
Paul Somerville	Woodward-Clyde Federal Services	Evaluator
Gabriel Toro	Risk Engineering	TF Team
Bob Youngs	Geomatrix Consultants	None

Table 4.3.3-1 Proponent Models

Atkinson and Boore	Point source stochastic
Campbell	Hybrid (empirical and point source Stochastic)
Frankel	Point source stochastic
Horton	Finite source numerical
EPRI	Point source stochastic
Somerville	Finite source numerical

Table 4.3.3-2 Point Estimate Matrix

DISTANCE ¹ (km)	DEPTH (KM)		
	5	10	20
0	x	x	x
10	x	x	x
20		x	x
70		x	
120		x	
200		x	

¹Horizontal distance from surface expression of fault (up-dip extension).

Table 4.3.3-3 ENA Velocity Profile

LAYER	DEPTH TO TOP (km)	V _S (km/s)	V _P (km/s)	DENSITY (g/cm ³)
1	0	2.83	4.9	2.52
2	1	3.58	6.2	2.73
3	80	3.81	6.6	2.79
4	220	4.1	7.1	2.87
5	1000	4.68	8.1	3.38

Source: EPRI (1993)

Table 4.3.3-4 Q Model

High	1000 $f^{0.3}$
Median	670 $f^{0.33}$
Low	400 $f^{0.4}$

Table 4.3.3-5 132 Case Definitions for Point Estimates

- (1) X-distance is the horizontal distance from the surface “trace” of the fault.
- (2) HW refers to hanging wall location in reverse faulting, FW to footwall location in reverse faulting, and SS to strike-slip faulting.
- (3) R_{Rupt} is rupture distance, the closest distance from the site to the fault rupture surface; R_{JB} is the Joyner-Boore distance, the closest distance to the surface projection of the rupture surface; R_{Seis} is seismogenic distance, the closest distance to the assumed seismogenic part of the rupture surface, here used as the part of the rupture surface that lies at least 3 km below the ground surface; R_{Hypo} is hypocentral distance.

132 case definitions for point estimates

CASE NO.	MAG	DEPTH (KM)	X-DISTANCE ¹ (KM)	FAULTING STYLE ²	R_{RUPT} ³ (KM)	R_{JB} ³ (KM)	R_{SEIS} ³ (KM)	R_{HYPO} ³ (KM)
1	5.0	5.0	0	FW	5.1	5.1	3.6	6.18
2	5.0	5.0	10	FW	14.1	14.1	13.6	14.51
3	6.0	5.0	0	FW	3.0	4.2	2.1	5.43
4	6.0	5.0	10	FW	12.3	13.3	12.1	13.12
5	7.0	5.0	0	FW	0.0	4.2	0.0	6.00
6	7.0	5.0	10	FW	10.0	13.3	10.0	11.66
7	7.5	5.0	0	FW	0.0	4.2	0.0	8.68
8	7.5	5.0	10	FW	10.0	13.3	10.0	13.24
9	5.0	10.0	0	FW	12.2	12.2	8.6	13.21
10	5.0	10.0	10	FW	20.5	20.5	18.6	21.14
11	5.0	10.0	20	FW	29.9	29.9	28.6	30.32
12	5.0	10.0	70	FW	79.1	79.1	78.6	79.26
13	5.0	10.0	120	FW	128.9	128.9	128.6	129.00
14	5.0	10.0	200	FW	208.8	208.8	208.6	208.90
15	6.0	10.0	0	FW	10.1	10.1	7.1	12.28
16	6.0	10.0	10	FW	18.6	18.6	17.1	19.83
17	6.0	10.0	20	FW	28.1	28.1	27.1	28.91
18	6.0	10.0	70	FW	77.5	77.5	77.1	77.77
19	6.0	10.0	120	FW	127.3	127.3	127.1	127.50
20	6.0	10.0	200	FW	207.3	207.3	207.1	207.40

132 case definitions for point estimates

CASE NO.	MAG	DEPTH (KM)	X-DISTANCE ¹ (KM)	FAULTING STYLE ²	R _{RUPT} ³ (KM)	R _{JB} ³ (KM)	R _{SEIS} ³ (KM)	R _{HYPO} ³ (KM)
21	7.0	10.0	0	FW	5.7	5.7	4.0	10.77
22	7.0	10.0	10	FW	14.6	14.6	14.0	17.20
23	7.0	10.0	20	FW	24.3	24.3	24.0	26.00
24	7.0	10.0	70	FW	74.1	74.1	74.0	74.6700
25	7.0	10.0	120	FW	124.1	124.1	124.0	124.40
26	7.0	10.0	200	FW	204.0	204.0	204.0	204.20
27	7.5	10.0	0	FW	1.9	4.2	1.3	10.09
28	7.5	10.0	10	FW	11.4	13.3	11.3	15.11
29	7.5	10.0	20	FW	21.4	23.2	21.3	23.55
30	7.5	10.0	70	FW	71.3	73.1	71.3	72.02
31	7.5	10.0	120	FW	121.3	123.0	121.3	121.70
32	7.5	10.0	200	FW	201.3	203.0	201.3	201.60
33	5.0	20.0	0	FW	26.3	26.3	18.6	27.33
34	5.0	20.0	10	FW	34.2	34.2	28.6	34.92
35	5.0	20.0	20	FW	42.9	42.9	38.6	43.50
36	6.0	20.0	0	FW	24.2	24.2	17.1	26.33
37	6.0	20.0	10	FW	32.1	32.1	27.1	33.70
38	6.0	20.0	20	FW	40.9	40.9	37.1	42.17
39	7.0	20.0	0	FW	19.8	19.8	14.0	24.41
40	7.0	20.0	10	FW	27.8	27.8	24.0	31.24
41	7.0	20.0	20	FW	36.8	36.8	34.0	39.44
42	7.5	20.0	0	FW	16.0	16.0	11.3	22.98
43	7.5	20.0	10	FW	24.1	24.1	21.3	29.23
44	7.5	20.0	20	FW	33.3	33.3	31.3	37.16
45	5.0	5.0	0	HW	5.1	5.1	3.6	6.18
46	5.0	5.0	10	HW	7.1	7.1	3.6	14.51
47	6.0	5.0	0	HW	3.0	4.2	2.1	5.43
48	6.0	5.0	10	HW	7.1	7.1	2.1	13.12

132 case definitions for point estimates

CASE NO.	MAG	DEPTH (KM)	X-DISTANCE ¹ (KM)	FAULTING STYLE ²	R _{RUPT} ³ (KM)	R _{JB} ³ (KM)	R _{SEIS} ³ (KM)	R _{HYPO} ³ (KM)
49	7.0	5.0	0	HW	0.0	4.2	0.0	6.00
50	7.0	5.0	10	HW	7.1	7.1	0.0	11.66
51	7.5	5.0	0	HW	0.0	4.2	0.0	8.68
52	7.5	5.0	10	HW	7.1	7.1	0.0	13.24
53	5.0	10.0	0	HW	12.2	12.2	8.6	13.21
54	5.0	10.0	10	HW	8.7	8.7	0.0	21.14
55	5.0	10.0	20	HW	14.1	14.1	8.6	30.32
56	5.0	10.0	70	HW	59.7	59.7	58.6	79.26
57	5.0	10.0	120	HW	109.2	109.2	108.6	129.00
58	5.0	10.0	200	HW	189.0	189.0	188.6	208.90
59	6.0	10.0	0	HW	10.1	10.1	7.1	12.28
60	6.0	10.0	10	HW	7.7	7.7	0.0	19.83
61	6.0	10.0	20	HW	14.1	14.1	7.1	28.91
62	6.0	10.0	70	HW	58.6	58.6	57.1	77.77
63	6.0	10.0	120	HW	107.9	107.9	107.1	127.50
64	6.0	10.0	200	HW	187.6	187.6	187.1	207.40
65	7.0	10.0	0	HW	5.7	5.7	4.0	10.77
66	7.0	10.0	10	HW	7.1	7.1	0.0	17.20
67	7.0	10.0	20	HW	14.1	14.1	4.0	26.00
68	7.0	10.0	70	HW	56.3	56.3	54.0	74.67
69	7.0	10.0	120	HW	105.2	105.2	104.0	124.40
70	7.0	10.0	200	HW	184.7	184.7	184.0	204.20
71	7.5	10.0	0	HW	1.9	4.2	1.3	10.09
72	7.5	10.0	10	HW	7.1	7.1	0.0	15.11
73	7.5	10.0	20	HW	14.1	14.1	1.3	23.55
74	7.5	10.0	70	HW	54.6	54.6	51.3	72.02
75	7.5	10.0	120	HW	103.0	103.0	101.3	121.70
76	7.5	10.0	200	HW	182.3	182.3	181.3	201.60

132 case definitions for point estimates

CASE NO.	MAG	DEPTH (KM)	X-DISTANCE ¹ (KM)	FAULTING STYLE ²	R _{RUPT} ³ (KM)	R _{JB} ³ (KM)	R _{SEIS} ³ (KM)	R _{HYPO} ³ (KM)
77	5.0	20.0	0	HW	26.3	26.3	18.6	27.33
78	5.0	20.0	10	HW	20.5	20.5	8.6	34.92
79	5.0	20.0	20	HW	18.7	18.7	0.0	43.50
80	6.0	20.0	0	HW	24.2	24.2	17.1	26.33
81	6.0	20.0	10	HW	18.6	18.6	7.1	33.70
82	6.0	20.0	20	HW	17.4	17.4	0.0	42.17
83	7.0	20.0	0	HW	19.8	19.8	14.0	24.41
84	7.0	20.0	10	HW	14.6	14.6	4.0	31.24
85	7.0	20.0	20	HW	15.2	15.2	0.0	39.44
86	7.5	20.0	0	HW	16.0	16.0	11.3	22.98
87	7.5	20.0	10	HW	11.4	11.4	1.3	29.23
88	7.5	20.0	20	HW	14.3	14.3	0.0	37.16
89	5.0	5.0	0	SS	3.1	3.1	0.0	6.18
90	5.0	5.0	10	SS	10.5	10.5	10.0	14.51
91	6.0	5.0	0	SS	0.9	3.0	0.0	5.43
92	6.0	5.0	10	SS	10.0	10.4	10.0	13.12
93	7.0	5.0	0	SS	0.0	3.0	0.0	6.00
94	7.0	5.0	10	SS	10.0	10.4	10.0	11.66
95	7.5	5.0	0	SS	0.0	3.0	0.0	8.68
96	7.5	5.0	10	SS	10.0	10.4	10.0	13.24
97	5.0	10.0	0	SS	8.1	8.1	0.0	13.21
98	5.0	10.0	10	SS	12.8	12.8	10.0	21.14
99	5.0	10.0	20	SS	21.6	21.6	20.0	30.32
100	5.0	10.0	70	SS	70.5	70.5	70.0	79.26
101	5.0	10.0	120	SS	120.3	120.3	120.0	129.00
102	5.0	10.0	200	SS	200.2	200.2	200.0	208.90
103	6.0	10.0	0	SS	5.9	5.9	0.0	12.28
104	6.0	10.0	10	SS	11.6	11.6	10.0	19.83

132 case definitions for point estimates

CASE NO.	MAG	DEPTH (KM)	X-DISTANCE ¹ (KM)	FAULTING STYLE ²	R _{RUPT} ³ (KM)	R _{JB} ³ (KM)	R _{SEIS} ³ (KM)	R _{HYPO} ³ (KM)
105	6.0	10.0	20	SS	20.9	20.9	20.0	28.91
106	6.0	10.0	70	SS	70.3	70.3	70.0	77.77
107	6.0	10.0	120	SS	120.2	120.2	120.0	127.50
108	6.0	10.0	200	SS	200.1	200.1	200.0	207.40
109	7.0	10.0	0	SS	1.5	3.0	0.0	10.77
110	7.0	10.0	10	SS	10.1	10.4	10.0	17.20
111	7.0	10.0	20	SS	20.1	20.2	20.0	26.00
112	7.0	10.0	70	SS	70.0	70.1	70.0	74.67
113	7.0	10.0	120	SS	120.0	120.0	120.0	124.40
114	7.0	10.0	200	SS	200.0	200.0	200.0	204.20
115	7.5	10.0	0	SS	0.0	3.0	0.0	10.09
116	7.5	10.0	10	SS	10.0	10.4	10.0	15.11
117	7.5	10.0	20	SS	20.0	20.2	20.0	23.55
118	7.5	10.0	70	SS	70.0	70.1	70.0	72.02
119	7.5	10.0	120	SS	120.0	120.0	120.0	121.70
120	7.5	10.0	200	SS	200.0	200.0	200.0	201.60
121	5.0	20.0	0	SS	18.1	18.1	0.0	27.33
122	5.0	20.0	10	SS	20.6	20.6	10.0	34.92
123	5.0	20.0	20	SS	26.9	26.9	20.0	43.50
124	6.0	20.0	0	SS	15.9	15.9	0.0	26.33
125	6.0	20.0	10	SS	18.8	18.8	10.0	33.70
126	6.0	20.0	20	SS	25.6	25.6	20.0	42.17
127	7.0	20.0	0	SS	11.5	11.5	0.0	24.41
128	7.0	20.0	10	SS	15.3	15.3	10.0	31.24
129	7.0	20.0	20	SS	23.1	23.1	20.0	39.44
130	7.5	20.0	0	SS	7.7	7.7	0.0	22.98
131	7.5	20.0	10	SS	12.6	12.6	10.0	29.23
132	7.5	20.0	20	SS	21.4	21.4	20.0	37.16

Table 4.3.3-6 D. L. Bernreuter: General Model Weighting Scheme

PROPONENT MODEL	WEIGHT		
	M 5	M 6	M 7 and 7.5
Atkinson and Boore	0.3	0.3	0.25
Campbell	0.4	0.2	0.25
EPRI	0.3	0.2	0.25
Frankel	0.0	0.0	0.0
Horton	0.0	0.0	0.0
Somerville	0.0	0.2	0.25

No period, distance, or mechanism dependence. Weights pertain to μ estimates only; EPRI model σ values adopted for σ estimates.

Table 4.3.3-7 D. M. BOORE: Model Weighting Scheme

PROPONENT MODEL	WEIGHT (μ)	WEIGHT (σ)
Atkinson and Boore	0.5	0.333
Campbell	0.0	0.333
EPRI	0.3	0.334
Frankel	0.0	0.0
Horton	0.1	0.0
Somerville	0.1	0.0

No magnitude, distance, period, or mechanism dependence.

**Table 4.3.3-8 K. W. CAMPBELL: General Model
Weighting Scheme**

PROPONENT MODEL	WEIGHT
Atkinson and Boore	0.17
Campbell	0.33
EPRI	0.08
Frankel	0.08
Horton	0.17
Somerville	0.17

No period or magnitude dependence. Campbell hybrid model is gradually downweighted at larger distances, see text for details. Weights pertain to μ estimates only. σ values are from the empirical western US attenuation relations considered in the hybrid model.

Table 4.3.3-9 K. JACOB: Model Weighting Scheme, μ Estimates (Unnormalized Values)

Strike-slip mechanism, m estimates:

PROPONENT MODEL	WEIGHTS		
	M 5	M 6	M 7 and 7.5
Atkinson and Boore	3	2	1
Campbell	2	2	2
EPRI	2	2	2
Frankel	2	2	1
Horton	3	3	3
Somerville	0	0	0

Reverse dip-slip mechanism, footwall:

PROPONENT MODEL	WEIGHTS		
	M 5	M 6	M 7 and 7.5
Atkinson and Boore	3	2	1
Campbell	2	2	2
EPRI	2	3	2
Frankel	2	2	1
Horton	0	0	0
Somerville	0	1	1

Reverse dip-slip mechanism, hanging wall:

PROPONENT MODEL	WEIGHTS		
	M 5	M 6	M 7 and 7.5
Atkinson and Boore	3	2	1
Campbell	2	2	2
EPRI	3	3	2
Frankel	2	2	3
Horton	2	2	3
Somerville	0	1	1

No period or distance dependence. Weights assigned correspond to ‘high’ (3), ‘medium’ (2), ‘low’ (1) and not applicable (0). Weights shown are not normalized; normalized values are obtained by dividing each weight by the sum of the weights for all proponent models at that magnitude.

Table 4.3.3-9 K. JACOB: Model Weighting Scheme, μ Estimates (Unnormalized Values) (cont'd)

Strike-slip mechanism:

PROPONENT MODEL	WEIGHTS	
	M 5	M 6, 7, and 7.5
Atkinson and Boore	2	1
Campbell	2	3
EPRI	2	2
Frankel	3	3
Horton	1	1
Somerville	0	0

Reverse dip-slip mechanism, footwall:

PROPONENT MODEL	WEIGHTS	
	M 5	M 6, 7, and 7.5
Atkinson and Boore	2	2
Campbell	2	2
EPRI	2	2
Frankel	3	3
Horton	0	0
Somerville	0	1

Reverse dip-slip mechanism, hanging wall:

PROPONENT MODEL	WEIGHTS	
	M 5	M 6, 7, and 7.5
Atkinson and Boore	2	2
Campbell	2	2
EPRI	2	2
Frankel	3	3
Horton	1	1
Somerville	0	1

No period or distance dependence. Weights assigned correspond to 'high' (3), 'medium' (2), 'low' (1) and not applicable (0). Weights shown are not normalized; normalized values are obtained by dividing each weight by the sum of the weights for all proponent models at that magnitude.

Table 4.3.3-10 P. G. SOMERVILLE: Model Weighting Scheme

Magnitude 5:

PROPONENT MODEL	WEIGHT
Atkinson and Boore	0.2
Campbell	0.4
EPRI	0.2
Frankel	0.2
Horton	0.0
Somerville	N/A

Magnitude 6, 7, 7.5:

PROPONENT MODEL	WEIGHT AT CLOSE DISTANCE	WEIGHT AT FAR DISTANCE
Atkinson and Boore	0.05	0.1
Campbell	0.4	0.4
EPRI	0.075	0.1
Frankel	0.075	0.1
Horton	0.0	0.0
Somerville	0.4	0.3

No period or mechanism dependence. Close distance defined as 10 km or less at M 6, 20 km or less at M 7 and 7.5. Far distance defined as 20 km or more at M 6, 70 km or more at M 7 and 7.5. Weights pertain to μ and σ estimates

Table 4.3.4-1A D. L. Bernreuter: Regression Coefficients Median Model

FREQUENCY (HZ)	a ₁	a ₂	a ₃	a ₄	a ₅	a ₆	a ₇	a ₈	SIGMA FIT
100	3.3522	0.2707	-1.4721	0.1816	0.138	0	0.0264	10.1	0.1089
25	4.9116	0.2707	-1.6716	0.1816	0.138	0.0085	-0.0114	11.8	0.1108
10	3.6617	0.2707	-1.3873	0.1816	0.138	-0.0085	0.0452	9.8	0.1165
2.5	2.444	0.2707	-1.1571	0.1816	0.138	-0.0742	0.0498	8.3	0.1248
1	1.4999	0.2707	-1.0754	0.1816	0.138	-0.1345	-0.0369	7.5	0.1341

Table 4.3.4-1B D. L. Bernreuter: Regression Coefficients Sigma Model

FREQUENCY (HZ)	b ₁	b ₂	b ₄	SIGMA FIT
100	0.6853	-0.0294	7.2	0.0749
25	0.6838	-0.0428	7.2	0.0764
10	0.6701	-0.0302	7.2	0.0745
2.5	0.7224	-0.0247	7.2	0.0502
1	0.7923	-0.0178	7.2	0.0447

Table 4.3.4-1C D. L. Bernreuter: Regression Coefficients Sigma-Mu Model

FREQUENCY (HZ)	c₁	c₂	c₃	c₄	c₅	c₆	SIGMA FIT
100	0.3772	-0.0521	-0.0328	0.009	0.0556	6	0.2537
25	0.4019	-0.0472	-0.0735	0.0156	0.0881	6	0.2368
10	0.3435	-0.001	-0.0449	0.0098	0.0708	6	0.2641
2.5	0.314	-0.0292	0.0527	-0.0018	-0.0198	6	0.3005
1	0.508	-0.013	0.1171	-0.0167	-0.051	6	0.2324

Table 4.3.4-1D D. L. Bernreuter: Regression Coefficients Sigma-Sigma Model

FREQUENCY (HZ)	d₁	d₂	d₄	SIGMA FIT
100	0.213	0.0302	7.2	0.0677
25	0.1732	0.0135	7.2	0.0635
10	0.2119	0.0294	7.2	0.0679
2.5	0.164	0.0218	7.2	0.0426
1	0.1477	0.0167	7.2	0.0373

Table 4.3.4-2A D. M. Boore: Regression Coefficients Median Model

FREQUENCY (HZ)	a ₁	a ₂	a ₃	a ₄	a ₅	a ₆	a ₇	a ₈	SIGMA FIT
100	3.2922	0.371	-1.4556	0.1554	0.1385	0	0.0595	8.5	0.1388
25	4.7198	0.371	-1.5974	0.1554	0.1385	0.0054	0.0325	9.7	0.1362
10	3.5246	0.371	-1.3287	0.1554	0.1385	-0.0076	0.0593	8.2	0.1418
2.5	2.0581	0.371	-1.0892	0.1554	0.1385	-0.0693	0.0946	6.9	0.1536
1	0.9888	0.371	-1.0009	0.1554	0.1385	-0.1306	0.0489	6.4	0.1742

Table 4.3.4-2B D. M. Boore: regression Coefficients Sigma Model

FREQUENCY (HZ)	b ₁	b ₂	b ₄	SIGMA FIT
100	0.6217	-0.0355	7.2	0.0374
25	0.6355	-0.0369	7.2	0.0352
10	0.6074	-0.0372	7.2	0.0363
2.5	0.6691	-0.0207	7	0.0324
1	0.7367	-0.0075	7	0.0363

Table 4.3.4-2C D. M. Boore: Regression Coefficients Sigma-Mu Model

FREQUENCY (HZ)	c ₁	c ₂	c ₃	c ₄	c ₅	c ₆	SIGMA FIT
100	0.3093	-0.0261	-0.0543	0.0066	0.0083	6	0.0798
25	0.3572	-0.0217	-0.0923	0.016	0.0184	6	0.0936
10	0.2436	-0.0067	-0.0403	0.008	0.0001	6	0.0759
2.5	0.17	-0.0171	0.0479	-0.0079	-0.0102	6	0.0898
1	0.2742	-0.0222	0.12	-0.023	-0.0388	6	0.1111

Table 4.3.4-2D D. M. Boore: Regression Coefficients Sigma-Sigma Model

FREQUENCY (HZ)	d ₁	d ₂	d ₄	SIGMA FIT
100	0.0511	0.0006	7.2	0.0017
25	0.0504	0.0002	7.2	0.0005
10	0.0503	0.0002	7.2	0.0005
2.5	0.05	-0.0002	7.2	0.0005
1	0.0503	-0.0014	7.2	0.0035

Table 4.3.4-3A K. W. Campbell: Regression Coefficients Median Model

FREQUENCY (HZ)	a ₁	a ₂	a ₃	a ₄	a ₅	a ₆	a ₇	a ₈	SIGMA FIT
100	3.2806	0.3029	-1.4378	0.0496	0.1521	0	-0.0068	9	0.1364
25	4.6735	0.3029	-1.5793	0.0496	0.1521	0.0132	-0.0907	10.4	0.1582
10	3.4706	0.3029	-1.3119	0.0496	0.1521	-0.0083	-0.0122	8.6	0.1454
2.5	2.4492	0.3029	-1.1509	0.0496	0.1521	-0.0745	0.0609	7.7	0.1486
1	1.6744	0.3029	-1.102	0.0496	0.1521	-0.1347	-0.0243	7.3	0.1673

Table 4.3.4-3B K. W. Campbell: Regression Coefficients Sigma Model

FREQUENCY (HZ)	b ₁	b ₂	b ₄	SIGMA FIT
100	0.568	-0.0232	7.2	0.0507
25	0.5798	-0.0214	7.2	0.056
10	0.5567	-0.0282	7.2	0.0433
2.5	0.6027	-0.0052	7.2	0.0514
1	0.666	0.0223	5.8	0.0557

Table 4.3.4-3C K. W. Campbell: Regression Coefficients Sigma-Mu Model

FREQUENCY (HZ)	c ₁	c ₂	c ₃	c ₄	c ₅	c ₆	SIGMA FIT
100	0.1719	-0.0056	-0.003	-0.0002	-0.0014	6	0.0178
25	0.2095	-0.0059	-0.0152	0.0009	0.0017	6	0.0359
10	0.1552	-0.0018	0.0057	-0.0013	-0.0013	6	0.0197
2.5	0.1657	-0.0046	0.0042	-0.0011	-0.0093	6	0.0268
1	0.1899	-0.0115	0.0254	-0.0056	-0.0201	6	0.0438

Table 4.3.4-3D K. W. Campbell: Regression Coefficients Sigma-Sigma Model

FREQUENCY (HZ)	d ₁	d ₂	d ₄	SIGMA FIT
100	0.0539	-0.0006	7	0.0079
25	0.0538	-0.0014	7	0.0102
10	0.0535	-0.0006	7	0.0068
2.5	0.0552	-0.0052	7	0.0106
1	0.0569	-0.0139	6.4	0.0146

Table 4.3.4-4A K. Jacob: Regression Coefficients Median Model

FREQUENCY (HZ)	a ₁	a ₂	a ₃	a ₄	a ₅	a ₆	a ₇	a ₈	SIGMA FIT
100	3.2113	0.3621	-1.4271	0.1079	0.1424	0	0.0048	8.6	0.1525
25	4.9629	0.3621	-1.6472	0.1079	0.1424	0.0089	-0.0973	11.2	0.181
10	3.6398	0.3621	-1.356	0.1079	0.1424	-0.0078	0.0042	9	0.1564
2.5	2.3168	0.3621	-1.1301	0.1079	0.1424	-0.0674	0.0841	7.5	0.1644
1	1.5657	0.3621	-1.0542	0.1079	0.1424	-0.1417	0.0073	6.9	0.1896

Table 4.3.4-4B K. Jacob: Regression Coefficients Sigma Model

FREQUENCY (HZ)	b ₁	b ₂	b ₄	SIGMA FIT
100	0.6277	-0.012	7	0.051
25	0.6104	-0.0164	7.1	0.0591
10	0.6146	-0.0174	7	0.0455
2.5	0.6523	0.0013	5.8	0.0457
1	0.7137	0.0115	7.2	0.0516

Table 4.3.4-4C K. Jacob: Regression Coefficients Sigma-Mu Model

FREQUENCY (HZ)	c ₁	c ₂	c ₃	c ₄	c ₅	c ₆	SIGMA FIT
100	0.4374	-0.0182	-0.0911	0.0113	-0.0043	6	0.1296
25	0.5841	-0.021	-0.1308	0.0207	-0.033	6	0.1775
10	0.3658	0.0144	-0.0594	0.0094	-0.023	6	0.1293
2.5	0.3034	-0.0198	0.0016	0.0004	-0.045	6	0.1413
1	0.4183	-0.0235	0.0428	-0.0077	-0.0365	6	0.1473

Table 4.3.4-4D K. Jacob: Regression Coefficients Sigma-Sigma Model

FREQUENCY (HZ)	d ₁	d ₂	d ₄	SIGMA FIT
100	0.1444	-0.0023	7	0.0597
25	0.1198	-0.0168	7	0.0835
10	0.1452	0.0156	5.8	0.0565
2.5	0.133	-0.0303	7	0.0664
1	0.1331	-0.0427	7.2	0.0808

Table 4.3.4.5A P. G. Somerville: Regression Coefficients Median Model

FREQUENCY (HZ)	a ₁	a ₂	a ₃	a ₄	a ₅	a ₆	a ₇	a ₈	SIGMA FIT
100	3.2482	0.159	-1.4498	0.1317	0.1596	0	-0.0078	10.1	0.1217
25	4.9854	0.159	-1.698	0.1317	0.1596	0.0128	-0.077	12.8	0.1484
10	3.6428	0.159	-1.3915	0.1317	0.1596	-0.0092	0.0096	10.1	0.1173
2.5	2.512	0.159	-1.1677	0.1317	0.1596	-0.075	0.0333	8.3	0.1395
1	1.6282	0.159	-1.0794	0.1317	0.1596	-0.1406	-0.0539	7.1	0.1508

Table 4.3.4.5B P. G. Somerville: Regression Coefficients Sigma Model

FREQUENCY (HZ)	b ₁	b ₂	b ₄	SIGMA FIT
100	0.5959	-0.0282	7	0.0409
25	0.6005	-0.03	7	0.046
10	0.5843	-0.0304	7	0.0358
2.5	0.6287	-0.0165	7	0.0342
1	0.7012	-0.0091	6.4	0.0337

Table 4.3.4.5C P. G. Somerville: Regression Coefficients Sigma-Mu Model

FREQUENCY (HZ)	c ₁	c ₂	c ₃	c ₄	c ₅	c ₆	SIGMA FIT
100	0.1873	-0.0109	-0.014	0.0019	0.0044	6	0.0351
25	0.2151	-0.0086	-0.0324	0.0063	0.0084	6	0.0581
10	0.1687	-0.0022	-0.0059	0.0009	0.0027	6	0.0253
2.5	0.1612	-0.0038	0.0021	0	-0.0067	6	0.0329
1	0.2247	-0.0135	0.0106	-0.0013	-0.041	6	0.063

Table 4.3.4.5D P. G. Somerville: Regression Coefficients Sigma-Sigma Model

FREQUENCY (HZ)	d ₁	d ₂	d ₄	SIGMA FIT
100	0.0562	-0.0021	5.8	0.0133
25	0.0593	-0.0027	6.5	0.0188
10	0.0564	0.0008	7.2	0.0125
2.5	0.0562	-0.0069	7	0.0159
1	0.0581	-0.0079	7	0.0212

Table 4.3.4-6A Expert Composite: Regression Coefficients Median Model

FREQUENCY (HZ)	a ₁	a ₂	a ₃	a ₄	a ₅	a ₆	a ₇	a ₈	SIGMA FIT
100	3.2672	0.2944	-1.4464	0.1265	0.1458	0	0.0153	9.2	0.1182
25	4.8347	0.2944	-1.6354	0.1265	0.1458	0.0097	-0.0487	11.1	0.129
10	3.5804	0.2944	-1.3535	0.1265	0.1458	-0.0082	0.0213	9.1	0.1223
2.5	2.349	0.2944	-1.1375	0.1265	0.1458	-0.0721	0.0646	7.7	0.132
1	1.4643	0.2944	-1.0608	0.1265	0.1458	-0.1363	-0.0117	7	0.1454

Table 4.3.4-6B Expert Composite: Regression Coefficients Sigma Model

FREQUENCY (HZ)	b ₁	b ₂	b ₄	SIGMA FIT
100	0.619	-0.0251	7.2	0.0378
25	0.6177	-0.0273	7.2	0.042
10	0.6058	-0.028	7.2	0.0336
2.5	0.6557	-0.0137	7	0.0283
1	0.7223	-0.0026	7	0.0286

Table 4.3.4-6C Expert Composite: Regression Coefficients Sigma-Mu Model

FREQUENCY (HZ)	c ₁	c ₂	c ₃	c ₄	c ₅	c ₆	SIGMA FIT
100	0.3097	-0.0208	-0.0485	0.0064	0.0207	6	0.1036
25	0.3882	-0.0162	-0.0846	0.0137	0.03	6	0.1236
10	0.2702	0.0016	-0.0375	0.0065	0.0148	6	0.1028
2.5	0.226	-0.0176	0.0291	-0.0037	-0.0246	6	0.1183
1	0.3599	-0.0148	0.0728	-0.0133	-0.0476	6	0.1152

Table 4.3.4-6D Expert Composite: Regression Coefficients Sigma-Sigma Model

FREQUENCY (HZ)	d ₁	d ₂	d ₄	SIGMA FIT
100	0.115	0.0055	7.2	0.0296
25	0.0919	-0.0084	7	0.0326
10	0.1143	0.0086	7.2	0.0297
2.5	0.102	-0.0095	7	0.0223
1	0.1008	-0.0153	7.2	0.0236

Table 4.4-1 Probability Distributions of the Upper Magnitude Cutoff M_u for Bollinger

EVA: **Gilbert BOLLINGER**

Elicitation of preliminary estimates for the seismicity rates and upper magnitude cutoffs for the zones in the composite seismic sources maps.

Date of the elicitation: 8-Jan-97

ELICITATION OF UPPER MAGNITUDE CUTOFFS: M_u

Names of Zones in the composite set of zonation maps	Magnitude Cutoff M_u				Comments
	Lower bound	Mode	Upper bound	Distribution shape	
3A	5.00	5.50	6.00	Uniform	Barely above background
3B-3A	4.50	5.00	5.50	Uniform	
3C	5.00	5.50	6.00	Uniform	
3B-3C	5.00	5.50	6.00	Uniform	
Charleston					
1A-(Characteristic)	7.00	7.30	7.60	Triangle	
1B-(3-blobs)	7.00	7.30	7.60	Triangle	Center blob has properties of 1A
1C-(ZRA)	7.00	7.30	7.60	Triangle	
1D-(Long--SW-NE)	7.00	7.30	7.60	Triangle	Same as 1B but different geometry
1E(2side.blobs+1A)	5.50	6.00	6.50	Triangle	Non characteristic part of 1A
Bckgnd to Charlstn					
6-Central-Virginia	6.00	6.30	6.60	Triangle	
7(Coast.Plain-CVSC)	4.50	5.00	5.50	Uniform	
8-Offshore	4.50	5.00	5.50	Uniform	
ETSZ					
4A-1	6.00	6.50	7.30	U taper	Based on 3 different methods
(4A-1)+(4A-2)	6.00	6.50	7.30	U taper	estimates: (1) Max Hist + Δ ,
(4A-1)+(4A-2)+(4A-3)	6.00	6.50	7.30	U taper	(2) 1000 yr reccur. extrapolation, and
4B-1	5.50	6.50	7.30	U taper	(3) estimate from fault length equat.
4B-2	6.00	6.00	6.80	U taper	4B-1=4A-1, 4B-2=(4A-2)+(4A-3)
4-C-(8-faults)	6.50	7.00	7.50	Triangle	8 faults system, see white paper
4-D-(varying-rates)				Triangle	
4-E-(rate-cylinders)	6.00	7.00	8.00	Triangle	same geometry as 4A, 10% PE
Backgrnd to ETSZ					
(5-1)	5.00	6.00	6.80	U taper	
(5-2)	5.00	6.00	6.80	U taper	
(5-1)+(5-2)	5.00	6.00	6.80	U taper	
(5-3)	5.00	5.00	5.50	Uniform	
(5-1)+(5-2)+(5-3)	4.50	6.30	7.00	U taper	

Table 4.4-2 Probability Distributions of the Upper Magnitude Cutoff M_u for Chapman

EVA: **Martin CHAPMAN**

Elicitation of preliminary estimates for the seismicity rates and upper magnitude cutoffs for the zones in the composite seismic sources maps.

Date of the elicitation: 19-Dec-96

ELICITATION OF UPPER MAGNITUDE CUTOFFS: M_u

Names of Zones in the composite set of zonation maps	Magnitude Cutoff M_u				Comments
	Lower bound	Mode	Upper bound	Distribution shape	
3A	6.00	6.50	7.00	Uniform	
3B-3A	6.00	6.50	7.00	Uniform	Complement to 3A
3C	6.00	6.50	7.00	Uniform	
3B-3C	6.00	6.50	7.00	Uniform	Complement to 3C
Charleston					
1A-(Characteristic)	6.90	7.20	7.50	Triangle	Lower & Upper based on A. Johnston
1B-(3-blobs)	6.50	7.20	7.50	U taper R	Center blob has properties of 1A
1C-(ZRA)	6.90	7.20	7.50	Triangle	Lower & Upper based on A. Johnston
1D-(Long--SW-NE)	6.50	7.20	7.50	U taper R	Same as 1B but different geometry
1E(2side.blobs+1A)					Non characteristic part of 1A
Bckgnd to Charlstn					
6-Central-Virginia	6.00	6.50	7.00	Uniform	Magn. vs. length considerations
7(Coast.Plain-CVSZ)	6.00	6.50	7.00	Uniform	Magn. vs. length considerations
8-Offshore	6.00	7.00	7.50	Uniform	Same as 6 & 7, NOT Characteristic
ETSZ					
4A-1	6.50	7.00	7.50	Uniform	Based on uncertainty on the max.
(4A-1)+(4A-2)	6.50	7.00	7.50	Uniform	length of the possible segments.
(4A-1)+(4A-2)+(4A-3)	6.50	7.00	7.50	Uniform	
4B-1	6.50	7.00	7.50	Uniform	4B is exclusive of 4A
4B-2	6.00	7.00	7.50	Uniform	
4C-(8faults)					
4D-(varying-rates)					
4E-(rate-cylinders)					
Backgrnd to ETSZ					
(5-1)	6.00	7.00	7.50	Uniform	
(5-2)	6.00	7.00	7.50	Uniform	
(5-1)+(5-2)	6.00	7.00	7.50	Uniform	
(5-3)	6.00	7.00	7.50	Uniform	
(5-4)					

Table 4.4-3 Probability Distributions of the Upper Magnitude Cutoff M_u for Coppersmith

EVA: **Kevin COPPERSMITH**

Elicitation of preliminary estimates for the seismicity rates and upper magnitude cutoffs for the zones in the composite seismic sources maps.

Date of the elicitation: 8-Jan-97

ELICITATION OF UPPER MAGNITUDE CUTOFFS: M_u

Names of Zones in the composite set of zonation maps	Magnitude Cutoff M_u				Comments
	Lower bound	Mode	Upper bound	Distribution shape	
3A	5.60	6.40	7.20	Triangle	See the SCR EPRI Study:
3B-3A	5.60	6.40	7.20	Triangle	Extended crust: 5.6, 6.4, 7.2
3C	5.90	6.30	6.70	Triangle	Non-extended crust: 5.9, 6.3, 6.7
3B-3C	5.60	6.40	7.20	Triangle	
Charleston					
1A-(Characteristic)	6.80	7.30	7.70	Triangle	Also account for any type of scenario. Handles the geological aspect
1B-(3-blobs)	6.80	7.30	7.70	Triangle	
1C-(ZRA)	6.80	7.30	7.70	Triangle	
1D-(Long--SW-NE)	6.80	7.30	7.70	Triangle	
1E(2side.blobs+1A)	6.80	7.30	7.70	Triangle	Same M_u for both blobs
Bckgnd to Charlstn					
6-Central-Virginia					
7(Coast.Plain-CVSZ)	5.60	6.40	7.20	Triangle	Extended crust
8-Offshore					
ETSZ					
4A-1	5.90	6.30	7.20	Triangle	5.9 from SCR, 7.2 from Chapman's long fault scenario.
(4A-1)+(4A-2)	5.90	6.30	7.20	Triangle	
(4A-1)+(4A-2)+(4A-3)	5.90	6.30	7.20	Triangle	
4B-1	5.90	6.30	7.20	Triangle	
4B-2	5.90	6.30	7.20	Triangle	
4-C-(8-faults)	5.90	6.30	7.20	Triangle	8 faults system, see white paper
4-D-(varying-rates)	5.90	6.30	7.20	Triangle	
4-E-(rate-cylinders)	5.90	6.30	7.20	Triangle	same geometry as 4A, 10% PE
Backgrnd to ETSZ					
(5-1)	5.90	6.30	6.70	Triangle	Non-extended crust, same as 3C
(5-2)	5.90	6.30	6.70	Triangle	
(5-1) + (5-2)	5.90	6.30	6.70	Triangle	
(5-3)	5.90	6.30	6.70	Triangle	
(5-1)+(5-2)+(5-3)	5.90	6.30	6.70	Triangle	

Table 4.4-4 Probability Distributions of the Upper Magnitude Cutoff M_u for Jacob

EVA: **Klaus JACOB**

Elicitation of preliminary estimates for the seismicity rates and upper magnitude cutoffs for the zones in the composite seismic sources maps.

Date of the elicitation: 19-Dec-96

ELICITATION OF UPPER MAGNITUDE CUTOFFS: M_u

Names of Zones in the composite set of zonation maps	Magnitude Cutoff M_u				Comments
	Lower bound	Mode	Upper bound	Distribution shape	
3A	6.50	7.00	7.50	Triangle	Excludes Charleston
3B-3A	6.00	6.50	7.00	Triangle	Complementary to 3A
3C	6.00	6.50	7.00	Triangle	Influenced w/seismicity, consistent
3B-3C	6.50	7.00	7.50	Triangle	with Virginia seismic zone
Charleston					
1A-(Characteristic)	7.00	7.50	7.80	Triangle	Jonston lower bound is 6.9
1B-(3-blobs)	7.00	7.50	7.80	Triangle	Does not exist
1C-(ZRA)	7.00	7.50	7.80	Triangle	
1D-(Long--SW-NE)	6.20	7.00	7.20	Triangle	Elongated with midle same as 1A
1E(2side.blobs+1A)	6.20	7.00	7.20	Triangle	Mu here, only for the side blobs
Bckgnd to Charlstn					
6-Central-Virginia	6.00	6.50	7.00		
7(Coast.Plain-CVSZ)	6.00	6.50	7.00		
8-Offshore	6.80	7.25	7.60		Only a characteristic earthquake
ETSZ					
4A-1	5.50	6.50	7.50	Triangle	
(4A-1)+(4A-2)	5.50	6.50	7.50	Triangle	Lower bound driven by seismicity +.5
(4A-1)+(4A-2)+(4A-3)	5.50	6.50	7.50	Triangle	than historical.
4B-1	5.50	6.50	7.50	Triangle	Upper bound driven by Chapman's
4B-2	5.50	6.50	7.50	Triangle	long fault scenario.
4-C-(8-faults)	5.50	6.50	7.50	Triangle	
4-D-(varying-rates)	5.50	6.50	7.50	Triangle	
4-E-(rates-cylinders)	5.50	6.50	7.50	Triangle	
Backgrnd to ETSZ					
(5-1)	6.00	6.50	7.00	Triangle	
(5-2)	6.00	6.50	7.00	Triangle	
(5-1)+(5-2)	6.00	6.50	7.00	Triangle	
(5-3)	6.00	6.50	7.00	Triangle	
(5-1)+(5-2)+(5-3)	6.00	6.50	7.00	Triangle	

Table 4.4-5 Probability Distributions of the Upper Magnitude Cutoff M_u for Talwani

EVA: Pradeep TALWANI

Elicitation of preliminary estimates for the seismicity rates and upper magnitude cutoffs for the zones in the composite seismic sources maps.

Date of the elicitation: 18-Dec-96

ELICITATION OF UPPER MAGNITUDE CUTOFFS: M_u

Names of Zones in the composite set of zonation maps	Magnitude Cutoff M_u				Comments
	Lower bound	Mode	Upper bound	Distribution shape	
3A	5.00	5.50	5.70	Triangle	Excludes Charleston
3B-3A	5.00	5.50	5.70	Triangle	Complementary to 3A
3C	5.00	5.50	5.70	Triangle	Runs along with Piedmont faults
3B-3C	4.80	5.00	5.50	Triangle	with Virginia seismic zone
Charleston					
1A-(Characteristic)	7.00	7.30	7.50	Triangle	
1B-(3-blobs)	7.00	7.30	7.50	Triangle	Delineation based on liquefaction
1C-(ZRA)	7.00	7.30	7.50	Triangle	
1D-(Long--SW-NE)	7.00	7.30	7.50	Triangle	Elongated with midle same as 1A
1E(2side.blobs+1A)	5.50	6.00	6.20	Triangle	
Bckgnd to Charlstn					
6-Central-Virginia	5.00	5.50	5.70		Same as 3C
7(Coast.Plain-CVSZ)	4.00	4.50	5.00		
8-Offshore					No input. Probability of existence=0
ETSZ					
4A-1	5.00	6.00	7.00	Triangle	Difficult to generate more than a
(4A-1)+(4A-2)	5.00	6.00	7.00	Triangle	m=6 because of the limited length of
(4A-1)+(4A-2)+(4A-3)	5.00	6.00	7.00	Triangle	possible fault scenarios. Mostly
4B-1	5.00	6.00	7.00	Triangle	based on historical seismicity, not
4B-2	5.00	6.00	7.00	Triangle	much weight of long N-S fault.
4-C-(8-faults)	5.00	6.00	7.00	Triangle	
4-D-(varying-rates)	5.00	6.00	7.00	Triangle	
4-E-(rate-cylinders)	5.00	6.00	7.00	Triangle	
Backgrnd to ETSZ					
(5-1)	4.50	5.50	5.70	Triangle	Without Giles County, which is
(5-2)	4.50	5.50	5.70	Triangle	localized and is treated separately.
(5-1)+(5-2)	4.50	5.50	5.70	Triangle	The 1916 N Alabama earthquake is
(5-3)	4.50	5.50	5.70	Triangle	a quarry blast (Bollinger, Stover)
(5-1)+(5-2)+(5-3)	4.50	5.50	5.70	Triangle	

Table 4.4-6 Probability Distributions of the Seismicity Rates $f(4)$ for Bollinger

EVA: Gilbert BOLLINGER

Elicitation of preliminary estimates for the seismicity rates and upper magnitude cutoffs for the zones in the composite seismic sources maps.
Date of the elicitation: 8-Jan-97

ELICITATION OF FREQUENCY RATES PER YEAR AT MAGNITUDE 4.0

Names of Zones in the composite set of zonation maps	Frequency rate per year for $M \geq 4.0$		Zone Area (km ²)	$f(4)$ (1/km ²) for $M \geq 4.0$		Return Periods (years)		Comments				
	Lower bound	Upper bound		Lower bound	Upper bound	Lower bound	Upper bound					
3A	0.02	0.0398	0.0667	Triangle	85307	2.344E-05	4.666E-05	7.819E-05	15.0	25.1	50.0	3A1 with Charleston & Bowman removed
3B-3A	0.0098	0.0195	0.0385	Triangle	89362	1.097E-05	2.182E-05	4.308E-05	26.0	51.3	102.0	JGR paper, use 95% confidence bounds, 3A1 removed
3C-Alternative-to-3A	0.05	0.08	0.15	Triangle	51988	9.619E-05	0.0001539	0.0002885	6.7	12.5	20.0	
3B-3C	0.0164	0.0195	0.0244	Triangle	130167	1.26E-05	1.498E-05	1.875E-05	41.0	51.3	61.0	3B with part of 3C in 3B, Bowman & Charleston 1A removed
Charleston												
1A (localized)	0.0122	0.0247	0.0526	Taper-Unif.	1924	0.0006341	0.0012838	0.0027339	19.0	40.5	82.0	Used LLNL regression fit provided
1B (3 blobs)	0.0196	0.0398	0.0847	Taper-Unif.	3098	0.0006341	0.0012838	0.0027339	11.8	25.1	50.9	
1C (ZRA)	0.0507	0.1026	0.2185	Taper-Unif.	7992	0.0006341	0.0012838	0.0027339	4.6	9.7	19.7	
1D (extended blobs)	0.057	0.1155	0.2459	Taper-Unif.	8996	0.0006341	0.0012838	0.0027339	4.1	8.7	17.5	
1E (2 side blobs + 1A)	0.0126	0.0256	0.0545	Taper-Unif.	1993	0.0006341	0.0012838	0.0027339	18.4	39.1	79.1	
Bkgnd-to-Charlston												
6-Central-Virginia	0.0204	0.0331	0.0667	Taper-Unif.	24926	8.184E-05	0.0001328	0.0002676	15.0	30.2	49.0	
7 (Coast Plain-CVSZ)	0.0053	0.0105	0.0208	Taper-Unif.	298749	1.774E-06	3.515E-06	6.962E-06	48.1	95.2	188.7	CVSZ removed
8-Offshore	0.0013	0.0026	0.0051	Taper-Unif.	72932	1.774E-06	3.515E-06	6.962E-06	196.9	390.1	772.9	
ETSZ												
4A-1	0.0537	0.085	0.1612	Taper-Unif.	15746	0.0003411	0.0005397	0.0010237	6.2	11.8	18.6	
(4A-1)+(4A-2)	0.0681	0.1078	0.2045	Taper-Unif.	19973	0.0003411	0.0005397	0.0010237	4.9	9.3	14.7	
(4A-1)+(4A-2)+(4A-3)	0.0833	0.1318	0.25	Taper-Unif.	24422	0.0003411	0.0005397	0.0010237	4.0	7.6	12.0	
4B-1	0.075	0.15	0.3	Taper-Unif.	15746	0.0004763	0.0009526	0.0019052	3.3	6.7	13.3	
4B-2	0.0035	0.0073	0.0139	Taper-Unif.	8676	4.008E-05	8.373E-05	0.0001603	71.9	137.7	287.6	
4C (8 faults)				Taper-Unif.					#DIV/0!	#DIV/0!	#DIV/0!	
4D (varying)-rates					24422	0	0	0	#DIV/0!	#DIV/0!	#DIV/0!	
4E (3 cyl./rate-zones)												
first cylinder-(4-1)	0.0655	0.1036	0.1965	Taper-Unif.	15746	0.0004159	0.0006581	0.0012482	5.1	9.7	15.3	
second cyl.-(4-2)	0.0132	0.0209	0.0396	Taper-Unif.	4227	0.0003119	0.0004935	0.0009362	25.3	47.9	75.8	
third cyl.-(4-3)	0.0046	0.0073	0.0139	Taper-Unif.	4449	0.000104	0.0001645	0.0003121	72.0	136.6	216.2	
Bkgnd-to-ETSZ												
(5-1)	0.0317	0.0662	0.1267	Uniform	79058	4.008E-05	8.373E-05	0.0001603	7.9	15.1	31.6	Giles County & 4A(1+2+3) removed
(5-2)	0.0683	0.1427	0.2733	Uniform	170435	4.008E-05	8.373E-05	0.0001603	3.7	7.0	14.6	
(5-1)+(5-2)	0.1	0.2089	0.4	Uniform	249493	4.008E-05	8.373E-05	0.0001603	2.5	4.8	10.0	
(5-3)				Uniform	81393	0	0	0	#DIV/0!	#DIV/0!	#DIV/0!	
(5-1)+(5-2)+(5-3)				Uniform	340000	0	0	0	#DIV/0!	#DIV/0!	#DIV/0!	
Large-Bowman-9A	0.0054	0.0107	0.0213	Uniform	922	0.0005857	0.0011605	0.0023102	46.9	93.5	185.2	

multiplicative factor for the size of unit area (in km²) =
100
100 km²
Thus the rates in columns 7, 8 and 9 are normalized for

Table 4.4-7 Probability Distributions of the Seismicity Rates f(4) for Chapman

EVA, Martin CHAPMAN

Elicitation of preliminary estimates for the seismicity rates and upper magnitude cutoffs for the zones in the composite seismic sources maps.
Date of the elicitation: 18-Dec-96

ELICITATION OF FREQUENCY RATES PER YEAR AT MAGNITUDE 4.0

Names of Zones in the composite seismic sources maps	Frequency rate per year for $M_s \geq 4.0$		Zone Area (km ²)	Distribution Shape	Return Periods (years)		Comments			
	Lower Bound	Upper Bound			Lower Bound	Upper Bound				
3A	0.037	0.073	8530.7	0.1468 Triangle	4.437E-05	8.5573E-05	0.0017115	6.8	13.7	27.0
3B-Comp-1b-3A	0.0175	0.035	8836.2	0.071 Triangle	1.958E-05	3.9167E-05	7.8333E-05	14.3	28.6	57.1
3C-Alternative-1b-3A	0.037	0.073	5198.8	0.143 Triangle	7.117E-05	0.0014042	0.0027508	7.0	13.7	27.0
3(A+3B)+3C	0.0175	0.035	13016.7	0.071 Triangle	1.344E-05	2.6889E-05	5.3777E-05	14.3	28.6	57.1
Charleston										
1A(localized1886)	0.027	0.053	192.4	0.1068 Triangle	0.0014033	0.00275468	0.00550936	9.4	18.9	37.0
1B(3b1b3b)	0.027	0.053	3098	0.1068 Triangle	0.0008715	0.00171078	0.00342166	9.4	18.9	37.0
1C(ZPA)	0.027	0.053	799.2	0.1068 Triangle	0.0003378	0.00066316	0.00132633	9.4	18.9	37.0
1D(3extended-bloks)	0.027	0.053	899.6	0.1068 Triangle	0.0003001	0.00058915	0.0011783	9.4	18.9	37.0
1E(2a1e-bbbs+1A)	0.008	0.017	199.3	0.0235 Triangle	0.0003001	0.00058915	0.0011783	42.6	85.2	167.2
Background-Charlstin										
6-Central-Virginia	0.022	0.044	2492.6	0.0988 Triangle	8.926E-05	0.00017652	0.008	11.4	22.7	45.5
7-Coastal-plan	0.015	0.03	29874.6	0.06 Triangle	5.021E-06	1.0042E-05	2.0084E-05	16.7	33.3	66.7
8-Offshore	0.0037	0.0073	7293.2	0.0148 Triangle	5.021E-06	1.0042E-05	2.0084E-05	68.3	136.5	273.1
ETZ										
(4-1)-----A	0.051	0.102	1574.6	0.204 Triangle	0.0003239	0.00064778	0.00129557	4.8	9.6	19.6
(4-1)(4-2)-----A	0.0558	0.1115	1997.3	0.2334 Triangle	0.0002739	0.0005585	0.001117	4.5	9.0	17.9
(4-1)(4-2)(4-3)-----A	0.0608	0.1216	2442.2	0.2432 Triangle	0.000249	0.00049791	0.00099582	4.1	8.2	16.4
(4-1)-----B	0.051	0.102	1574.6	0.204 Triangle	0.0003239	0.00064778	0.00129557	4.8	9.6	19.6
(4-2)(4-3)-----B	0.0098	0.0196	867.6	0.0392 Triangle	0.000113	0.00022591	0.00045182	25.5	51.0	102.0
4C-(8-faults)	0.0608	0.1216	100	0.2432 Triangle	0.0608	0.1216	0.2432	4.1	8.2	16.4
4D-(varying-rates)			2442.2	Triangle						
4E-(3.0)/(rate-zones)										
--first-cy-(4-1)	0.0478	0.0956	1574.6	0.1912 Triangle	0.0003036	0.00060713	0.00121427	5.2	10.5	20.9
--second-cy-(4-2)	0.0098	0.0192	422.7	0.0385 Triangle	0.0002277	0.00045535	0.0009107	26.0	52.0	103.9
--third-cy-(4-3)	0.0034	0.0068	444.8	0.0138 Triangle	7.588E-05	0.00015178	0.00030357	74.0	148.1	296.2

Basic estimate. Others in module 4 are proportional to areas.

Rates are estimated on a (10km x 10km) grid basis.

Table 4.4-8 Probability Distributions of the Seismicity Rates $f(4)$ for Coppersmith

EVA: Kevin COPPERSMITH

Elicitation of preliminary estimates for the seismicity rates and upper magnitude cutoffs for the zones in the composite seismic sources maps.

Date of the elicitation: 8-Jan-97

ELICITATION OF FREQUENCY RATES PER YEAR AT MAGNITUDE 4.0

Frequency rate per year for $M \geq 4.0$		Zone Area (km ²)	Distribution shape	$f(4)$ (km ⁻²) for $M \geq 4.0$		Mean	Upper bound	Lower bound	Return Periods (years)		Comments
Mode	Upper bound			Lower bound	Mode				Upper bound		
0.04	0.1	85307	0.2 Triangle	4.68895E-05	0.000117224	0.000234447	5.0	10.0			
0.045	0.04	89362	0.06 Triangle	1.67857E-05	4.47618E-05	6.74426E-05	16.7	25.0			
0.05	0.09	51988	0.15 Triangle	9.6176E-05	0.000173117	0.000288628	6.7	11.1			
		130167		0	0	0					
0.035	0.06	1924	0.1 Triangle	0.001819127	0.003118503	0.005197505	10.0	16.7			
0.035	0.06	3098	0.1 Triangle	0.001129761	0.001936733	0.003227889	10.0	16.7			
0.035	0.06	7992	0.1 Triangle	0.000437938	0.000750751	0.001251251	10.0	16.7			
		8996		0	0	0					
		1993		0	0	0					
0.022	0.044	24926	0.088 Triangle	8.82613E-05	0.00176523	0.003530464	11.4	22.7		45.5 Based on LLNL calculations	
0.015	0.03	298749	0.06 Triangle	5.02094E-06	0.00419E-05	2.00897E-05	16.7	33.3		66.7 Based on LLNL calculations	
0.0027	0.0053	72932	0.016 Triangle	3.70208E-06	2.6704E-06	2.19382E-05	62.5	188.7		370.4 Based on LLNL calculations	
0.07	0.15	15746	0.2 Triangle	0.000444557	0.000952623	0.00170464	5.0	6.7		14.3 Represent the entire seismicity	
0.07	0.15	19973	0.2 Triangle	0.000350473	0.000751014	0.001402028	5.0	6.7		14.3 of the ETSZ, regardless of boundary	
0.07	0.15	24422	0.2 Triangle	0.000286627	0.0006142	0.001128442	5.0	6.7		14.3 location.	
0.045132	0.096742	15746	0.289493 Triangle	0.000286627	0.0006142	0.001128442	7.8	10.3		22.2 Apportion by areas, total of 4B-1	
0.024868	0.053288	8676	0.0710507 Triangle	0.000286627	0.0006142	0.001128442	14.1	18.8		40.2 and 4B-2 equals 4a(1+2+3)	
		24422		0	0	0					
0.055033	0.117927	15746	0.572359 Triangle	0.000349502	0.000748933	0.001497866	6.4	8.5			
0.01108	0.03743	4227	0.0516574 Triangle	0.000262126	0.00056617	0.001132342	31.6	42.1			
0.03887	0.08633	4449	0.0811067 Triangle	2.73755E-05	0.000187233	0.000249644	90.0	120.0			
		79058		0	0	0					
		70435		0	0	0					
		29493		0	0	0					
		11393		0	0	0					
0.25	0.5	340000	0.25 Triangle	7.35294E-05	0.000147059	0.000205882	1.4	2.0			

size of unit area (in km²) =
7, 8 and 9 are normalized for

Table 4.4-9 Probability Distributions of the Seismicity Rates f(4) for Jacob

EVA: Klaus JACOB

Elicitation of preliminary estimates for the seismicity rates and upper magnitude cutoffs for the zones in the composite seismic source maps.
Date of the elicitation: 19-Dec-96

ELICITATION OF FREQUENCY RATES PER YEAR AT MAGNITUDE 4.0

Names of Zones in the composite set of zonation maps	Frequency rate per year for $M_p \geq 4.0$		Zone Area (km ²)	f(4)/(km ²) for $M_p \geq 4.0$		Return Periods (years)		Comments	
	Lower bound	Upper bound		Lower bound	Upper bound	Lower bound	Upper bound		
3A-1	0.05	0.1	85307	5.861E-05	0.00011722	0.00023444	5.0	10.0	20.0
3B-3A	0.05	0.08	89362	5.595E-05	0.0001679	0.0001679	6.7	12.5	20.0
3C-Alternative-to-3A	0.045	0.083	51988	8.666E-05	0.00015965	0.0002885	6.7	12.0	22.2
3B-3C	0.02	0.05	130167	1.536E-05	3.8412E-05	6.146E-05	12.5	20.0	50.0
Charleston									
1A(localized1886)	0.05	0.07	1924	0.0025988	0.00363825	0.0051975	10.0	14.3	20.0
1B(3blobs)	0.05	0.07	3098	0.0016139	0.00225952	0.0032279	10.0	14.3	20.0
1C(ZRA)	0.05	0.07	7992	0.0006256	0.00087588	0.0012513	10.0	14.3	20.0
1D(3extended-blobs)	0.05	0.07	8996	0.0005558	0.00077812	0.0011116	10.0	14.3	20.0
1E(2side-blobs+1A)	0.05	0.07	1993	0.0025088	0.00351229	0.0050176	10.0	14.3	20.0
Backgd-to-Charlstin									Two side blobs. non characteristic part
6-Central-Virginia	0.03	0.08	24926	0.0001204	0.00032095	0.12	8.3	12.5	33.3
7(CoastPlain-CV5Z)	0.01	0.025	298749	3.347E-06	8.3682E-06	1.674E-05	20.0	40.0	100.0
8-Offshore			72932	0	0	0	#DIV/0!	#DIV/0!	#DIV/0!
ET5Z									
4A-1	0.0387	0.0967	15746	0.0002457	0.0006142	0.0010237	6.2	10.3	25.8
(4A-1)+(4A-2)	0.0491	0.1227	19973	0.0002457	0.0006142	0.0010237	4.9	8.2	20.4
(4A-1)+(4A-2)+(4A-3)	0.06	0.15	24422	0.0002457	0.0006142	0.0010237	4.0	6.7	16.7
4B-1	0.0387	0.0967	15746	0.0002457	0.0006142	0.0010237	6.2	10.3	25.8
4B-2	0.0213	0.0533	8676	0.0002457	0.0006142	0.0010237	11.3	18.8	46.9
4C-(8-faults)	0.06	0.15	100	0.06	0.15	0.25	4.0	6.7	16.7
4D-(varying)-rates			24422	0	0	0	#DIV/0!	#DIV/0!	#DIV/0!
4E-(3.cyl.rate-zones)									
--firstcylinder-(4-1)	0.0472	0.1179	15746	0.0002996	0.00074893	0.0012482	5.1	8.5	21.2
--second-cyl-(4-2)	0.0095	0.0237	4227	0.000247	0.0005617	0.0009362	25.3	42.1	105.3
--third-cylind-(4-3)	0.0033	0.0083	4449	7.489E-05	0.00018723	0.0003121	72.0	120.0	300.1
Backgd-to-ETSZ									
(5-1)			79058	0	0	0	#DIV/0!	#DIV/0!	#DIV/0!
(5-2)			170435	0	0	0	#DIV/0!	#DIV/0!	#DIV/0!
(5-1)+(5-2)			249493	0	0	0	#DIV/0!	#DIV/0!	#DIV/0!
(5-3)			81393	0	0	0	#DIV/0!	#DIV/0!	#DIV/0!
(5-1)+(5-2)+(5-3)			340000	0	0	0	#DIV/0!	#DIV/0!	#DIV/0!

multiplicative factor for the size of unit area (in km²) =
100
100 km²
Thus the rates in columns 7, 8 and 9 are normalized for

Table 4.4-10 Probability Distributions of the Seismicity Rates f(4) for Talwani

EVA: Pradeep TALWANI

Elicitation of preliminary estimates for the seismicity rates and upper magnitude cutoffs for the zones in the composite seismic sources maps.
Date of the elicitation: 26-Jan-97

ELICITATION OF FREQUENCY RATES PER YEAR AT MAGNITUDE 4.0

Names of Zones in the composite set of zonation maps	Frequency rate per year for $M_p \geq 4.0$		Zone Area (km ²)	f(4)(/km ²) for $M_p \geq 4.0$		Return Periods (years)			Comments			
	Lower bound	Mode		Upper bound	Lower bound	Mode	Upper bound					
3A	0.07	0.0813	0.0955	Triangle	85307	8.206E-05	9.528E-05	0.00011195	10.5	12.3	14.3	
3B-3A	0.0182	0.0257	0.0955	Triangle	89362	2.037E-05	2.876E-05	0.00010687	10.5	38.9	54.9	
3C-Alternative-to-3A	0.03	0.0407	0.0832	Triangle	51988	5.771E-05	7.829E-05	0.00016004	12.0	24.6	33.3	
3B-3C	0.025	0.0309	0.0955	Triangle	130167	1.921E-05	2.374E-05	7.3367E-05	10.5	32.4	40.0	
Charleston												
1A(localized-fault)	0.0372	0.0407	0.0646	Triangle	1924	0.0019309	0.0021175	0.00335759	15.5	24.5	26.5	
1B(3blobs)				Triangle	3098	#VALUE!	#VALUE!	#VALUE!	#VALUE!	#VALUE!	#VALUE!	
1C(ZBA)				Triangle	7992	#VALUE!	#VALUE!	#VALUE!	#VALUE!	#VALUE!	#VALUE!	
1D(3extended-blobs)				Triangle	8936	0	0	0	#DIV/0!	#DIV/0!	#DIV/0!	
1E(2side-blobs+1A)				Triangle	1993	0	0	0	#DIV/0!	#DIV/0!	#DIV/0!	
Backgd-to-Charlston												
6-Central-Virginia	0.0316	0.0525	0.0589	Triangle	24926	0.0001269	0.0002105	0.00023622	17.0	19.1	31.6	Based on LLNL calculations
7(Coast-Plain-CVSW)	0.01	0.0148	0.0251	Triangle	298749	3.347E-06	4.951E-06	8.4084E-06	39.8	67.6	100.0	Based on LLNL calculations
8-Offshore				Triangle	72932	#VALUE!	#VALUE!	#VALUE!	#VALUE!	#VALUE!	#VALUE!	Based on LLNL calculations
ETSZ												
4A-1				Triangle	15746	#VALUE!	#VALUE!	#VALUE!	#VALUE!	#VALUE!	#VALUE!	Represent the entire seismicity of the ET SZ, regardless of boundary location.
(4A-1)+(4A-2)				Triangle	19973	#VALUE!	#VALUE!	#VALUE!	#VALUE!	#VALUE!	#VALUE!	
(4A-1)+(4A-2)+(4A-3)	0.07	0.0866	0.1412	Triangle	24422	0.0002866	0.0003546	0.00057817	7.1	11.5	14.3	
4B-1				Triangle	15746	#VALUE!	#VALUE!	#VALUE!	#VALUE!	#VALUE!	#VALUE!	Apportion by areas, total of 4B-1 and 4B-2 equals 4a(1+2+3)
4B-2				Triangle	8676	#VALUE!	#VALUE!	#VALUE!	#VALUE!	#VALUE!	#VALUE!	
4C-(8-faults)				Triangle					#DIV/0!	#DIV/0!	#DIV/0!	
4D-(varying)-rates				Triangle	24422	0	0	0	#DIV/0!	#DIV/0!	#DIV/0!	
4E-(3.cyl.rate-zones)												
-first cylinder-(4-1)	0.055	0.0681	0.111	Triangle	15746	0.0003495	0.0004324	0.000705	9.0	14.7	18.2	
-second-cyl.-(4-2)	0.0111	0.0137	0.0224	Triangle	4227	0.0002621	0.0003243	0.00052875	44.7	73.0	90.3	
-third-cylind.(4-3)	0.0039	0.0048	0.0078	Triangle	4449	8.738E-05	0.0001081	0.00017625	127.5	207.9	257.2	
Backgd-to-ETSZ												
(6-1)	0.0778	0.1177	0.1518	Triangle	79058	9.84E-05	0.0001489	0.00019199	6.6	8.5	12.9	
(6-2)	0.1677	0.2538	0.3272	Triangle	170435	9.84E-05	0.0001489	0.00019199	3.1	3.9	6.0	
(6-1)+(5-2)	0.2455	0.3715	0.472	Triangle	249493	9.84E-05	0.0001489	0.00019199	2.1	2.7	4.1	
(6-3)	0.0811	0.1227	0.1582	Triangle	82393	9.84E-05	0.0001489	0.00019199	6.3	8.2	12.3	
(6-1)+(5-2)+(5-3)	0.3346	0.5063	0.6528	Triangle	340000	9.84E-05	0.0001489	0.00019199	1.5	2.0	3.0	

multiplicative factor for the size of unit area (in km²) =
100
Thus the rates in columns 7, 8 and 9 are normalized for
100 km²

Table 4.4-11 Probability Distributions of the Seismicity Rates f(m₁) for Bollinger

EVA: Gilbert BOLLINGER

Elicitation of preliminary estimates for the seismicity rates and upper magnitude cutoffs for the zones in the composite seismic sources maps.
Date of the elicitation: 8-Jan-87

ELICITATION OF FREQUENCY RATES PER YEAR AT MAGNITUDE M₁

Names of zones in the composite set of zonation maps	M ₁	Frequency rates per year for m>=M ₁		Distribution shape	Zone Area (km ²)	f ₀ (km ³) for m>=M ₁		Return Periods (years)		Comments		
		Lower bound	Mode			Upper bound	Lower bound	Upper bound	Mode		Lower bound	Upper bound
3A(1+2)	5.00	2.500E-03	4.900E-03	9.600E-03	Triangle	85307	2.931E-06	5.744E-06	1.125E-05	104.2	204.1	400.0
3B-3A	5.00	1.700E-03	3.300E-03	5.000E-03	Triangle	89362	1.902E-06	3.693E-06	5.595E-06	200.0	303.0	588.2
3C-Alternative-to-3A	6.00	1.000E-04	3.000E-04	1.100E-03	Triangle	51989	1.924E-07	5.771E-07	2.116E-06	909.1	3333.3	10000.0
3B-3C	4.50	4.357E-04	8.278E-04	1.699E-03	Triangle	130167	3.347E-07	6.360E-07	1.305E-06	588.5	1208.0	2295.1
Charleston												
1A(Localized1886)	6.00	1.000E-04	4.000E-04	1.100E-03	U-taper	1924	5.198E-06	2.079E-05	5.717E-05	909.1	2500.0	10000.0
Charleston-Charact.	7.30	2.000E-04	1.000E-03	1.667E-03	U-taper	1924	3.848E-03	1.924E-02	3.207E-02			
1B(3blobs)	6.00	1.000E-04	4.000E-04	1.100E-03	U-taper	3096	3.228E-06	1.291E-05	3.551E-05	909.1	2500.0	10000.0
1C(ZERA)	6.00	1.000E-04	4.000E-04	1.100E-03	U-taper	7992	1.251E-06	5.005E-06	1.376E-05	908.1	2500.0	10000.0
1D(extended-blobs)	6.00	1.000E-04	4.000E-04	1.100E-03	U-taper	8996	1.112E-06	4.446E-06	1.223E-05	909.1	2500.0	10000.0
1E(2side-blobs+1A)	6.00	1.000E-04	4.000E-04	1.100E-03	U-taper	1993	5.018E-06	2.007E-05	5.519E-05	909.1	2500.0	10000.0
Backgnd-to-Charlstin												
5-Central-Virginia	5.50	1.600E-03	3.000E-03	4.170E-03	Taper-U	24926	6.419E-06	1.204E-05	4.170E-05	24.0	333.3	625.0
7(CoastPlain-CV/SZ)	4.50	1.000E-03	1.900E-03	3.900E-03	Triangle	288748	3.347E-07	6.360E-07	1.305E-06	256.4	526.3	1000.0
8-Offshore	4.50	2.441E-04	4.638E-04	9.521E-04	Triangle	72932	3.347E-07	6.360E-07	1.305E-06	1050.3	2155.9	4096.3
ETSZ												
4A-1	6.00	1.032E-03	1.354E-03	1.934E-03	Uniform	15746	6.551E-06	8.599E-06	1.228E-05	517.0	736.6	969.4
4A-1)+(4A-2)	6.00	1.309E-03	1.777E-03	2.453E-03	Uniform	19973	6.551E-06	8.599E-06	1.228E-05	407.6	562.3	764.2
4A-1)+(4A-2)+(4A-3)	6.00	1.600E-03	2.100E-03	3.000E-03	Uniform	24422	6.551E-06	8.599E-06	1.228E-05	333.3	476.2	625.0
4B-1	6.00	2.750E-04	1.100E-03	4.400E-03	Uniform	15746	1.746E-06	6.986E-06	2.794E-05	227.3	909.1	3636.4
4B-2	6.00	1.515E-04	6.061E-04	2.400E-03	Uniform	8676	1.746E-06	6.986E-06	2.766E-05	4.17E+02	1.65E+03	6.60E+03
4C-(6-faults)												
4D-(varying)-rates												
4E-(3-cyl./rate-zones)												
1st-cyl/ndr-(4-1)	6.00	1.288E-03	1.651E-03	2.359E-03	Triangle	15746	7.989E-06	1.049E-05	1.498E-05	424.0	605.7	795.0
second-cyl-(4-2)	6.00	2.533E-04	3.324E-04	4.749E-04	Triangle	4227	5.991E-06	7.864E-06	1.128E-05	2105.9	3008.4	3848.5
3rd-cyl/ndr-(4-3)	6.00	8.895E-05	1.166E-04	1.666E-04	Triangle	4449	1.997E-06	2.621E-06	3.745E-06	6002.4	8574.9	11254.5
Backgnd-to-ETSZ												
5(1)	5.50	1.933E-03	2.408E-03	4.816E-03	Uniform	79058	2.445E-06	3.046E-06	6.092E-06	207.6	415.2	517.3
5(2)	5.50	4.167E-03	5.192E-03	1.039E-02	Uniform	170435	2.445E-06	3.046E-06	6.092E-06	96.3	192.6	240.0
5(1)+(5-2)	5.50	6.100E-03	7.600E-03	1.520E-02	Uniform	249493	2.445E-06	3.046E-06	6.092E-06	65.8	131.6	163.9
5(3)	5.50				Uniform	81393	0.000E+00	0.000E+00	0.000E+00	#DIV/0!	#DIV/0!	#DIV/0!
5(1)+(5-2)+(5-3)	5.50				Uniform	340006	0.000E+00	0.000E+00	0.000E+00	#DIV/0!	#DIV/0!	#DIV/0!
Large-Bowman-9A	5.50	1.300E-03	2.700E-03	5.400E-03	Uniform	92.2	1.410E-04	2.928E-04	5.857E-04	185.2	370.4	769.2

multiplicative factor for the size of unit area (in km²) = 100
Rates in columns 7, 8 and 9 are normalized for 100 km²

Table 4.4-12 Probability Distributions of the Seismicity Rates f(m) for Chapman

EVA: Martin CHAPMAN

Elicitation of preliminary estimates for the seismicity rates and upper magnitude cutoffs for the zones in the composite seismic sources maps.
Date of the elicitation: 19-Dec-96

ELICITATION OF FREQUENCY RATES PER YEAR AT MAGNITUDE M_i

Names of Zones in the composite set of zonation maps	M _i		Frequency rate per year for m>=M _i		Distribution shape	Zone Area (km ²)	(d)/(km ²) for m>=M _i		Return Periods (years)		Comments
	Lower bound	Upper bound	Mode	Upper bound			Lower bound	Mode	Lower bound	Upper bound	
3A	5.90	3.00E-04	1.00E-03	3.00E-03	Triangle	85307	3.517E-07	1.172E-06	333.3	1000.0	3333.3
3B-3A	6.00	2.670E-05	1.060E-04	4.250E-04	Triangle	89362	2.988E-08	1.186E-07	2352.9	9434.0	37453.2
3C-Alternative-to-3A	6.00	5.500E-05	2.200E-04	8.800E-04	Triangle	51988	1.058E-07	4.232E-07	1136.4	4545.5	18181.8
3B-3C	6.00	2.670E-05	1.060E-04	4.250E-04	Triangle	130167	2.051E-08	8.143E-08	2352.9	9434.0	37453.2
Charleston											
1A (localized 1888)	6.50	1.450E-04	2.900E-04	5.800E-04	Triangle	1924	7.536E-06	1.507E-05	1724.1	3448.3	6896.6
Charleston-Charard	7.20	5.000E-04	1.000E-03	1.198E-03	Uniform	1924	9.620E-03	1.924E-02	#DIV/0!	#DIV/0!	#DIV/0!
1B (3blobs)					Triangle	3098	0.000E+00	0.000E+00	#DIV/0!	#DIV/0!	#DIV/0!
1C (ZRA)	6.50	5.000E-04	1.000E-03	1.198E-03	Uniform	7992	6.256E-06	1.251E-05	834.7	1000.0	2000.0
1D (3extended-blobs)					Triangle	8996	#VALUE!	0.000E+00	#DIV/0!	#DIV/0!	#VALUE!
1E (2side-blobs+1A)					Triangle	1993	0.000E+00	0.000E+00	#DIV/0!	#DIV/0!	#DIV/0!
Background-to-Charlston											
6-Central-Virginia	6.00	6.000E-04	2.400E-03	9.500E-03	Triangle	24926	2.407E-06	9.629E-06	105.3	416.7	1666.7
7-Coast Plain-CV(SZ)	6.00	1.000E-04	3.000E-04	1.400E-03	Triangle	298749	3.347E-08	1.004E-07	714.3	3333.3	10000.0
8-Offshore	6.00	1.800E-05	7.324E-05	2.470E-04	Triangle	72932	2.468E-08	1.004E-07	4048.6	13654.2	55555.6
ETSZ											
4A-1	6.00	1.853E-04	7.413E-04	2.965E-03	Triangle	15746	1.177E-06	4.708E-06	337.3	1349.0	5396.7
(4A-1)+(4A-2)	6.00	1.717E-04	5.275E-04	2.128E-03	Triangle	19973	8.599E-07	2.641E-06	470.3	1895.7	5822.6
(4A-1)+(4A-2)+(4A-3)	6.00	2.100E-04	6.450E-04	2.600E-03	Triangle	24422	8.599E-07	1.065E-05	384.6	1550.4	4761.9
4B-1	6.00	2.750E-04	1.100E-03	4.400E-03	Triangle	15746	1.746E-06	6.986E-06	227.3	909.1	3636.4
4B-2	6.00	3.560E-05	1.422E-04	5.690E-04	Triangle	8676	4.103E-07	1.639E-06	1.76E+03	7.03E+03	2.81E+04
4C-(6 faults)					Triangle				#DIV/0!	#DIV/0!	#DIV/0!
4D-(varying)-rates					Triangle	24422	0.000E+00	0.000E+00	#DIV/0!	#DIV/0!	#DIV/0!
4E-(3 cyl-rate-zones)					Triangle						
first-cylinder-(4-1)	6.00	1.651E-04	5.071E-04	2.044E-03	Triangle	15746	1.049E-06	3.220E-06	489.2	1972.1	6057.0
second-cyl-(4-2)	6.00	3.324E-05	1.021E-04	4.115E-04	Triangle	4227	7.864E-07	2.415E-06	2429.9	9794.8	30084.0
third-cylind-(4-3)	6.00	1.166E-05	3.582E-05	1.444E-04	Triangle	4449	2.621E-07	8.051E-07	6925.8	27918.1	85748.5
Background-to-ETSZ											
(5-1)	6.00	6.000E-04	2.500E-03	1.010E-02	Triangle	79058	7.589E-07	3.162E-06	9.90E+01	4.00E+02	1.67E+03
(5-2)	6.00	3.100E-03	1.250E-02	5.000E-02	Triangle	170435	1.819E-06	7.334E-06	2.00E+01	8.00E+01	3.23E+02
(5-1)+(5-2)	6.00	6.500E-03	2.620E-02	1.050E-01	Triangle	249493	2.605E-06	1.050E-05	9.52E+00	3.82E+01	1.54E+02
(5-3)	6.00	1.880E-04	7.500E-04	3.000E-03	Triangle	81393	2.310E-07	9.215E-07	333.3	1333.3	5319.1
(5-1)+(5-2)+(5-3)	6.00				Triangle	340000	0.000E+00	0.000E+00	#DIV/0!	#DIV/0!	#DIV/0!

100

100 km²

multiplicative factor for the size of unit area (in km²) = Rates in columns 7, 8 and 9 are normalized for

Table 4.4-13 Probability Distributions of the Seismicity Rates $f(m)$ for Coppersmith

EVA: Kevin COPPERSMITH

Elicitation of preliminary estimates for the seismicity rates and upper magnitude cutoffs for the zones in the composite seismic sources maps.
Date of the elicitation: 8-Jan-07

ELICITATION OF FREQUENCY RATES PER YEAR AT MAGNITUDE M_i

Names of Zones in the composite set of zonation maps	M_i	Frequency rate per year for $m > M_i$			Zone Area (km ²)	$f(m)$ (1/km ²) for $m > M_i$			Return Periods (years)			Comments
		Lower bound	Mode	Upper bound		Distribution shape	Lower bound	Mode	Upper bound	Lower bound	Mode	
3A	6.00	1.500E-04	4.000E-04	1.000E-03	85307	1.759E-07	4.689E-07	1.172E-06	1000.0	2500.0	6666.7	
3B-3A	5.50	2.000E-04	5.000E-04	1.500E-03	89362	2.238E-07	5.595E-07	1.679E-06	666.7	2000.0	5000.0	
3C-Alternative-to-3A	5.50	3.000E-04	9.000E-04	2.500E-03	51988	5.771E-07	1.731E-06	4.809E-06	400.0	1111.1	3333.3	
3B-3C	5.50	2.000E-04	5.000E-04	1.500E-03	130167	1.536E-07	3.841E-07	1.152E-06	666.7	2000.0	5000.0	
Charleston												
1A(localizer/1886)	6.50	1.000E-04	3.500E-04	2.000E-03	1924	5.199E-06	1.819E-05	1.040E-04	500.0	2857.1	10000.0	
Charleston-Charad.	7.30	4.000E-04	1.000E-03	3.300E-03	1924	7.696E-03	1.924E-02	6.407E-02				
1B(3blobs)				Triangle	3098	0.000E+00	0.000E+00	0.000E+00	#DIV/0!	#DIV/0!	#DIV/0!	
1C(ZFA)	6.50	1.000E-04	3.500E-04	2.000E-03	7992	1.251E-06	4.379E-06	2.503E-05	500.0	2857.1	10000.0	
1D(3extended-blobs)				Triangle	8996	#VALUE!	0.000E+00	0.000E+00	#DIV/0!	#DIV/0!	#VALUE!	
1E(2side-blobs+1A)				Triangle	1993	0.000E+00	0.000E+00	0.000E+00	#DIV/0!	#DIV/0!	#DIV/0!	
Seignod-to-Charlism												
3-Central-Virginia				Triangle	24926	#VALUE!	#VALUE!	#VALUE!	#VALUE!	#VALUE!	#VALUE!	
7(Coast Plain-CV/SZ)				Triangle	298749	#VALUE!	#VALUE!	#VALUE!	#VALUE!	#VALUE!	#VALUE!	
3-Offshore				Triangle	72932	#VALUE!	#VALUE!	#VALUE!	#VALUE!	#VALUE!	#VALUE!	
ETSZ												
4A-1	6.00	9.671E-05	2.578E-04	6.447E-04	15746	6.142E-07	1.638E-06	4.095E-06	1551.0	3877.5	10340.0	
4A-1)+(4A-2)	6.00	1.227E-04	3.271E-04	8.178E-04	19973	6.142E-07	1.638E-06	4.095E-06	1222.8	3056.9	8151.7	
4A-1)+(4A-2)+(4A-3)	6.00	1.500E-04	4.000E-04	1.000E-03	24422	6.142E-07	1.638E-06	4.095E-06	1000.0	2500.0	6666.7	
4B-1	6.00	9.671E-05	2.579E-04	6.447E-04	15746	6.142E-07	1.638E-06	4.095E-06	1551.0	3877.5	10340.0	
4B-2	6.00	5.329E-05	1.421E-04	3.583E-04	8676	6.142E-07	1.638E-06	4.095E-06	2.81E+03	7.04E+03	1.88E+04	
4C-(8-faults)				Triangle					#DIV/0!	#DIV/0!	#DIV/0!	
4D-(varying)-rates				Triangle	24422	0.000E+00	0.000E+00	0.000E+00	#DIV/0!	#DIV/0!	#DIV/0!	
4E-(3.cyl.rate-zones)												
first-cylinder-(4-1)	6.00	1.179E-04	3.145E-04	7.862E-04	15746	7.489E-07	1.997E-06	4.993E-06	1272.0	3179.9	8479.8	
second-cyl-(4-2)	6.00	2.374E-05	6.331E-05	1.583E-04	4227	5.617E-07	1.498E-06	3.745E-06	6317.6	15794.1	42117.6	
third-cyl-(4-3)	6.00	8.330E-06	2.221E-05	5.563E-05	4449	1.872E-07	4.993E-07	1.248E-06	18007.2	45018.0	120048.0	

Table 4.4-14 Probability Distributions of the Seismicity Rates $\lambda(m)$ for Jacob

EVA: Klaus JACOB

Elicitation of preliminary estimates for the seismicity rates and upper magnitude cutoffs for the zones in the composite seismic sources maps.
Date of the elicitation: 19-Dec-96

ELICITATION OF FREQUENCY RATES PER YEAR AT MAGNITUDE M_i

Names of Zones in the composite set of zonation maps	M _i	Frequency rate per year for m > M _i		Zone Area (km ²)	$\lambda(m)$ (1/km ²) for m > M _i		Return Periods (years)		Comments
		Lower bound	Mode		Upper bound	Lower bound	Mode	Upper bound	
3A	6.50	5.00E-05	1.600E-04	85307	5.861E-08	1.876E-07	1.172E-06	6250.0	20000.0
3B-3A	6.00	8.000E-05	1.500E-04	89362	8.952E-08	1.679E-07	8.952E-07	6666.7	12500.0
3C-Alternative-to-3A	6.00	1.000E-04	3.000E-04	51988	1.924E-07	5.771E-07	1.924E-06	3333.3	10000.0
3B-3C	6.00	1.000E-04	9.000E-04	130167	7.682E-08	6.914E-07	1.538E-06	1111.1	10000.0
Charleston									
1A(localized/886)	6.00	5.000E-04	2.000E-03	1924	2.599E-05	1.040E-04	1.715E-04	500.0	2000.0
Charleston-Charact	7.50	7.100E-04	1.600E-03	1924	1.366E-02	3.078E-02	5.772E-02	625.0	1408.5
1B(3blobs)									
1C(ZRA)	7.50	5.000E-04	2.000E-03	3098	#VALUE!	#VALUE!	0.000E+00	#VALUE!	#VALUE!
1D(3extended-blobs)	6.00	7.100E-04	1.600E-03	7992	6.256E-06	2.503E-05	4.129E-05	500.0	2000.0
1E(2side-blobs+1A)	6.00	7.100E-04	1.600E-03	8996	7.892E-06	1.779E-05	3.335E-05	625.0	1408.5
Beckand-to-Charlston									
6-Central-Virginia	6.00	2.000E-04	1.300E-03	24926	8.024E-07	5.216E-06	4.000E-03	769.2	5000.0
7-Coast-Plain-CVNSZ	6.00	1.500E-04	4.500E-04	298749	5.021E-08	1.506E-07	4.017E-07	2222.2	6666.7
8-Ofishore									
ETSZ									
4A-1	6.00	1.900E-04	1.300E-03	15746	1.207E-06	8.266E-06	2.032E-05	312.5	5263.2
4A-1+H(4A-2)	6.00	2.400E-04	1.600E-03	19973	1.202E-06	8.011E-06	2.053E-05	243.9	4166.7
4A-1+4A-2+H(4A-3)	6.00	3.000E-04	2.000E-03	24422	1.228E-06	8.189E-06	2.047E-05	200.0	3333.3
4B-1	6.00	1.900E-04	1.300E-03	15746	1.207E-06	8.266E-06	2.032E-05	312.5	5263.2
4B-2	6.00	1.070E-04	7.100E-04	8676	1.233E-06	8.183E-06	2.052E-05	1.41E+03	9.33E+03
4C-(8-faults)									
4D-(var/ing)-rates									
4E-(3 CVL rates-zones)									
first-cylinder-(4-1)	6.00	2.368E-04	1.577E-03	15746	1.502E-06	1.001E-05	2.503E-05	253.7	4226.2
second-cyl-(4-2)	6.00	4.762E-05	3.175E-04	4227	1.127E-06	7.510E-06	1.878E-05	3150.1	21000.4
third-cyl-(4-3)	6.00	1.671E-05	1.114E-04	4449	3.755E-07	2.503E-06	6.258E-06	3591.5	59857.6
Beckand-to-ETSZ									
(5-1)	6.00	3.200E-02	6.500E-02	79958	4.048E-05	8.222E-05	2.530E-05	5.00E+01	3.13E+01
(5-2)	6.00	4.500E-03	9.600E-03	170435	2.640E-06	5.633E-06	1.584E-05	3.70E+01	1.04E+02
(5-1)+(5-2)	6.00	8.100E-03	1.600E-02	249493	3.247E-06	6.413E-06	1.924E-05	2.08E+01	6.25E+01
(5-3)	6.00	1.900E-03	3.800E-03	82393	2.306E-06	4.612E-06	1.396E-05	263.2	526.3
(5-1)+(5-2)+(5-3)	6.00	1.000E-02	2.000E-02	340000	2.941E-06	5.882E-06	1.765E-05	16.7	100.0

100

100 km²

multiplicative factor for the size of unit area (in km²) =
Rates in columns 7, 8 and 9 are normalized for

Table 4.4-15 Probability Distributions of the Seismicity Rates $\lambda(m)$ for Talwani

EVA: Pradeep TALWANI

Elicitation of preliminary estimates for the seismicity rates and upper magnitude cutoffs for the zones in the composite seismic sources maps.
Date of the elicitation: 20-Jan-97

ELICITATION OF FREQUENCY RATES PER YEAR AT MAGNITUDE M_1

Names of Zones in the composite set of zonation maps	M_1	Frequency rate per year for $m > M_1$			Distribution shape	Zone Area (km ²)	$\lambda(m)$ for $m > M_1$			Return Periods (years)			Comments
		Lower bound	Mode	Upper bound			Lower bound	Mode	Upper bound	Lower bound	Mode	Upper bound	
3A	5.00	6.46E-03	6.92E-03	1.51E-02	Triangle	77241	8.36343E-06	8.95697E-06	1.9601E-05	66.1	144.5	154.8	
3B-3A	5.00	1.41E-03	3.16E-03	1.51E-02	Triangle	100274	1.40615E-06	3.15137E-06	1.50986E-05	66.1	316.5	709.2	
3C-Alternative-to-3A	5.00	2.50E-03	3.09E-03	1.29E-02	Triangle	52780	4.73664E-06	5.85449E-06	2.44032E-05	77.6	323.6	400.0	
3B-3C	4.50	9.23E-03	9.77E-03	3.43E-02	Triangle	132203	6.98169E-06	7.39015E-06	2.59298E-05	29.2	102.4	108.3	
Charleston													
1A(localized1886)	6.80	1.00E-04	1.23E-04	2.00E-03	Triangle	1924	5.19751E-06	6.39293E-06	0.00010395	500.0	8130.1	10000.0	
Charleston-Charact.	7.30		2.00E-03		Uniform	1924	#VALUE!	0.03848	#VALUE!				
1B(blobs)					Triangle	4985	#VALUE!	#VALUE!	0	#DIV/0!	#VALUE!	#VALUE!	
1C(ZRA)					Uniform	11920	#VALUE!	#VALUE!	#VALUE!	#VALUE!	#VALUE!	#VALUE!	
1D(extended-blobs)					Triangle	15266	#VALUE!	#VALUE!	#VALUE!	#VALUE!	#VALUE!	#VALUE!	
1E(2side-blobs+1A)					Triangle	3060	#VALUE!	#VALUE!	#VALUE!	#VALUE!	#VALUE!	#VALUE!	
Background-Charlstin													
6-Central-Virginia	5.00	0.00589	7.69E-03	0.01	Triangle	24926	2.36299E-05	3.04501E-05	0.01	100.0	131.8	169.8	
7(Coast.Plain-CVNSZ)	4.00	1.00E-02	1.48E-02	0.02512	Triangle	323675	3.08952E-06	4.5694E-06	7.76087E-06	39.5	67.6	100.0	
8-Offshore						57200							
ETSZ													
4A-1	5.50	5.68E-04	8.00E-04	4.07E-03	Triangle	15746	3.60785E-06	5.07801E-06	2.58405E-05	245.8	1250.7	1760.3	
(4A-1)+(4A-2)	5.50	7.21E-04	1.01E-03	5.16E-03	Triangle	19973	3.60785E-06	5.07801E-06	2.58405E-05	193.8	986.0	1387.7	
(4A-1)+(4A-2)+(4A-3)	5.50	8.81E-04	1.24E-03	6.31E-03	Triangle	24419	3.60785E-06	5.07801E-06	2.58405E-05	158.5	806.5	1135.1	
4B-1	5.50	5.68E-04	8.00E-04	4.07E-03	Triangle	15746	3.60785E-06	5.07801E-06	2.58405E-05	245.8	1250.7	1760.3	
4B-2	5.50	3.13E-04	4.41E-04	2.24E-03	Triangle	8676	3.60785E-06	5.07801E-06	2.58405E-05	4.46E+02	2.27E+03	3.19E+03	
4C-(8-faults)					Triangle								
4D-(varying)-rates					Triangle	15746	0	0	0				
4E-(3.cyl.rate-zones)					Triangle								
first cylinder-(4-1)	5.50	0.00069295	0.000974899	0.00496098	Triangle	15746	4.3989E-06	6.19141E-06	3.15063E-05	201.6	1025.7	1443.7	
second-cyl-(4-2)	5.50	0.000139456	0.000196283	0.000998828	Triangle	4227	3.29917E-06	4.64356E-06	2.36297E-05	1001.2	5094.7	7170.7	
third-cylind-(4-3)	5.50	4.89267E-05	6.8664E-05	0.000350428	Triangle	4449	1.09972E-06	1.54785E-06	7.67657E-06	2853.6	14521.4	20438.7	
Background-ETSZ													
(5-1)	5.00	1.49E-02	1.87E-02	1.96E-02	Triangle	110000	1.35154E-05	1.70152E-05	1.78192E-05	5.10E+01	5.34E+01	6.73E+01	
(5-2)	5.00	2.08E-02	2.62E-02	2.74E-02	Triangle	154000	1.35154E-05	1.70152E-05	1.78192E-05	3.64E+01	3.82E+01	4.80E+01	
(5-1)+(5-2)	5.00	3.72E-02	4.68E-02	4.90E-02	Triangle	274872	1.35154E-05	1.70152E-05	1.78192E-05	2.04E+01	2.14E+01	2.69E+01	
(5-3)	5.00	0.008784998	0.011059875	0.011562482	Triangle	65000	1.35154E-05	1.70152E-05	1.78192E-05	86.2	90.4	113.8	
(5-1)+(5-2)+(5-3)	5.00	0.045952298	0.057851655	0.060585291	Triangle	340000	1.35154E-05	1.70152E-05	1.78192E-05	16.4	17.3	21.8	

100

100 km²

multiplicative factor for the size of unit area (in km²) =
Rates in columns 7, 8 and 9 are normalized for

REFERENCES

- Abrahamson, N.A. and K.M. Shedlock. "Overview." *Seismological Research Letters*. Vol. 68, No. 1, p. 9-23: 1997.
- Abrahamson, N.A. and W.J. Silva. "Empirical Response Spectral Attenuation Relations for Shallow Crustal Earthquakes." *Seismological Research Letters*. Vol. 68, No. 1, p. 94-127: 1997.
- Atkinson, G. and Boore, P. "Ground Motion Regulations for Eastern North America." *Bulletin of the Seismological Society of America*. Vol. 85, p. 17-30: 1995.
- Boore, D.M., W.B. Joyner, and T.E. Fumal. "Equations for Estimating Horizontal Response Spectra and Peak Acceleration From Western North American Earthquakes: A Summary of Recent Work." *Seismological Research Letters*. Vol. 68, No. 1, p. 128-153: 1997.
- Campbell, K.W. "Empirical Near-Source Attenuation Relationships for Horizontal and Vertical Components of Peak Ground Acceleration, Peak Ground Velocity, and Pseudo-Absolute Acceleration Response Spectra." *Seismological Research Letters*. Vol. 68, No. 1, p. 154-179: 1997.
- Electric Power Research Institute (EPRI). "Guidelines for Site Specific Ground Motions." EPRI, Palo Alto, California. TR-102293. 1993.
- Frankel, A., Burnhard, C., Perkins, D., Leyendecker, E.V., Dickman, N., Hanson, S. and Hopper, M. "National Seismic Hazard Maps: Documentation." U.S. Geological Survey. Open-File Report 96-532, 110 p. 1996.
- Idriss, I.M. "Procedures for Selecting Earthquake Ground Motions at Rock Sites." National Institute of Standards and Technology, Gaithersburg, Maryland. Report No. NIST GCR 93-625. 1991.
- Idriss, I.M. "Equations for Peak Horizontal Acceleration," written communication to N.A. Abrahamson, 4 November 1996.
- Horton, S.P., Dr. de Polo and W.R. Walter: "Source Parameters and Tectonic Setting of the 1990 Lee Vining, California Earthquake Sequence." *Bulletin of the Seismological Society of America*. Vol. 87, pp. 1035-1045: 1997.
- Joyner, W.B. and D.M. Boore. "Measurement, Characterization, and Prediction of Strong Ground Motion." Proceedings Conference on Earthquake Engineering and Soil Dynamics II—Recent Advances in Ground-Motion Evaluation, J.L. Von Thun, ed., Park City, Utah, June 27-30, 1988. Geotechnical Special Publication No. 20, p. 43-102. American Society of Civil Engineers: New York. 1988.
- National Research Council, NAS/NRC. "Review of: 'Recommendations for Seismic Hazard Analysis: Guidance on Uncertainty and Use of Experts.'" National Academy Press. 1997.
- Nuclear Regulatory Commission (U.S.) (NRC). NUREG-1563, "Branch Technical Position on the Use of Expert Elicitation in the High Level Radioactive Waste Program." NRC: Washington, D.C. 1996.
- Nuclear Regulatory Commission (U.S.) (NRC). NUREG/CR-6372, "Recommendations for Probabilistic Seismic Hazard Analysis: Guidance on Uncertainty and Use of Experts." NRC: Washington, D.C. 1997.
- Sadigh, K., C.-Y. Chang, J.A. Egan, F. Makdisi, and R.R. Youngs. "Attenuation Relationships for Shallow Crustal Earthquakes Based on California Strong Motion Data." *Seismological Research Letters*. Vol. 68, No. 1, p. 180-189: 1997.
- Savy, J., Boissonnade, A., Mensing, R. and Short, S. "Eastern U.S. Seismic Characterization Update." UCRL-ID-115111. Lawrence Livermore National Laboratory: Livermore, CA. June 1993.

Silva, W.J. and K. Lee. "WES RASCAL Code for Synthesizing Earthquake Ground Motions." *State-of-the-Art for Assessing Earthquake Hazards in the United States*. Miscellaneous Paper S-73-1, Report 24. U.S. Army Engineers Waterways Experiment Station: Vicksburg, Mississippi. 1987.

Somerville, P. and N. Abrahamson. "Prediction of Ground Motion for Thrust Earthquakes,

Report to California." Strong Motion Instrumentation Program (SMIP), Sacramento, CA: 1995.

Wells, D.L. and K.J. Coppersmith. "New Empirical Relationships Among Magnitude, Rupture Length, Rupture Width, Rupture Area, and Surface Displacement." *Bulletin of the Seismological Society of America*. Vol. 84, p. 974-1002: 1994.

**APPENDIX A: WHITE PAPERS DEVELOPED ASA RESULT OF ISSUES
RAISED IN WORKSHOP #1**

Discreet Charleston earthquake source.

Pro: Pradeep Talwani

Con: Gill Bollinger

Discreet fault sources within the ETSZ.

Pro: Martin Chapman

Con: Klaus Jacob

Discreet local fault sources for Vogtle

Pro Kevin Coppersmith

Con: Pradeep Talwani

(DRAFT)

**ARGUMENTS FOR A DISCRETE CHARLESTON, SOUTH CAROLINA,
EARTHQUAKE SOURCE ZONE**

by
**Pradeep Talwani
and
Ronald Marple**

Sections a – c are intentionally not included

d. Stratigraphy

Auger-hole and well data along the ZRA to the north and south of Lake Moultrie reveal uplifted stratigraphy. Investigation of the anomalously-oriented, early Pleistocene Summerville barrier and underlying shallow marine sediments near Summerville reveals that they were deposited on a NNE-trending, buried structural high, which is reflected in the pre-Plio-Pleistocene surface near Summerville (Weems and Obermeier, 1990) (Fig. 3).

In northeastern South Carolina, the base of a prominent, widespread clay unit (lagoonal/bay environment, Woollen, 1978) within the Black Creek Formation (Upper Cretaceous) is upwarped ~45 m beneath the northern end of the ZRA between the Lynches and Pee Dee rivers (Fig. 4). Further south along the east side of the ZRA between the Lynches and Santee rivers, this Upper Cretaceous horizon exhibits a west-side-up flexure, which suggests faulting or folding of this horizon. However, the contours in the southwestern part of the map area are poorly constrained due to the lack of subsurface data in this area. This linear, NNE-trending area of upwarped, Upper Cretaceous sediments between the Santee and Pee Dee rivers is aligned with the inferred uplift associated with the Summerville barrier to the south (Fig. 3).

e. Shallow seismic reflection data

Shallow seismic reflection data are available along certain portions of the ZRA. The EXXON Exploration Company acquired a seismic reflection profile across the South Carolina Coastal Plain (unpublished data) during the mid 1980s that traverses the ZRA between the Black and Lynches rivers (Fig. 5). These data reveal two steeply-dipping faults about 3.8 km apart that are approximately centered on the ZRA (Fig. 5). Displacements along the steep, west-dipping fault toward the east side of the ZRA decrease from about 20 ms (about 20 m) for the deepest (720 ms, about 720 m) continuous reflector (Jurassic-age basalt flow?) to about 8 ms (8 m) for the reflector at about 320 ms (~320 m) depth (Fig. 5). The reflectors above appear gently upwarped. The fault to the west dips steeply to the east and displays small (< 10 ms) displacements to within about 340 ms (~340 m) of the surface. These two faults are nearly centered on the upwarped Upper Cretaceous sediments along the ZRA (Fig. 5), which suggests that the two faults on the EXXON profile are part of a buried active fault system, uplift along which produced the upwarped Upper Cretaceous sediments and the ZRA.

Additional shallow seismic reflection surveys were acquired near Summerville. Three seismic reflection surveys acquired by the U.S. Geological Survey in the early 1980s near Summerville (e.g., SC-4, SC-6, and SC-10; Fig. 2) revealed three possible faults (Gants and Cooke faults, and the edge of the missing 'J' of Fig. 2; Hamilton et al., 1983) that are nearly centered on the ZRA. The Gants and Cooke faults, both of which coincide with the linear aeromagnetic anomaly, are characterized by west-side-up offsets of about 50 m in a Jurassic-age basalt layer at a depth of about 700 to 750 m (Hamilton et al., 1983). Marple and Talwani (1993) reinterpreted the edge of the missing 'J' as an offset in the Jurassic-age basalt at about 750 m depth. Three shallow, high resolution seismic reflection profiles that were acquired across the ZRA near Summerville in 1993 by the University of South Carolina also revealed

buried faults with small west-side-up offsets and/or upwarped sediments (Marple, 1994) (Fig. 2). A few of these coincide with the linear magnetic anomaly (Fig. 2), which suggests the presence of a NNE-trending buried fault zone beneath the ZRA near Summerville.

f. Microseismicity

Using instrumentally-recorded seismicity data from the MPSSZ, Talwani (1982, 1986) identified two intersecting faults in the Summerville area, the north-northeast-trending Woodstock fault and the northwest-trending Ashley River fault (Fig. 3). The Woodstock fault dips steeply to the west and is associated with right-lateral, oblique, strike-slip motion whereas the Ashley River fault is associated with reverse motion, upthrown to the southwest (Madabhushi and Talwani, 1993). During the period between 1980 and 1990 the seismicity was concentrated primarily near the intersection of these faults (Madabhushi and Talwani, 1993). Although the seismicity between 1991 and early 1995 was located near the main cluster of microseismic activity, more recent seismicity (1995 and 1996) lies farther from this cluster along the trend of the Woodstock fault as defined by Talwani (1982).

g. Paleoseismology

Recent analyses of all available paleoseismological data suggest that there may have been at least six and possibly 7 paleoearthquakes in the outer South Carolina Coastal Plain. A search was carried out for paleoliquefaction features within fluvial deposits inland near the Edisto River and Bowman, although none were found. The only paleoliquefaction features that have been found in South Carolina lie along the coast northeast and southwest of Charleston (Weems et al., 1986; Amick and Gelinis, 1991; Rajendran and Talwani, 1993). The ages of the paleoearthquakes are $110, 546 \pm 17$, 1001 ± 33 , 1641 ± 89 , 3548 ± 66 , 5038 ± 166 and 5300 - 6300 years before present (Talwani and Amick, in preparation). The discovery of sandblows of similar ages near Charleston and to its northeast and southwest argue for a source near Charleston. However, sandblows for the event dated at 1641 ± 89 were found only in the north near Georgetown and Myrtle Beach, and not near Charleston, which argues for a seismic source north of Charleston. These observations suggest that the seismic source associated with the seismicity near Charleston extends to the northeast, possibly along the Woodstock fault. No evidence of a source of prehistoric earthquakes was found towards the northwest.

h. Conclusions

Based on all the data presented in the sections above, we conclude that the seismic activity in Charleston is associated with a NNE-trending fault along the ZRA. A fault length of 50 to 60 km is required to generate an Mw 7.3 earthquake (Johnston's (1996) estimate of the 1886 Charleston earthquake). The extent of the buried fault associated with the ZRA and other features described above provide an adequate length for an Mw 7.3 earthquake.

III. EVIDENCE OF TECTONIC ACTIVITY

Evidence of tectonic activity is divided into loosely-defined time scales, which cover the last 1,000,000 years. These different lines of evidence include the ZRA, upwarped Plio-Pleistocene deposits, paleoearthquakes, releveling, current seismicity and GPS investigations.

a. Holocene to 1,000,000 years

Evidence of tectonic activity along the ZRA during this time range comes from a variety of observations. The upwarped floodplains along the Santee, Lynches and Pee Dee rivers (Fig. 1) indicate tectonic activity between about 100,000 years and Holocene time. Observations of surficial deposits combined with changes in the cross-valley shapes of the Santee and Lynches river valleys along their arc-shaped curves suggest local uplift along the ZRA since at least Penholoway time (~750,000 years, McCartan et al., 1990) and through Holocene time.

b. Thousands of years to present

Paleoliquefaction data suggest that there was earthquake activity at least as far back as 5,000 years. Historical seismicity has been documented for about the last 300 years. In view of the current seismicity we conclude that there has been tectonic activity for at least the last 5,000 years. Additional evidence of local tectonic activity for the last 100 years comes from an evaluation of the releveling data in the area. These data suggest localized uplift south of Summerville.

Results of recent GPS surveys show that there is localized high strain accumulation in the MPSSZ. The calculated strain rate is about two orders of magnitude greater than the background. The direction of compression obtained from GPS is in good agreement with the direction of SHmax inferred from other data (e.g., Zoback et al., 1986).

c. Conclusions

Data presented above provide evidence for tectonic activity over approximately the last 1,000,000 years.

IV. EVIDENCE FOR A DISCRETE SOURCE

Between Summerville and Middleton Place we have evidence of a northwest-trending fault along the Ashley River. The northwest trend terminates near Summerville along the north-northeast trend of the Woodstock fault/ZRA. No evidence for a NW-trending fault was found northwest of Summerville. In the sections above we showed that integration of a variety of data support the existence of a NNE-trending buried fault along the ZRA. The length of this NNE-trending Woodstock fault/ZRA is adequate to generate the Mw 7.3 estimated for the 1886 Charleston, SC, earthquake. A variety of data indicate that there has been tectonic activity on this feature for at least 1,000,000 years. Currently, the most seismically active part of this feature is its southern end where it intersects with the Ashley

River fault. This is also where localized high strain accumulation was observed by a GPS study. SHmax is favorably oriented with respect to the Woodstock fault to generate right-lateral strike slip faulting.

Based on all these observations we conclude that the seismicity near Charleston is associated with a discrete, ~50-km-long, NNE-trending source--the Woodstock fault.

REFERENCES

- Amick, D.C., and Gelinas, R., 1991, The search for evidence of large prehistoric earthquakes along the Atlantic seaboard: *Science*, v. 251, no. 4994, p. 655-658.
- Hamilton, R.M., Behrendt, J.C., and Ackermann, H.D., 1983, Land multichannel seismic reflection evidence for tectonic features near Charleston, South Carolina, in Gohn, G.S., ed., *Studies related to the Charleston, South Carolina, earthquake of 1886; tectonics and seismicity*: U.S. Geological Survey Professional Paper 1313, p. II-II8.
- Johnston, A.C., 1996, Seismic moment assessment of earthquakes in stable continental regions—III. New Madrid 1811-1812, Charleston 1886 and Lisbon 1755: *Geophysical Journal International*.
- Madabhushi, S., and Talwani, P., 1993, Fault plane solutions and relocations of recent earthquakes in Middleton Place Summerville seismic zone near Charleston, South Carolina: *Bulletin of the Seismological Society of America*, v. 83, no. 5, p. 1442-1466.
- Marple, R.T., 1994, Discovery of a possible seismogenic fault system beneath the Coastal Plain of South and North Carolina from an integration of river morphology and geological and geophysical data [Ph.D. dissert.]: Columbia, University of South Carolina, 354 p., 13 plates.
- Marple, R.T., and Talwani, P., 1993, Evidence of possible tectonic upwarping along the South Carolina coastal plain from an examination of river morphology and elevation data: *Geology*, v. 21, no. 7, p. 651-654.
- McCartan, L., Weems, R.E., and Lemon, E.M., Jr., 1990, Quaternary stratigraphy in the vicinity of Charleston, South Carolina, and its relationship to local seismicity and regional tectonism, in *Studies Related to the Charleston, South Carolina, Earthquake of 1886-Neogene and Quaternary Lithostratigraphy and Biostratigraphy*: U.S. Geological Survey Professional Paper 1367-A, p. A1-A39.
- Phillips, J.D., 1988, Buried structures at the northern end of the early Mesozoic South Georgia basin, South Carolina, as interpreted from aeromagnetic data, in Froelich, A.J., and Robinson, G.R., eds., *Studies of the early Mesozoic basins of the eastern United States*: U.S. Geological Survey *Bulletin* 1776, p. 248-252.
- Rajendran, C.P., and Talwani, P., 1993, Paleoseismic indicators near Bluffton, South Carolina: An appraisal of their tectonic implications: *Geology*, v. 21, p. 987-990.
- Talwani, P., 1982, An internally consistent pattern of seismicity near Charleston, South Carolina: *Geology*, v. 10, p. 655-658.
- Talwani, P., 1986, Seismotectonics of the Charleston region, in *Proceedings, National Conference on Earthquake Engineering, 3rd: Earthquake Engineering Research Institute*, v. 1, p. 15-24.
- Weems, R.E., and Obermeier, S.F., 1990, The 1886 Charleston earthquake -- An overview of geologic studies, *Proceedings, Water Reactor Safety Information Meeting, 17th*: U.S. Nuclear Regulatory Commission NUREG/CP-0105, p. 289-313.

- Weems, R.E, Obermeier, S.F., Pavich, J.J., Gohn, G.S., Rubin, M., Phipps, R.L., and Jacobson, R.B., 1986, Evidence for three moderate to large prehistoric Holocene earthquakes near Charleston, South Carolina: Proceedings, 3rd U.S. National Conference on Earthquake Engineering, Earthquake Engineering Research Institute, v. 1, p. 197-208.
- Woollen, I.D., 1978, Structural framework, lithostratigraphy and depositional environments of Upper Cretaceous sediments of eastern South Carolina [Ph.D. dissert.]: Columbia, University of South Carolina, 276 p.
- Zoback, M.L., Nishenko, S.P., Richardson, R.M., Hasegawa, H.S., and Zoback, M.D., 1986, Mid-plate stress, deformation and seismicity, *in* Vogt, P.R., and Tucholke, B.E., eds., *The Geology of North America*, volume M: Boulder, Colorado, Geological Society of America, The Western North Atlantic region, p. 297-312.

FIGURE CAPTIONS

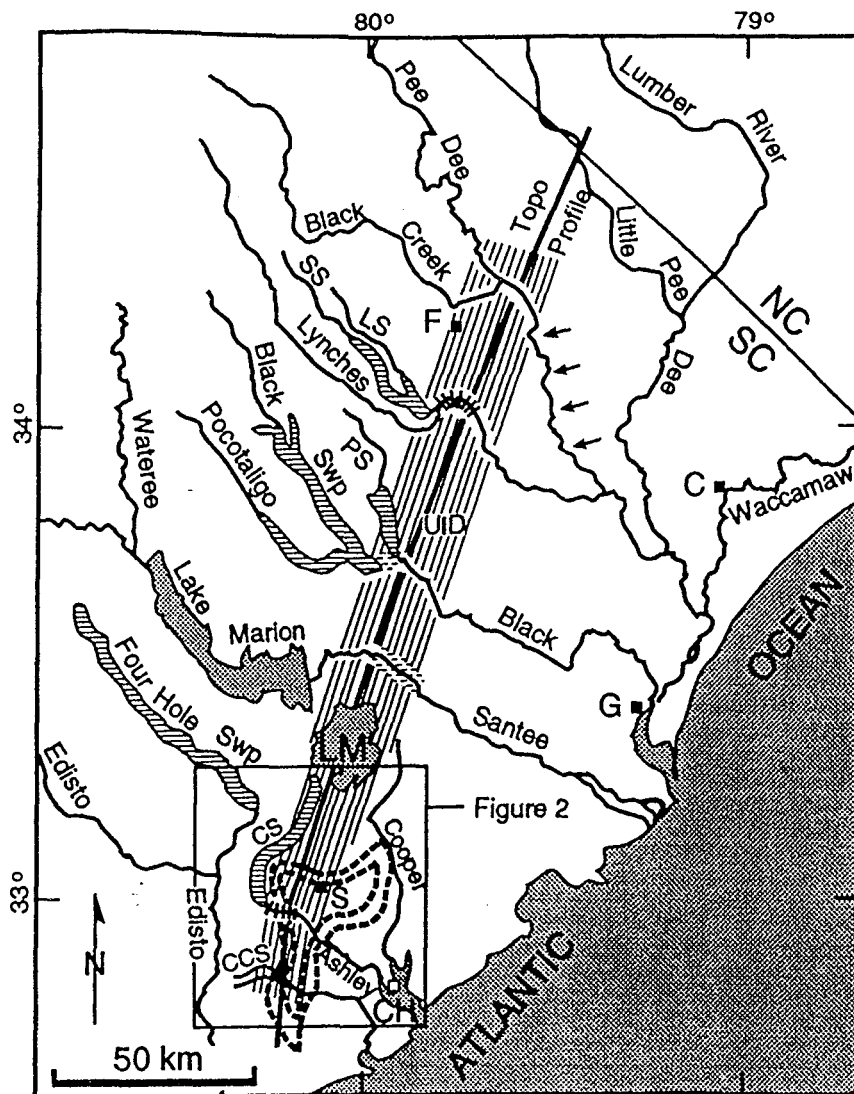
Figure 1: The "zone of river anomalies" (ZRA, NNE-trending striped area), anastomosing stream patterns, pre-1886 sand blow sites (stars, modified from Obermeier et al., 1987, and Prowell and Obermeier, 1991) and Sloan's isoseismals of the 1886 Charleston, S.C., earthquake (dashed closed contours near Summerville-S, after Dutton, 1890). The arrows along the north side of the Pee Dee River downstream of the ZRA denote that part of the river that is flowing against the southwest side of its valley. U/D denotes location of the easternmost fault of the two buried faults inferred on the EXXON seismic reflection profile (unpublished data) (see Fig. 5). C-Conway, CCS-Caw Caw Swamp, CH-Charleston, CS-Cypress Swamp, F-Florence, G-Georgetown, LM-Lake Moultrie, LS-Lake Swamp, PS-Pudding Swamp, S-Summerville, SS-Sparrow Swamp. Location of figure 2 is shown.

Figure 2: Locations of seismicity (1974-1996, black dots) compared with the "zone of river anomalies" (ZRA, NNE-trending stripes) and locations of various geological features. Ashley River fault (ARF) and Woodstock fault (WF) shown as dashed lines (from Talwani, 1986). Gray area denotes topographically high areas inferred from topographic profiles (see Fig. 4 of Marple and Talwani, 1993). Line 9 shows part of releveled line from Yemassee (Y) to Charleston (Ch) (from Poley and Talwani, 1986). The area of uplift inferred along Line 9 is dashed. Buried faults and areas of upwarped sediments inferred from seismic reflection data are denoted by U/D and U?, respectively. J-western edge of missing 'J' horizon, C-Cooke fault, G-Gants fault (Hamilton et al., 1983). Ch-Charleston, LM-Lake Moultrie, ML-linear magnetic anomaly inferred from aeromagnetic data of Phillips (1988), S-Summerville.

Figure 3: Spatial comparison of Summerville barrier (bold contour), ZRA (between parallel dashed lines), and linear aeromagnetic anomaly (ML) with the contour map of the base of the Plio-Pleistocene deposits (from Weems and Obermeier, 1990) in the Summerville area. Note the coincidence of the linear magnetic anomaly, Summerville barrier, ZRA, and the NNE-trending structural high on the base of the Plio-Pleistocene sediments (black area, >40 ft contour) between Lake Moultrie and Summerville. LM-Lake Moultrie, M-Moncks Corner, S-Summerville.

Figure 4: Spatial comparison of the ZRA (striped area) with the structure contour map of the base of a clay unit in the Black Creek Formation in northeastern South Carolina and the postulated area of uplift between Lake Moultrie and the Ashley River (black area). Contours in hundreds of feet with respect to mean sea level. Contours modified from Woollen's (1978) map (figure 6.8.8, p. 207). Note the distortion of the contours along or just east of the ZRA. CS-Cypress Swamp, S-Summerville.

Figure 5: Portion of seismic reflection profile acquired by EXXON (unpublished data) that crosses the ZRA. Note the two steeply-dipping buried faults (steeply dipping thin lines) about 3.8 km apart. See figure 1 for location of fault on the east side of this profile.



LEGEND

- +++++ incised river channel
- ||||| dissected floodplain
- ||||| anastomosing stream patterns

Figure 1

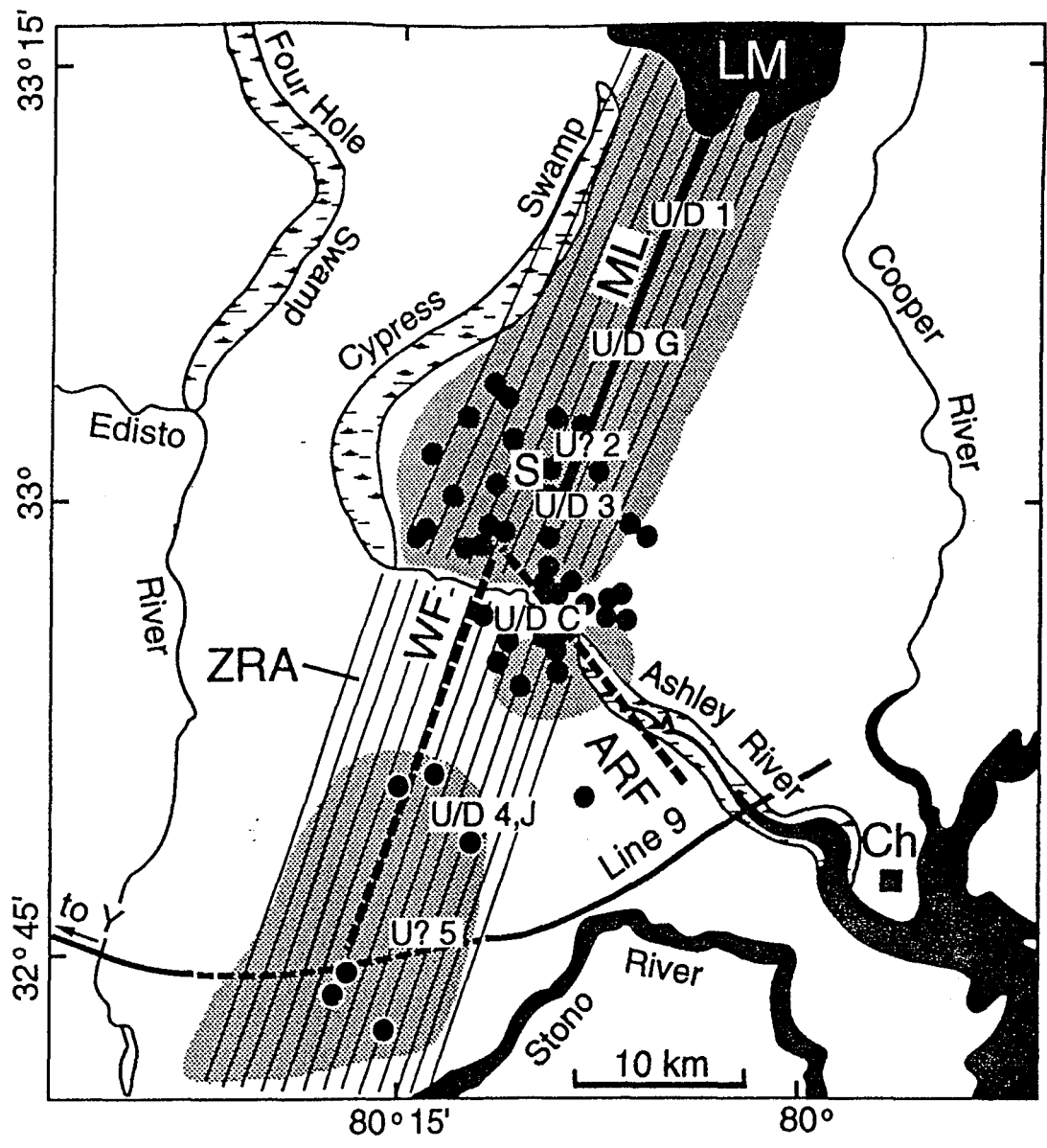


Figure 2

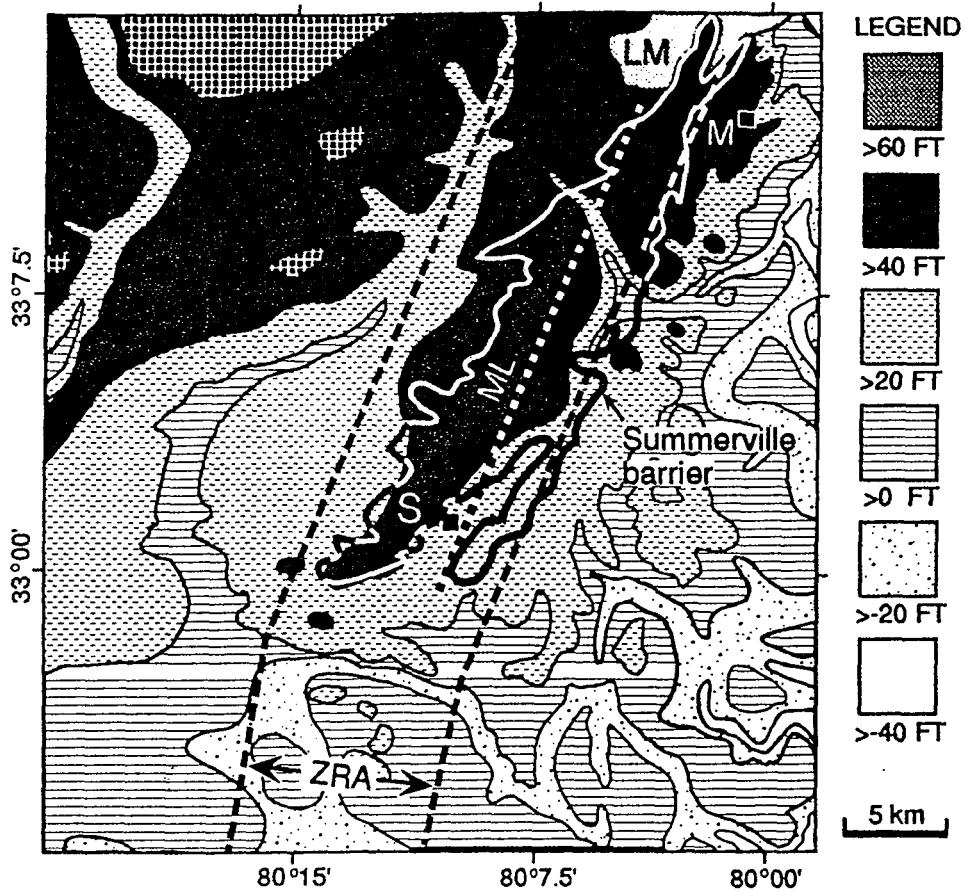


Figure 3

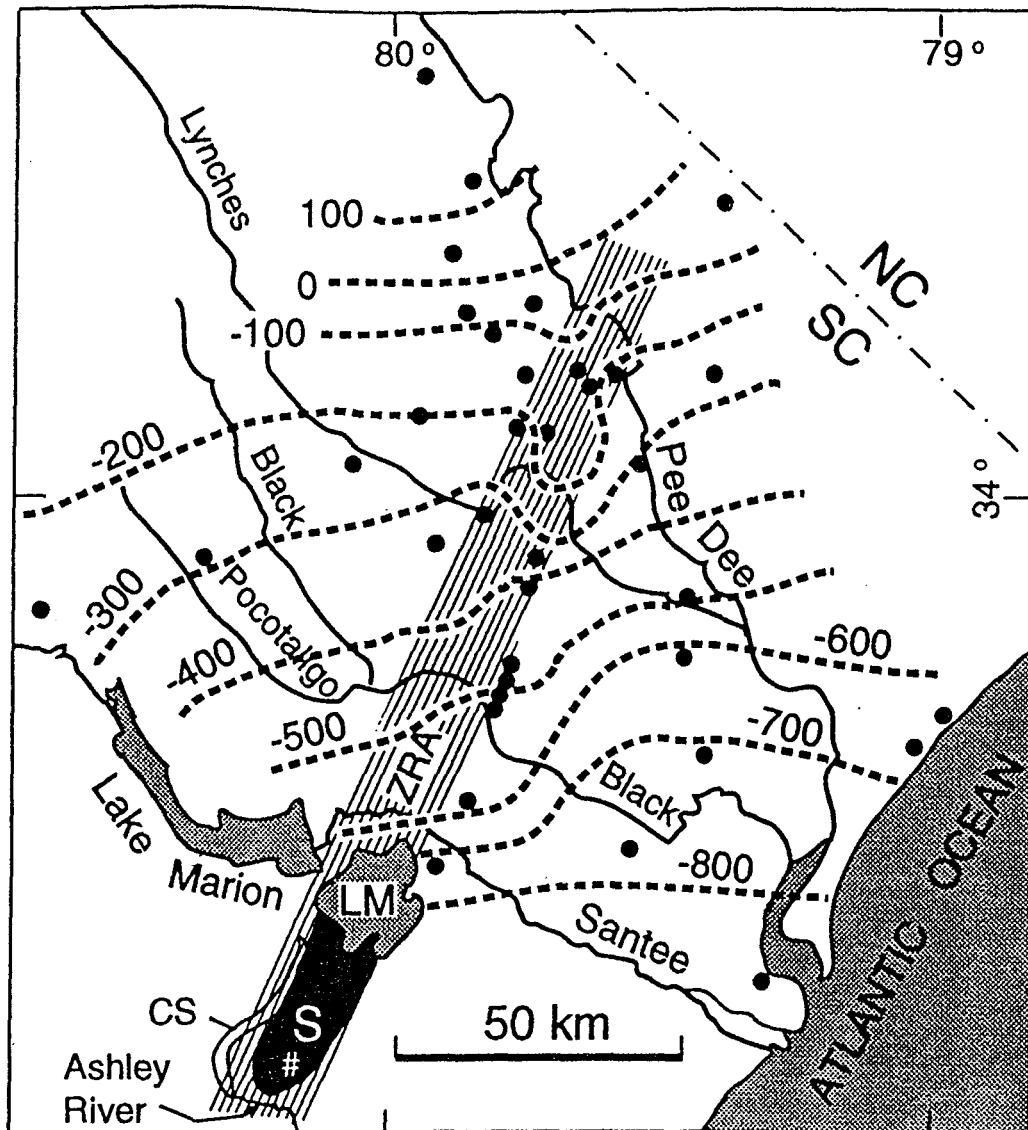


Figure 4

Courtesy of EXXON Exploration Company, Houston

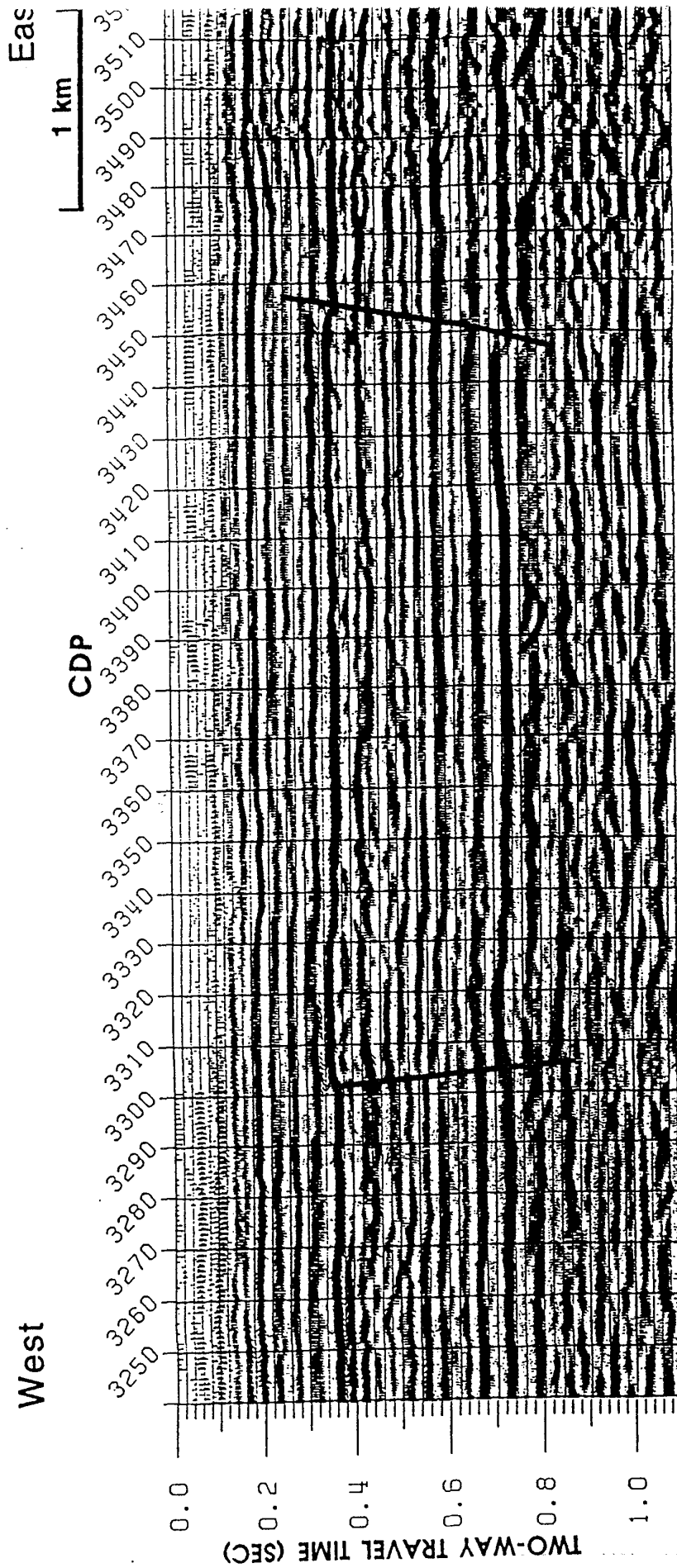


Figure 5

THE CASE FOR A LARGE EARTHQUAKE (M=7+) IN SOUTH CAROLINA AWAY FROM THE CHARLESTON AREA

Gil Bollinger

Introduction

The large 1886 Charleston, South Carolina earthquake (M 7.3, MMI X) dominates the seismicity of that state and its host region. It is an especially singular event in that the next largest earthquake, the 1897 Giles County, Virginia shock, was some one-and-a-half magnitude units and two MMI levels smaller (M 5.7, MMI VIII). South Carolina has a further seismological distinction in that the entire state exhibits a low level of diffuse historical and recent earthquake activity while adjoining North Carolina and Georgia are much less active. I emphasized this fact in a 1973 BSSA paper with the definition of a northwest trending South Carolina-Georgia Seismic Zone. Subsequent instrumental and network monitoring has continued to document earthquake occurrence both in the Charleston area and throughout that northwest zone, including episodes of reservoir-induced seismicity.

Given the singular occurrence of a large earthquake at the apparent terminus of a relatively isolated zone of seismicity the question of the earthquake potential throughout the remainder of that zone arises naturally. This paper will argue that the entire zone should be considered to have a M 7+ capability.

Spatial Considerations

The spatial character of historical and recent seismicity in South Carolina can be characterized as clusters at Charleston and Bowman and a diffuse distribution throughout the remainder of the state, particularly in the Piedmont portion. Comparison of my original definition of seismic zones based primarily on historical seismicity with recent SEUSSN Bulletins showing the activity over the past two decades documents the spatial stationarity of earthquake occurrence in South Carolina over that time period. The only 'newcomer' is the low energy level cluster at Bowman

which has an on again/off again habit since its initial activity in the early 1970's. In terms of energy release, however, the Charleston Zone accounts for some 90+% of the state's strain energy release budget.

As noted above, in 1973 I zoned all of the seismicity in South Carolina, plus a small amount in Georgia, into a South Carolina-Georgia Seismic Zone. In 1992 (USGS Bulletin 2017), given the increase in locational accuracy by the region's networks, I separated the clusters and the diffuse activity into three separate zones labeled Charleston, Bowman and South Carolina Piedmont & Coastal Plain. Recent paleoseismic results indicate possible prehistoric liquefaction producing loci northeast of Charleston and maybe southwest of Charleston also. Both of those sites are in the Coastal Plain and should be considered for zonal status even though one possible explanation for the paleoliquefaction there is amplification by some form of crustal focusing.

The spatial isolation of South Carolina seismicity with respect to the northeast, southwest and southeast directions defines a distinct seismotectonic regime that includes the region's largest known earthquake at its southeast terminus. Charleston's seismic activity appears to be due to a set of intersecting structures. Talwani and his co-workers (Eqke Notes, 1986) have presented extensive evidence for two intersection faults which they term the Woodstock and Ashely River faults. Phillips (USGS Bull. 1776, 1988) interpreted potential field data to show a circular impact-type structure intersecting a throughgoing Triassic basin border fault at Summerville, near the presumed epicenter of the 1886 shock. An intersection feature would certainly explain the concentrated character of the recent seismicity. The sporadic earthquakes at Bowman are also clustered but no probable structures have been identified there.

At least some portion of the diffuse South Carolina Piedmont seismicity carries one or two proposed explanations. Zoback et al (GSA Geol. No. Am., 1986) finds a very high level of horizontal stress in the upper few kilometers of the high-velocity crystalline Piedmont rocks. He argues that this stress regime could result in a 'skin effect' of shallow microseismicity that has no associated large earthquake potential. Talwani (see, e.g., Seism.

Res. Ltrs., 1996) has studied the small central Piedmont and upper Coastal Plain earthquakes (M about 4 or less) with respect to their tectonic and potential field settings. He finds such earthquakes often located on the flanks of intrusive structures and invokes a stress-concentration type of causality - again without large earthquake potential. Finally, the South Carolina Piedmont is unique in the host southeastern U.S. because of its multiple instances of reservoir-induced seismicity (see, e.g., Talwani, Pure & Appld. Geoph., 1984) which also tends to be shallow and associated with high stress levels.

If all of the spatially diffuse South Carolina Piedmont is indeed due to one or both of the proposed mechanisms then only the Charleston locale and perhaps the paleoliquefaction sites have the capability to generate a large earthquake within the state. There are, however, a number of throughgoing structural features in the state, e.g., Triassic basin marginal faults, Modoc fault, etc. that require only an intersecting fault, intrusion or dike to have an adequate strain volume for a Charleston-sized shock. In principle, the Bowman cluster or any of the skin effect/stress amplification earthquakes could be at such an intersection that is currently only experiencing only a very low rate of strain deformation. This type of situation would be similar to the lack of historic and current seismicity that presently exists at the non-Charleston paleoliquefaction sites within the state.

Temporal Considerations

The temporal behavior of South Carolina's seismicity displays the following three different habits :

- (1) Charleston locale - Some 300 years of persistent seismicity (earliest earthquake 1698) with one large historic shock 110 years ago,
- (2) Coastal Plain northeast and southwest of Charleston - Paleoliquefaction sites indicating focusing from Charleston and/or the occurrence of moderate to large prehistoric earthquakes. There is little or no associated historic or recent earthquake activity at these sites and
- (3) Coastal Plain and Piedmont northwest of Charleston - 200+ years of sporadic, low energy level earthquakes and no large historic earthquake.

No prehistoric data available. On/off clustered activity in the Bowman area.

In terms of recurrence rates, we have the following (Bollinger, USGS Bull. 2017, 1992) :

Charleston Zone	Log Nc = 1.69 - 0.77mb	Observed Mmax ~ 7.3
Bowman Zone	Log Nc = 1.34 - 0.78mb	Observed Mmax ~ 4.5
SC P/CP Zone	Log Nc = 1.86 - 0.80mb	Observed Mmax ~ 4.8

Interestingly, while there is the expected large difference in the zonal observed Mmax's and seismicity levels (a-values), the proportions of small to large shocks that have occurred are all at a b-value of about 0.8. Comparing these a-values and b-values with those from the host region (SE US) and geological provinces (Coastal Plain and Piedmont) (Bollinger, JGR,1989) :

SE US	Log Nc = 3.12 - 0.84mb,
Piedmont	Log Nc = 2.18 - 0.81mb,
Coastal Plain	Log Nc = 2.22 - 0.78mb,

we again find the same b-value (0.8) and the expectably very different a-values. Thus, within the resolution of the historical seismicity data base, significant differences are not found between the region and its various subdivisions in the small-to-large earthquake proportions. This provides no spatial or temporal constraints or preferences on the occurrence of a large earthquake in the region.

Geologic Considerations

The tectonic setting at Charleston is almost certainly non-unique. Therefore, similar settings probably exist elsewhere in the region - perhaps in the South Carolina Piedmont - and are candidates for future large shocks.

The rate of the Charleston source, about 1/500 yr, would leave obvious structural evidence (Cenozoic mountains) over geologic time frames. Such evidence is not found at Charleston which implies an episodic, 'on/off' source. This allows for the presence of currently 'off' sources elsewhere in

the region, including the South Carolina Piedmont, that can turn 'on' in the future.

Given the same plate motions driving the seismicity over much of the past few tens of millions of years (Klitgord and Schouten, GSA, The Geol. of No. Am., 1986) then the eastern U.S. seaboard, including Charleston, has probably maintained the same approximate rate of seismicity over that time interval. Therefore, before Charleston turned on, any accumulated strain deformation was released elsewhere, most likely along the belt of Mesozoic extensional faults which includes the South Carolina Piedmont (R. Wheeler, written comm., 1996). Such sources can, in principle, turn 'on' again.

In high strain-rate interplate areas the faulting tends to be rather organized with earthquakes repeating themselves - but there are occasional outliers. It may be that in low strain-rate intraplate areas the long term variance of the faulting process is very large which results in a spatially uniform, long term seismicity (M. Chapman, written comm., 1996). Surely, there should also be the occasional 'outlier' shocks there. Such a seismic environment could host more than one large earthquake source in an area the size of the state of South Carolina.

Possible Locations for Large South Carolina Earthquakes

If the the temporal habits described above are indeed applicable to South Carolina's next large earthquake then assigning a large earthquake potential outside of the Charleston locale requires either that,

- (1) The new source area(s) have exhibited persistent historical seismicity similar to the Charleston area or,
- (2) They have exhibited no appreciable strain release during historic and recent time similar to the paleoliquefaction sites.

If the previously discussed spatial habits are diagnostic, then,

- (3) Only the recent clustered activity at Bowman allows for a possible new large earthquake site.

The geologic considerations presented have argued that,

(4) The Charleston source's tectonic non-uniqueness, 'on/off' recurrence nature from lack of structural/topographic features, the probable presence of other pre-Charleston 'on/off' sources elsewhere in response to long-term, uniform plate motions and low, intraplate strain-rate effects in the region all allow for the occurrence of a large earthquake in the South Carolina Piedmont.

The (1) and (3) possibilities restrict new sources to the Bowman locale. In the (2) possibility, however, the prehistorically active and historically inactive paleoliquefaction sites, if due at least in part to large earthquakes, open the entire South Carolina Coastal Plain area to that level of hazard. Possibility (4) and the fact that there are no prehistoric indicators on the South Carolina Piedmont to define seismicity there argue for the potential occurrence of a large (M 7+) in the South Carolina Piedmont.

AN ARGUMENT IN SUPPORT OF THE CONTENTION THAT A MAJOR
EARTHQUAKE COULD OCCUR IN EASTERN TENNESSEE

by
Martin C. Chapman

Introduction

The eastern Tennessee seismic zone is defined primarily on the basis of small, instrumentally recorded earthquakes that have occurred since regional seismic networks became operational in the area beginning in 1981. The zone lies mostly within the Valley and Ridge province of eastern Tennessee, but extends from northwestern Georgia to near the intersection of the Tennessee, Virginia and Kentucky borders (e.g., Powell et al., 1994). For the period 1981 through 1994, this zone has dominated the recorded seismicity of the southeastern U.S., in sheer number of events. This is partly due to the network detection capability. But when one examines only the larger shocks (Figure 1) the zone remains the most outstanding feature on the regional seismicity map.

Most, if not all of the earthquakes occur beneath the Appalachian thrust sheets, at depths from 5 to 20 km, and therefore indicate a relatively thick section of seismogenic (brittle) crust (Bollinger et al., 1985, 1991; Vlahovic et al 1996). No surface expression of the seismicity has been recognized.

Focal mechanisms indicate that strike-slip is the dominant mode of faulting throughout the seismic zone, with most well-constrained mechanisms showing right-lateral or left-lateral motion on N-S or E-W striking planes, respectively (Johnston et al, 1985, Teague et al 1986, Davison, 1988; Li, 1994; Chapman et al., 1996). A smaller population of events exhibit right-lateral and left-lateral motion on planes striking NE-SW or NW-SE,

respectively (Chapman et al. 1996). The largest historical shock in the zone is mblg 4.6. (Bollinger, 1973; Bollinger et al., 1976; Reinbold and Johnston, 1987).

The Potential for Large Shocks

Kagan and Jackson (1994) give, for the general case, the following conditions that seem reasonable pre-requisites for assigning a high likelihood for future large earthquakes.

- 1) Geological evidence of large earthquakes in the past few thousand years.
- 2) Geodetic or geological evidence of stress accumulation.
- 3) Seismological evidence of large earthquakes in the last few centuries (historical seismicity).
- 4) Seismological evidence of earthquakes in the last few years or decades.

As noted by Kagan and Jackson (1994), the conditions often give contradictory signals. The following discussion will deal with these four conditions in turn.

1) Geological Evidence

We have no geological evidence for past large earthquakes in eastern Tennessee. In assessing the implication of this, the observation that seismicity is occurring at depth, beneath a detachment surface must be considered. This, combined with the great thickness of brittle crust, may represent a situation where the rupture of a magnitude 7.0 shock could be contained entirely within the basement. Given the intra-plate setting, surface expression of repeated shocks might be masked or removed

entirely by erosion, particularly if mechanisms were strike-slip with return periods on the order of several thousand years. Also, lack of geological evidence is relevant to this issue only if it can be argued, with reasonable confidence, that evidence would be in hand if the requisite geologic features actually exist. Clearly, the extent to which geological investigations have been made, or are possible, is an important consideration. For example, the fact that no paleoliquefaction relics have been recognized to date may reflect a lack of deposits susceptible to liquefaction, rather than the absence of large shocks in the past.

2) Stress Accumulation

Accurate geodetic estimates of strain rate are not available for eastern Tennessee. There is some geological evidence for post Cretaceous uplift in the region, based on erosion rates of the order 40m/million yr (Bartholomew and Mills, 1993).

3) Historical Seismicity

The earliest recorded shock in eastern Tennessee was in 1777. There is no record of an eastern Tennessee earthquake with magnitude exceeding 4.6. The lack of moderate earthquakes in the historical past is a potential argument against future large shocks in the seismic zone. To examine this, I use the Virginia Tech catalog of southeastern U.S. earthquakes to develop a recurrence relation for the area shown by the dashed lines in Figure 1. After removing obvious dependent events, the numbers of earthquakes are summed by decade and binned by magnitude as shown in Table 1.

TABLE 1
 Number of Earthquakes by decade
 Eastern Tennessee Seismic Zone

date	Magnitude mblg					
	2.0-2.4	2.5-2.9	3.0-3.4	3.5-3.9	4.0-4.4	4.5+
1994-90	35	19	5	0	0	0
1989-80	59	27	15	4	2	0
1979-70	1	3	2	4	0	1
1969-60	0	3	1	2	1	0
1959-50	0	0	6	4	3	0
1949-40	0	3	2	2	1	0
1939-30	0	0	1	2	0	0
1929-20	0	0	0	2	0	0
1919-10	0	2	3	3	1	0
1909-00	0	0	1	2	1	0
1899-90	0	0	0	0	0	0
1889-80	1	0	1	0	0	0
1879-70	0	2	0	0	1	0
1869-60	0	1	0	0	0	0
1859-50	0	0	0	0	0	0
1849-40	0	0	0	1	0	0
-----	-	-	-	-	-	-
1777	0	0	1	0	0	0

1981

Assuming stationary temporal behavior, I judge (from Table 1) that the catalog is ~~complete for magnitudes 2.0 to 3.5 for the past 15 years; for magnitudes 3.5 to 3.9 it appears complete back to 1900; for magnitudes greater than 4.0 it appears complete to 1870.~~ A least squares fit to the logarithms of the cumulative annual rates gives $\text{Log } N = 3.23 - 1.07 \text{ mblg}$. The data and the regression line are shown in Figure 2. Further assuming that the earthquakes represent a Poisson process, with rates for various magnitudes given by the above equation, I address the question of whether or not the lack of moderate shocks in the historical record has any real significance to the issue of possible large shocks in eastern Tennessee. I ask: how far back in time would the historical record of (complete) seismicity have to extend in order for it to have a more than 0.5 probability of recording the occurrence of at least 1 event

of say, M greater than 7.0? The probability of one or more events in time t is given by $P = 1 - \exp(-Nt)$. Solving for t with $N = 5.5 \times 10^{-5}$ (for mblg = 7.0) and $P = 0.5$ gives $t = 12,600$ years. Results for mblg = 6.0 and mblg = 5.0 are 1,030 and 88 years, respectively. The required catalog dates are as follows:

$t(m=7.0|P=0.5) = 12,600$ years, 10,604BC,
 $t(m=6.0|P=0.5) = 1,066$ years, 930AD,
 $t(m=5.0|P=0.5) = 91$ years, 1905AD.

Clearly, the existing catalog is much too short to have any relevance for magnitudes 6 and greater. However, it appears that at the magnitude 5 level, the catalog MAY be long enough to yield some marginally significant information. It is likely that the catalog is in fact complete for $M > 5$ back to at least 1870, and possibly somewhat earlier. Using the 1870 date as the completeness limit (i.e., setting $t = 126$ years) we get:

$P(\text{at least 1 } M > 5.0 \text{ event} | 126 \text{ years}) = 0.62.$

This is another way of saying that the return period of $M > 5.0$ is 126 years. Let us consider the possibility that the catalog is complete for $M = 5.0$ all the way back to 1840.

$P(\text{at least 1 } M > 5.0 \text{ event} | 156 \text{ years}) = 0.69.$

Although 0.69 is large enough to suggest that eastern Tennessee is slightly overdue for the occurrence of a magnitude 5.0 or larger shock, it is not a statistically significant basis for an argument in favor of a limited maximum magnitude.

For the seismic history to have any bearing on the "Large Earthquake" problem, we need a catalog of length such that the absence of $M > 5$ events is significant at (the very least) the 90%

level: i.e, the catalog would have to be complete for magnitude 5.0 (and contain no $M > 5.0$ events) back to

$t(m=5.0 | P=0.9) = 303 \text{ years, } 1693\text{AD.}$

Assuming that a catalog complete to the days of earliest colonial presence in the area was in hand, an argument favoring a limited maximum magnitude on the basis of that catalog would have to recognize that the Poisson process is a critical assumption.

In summary, there is an appreciable probability of not observing moderate or large shocks during the historical period, and arguments either for (or against) the likelihood of earthquakes significantly larger than the historical maximum of 4.6 are highly equivocal, if based on the catalog alone. Finally, it is worth mentioning that the magnitude 5.0+ earthquake of February 21, 1916 which is listed in most catalogs (e.g., Stover and Coffman, 1993) as centered near Waynesville, North Carolina, produced very nearly the same maximum intensity effects over an extended area of Sevier County, Tennessee, well to the west (Figure 3). In my opinion, the possibility exists that this shock actually occurred somewhere in the Smoky Mountains near the Tennessee - North Carolina border.

4) Recent Seismicity

On the basis of the above arguments, I contend that the information provided by the instrumentally recorded seismicity during the past 15 years currently represents the most viable basis for assessing the potential for large shocks in eastern Tennessee.

In addition to the salient features mentioned in the introduction, the instrumentally located seismicity exhibits other properties which are pertinent to this discussion.

- Unequivocal correlation of the seismicity with major potential field anomalies and crustal velocity anomalies.
- A high degree of consistency of focal mechanism solutions within the spatially extended seismic zone.
- Correlation and mutual consistency of earthquake spatial location, epicenter directional alignment, and focal mechanism solutions.

The correlation between seismicity and the New York - Alabama potential field anomaly is well known (King and Zietz, 1978; Johnston et al., 1985; Powell et al. 1994). Johnston et al. (1985) interpreted the early results of network monitoring as suggesting the existence of a seismogenic crustal block bounded on the northwest by the NY-AL anomaly and on the southeast by the Clingman Lineament (Nelson and Zietz, 1983). After more than a decade of additional monitoring, this conceptual model can be refined.

On the basis of a statistical examination of the epicenter locations and focal mechanism solutions, Chapman et al., (1996) find that much of the seismicity is organized along several NE-trending, en-echelon alignments, which lie along and to the southeast of the potential field anomaly. The NE-trending alignments are responsible for the overall trend of the seismic zone, but do not tell the whole story. The picture is complicated by evidence for easterly-trending alignments, the most prominent of which is at 35.5 deg. N, where a significant number of earthquakes have occurred on both sides of the NY-AL anomaly.

Chapman et al. (1996) interpret the network data as suggesting the existence of a set of northeast-trending basement faults intersected by an east-trending conjugate set (Figure 4). The faults are inferred to be steeply dipping, with mostly right

lateral motion on the NE set, whereas left-lateral slip is inferred for the east-trending set. It is important to note that this interpretation is based on the entire data set, including earthquakes as small as magnitude 0.0; however, as shown in Figure 4, the larger magnitude shocks have occurred along and near the intersections of the inferred faults.

A 3D velocity inversion of the network data by Vlahovic et al. (1996) indicates that the potential field anomalies are spatially correlated with velocity anomalies that extend vertically through the inversion volume (25 km). An integrated interpretation of the velocity and potential field data is being performed by Gordana Vlahovic. At this point, it appears that the juxtaposition of crustal scale potential field and velocity anomalies with a spatially extensive and highly organized zone of seismicity is no coincidence. I argue here that the recent shocks are illuminating two sets of basement faults, one of which trends sub-parallel to major structural/lithologic elements of the crust. The relationship between the faults inferred on the basis of the seismicity and the large scale crustal features responsible for the potential field and velocity anomalies is likely complex, due to the very complex tectonic history of the Appalachians. In fact, there is no strong, presumptive reason to expect anything approaching a one-to-one correlation between the gross structural framework of the crust (that is probably responsible for the potential field/velocity anomalies) on the one hand, and currently seismogenic faults on the other. The reason is that the modern stress field will act to preferentially re-activate favorably oriented faults. In this particular case a clear correlation does exist, involving the NE-trending inferred faults. The east-west trending epicenter alignments may be illuminating (comparatively minor?) cross cutting features more favorably aligned to the modern direction of maximum shear stress. Regardless of the likely complex relationships between currently

seismogenic structures and the gross tectonic fabric, the lengths of the inferred faults are more than sufficient to produce a major shock. In my opinion, this is to be expected given that the velocity and potential field data suggest that this area may be the site of a major Late Paleozoic (or Precambrian) shear zone or Eocambrian zone of extension (Powell et al., 1994).

References

- Bartholomew, M.J. and H.M. Mills, (1993). Old courses of the New River: Its Cenozoic migration and bedrock control inferred from high level stream gravel, *Bull. Geological Soc. Am.*, 103, 73-81.
- Bollinger, G.A. (1973). Seismicity of the southeastern United States, *Bull. Seism. Soc. Am.*, 63, 1785-1808.
- Bollinger, G.A., C.J. Langer and S.T. Harding (1976). The eastern Tennessee earthquake sequence of October through December, 1973, *Bull. Seism. Soc. Am.*, 66, 525-547.
- Bollinger, G.A., M.C. Chapman, M.S. Sibol and J.K. Costain (1985). An analysis of earthquake focal depths in the southeastern U.S., *Geophysical Research Letters*, 12, 785-788.
- Bollinger, G.A., A.C. Johnston, P. Talwani, L.T. Long, K.M. Shedlock, M.S. Sibol and M.C. Chapman (1991). Seismicity of the southeastern United States; 1698 to 1986, in Slemmons, D.B., E.R. Engdahl, M.D. Zoback and D.D. Blackwell, eds., *Neotectonics of North America, Decade Map Vol. 1*, Geological Society of America, Boulder Co., 498 p.
- Chapman, M.C., C.A. Powell, G. Vlahovic, and M.S. Sibol (1996). The nature of faulting in eastern Tennessee inferred from a statistical analysis of focal mechanisms and epicenter location, submitted to *Bull. Seism. Soc. Am.*.

- Davison, F.C. (1988). Stress Tensor Estimates Derived from Focal Mechanism Solutions of Sparse Data Sets: Applications to Seismic Zones in Virginia and Eastern Tennessee, Ph.D. thesis, Virginia Polytechnic Institute and State University, Blacksburg, VA, 189 p.
- Herrmann, R.B. (1979). Surface wave focal mechanisms for eastern North American earthquakes with tectonic implications, *Journ. Geophys. Res.*, 84, 3543-3552.
- Johnston, A.C., D.J. Reinbold and S.I. Brewer, (1985). Seismotectonics of the southern Appalachians, *Bull. Seism. Soc. Am.*, 75, 291-312.
- Kagan, Y.Y. and D.D Jackson (1994). Long-term probabilistic forecasting of earthquakes, *Journal of Geophysical Research*, 99, B7, 13,685-13,700.
- King, E.R., and I. Zietz (1978). The New York - Alabama lineament: geophysical evidence for a major crustal break beneath the Appalachian basin, *Geology*, 6, 312-318.
- Li, Hongsheng (1994). Focal Mechanism Analysis of Eastern Tennessee Seismic Zone Earthquakes, Master's Degree thesis, University of Memphis, Memphis, TN.
- Nelson, A.E. and I. Zietz (1983). The Clingman lineament, other aeromagnetic features and major lithotectonic units in part of the southern Appalachian mountains, *Southeastern Geology*, 24, 147-157.
- Powell, C.A., G.A. Bollinger, M.C. Chapman, M.S. Sibol, A.C. Johnston and R.L. Wheeler (1994). A seismotectonic model for the 300 kilometer long eastern Tennessee seismic zone, *Science*, 264, 686-688.
- Reinbold, D.J. and A.C. Johnston (1987). Historical seismicity in the southern Appalachian seismic zone, *U.S. Geological Survey Open-File Report 87-433*, 859 p.
- Stover, C.W and J.L. Coffman (1993). Seismicity of the United States, 1568-1989 (Revised), *U.S. Geological Survey Prof. Paper 1527*.

Teague, A.G., G.A. Bollinger and A.C. Johnston (1986). Focal mechanism analyses for eastern Tennessee earthquakes (1981-1983), *Bull. Seism. Soc. Am.*, 76, 95-109.

Vlahovic, G, C.A. Powell, M.C. Chapman and M.S. Sibol (1996). P and S wave velocity structure and hypocenter locations in the eastern Tennessee seismic zone, *Abst., Sesimological Research Letters*, 67, no.2, 59.

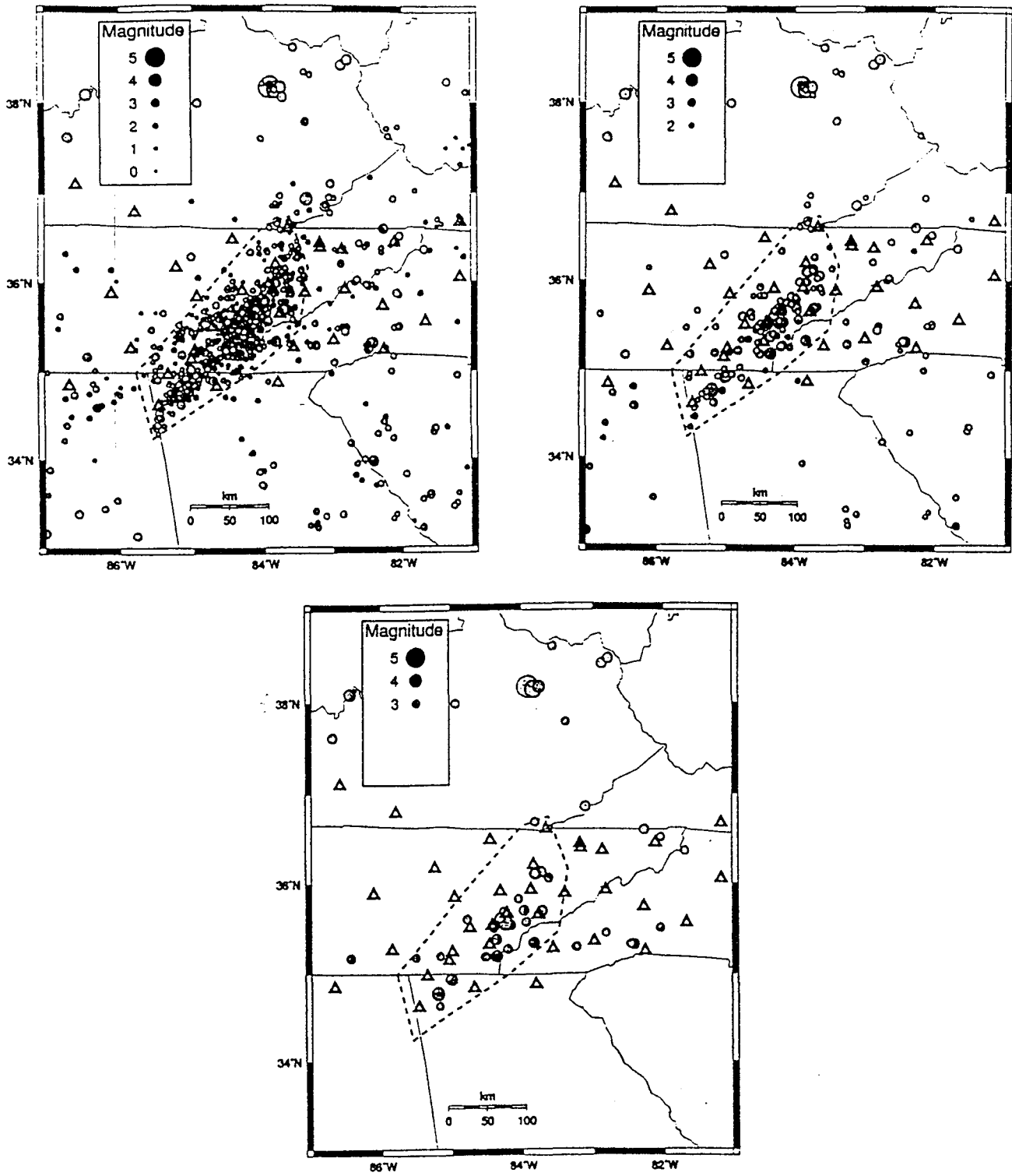


Figure 1: Circles indicate the epicenters of instrumentally detected and located earthquakes in eastern Tennessee and the surrounding region 1977-present. Three different magnitude thresholds are shown, to illustrate the effect of network detection capability. The eastern Tennessee seismic zone is indicated by the dashed line. TVA and University of Memphis seismic network stations are shown by the triangles.

Eastern Tennessee Seismic Zone

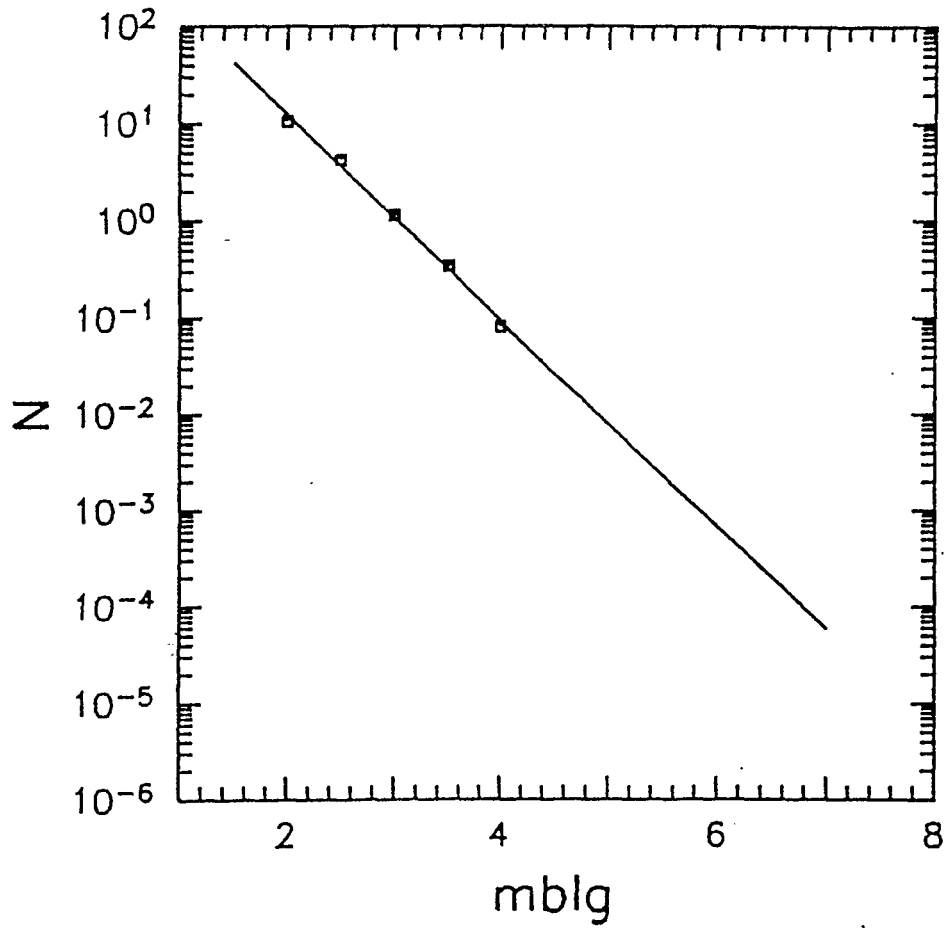


Figure 2: Estimated cumulative annual rates for earthquakes in the eastern Tennessee seismic zone, versus mblg magnitude. The solid line shows a least squares fit to the data, which are shown by the squares.

Figure intentionally omitted

Figure 3: Isoseismal map for the February 21, 1916 earthquake in the southern Appalachians. (from Stover and Coffman, 1993).

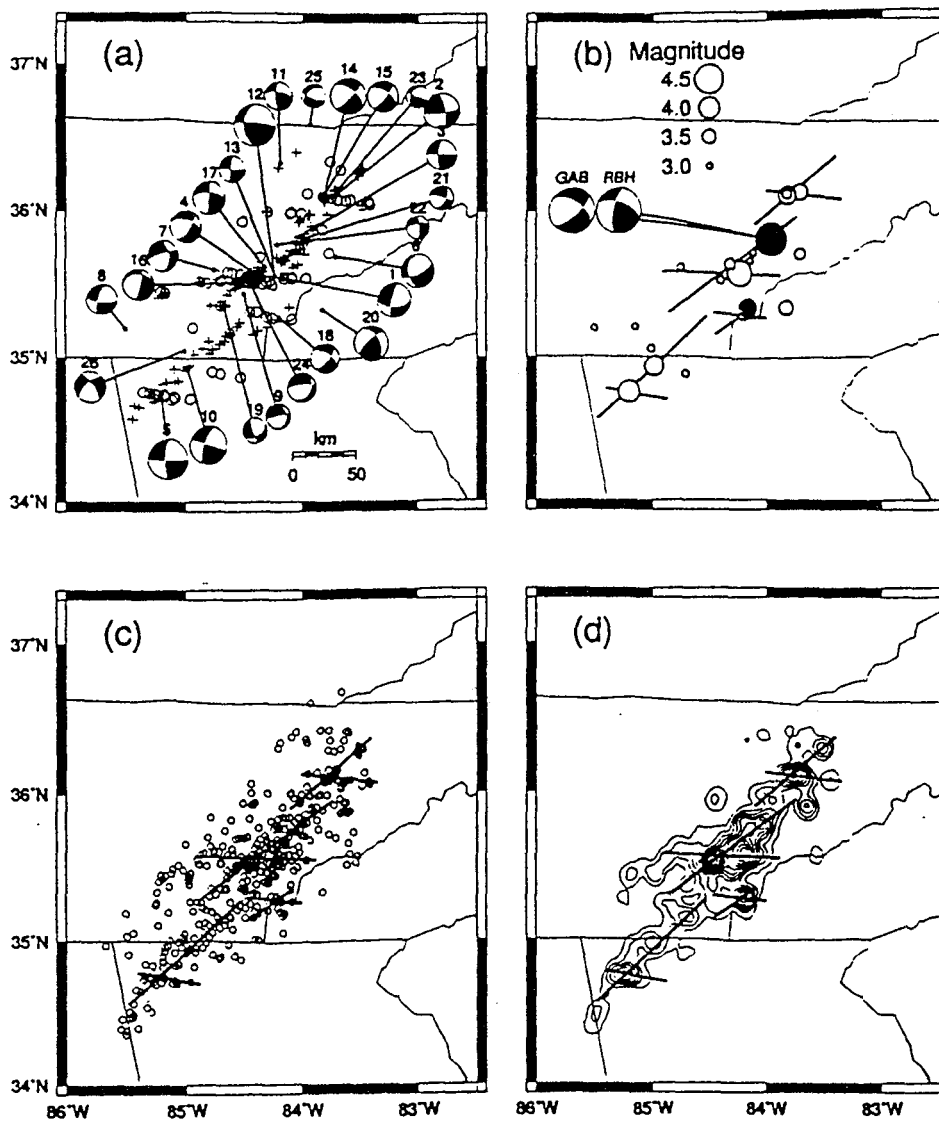


Figure 4: (a) Combined results of sorting the eastern Tennessee earthquake catalog using scale lengths of 20 and 30 km, for 20 degree azimuth ranges centered on N50E (crosses) and N95E (circles). Lower hemisphere focal mechanism solutions have the compressional quadrants shaded. (b) Bold lines indicate faults inferred from (a). The unshaded circles indicate epicenters of instrumentally located earthquakes with magnitudes greater than 3.0, 1983-1995. The large shaded circles represents the Nov. 30, 1973 Maryville earthquake. The smaller shaded circle represents the July 5, 1995 Tellico Plains earthquake. Focal Mechanisms of the Maryville shock derived by Bollinger et al., (1976) and Herrmann (1979) are indicated by GAB and RBH, respectively. (c) Circles show the 474 relocated epicenters. (d) Contours depict the epicenter density function derived using a 10 km kernel half-width.

DRAFT DRAFT DRAFT DRAFT

Invited Arguments Against the Hypothesis that
Major Earthquakes Occur in the Eastern Tennessee Seismic Zone
(ETSZ)

OR:

ESTIMATING THE UPPER-BOUND MAGNITUDE OF THE ETSZ.

by

Klaus H. Jacob
Lamont-Doherty Earth Observatory of Columbia University
Palisades NY 10964
E-mail: jacob@ldeo.columbia.edu

PREAMBLE.

The author was assigned to the task of presenting the arguments AGAINST the likelihood for a large earthquake in the ETSZ. Martin Chapman was assigned to the task to present the opposite arguments, i.e. IN SUPPORT of the notion that the ETSZ can produce "major" earthquakes. That paper is referred to simply as Chapman, (1996) or "PRO" paper.

SUMMARY

In search for arguments for a low upper-bound magnitude M_u for the ETSZ, the low maximum magnitude of $M_{blg}=4.6$ historically observed is the only strong argument in favor of low upper-bound magnitude levels for the ETSZ. Most other arguments lead to M_u values in excess of $M=6$. For this reason we propose a wide range of M_u values, from $M_u = 5$ to 8, to which we assign subjective weights for use in a logic-tree approach.

Introduction.

The ETSZ is at most 300 km long, about 50 km wide, and extends in depth from about 3 to 25 km, with most of the seismicity located below the Paleozoic thrust decollement in presumably cratonic basement which is likely to be at least 1 Billion years old. The tectonic province is known as the Valley and Ridge province of the Appalachians formed of Paleozoic metasedimentary folded thrust sheets above the decollement. The largest event observed for the ETSZ in historic time is the $M_{blg}=4.6$ of 1973 earthquake near Alcoa-Maryville (Bollinger et al, 1991).

What is the upper-bound magnitude earthquake that can be generated by the ETSZ ?

There are several fundamental ways to argue about the upper-bound magnitude M_u of a seismic source zone or seismotectonic province. Possible constraints include:

(1) Catalogs and Seismicity - Magnitude extrapolations to Long Recurrence Periods. A common procedure is to use earthquake catalogs for a region and extrapolating by some statistical procedure or recurrence period argument what the upper bound M_u would or should be. Examples are work by Veneziano (1988?) as part of the EPRI and NCEER studies of seismicity in the CEUS. Martin Chapman (1996), in his PRO paper, used simple recurrence relations assuming the Poisson model

of seismicity and the exponential Gutenberg Richter relation of frequency of occurrence vs. magnitude. He estimated the probabilities of observing certain threshold magnitudes during various (past) periods of exposure time, most of them much longer than the actual catalog duration. Extrapolating a least-square-fit recurrence relation for the entire ETSZ to annual probabilities of $10^{-2}/\text{yr}$ yields magnitudes of about $M_{blg}=5.1$; for $10^{-3}/\text{yr}$ it yields about $M_{blg}=6.0$; and for $10^{-4}/\text{yr}$ it yields about $M_{blg}=6.8$.

(2) Geological Province Arguments. In this case the seismic zone is placed into a type of geological province for which global statistical evaluations have been made. The principle is to replace limited catalog time with plenty of (global) space in the hope to catch the largest possible earthquakes elsewhere in a comparable geologic setting. An example is the approach that EPRI (1994) took for its study of the large-earthquake potential in stable continental regions (SCR). The ETSZ is located in the Appalachian Valley and Ridge province which can be categorized as a Paleozoic thrust and fold belt underlain by unextended cratonic crust. The EPRI (1994) study assigns an upper bound $M=6.8\pm 0.3$ to non-extended crust, craton; and a $M=6.4\pm 0.2$ to non-extended crust, fold belt (Paleozoic- Mesozoic). The latter choice seems the most fitting category for the ETSZ (i.e. upper bound $M=6.4 \pm 0.2$).

(3) Strain energy arguments. Geodetic strain rates in the eastern US, although not known for the ETSZ in particular, are estimated from VLBI and GPS measurements to be of the order of 10^{-14} to 10^{-15} /sec which implies about 0.3 to 0.03 microstrains / year. For instance: recent GPS measurements in the NMSZ (Zoback et al., 1996, unpublished data) indicate a mean of 0.11 microstrain / year (95 % confidence intervals are from 0.04 to 0.20 microstrains / year) for a region about 55km in width across the NMSZ.

Annual strain rate, $\partial e/\partial t$, and annual moment rate, $\partial Mo/\partial t$, are related by

$$\partial Mo/\partial t = 2\mu V \partial e/\partial t$$

where V, the strained Volume, is assumed to have an average shear modulus μ .

The strain rate for the ETSZ is not known. But if we assume for the moment that the geodetic rate were the same as that for the NMSZ (!); and if we assume the volume V of the ETSZ proper to be about 300 by 50 by 20 km cubed or $V=3 \times 10^5 \text{ km}^3 = 3 \times 10^{20} \text{ cm}^3$, and the shear modulus to be of the order $\mu = 3.7 \times 10^{11} \text{ dyne/cm}^2$. This combined with the relation

$$M = 2/3 \log Mo \text{ (dyne cm)} - 10.7$$

would imply an average annual rate of moment of $2.22 \times 10^{25} \text{ dyne cm /y}$ or the equivalent of a $M_w=6.2$ every year (!), which obviously is not even achieved by the NMSZ. If no seismic moment would be released in the ETSZ by smaller earthquakes, this moment rate would imply every thousand years a magnitude $M=8.2$. Such events would have most likely be detected by their paleo-seismic / geologic effects in the ETSZ area and beyond. Hence we do not believe such high strain rates are currently accumulating, which -by the way- would be geodetically detectable in a decade or less. On the other hand we are not certain whether sufficient paleoseismic and geologic work has been done in and around the ETSZ to exclude that $M=7$ to 8 earthquakes have not occurred in the last 10,000 years or so.

The historically detectable seismic moment rate (determined from the seismic network data), according to Chapman (1996, Figure 2) is about one $M_{blg}=4$ event every 10 years. If we equate (for convenience rather than accuracy) M_{blg} with M, then this level of seismicity corresponds to a moment release on the order of

$$\partial Mo/\partial t = 1.122 \times 10^{21} \text{ dyne cm / y}$$

and to a "seismic" strain rate of only

$$\partial e/\partial t = \partial Mo/\partial t / (2\mu V) = (1.122 \times 10^{21} \text{ dyne cm / y}) / (2 \times 3.7 \times 10^{11} \text{ dyne /cm}^2 \times 3 \times 10^{20} \text{ cm}^3)$$

$$\partial e/\partial t \approx 5 \times 10^{-6} \text{ microstrain / y}$$

or five orders of magnitude lower than what is currently being observed in the NMSZ. This seems an extraordinarily small strain rate. Almost certainly there is more strain either being accumulated elastically, or being released by aseismic creep in the ETSZ than is being released seismically. This clearly warrants future GPS measurements in the area.

One possible analogy comes to mind in this context. The region may be -for one reason or another- a "creeping inclusion" into the generally competent fully brittle eastern US crust. Similarly the creeping section of the Andreas Fault (SAF) north of Parkfield CA, is an anomaly amongst the otherwise brittle segments of the SAF. Creep in the ETSZ could be induced by pressure solution. The surrounding rock matrix may respond to stress changes related to the volume changes associated with the pressure solution by limited brittle stress release in relatively small earthquakes. The creeping section of the San Andreas fault is by number of earthquakes the most seismically active, and most well defined fault segment of the SAF, but only for earthquakes in the order of $M=3$ or less. No larger earthquakes ($M>5$) are known to have ever occurred on this SAF segment. Why the process of creep in the ETSZ volume -if present- should be activated there and not elsewhere in the eastern US crust or along other portions of the New York - Alabama lineament remains of course a mystery. But so is the reason for the creeping section of the SAF.

Another option to explain the ETSZ activity is analogous to what is known for the NMSZ and the Charlevoix/St. Lawrence River SZ in Quebec, Canada. The current small-earthquake activity in these active areas is "aftershock" seismicity to recent large $M=7$ to 8 earthquakes. In the case of the ETSZ the large earthquake would have occurred recently, yet prehistorically. But once again we have to ask: where is the paleoseismic / geologic evidence for this past large earthquake (or sequence of quakes).

To close this issue, the strain argument is inconclusive in providing constraints on the size of future earthquakes in the ETSZ, at least until geodetic / GPS measurements are being made at and surrounding the ETSZ. Such geodetic measurements would hopefully indicate whether and how strain accumulates elastically in the ETSZ compared to what strain is being seismically released; or whether and how strain is aseismically released; and how strain rates in the ETSZ compare to measured rates in regions outside the ETSZ. We would expect that GPS can elucidate the issue whether the ETSZ coincides with a strain rate anomaly in the CEUS, and whether the observed strain is compatible with the seismic strain release during the last few decades, or not. Additionally, paleoseismic studies may need to be intensified in and around the ETSZ.

At this time we do not feel that magnitude constraints can be inferred from the strain argument.

4. Detailed Seismicity and Focal Mechanism Patterns.

Chapman et al. (1996) have analyzed and correlated the strike of focal mechanism planes in the ETSZ with spatial patterns of epicenters (but not of hypocenters) to infer the existence of extended faults, and their dimensions and orientations. They find two preferred orientations of subvertical strike-slip faults: (1) a NE striking right-lateral strike-slip set of en-echelon faults whose individual strikes virtually coincide with the maximum horizontal stress direction S_1 (about N56E; personal communication by L. Seeber, based on inversion of the 26 focal mechanisms presented by

Chapman et al., 1996). In order for these NE striking faults to slip, one must infer very low effective stress to be associated with them, i.e. they appear to be very weak, possibly implying high pore pressure. (2) a nearly E-W striking, left-lateral-slipping set which is oriented at about 40 degrees with respect to the maximum horizontal compressional axis S1 (and with respect to the first set of faults as well). Since the volume of ETSZ basement rock appears to undergo NE-SW compression, then these E-W striking left-lateral, left-stepping faults could be considered a set of cross faults in an overall right-lateral NE-trending ETSZ shear zone. These cross faults may indicate blocks in a "bookshelf" tectonic regime where the individual blocks undergo clockwise rotation.

The length of the E-W striking fault sets appears somewhat shorter (<30km) than that of the NE-striking sets (>50km). This inference needs to be qualified since only 2-d epicenter information instead of 3-d hypocenter information was analyzed for alignment by Chapman et al. (1996).

While from the pattern of apparent fault alignment it appears unlikely that there exists a single through-going NE-striking fault, the apparent sub-fault dimensions of $L \approx 50\text{km}$ length towards NE, and up to $L \approx 30\text{km}$ towards E, if activated in single ruptures, could accommodate earthquakes with moments on the order of:

$$M_o = k \Delta s w^2 L$$

where k is a constant with an amplitude of order of $k=1$; it varies in detail for dip-slip and strike-slip fault geometries and for different ratios of fault width w to fault length L ; with reasonable assumptions for k , w , L and stress drop Δs ,

$$\begin{aligned} M_o &= k \Delta s w^2 L \\ &\approx 1 \times 50\text{bar} \times (20\text{km})^2 \times 40\text{km} = \\ &\approx 1 \times 50 \times 10^6 \text{ dyne/cm}^2 \times (2.0 \times 10^6 \text{ cm})^2 \times 4.0 \times 10^6 \text{ cm} = \\ &\approx 8 \times 10^{26} \text{ dyne cm.} \end{aligned}$$

This moment corresponds to a (moment-) magnitude of $M = 7.2$. Hence, fault length segmentation as presented by Chapman et al. (1996) for the ETSZ is hardly an argument to advocate that the ETSZ is capable of only moderate ($M \leq 6$) earthquakes.

Conclusions.

1. The strongest argument for small values for the upper-bound magnitude M_u is the fact that observed historic and recent network seismicity in the ETSZ did probably not exceed magnitudes of $M_{blg} = 4.6$. Extrapolation of the Gutenberg-Richter relation $\log N = a - bM$ to recurrence periods of 100, 1,000 and 10,000 years imply M_{blg} magnitudes on the order of 5.1, 6.0 and 6.8, respectively, for the ETSZ. This presumes a temporally stationary, exponential and Poissonian-, rather than characteristic-earthquake, behavior out to these magnitudes.

2. The tectonic-province categorization using global correlations from EPRI (1994) would suggest an upper-bound magnitude of about $M=6.4 \pm 0.2$.

3. Strain arguments are inconclusive since independent (geodetic or GPS) strain data are not available for the ETSZ and surrounding areas.

4. Focal mechanisms combined with spatial patterns of hypocenter alignments give potential maximum fault lengths on the order of at least 20 to 30 km if not 50km, especially for the NE-striking alignment directions within the ETSZ. Such fault-lengths, when combined with moderate stress drop assumptions (≈ 50 bar), yield moment magnitudes in excess of $M=7$. Hence analysis of seismicity and focal mechanism patterns does not provide viable arguments for low upper-bound magnitude values.

In summary, we infer that maximum magnitudes for the ETSZ lie in the range from 5 to 7 and must be considered seriously, and those beyond $M=7$ marginally. For a logic-tree representation we suggest the following weighting scheme:

Upper-Bound Magnitude μ	Weight w
5.0	0.10
5.5	0.20
6.0	0.30
6.5	0.20
7.0	0.10
7.5	0.07
8.0	<u>0.03</u>
Total:	1.00

References.

- Bollinger, G.A. et al. (1991). Seismicity in the southeastern U.S.; 1698 to 1986; pp. 291-308; Chapter 16 in: Neotectonics of North America; Decade Map Volume to accompany the Neotectonic Maps, Part of DNAG; Slemmons, D.B. et al. (Editors); The Geolog. Soc. of America. 1991.
- Chapman, M.C. (1996) An argument in support of the contention that a major earthquake could occur in eastern Tennessee. pp. 15; prepared for LLNL SSHAC implementation study. July (?) 1996.
- Chapman, M.C., C.A. Powell, G. Vlahovic and M. Sibol (1996). The nature of faulting in eastern Tennessee inferred from statistical analysis of focal mechanisms and epicenter locations. subm. to Bull. Seism. Soc. Am. pp. 29, April 12, 1996.
- EPRI (1987) Working Report: Methods for Assessing Maximum Earthquakes in the Central and Eastern US. EPRI Research Project 2556-1. Prepared by K.J. Coppersmith et al., based on a EPRI workshop held at Palo Alto in June 20 & 21, 1985; published January, 1987.
- EPRI (1994). The earthquakes of stable continental regions. Volume 1: Assessment of large earthquake potential. And Volume 5: Database and Maps. EPRI Report TR-102261-V1 to V5. Prepared by A.C. Johnston et al.; Dec 1994.
- Powell, C.A. et al (1994). A seismotectonic model of the 300-kilometer-long ETSZ. Science, 264. 686-688; April 29, 1994.
- Veneziano, D. (ca 1987 or 88 ?); A random-effects model for maximum earthquake magnitude. Unpublished (?) script; pp. 27; ca. 1987 or 1988 ? based on work supported by NCEER and EPRI.

DRAFT

**DOES THE PEN BRANCH FAULT POSE A
SEISMIC HAZARD?**

Dr. Pradeep Talwani

PEN BRANCH FAULT

Here I present an extended outline of the arguments against the Pen Branch Fault (PBF) being a major player contributing to seismic hazard potential at the Vogtle plant. In my view the seismic hazard presented by the PBF is at a level equal or less than the regional background for the area, i.e., $M_{\max} \leq 4.5$.

1. Depth Constraints

The depth extent of the Pen Branch Fault and the Dunbarton basin has been obtained from a variety of seismic reflection and refraction data. These include the following:

- a. Various seismic reflection data acquired on the Savannah River Plant in the 1960s (various reports by I.W. Marine).
- b. Seismic reflection data on SRS acquired and processed by CONOCO (Chapman and DiStefano, 1989).
- c. CONOCO data reprocessed by VPI (Domoracki, 1995; Sen and Çoruh, 1992).
- d. An analyses of these data by Stieve and Stephenson, S.E. Geology, 1995; Domoracki et al., preprint and Dale Stephenson's and Alice Stieve's presentations at the Augusta meeting, 1996 (Figure 1).
- e. Seismic reflection line along the Savannah River by U.S.G.S.
- f. Seismic refraction data acquired between two wells in New Ellenton and Walterboro (Luetgert et al., SRL, 1994).
- g. COCORP reflection profile in Georgia just across the SC-GA border (Peterson et al., 1984).

Synthesis of these data (see e.g., Domoracki et al., preprint) and Figures 2 and 3 from Luetgert et al., 1994) all show that the Dunbarton basin is very shallow (~ 3-4 km) (Çoruh, Pers. Comm. to Dale Stephenson). The data also show that the PBF is also very shallow and does not wrap into the decollement.

To generate a moderate earthquake, $M \geq 5.0$ would require larger depth extent (in order to store the needed stresses). Usually a $M \sim 5.0$ event occurs at depths greater than about 10 km in southeast US.

Conclude that available data do not support the PBF having adequate depth extent to generate a $M \geq 5.0$ earthquake.

2. Geologic Constraints

Detailed geologic data have been acquired as a result of confirmatory drilling (Stieve et al., Conf. Drilling Report, 1994; Stieve and Stephenson, S.E. Geology, 1995 and Stieve, Augusta presentation, 1996).

- a. The PBF lies below the Williamsburg unconformity. Examination of sediments revealed no evidence of deformation above the unconformity. The undeformed Williamsburg unconformity is approximately 50 Ma old. Deformation on the PBF was found only below the unconformity. (The Upland unconformity is shallower than the Williamsburg unconformity).
- b. Stieve in her presentation at Augusta, also concluded that "Faulting on the PBF is older than 500 K years and therefore the PBF is a non-capable fault per 10 CFR 100 Appendix A".
- c. Investigations of quaternary geology (Geomatrix, Hanson and Bullard, 1992) consisted of longitudinal profiles of stream-channel and river terraces along the Savannah River and other tributaries crossing the PBF. They showed no nick points. The authors concluded that there was no deformation within a resolution of 3 m.

These geological observations suggest that PBF has not moved recently, or with measurable displacement. Thus they provide support for the conclusion that the PBF (or other structures) are not capable of producing $M \geq 5.0$ earthquakes.

3. Orientation With Respect to S_{Hmax}

The region is under a compressional stress regime, as such the seismogenic potential of a structure depends on its orientation with respect to S_{Hmax} . Various *in situ* data (e.g., Moos and Zoback, 1993) show that the PBF is parallel to S_{Hmax} in the area. This orientation is the least likely to produce an earthquake. Sibson (1992) has shown that for faults oriented at very small angles with respect to S_{Hmax} , extremely high pore pressures (approaching lithostat) are needed to trigger earthquakes. No evidence exists for large pore pressures at the depths at which the two small earthquakes have been located within the SRS. Thus from a purely mechanical point of view, PBF does not pose much of a seismic hazard. It also does not show a capability of generating $M \geq 5.0$ earthquakes.

We have interpreted the small earthquakes that occurred within the SRS to have occurred on small, suitably oriented, cross faults. The dimensions of these cross structures preclude earthquakes $M \geq 3.0$.

Based on the arguments presented above, I consider the Pen Branch Fault incapable of generating $M \geq 5.0$ events. Consequently I suggest that a "regional event" with $M \leq 4.5$ is adequate to cover the seismic hazard posed by PBF or other small faults encountered near SRS.

Figure intentionally omitted

Figure 1. Figure 13 of Stieve, 1996. Geologic cross-section of northwest to southeast transect through SR5 to the coast.

Figure intentionally omitted

Figure 2. From Luetgert et al. (1994).

Figure intentionally omitted

Figure 3. From Luetgert et al. (1994).

**WHITE PAPER FOR TRIAL IMPLEMENTATION PROJECT
POSITION: "INCLUDE THE PEN BRANCH AND OTHER LOCAL
FAULTS IN THE PSHA"**

Kevin J. Coppersmith

Disclaimer: The following white paper--much like a lawyers legal argument--presents a particular position and seeks only to support that position. I have intentionally tried to present an unbalanced case, giving only lip service to counter-arguments that my worthy opponent (the esteemed Prof. Talwani) will likely present. Further, I have done a poor job of citing references and providing supporting data to many of my arguments. Nevertheless, I trust that the paper will at least spark some thinking and help us reach our ultimate goal: staying awake at the next workshop.

Position: The seismic hazard analysis at the Vogtle site should include a consideration of the faults mapped in the local site vicinity as potential seismic sources.

Background

Numerous studies have been conducted in the past nine years (see Domoracki, et al., in press and A. Stieve vu-graphs for summary of geologic and geophysical studies) aimed at identifying and characterizing faults in the local SRS site vicinity. These are probably the most intensive studies ever conducted of Mesozoic normal faulting anywhere along the eastern seaboard. The studies include deep seismic reflection, shallow high-resolution seismic reflection, heat-flow interpretations, seismicity analyses from a local seismic network, geologic mapping, Quaternary geologic studies, in-situ stress measurements, etc.

The available studies indicate that the major bedrock faults in the site vicinity developed during the extensional tectonic regime associated with Mesozoic continental rifting. This rifting event was a profound orogenic event that is documented in the geologic record throughout the continental margin of eastern North America and included parts of the present mid-continent including the New Madrid region. As a profound tectonic event, the faults that accommodated the extension persisted throughout the width (thickness) of the crust. Very deep seismic reflection profiles across the continental margin document the persistence downdip of the major normal faults to at least mid-crustal depths. In many cases, no doubt, the extensional faults reactivated reverse faults associated with the compression that accompanied continental collision during the Paleozoic. However, because normal faults tend to display relatively steep dips in at least the brittle upper crust, the higher-dip Mesozoic normal faults probably only reactivated the higher-dip components of Paleozoic reverse faults.

It is not clear that *every* Mesozoic normal fault is a fault that exists throughout the entire crust. No doubt, many faults are antithetic to major normal faults; others could be secondary splays.

The faults identified in the local site vicinity display the classic expression of Mesozoic normal faults: east-dipping normal faults showing a down-dropped basement and bounding Triassic-age arkosic "red-beds" associated with the in-filling of these basins (in this case the Dunbarton basin). Subsequent deposition of the Cretaceous and younger Coastal Plain sediments has buried the basin. The Dunbarton Basin formed as a tilted fault block with faulting along the western margin. It is a relatively small basin compared to other mapped Triassic basins (about 30 km long) although crustal extension was sufficient to result in a minimum of ----- meters of normal slip and deposition of about ----- meters of Triassic sediment. As such, the faults bounding--and responsible for--the Dunbarton basin were large, significant faults during the time that they accommodated this extension. Based on this assessment, there is a good chance that the east-facing border fault bounding the Dunbarton Basin (known in the Coastal Plain section as the Pen Branch fault) is a significant fault that likely transects the entire continental crust. Interpretations of seismic reflection data by Domoracki et al. (in press) suggest that the Pen Branch fault may be related to the updip part of large Paleozoic reverse faults such as the Augusta fault.

As discussed by Alice Stieve and Dale Stephenson at the first TIP workshop, other faults besides the Pen Branch fault have been interpreted at the top of basement and within the Coastal Plain sediment in the SRS vicinity. These local faults, as well as the Pen Branch fault, should be considered as potential seismic sources for the TIP-PSHA for the following reasons.

1. Mesozoic normal faults persist throughout the crust and extended crust can be important to large-earthquake potential. As discussed above, the faults associated with Mesozoic continental extension are likely deep-seated high-angle structures that persist downdip throughout the seismogenic crust. Although there are probably some minor normal faults that were antithetic or secondary to the major normal faults, those faults that are clearly related to and bound known Mesozoic basins are clearly the most likely to have been the major structures (i.e., have the most cumulative slip) accommodating continental extension. An example of such a basin-bounding normal fault is the Ramapo fault that forms the northwesterly boundary of the Newark Basin.

Because the Pen Branch and associated normal faults bound the Dunbarton Basin, they are likely significant structures within the seismogenic crust (upper 15 to 20 km). That is, they likely persist as fairly high-angle (approximately 60 degree dipping) faults throughout the depth of the seismic reflection profiles given in Domoracki et al. (in press). Domoracki et al. suggest that the Pen Branch may be related to--and perhaps an extensional reactivation of--Paleozoic reverse faults such as the Augusta. They do not, however, clearly identify the Pen Branch fault at mid- to upper-crustal depths on their profiles. This is not surprising for several reasons: 1) seismic reflection data commonly

do not image steeply dipping structures well (e.g., high-angle faults are usually identified from the vertical separation and discontinuity of reflectors, rather than from reflections off the fault plane), 2) the cumulative normal slip on the Pen Branch fault is relatively small compared to that of the Augusta fault, and 3) the intensity of deformation associated with the extensional tectonism was probably far less than that associated with Paleozoic compression (e.g., the development of duplex structures postulated by Domoracki et al.). As a result the downdip extent of the Pen Branch fault is not well-imaged in the seismic data. This is a common problem in the Basin and Range province in which seismic reflection profiles provide clear images of low-angle reverse faults but rarely image the high-angle normal faults that are well-known at the surface (e.g., Smith and Bruhn).

The normal faulting associated with Mesozoic extension--represented locally by the Pen Branch fault and regionally by a domain of extensional features along the eastern seaboard--is indicative of significantly extended continental crust. Studies of large earthquakes that have occurred within stable continental regions (SCR; Johnston et al.) show that all of the largest ($M > 7$) events have occurred within extended crust. Admittedly, the correlations given in Johnston et al. between the earthquakes and their tectonic associations were regional (that is, typically the large SCR earthquake can only be associated with a regional 'tectonic domain' and not with an individual fault--like the Pen Branch). Nevertheless, regardless of our inability to identify the exact causative fault, large SCR earthquakes must be occurring on faults and candidate causative faults within a domain can be identified.

2. The Pen Branch fault displays clear evidence for reactivation as a reverse fault. Geologic and geophysical studies of the Pen Branch fault provide perhaps the best documented evidence of reactivation of a Mesozoic normal fault as a post-Mesozoic reverse fault. This confirms that the fault was involved not only in the accommodation of regional extension associated with continental rifting, but, since then, has responded to post-rifting compressional stresses. These stresses were presumably induced by ridge-push forces following complete continental separation and continue to exist today in the continental crust of eastern North America. Detailed studies of some other Mesozoic normal faults (e.g., Ramapo fault) have shown that the most recent episode of brittle deformation occurred as normal faulting and did *not* include subsequent reactivation in a reverse sense (Ratcliffe).

The concept that Mesozoic normal faults might be reactivated as reverse faults--and might represent a contemporary seismic hazard--was first proposed by Wentworth and Mergner-Keefer. Based on the observation that the contemporary stress field appeared to be compressional and the--anecdotal at the time--limited evidence of recent faulting appeared to be along reverse faults, they suggested that a domain of reactivated reverse faults exists along the continental margin of the East Coast marked by Mesozoic basins. In the absence of much direct evidence, they postulated that future detailed studies of the basin-bounding faults might/would show evidence for reactivation in a reverse sense and, thus, an indication of potential activity in the present tectonic regime.

The Pen Branch fault clearly meets the conditions that are part of Wentworth and Mergner-Keefe's hypothesis (i.e., reverse reactivation of a Mesozoic normal fault), although, at the time, they believed that the maximum horizontal crustal stress direction was northwest-southeast, perpendicular to the northeasterly strike of the Mesozoic normal faults. We now have independent data that show that the axis of maximum horizontal compression lies in the northeast quadrant--essentially parallel to the strike of the Pen Branch fault. This orientation is probably most conducive to strike-slip faulting, with some component of reverse displacement. At present, there are virtually no data that confirm or deny a significant lateral component of post-Cretaceous slip on the Pen Branch fault. Therefore, the Pen Branch fault could well be a strike-slip fault, with a reverse component, consistent with the present tectonic crustal stress regime.

3. Dimensions of the Dunbarton Basin are sufficient to suggest the potential to generate significant earthquakes. The dimensions of a fault (downdip width and fault length) are an indication of the size of earthquakes that might be generated by the fault. It is also well-known that the dimensions directly scale with moment magnitude (e.g., Wells and Coppersmith). As discussed previously, the downdip width of the fault is likely crustal in extent because the Dunbarton Basin is a significant basin associated with continental extension and rifting. The thickness of the seismogenic crust in the vicinity of SRS is about 15 to 20 km thick. It is therefore suggested that the downdip width of the Pen Branch fault is also approximately of this dimension.

It could be argued that the Pen Branch possibly connects downdip with the Augusta fault and soles out at relatively shallow depth into a low angle fault. Assuming that only the updip high-angle part of the fault is seismogenic (i.e., that the low-angle part of the Augusta fault has not been reactivated since the Paleozoic), this would limit the downdip dimensions--and, hence, maximum earthquake potential--of the Pen Branch fault. However, as discussed earlier, a common problem with the interpretation of seismic reflection data in extensional regimes superimposed on compressional regimes is that the low-angle reverse faults are the dominant reflectors in the seismic data (Smith and Bruhn). For example, deep reflection profiles across large, active normal faults such as the Wasatch fault, Utah, and the Lost River fault, Idaho, image large regional low-angle reverse faults associated with previous episodes (primarily Laramide) of compressional deformation. Often, these reverse faults sole into regional detachments at relatively shallow depths (5-10 km). In most cases the active normal faults at the surface can be projected downdip to the steeper portions of the reverse faults but they are not well-imaged in the reflection data.

For example, in the case of the Lost River fault, the coseismic fault plane is well-imaged from the pattern of aftershocks to the 1983 Borah Peak earthquake. The coseismic fault dips steeply (~45-50 degrees) to the east and extends downdip to depths of about 15 km. There is no sign that the dip is listric. In contrast, seismic reflection profiles across the Lost River fault image an east-dipping Laramide reverse fault that is listric and soles into a subhorizontal reflector at depths of about 8 km. There is simply no good agreement between the faulting interpreted in the reflection data and the seismogenic fault mapped at

the surface and in the subsurface from aftershocks. It is suggested that a similar circumstance could be the case with the Pen Branch fault. The seismic reflection data clearly image the compressional Paleozoic structures and the high-angle (probably lesser cumulative slip) Mesozoic extensional structures are not well-imaged. However, the tectonic role that the normal faults played in continental rifting suggest that they do, in fact, extend to significant depth.

In addition to the width, the *length* of the Pen Branch fault is also likely significant enough to allow for the generation of moderate-to-large earthquakes. The location and length of the Dunbarton Basin is interpreted from geophysical data and subsurface geologic data to be about 30 km long. Although it is not known with certainty that the Pen Branch fault extends along the entire length of the basin, the tectonic position of the fault in the vicinity of SRS --a basin bounding normal fault-- would suggest that it does bound the entire length of the basin. Further, the seismic reflection line that runs down the Savannah River indicates the presence of the fault at least beyond the boundary of the SRS.

The combination of a 15-20 km downdip width and a 30 km length would imply a potential rupture area that is about 450-600 km². This area would be capable of sustaining a moment magnitude of about 6 1/2 to 7, based on the empirical regressions between rupture area and magnitude given in Wells and Coppersmith (1994).

4. The absence of observed seismicity is not a good indicator of the lack of future earthquake potential. The Pen Branch fault and the Dunbarton Basin lie within a diffuse regional zone of seismicity, as noted by Domoracki et al. Although there is some chance that the two small local earthquakes recorded at the SRS may have been associated with the Pen Branch fault (Domoracki et al.), there is no clear alignment or association of seismicity with the fault over and above the levels of the diffuse zone.

A clear association of seismicity with a fault is a good indication of its future earthquake potential (if not in magnitude, at least in terms of whether or not the fault is seismogenic). In contrast, the absence of observed seismicity may or may not be an indication of future earthquake potential. Numerous cases can be found--particularly along Quaternary-active normal faults of the Basin and Range province--where clearly "active" (i.e., Quaternary) faults are not associated with observed seismicity. This may be the case for the Pen Branch fault.

In the absence of observed associated seismicity, other information (e.g., geologic evidence for the recency of faulting, tectonic relationships, etc.) become the primary mechanism for assessing whether or not a fault should be considered potentially seismogenic. Quaternary geologic studies conducted thus far for the Pen Branch fault suggest that the Pen Branch fault has not displaced Quaternary deposits of the Savannah River and, therefore, is not a Quaternary-active fault. Unfortunately, these studies are preliminary and the level of resolution of the geologic mapping could allow for a small amount of Quaternary deformation below the threshold of resolution of the geologic and geomorphic techniques that have been applied thus far.

5. Probabilistic seismic hazard analyses should incorporate a wide range of tectonic hypotheses. Despite the brilliant (if not persuasive) arguments made in this white paper for why the Pen Branch fault is, in fact, a seismogenic fault, there is admittedly significant uncertainty surrounding the issue. A key goal to any PSHA should be to properly characterize alternative tectonic hypotheses and to quantify the associated uncertainties in a manner that is appropriate to hazard analysis. Popular counter-arguments to the notion of actually attempting to include the tectonic hypotheses in the analysis is that “it probably won’t affect the hazard results anyway” or “a local source zone should cover the possibility of a local fault.”

Purely from the standpoint of hazard analysis (i.e., mean hazard), these arguments are often correct. For example, most of the arguments surrounding the Pen Branch fault deal with whether or not it is seismogenic (that is capable of generating significant earthquakes). Even allowing for this uncertainty, the Quaternary geologic studies that have been done in the SRS area would suggest that, if the fault is active in Quaternary time, its rate of slip during the this time has been very low. Thus, a PSHA that uses slip rate as a constraint on earthquake recurrence rate (as most do these days) would show that, because of the low recurrence rate, the Pen Branch fault makes an insignificant contribution to the hazard at the Vogtle site. Therefore, “it doesn’t affect the hazard results anyway.”

This is true but there is some real value in properly and comprehensively incorporating all credible tectonic models and hypotheses into the PSHA. The arguments are the following. First, our intuition about what is important and unimportant to PSHA is not always correct. PSHA is a complicated convolution of the probability of activity, source-to-site distances, earthquake recurrence rates, and ground motion attenuation laws. Even the most sage hazard analysts are occasionally surprised by the results. Second, including all tectonic hypotheses can help satisfy the larger technical community that all viewpoints have been considered and--indeed--represented in the hazard analysis. This can enhance the technical credibility of the study and help diffuse contention and polarization about controversial issues. Third, although a particular model or hypothesis may not affect the mean hazard at certain probability levels, it could significantly affect the uncertainty distribution of the hazard and might have significance at other probability levels of interest. For example, the concept of a large-magnitude earthquake rupturing the regional Paleozoic detachment along the eastern seaboard (an hypothesis that has lost favor in recent years) might only be significant to calculated hazard at low probability levels (say, 10^{-4} per year). Finally, often the best way to show that a particular tectonic hypothesis is insignificant to hazard is, in fact, to include it in the analysis. Sensitivity studies can then isolate its contribution to the hazard results and, if found to be significant, can identify those aspects that are most important. For example, once the Pen Branch fault is included in a PSHA for the Vogtle site, it may be shown that the fault is a minor contributor to the hazard; or, if it is significant, that the most important aspect of its characterization is the assessment of whether or not it is seismogenic. This type of sensitivity analysis can help to focus subsequent data-collection efforts.

Conclusion

The Pen Branch fault--and perhaps other local faults--should be considered as potential seismic sources in the PSHA. This is a tectonic hypothesis that should be properly included in the analysis. We can debate the alternative ways that this hypothesis might best be represented (e.g., a discrete fault, a local source zone, a zone of faults, etc.).

APPENDIX B: WHITE PAPERS ASSIGNED TO EXPERTS IN PREPARATION OF WORKSHOP #3

Extrapolating rates for small magnitudes to large magnitudes

Pro: Klaus Jacob

Con: Martin Chapman

Estimating maximum magnitude

— Strong position on using fault plane area/length for ETSZ Gil Bollinger

—Using global data (not developed)

Estimating magnitudes from Paleoliquefaction

Pradeep Talwani

LIMITATIONS TO ESTIMATING THE RATE OF LARGE EARTHQUAKES FROM THE RATES OF SMALL EVENTS.

Klaus H. Jacob

Lamont-Doherty Earth Observatory of Columbia University, Palisades NY 10964

E-mail: jacob@ldeo.columbia.edu

PREAMBLE.

The author was assigned to the task of presenting the arguments AGAINST the widely held opinion that one can readily infer the rate of occurrence of large earthquakes from the rates of smaller earthquakes. Martin Chapman (1997) was assigned to the task of presenting the opposite arguments, i.e. IN SUPPORT of the notion that such extrapolations can be readily made.

Note: In this script we use the following notations: m is magnitude; M stands for seismic moment; the symbol \sim means "proportional to", and $^{\wedge}$ implies "raised to power" (of what ever follows in parentheses).

Summary

It is shown that if self-organized criticality is a process that applies to earthquake phenomena, than one needs to know the mode of criticality of the strain release process before one can decide whether it is possible to extrapolate from the rate of small earthquakes to the rate of the largest possible earthquakes in any given region.

Introduction.

In the interior of plates and "stable continental regions" (SCR) the sparse seismicity is -by definition- not associated with plate boundaries whose relative plate motion rates are generally well constrained; nor is such SCR seismicity generally associated with major through-going fault systems whose slip rates are constrained from geologic or geodetic data. Therefore geologic/geodetic constraints do not generally exist for the moment rate that may be released by earthquakes. Since *large* earthquakes tend to release most of the strain energy available, while small earthquakes contribute little to the strain release, there are little useful constraints on the occurrence rate of potentially large earthquakes other than what can be learned and inferred from the instrumental, historic, or paleoseismic record of the earthquakes themselves. However, in most regions of the eastern U.S. (i.e. east of the Rockies), the historic record is at best only 200 to 300 years old which is thought to be only a small fraction of the recurrence times of the largest earthquakes. And only in a few regions paleoseismicity has produced data for longer exposure times. Moreover, the paleoseismicity studies are geographically sparsely distributed; the

completeness of the record of large earthquakes detectable by paleoseismic methods is difficult to assess; and the spatio-temporal resolution of paleoseismically inferred events is often quite poor.

For these reasons, seismologists have been tempted to infer the expected rate of occurrence of potentially larger earthquakes (say, $m \geq 6$) from the rate of occurrence of smaller events (typically with magnitudes $m \leq 4$) by extrapolating the well known Gutenberg-Richter (G-R) relation

$$\log N = A - bm \quad (1)$$

to magnitude ranges $m \geq m^*$ where m^* is the magnitude of the largest earthquake so far observed at least once in the sample record for the specific region or seismic source zone under consideration. The validity of extrapolations to $m \geq m^*$ hinges critically on a number of assumptions. One of these is the notion that the slope b in the (G-R) relation (1) is constant over a sufficiently wide range of magnitudes that includes both the observed magnitudes and the magnitudes $m \geq m^*$ to which we wish to extrapolate.

Let us therefore look at some of the arguments that have been made in the literature about the validity of a constant b -value, deviations from constant- b models, and relevant observations and theoretical arguments. This brief commentary is only a sampling of the literature and does not claim to be a balanced and exhaustive survey; hence it may not be fully representative of the variety of arguments that may have been made on this subject.

Also, we do not touch here on other difficulties that can arise in addition to the question whether b is constant or not. These other difficulties tend to control the *uncertainties* associated with determining the A - and b -values of the G-R relation, stemming often from the related problems of catalog incompleteness, and of non-unique definitions of the magnitude and intensity scales. These practical issues do not call by themselves in question the existence of the constancy of b in the Gutenberg-Richter relation; but they can contribute to the uncertainty with which b can be determined and thus may make it impossible to resolve whether a constant b slope exists or not, over the range of magnitudes of interest.

The Physical Need for an Upper Magnitude Limit.

It has been shown by many authors (e.g. Main, 1995) that the seismic energy E (or moment M) is related to magnitude m and fault length L by relations of the form

$$\log E = cm + d \quad (2)$$

and

$$E \sim L^a \quad (3)$$

It can be shown that (1) through (3) imply a power law frequency distribution of energy

$$N(E) \sim E^{-B} \quad (4)$$

with $B = b/c$.

It also can be shown that for typically observed b-values $0.5 \leq b \leq 1.5$ a finite maximum earthquake size must exist, otherwise there would be infinite seismic energy release for a finite strain rate in the presence of the G-R law (1) and power-law distribution (4). Hence, finiteness of strain energy requires a truncation at some upper magnitude level, at least for typically observed b-value slopes.

Observations and Arguments For and Against a Constant b-Value.

Observations: Limited fault or source zone vs. "global" fault or source zone statistics.

A constant b-value slope in the powerlaw distribution follows if self-similarity applies to the earthquake process, i.e. if the processes involved apply equally regardless of scale.

Wesnousky et al. (1983) found from combining geologic, geodetic and seismicity data, that in Japan for a single fault zone, the frequency-magnitude distribution does not follow the classic constant b-value model. In particular they found, that the largest moment on a fault is substantially larger than that predicted from a G-R type relation. Similar results are known from the Mexican subduction zone seismicity, or from a European graben system (Lower Rhine embayment in the Netherlands / German border region) with low seismicity and events thought to be limited to about $m \leq 6.5$ (Camelbeeck and Meghraoui, 1996).

Schwartz and Coppersmith (1984) proposed the concept of "characteristic earthquakes" based on observations on the Wasatch (Utah) and San Andreas (CA) faults. The geologically inferred recurrence rates of the characteristic earthquakes were higher than those inferred from the known historic and instrumental seismicity (see attached **Figures A**).

Davison and Scholz (1985) used catalogs from the Alaska Aleutian arc to make the point that if one uses the catalog data from limited rupture zones, then the extrapolation from small earthquakes always underpredicts the moment rate implied by the occurrence of the largest earthquakes in this

subzone. If, on the other hand, all events, i.e. small and characteristic events are used in a single "global" Alaska-Aleutian arc seismic zone, than the rate of the largest earthquakes (in this case of the 1964 moment magnitude 9.2 Gulf of Alaska earthquake) is well predicted by the occurrence of all other earthquakes. The same holds for a global catalog which correctly "predicts" the largest known earthquake, the 1960 Chile earthquake (see attached **Figures B**).

It is interesting to note that Bollinger et al. (1989) tested the seismicity catalog for the southeastern U.S. (SEUS) as a whole, and for subregions of it, and came to what appears to be a somewhat differing conclusion for this SCR region: that if the entire SEUS catalog (exclusive of Charleston S.C.) is used, a higher rate of Charleston-type earthquakes is inferred for this region using a G-R type relation for the moderate and smaller earthquakes, than the local small-magnitude seismicity data would allow one to infer for the Charleston area (which in turn provides recurrence rates roughly consistent with the paleoseismic results for Charleston). The authors argue that therefore the local data for Charleston may provide a better estimate of the recurrence rate of the maximum-size event in the Charleston area, and that using the entire SEUS data, i.e. the "global" data in our earlier terminology, would over- (rather than under-) estimate the recurrence rate of Charleston-type events in the entire SEUS, if such events can occur outside the Charleston area proper.

In many other regions investigators often find general applicability of the G-R relations, i.e. that the occurrence rates of the largest events can be reasonably accurately inferred from the rates of smaller earthquakes. However, as pointed out by Pacheco and Sykes (1992) based on empirical data, caution must be exercised when the size of ruptures becomes so large (moment magnitudes ≥ 7.5) that they approach the down-dip dimension of the seismogenic zone of the crust and uppermost mantle. Many seismic scaling relations appear to change at this magnitude threshold, including the b-value slope of global seismicity catalogs from $b=1.04$ for moment magnitudes $7.0 \leq m \leq 7.5$, to $b=1.51$ for magnitudes $7.6 \leq m \leq 8.0$ (see attached **Figures C**).

In summary, we find cases of overestimating, underestimating or correctly estimating the rates of large events from the rates of smaller events. What are the possible explanations for and inferences from these seemingly diverging observations, for reasons other than those presented by Pacheco and Sykes (1992) ?

Fractals, Rock Mechanics, Physical Models, Computer Simulations. In the last two decades or so the earthquake process has been investigated from the different vantage points of a variety of disciplines: chaos theory for linear and nonlinear systems; rock mechanics; statistical mechanics;

fractal concepts; and computer simulations of the earthquake-loading and strain-release cycles of large coupled systems (so-called "automatons"). From these approaches has emerged the realization that earthquakes may represent a class of stochastic processes known as "self organized critical (SOC) phenomena" (e.g. Ito and Matsuzaki, 1990). However, deviation from strict SOC behavior is needed to explain the diverse observations. Such modified SOC processes can "explain", or at least mimic, the sometimes quasi-cyclic behavior, foreshock and aftershock sequences, size distributions, "characteristic events" and other features frequently observed in seismicity. In a recent paper, Main (1995) reviews several of the salient features of these models and some of their implications for seismic hazard assessments.

Following Rundle and Klein (1993) three states are distinguishable in such modeling efforts: subcritical, critical and supercritical. The three types of behavior are illustrated in Figures D taken from Main (1995). The three types of behavior can be analytically described by a generalized power-law (fractal) distribution for small events if modified by an exponential (Boltzmann) tail with negative, zero, or positive exponent of the form:

$$N(E) \sim E^{(-b)} e^{(-E/E_0)} \quad (5)$$

where E_0 is a characteristic energy (or moment) "reflecting the probability of occupying the different energy states E ". In computer modeling experiments, E_0 tends to increase with driving velocity, i.e. the rate of the tectonic strain loading. The cumulative or integrated form of the density distribution (5) is a generalized gamma distribution (for details see Main, 1995). If the distribution is subcritical ($1/E_0 > 0$), then the system sets its own upper magnitude and one obtains the exponentially truncated frequency-magnitude distribution currently most commonly used in seismic hazard analyses. If the system is precisely critical ($1/E_0 = 0$), then all states have equal chance of being occupied up to the limiting state, and a fixed sharp drop-off at a well defined maximum energy (i.e. moment magnitude) is needed to preserve total final energy. If the system is supercritical ($1/E_0 < 0$) there is a greater potential for the largest earthquake than expected from the power-law distribution of the smaller events, i.e. energy is deprived to occupy the fractal- or powerlaw-controlled energy states of smaller events. This supercritical mode corresponds to the characteristic earthquake model. The three cases are schematically illustrated in Figures E taken from Main (1995) and referred to as case (a) = subcritical, (b) = exactly critical and (c) = supercritical, with their corresponding probability (or frequency) density distribution (left) and moment density distribution (right) indicated. For details see Main (1995).

Discussion.

The simple analytical model of an exponentially tailored power law described above by (5) is based largely on equivalents to thermodynamic processes. But relatively simple automaton computer models of systems of sliding masses, springs and damping components, can simulate artificial "earthquake data" with properties that largely reproduce the classes of observations from real earthquakes made for many parts of the world.

If this type of modified self-organized critical model does indeed apply to the earthquake process, which at this time is an unproven hypothesis, then such models would have great implications for quantitative seismic hazard assessments. Also not known at this time is which of the possible tectonic factors control the mode of criticality, i.e. under what tectonic circumstances does the subcritical, critical, or supercritical case apply. Strain rates seem to have some controlling influence, but not solely. The degree of material heterogeneities may contribute among many other possible factors.

All three modes of energy release (subcritical, critical, and supercritical) require a truncated frequency vs. moment (or magnitude) distribution. But only in the subcritical and critical cases it is possible to use the fractal portion (the power-law or G-R portion) of the frequency-magnitude distribution to estimate from the rate of small earthquakes the rate of the largest earthquakes with reasonable confidence. Without knowing the critical energy E_0 and/or its controlling tectonic factors, it will be unknown whether the common practice of using the simple G-R relations for estimating large earthquakes is valid and applicable in any specific case. While it is likely that more often than not subcritical to critical conditions exist, there is currently no method available to assess *a priori* the mode of criticality, and hence one cannot exclude the possibility that a characteristic earthquake model may apply in any given region due to supercritical conditions tending to produce characteristic earthquake occurrences. If such supercritical conditions apply, the extrapolation of the G-R relation to large magnitudes under the assumption of a constant b-slope would tend to underestimate the rates of the largest (characteristic) earthquakes.

References.

- Bollinger, G.A., F.C. Davison, M.S. Sibol, and J.B. Birch (1989). Magnitude recurrence relations for the Southeastern United States and its subdivisions. *JGR* 94, 2857-2873, March 10, 1989.
- Camelbeeck, T. and M. Meghraoui (1996). Large Earthquakes in Northern Europe more likely than once thought. *EOS, Transactions of the Am. Geophys. Union*, Vol. 77, No. 42, October 15, 1996, pp. 405 & 409.
- Chapman, M.C. (1996). Can small magnitude shocks be used to infer the occurrence rates and locations of future damaging shocks? White paper for LLNL - TIP, Jan 7, 1997.
- Davison, F.C. and C.H. Scholz (1985). Frequency-moment distribution of earthquakes in the Aleutian Arc: A test of the characteristic earthquake model. *BSSA* 75, 1349-1362, October 1985.
- Ito, K. and M. Matsuzaki (1990). Earthquakes as self-organized critical phenomena. *JGR* 95, 6853-6860, May 10, 1990.
- Main, I.G. (1995). Earthquakes as critical phenomena: implications for probabilistic seismic hazard analysis. *BSSA* 85, 1299-1308, October 1995.
- Pacheco, J.F. and L.R. Sykes (1992). Seismic moment catalog of large shallow earthquakes, 1900 to 1989. *BSSA* 82, 1306-1349, June 1992.
- Rundle, J.B. and W. Klein (1993). Scaling and critical phenomena in a cellular automaton slider-block model of earthquakes. *J. Stat. Phys.*, 72, 405-413.
- Schwartz, D.P. and K.J. Coppersmith (1984). Fault behavior and characteristic earthquakes: examples from the Wasatch and San Andreas fault zones. *JGR* 89, 5681-5698, July 10, 1984.
- Wesnousky S., C.H. Scholz, K. Shimazaki and T. Matsuda (1983). Earthquake frequency distribution and the mechanics of faulting. *JGR* 89, 9331-9340.

Figure intentionally omitted

Figures A: from Schwartz, D.P. and K.J. Coppersmith (1984). Fault behavior and characteristic earthquakes: examples from the Wasatch and San Andreas fault zones. JGR 89,568 1-5698, July 10, 1984.

Figure intentionally omitted

Figures B: from Davison, F.C. and C.H. Scholz (1985). Frequency-moment distribution of earthquakes in the Aleutian Arc: A test of the characteristic earthquake model. BSSA 75, 1349-1362, October 1985.

Figure intentionally omitted

Figures B (continued).

Figure intentionally omitted

Figure B (continued).

Figure intentionally omitted

Figures C: from Pacheco, J.F. and L.R Sykes (1992). Seismic moment catalog of large shallow earthquakes, 1900 to 1989. BSSA 82,1306-1349, June 1992.

Figure intentionally omitted

Figures D: from Main, I.G. (1995). Earthquakes as critical phenomena: implications for probabilistic seismic hazard analysis. BSSA 85, 1299- 1308, October 1995.

Figure intentionally omitted

Figures E: from Main, I.G. (1995). Earthquakes as critical phenomena: implications for probabilistic seismic hazard analysis. BSSA 85,1299-1308, October 1995.

Can Small Magnitude Shocks be Used to Infer the Occurrence Rates and Locations of Future Damaging Shocks?

by

Martin C. Chapman

Jan. 7, 1997

Summary

Yes, if it can be assumed that certain elements of the seismogenic process are scale-invariant and stationary. Under those assumptions, extrapolation of small magnitude occurrence rates to higher magnitudes is consistent with hazard models wherein the locations of larger shocks are represented by area sources.

Introduction

Seismogenic sources in most areas of the eastern United States must be inferred indirectly from geophysical data, which in most cases is gleaned from small magnitude earthquakes. Given a data set consisting largely of the locations and dates of occurrence of small magnitude shocks, what if anything can be said, in a statistical sense, about the future occurrence times and locations of larger (potentially damaging) shocks? I argue below that because the seismogenic process is fundamentally scale invariant and stationary, the locations and occurrence rates of small magnitude shocks, can in principle, be used to infer the rates and locations of future large shocks.

Discussion

Scale invariance implies that a process has the same appearance, regardless of the magnification used to examine it. For this discussion, the process in question is faulting, and the key measurement is the size of the earthquake source (expressed as a rupture length, or area, or indirectly as seismic moment) and the length(s) of seismogenic faults. Stationarity implies that statistical properties of the process are constant. Stationarity is a basic

assumption of hazard analysis. It is assumed that occurrence rates (as well as the locations) of future damaging shocks can be predicted, in a probabilistic sense, using a data set comprised of past observations.

Scale invariance is a property of fractal sets, and implies a power law frequency distribution of the lengths of objects comprising the set. Several important attributes of seismicity (faulting) exhibit this property. For example, fault lengths in a given region have a power law frequency distribution. The Gutenberg-Richter frequency versus magnitude relationship is also a power law, when expressed in terms of seismic moment rather than magnitude. Earthquakes are scale invariant in terms of stress drop. Observations show a range of stress drop between a few 10's of bars to a few hundreds of bars, over several orders of magnitude of seismic moment.

Spatial Behavior:

Earthquakes exhibit clustering, both temporally and spatially. In particular, it is well established from observation in regions with high deformation rates that seismic energy release at all magnitude levels tends to occur on large, dominant faults. Some recent studies of the (statistical) physics of crustal scale deformation suggest that the evolution of the faulting process in a given volume results in the spontaneous emergence of spatially organized, dominant faults. For example, Cowie et al. (1993) developed a numerical rupture model to simulate the growth of crustal scale faults. The conceptual model was comprised of a lattice of 10x10 km crustal blocks interacting through both short and long range elastic forces, in response to a constant driving velocity at the model boundary. Initially, the lattice deforms by uncorrelated nucleation of small faults, reflecting the random, uncorrelated distribution of the material properties in the model. But as time progresses areas of the lattice become silent, while other areas contain all activity. The deformation is increasingly concentrated on large, dominant through-going faults. This occurs in spite of the fact that stress is simultaneously high elsewhere in the model grid. The system is driven to failure less often between the major faults. The faults in the simulation have a power law scaling, both of their size distribution and in the sizes of the earthquakes they

generate (Cowie et al., 1995). The results indicate that the (eventual) localization of rupture in space does not require preexisting zones of weakness.

The results of Cowie et al. are derived from two-dimensional, thin plate models: all faults in their simulations rupture the conceptualized brittle crust. Deformation rates used in the modeling are compatible with plate boundary rates. If similar results hold for a large range of scale lengths in 3-dimensions and for a range of strain rates, they may have important practical implications. For example, in a system that has evolved sufficiently, a short term snapshot of the recent seismic history could in principle be very useful for hazard analysis purposes: the locations of small shocks tend to illuminate the dominant faults, upon which large shocks will tend to occur. Thus, the results provide an experimental justification for the common practice in hazard assessment of using low magnitude seismicity to define potential sources of large shocks. Equally important however, is the result that for a system in some earlier state of evolution, the spatial correlation between the locations of the smallest shocks and largest faults could be very weak. In the context of the modeling results above, the usefulness of the historical catalog of seismicity in the southeast depends upon whether or not deformation in the region is in a stable: i.e., stationary, "self-organized" state.

The evolution of the model of Cowie et al. leads eventually to asymptotic behavior, where deformation occurs on a few through-going faults (which may be structurally complex). Areas between these major faults are stable. While this situation may be analogous to California, for example, it is not analogous to the east, at least for the scales conceptualized in the experiments. Clearly, the intraplate setting of the east does not represent the ultimate evolutionary state of the model. However, the point here is that in the model experiments, the transition from uniform "disorganized" deformation on small faults to "organized" deformation occurs at an early stage, and corresponds to a change in fault lengths from an exponential to a power-law frequency distribution.

The Gutenberg-Richter relationship for the southeastern U.S. is consistent with a power-law, with a "normal" b value of about 0.8 to 0.9, determined over

magnitudes from 2.0 to 7.0 (Bollinger et al., 1989). This suggests that seismicity in the region has indeed reached a state such that at least some clustering along dominant faults is occurring. This is supported by the observation that the instrumentally located shocks occurring during the past 20 years are obviously correlated with the pre-1976 seismicity pattern, which is distinctly non-uniform. Also, small magnitude shocks in the New Madrid seismic zone define a highly organized zone of crustal scale faulting. Similarly, seismicity in Giles County, VA indicates a steeply dipping planar zone, suggesting a crustal scale fault zone. The same situation applies to Charleston, SC. These examples represent seismicity in the "shadow" of relatively recent, large shocks. The New Madrid, Charleston and Giles County earthquakes occurred 187, 110 and 100 years ago, respectively, and it is conceivable that the current seismicity is somehow due to stress redistribution following the larger shocks. However, it is at least equally plausible the observed activity is in fact representative of an (approximate) steady-state rate of earthquake occurrence in those areas. The temporal stationarity of the seismicity is an important issue, to be addressed below. However, regardless of that aspect, small magnitude shocks in New Madrid, Giles County and Charleston tend to occur on planar features that in all likelihood represent seismogenic crustal scale faults. So, it would seem that for the purpose of predicting the locations of future damaging shocks, the locations of small magnitude shocks represent a highly relevant data set.

Temporal Behavior:

If seismicity were indeed a temporally stationary, scale invariant process, the accuracy of predicted rates of large earthquakes would depend only on random error in observed earthquake rates, which in principle could be estimated with no bias from small magnitude events. Unfortunately, the physics of the problem on a fault-specific scale indicates a very complex process. A finite maximum magnitude must exist for any given fault. The elastic rebound theory implies that strain energy is stored and released in a manner such that slip rates on faults in a given region must reflect the regional tectonic deformation rate. It is generally assumed that the regional rates are constant on the long term (several thousand years), because they are due to the mechanics of plate motion

and interaction. However, a (constant) regional deformation rate in principle might not be accurately represented by the frequency of the smaller shocks, because the deformation is dominated by slip that occurs in the largest shocks. Furthermore, comparisons of rates of large magnitude shocks with rate of smaller magnitude, recent shocks often show a discrepancy. The characteristic earthquake model for the largest shocks on a fault (Schwartz and Coppersmith, 1984; Youngs and Coppersmith, 1985) implies clustering of interevent times, and higher rates than would be predicted from a linear extrapolation of the observed Gutenberg-Richter relationship at small magnitudes.

Given the above, do rate estimates derived from catalogs containing only small magnitude events have any practical value for hazard assessment? Yes, I think they do have value. Although the linear Gutenberg-Richter relationship may break down on a fault specific basis, most seismic sources in the eastern U.S. are modeled as composites (i.e. as areas), representing assemblages of individual seismogenic faults. This spatial averaging invariably produces a linear recurrence relationship, for the population of faults. This population average is compatible with the use of a hazard model wherein the location of future damaging shocks is treated as a random variable.

References

- Bollinger, G.A., F.C. Davison, M.S. Sibol and J.B. Birch (1989), Magnitude recurrence relations for the southeastern United States and its subdivisions, *Journ. Geophys. Res.*, 94, B3, 2857-2873.
- Cowie, P.A., C. Vanneste, and D. Sornette (1993), Statistical physics model for the spatiotemporal evolution of faults, *Journ. Geophys. Res.*, 98, B12, 21,809-21,821.
- Cowie, P.A. D. Sornette and C. Vanneste (1995), Multifractal scaling properties of a growing fault population, *Geophys. J. Int.*, 122, 457-469.

Schwartz, D.P. and K.J. Coppersmith (1984), Fault behavior and characteristic earthquakes: examples from the Wasatch and San Andreas fault zones, Journ. Geophys. Res., 89, 5681-5698.

Youngs, R.R and K.J. Coppersmith (1985), Implications of fault slip rates and earthquake recurrence models to probabilistic seismic hazard estimates, Bull. Seism. Soc. Am., 75, 939-964.

USE OF FAULT LENGTH AND AREA IN THE ESTIMATION OF MAXIMUM MAGNITUDES FOR THE EASTERN TENNESSEE SEISMIC ZONE

G. A. Bollinger

LLNL SSHAC Project White Paper - November 1996

INTRODUCTION

A key parameter for seismic hazard analysis is an estimate of the maximum possible earthquake for the fault segment or seismic zone under consideration. For some high strain-rate, interplate regions, e.g., California, estimates for specific segments of the causal fault system (San Andreas) can often be made with reasonable confidence. For low strain-rate, intraplate areas such as the eastern U.S., the lack of understanding of the causes of intraplate seismicity in general and the lack of knowledge concerning individual fault segments in particular are major problems in this estimation process.

A principal technique applied in both interplate and intraplate areas for the maximum magnitude estimation process involves the use of empirical relationships between magnitude and fault parameters. Tocher (BSSA, 1958) was probably the first to show quantitatively that such a correlation existed. Since that initial study, there have been numerous published relationships relating magnitude to various fault parameters. The most recent of these is a 1994 study by Wells and Coppersmith (BSSA). This is an especially thorough, well done investigation. From a worldwide data base of source parameters for 421 earthquakes (Shallow - less than 40 km), continental interplate and intraplate shocks with magnitudes greater than about 4.5, 244 earthquakes were selected for analysis. Log-linear regressions were developed between earthquake magnitude and surface/subsurface rupture lengths and rupture areas that are especially well-correlated, having standard deviations of 0.25-0.35 magnitude units. That standard deviation is comparable to what is observed in the worldwide measurements reported for an individual earthquake. The authors conclude that since the magnitude-fault length and fault area

measurements have a large enough data base to exhibit a statistical stability that makes it unlikely that the regressions obtained would change significantly in response to additional data.

Of special importance to this study, Wells and Coppersmith (1994) also investigated the possible effect of tectonic setting. They used t-statistics to demonstrate that, at the 95% significance level, there was no difference in the regressions between extensional and compressional stress regimes. They also investigated for possible differences in earthquakes occurring in stable continental regions (SCR) with those from non-SCR regions. They found that, at the 95% significance level, the differences in the regressions for those two very different tectonic environments resulted in an expected magnitude difference of less than 0.2M. I agree with their final conclusion that subdividing the data set according to various geographic regions or tectonic settings would not typically improve the statistical significance of the regressions.

Accordingly, we will use herein the Wells and Coppersmith (1994) regressions between Moment magnitude (M) and subsurface rupture length, subsurface rupture width and rupture area. Those regressions are :

$$\text{Subsurface Rupture Length (SRL ; km)} \quad M = 4.38 + 1.49 \log (\text{SRL}) \quad (1)$$

$$\text{Subsurface Rupture Width (SRW ; km)} \quad M = 4.06 + 2.35 \log (\text{SRW}) \quad (2)$$

$$\text{Rupture Area (RA ; sq km)} \quad M = 4.04 + 0.98 \log (\text{RA}) \quad (3)$$

Use of these relationships to make estimates of maximum magnitudes obviously requires that the input rupture parameter estimates themselves be maxima. Also, it is preferable to make multiple estimates for the same fault if at all possible. This provides a qualitative indication of the stability and range of maximum magnitude estimates that the fault measurements at hand provide and it can also contribute to uncertainty assessments.

sub-vertical. Chapman provided two sets of plots at different foci gather distances (20 and 30 km) and I selected the width dimension that was the larger between them. A fault plane area is then determined by the product of the length and downdip values. Application of equations (2) and (3) produces the following results :

<u>Fault</u>	<u>Downdip Length (km)</u>	<u>(M)</u>	<u>Fault Area (sq km)</u>	<u>(M)</u>
EW1	17	7.0	1,037	7.0
EW2	16	6.9	1,520	7.2
EW3	10	6.4	420	6.6
EW4	17	7.0	510	6.7
NS1	17	7.0	1,428	7.1
NS2	20	7.1	2,500	7.4
NS3	(Not available)		(Not available)	
NS4	10	6.4	1,180	7.1

Again, we have magnitude values in the 6 1/2 to 7 1/2 range.

A comparison of the three magnitude estimates derived for all the faults except one (NS3) is as follows :

<u>Fault</u>	<u>Rupture Length M</u>	<u>Downdip Length M</u>	<u>Fault Area M</u>
EW1	7.0	7.0	7.0
EW2	7.3	6.9	7.2
EW3	6.8	6.4	6.6
EW4	6.6	7.0	6.7
NS1	7.2	7.0	7.1
NS2	7.5	7.1	7.4
NS3	6.7	NA	NA
NS4	7.5	6.4	7.1

The three values for each fault generally agree very well with each other. The average difference within the sets of three values is 0.28. Excluding NS4, whose downdip length estimate is anomalous with respect to the other to values, that average is 0.20. This remarkable consistency indicates that the horizontal length/downdip length of the Eastern Tennessee Seismic Zone faults is in accord with what has been observed for seismogenic faults worldwide.

I judge these estimates to be very useful to the process of determining maximum magnitudes estimates for the Eastern Tennessee Seismic Zone. In particular, they demonstrate that the crustal seismogenic zone present there is unusually thick (17 km), that it extends to mid-crustal depths of 22 km. and, according to worldwide earthquake fault data, is, in principle, capable of generating shocks in the large (7 1/2) range.

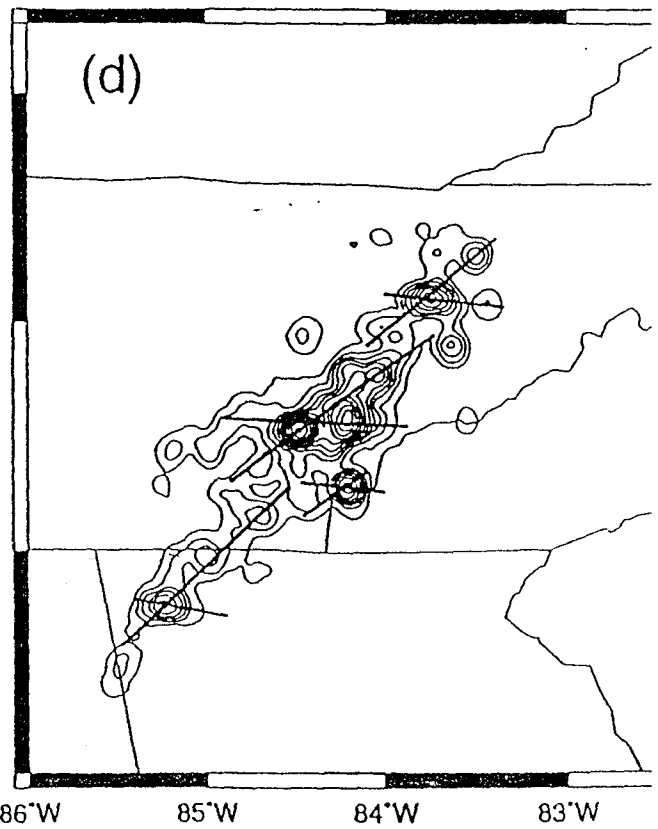
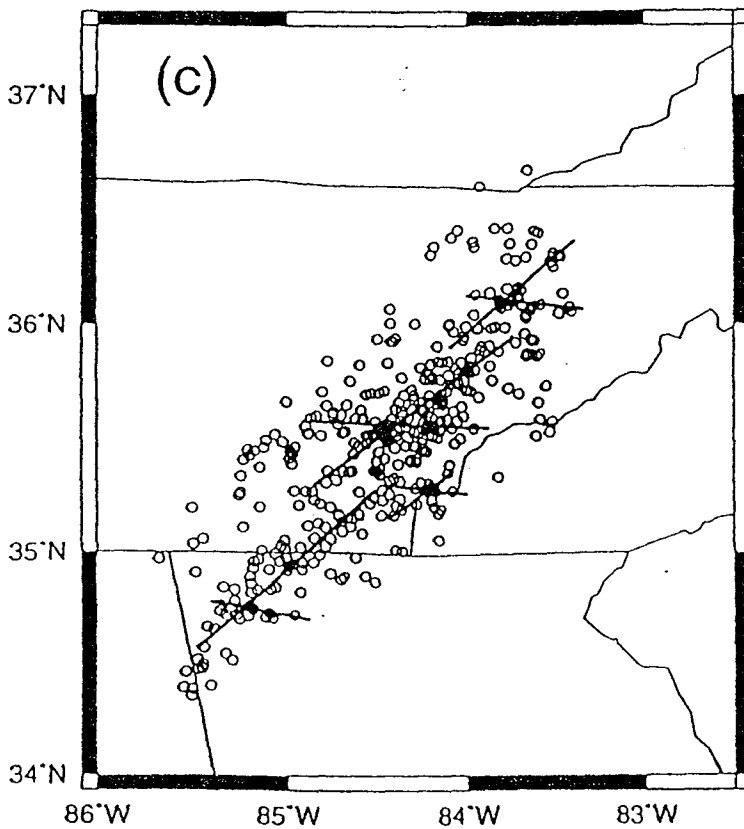
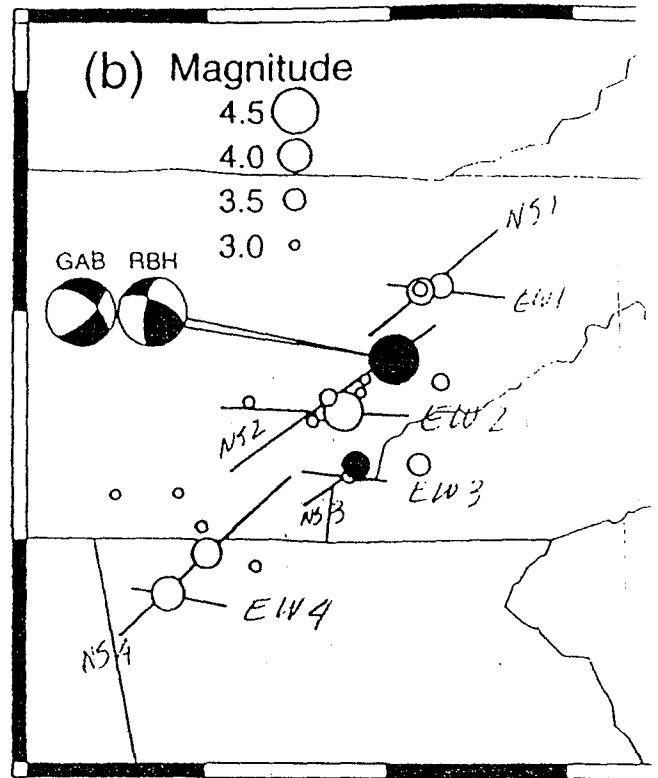
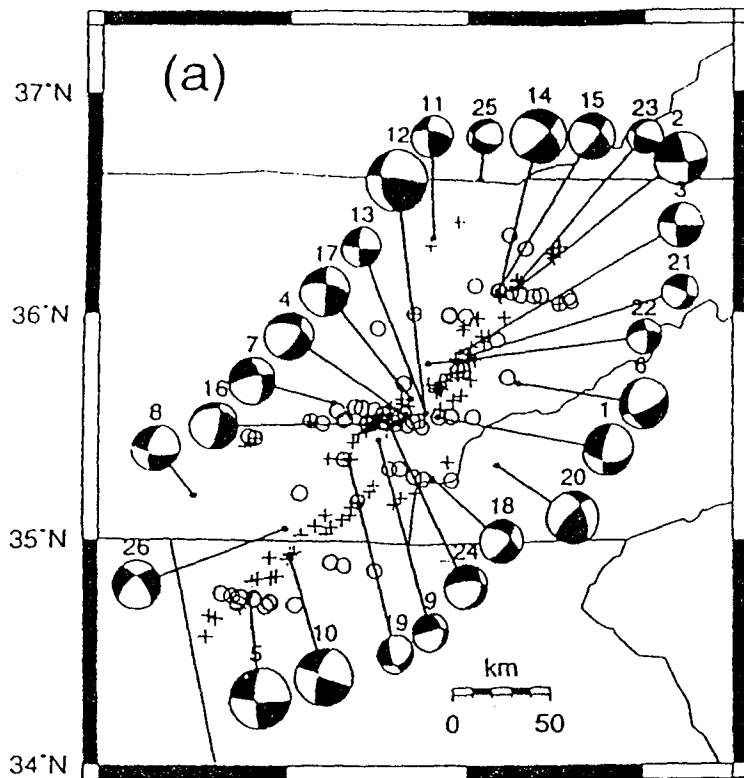


Figure 1

APPENDIX

Foci Plots for the Eastern Tennessee Seismic Zone Showing Horizontal and Vertical Distributions

(Provided by Martin Chapman, Oct 1996)

Figures on the following pages B-29 through B-40 were intentionally removed

Figure intentionally omitted

DRAFT

Estimating Magnitudes of Earthquakes From Paleoliquefaction

by

Pradeep Talwani

January 1997

1. Seismically induced liquefaction (SIL) features - lateral flows, explosion craters - are widely observed. The geometry, size and distance of these features from the earthquake source varies greatly attesting to the fact that seismically induced liquefaction is a very intricate process. Earthquakes of magnitude as low as 4.5 have been known to have caused liquefaction. Great earthquakes, e.g., 1905 Kangra, India are known to have caused widespread liquefaction at distances over 200 km, and there was an absence of liquefaction features at lesser distances. These observations are just to make a point that several factors control the location and incidence of liquefaction due to an earthquake. Contrariwise, determining the size and nature of an earthquake from an examination of SIL feature is problematic.
 - 2.1. The occurrence of liquefaction at any site is controlled by several factors. These include:
 - a. Geotechnical characteristics of the soil - grain size, saturation, packing density, effective stress conditions, etc.
 - b. Thickness and density of overlying soil column.
 - c. Depth to the water table.
 - d. Amplitude of strong ground motion.
 - 2.2. The amplitude of strong ground motion at any site, (besides the site conditions described in (i) above,) also depends on seismological factors:
 - a. The earthquake magnitude.
 - b. The hypocentral distance from the source.
 - c. The peak and duration of horizontal acceleration.
 - d. The crustal structure between the source and site. Several examples attest to this conclusion. Liquefaction occurred at distances 100 km or greater following the 1989 Loma Prieta, California, 1905 Kangra, India,

1934 and 1988 Bihar-Nepal, earthquakes. Catchings and Kohler (1996) showed that focussing of seismic waves, can amplify strong ground motion at large distances.

3. The above observations are made to point out that it is not a simple or easy task to estimate the magnitude of an earthquake from an examination of liquefaction features. However, if certain conditions are met it is possible to obtain a qualitative estimate of the size of a prehistoric earthquake. These include:
 - a. Knowledge of the location of the earthquake.
 - b. Widespread observation of liquefaction features relatable to a source.
 - c. Availability of a calibration earthquake, i.e., an earthquake whose location and magnitude are known and whose liquefaction effects can be compared with those of paleoearthquakes.

An example of such an earthquake is the 1886 Charleston earthquake which was associated with widespread liquefaction and various paleoearthquakes were associated with a similar distribution of paleoliquefaction features.

Obermeier and others (1989) noted that the dimensions and frequency of sand blows decreased away from Charleston. They interpreted that observation to suggest that the source of the prehistoric earthquakes was near Charleston.

4. Once the location of the source is known, under favorable circumstances, three methods can be used to obtain an estimate of the magnitude of a prehistoric earthquake from an examination of liquefaction features.
 - a. From the size and frequency of sand blows of the same age.
 - b. From Liquefaction Severity Index (Youd and Perkins, 1987).
 - c. From geotechnical measurements.

These are briefly described below:

- 4.a. The 1886 M_w 7.3 Charleston earthquake, was associated with liquefaction near Bluffton and near Georgetown, located 100 km to SW and NE of Charleston (Figure 1). The prehistoric earthquakes of 546, 1000, 3550 YBP were also associated with sand blows at these three locations. This observation was used to infer the size of the prehistoric earthquakes as being comparable to the 1886 event. The 1641 YBP paleoearthquake was only encountered in the sand

blows between Myrtle Beach and Georgetown and not near Charleston. It was assigned a M_w 6.0.

- 4.b. Using the size and nature of deformation of sedimentary features in a continuous distribution of liquefaction features away from sources of earthquakes in western US, Youd and Perkins (1987) developed the Liquefaction Severity Index (LSI) as a measure of horizontal ground displacement associated with subsurface liquefaction. By comparing epicentral distances to different liquefaction features for different magnitude earthquakes, they obtained LSI attenuation curves (Figure 2). These in turn can be used to estimate the magnitude of paleoearthquakes. However by comparing the LSI data for the instrumentally located Saguenay earthquake, Tuttle (1994) showed that the LSI curves are limited in their usefulness for estimating magnitudes for prehistoric earthquakes unless the source area can be defined.
- 4.c. Estimates of magnitudes from geotechnical tests. Magnitude estimates can also be obtained by comparing the results of geotechnical tests in areas of liquefaction (see e.g., Seed and Idriss (1982), Martin (1990), Amick and Talwani (1991) and Tuttle (1994)).

Based on an extensive body of data empirical correlations were obtained relating the occurrence and nonoccurrence of liquefaction to the intensity of ground shaking and the principal characteristics of cohesionless soils. Figure 3 shows the data for earthquakes with a $\sim M$ 7.5. Each point corresponds to one boring record. The intensity of ground motion at a site is represented by the vertical ordinate, τ_{av}/σ'_0 where τ_{av} is the average peak shear stress and σ'_0 is the initial vertical effective stress. The soil resistance is represented by the horizontal abscissa $(N_1)_{60}$ which is the blow count in a standard penetration test (SPT) corrected for the depth of the overburden.

The curve drawn in Figure 3 is used to divide zones of liquefaction and non-liquefaction. Using similar data for other earthquakes, Seed and Idriss (1982) obtained a family of curves for different magnitudes (Figure 4).

For a paleoliquefaction site, the results of SPT tests can be used to obtain the penetration resistance, and other tests are used to estimate the ground acceleration associated with the liquefaction (vertical ordinate), and hence the magnitude of the earthquake (see e.g., Martin 1990). These curves are generic and local site conditions can modify the results.

References

1. Amick, D.C. and P. Talwani (1991). The Use of Paleoliquefaction Features to Estimate Prehistoric Levels of Ground Motion. Proceedings of the Second International Conference on Recent Advances in Geotechnical Earthquake Engineering and Soil Dynamics, St. Louis, Missouri, March 11-15, 1991.
2. Catchings, R.D. and Kohler, W.M., (1996). Reflected Seismic Waves and Their Effect on Strong Shaking During the 1989 Loma Prieta, California Earthquake, *Bull. Seis. Soc. Am.*, **86**, 1401-1416.
3. Martin, J.R. (1990). Implications From a Geotechnical Investigation of Liquefaction Phenomena Associated With Seismic Events in the Charleston, South Carolina Area. Ph.D. Dissertation, Virginia Polytechnic Institute and State University, 414 p.
4. Obermeier, S.F., Weems, R.E., Jacobson, R.B. and Gohn, G.S. (1989). Liquefaction Evidence for Repeated Holocene Earthquakes in the Coastal Region of South Carolina: *Annals of the New York Academy of Sciences*, **558**, 183-195.
5. Seed, H.B. and I.M. Idriss (1982). Ground Motions and Soil Liquefaction During Earthquakes. EERI Monograph Series, Vol. 5, 134 p.
6. Tuttle, M.P. (1994). The Liquefaction Method for Assessing Paleoseismicity: Technical Report NUREG/CR-6258, Nuclear Regulatory Commission, Washington, D.C., 38 p.
7. Youd, T.L. and D.M. Perkins (1987). Mapping of Liquefaction Severity Index. *Journal of Geotechnical Engineering*, Vol. **113**, No. 11, 1374-1392.

Figure intentionally omitted

Figure I Shows the location of paleoliquefaction sites from where radiocarbon dates have been obtained. Isoseismal lines for the 1886 Charleston earthquake are taken from Bollinger (1977).

Figure intentionally omitted

Figure 2 Liquefaction severity index (LSI versus distance for the 1988 Saguenay, Quebec, 1886 Charleston, SC, and 1811 New Madrid, MO, earthquakes, with least squares fit lines for each earthquake, as well as LSI for western US earthquakes (dashed lines) of equivalent magnitude (from, Youd et al., 1989). (Figure from Tuttle, 1994.)

FIGURE -3 Relationship between stress ratios causing liquefactibn and (N1)60 values for clean sands for magnitude 7.5 earthquakes. Source: Seed et al. (1984).

Figure intentionally omitted

Figure 4- Chart for evaluation of liquefaction potential of sands for earthquakes of different magnitudes.
Source: Seed and Idriss (1982).

**APPENDIX C: PRELIMINARY SOURCE GEOMETRIES DEVELOPED
BY THE EXPERTS IN PREPARATION OF THE SEISMIC SOURCE
EXERCISE OF WORKSHOP #2**

Some of the maps displayed here were actually drawn by the experts during Workshop #1, then modified and documented for Workshop #2.

The remaining pages in Appendix C were copied from other sources.

DOCUMENTATION FOR SEISMIC SOURCE MAPS

by

Gil Bollinger

August 1996

for

Trial Implementation of SSHAC Guidelines Project - LLNL/FESSP

The basic rationale for my approach to the definition of Seismic Source Zones in the Southeastern U. S., along with detailed discussions for specific examples, is given in the *USGS Bulletin 2017*, 1992. In brief, my technique places primary emphasis on areas of concentrated historical and instrumental seismicity. That emphasis is based from three factors :

- (1) Those areas are the currently most active,
- (2) McGuire's 1979 study of the 1900-yr long Chinese catalog concluded that the most recent 50-100 year period was the best predictor of the felt-shaking hazard for the next 50 years,
- (3) There is good agreement spatially between the 200-yr+ historical seismicity and the most recent 20-years of network/instrumental seismicity in the southeastern U.S.

Points 2 and 3 bear directly on PSHA for structures with 50 yr and 100 yr lifetimes. However, current strain rate estimates for the eastern U.S. are too large to be sustained over geologic time - therefore, there must be some type of cyclicity or on/off character in the region's earthquake activity. Right now, we can only say that it is longer than 200 years. Since the much more active China region had a 300-yr periodicity, perhaps the much less active eastern U.S. will have even longer periods of variations in strain energy release.

I use data and results from Seismology, Geology, Geophysics and Tectonics to supplement the seismicity data for zonal boundary definition and parameter estimation on a case-by-case basis.

Instead of the use of alternate source zones to express uncertainty, I prefer to assign probabilities of existence (pe) to each zone - the more uncertain the zone the lower its pe.

A simple zonal boundary such as a closed-curve or a polygonal figure is judged to be adequate because :

- (1) When the epicenter error ellipses are plotted they occupy a much larger area than that of the epicentral point estimates,
- (2) The Southeastern US epicenter concentrations generally have a 'halo' type of surrounding activity thereby making the exact boundary of the zonal concentration less clearly defined, and
- (3) As the 1988 Saguenay earthquake demonstrated, moderate shocks can occur at appreciable distances from the main zonal epicenter concentrations (75 km from Charlevoix Zone).

The principal concentrations I identify as Seismic Source Zones in the Southeastern US are the sites of the two largest historical shocks in the region, the spatially largest epicenter concentration and a small cluster separate from the site of the region's largest earthquake :

- The Giles County, VA Zone (Zones RZ3 and RZ3A)
- The Eastern Tennessee Zone (Zones RZ1, RZ1A and RZ1B)
- The Charleston, SC Zone (Zones LZ1, LZ1A and LZ1B))
- The Bowman Zone (Zone LZ2)

More diffuse seismicity concentrations are identified as source zones in :

- Central Virginia (Zone RZ4)
- Central Appalachians (Zone RZ5)
- Western North Carolina (Zone RZ2)
- South Carolina. (Zones LZ3, LZ3A and LZ4)

Finally, because of their great seismic potential, zones should also be considered for :

- New Madrid, MO (Zone RZ6)
- Wabash Valley, IL-ID (Zone RZ7)

Documentation for Southeastern U. S. Seismic Source Zones

Following is a listing of each Zones' principal diagnostic features.

Giles County, VA Source Zone (RZ3 - pe 100%) :

Concentrated linear zone of well-located instrumental seismicity -

Also, Define a causal fault zone (RZ3A - 75% pe)

Zone of historical/poorly located seismicity ; Largest shock mb 5.6* in 1897.

P and S reflection seismic data define steeply-dipping basement faulting in agreement with focal mechanism nodal planes, Well-constrained focal depths 4-15** km - Implies average seismogenic crustal thickness and location beneath the Appalachian Overthrust,

General agreement between NE strike of zone and strike of focal mechanism nodal planes - that strike is rotated some 20 deg from the ENE strike of the Appalachian structural grain,

General uniformity of focal mechanisms - mixed strike-slip and reverse with northeasterly trending P-axes and

Possible North-South intersection structure from instrumental seismicity.

* - Magnitudes herein from Stover & Coffman, USGS Paper 1527, 1992.

** - Focal Depths throughout are 10% and 90% fractile depths from Bollinger, 1992.

Eastern Tennessee Source Zone (RZ1 - pe 100%) :

Concentrated 300+ km long linear zone of well-located instrumental seismicity,

Zone of historical/poorly located seismicity ; Largest shock a mb 5.0 in 1865 (Chapman argues this shock was not in NC but rather near the NC-TN border),

Well-constrained focal depths 8-21 km - Implies thick seismogenic crust below the Appalachian Overthrust rocks,

Two groups of strike-slip, steeply dipping focal mechanisms : N-S/E-W and NE-SW/NW-SE, i.e., oblique and parallel to the zone, with well based preference for the NE-SW and E-W nodal planes as a conjugate set of causal faults,

General uniformity of focal mechanism P-axes - northeasterly trend,

Very distinct correlation with regional through-going aeromagnetic anomaly lineations,

Define (1) A specific fault source zone (Chapman et al, subm BSSA, 1996) designated as RZ1A with a pe of 50% and also

(2) A low probability of existence (RZ1B - pe 10%) Zone for the possible development of a fault the full length of the zone resulting in a great earthquake (Mw 8).

Charleston, SC Source Zone (LZ1) - pe 100% :

Concentrated cluster of well-located seismicity,

Zone of historical/poorly located seismicity ; Largest shock a Mw 7.3 in 1886,

Focal depths to 5-10 km - Average seismogenic crustal thickness, Focal mechanisms variable plus concentrated nature of recent seismicity suggests some type of intersection structure operative in localizing the strain.

Coastal Plain sedimentary wedge causes enhanced Intensity effects to the NW and reduced effects to the NE-SW and

Possible associated sources (or crustal amplification sites from the Charleston Source) from local liquefaction features northeast (Georgetown area - LZ1A - pe 50%) and southwest (Bluffton area - LZ1B - pe 25%) of the Charleston locale.

Bowman, SC Source Zone (LZ2 - pe 50%):

Concentrated zone (NW trend ?) of well-located seismicity ; Largest shock a mb 4.5 in 1972,

Not a historical zone - Has exhibited an 'on again/off again' habit since the early 1970's,

No focal mechanisms - Focal depths 2-6 km,

Only a few, small (M mostly less than 4) earthquakes and

Approximately 70 km from the Charleston source ; the 1988 Saguenay earthquake was some 75 km from the Charlevoix Zone.

South Carolina Piedmont & Coastal Plain Source Zone (LZ3 - pe 100%)

Diffuse seismicity of generally low-level ; Largest shock a mb 4.8 in 1913,

Persistent strain release throughout the historical record,

Reflection seismic data indicate structural/seismicity similarities with the Central Virginia Seismic Zone where strain release is occurring on multiple splay faults off a major detachment fault, Multiple sites of Reservoir-Induced Seismicity (RIS) and borehole stress measurements suggests high stress levels at shallow depths in the host crystalline Piedmont rocks, Presence of many intruded plutons in the basement rocks allows for sites of stress amplification and Alignment of RIS and other epicenter concentrations suggest the possibility of a Fall Line Seismic Zone (LZ3A - pe 20%).

Savannah River Site and Vogtle Seismic Zone (LZ4 - pe 20%)

Extensive geological, geophysical and seismological investigations at these two important sites have revealed the presence of multiple faults and other structural features, e.g., the Triassic Dunbarton basin and Pen Branch Fault, that are typical of the entire host Piedmont Province,

Very low level seismicity ; Largest shock an mb 3.3 in 1974 with mb 3.2's in 1972 and 1993,

Earthquake occurrences here have been interpreted as due to pockets of relatively high stress concentrations in the vicinity of buried plutons and/or a 'skin effect' of high stress regimes in the uppermost few kilometers of the high velocity Piedmont crystallines and

Recognized herein as a zone, with a pe of 20%, because of the known geologic structures and the critical facilities and storage materials present.

Western North Carolina Seismic Zone (RZ2 - pe 75%)

Diffuse earthquake activity of generally low level with larger shocks in 1861 (mb 5.0) and 1916 (mb 5.2),

Zone more active in pre-instrumental period prior to about 1960 than subsequently and

First identified as a zone by Gerald R. MacCarthy in 1956.

Central Virginia Seismic Zone (RZ4 - pe 100%)

Spatially isolated, coin-shaped seismogenic volume of persistent, low-level activity in the Virginia Piedmont,

Largest shock an mb 5.0 in 1875,
Focal mechanisms exhibit widely variable parameters and
Earthquake hypocenters and reflection seismic data show
excellent correlation with splay faults off the western flank of
a regional antiform structure (Foci shallower (3-7 km) and NE
trending focal mechanism P-axes) and with a separate, near-
vertical diabase dike swarm of Mesozoic age (Deeper foci (8-13
km and NW P-axes).

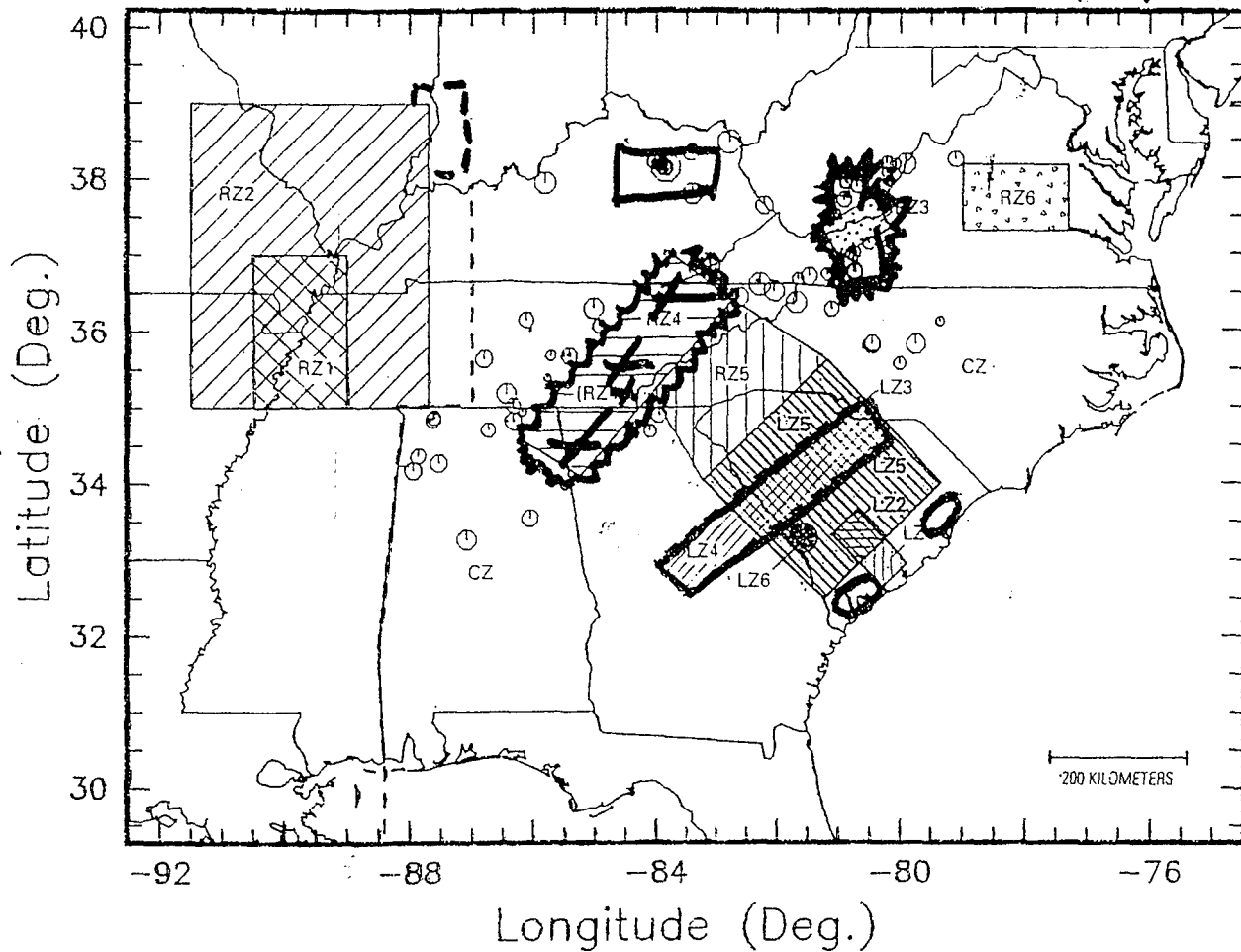
Appalachian Seismic Zone (RZ5 - pe 50%)

Diffuse earthquake occurrences that forms a regional 'halo effect'
about the area's more well-defined zones (Giles County, Eastern
Tennessee and Western North Carolina) and
Largest shock less than mb about 4 ; Low level seismicity historically
persistent.

New Madrid, MO Source Zone (RZ6 - pe 100%):

Concentrated zone - a complex 4-segmented zone of well-located
seismicity,
Zone of historical/poorly located seismicity ; Three largest shocks in
1811-12 in the Mw 7+ to 8 range,
Focal depths to 12 km. - Average seismogenic crustal thickness,
Focal mechanisms variable but uniform within each segment
Wabash Valley seismicity plus paleoliquefaction evidence argues
strongly for its own Seismic Source Zonal status (RZ7 - pe of
100%).

Bollinger
6/18/96



EXPLANATION

<table border="1" style="width: 100%; border-collapse: collapse;"> <tr><td style="text-align: center;">CZ</td><td>Complementary Zone</td></tr> <tr><td style="text-align: center;">LZ1</td><td>Local Zone 1</td></tr> <tr><td style="text-align: center;">LZ2</td><td>Local Zone 2</td></tr> <tr><td style="text-align: center;">LZ3</td><td>Local Zone 3</td></tr> <tr><td style="text-align: center;">LZ4</td><td>Local Zone 4</td></tr> <tr><td style="text-align: center;">LZ5</td><td>Local Zone 5</td></tr> <tr><td style="text-align: center;">LZ6</td><td>Local Zone 6</td></tr> <tr><td style="text-align: center;">RZ1</td><td>Regional Zone 1</td></tr> <tr><td style="text-align: center;">RZ2</td><td>Regional Zone 2</td></tr> <tr><td style="text-align: center;">RZ3</td><td>Regional Zone 3</td></tr> <tr><td style="text-align: center;">RZ4</td><td>Regional Zone 4</td></tr> <tr><td style="text-align: center;">RZ5</td><td>Regional Zone 5</td></tr> <tr><td style="text-align: center;">RZ6</td><td>Regional Zone 6</td></tr> </table>	CZ	Complementary Zone	LZ1	Local Zone 1	LZ2	Local Zone 2	LZ3	Local Zone 3	LZ4	Local Zone 4	LZ5	Local Zone 5	LZ6	Local Zone 6	RZ1	Regional Zone 1	RZ2	Regional Zone 2	RZ3	Regional Zone 3	RZ4	Regional Zone 4	RZ5	Regional Zone 5	RZ6	Regional Zone 6	<p>Background</p> <p>Charleston, South Carolina, seismic zone</p> <p>Bowman, South Carolina, seismic zone</p> <p>South Carolina Piedmont and Coastal Plain seismic zone</p> <p>South Carolina Fall Line seismic zone</p> <p>Area of Local Zone 3 minus area of Local Zone 4</p> <p>Savannah River Site</p> <p>New Madrid, Missouri, seismic zone (small)</p> <p>New Madrid, Missouri, seismic zone (large)</p> <p>Giles County, Virginia, seismic zone</p> <p>Eastern Tennessee seismic zone (RZ4A the same area as RZ4)</p> <p>Northwestern South Carolina and southwestern North Carolina seismic zone</p> <p>Central Virginia seismic zone</p>	<p>MAGNITUDE</p> <p>⊕ 5</p> <p>⊙ 4</p> <p>⊖ 3</p> <p>○ 2</p> <p>◦ 1</p> <p>• 0</p>
CZ	Complementary Zone																											
LZ1	Local Zone 1																											
LZ2	Local Zone 2																											
LZ3	Local Zone 3																											
LZ4	Local Zone 4																											
LZ5	Local Zone 5																											
LZ6	Local Zone 6																											
RZ1	Regional Zone 1																											
RZ2	Regional Zone 2																											
RZ3	Regional Zone 3																											
RZ4	Regional Zone 4																											
RZ5	Regional Zone 5																											
RZ6	Regional Zone 6																											

Preliminary Source Geometry

Martin Chapman

August 25, 1996

Zonation 1:

Spatial smoothing of seismicity, with source areas for the New Madrid and the Wabash Valley seismic zones (Figure 1).

Zonation 2:

Areas defined for all sources, with no spatial smoothing (Figure 2).

Zonation 3:

Modification to Zonation 2 above, where fault sources replace source areas A and D. Areas N and M replace areas C and E (Figure 3).

Discussion

Source A: (Eastern Tennessee Area Source)

The Valley and Ridge province of eastern Tennessee has been the most seismically active area in the southeastern United States since instrumental monitoring of the region became approximately uniform in the early 1980's. The pattern of epicenters defines a northeast trending zone, which correlates with regional scale potential field anomalies (King and Zietz, 1978; Nelson and Zietz, 1983, Powell et al., 1994). The earthquakes in eastern Tennessee show similarities to the seismicity of the Giles County, Virginia, zone (Bollinger et al., 1991). Focal depths are beneath the Appalachian sedimentary section in Precambrian basement.

Intentionally blank

Source A alternative: (basement faults)

The basement faults inferred by Chapman et al., (1996) are modeled as an alternative to a uniform area source.

Source B:

This source includes southwestern Virginia, western North Carolina, northeastern Tennessee, and northwestern South Carolina. Instrumental data from shocks in this area suggest that the earthquakes occur beneath the Appalachian thrust sheets, in Precambrian basement rock, as in Giles County Virginia and the adjoining eastern Tennessee seismic zones. The region overlies the inferred Eocambrian margin of North America, and reactivation of extensional faults that originally developed during the opening of the proto-Atlantic ocean may be responsible for modern seismicity (Bollinger and Wheeler, 1988).

The largest historical shock in this source area occurred on February 21, 1916. The epicenter of this shock is uncertain: it was strongly felt in Waynesville, North Carolina, which is the attributed epicenter. However, the shock was also strongly felt on the western side of the Smoky Mountains, in Sevierville, Tennessee. Stover and Coffman (1993) list a magnitude value of 5.2 (m_b/g), based on felt area.

Source C South Carolina - Georgia Piedmont.

A section of the Piedmont in South Carolina and eastern Georgia has experienced a higher level of seismicity than the Piedmont-Coastal Plain region as a whole. Probably the largest historical shock in the entire Piedmont occurred near Union, South Carolina on January 1, 1913. That shock threw down numerous chimneys in the epicentral area. The magnitude is estimated as 4.8 (Stover and Coffman, 1993). Source area C is defined here on the basis of historical and recent levels of seismicity.

Source D Charleston (1886 epicenter area)

Geological investigations have revealed evidence for several pre-1886 earthquakes in the coastal South Carolina area (Talwani and Cox, 1985; Obermeier et al., 1985; Weems and Obermeier, 1989; Amick et al., 1990; 1991, Rajendran and Talwani, 1993, Gelinis et al., 1994,). The evidence suggests that seismicity is recurrent in the immediate area near the epicenter of the 1886 shock. The area source D models the hypothesis of an active source limited to the epicentral area of the 1886 shock.

ZRA: (Alternative to Source D).

The fault models a potentially seismogenic structure associated with the zone of river anomalies discussed by Marple and Talwani (1993) and Marple (1994).

Source E: Piedmont and Coastal Plain

The Piedmont and Atlantic Coastal Plain areas exclusive of South Carolina and central Virginia exhibit a low level of seismic activity.

Source F: Central Virginia

The central Virginia seismic zone is an area of persistent seismicity that roughly trends along the James River. The largest historical shock was approximately magnitude 5.0 (mblg) on December 22, 1875, in Goochland County. The seismic zone has been instrumentally monitored since 1978. The data indicate a more complicated stress regime than that inferred for the Giles County, VA and eastern Tennessee seismic zones to the west. Also, central Virginia shocks tend to be at shallower depth, extending from the surface to mid-crustal depth.

Results to date indicate that the geologic causes of seismicity in central Virginia are substantially different from those operative to the west in the Appalachian mountain regions. Seismicity in central Virginia is related to

intensely deformed structures in the detached upper crustal rocks, whereas less deformed Grenville basement is aseismic. Much the opposite is the case in the Appalachian mountain region (Valley and Ridge and Blue Ridge), where the shallow crust above the detachment is aseismic, and earthquakes are inferred to occur due to reactivation of faults in Grenville basement.

Source G: Northern Virginia.

This area includes the Valley and Ridge and Blue Ridge areas of the central Appalachians. The area has a low level of historical seismicity.

Source H: Appalachian Foreland

This source area is simply defined on the basis of sparse historical seismicity. It represents the average seismicity characteristics of a large portion of the central United States.

Source I: Alabama

This source area includes the moderately active Appalachian Valley and Ridge province of Alabama and the extension beneath the coastal plain.

Source J: Giles County Virginia

The "Giles County" seismic zone is an area of concentrated seismicity near the West Virginia-Virginia border, lying mostly within Giles County, Virginia. This is the location of the second largest earthquake to have occurred in the southeastern United States during the historical period. It occurred on May 31, 1897, with an estimated magnitude of 5.8 (mblg). It caused intensity VIII MM damage in the epicentral area, near Pearisburg. The largest shock in recent times was mblg 4.6 on November 11, 1969.

Earthquakes occur at depths between 5 and 25 km and appear to define a 40 km long, steeply dipping structure which trends NNE, about 20 degrees

counterclockwise to the trend of the detached sedimentary structures mapped at the surface. The earthquakes are apparently unrelated to structure exposed at the surface, and are confined to the Grenville basement beneath the Paleozoic detachment. It has been proposed that seismicity in the zone is the result of reactivation of one or more Eocambrian extensional faults (Bollinger et al., 1993, 1991; Bollinger and Wheeler, 1988).

Source K: Wabash Valley

This area models the potential for large shocks in the Wabash Valley. Recent paleoseismic studies have discovered evidence for several large pre-historic shocks in this area (e.g., Obermeier, 1996).

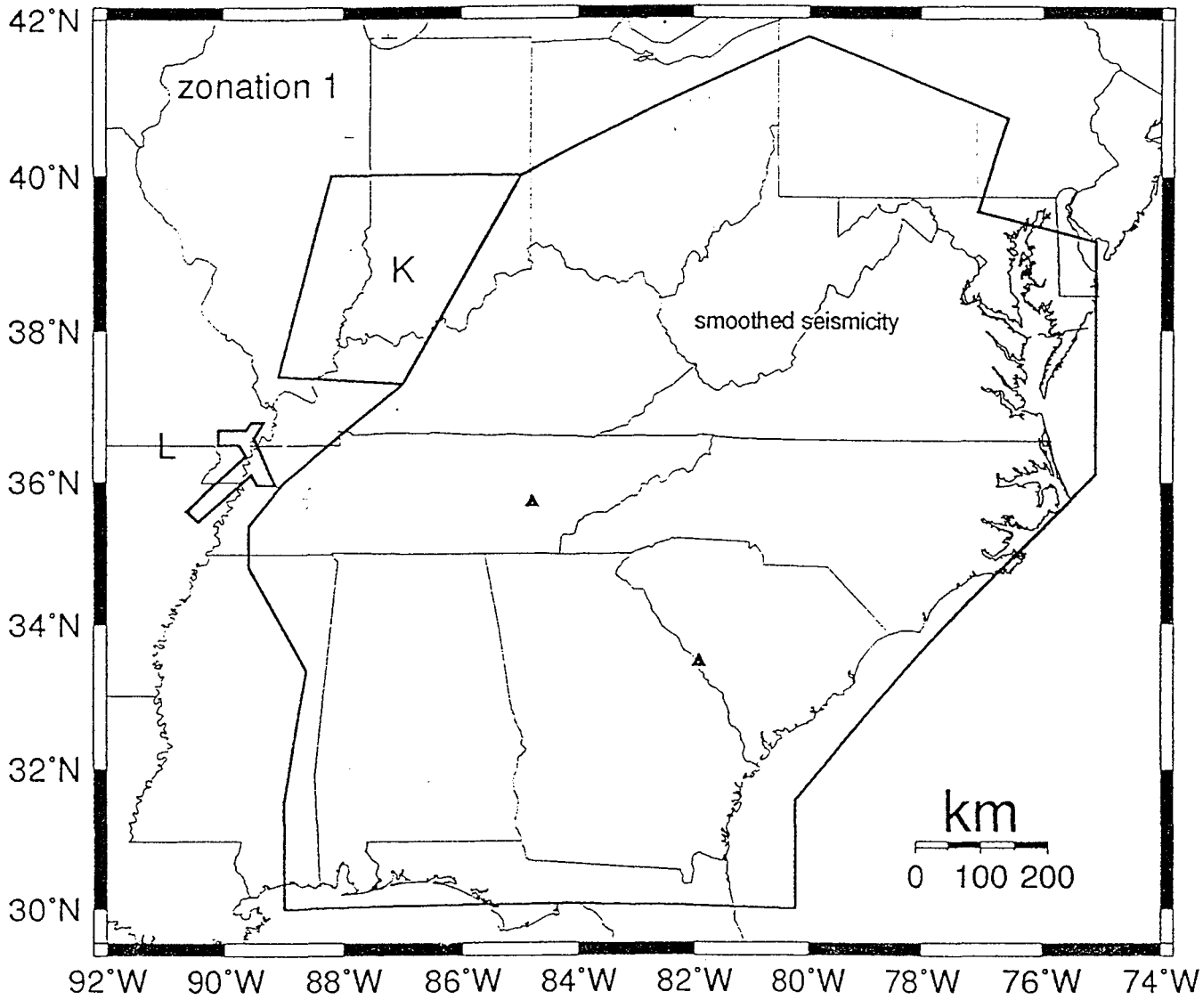
Source L: New Madrid

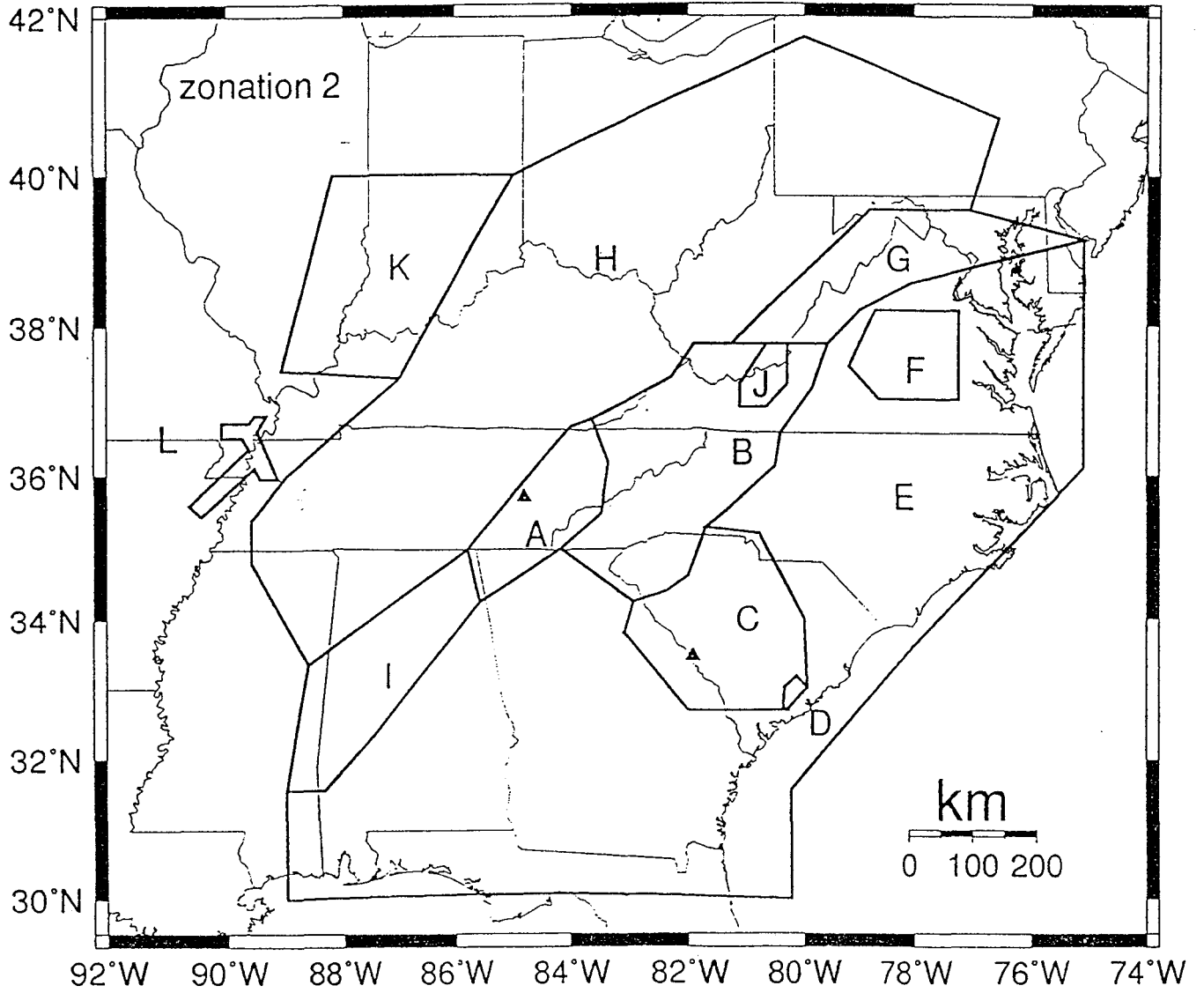
This source area models the seismogenic basement faults in the New Madrid seismic zone.

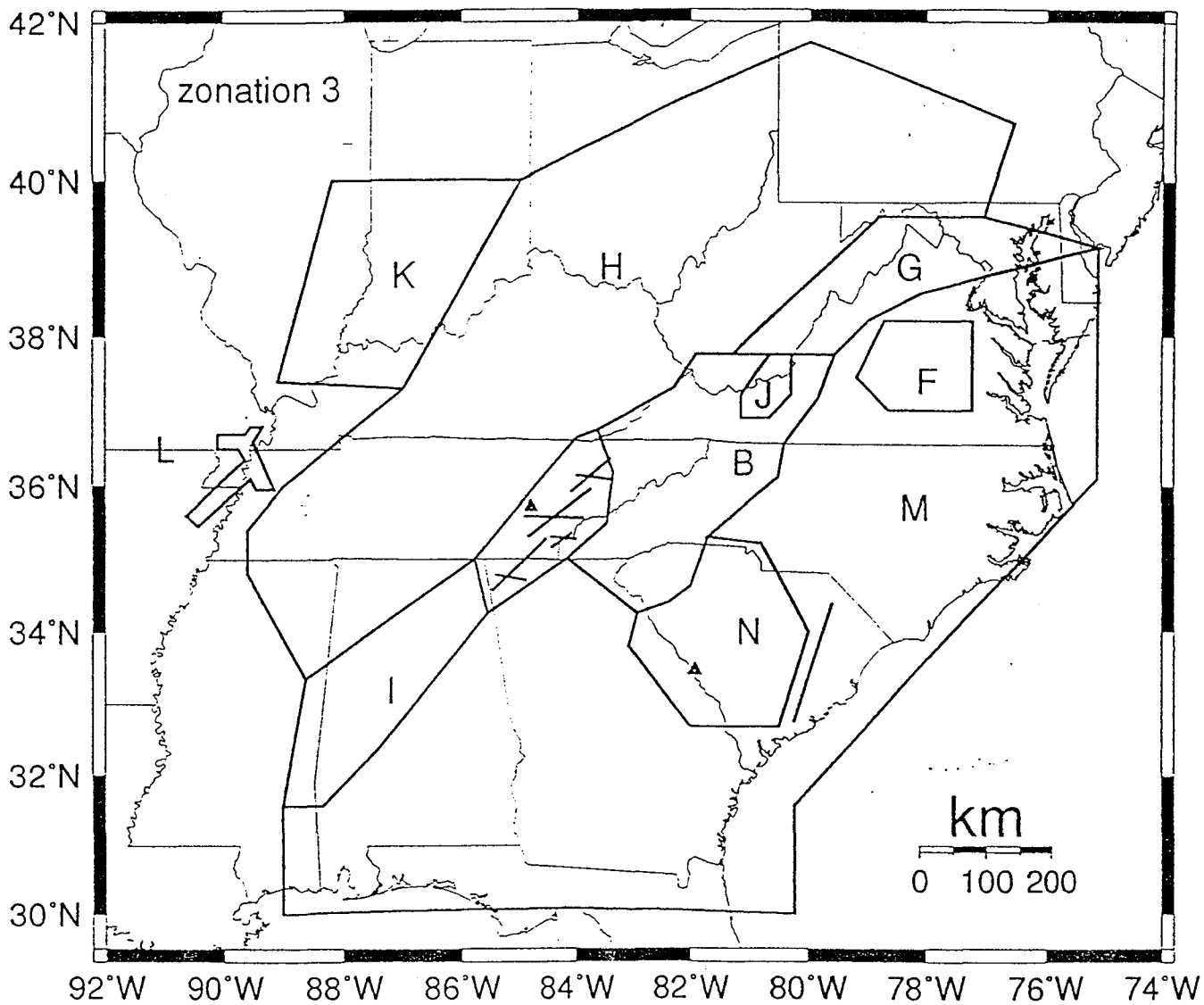
Source M: Alternative to Source E

Source N: Alternative to Source C

This slight modification is to be used in association with the ZRA source for Charleston and source E for the greater Piedmont areas.







References

- Amick, D., G. Maurath, and R. Gelinas, (1990), Characteristics of seismically induced liquefaction sites and features located in the vicinity of the 1886 Charleston, South Carolina, earthquake, Seismological Research Letters, v. 61, no. 2, pp. 117-118.
- Amick, D., R. Gelinas, and K. Cato, (1991), Magnitudes, locations and return periods of large prehistoric earthquakes occurring in coastal South Carolina, Seismological Research Letters, v. 62, no. 3-4, p. 161.
- Bollinger, G. A. and R. L. Wheeler, (1988), The Giles County, Virginia, seismic zone - Seismological results and geological interpretation, U.S. Geological Survey Professional Paper 1355, 85 p.
- Bollinger, G. A., A. C. Johnston, P. Talwani, L. T. Long, K. M. Shedlock, M. S. Sibol, and M. C. Chapman, (1991), Seismicity of the Southeastern United States; 1698 to 1986, in Neotectonics of North America, D. B. Slemmons, E. R. Engdahl, M. D. Zoback, and D. D. Blackwell, editors, Geological Society of America, Boulder, CO, Decade volume 1, pp. 291-308.
- Chapman, M. C., Powell, C. A., Vlahovic, G., and M. S. Sibol, (1996), The nature of faulting in eastern Tennessee inferred from a statistical analysis of earthquake epicenters and focal mechanisms, submitted to Bulletin of the Seismological Society of America, 1996.
- Gelinas, R., K. Cata, D. Amick and H. Kemppinen, (1994), Paleoseismic studies in the southeastern United States and New England, NUREG/CR-6274, Division of Engineering, Office of Nuclear Regulatory Research, U.S. Nuclear Regulatory Commission, Washington, D.C.
- King, E. R. and Zietz, I., (1978), The New York - Alabama lineament; Geophysical evidence for a major crustal break in the basement beneath the Appalachian basin, Geology, v. 6, pp. 312-318.

- Marple, R. T., (1994), Discovery of a possible seismogenic fault system beneath the Coastal Plain of South and North Carolina from an integration of river morphology and geological and geophysical data (Ph.D dissertation), Univ. South Carolina, 354 p.
- Marple, R. T., and P. Talwani, (1993), Evidence of possible tectonic upwarping along the South Carolina coastal plain from an examination of river morphology and elevation data, Geology, 21, p. 651-654.
- Nelson, A. E. and I. Zietz, (1983), The Clingman lineament, other aeromagnetic features, and major lithotectonic units in part of the southern Appalachian Mountains, Southeastern Geology, v. 24, pp. 147-157
- Obermeier, S. F., (1996), Seismically Induced Paleoliquefaction Features in Southern Illinois, (abst), Seismological Research Letters, 67 no. 2, p 49.
- Obermeier, S. F., G. S. Gohn, R. E. Weems, R. L. Gelinas, and M. Rubin, (1985), Geologic evidence for recurrent moderate to large earthquakes near Charleston, South Carolina, Science, v. 227, pp. 408-411.
- Powell, C.A., G.A. Bollinger, M.C. Chapman, M.S. Sibol, A.C. Johnston and R.L. Wheeler (1994). A seismotectonic model for the 300 km long eastern Tennessee seismic zone, Science, 264, 686-688.
- Rajendran, C. P., and P. Talwani, (1993), Paleoseismic indicators near Bluffton, South Carolina: An appraisal of their tectonic implications, Geology, 21, 987-990.
- Stover, C. W. and J. L. Coffman, (1993), Seismicity of the United States 1568-1989 (Revised), U.S. Geological Survey Professional Paper 1527, p. 418.

Talwani, P. and J. Cox, (1985), Paleoseismic evidence for recurrence of earthquakes near Charleston, South Carolina, Science, v. 229, pp. 379-381.

Weems, R. E. and S. F. Obermeier, (1989), The 1886 Charleston earthquake - an overview of geologic studies, in, Proceedings of the 17th Water Reactor Safety Information Meeting, v. 2, U.S. Nuclear Regulatory Commission, pp. 289-313.

**PRELIMINARY DEFINITION OF SEISMIC SOURCES
FOR THE VOGTLE AND WATTS BAR SITES**

TIP Project

Kevin Coppersmith

August 26, 1996

Regional Characterization (applies to both sites)

(See Map KC-1 for identification of sources)

Key Sources

- 1) MERR- Mississippi Embayment-Reelfoot Rift
- 2) New Madrid
- 3) Non-extended Craton
- 4) Ocoee Block
- 5) Iapetan rifted margin zone
- 6) Giles County
- 7) Central Virginia

Vogtle Characterization

(See map KC-1)

- 8) Extended crustal margin zone (runs east to slope break and East Coast magnetic anomaly)
- 9) NW seismicity zone
- 10) Model as either: Pen Branch fault (discrete fault along western boundary of Dunbarton Basin) or as a local source zone (as shown with dotted line)
- 11) Charleston mesoseismal zone
- 12) Marple's zone of river anomalies

Watts Bar Characterization

Three methods are suggested to characterize the spatial distribution of future seismicity in the Watts Bar region:

1. *Spatial smoothing* of observed seismicity, with the following characteristics: Epanechnikov kernel, smoothing distance of 30 km, smooth counts (not 'a-values') including all events in the catalog (including dependent events)
2. *Seismic sources*, including the following sources (shown in Figure KC-2):
 - 1) Northeast-trending discrete faults (probability of activity of 0.3)
 - 2) East-west discrete faults (prob. activity of 0.2)

- 3) Red source zone (prob. activity of 1.0)
- 4) Yellow source zone (prob. activity of 1.0)

Dependences among the sources are the following:

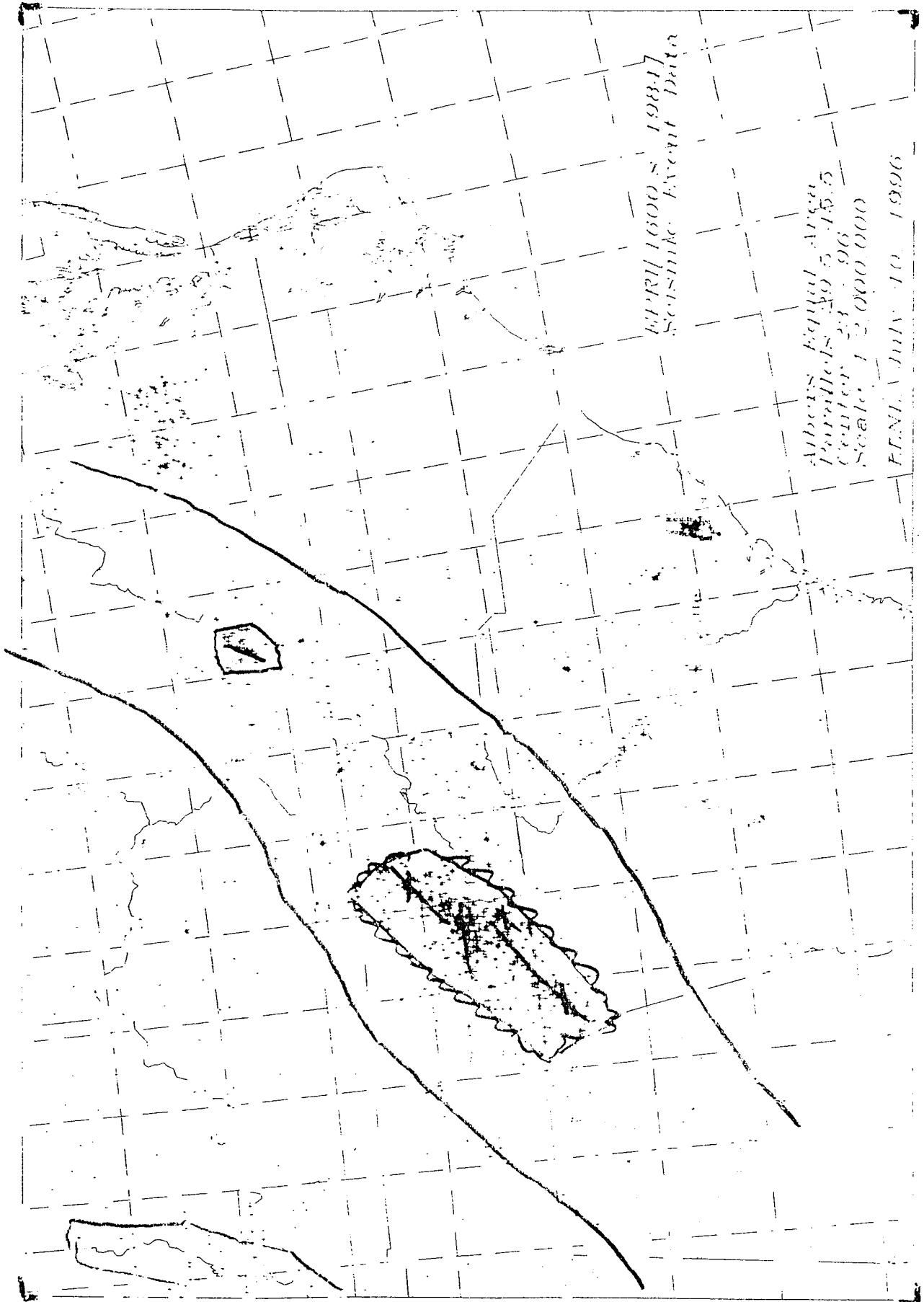
- Sources 1 and 2 are mutually exclusive.
- Sources 3 and 4 are alternative interpretations with weights of 0.4 and 0.6, respectively
- Sources 1&2 and 3&4 are mutually exclusive with each other

3. Probability Density

The contours drawn in Figure KC-3 are assumed to contain 70%, 95% and 100% of the probability density for the occurrence of future events (see attached pages for explanation)

M. CHAPMAN

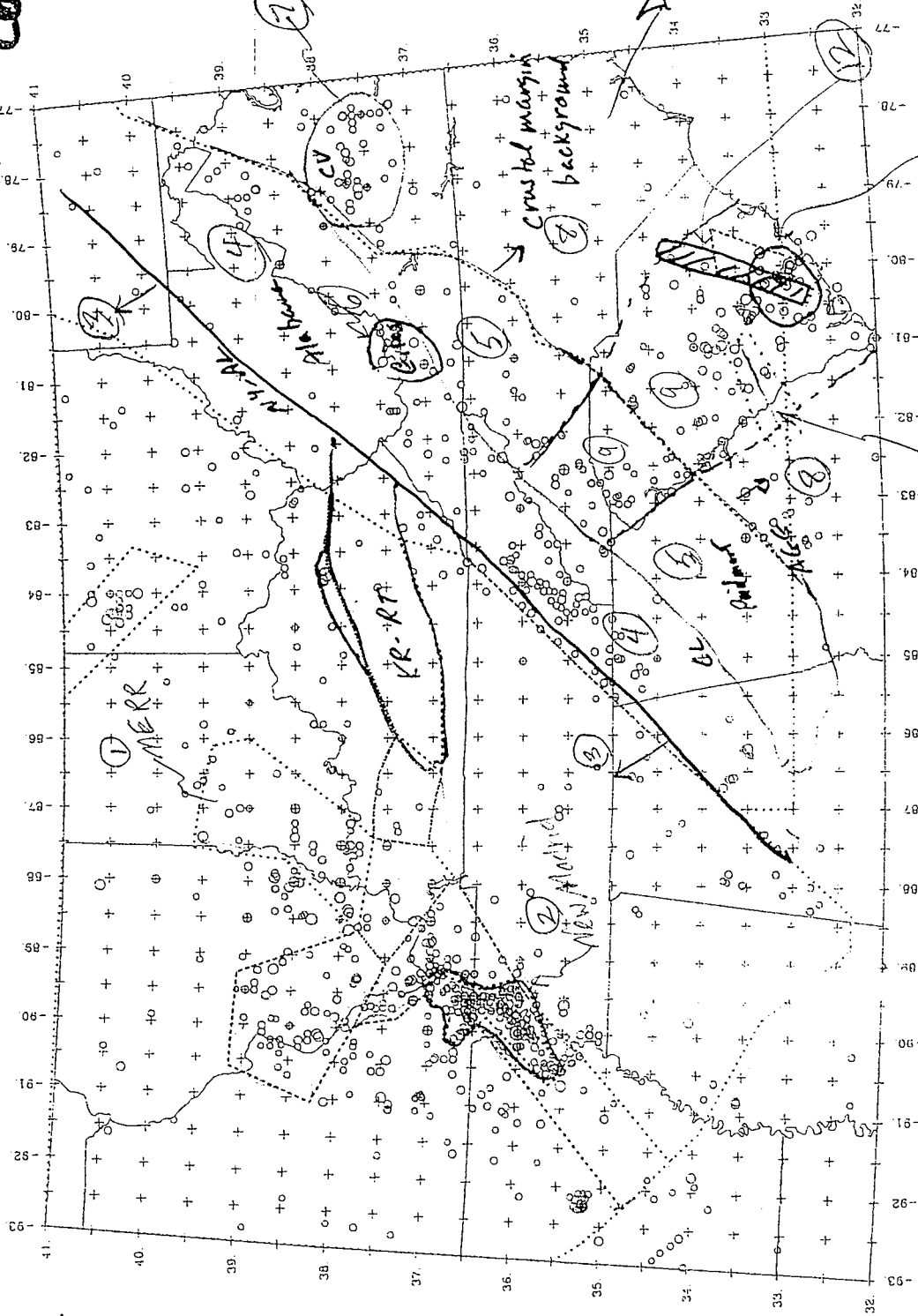
Test Implementation Project - Map #2



Coppersmith
1/13 6/18/14

Magnitude Scale

○	Mag 8	◇	Int XI
○	Mag 7	◇	Int X
○	Mag 6	◇	Int IX
○	Mag 5	◇	Int VIII
○	Mag 4	◇	Int VII
○	Mag 3	◇	Int VI
○	Mag 2	◇	Int V
○	Mag 1	◇	Int IV
○	Mag n/a	◇	Int III
○		◇	Int II



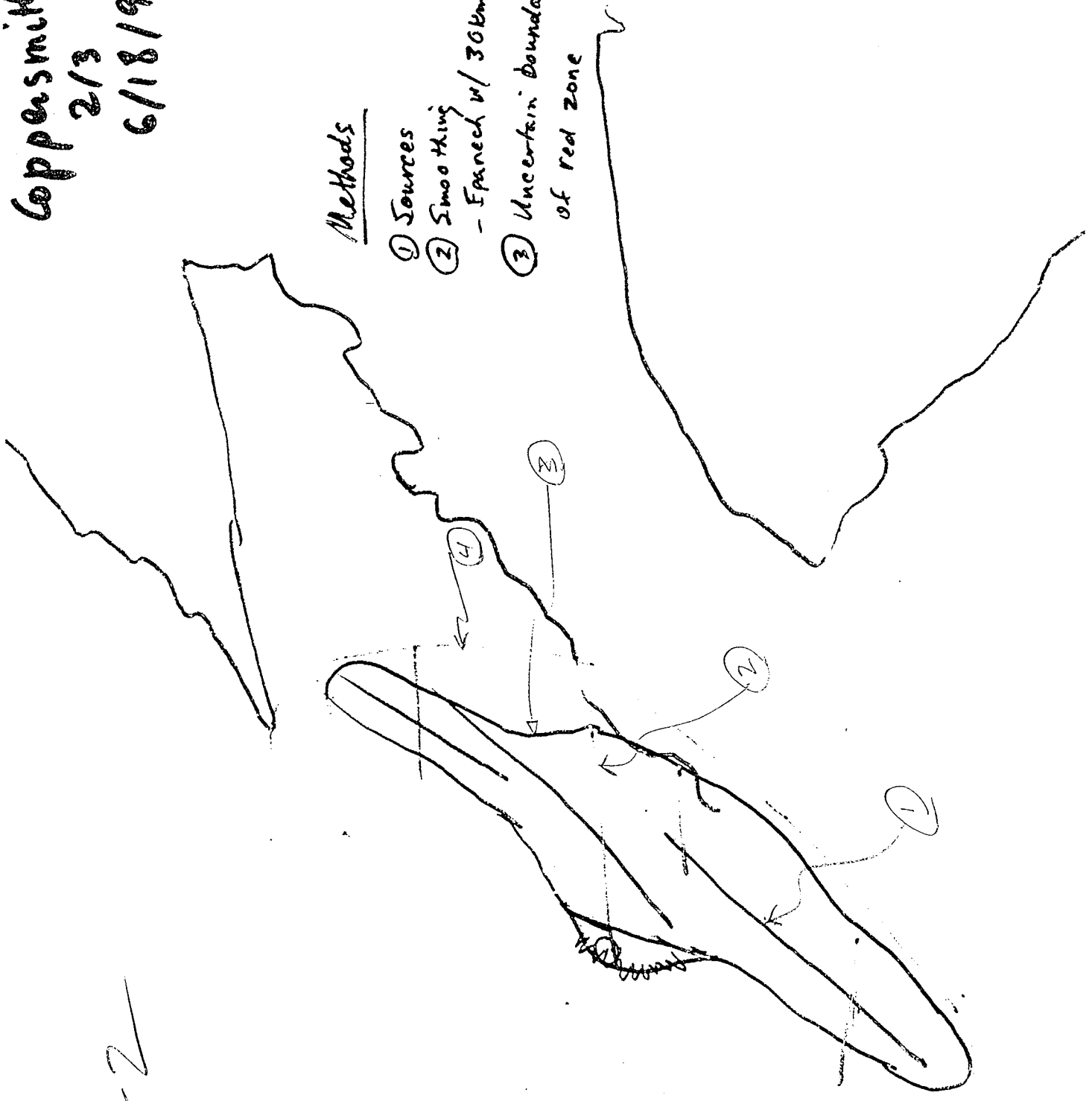
New Branch
Dry water

MAP KC-1

Coppersmith
2/3
6/18/96

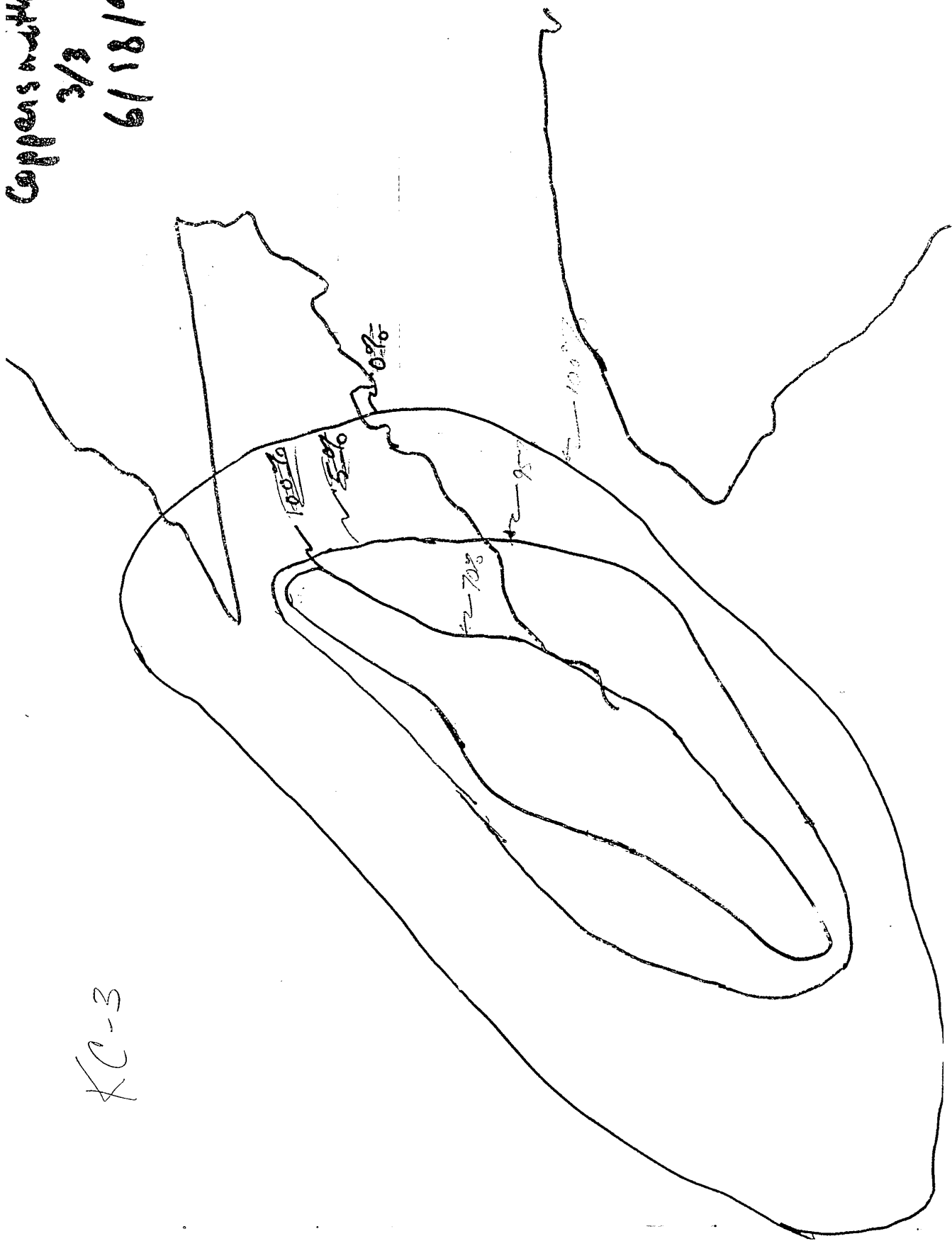
Methods

- ① Sources
- ② Smoothing
- Franck w/ 30km = h
- ③ Uncertain boundary
of red zone



KC-2

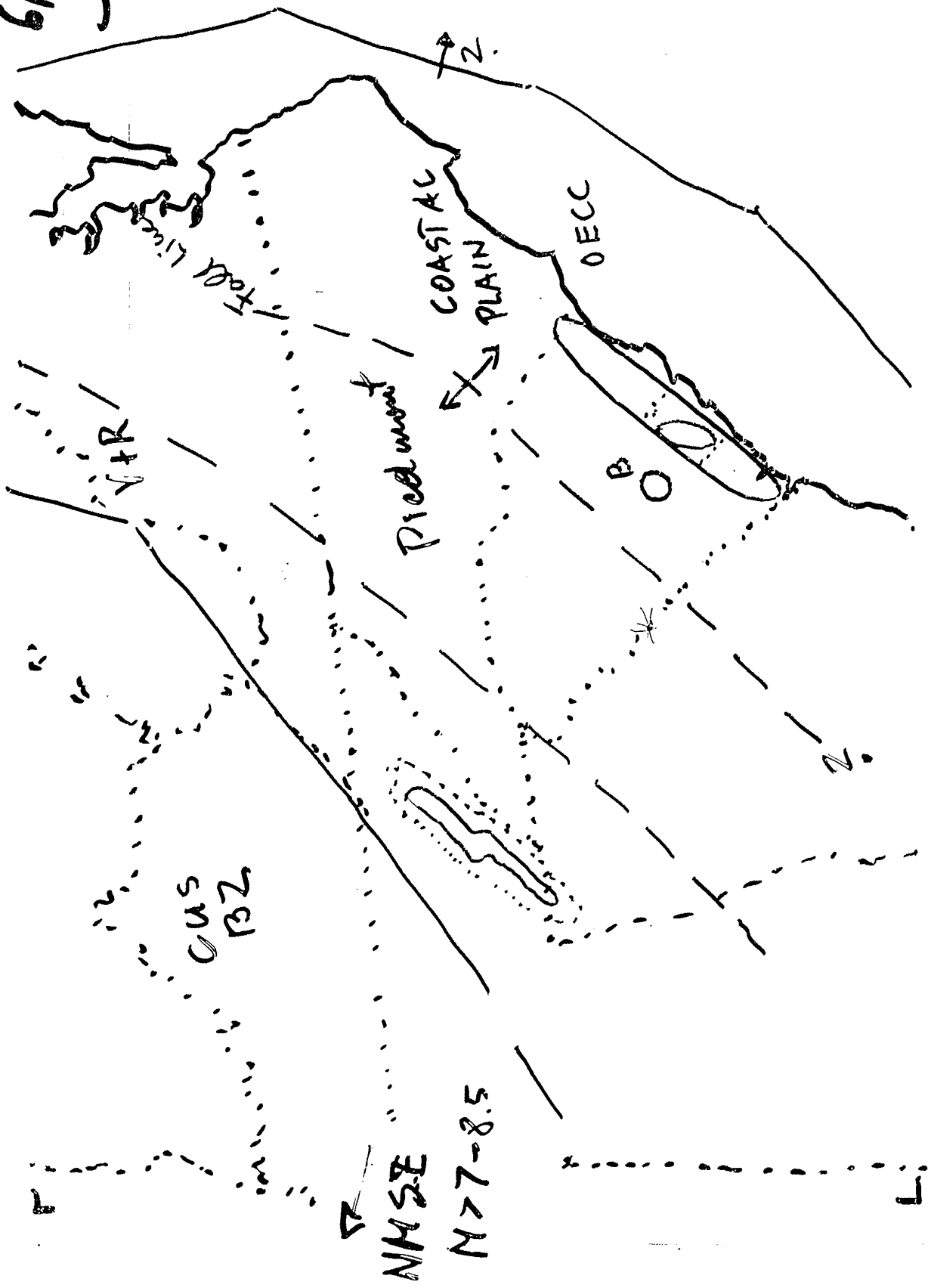
Coppersmith
3/3
6/18/96



KC-3

6/18/96
Jacob

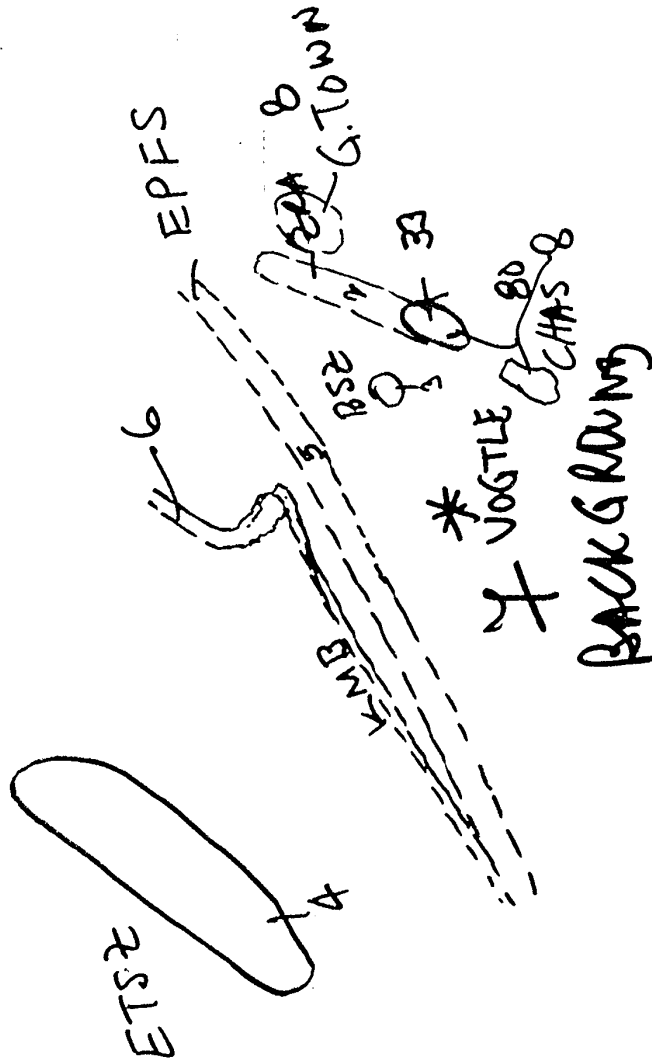
7



(ALW, W) +
6/18/96

+

87
+39



+34
+35

+

- 1. Charleston 7.5
- 2. RA 7.5
- 3. BSE 5.0
- 4. ETSZ 6.0
- 5. EPFS 5.0
- 6. KMB 5.0
- 7. BACKGROUND
- 8. RA EITON 4.5
- 9. +670W

+

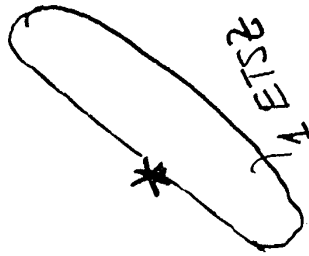
TALWANI +

6/18/96

O²
GCSZ

+34
81
f³

37 +
85



WATTS
BAR

+

3. ZRA/CHARLESTON 7.5

- 1. ETSZ 6.0
- 2. GCSZ 6.0

+

**APPENDIX D: GROUND MOTION UNCERTAINTY IN
PROBABILISTIC HAZARD ANALYSES**

APPENDIX D: GROUND MOTION UNCERTAINTY IN PROBABILISTIC HAZARD ANALYSES

D.1 Introduction

In seismic hazard analyses all uncertainty may be categorized as either *aleatory variability* (not controlled by data) or *epistemic uncertainty* (controlled by the amount of available data. If it relates to limitations in the model, then it may also be labeled as *modeling*; if related to the chosen parameterization, then *parametric*. A convenient tool to visualize these decompositions is an uncertainty grid with one axis accounting for the classification as aleatory or epistemic, and the second for modeling or parametric. Aleatory variability is denoted by σ and epistemic uncertainty by U:

		Aleatory	Epistemic	
			Median	Standard Deviation
Modeling	σ_{model}		$U_{\mu\text{-model}}$	$U_{\sigma\text{-model}}$
Parametric	σ_{params}		$U_{\mu\text{-params}}$	$U_{\sigma\text{-params}}$

Although the terms variability and epistemic uncertainty may be unfamiliar, their use encourages precision in communication.

The following begins with a basic discussion of what aleatory variability and epistemic uncertainty are. Although simple in structure, the subject of uncertainty can rapidly become complex and confusing. To prevent the abstract aspects from becoming unwieldy, concrete examples are presented. These examples are all posed in terms of the development of strong ground motion attenuation relations, but the principles are equally relevant in other modeling applications.

D.2 Classification of uncertainty as aleatory or epistemic

Epistemic uncertainty is the uncertainty due to limitations of available data and is familiar to most scientists. Many parameters have a single, actual, true value based in physical reality. Some examples are the shear-wave velocity at a specific location in the real world, the mean of a distribution, and the probability distribution of a real-world population. Such items would be determinable to a near-certainty given perfect data, but as a practical matter we can only estimate what they are given existing data. Epistemic uncertainty is often called *scientific uncertainty* or, generically, *uncertainty*.

Aleatory variability cannot be eliminated by additional data and accounts for inherent limitations in the model. For instance, if faulting style is not a parameter in a simple magnitude-distance attenuation relation, the predicted ground motions will fit the data more poorly than if faulting style were included. This spread is aleatory variability due to *unmodeled effects* (σ_{model}): additional data will not remove the model shortcoming. Aleatory variability also may arise from model parameters that are multivalued by nature, when this attribute is not specified in the question asked. For instance, if stress drop is not specified, then the attenuation model predicts the ground motion for a “generic” stress drop, and uncertainty is introduced; this is described in greater detail in a later section. Aleatory variability is

sometimes termed *random* or *inherent*, perhaps because the ground motion that is unpredicted by the model looks like random scatter to the model and cannot be eliminated with this model. It may also be termed *random* because the actual stress drop associated with faulting in a future event (the stress drop value that “should” be used in the model) has no “true” value but only potential values, is not determinable at this time, and so in a sense will occur randomly.

In general, to decide if a contribution to uncertainty is aleatory or epistemic, consider if there is a single correct value of the parameter being considered. If a single, correct, factual value exists for a model parameter, but we simply don't know it due to lack of data, then there is epistemic uncertainty in the estimated value we use. If the parameter is not single-valued but rather has a range of potential values, and if the multi-valued nature is not included in the model, then the range causes aleatory variability. We also briefly note here, and explain in detail later, that *context* determines whether a parameter introduces aleatory variability or epistemic uncertainty into the model.

D.3 Three easy steps for empirical attenuation models

At this point, calculating uncertainty for empirical attenuation models can be tackled. The classification grid makes assessing uncertainty for empirical attenuation models easy and systematic, and the divisions quite naturally reflect the structure of the problem. Any specific case will fit into one of three prototypes described below.

For a given magnitude and distance, an empirical attenuation relation produces an estimate of the median ground motion, μ , and the standard deviation of the ground motion, σ . A database of recordings at several sites for N earthquakes is used to construct the model. Known are some subset of the following: magnitude (M_j), faulting style (F_j), and stress drop (Δs_j) for each earthquake j , distance (d_{ij}), site factor (S_i), and recorded ground motion (y_{ij}) for each site i .

In each case below, the question we ask is "what is the predicted ground motion given a magnitude, faulting style, distance and site type (M, F, d, S)?"

D.3.1 Case 1 : Inputs specified exceed model parameters

In Case 1, our model has three parameters, M, d , and S . Since by assumption the inputs specified are M, F, d , and S , in this case the inputs specified exceed model parameters.

The modeling aleatory variability, σ_{model} , is the amount of scatter not modeled, i.e. the data not matched by the model. It is given by the standard error of the model:

(eqn 1)

where y_{ij} is the predicted ground motion, y is the mean ground motion of all the recordings, and M_j is the number of recordings for event N .

The parametric aleatory variability, σ_{params} , is zero since we have specified a value for each model parameter. The parametric epistemic uncertainty, U_{params} , is similarly zero.

The modeling epistemic uncertainty is caused by a lack of data. With an infinite number of recordings we would know the true median ground motion and the true scatter about it. The limited data leads to uncertainty in our estimated values (denoted U_μ and U_σ). For now we assume U_μ and U_σ can be estimated by comparing credible models and by judgment.

Our uncertainty grid for Case 1 is:

	Aleatory	Epistemic	
		Median	Standard Deviation
Modeling	σ_{model}	U_{μ}	U_{σ}
Parametric	none	none	none

D.3.2 Case 2 : Inputs specified equal model parameters

In Case 2, our model has four parameters, M, d, F and S. The assumed inputs specified are still M, d, F and S. Thus in this Case values for each model parameter, and no extra parameters, are specified.

The uncertainty analysis is identical to Case 1 and the uncertainty grid for Case 2 is:

	Aleatory	Epistemic	
		Median	Standard Deviation
Modeling	σ_{model}	U_{μ}	U_{σ}
Parametric	none	none	none

D.3.3 Case 3 : Inputs specified exceed model parameters

In Case 3, our model has five parameters, M, d, F, Δs and S. The inputs specified are still M, F, d, and S. In this Case the inputs specified are fewer than model parameters: Δs is unspecified.

The modeling aleatory variability, σ_{model} , is still given by the standard error of the model as in equation 1 above.

The parametric aleatory variability, σ_{params} , for the parameters M, d, F, and S is zero since their values are specified. However, there is a non-zero $\sigma_{\Delta s}$. The parametric aleatory variability in Δs is given by the standard error in the predicted ground motion due to varying Δs. This is calculated by making multiple runs of the model and for each run picking a "random" Δs from a "known" distribution function of Δs:

(eqn 3)

Written in continuous terms,

(eqn 4)

As above, the modeling epistemic uncertainty due to limited data is U_{μ} and U_{σ} . The parametric epistemic uncertainties are due to uncertainty in knowing the true distribution function of Δs ($\mu(\Delta s)$ and $\sigma(\Delta s)$).

Our uncertainty grid for Case 3 is:

		Aleatory	Epistemic	
			Median	Standard Deviation
Modeling	σ_{model}		U_{μ}	U_{σ}
Parametric	$\sigma_{\Delta s}$		$U_{\mu(\Delta s)}$	$U_{\sigma(\Delta s)}$

D.3.4 Observations on uncertainty for empirical attenuation relations

The total aleatory variability for a given question cannot be reduced by addition of parameters beyond those specified in the question. Additional parameters merely shift uncertainty from aleatory modeling variability to aleatory parametric variability.

Models having more parameters will have less standard error than models with less parameters:

$$\sigma_{model}^{(3)} < \sigma_{model}^{(2)} < \sigma_{model}^{(1)}$$

is less than the modeling component of the aleatory variability for

$\mu^{(2)}$, the parametric aleatory error balances it out:

$$\sigma_{total}^{(2)} = \sigma_{total}^{(3)}$$

because

(eqn 5)

and

(eqn 6).

A summary of our results for a question in which 4 parameters are specified for model 1 (3 parameters), model 2 (4 parameters), and model 3 (5 parameters) is given below.

Calculation of σ_{total} :

$$\sigma_{total}^{(1)} = \sigma_{model}^{(1)}$$
$$\sigma_{total}^{(2)} = \sigma_{model}^{(2)}$$
$$\sigma_{total}^{(3)} = [\sigma_{model}^{(3)}]^2 + [\sigma_{\Delta s}^{(3)}]^2$$

Relations between models:

$$\sigma_{model}^{(3)} < \sigma_{model}^{(2)} < \sigma_{model}^{(1)}$$
$$\sigma_{total}^{(1)} > \sigma_{total}^{(2)}, \sigma_{total}^{(3)}$$
$$\sigma_{total}^{(2)} = \sigma_{total}^{(3)}$$

D.3.5 Calculation of the epistemic uncertainty for empirical attenuation models

Epistemic uncertainties in μ and σ arise because of the limited number of records in the data set used to develop the model. In practice U_μ and U_σ are usually not estimated explicitly, but rather are represented by using multiple attenuation relations with weights. This approach assumes that credible attenuation relations developed by different people represent both U_μ and U_σ . Although it may sound overly esoteric to talk about U_σ , the epistemic uncertainty in the aleatory variability, it is of practical importance to estimate how well we know the scatter of the ground motions. (For instance, this tells us about the possibility of extremely high accelerations.) In this approach the epistemic uncertainty is represented by alternative models and the aleatory variability is given by the standard deviation provided with the attenuation relation. This is a natural separation of uncertainty.

The main drawback to using alternative models with weights to represent the epistemic uncertainty is that many of the models are developed from similar data sets. The differences in the models may not be representative of the true underlying scientific uncertainty due to small data set sizes. For example, consider the four alternative attenuation models for soil sites in California: Abrahamson and Silva (1997), Boore et al (1997), Campbell et al (1997), and Sadigh et al (1997). These attenuation models for peak acceleration are shown in Figure A-1 for magnitudes 5.0 and 7.0.

Figure 1 shows that the models all produce similar ground motion values for a magnitude 7.0 event at short distances; however, there is very little data in this magnitude-distance range. The agreement of the median predictions by the models does not necessarily imply that the value for the median is well known; the epistemic uncertainty, U_μ , should not necessarily be small.

Explicitly asking for estimates of U_μ forces us to think about epistemic uncertainty due to limitations of data that may not be accurately represented by alternative attenuation relations. Basically, it is another way of asking how confident we are of their estimates. The same can be said for U_σ .

D.4 Further discussion of aleatory and epistemic uncertainty

In words, the above example implies the sources of uncertainty are:

		Aleatory	Epistemic	
			Median	Standard Deviation
Modeling	Unmodeled effects		Uncertainty in estimate of μ due to finite number of recordings	Uncertainty in estimate of σ due to finite number of recordings
Parametric	none		Uncertainty in distributions of parameters for which values are not specified	Uncertainty in distributions of parameters for which values are not specified

D.4.1 Application of these classifications to modeling

It is tempting to conclude that all uncertainty in ground motion attenuation is epistemic. That is, if we had the right model (exact description of the source process, 3-D crustal structure, and site properties) then we could compute the ground motions exactly. This is the concept of the perfect model with perfect data. Perfect data will eliminate epistemic uncertainty. A perfect model will eliminate the problem of inherent aleatory variability due to unmodeled effects. If a very simple or very specific question is asked, aleatory variability associated with “random” variables will not be present. There would be no uncertainty in the predicted ground motion.

Unfortunately, once the question is moderately interesting or general, the perfect model cannot eliminate the uncertainty associated with “random” variables. For instance, we know that stress drop affects the ground motions. Therefore the perfect model must include a parameter for stress drop. However, since it is impossible to uniquely determine the correct value of a future stress drop from current conditions, perfect data will not enable us to determine what value to use for stress drop, and we cannot eliminate this aleatory variability. We could eliminate this particular uncertainty if we pose the relatively less useful and more specific question of predicting ground motions for an earthquake with a stress drop of 50 bars.

More importantly, on a practical level, the problem with the “perfect model” concept is that it does not consider the limitations of the information that is provided. Typically, the independent variables provided are simply tectonic region, earthquake magnitude, focal mechanism, site-to-source distance, and site classification. Since these simple parameters are not sufficient to completely characterize the source, path, and site effects, we cannot develop a perfect model of ground motion. Although with an infinite number of recordings we can reduce the uncertainty in our estimate of the median ground motion to zero, there will still be variability due to unmodeled effects such as the range of source properties, crustal velocities, and site properties that all have the same region, magnitude, mechanism, distance, and site class. This inherent variability due to unmodeled effects is aleatory variability.

D.4.2 Context-dependence of classification of uncertainty

The question that is asked by the model determines whether a model parameter contributes epistemic or aleatory variability. For example, if we want to know what ground motions will be generated by an event on the Whittier Fault and we think the dip is around 60°, the dip parameter introduces epistemic uncertainty that could be settled as a factual matter by digging a very deep trench (assuming a planar fault). On the other hand, if our question is what the ground motion will be from a generic earthquake, then the dip parameter introduces aleatory variability, because we do not uniquely specify the dip. (As an aside, the assumption of a planar fault introduces aleatory variability from unmodeled effects to the extent that the assumption does not reflect the real world, which is accounted for under the model's randomness, σ_{model} .)

D.5 Modeling and parametric uncertainty related to numerical models

We have implicitly discussed and made use of the division of uncertainty into modeling and parametric uncertainty in the above discussion. For complex models such as arise in numerical modeling procedures there are many components to each of our four basic uncertainties σ_{model} , σ_{params} , U_{model} and U_{params} .

D.5.1 Modeling uncertainty

Modeling uncertainty represents the limitations of the ground motion model. That is, even when the model parameters are optimized for a particular past earthquake, there are still differences between the predicted motions and observed motions (for example, the residuals are not all zero). These differences are attributed to the use of a simplified model of a complicated process.

Since modeling uncertainty is a measure of the limitations of the ground motion model, the only way we can measure it is through comparisons with ground motions from previous earthquakes. The comparison of the model predictions with recordings from past earthquakes has been called model *validation*, but it is more than that. Validation is also necessary to estimate the modeling uncertainty component of the total uncertainty of the ground motion predictions for future earthquakes.

The standard error of the residual represents uncertainty of the ground motions that is not predictable by the simple model. This uncertainty is considered to be random variation (aleatory) for that particular model. (As far as that particular model is concerned, these variations are random.) When predicting ground motions for a future earthquake, we need to account for this random variation that is not captured by the model (part of aleatory σ). There is also epistemic uncertainty due to the uncertainty in our estimation of the value of the standard error due to the limited number of recordings and earthquakes used in the validation exercise (component of U_e). In general, there is also uncertainty in the form of the probability distribution (e.g. other than lognormal), but that is outside the scope of this discussion.

Since modeling uncertainty is computed from comparisons to data, the modeling uncertainty is a catchall that in principle covers all of the shortcomings of the numerical simulation procedure. This is true only to the extent that the events used in the validation exercise are representative of future earthquakes. As the numerical models become more complete, the modeling uncertainty will be reduced, but the parametric uncertainty should then be increased because more event-specific parameters need to be randomized, as described below.

D.5.2 Parametric Uncertainty

The parametric uncertainty represents the uncertainty of ground motion due to variations of the parameters for future earthquakes. This variability comes from multiple realizations of the model with different values of the source parameters. Those source parameters that were optimized for individual events in the validation study are varied for future earthquakes. Parameters that are fixed in the model (either to constant value or constant scaling relations) are not varied because the effect of their variations is already captured as part of the modeling uncertainty if a sufficient number of events is used in the validation study. (The same holds for site and path parameters.)

We discussed above how parametric aleatory variability arises from unspecified values for a parameter with a range of potential values. There is also parametric epistemic uncertainty in the assumed distributions for the source parameters (mean and standard deviation of the source parameters).

D.6 Uncertainty in numerical simulation models

For numerical simulations, there are two parts to the modeling uncertainty: the mean of the residuals and the standard error of the residuals. The mean residual is an estimate of the bias of the model, i.e. whether or not the model tends to systematically over-predict or under-predict the ground motion. If there is a large bias, then the model may not be acceptable. The evaluation of the model bias is really what is commonly taken as the model validation. If the bias is acceptably small, then the model is said to be validated. If there is a significant model bias, then the model could be revised (improved) in the future to correct for this bias. Because the bias is reducible with additional information, the bias is considered as part of the epistemic uncertainty (a component of U_e).

For numerical simulations, there are two parts to the parametric uncertainty. Parametric aleatory variability is caused by not specifying values for the source parameters of the future event. Uncertainty in the values contributes epistemic uncertainty to U_e .

The sources of uncertainty for numerical modeling are:

	Aleatory	Epistemic	
	σ	U_μ	U_σ
Modeling (From comparisons with data)	σ_{model}	$\sigma_{\mu\text{-method}}$ σ_{bias}	$\sigma_{\sigma\text{-method}}$ $\sigma_{\sigma\text{-model}}$
Parametric (From multiple realizations of the model)	σ_{source}	σ_{dip}	Not considered

D.7 Total uncertainty

The total aleatory variability is given by summing the modeling variance and parametric variance:

$$\sigma_{\text{total}} \approx \sqrt{\sigma_{\text{model}}^2 + \sigma_{\text{param}}^2}$$

This assumes that the covariance between the modeling and parametric terms is zero, i.e. that they are independent variables.

In a hazard analysis, the epistemic and aleatory components of the uncertainty are kept separate. However, for an 84th percentile ground motion estimate, the total uncertainty is given by summing the aleatory variance and the variance in the median:

$$\sigma_{\text{total}} \approx \sqrt{\sigma_{\text{model}}^2 + \sigma_{\text{param}}^2 + \sigma_\mu^2}$$

D.8 Complex versus simple models

As more complex models are used, the modeling uncertainty is reduced, but there is a counteracting increase in the parametric uncertainty. That is, the total uncertainty cannot be reduced by adding more event-specific parameters to the model.

The advantage of using a complex model with additional event- and site-specific parameters is that it better explains past earthquakes. It provides a physical basis for the variations in the ground motion. We intuitively have more confidence in the model when we can explain the variations rather than just say that they are random.

The disadvantage of using a more complex model is that we need to develop *joint* probability distributions for all of the event-specific parameters used in the model. It is sufficiently difficult to develop probability distributions for the parameters independently from the limited data available; once we have multiple source parameters, we must develop joint distributions to account for their correlation. If the correlation of source parameters is ignored, then the variability will likely be overestimated.

**APPENDIX E: DOCUMENTATION OF EXCEL 5.0
SPREADSHEETS AND FORTRAN CODES FOR DEVELOPING
HYBRID EMPIRICAL GROUND-MOTION ESTIMATES FOR THE
MIDCONTINENT OF THE EASTERN UNITED STATES**

APPENDIX E: DOCUMENTATION OF EXCEL 5.0 SPREADSHEETS AND FORTRAN CODES FOR DEVELOPING HYBRID EMPIRICAL GROUND-MOTION ESTIMATES FOR THE MIDCONTINENT OF THE EASTERN UNITED STATES

Kenneth W. Campbell
EQE International, Inc.
2942 Evergreen Parkway, Suite 302
Evergreen, Colorado 80439

INTRODUCTION

I have developed several EXCEL 5.0 spreadsheets and a Fortran 77 code for calculating the various distance measures, adjustment factors, and empirical ground-motion estimates for application of the hybrid empirical ground-motion model, hereafter referred to as the Hybrid Model, to the Midcontinent region of the Eastern United States (EUS). The spreadsheets allow the user to interactively add distances and ground-motion parameters for which the estimates are to be made as well as to change the weights assigned to the various relationships and adjustment factors. The Fortran code allows the user to compute theoretical median adjustment factors and their standard deviations for specific values of seismological and crustal parameters. A brief description of the spreadsheets and Fortran code are given below.

DESCRIPTION OF SPREADSHEETS AND FORTRAN CODE

DIST_D5.XLS, DIST_D10.XLS, and DIST_D20.XLS

These spreadsheets calculate the three fault-distance measures required to estimate empirical ground motions using contemporary empirical strong-motion attenuation relationships for shallow-focus (DIST_D5.XLS), intermediate-focus (DIST_D10.XLS), and deep-focus (DIST_D20.XLS) earthquakes. Each spreadsheet contains two worksheets for fault dips of 90 and 45 degrees. Distances for other fault dips can be calculated by simply changing the value of the fault dip on any of the worksheets or by copying an existing worksheet to a new worksheet and changing the fault dip to the desired value. Significant parameters in these spreadsheets are defined below. Only those parameters that are required to use the spreadsheets are described. All depths, widths, and distances have units of kilometers.

alpha. The dip of the fault plane measured from the horizontal plane in degrees. The fault dips of 90 and 45 degrees were specified by the facilitation team.

d. Depth to the center of the fault-rupture plane. This depth is held constant for all rupture scenarios. These depths were defined as 5 km (shallow-focus earthquakes), 10 km (intermediate-focus earthquakes), and 20 km (deep-focus earthquakes) by the facilitation team.

dmax. Maximum depth of fault rupture. This depth was assumed to be 35 km to be consistent with rupture scenarios defined in the ground-motion study conducted by EPRI (1993) for the Midcontinent region of the EUS. This depth is also consistent with the maximum depth of faulting estimated by Arch Johnston (personal communication, 1997) for the 1811-1812 New Madrid, Missouri, earthquakes.

dseis. Depth to the top of the seismogenic portion of the fault. The seismogenic zone of rupture is not allowed to propagate to depths shallower than this value. This depth is set at 3 km, the minimum value recommended by Campbell (1997). The use of a smaller value may lead to unrealistic amplitudes of ground-motion parameters and should be used with caution.

Magnitude. Moment magnitude, M_w . The values of M_w and the corresponding values of horizontal distance (see below) were specified by the facilitation team.

Fault Width. The median estimate of the fault rupture width for the given value of moment magnitude (M_w). This width is calculated using a relationship between rupture width and moment magnitude developed by Wells and Coppersmith (1994) for all faulting mechanisms. This width is assumed to be centered about d unless constrained by the surface trace of the fault or by d_{max} , in which case the remaining width is accommodated by the unconstrained portion of the fault. When the width fills the entire fault plane, the excess width, if any, is disregarded.

Horizontal Distance. The horizontal distance (defined in other spreadsheets as R_{hor}) from the site to the surface trace of the fault. The values of R_{hor} and M_w were specified by the facilitation team.

Reps. The distance from the site to an equivalent point source defined as the down-dip center of the fault rupture plane. This is the distance measure used in the BLWN-RVT point-source stochastic simulation model (Silva and Lee, 1987) used to calculate the theoretical adjustment factors.

Rjb. The shortest distance from the site to the projection of the fault rupture plane on the surface of the earth. This is the distance measure used by Joyner and Boore (1988) and Boore et al. (1997). See Abrahamson and Shedlock (1997) for a brief description of this distance measure.

Rrup. The shortest distance from the site to the fault rupture plane. This is the distance measured used by Abrahamson and Silva (1997), Idriss (1991, 1996), and Sadigh et al. (1997). See Abrahamson and Shedlock (1997) for a brief description of this distance measure.

Rseis. The shortest distance from the site to the seismogenic part of the fault rupture plane. This is the distance measure used by Campbell (1997). See Abrahamson and Shedlock (1997) for a brief description of this distance measure.

HYBRD_5.XLS, HYBRD_10.XLS, and HYBRD_20.XLS

These spreadsheets calculate hybrid empirical ground-motion parameters for shallow-focus (HYBRD_5.XLS), intermediate-focus (HYBRD_10.XLS), and deep-focus (HYBRD_20.XLS) earthquakes using contemporary empirical strong-motion attenuation relationships for California and adjustment factors for applying the California ground-motion estimates to the Midcontinent EUS. The adjustment factors were calculated using the band-limited white noise (BLWN) point-source stochastic simulation model with ground-motion parameters estimated from random vibration theory (RVT). A single estimate of these parameters were developed for California for each magnitude and distance of interest using model parameters developed by Walt Silva (personal communication, 1997), which he developed by calibration to strong-motion recordings and to the ground-motion estimates given by the empirical attenuation relationship of Abrahamson and Silva (1997). A single estimate of these parameters were developed for the EUS for each focal depth using the median model parameters for the Midcontinent region given by EPRI (1993), the crustal model (shear-wave velocity and density as a function of depth) specified by the facilitation team, and a relationship between stress drop and shear-wave velocity in the source region specified by Norm Abrahamson (personal communication, 1997). Uncertainty in the adjustment factors were taken directly from EPRI (1993) and were not calculated independently.

Each spreadsheet contains five worksheets. The first three worksheets give empirical estimates for the specified ground-motion parameters, magnitudes, and horizontal distances for fault dips of 90 and 45 degrees, the latter for both the hanging wall and the foot wall of the fault plane (not the earthquake rupture plane). The fourth worksheet (Factors) gives the calculated adjustment factors and their standard deviations. The standard deviations are 0 because only one estimate is calculated for each stress drop. The

fifth worksheet (*Hybrid Estimates*) gives the calculated hybrid empirical estimates for the same set of ground-motion parameters, magnitudes, and distances.

Significant parameters in these spreadsheets are defined below. Only those parameters that are required to use the spreadsheets are described. Parameters common to more than one worksheet are defined only once.

Empirical Estimates Worksheets (Dip=90; Dip=45, Hanging Wall; Dip=45, Foot Wall)

Attenuation Relationships. Identification of the attenuation relationships used to develop the empirical ground-motion estimates. Attenuation relationships developed by Abrahamson and Silva (1997), Boore et al. (1997), Campbell (1997), Idriss (1991,1996), Sadigh et al. (1997), and Joyner and Boore (1988) are included. The user can add additional relationships if desired. The Joyner and Boore (1988) relationships, although superseded by Boore et al. (1997), are included because they include a relationship for peak ground velocity. All of the listed relationships can be considered to represent California strong-motion recordings.

Dip. The dip of the fault plane measured from the horizontal plane in degrees.

Style of Faulting (F). The style of faulting parameter F used in all of the empirical attenuation relationships. $F = 0$ corresponds to strike-slip faulting. Most relationships do not include many normal-faulting earthquakes, but the authors of these relationships generally recommend that $F = 0$ be used for normal-faulting events. All of the authors recommend $F = 1$ be used for reverse and thrust-faulting earthquakes. Some authors recommend $F = 0.5$ be used for reverse-oblique faulting. The BLWN-RVT model parameters for California were determined for an average faulting mechanism, consistent with $F = 0.5$, and a median stress drop of 59 bars (Walt Silva, personal communication, 1997). In these worksheets, a value of $F = 0.5$, to be consistent with the way the California model parameters were developed, is used with median stress drops developed independently for the EUS by EPRI (1993) and Gail Atkinson (Norm Abrahamson, personal communication, 1997).

Depth to Hard Rock (D). The depth to basement (hard) rock defined by Campbell (1997). This parameter was set to 2.0 km, which is believed to be generally representative of the “generic” rock site used to calibrate the California BLWN-RVT point-source model parameters used to estimate the adjustment factors. The appropriate value of D for the Midcontinent EUS is inherently incorporated in the crustal model used to estimate the adjustment factors.

M_w. Moment magnitude. This magnitude measure was specified by the facilitation team.

R_{hor}. Horizontal distance to the surface trace of the fault plane. The values of these distances were specified by the facilitation team..

Reps, Rjb, Rrup, Rseis. The equivalent point-source and fault-distance measures defined previously. The values are those calculated in the DIST_D5.XLS, DIST_D10.XLS, and DIST_D20.XLS spreadsheets for the specified values of M_w and R_{hor} .

PSA. The average horizontal component of 5%-damped pseudo-absolute acceleration in g for the oscillator frequencies specified by the facilitation team (i.e., 1.0, 2.5, 10.0, and 25.0 Hz).

PGA. The average horizontal component of peak ground acceleration in g.

PGV. The average horizontal component of peak ground velocity in cm/sec. This parameter was not requested by the facilitation team. It is included for information only.

Median Ground Motion Estimates. The median estimates of PSA, PGA, and PGV from the selected attenuation relationships. Only Campbell (1997) and Joyner and Boore (1988) developed attenuation relationships for PGV. The values of PSA at a frequency of 25 Hz were estimated by interpolating between estimates at 20 Hz and PGA (assumed to represent a frequency of 33 Hz) for those relationships that did not have coefficients for 25 Hz.

Standard Errors. The standard errors (i.e., aleatory uncertainty) associated with the empirical estimates of PSA, PGA, and PGV. Interpolation was used to estimate standard errors at 25 Hz as discussed above for *Median Ground Motion Estimates*.

Subjective Weights. The weights assigned to each of the attenuation relationships and each of the ground-motion parameters. These weights must add up to 1, but can be 0 for those attenuation relationships which are not used. The user should select these weights according to his or her belief that the relationship is appropriate for the given ground-motion parameter, magnitude, and distance. Equal weights are assumed. The Joyner and Boore (1988) relationship is not used to estimate PSA and PGA because it has been superseded by Boore et al. (1997). It is used only to estimate PGV. Changing the weights will automatically adjust the weighted estimates in the spreadsheet.

Weighted Median. There are two sets of weighted medians, each weighted by the subjective weights assigned to the attenuation relationships: (1) the weighted median of the median ground-motion estimates, with weights applied to the logarithm of the ground-motion parameters assuming a lognormal distribution of medians; and (2) the weighted median of the standard errors (i.e., aleatory uncertainty), with weights applied to the standard errors assuming a normal distribution of standard errors. An attempt to provide 'unbiased' estimates for the median and standard error of PGV was implemented by applying the median ratio of these estimates with respect to PGA to the weighted median estimate for PGA estimated from all of the attenuation relationships selected by the user. The estimates of aleatory uncertainty are provided for information only. The calculated values of this uncertainty were not used in the hybrid estimates. Instead, the "randomness" component of standard deviation specified by EPRI (1993), which includes both parametric and modeling aleatory uncertainty, was used to estimate total aleatory uncertainty.

σ . There are two sets of σ s: (1) the standard deviation of the median ground-motion estimates (i.e., epistemic modeling uncertainty), and (2) the standard deviation of the standard errors. The σ s are not weighted, instead they are calculated from the total number of estimates that are available in order to avoid predicting too small a standard deviation if too few attenuation relationships are selected. The σ s are adjusted by the number of degrees of freedom (i.e., $N-1$, where N is the number of values used to determine the median). When $N = 1$, the number of degrees of freedom is assumed to be equal to 0.5. The estimates of epistemic modeling uncertainty are provided for information only. The calculated values of this uncertainty were not used in the hybrid estimates. Instead, the "uncertainty" component of standard deviation specified by EPRI (1993), which includes both parametric and modeling epistemic uncertainty, was used to estimate total epistemic uncertainty.

Adjustment Factors Worksheet (Factors)

$\Delta\sigma$. Stress drop in bars. Calculations were done for median stress drops of 120, 150, and 180 bars, consistent with the shear-wave velocity in the source region of the three focal depths. The median stress drops of 120 and 180 bars correspond to focal depths of 5 km ($V_s = 3.52$ km/sec) and 20 km ($V_s = 3.75$ km/sec), respectively. The smaller value is consistent with the shear-wave velocity of about 3.5 km/sec and the median stress drop of 120 bars specified by EPRI (1993) for the Midcontinent region of the EUS. The larger value is consistent with the shear-wave velocity of about 3.8 km/sec and the median stress drop of 180 bars specified by Gail Atkinson (Norm Abrahamson, personal communication, 1997) for northeastern North America. The intermediate values correspond to a focal depth of 10 km, near the boundary of the lower-velocity and higher-velocity source regions. Although adjustment factors for all

three stress drops are included in each spreadsheet, the value that is consistent with the appropriate focal depth is selected through use of a weighting factors (see *Subjective Weights* below). Each stress drop corresponds to a consistent value of shear-wave velocity and density in the source region and an associated crustal model (i.e., set of crustal amplification factors).

Adjustment Factors. The multiplicative adjustment factors for estimating ground-motion parameters for the EUS from the parameters estimated for California. These factors were developed using the BLWN-RVT stochastic simulation model as described above. The median represents the estimates obtained from the median model parameters for California and the EUS. The σ represents the standard deviation of the median factors (i.e., epistemic parametric uncertainty), assuming no uncertainty in the California model parameters. This value is 0 because the uncertainty in these factors resulting from the EUS model were adopted from EPRI (1993) and were not calculated independently. The assumption of no uncertainty in the California model should be evaluated by the user. The reasons for not including any uncertainty in the California model estimates are: (1) the model parameters were constrained by calibrating the model to the California strong-motion records and the Abrahamson and Silva (1997) attenuation relationship, so modeling uncertainty that would result from calibrating these parameters to other attenuation relationships is believed to be already accounted for in the parametric modeling uncertainty calculated by EPRI (1993) (Note that there may be a bias between the ground-motion estimates from this attenuation relationship and the weighted median of all of the attenuation relationships which has not been included); (2) the set of California parameters cannot be replaced with independent assessments of these parameters because of inter-parameter correlation, and (3) the same model is applied in both California and the EUS, so presumably uncertainty in the appropriateness of the stochastic simulation model does not contribute significantly to the modeling uncertainty in the calculated adjustment factors, provided that the source scaling relations are the same in both regions.

Subjective Weights. The weights assigned to each of the stress drops. This weight must be 1 for the stress drop that corresponds to the specified focal depth and must be 0 for all other stress drops.

Weighted Median. The weighted median of the median adjustment factors. This is simply the value that corresponds to the specified focal depth, selected by the use of the *Subjective Weights*.

Example Hybrid Estimates Worksheet (Hybrid Estimates)

Median. The weighted median empirical ground-motion estimate times the weighted median adjustment factor for the given ground-motion parameter, magnitude, and horizontal distance. Estimates are provided for all of the ground-motion parameters, magnitudes, and horizontal distances specified by the facilitation team for a vertical strike-slip fault and for the hanging wall and the foot wall of a 45-degree dipping fault plane. As requested by the facilitation team, estimates are also provided for a site randomly located on the hanging wall and foot wall. The user can modify or extend this table to include other magnitudes and distances of interest. This may require that additional empirical estimates be developed in the first three worksheets.

σ . The standard deviations of the empirical ground-motion estimates (aleatory uncertainty), the hybrid empirical estimates (epistemic uncertainty), and the aleatory standard errors (σ) for the given ground-motion parameter, magnitude, and horizontal distance. All of the standard deviations are given in terms of the natural logarithm (log base e). Except for PGV, the aleatory and epistemic uncertainty was taken from EPRI (1993). The aleatory uncertainty for distances greater than 20 km was used at shorter distances because the increased uncertainty at short distances given by EPRI was due to uncertainty in focal depth, whereas, for this application, the focal depth was specified by the facilitation team. Since EPRI did not provide uncertainty estimates for PGV, estimates of aleatory and epistemic uncertainty for this parameter were taken to be the same as that for the 2.5-Hz PSA for $M_w = 5.0$ and 6.0 and the average of the square root of the variances of the 1.0 Hz and 2.5 Hz PSA for $M_w = 7.0$ and 7.5 , consistent with the empirical

attenuation relationships. The standard deviation of σ is the standard deviation of the weighted standard errors of the empirical ground-motion estimates.

Ratios. Ratios of PGV to PGA are provided for information.

FACTORS.FOR

This Fortran 77 computer code calculates the theoretical adjustment factors between the Midcontinent EUS and California for the ground-motion parameters of interest. It requires one additional executable Fortran code, EQERASCL.EXE, for calculating ground-motion parameters using the band-limited white noise (BLWN), random vibration theory (RVT), point-source stochastic simulation model developed by Silva and Lee (1987), with modifications recommended by Walt Silva (personal communication, 1995). EQERASCL.EXE is called from within FACTORS.FOR. This may require replacing the Lahey Fortran system call to DOS with the equivalent system call for the Fortran used to compile the code. The executable file, FACTORS.EXE, is provided to avoid having to recompile the code. FACTORS.FOR also requires an input file that lists the moment magnitudes and equivalent point-source distances for which the adjustment factors are calculated.

Input File

The name of the input file is provided by the user in response to a screen request when the main program is run. Only the main file name should be provided, not the extension (i.e., the part of the filename to the right and inclusive of the decimal point). The file extension for this input file must be '.IN' (e.g., FACT_D5.IN, FACT_D10.IN, or FACT.D20.IN). This file is free format so the only formatting constraint is that multiple entries on a given line be separated by one or more spaces. The data required in this input file are as follows:

First Line. The number of magnitudes followed by the number of distances for each magnitude.

Second Line. The moment magnitudes.

Third and Subsequent Lines. The horizontal distances (*Rhor*) followed by the equivalent point-source distances (*Reps*) corresponding to the horizontal distances (one line for each magnitude). The values of *Reps* are computed in the spreadsheets DIST_D5.XLS, DIST_D20.XLS, and DIST_D20.XLS.

Output Files

Two output files are generated, each with the main file name specified upon program execution, one with an extension of '.OUT' and one with an extension of '.DAT'. Each file is comma delimited for ease in importing to other programs (e.g., EXCEL). A description of these files are as follows:

'OUT' File. This file contains the following parameters: magnitude (MW); horizontal distance (RHOR); stress drop (SDROP); Q at 1 Hz (Q0); the exponent of frequency in the power-law Q function (ETA); the number of the crustal amplification model ('CRUST' ISDROP); the upper crustal attenuation parameter (KAPPA); calculated horizontal spectral accelerations (PSA) for all frequencies of interest (ordered from low to high frequency), peak horizontal ground acceleration (PGA), and peak horizontal ground velocity (PGV) for the Midcontinent EUS; the same ground-motion parameters (H_PSA, H_PGA, and H_PGV) for California; and the adjustment factors, or ratios between the ground-motion parameters listed in the same order as above, between the Midcontinent EUS and California (FACTOR). There is one line for each combination of magnitude, distance, and model parameters.

'DAT' File. This file contains the following parameters: magnitude (MW); horizontal distance (RHOR); stress drop (SDROP); and, for PSA at all frequencies of interest (ordered from low to high frequency),

PGA, and PGV, the median (AVG) and standard deviation (STDDEV) of the calculated adjustment factors. There is one line for each combination of magnitude, distance, and stress drop.

EQERASCL Files

There is one file that is provided by the user and several files that are automatically generated for use with EQERASCL. These files are described as follows:

FREQ.DAT. This file contains the frequencies for which ground-motion parameters are calculated by EQERASCL. The first two values in this file are “dummy” values that indicate PGA and PGV. The remaining values are the frequencies at which PSA and other spectral parameters are calculated. This file must be provided by the user.

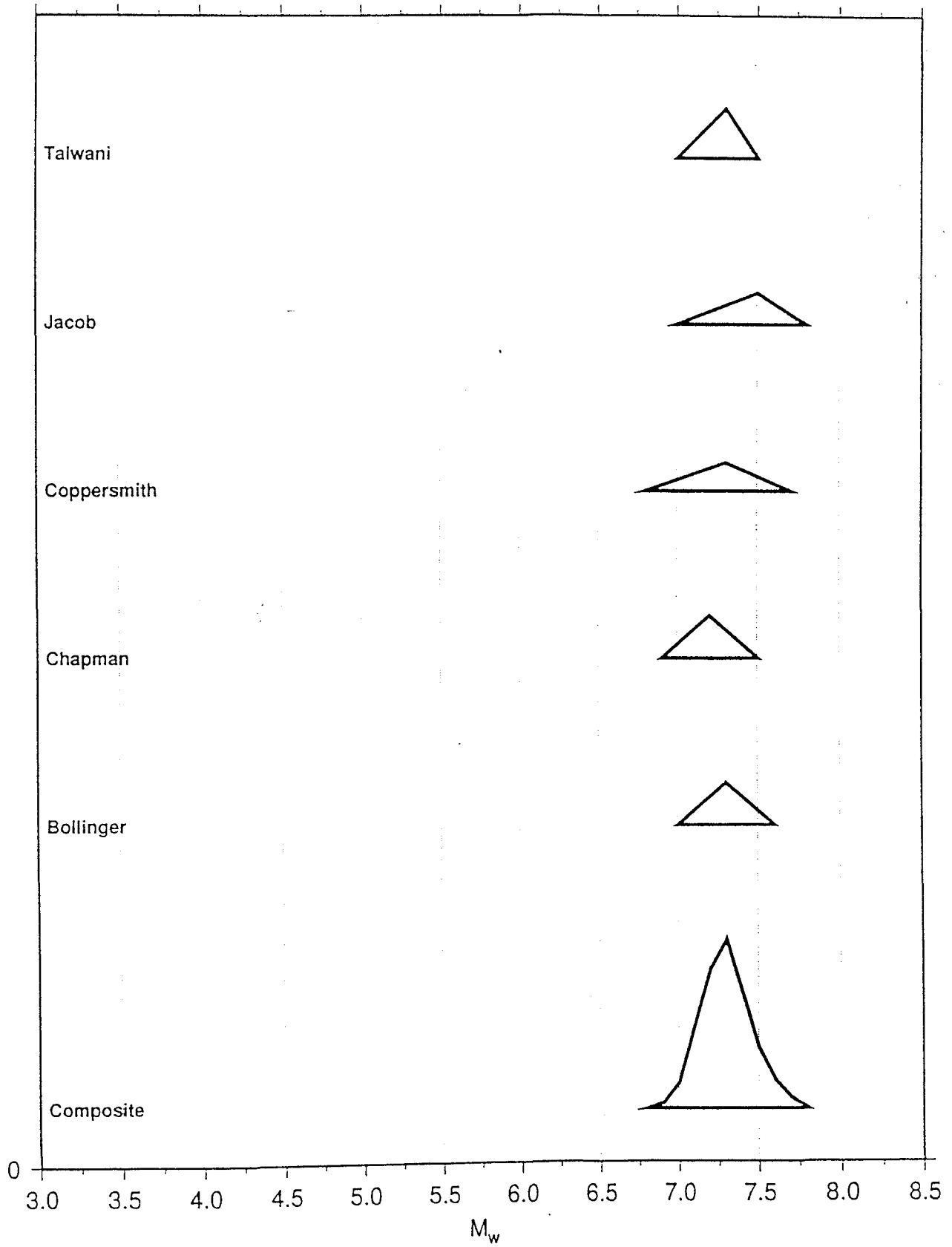
INPUT.TXT. This file contains the names of the generic file names that are opened by EQERASCL (generated by FACTOR).

INPUT.DAT. This file contains the input data file for EQERASCL (generated by FACTOR).

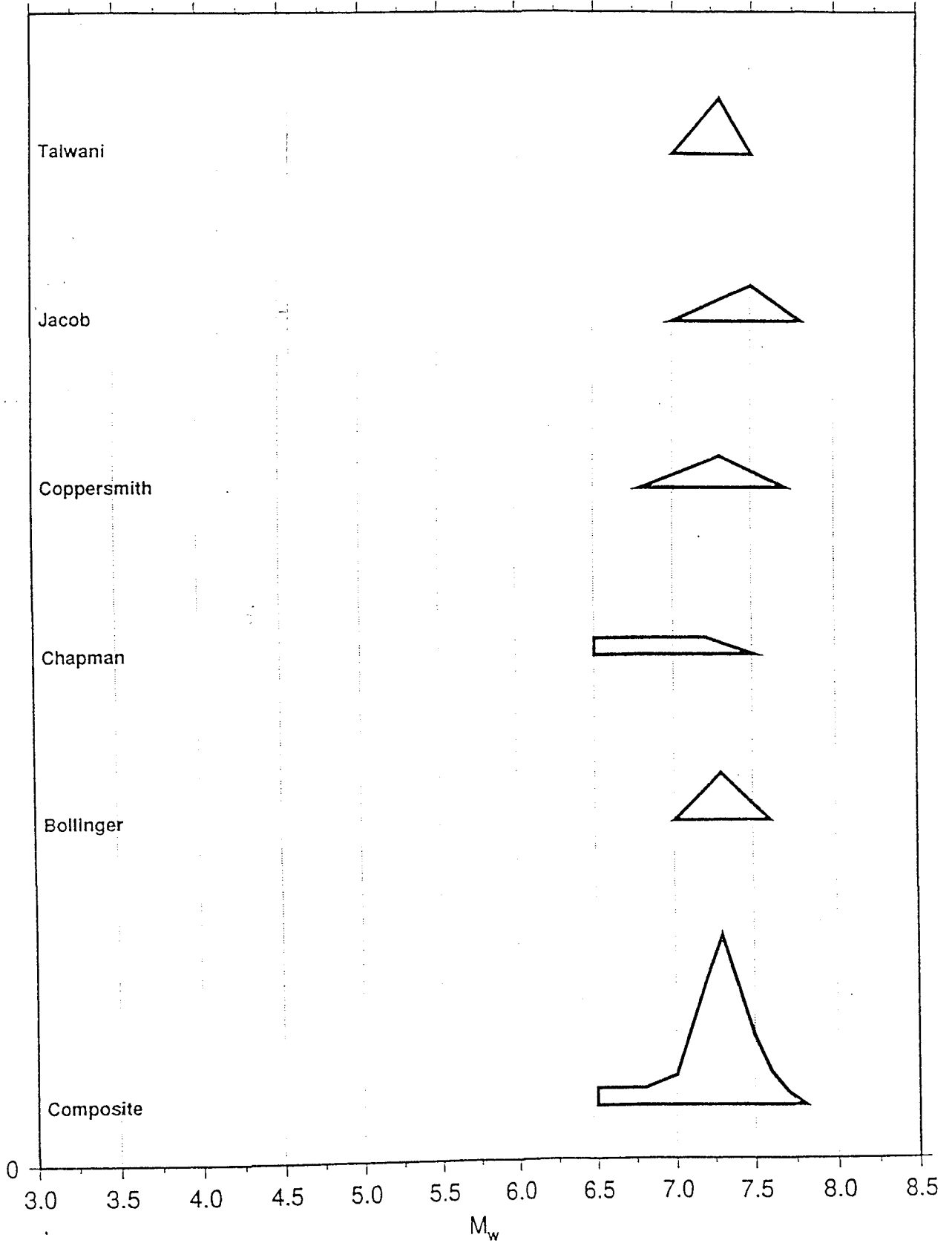
OUTPUT.DAT. This file contains the output file from EQERASCL (generated by FACTOR).

**APPENDIX F: TRIAL IMPLEMENTATION PROJECT—PLOTS OF
MAXIMUM MAGNITUDE AND RECURRENCE RATE ESTIMATES FOR
EACH EXPERT, AND COMPOSITE PROBABILITY DISTRIBUTION
FUNCTION**

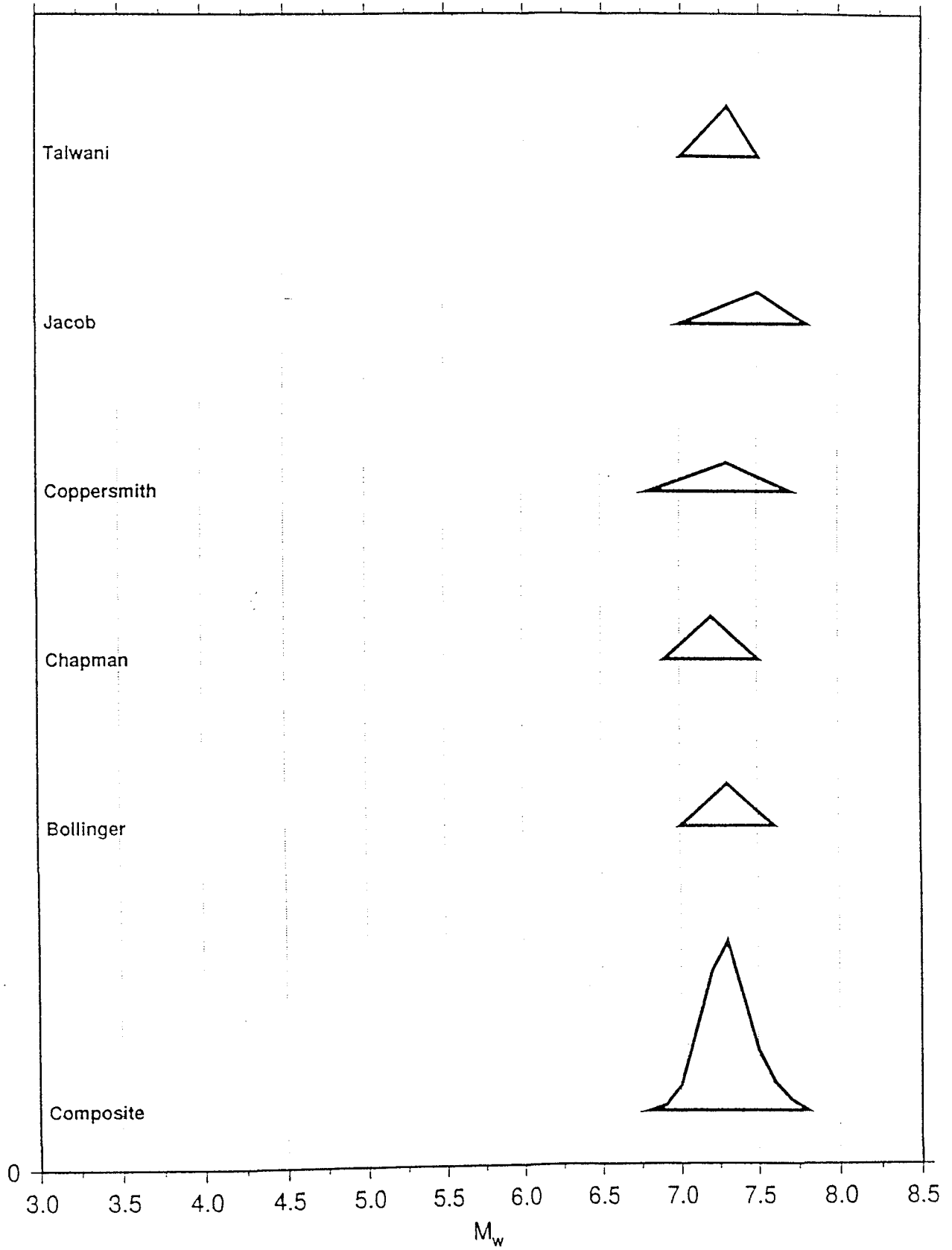
M_u ; ZONE 1a



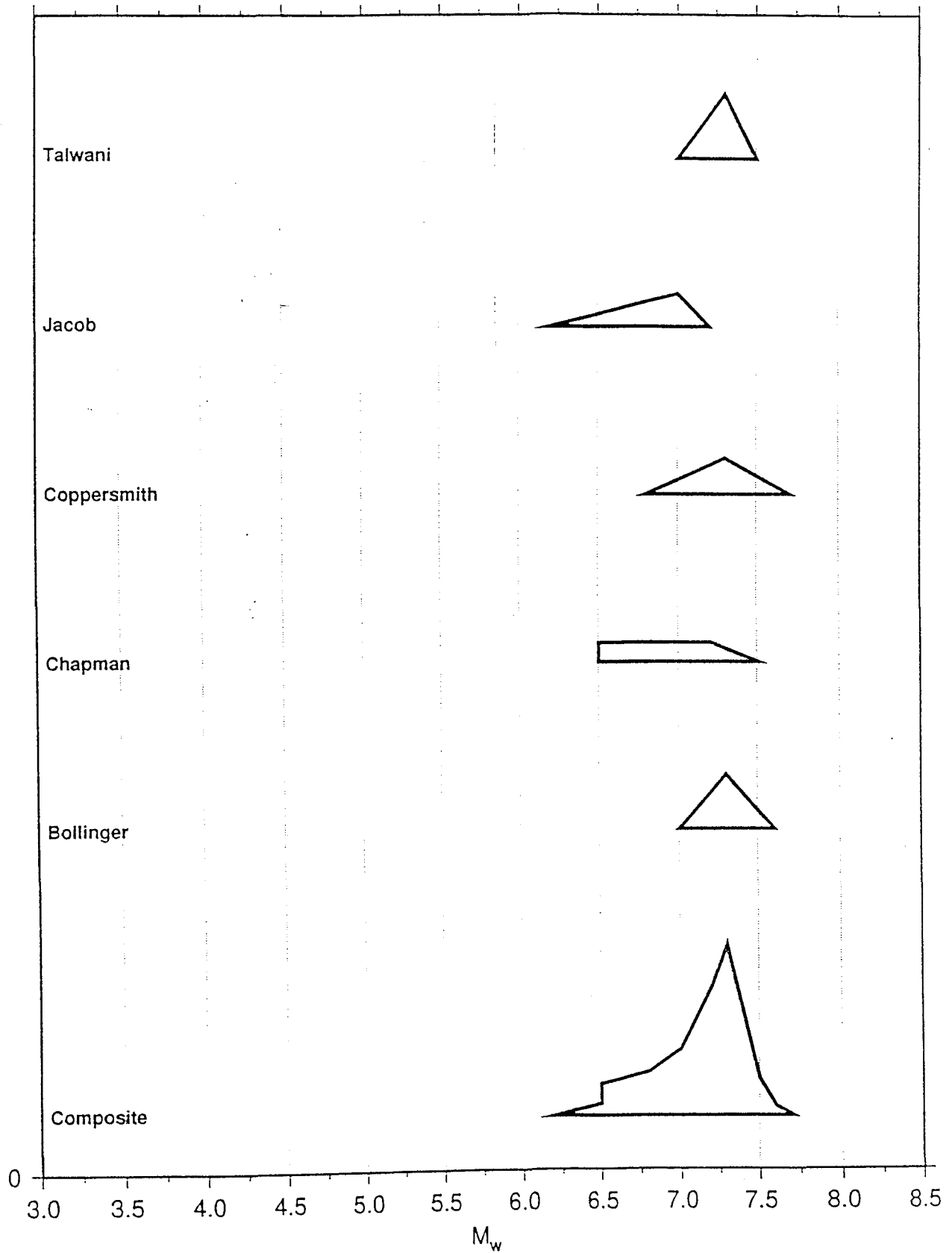
M_u ; ZONE 1b



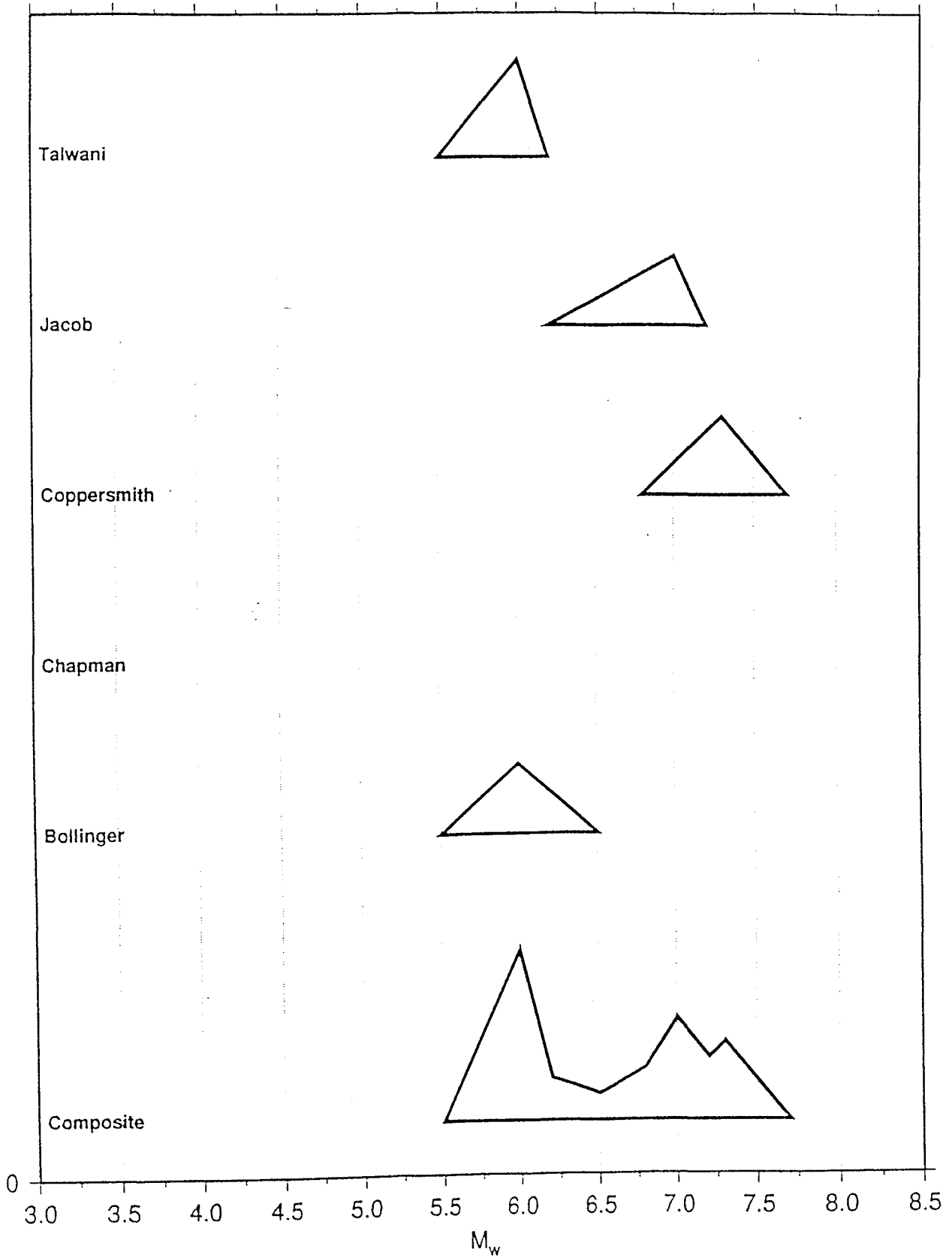
M_U ; ZONE 1c



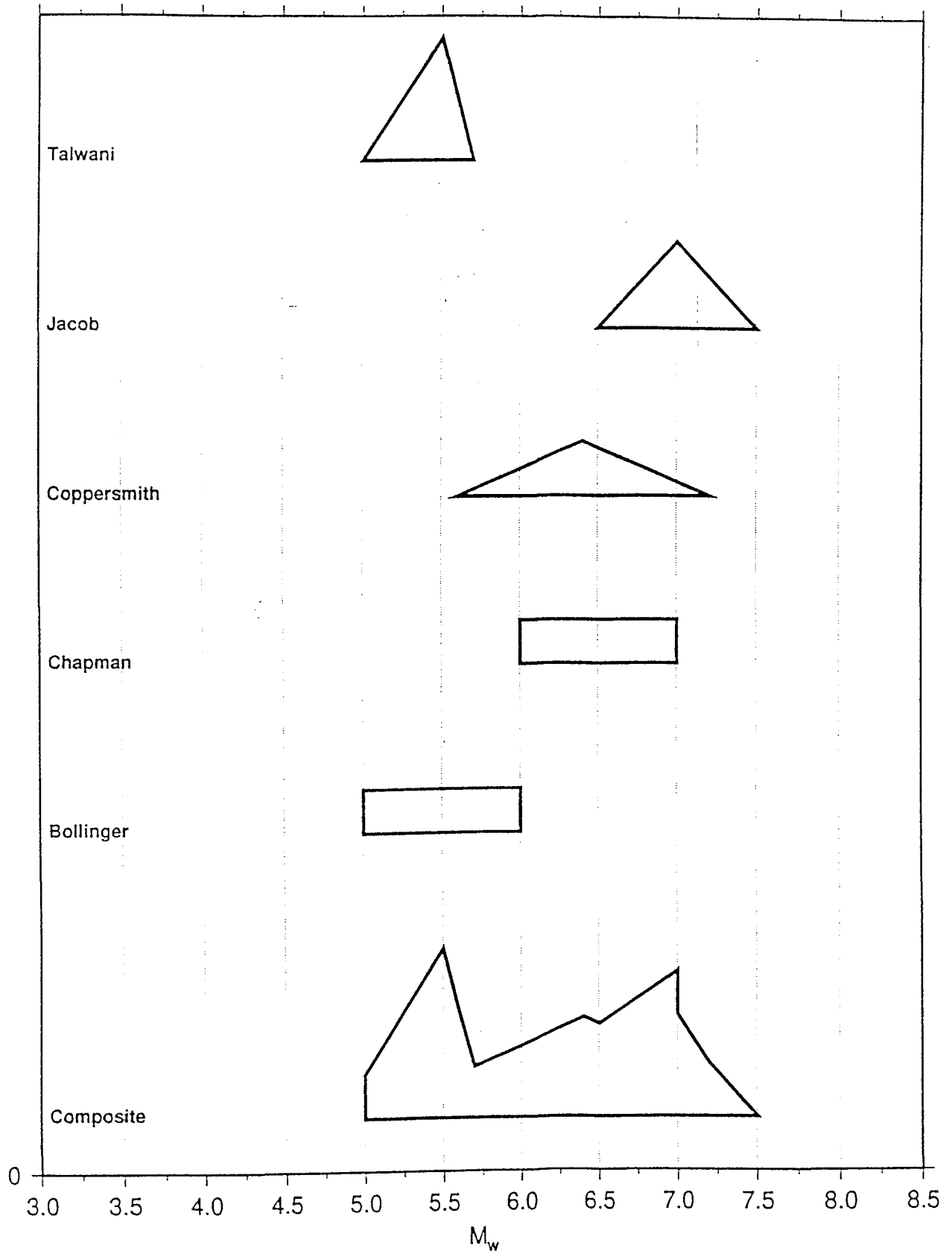
M_u ; ZONE 1d



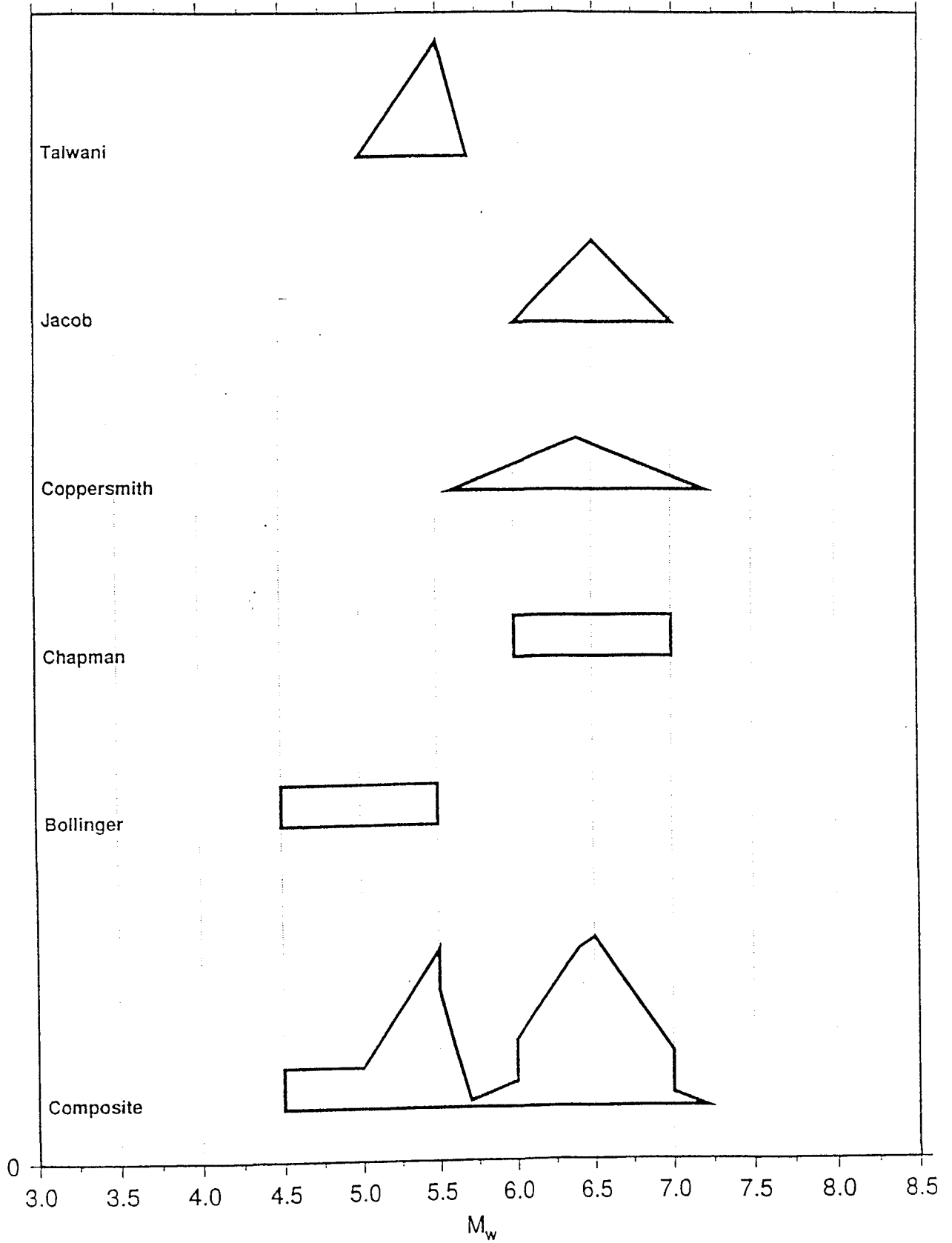
M_U ; ZONE 1e



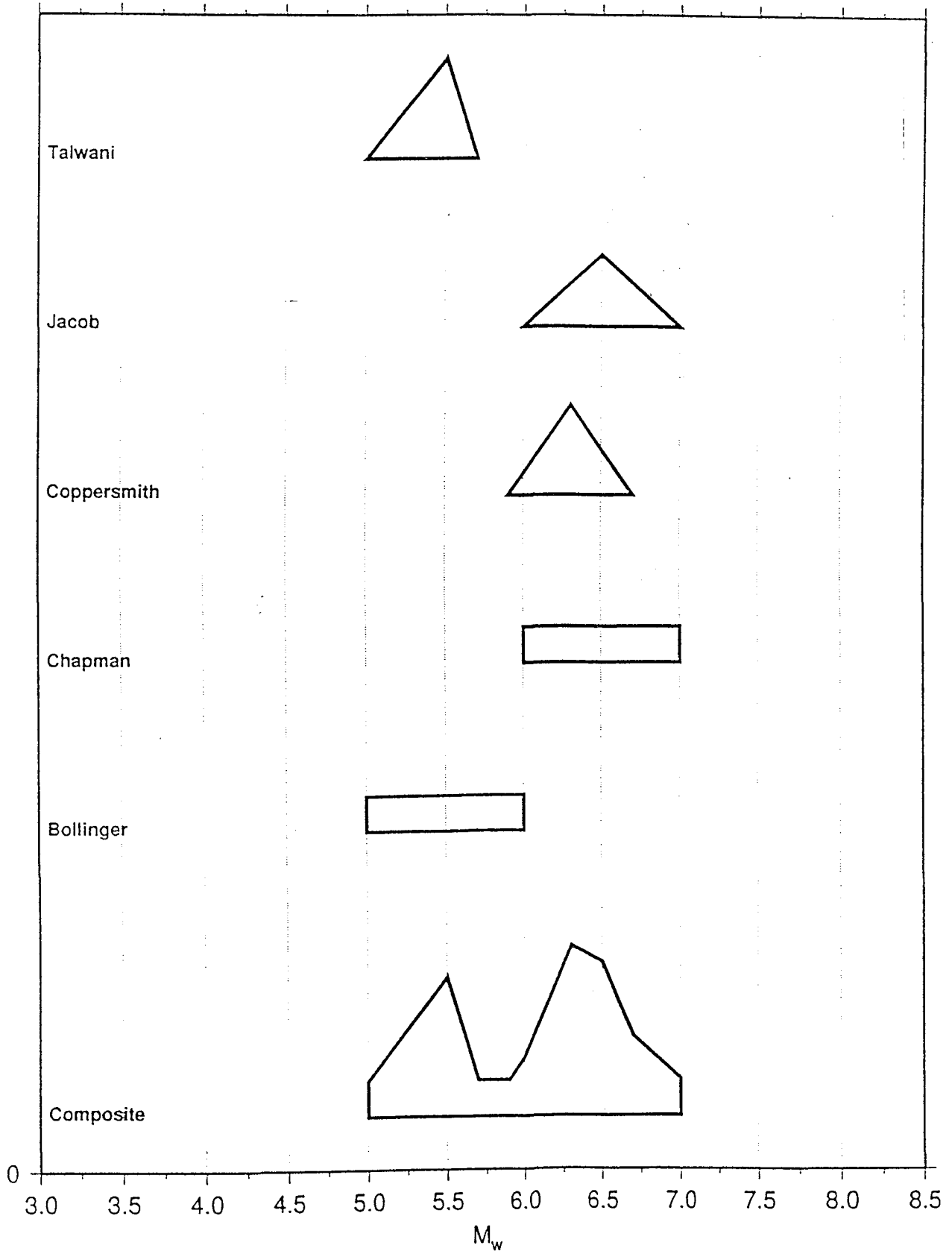
M_U ; ZONE 3a



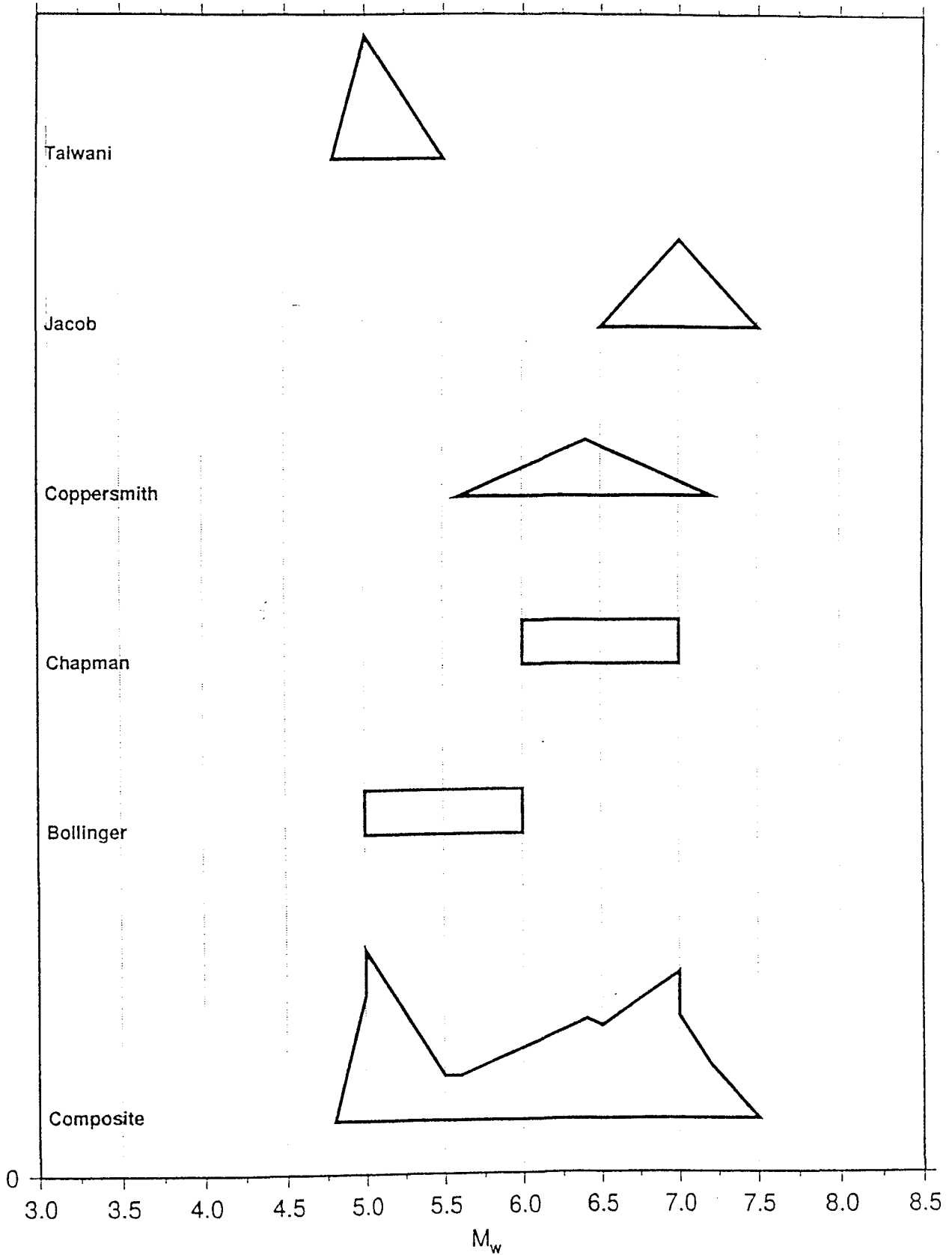
M_u ; ZONE 3b-3a



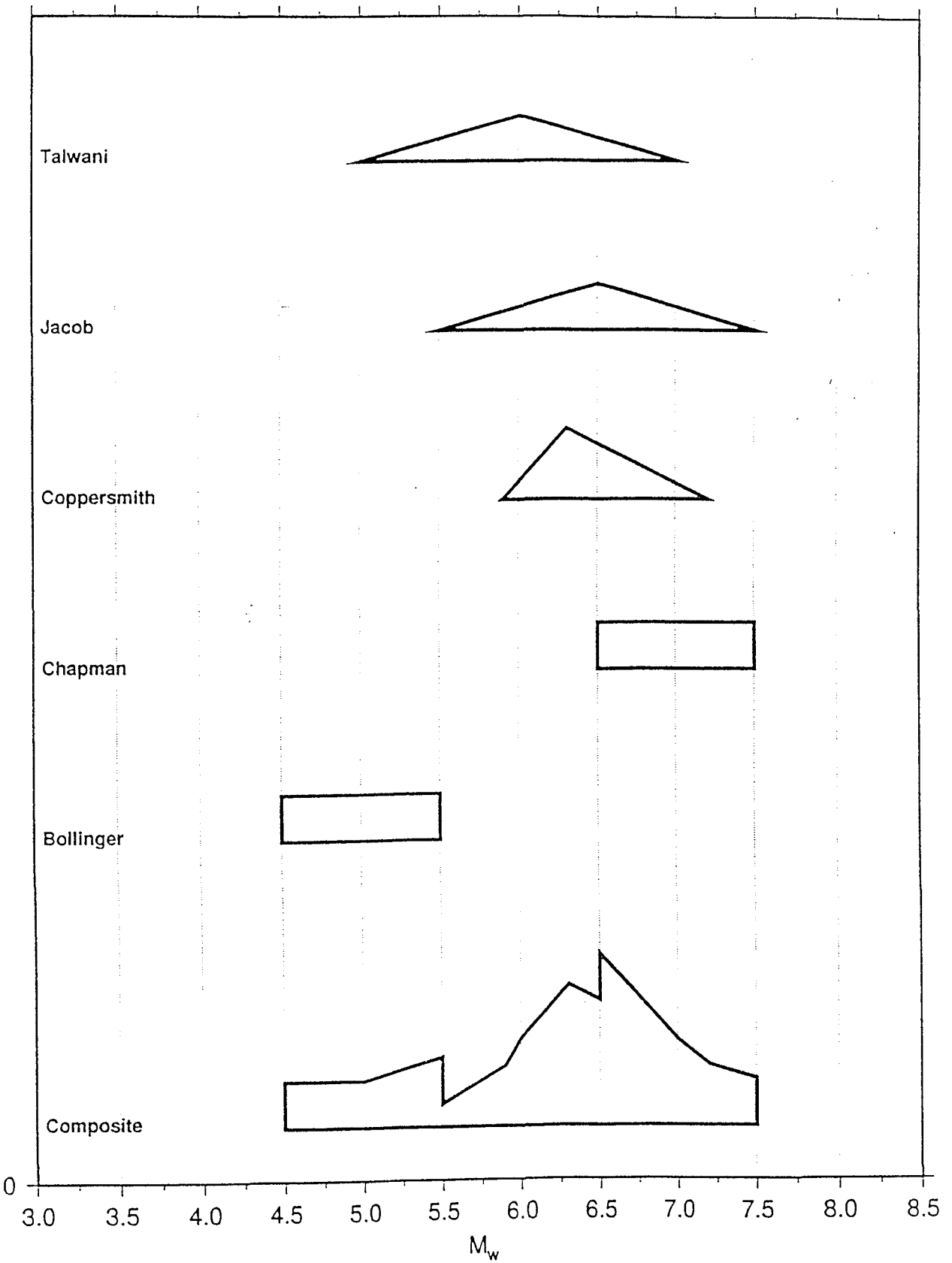
M_U ; ZONE 3c



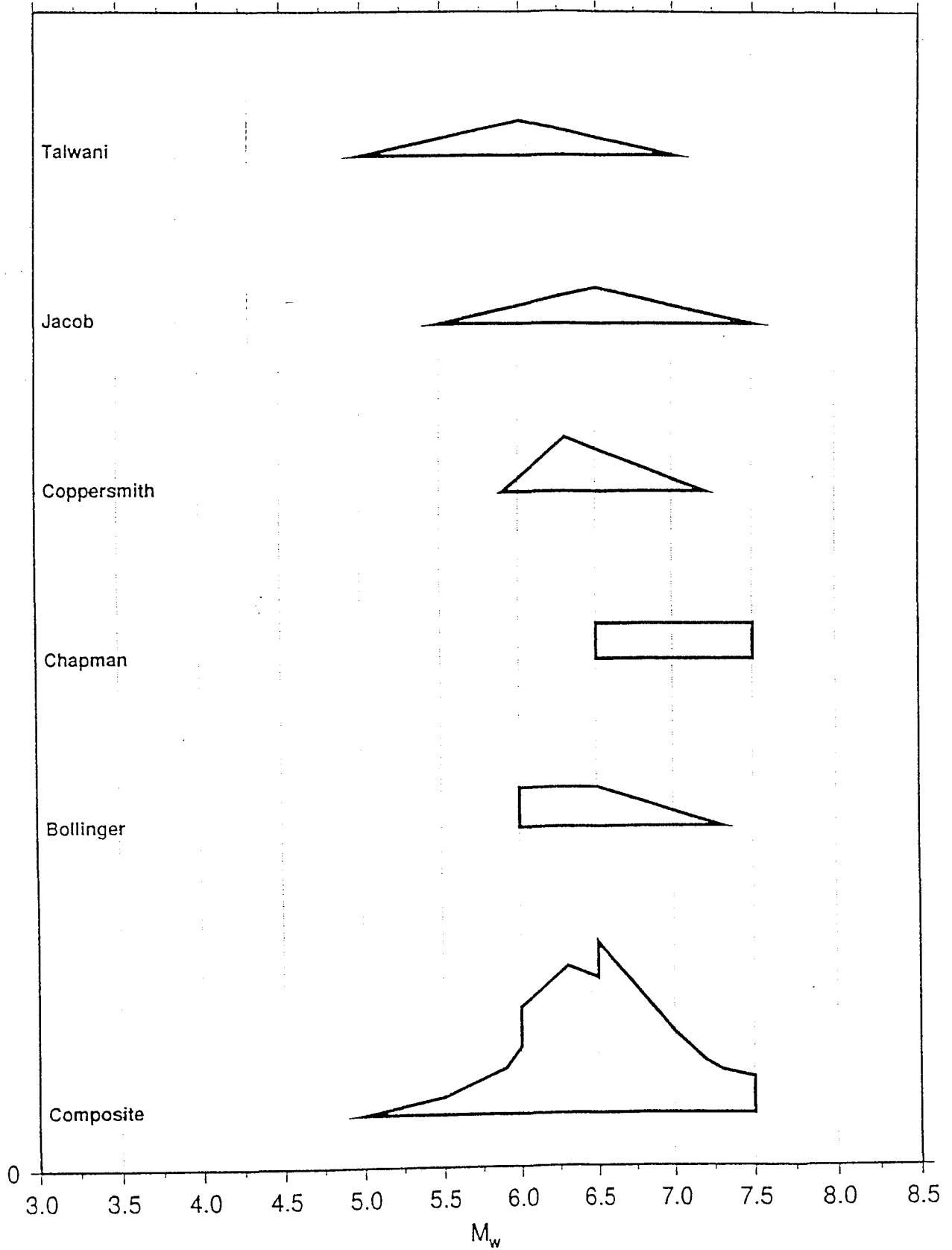
M_u ; ZONE 3b-3c



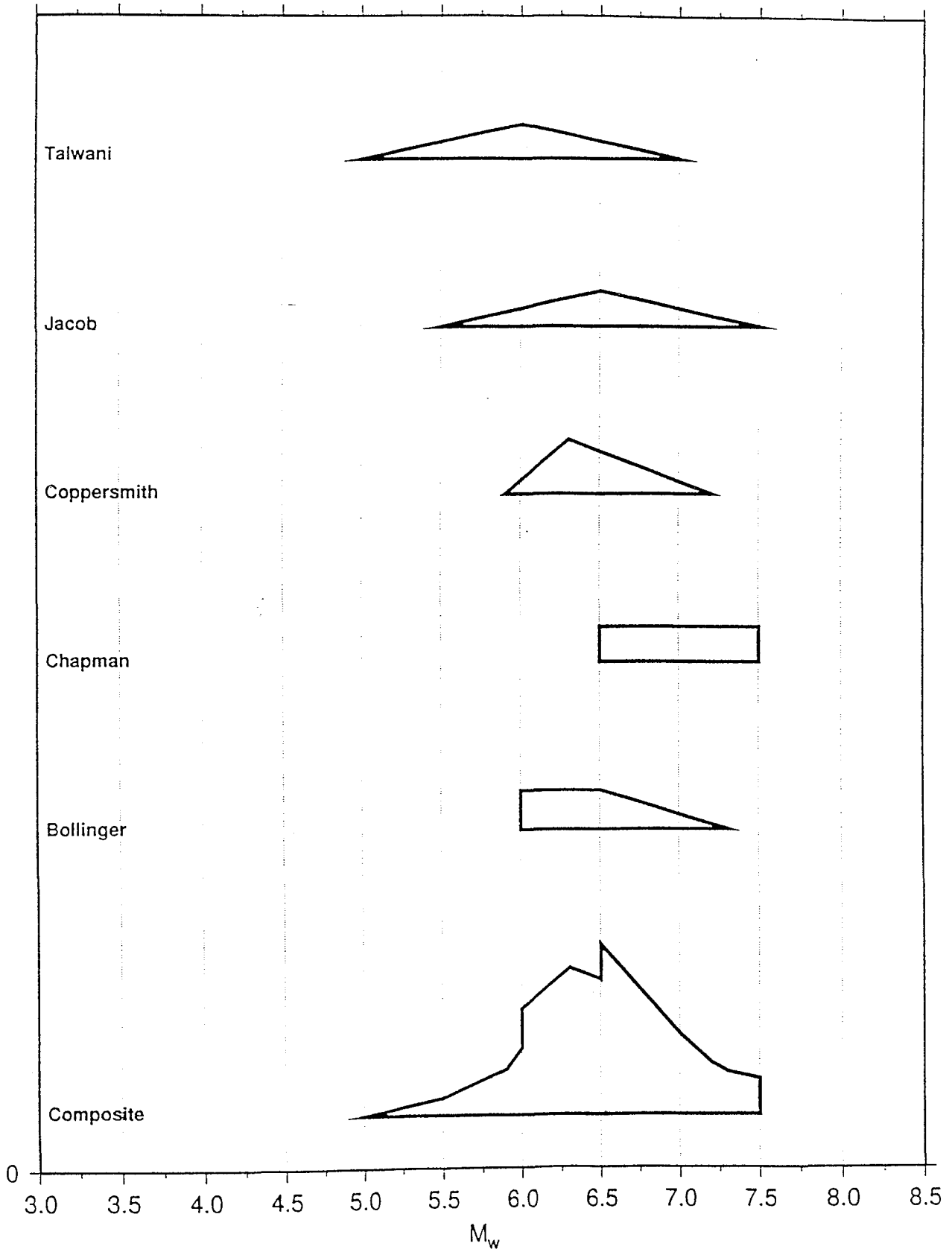
M_U ; ZONE 4a1



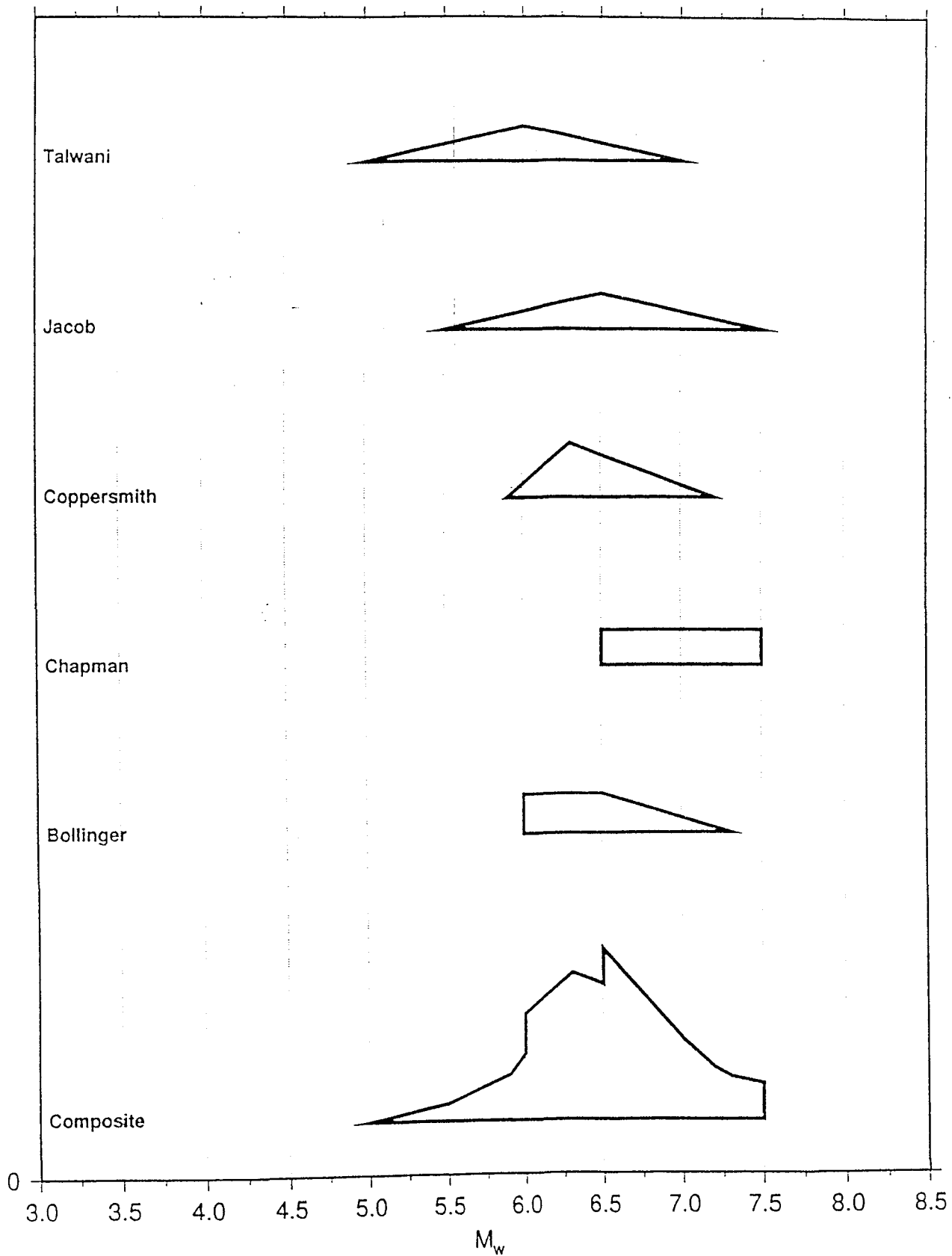
M_U ; ZONE 4a1+2



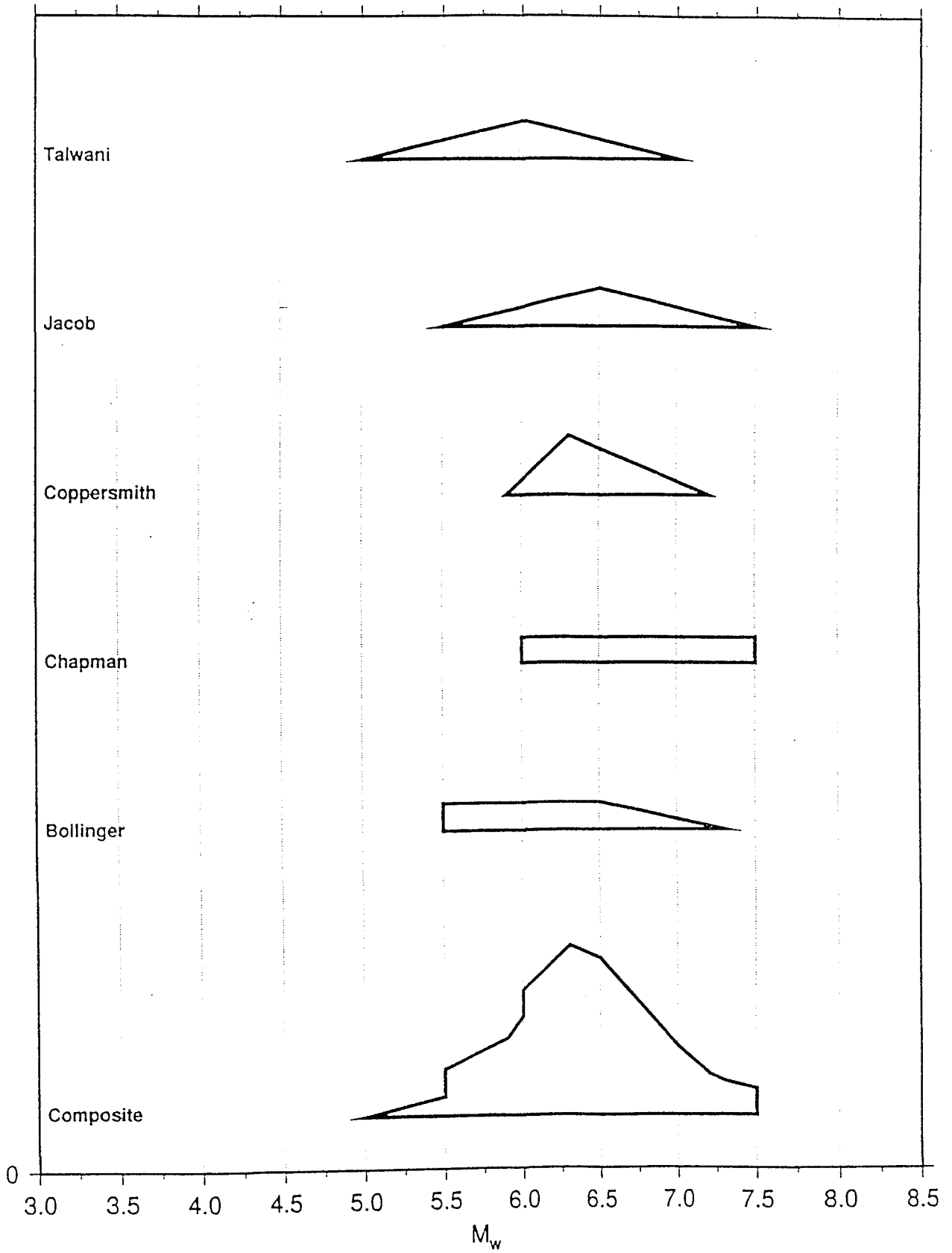
M_U ; ZONE 4a1+2+3



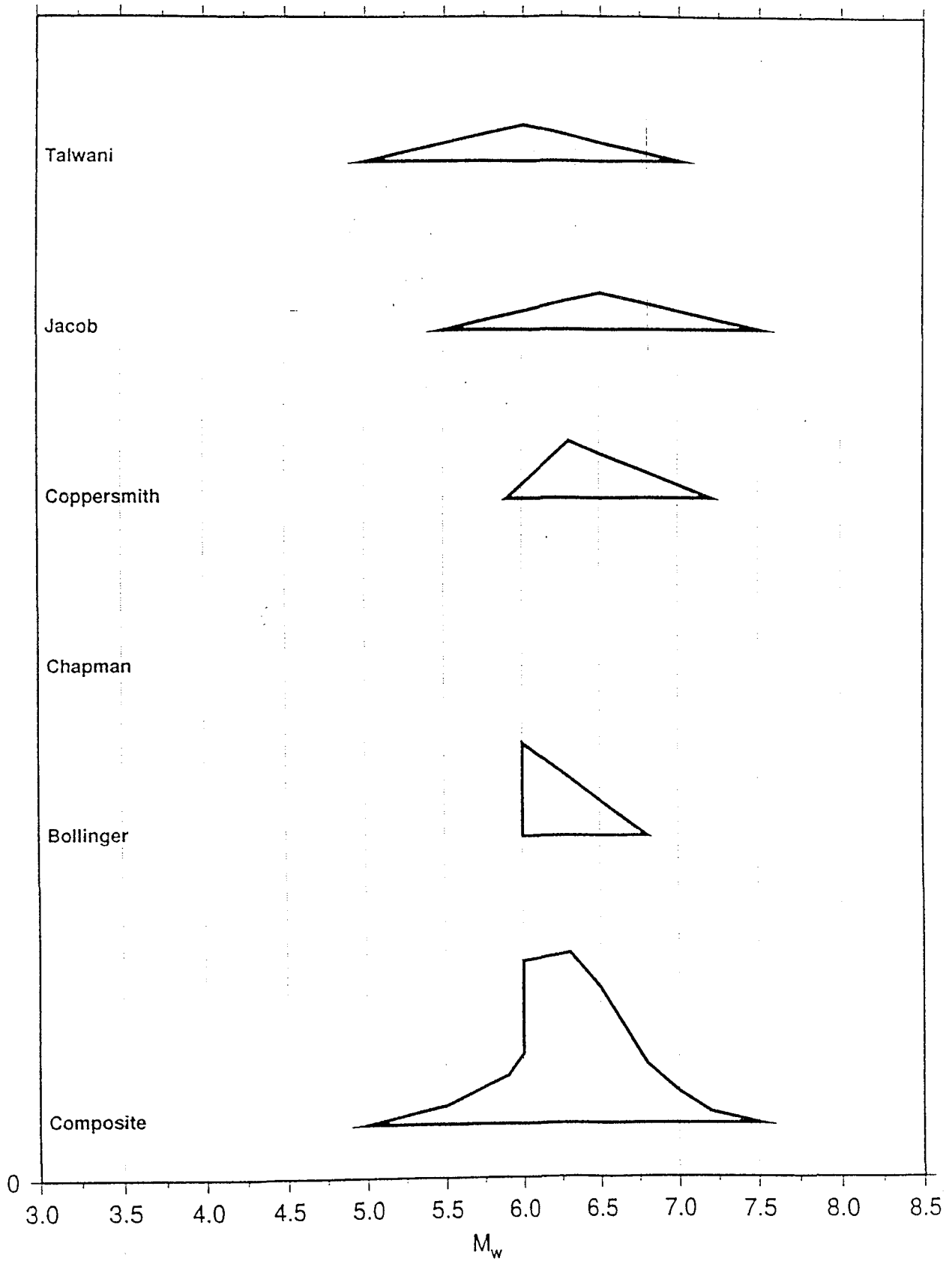
M_u ; ZONE 4b1



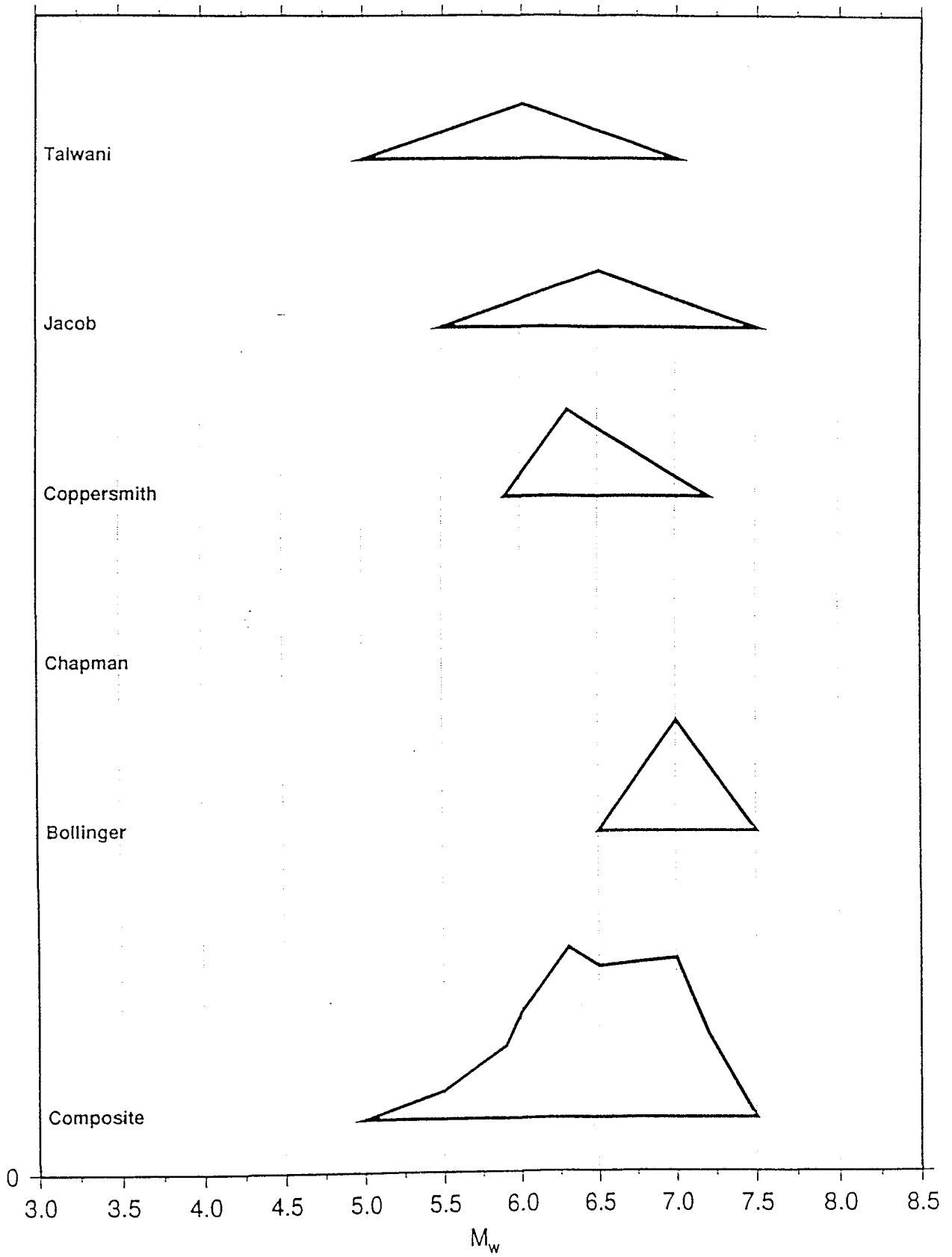
M_u ; ZONE 4b2



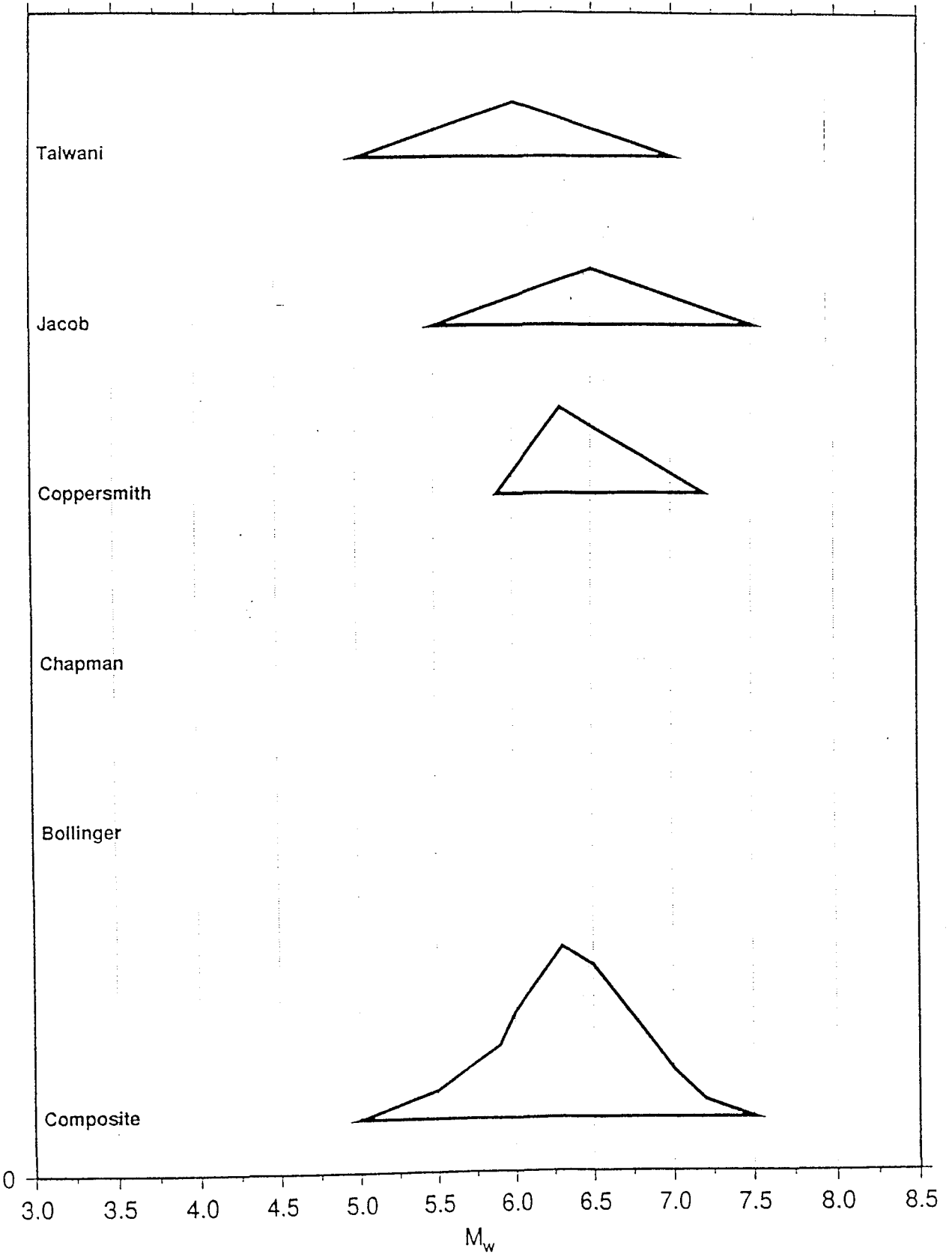
M_U ; ZONE 4c



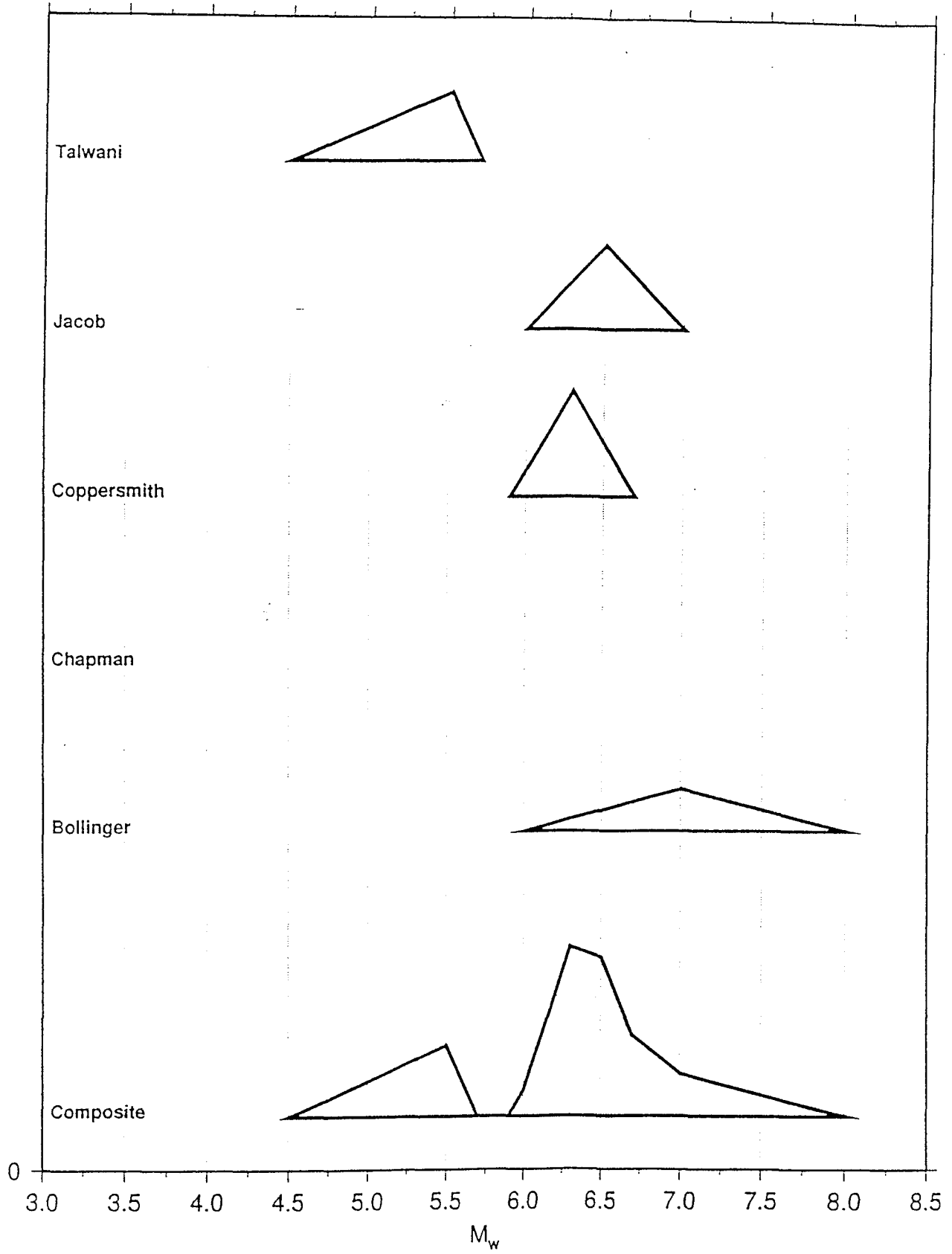
M_u ; ZONE 4d



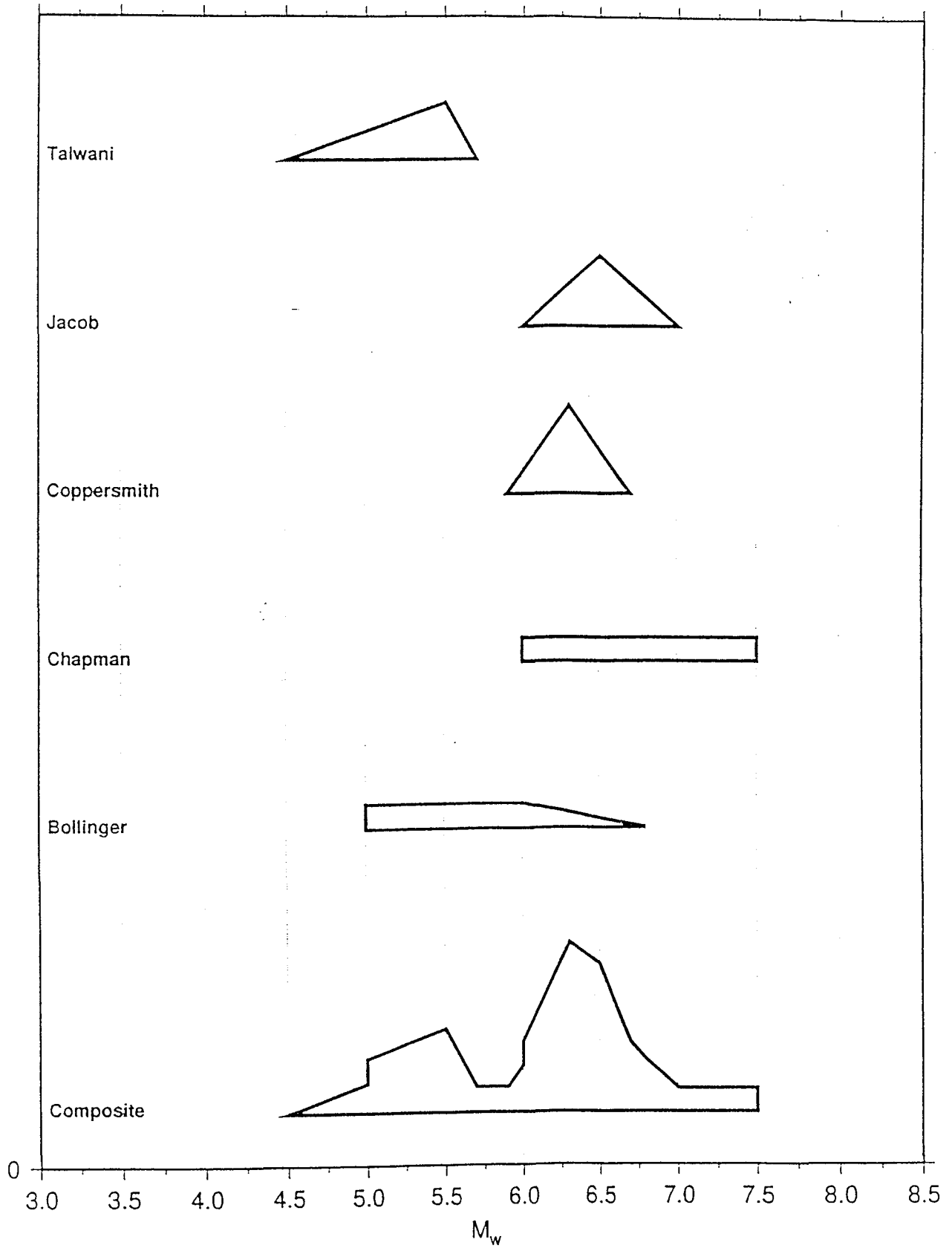
M_u ; ZONE 4e



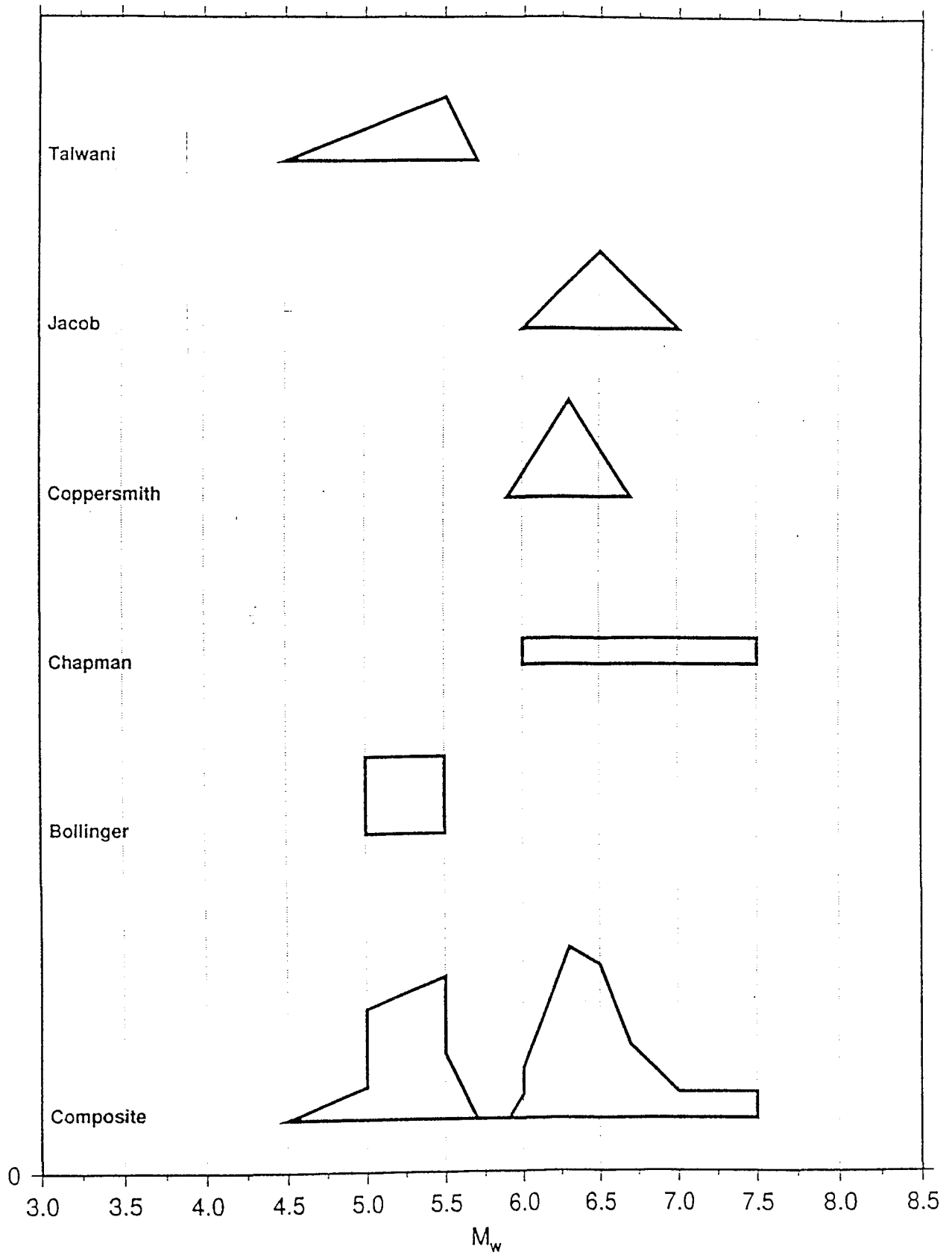
M_U ; ZONE 5-1



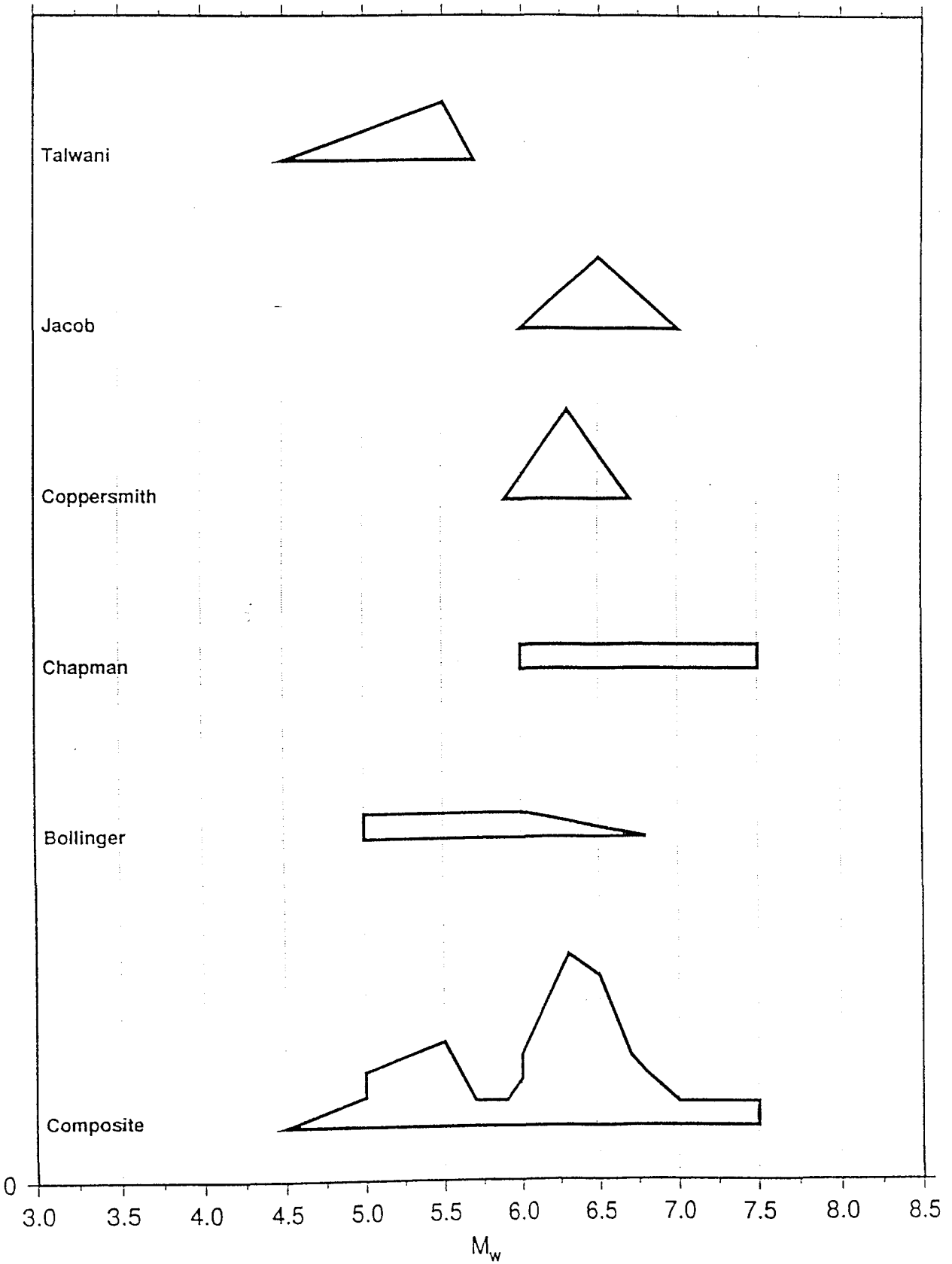
M_U ; ZONE 5-1+2



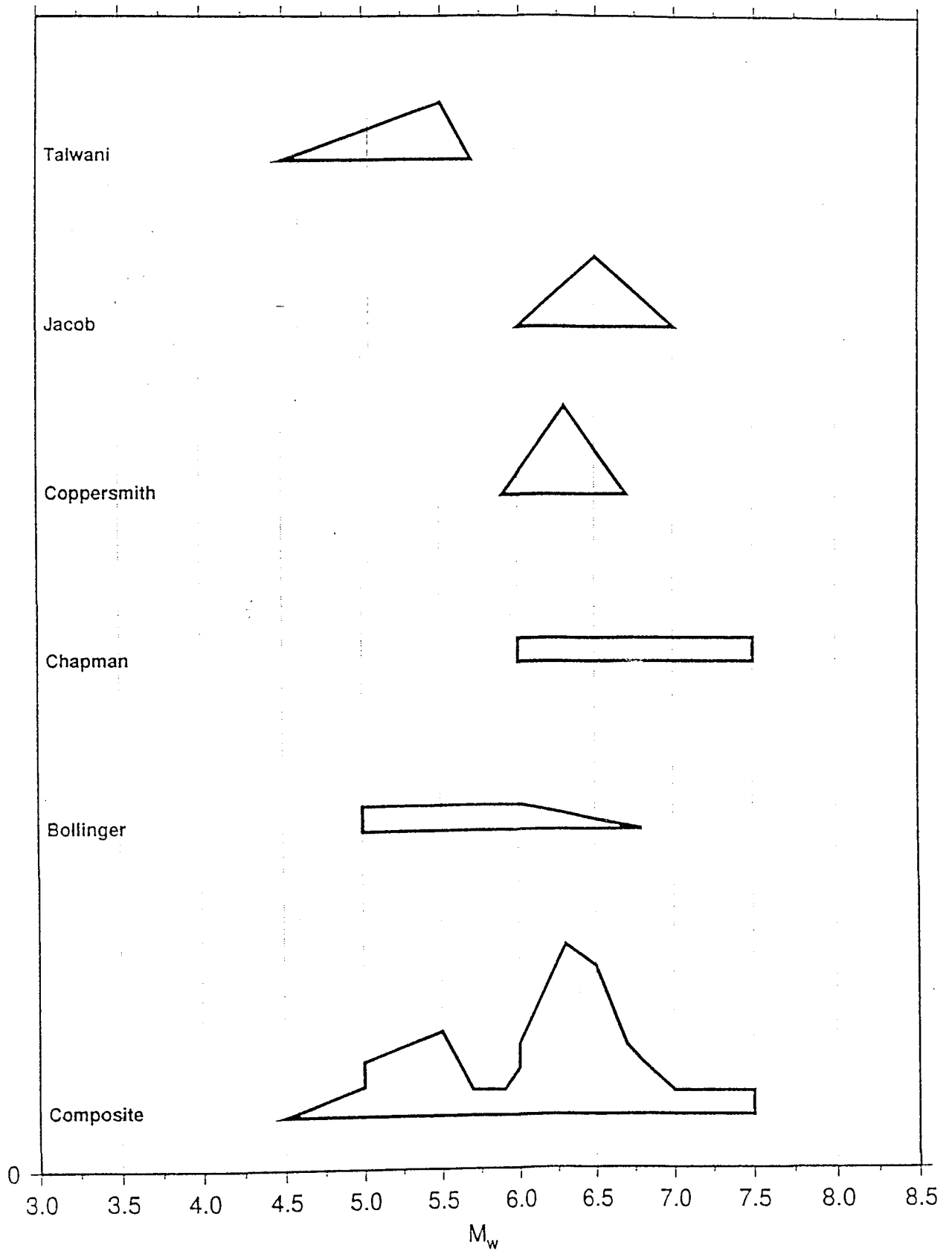
M_u ; ZONE 5-1+2+3



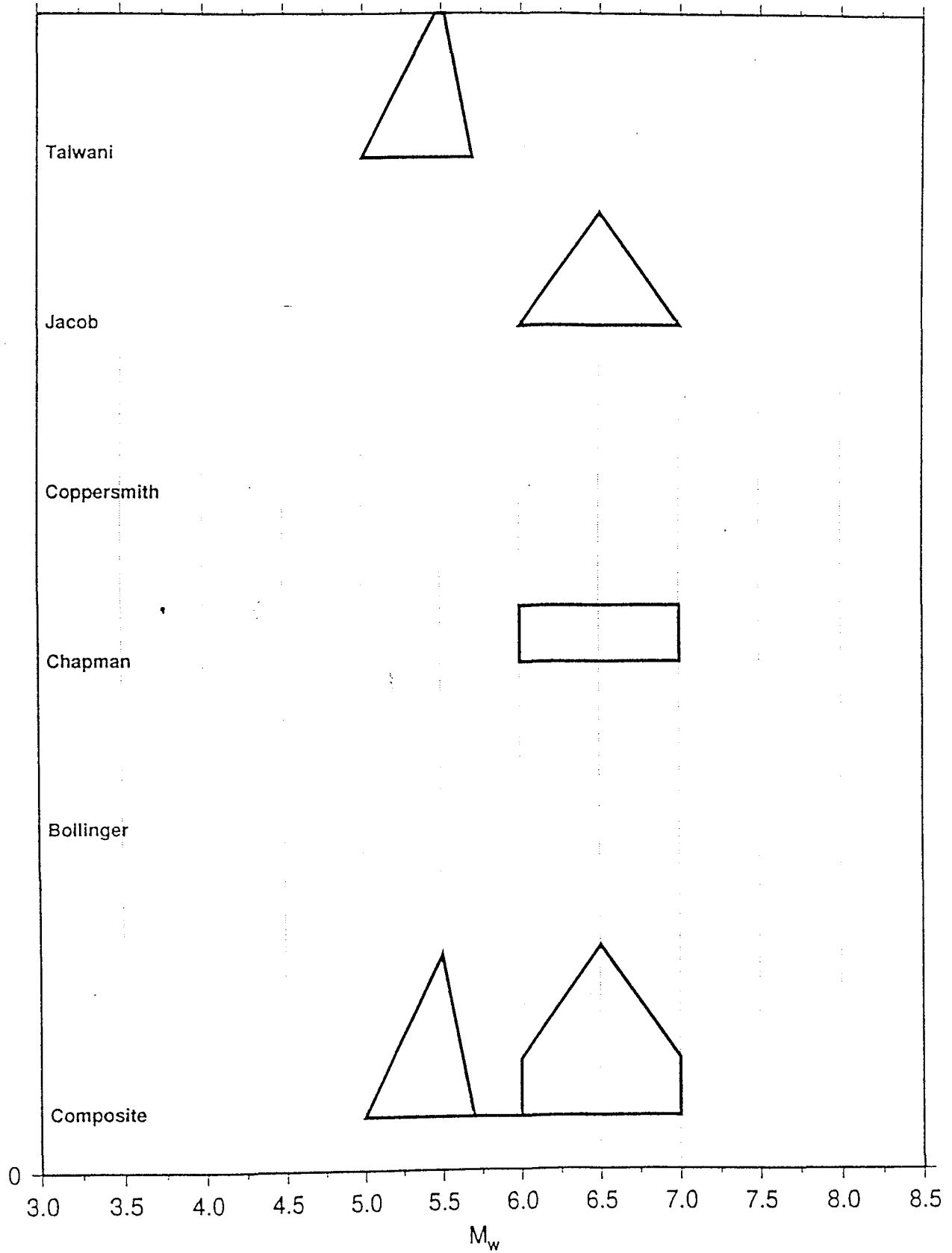
M_u ; ZONE 5-2



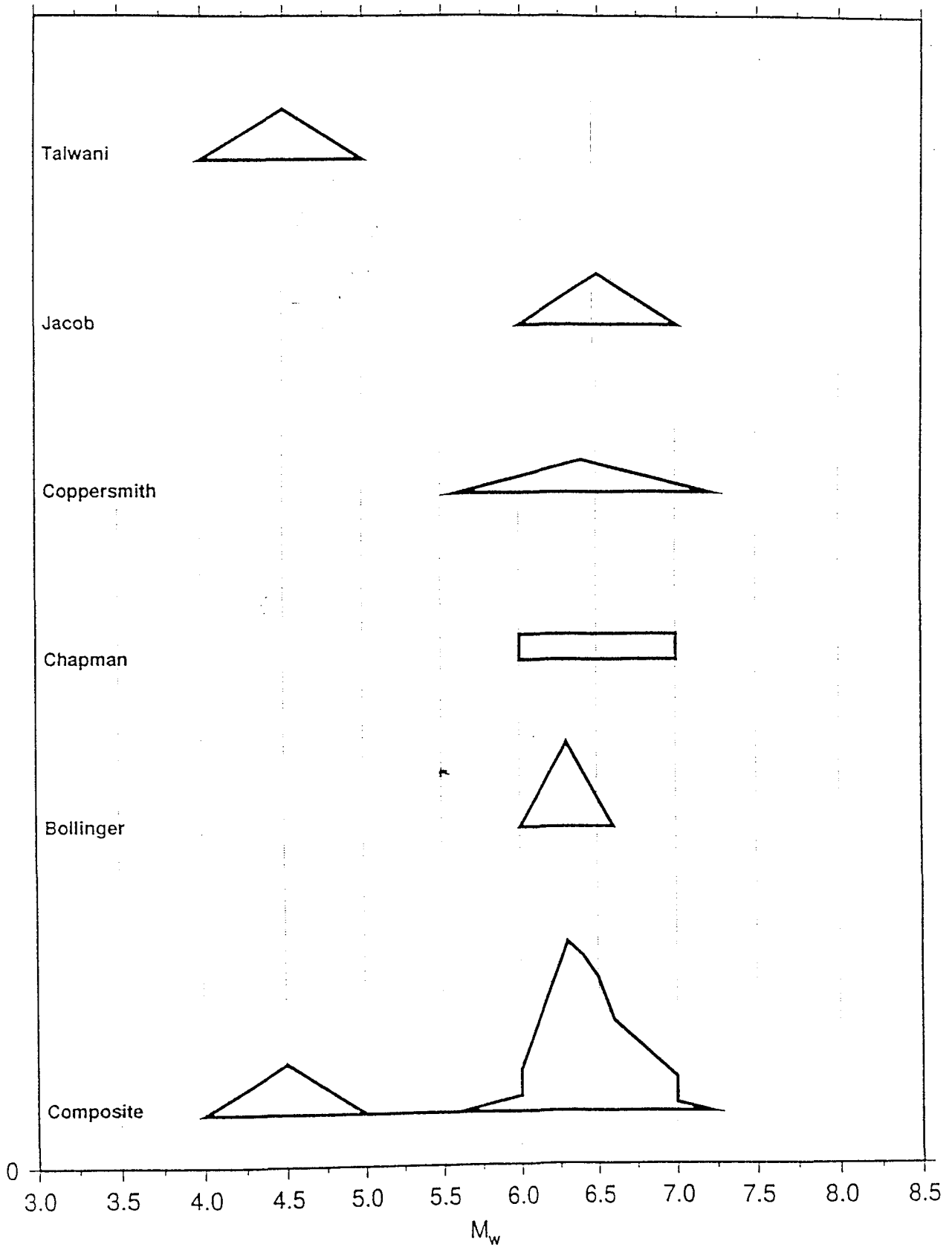
M_U; ZONE 5-3



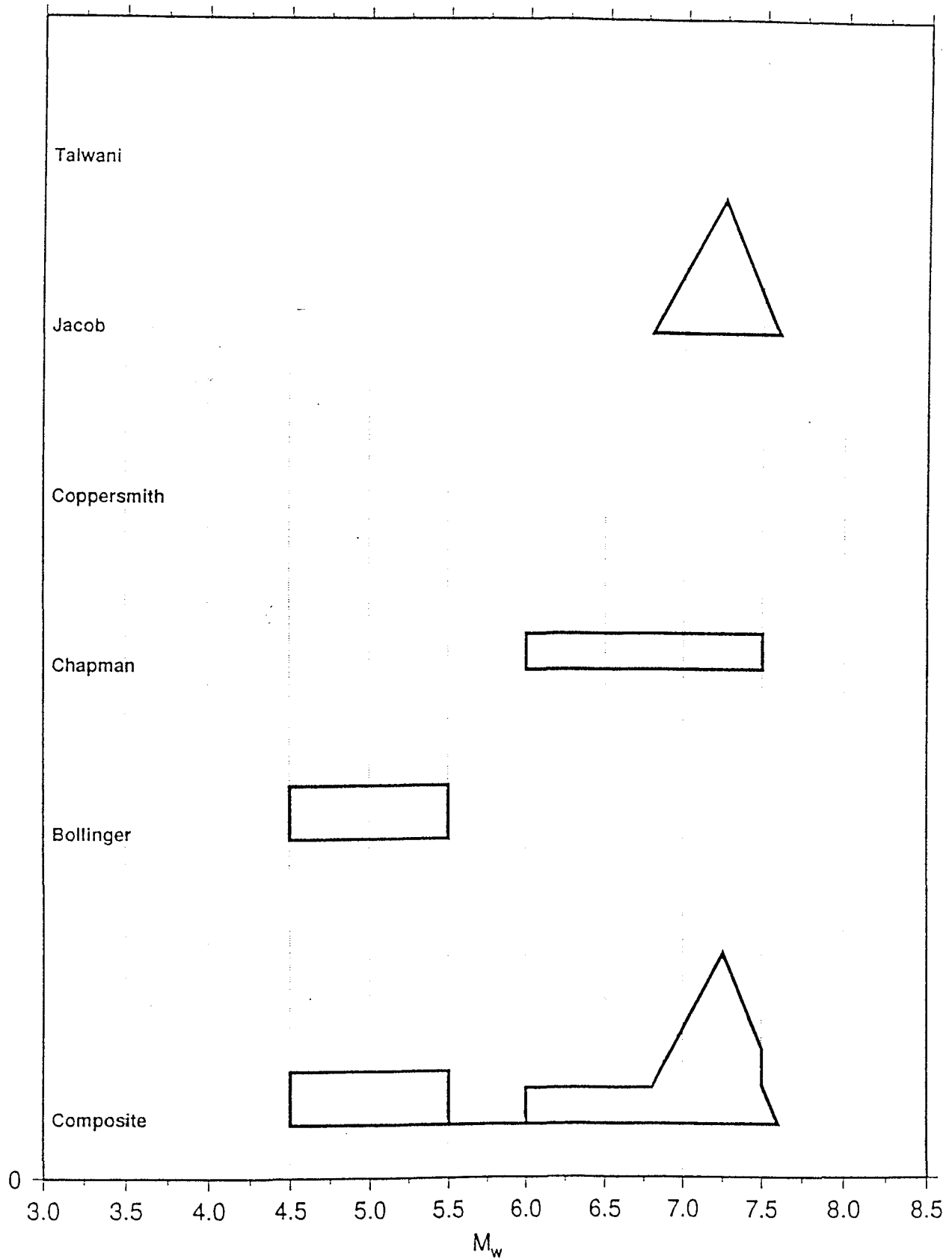
M_U ; ZONE 6



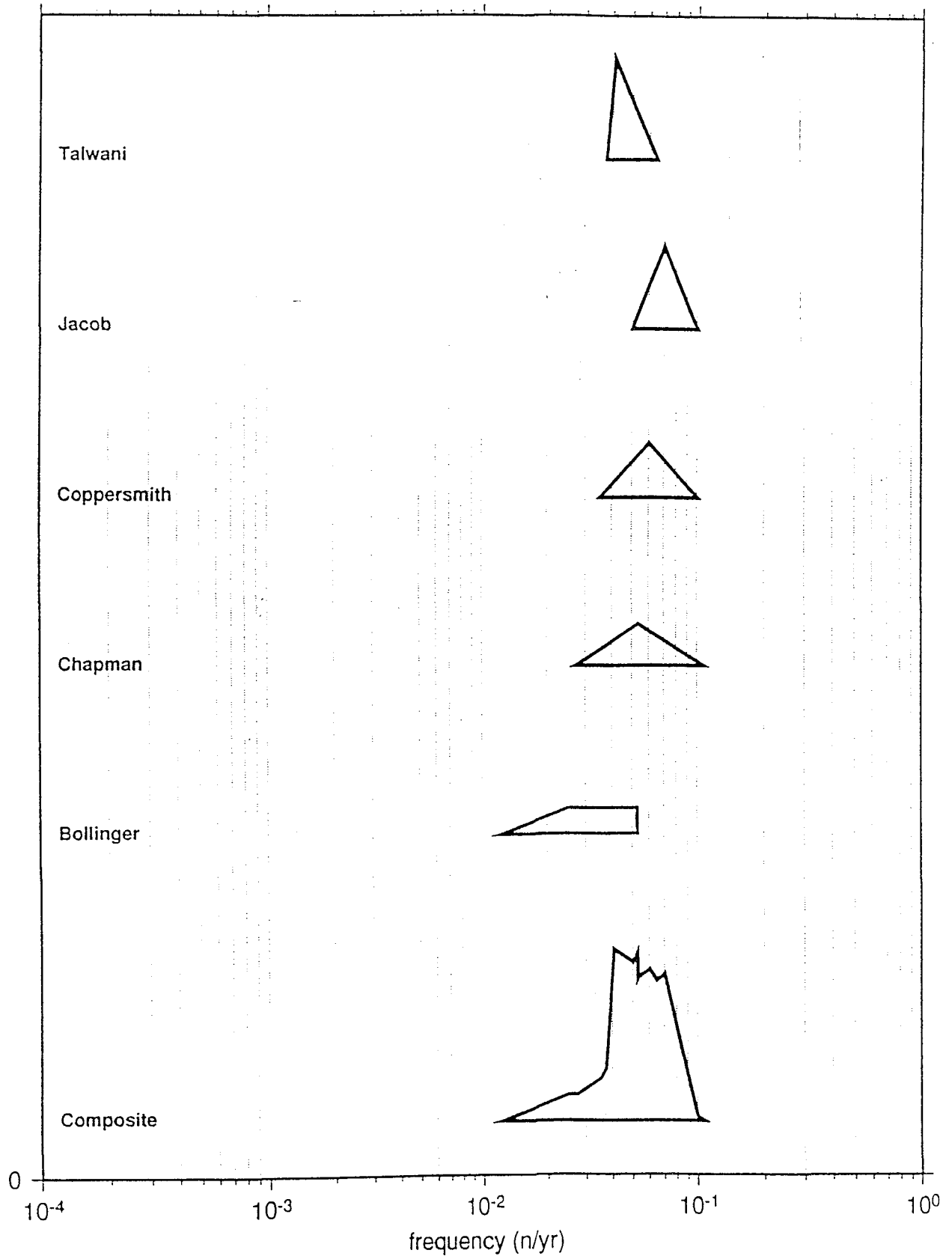
M_U ; ZONE 7



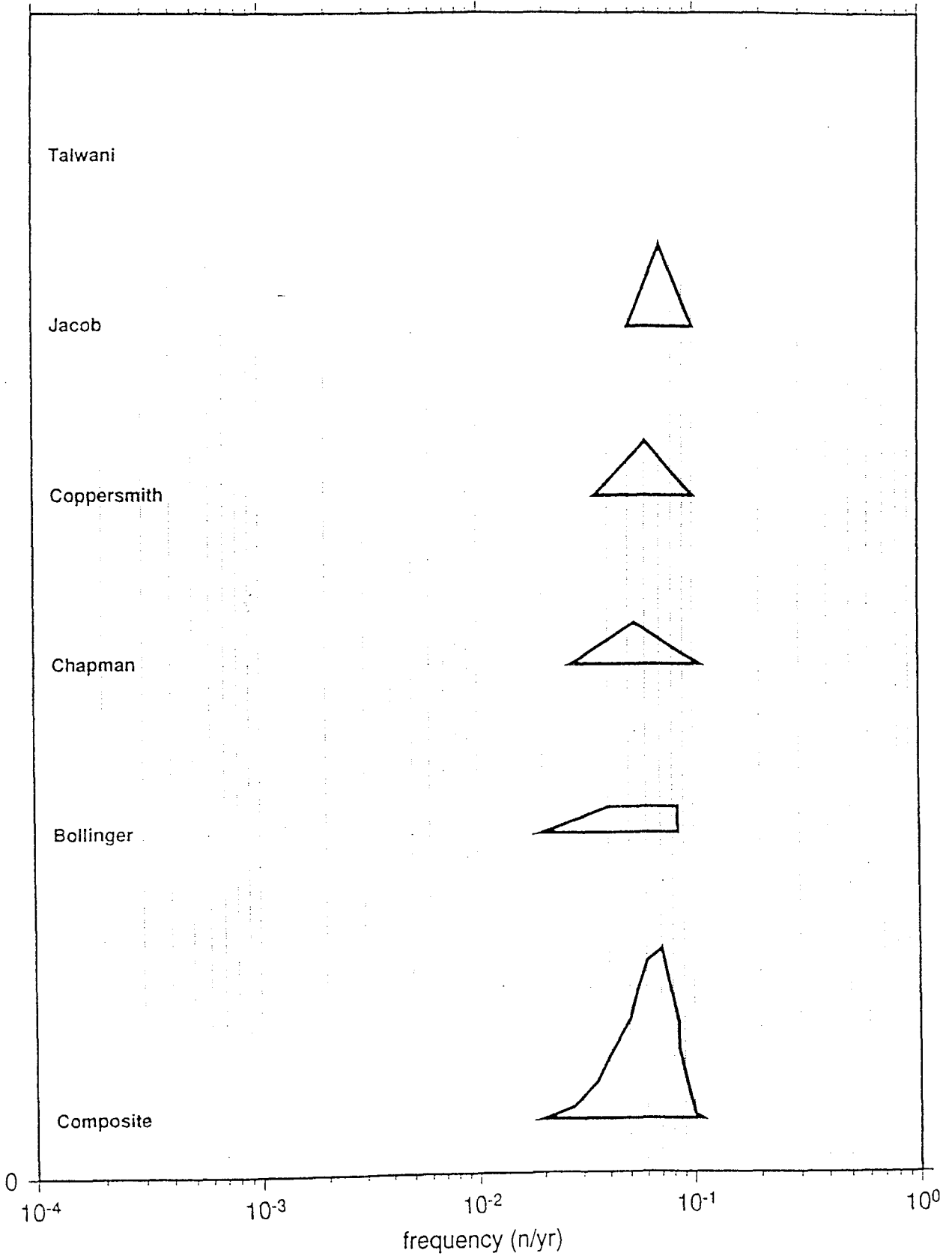
M_U ; ZONE 8



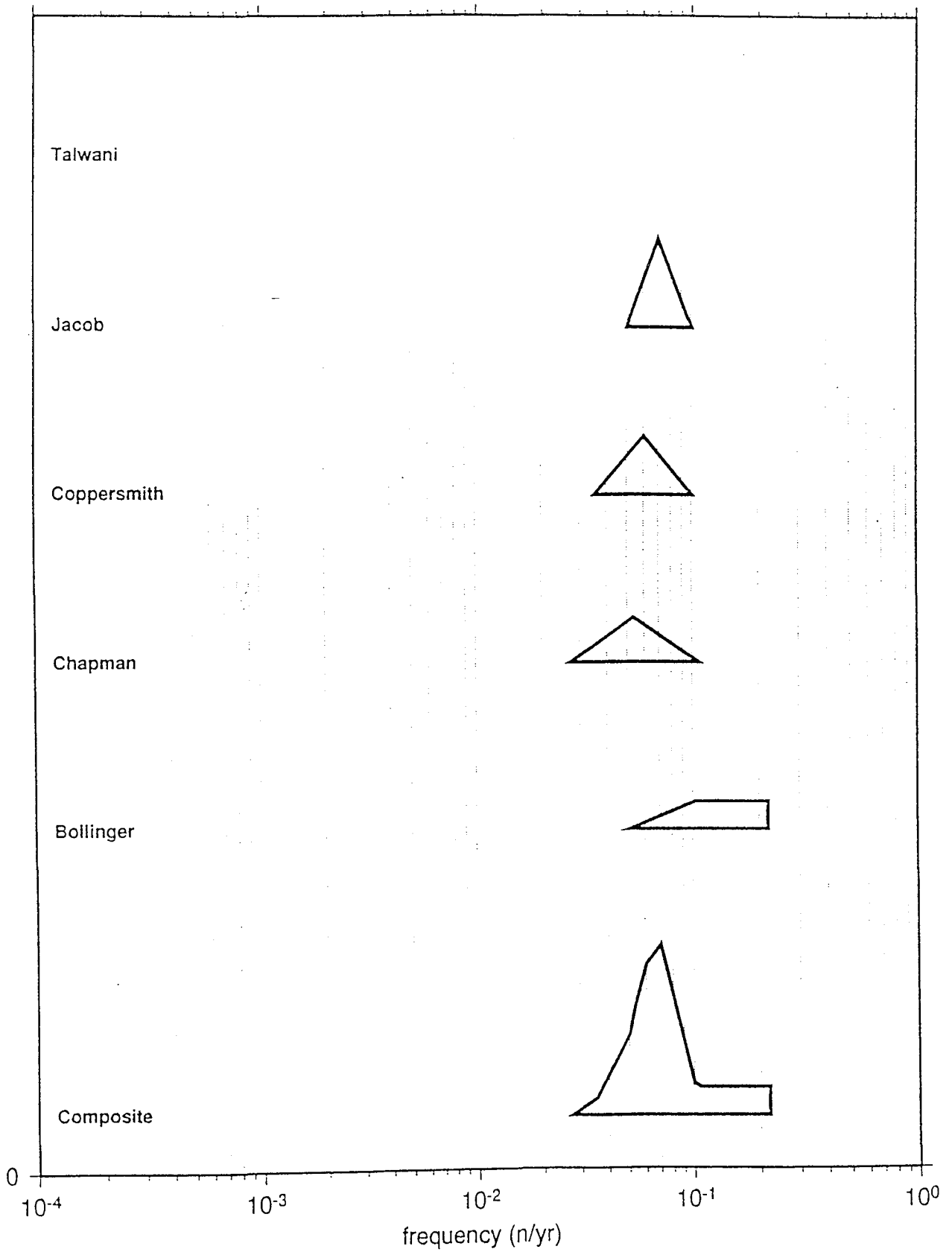
FREQUENCY at M4 ; ZONE 1a



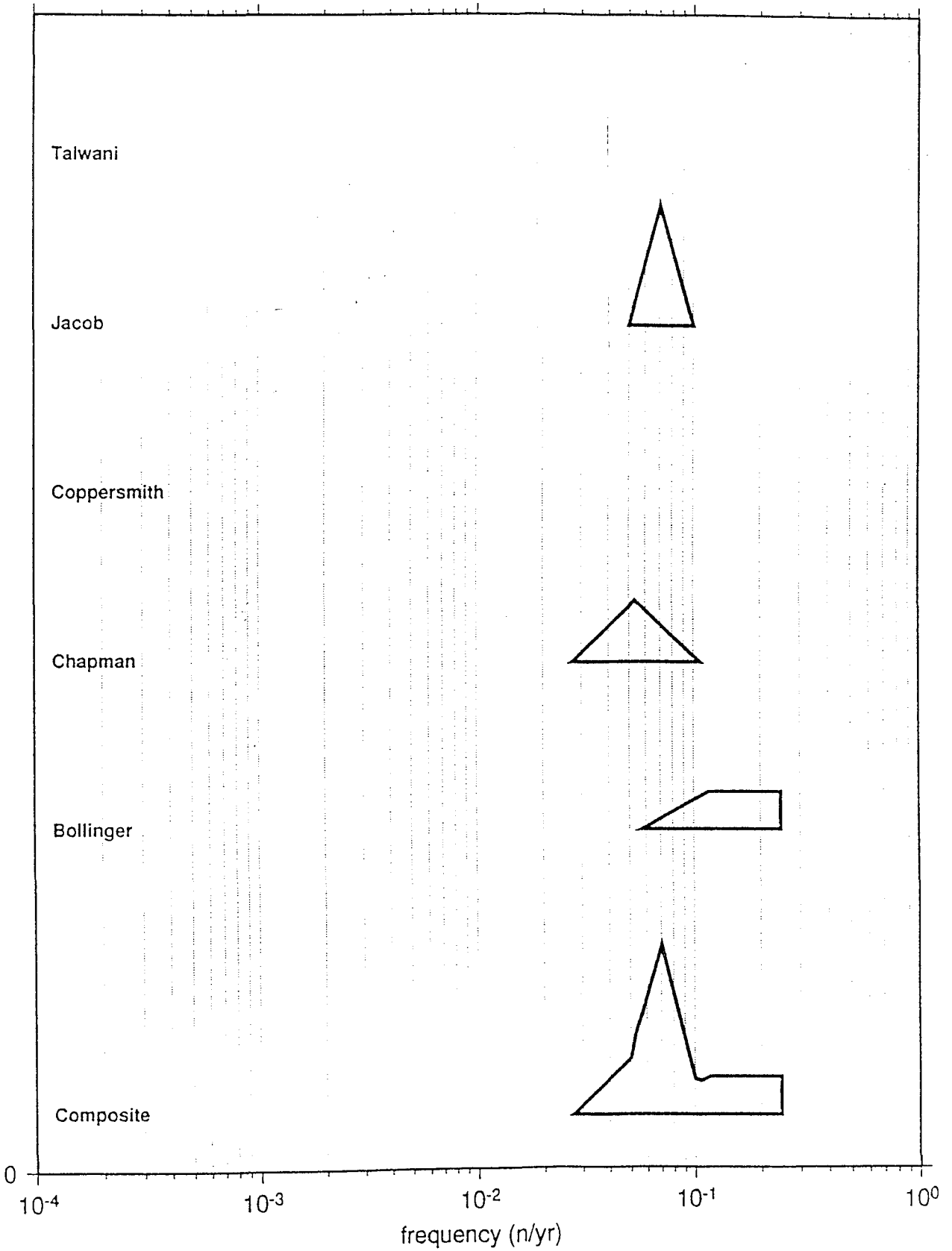
FREQUENCY at M4 ; ZONE 1b



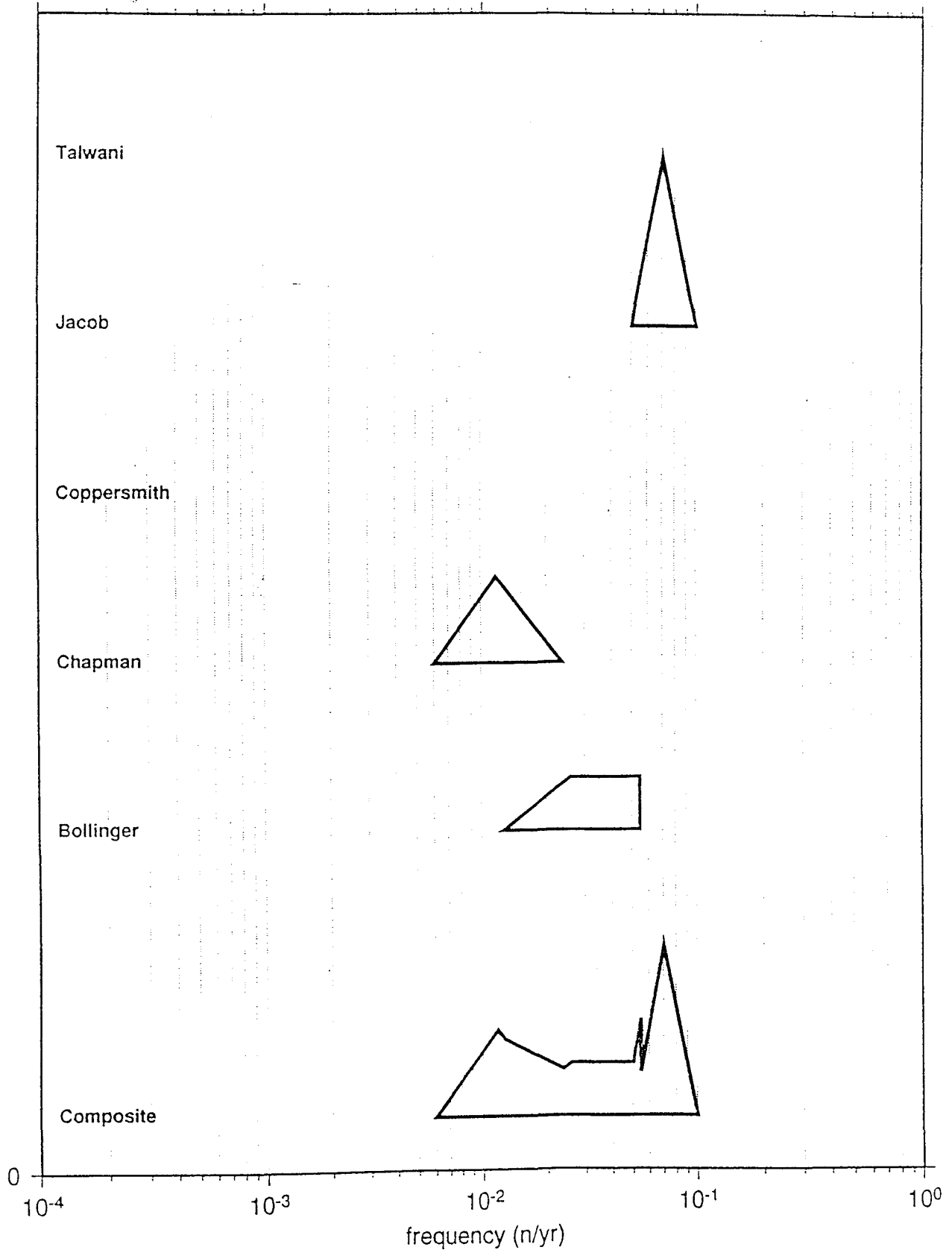
FREQUENCY at M4 ; ZONE 1c



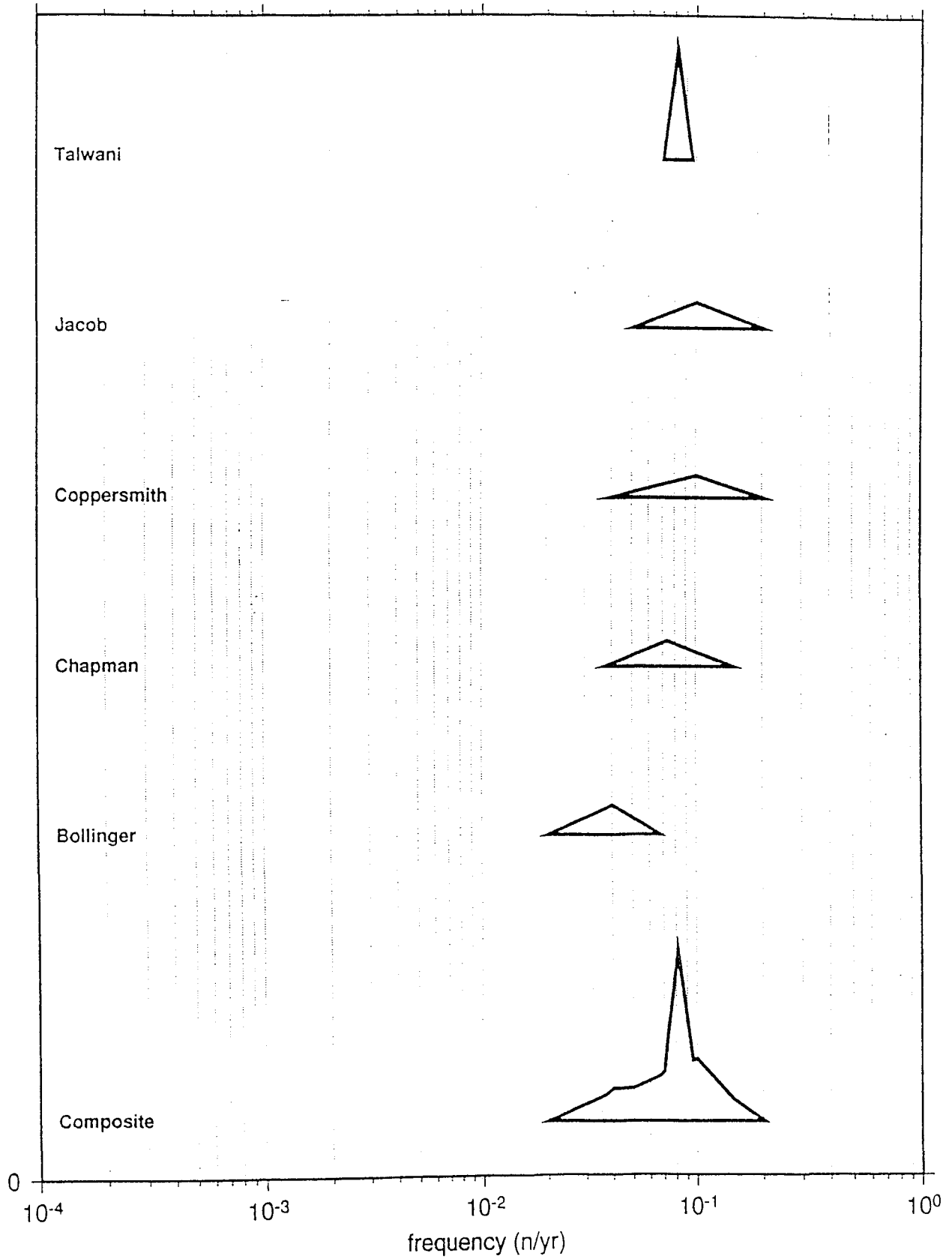
FREQUENCY at M4 ; ZONE 1d



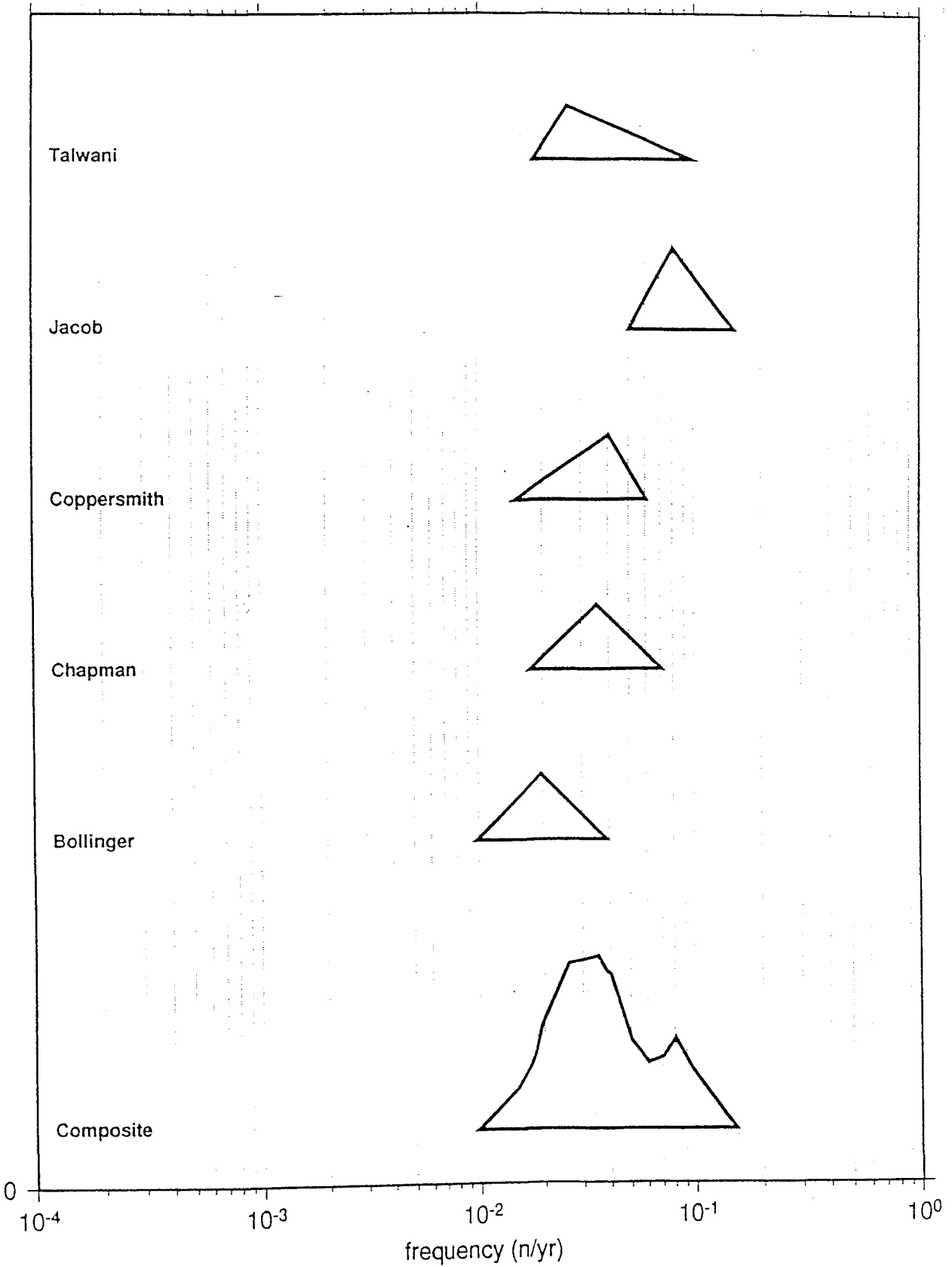
FREQUENCY at M4 ; ZONE 1e



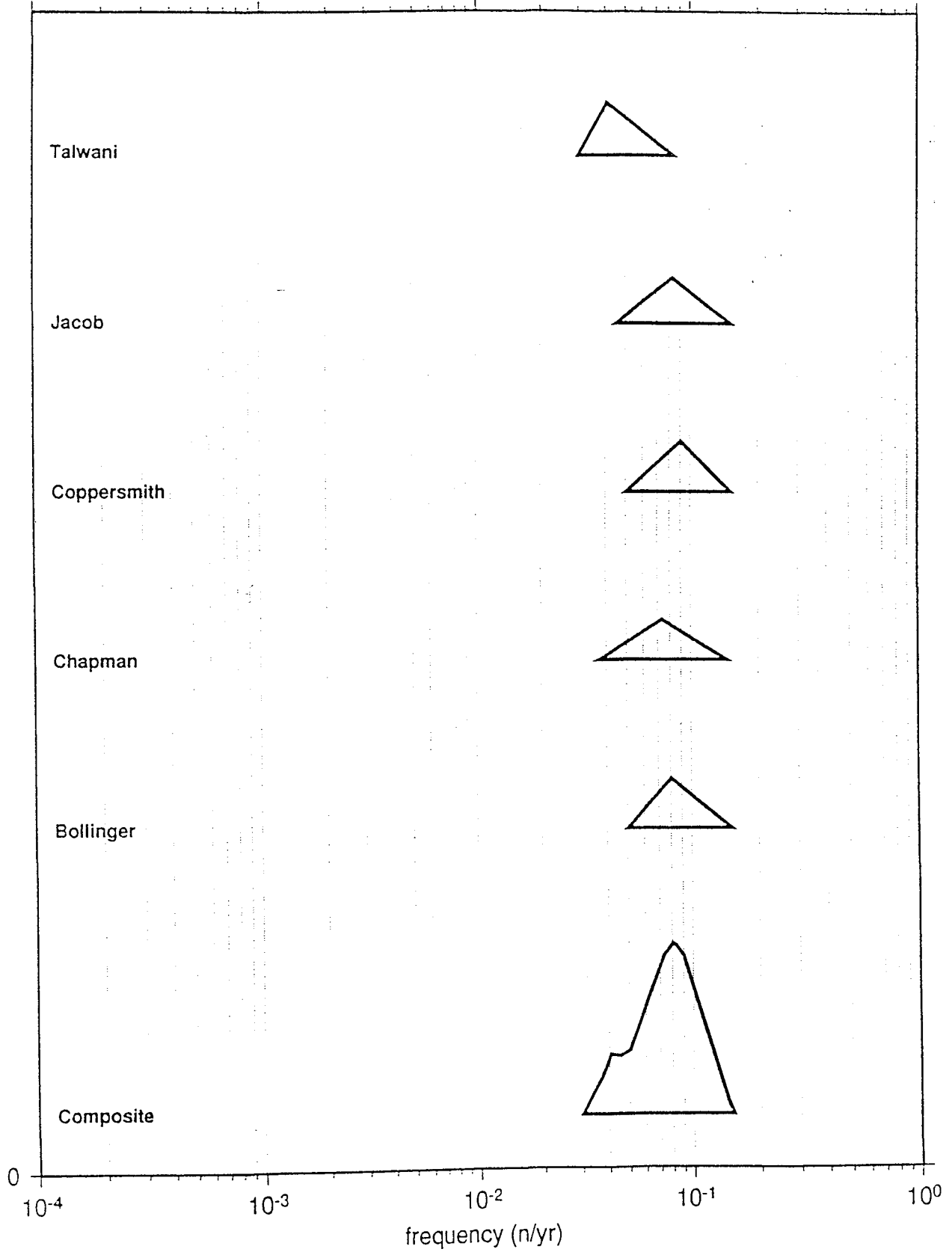
FREQUENCY at M4 ; ZONE 3a



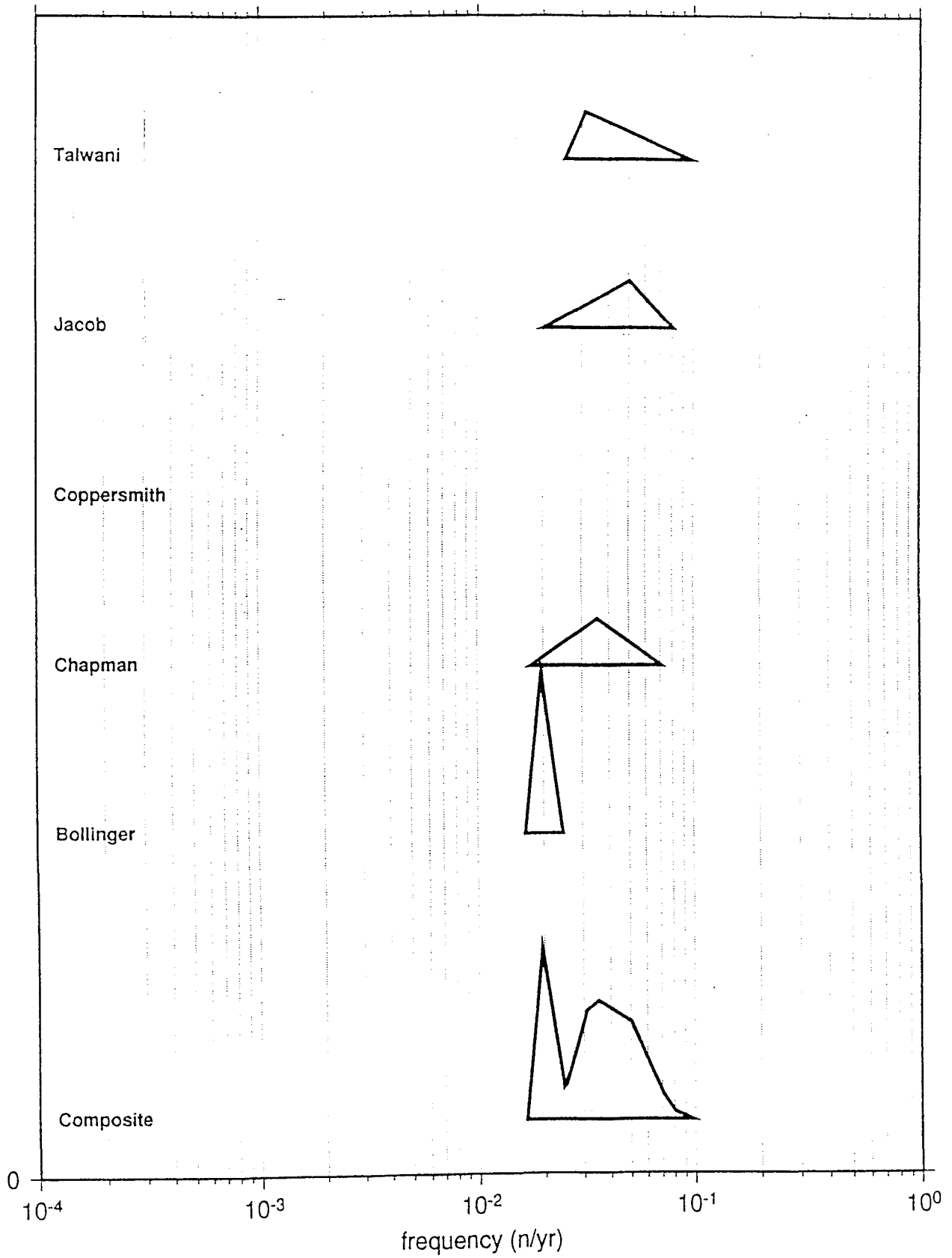
FREQUENCY at M4 ; ZONE 3b-3a



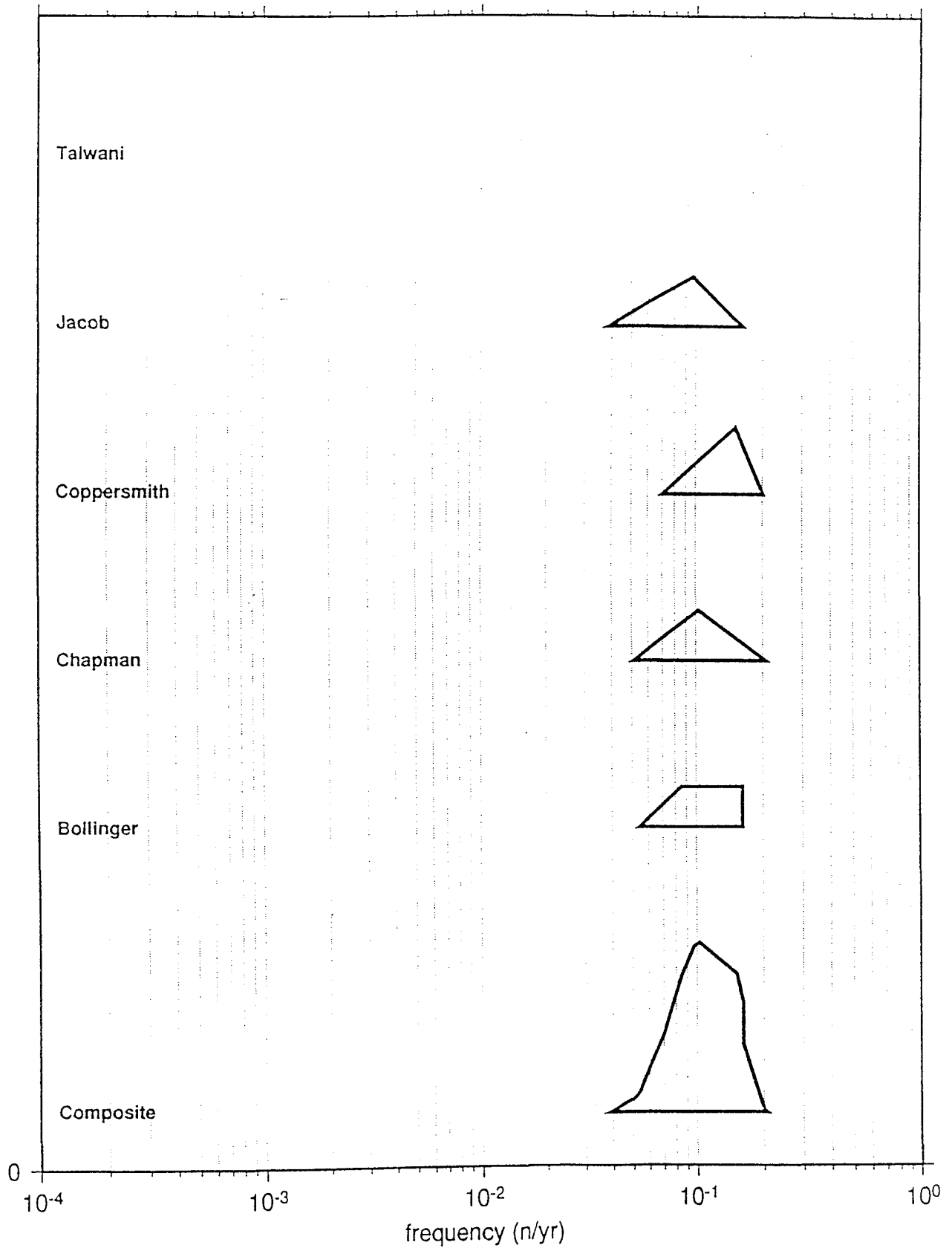
FREQUENCY at M4 ; ZONE 3c



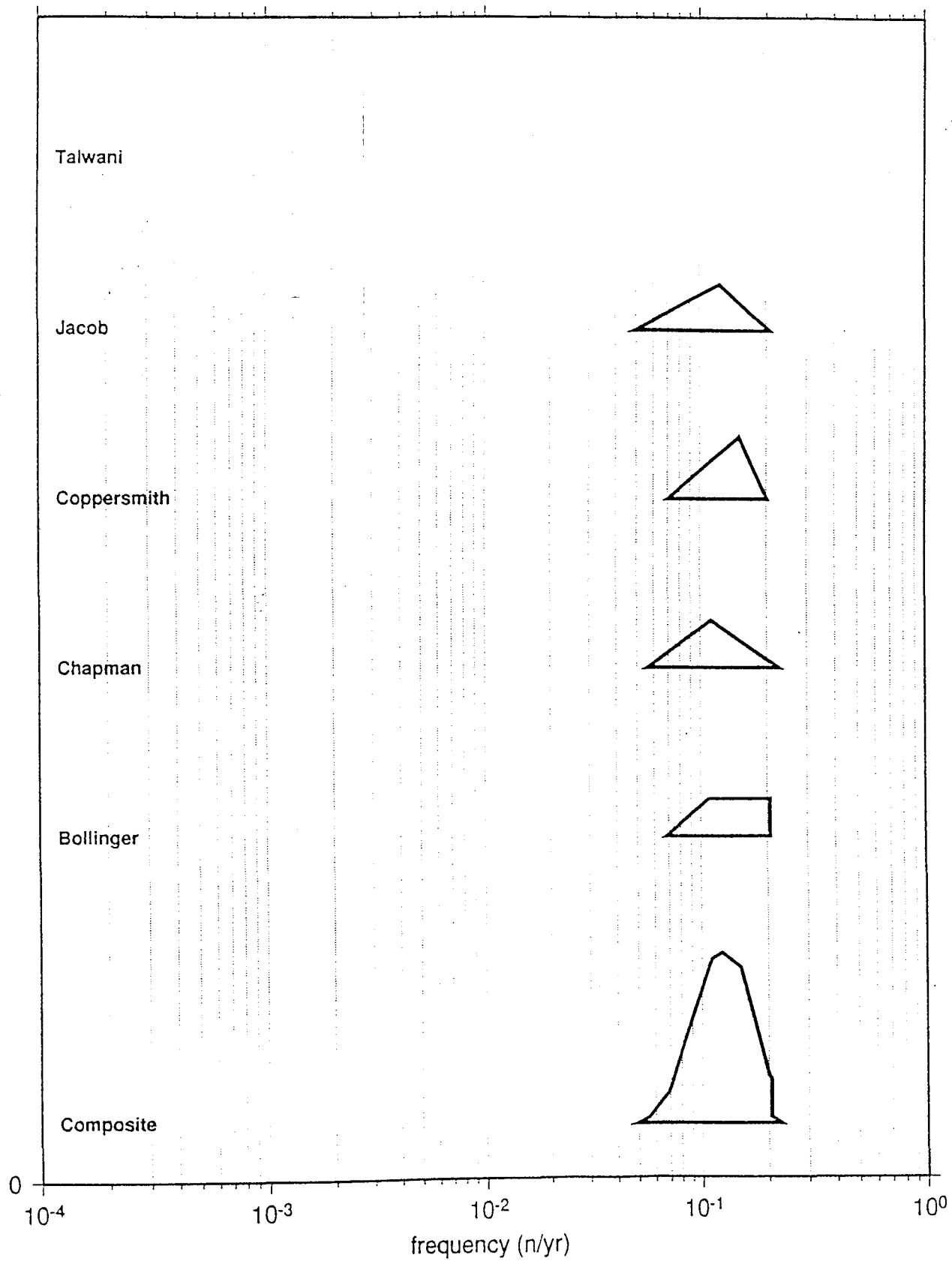
FREQUENCY at M4 ; ZONE 3b-3c



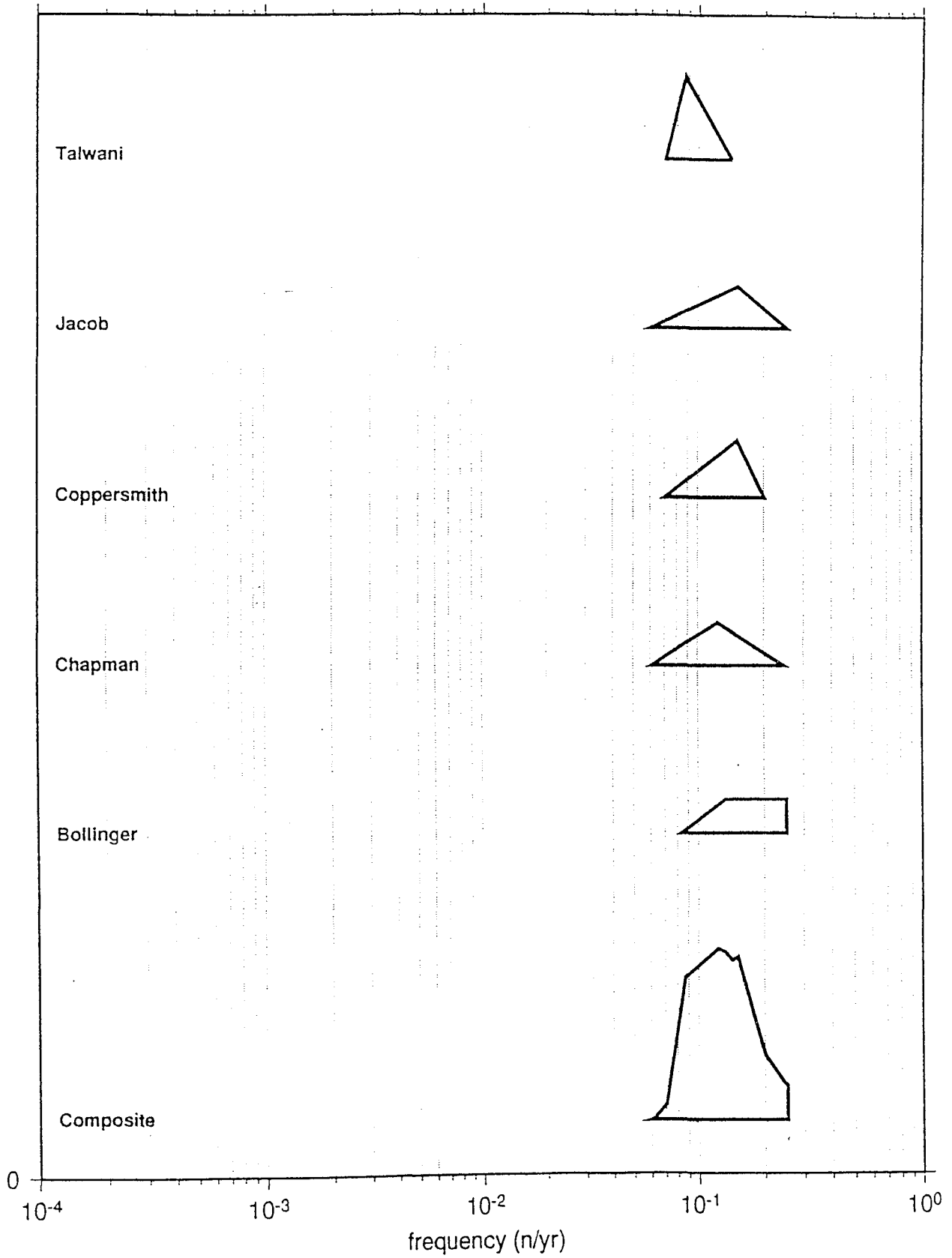
FREQUENCY at M4 ; ZONE 4a1



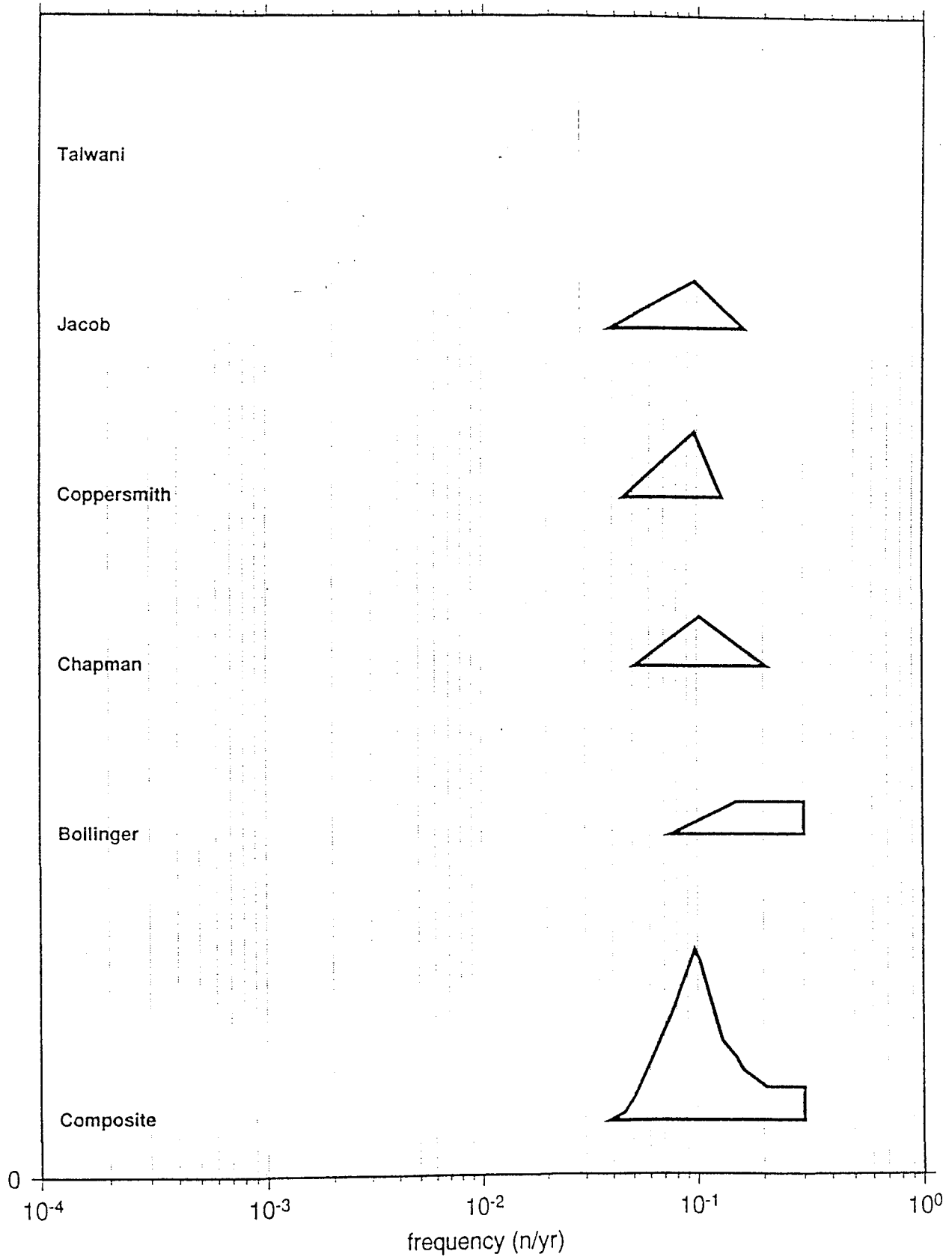
FREQUENCY at M4 ; ZONE 4a1+2



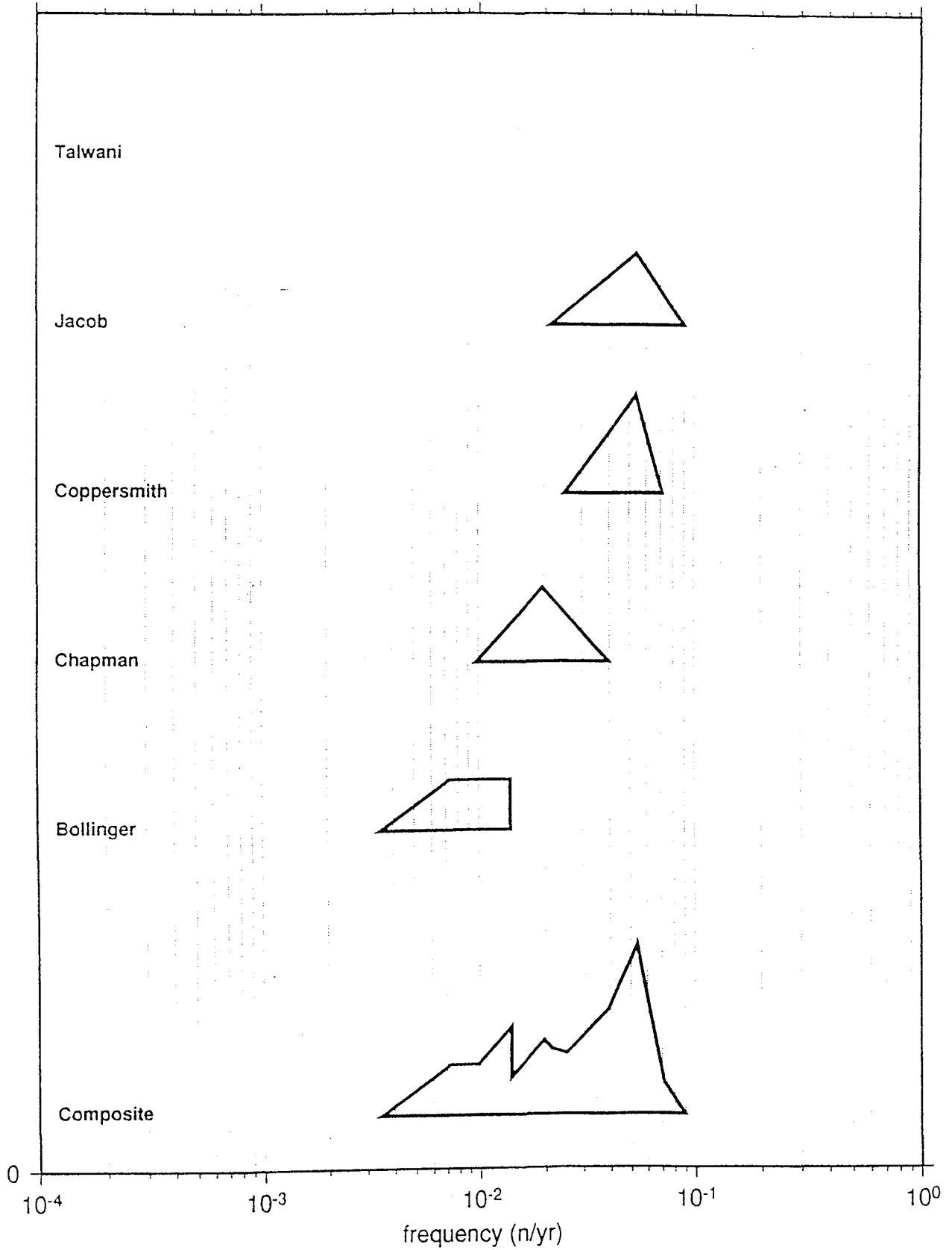
FREQUENCY at M4 ; ZONE 4a1+2+3



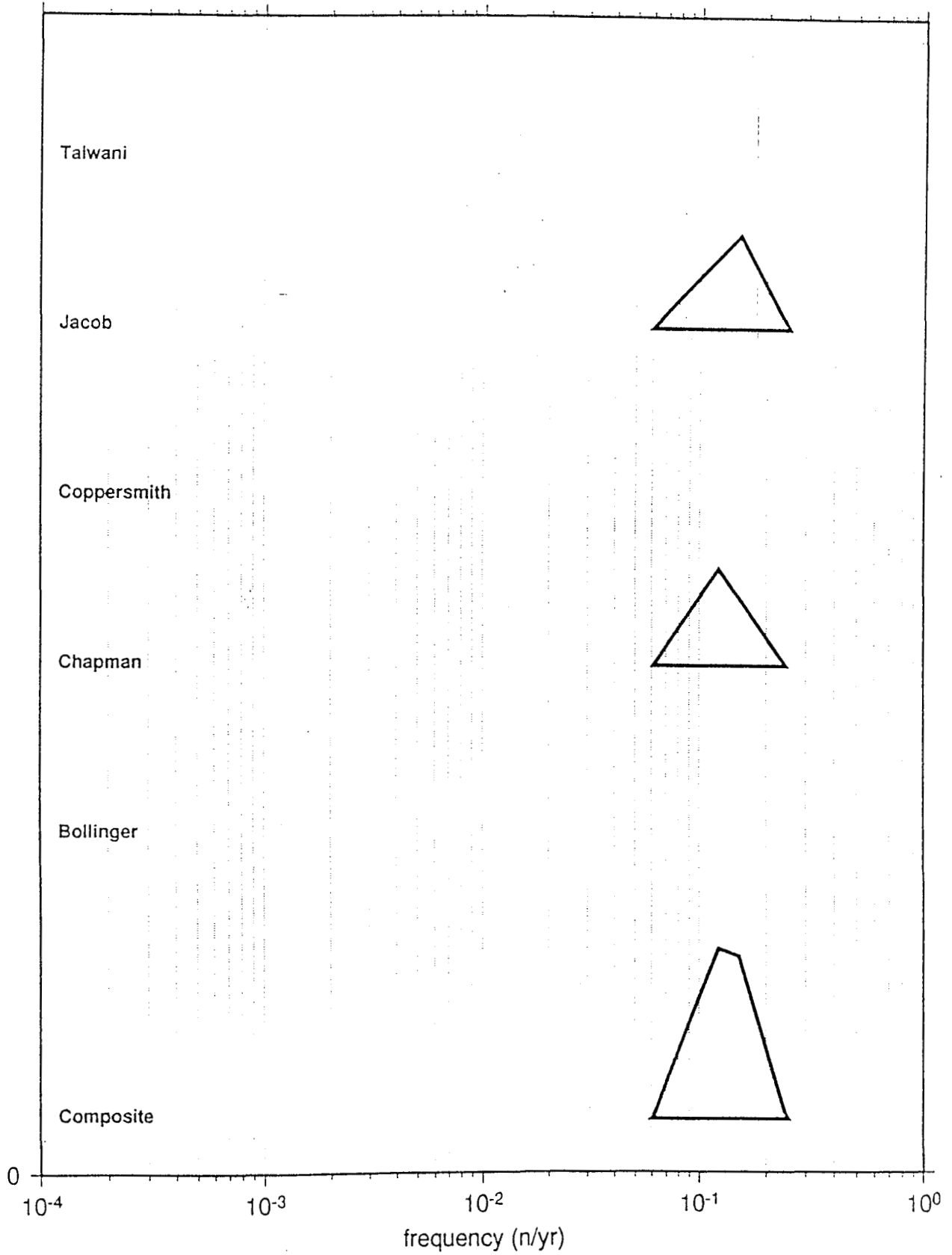
FREQUENCY at M4 ; ZONE 4b1



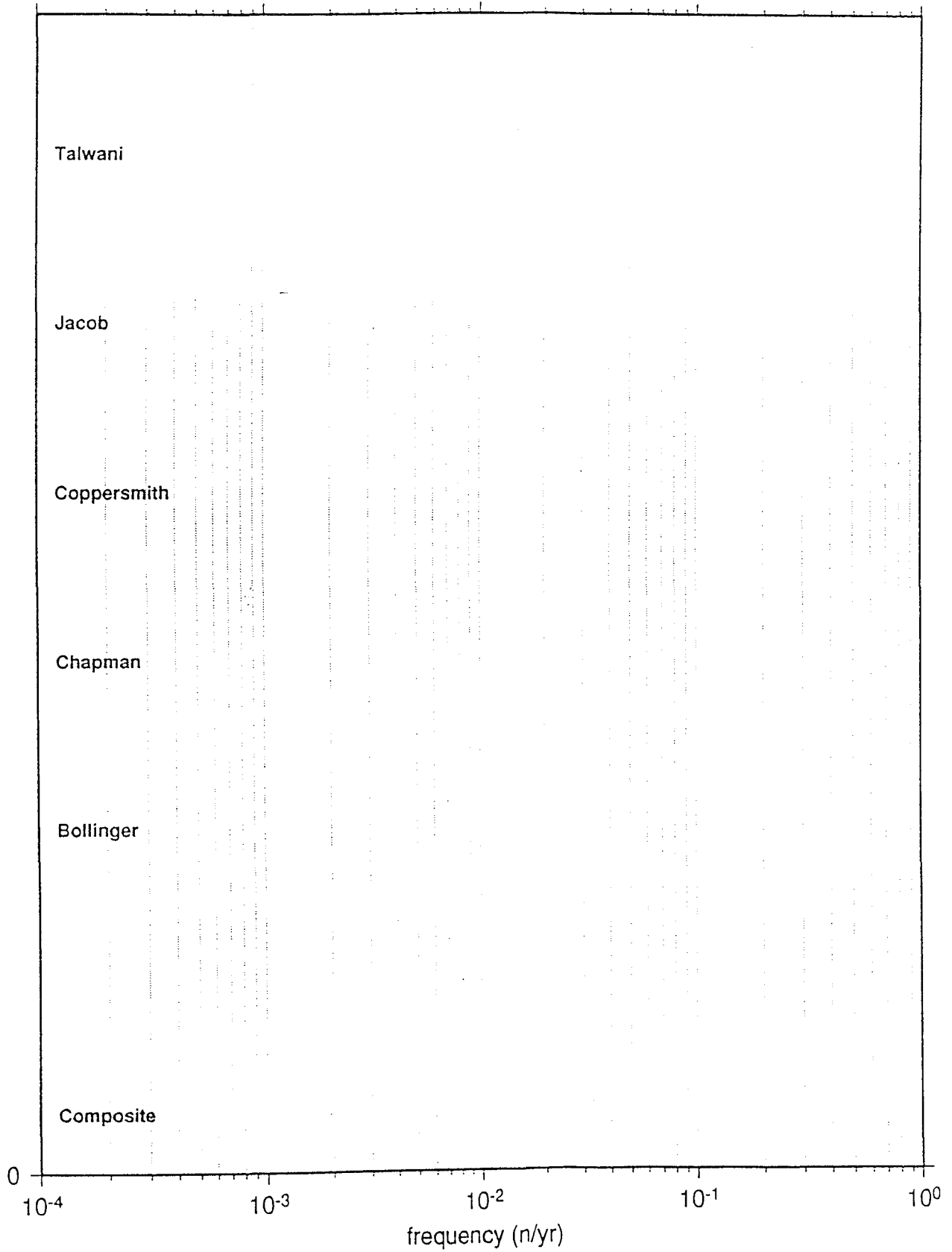
FREQUENCY at M4 ; ZONE 4b2



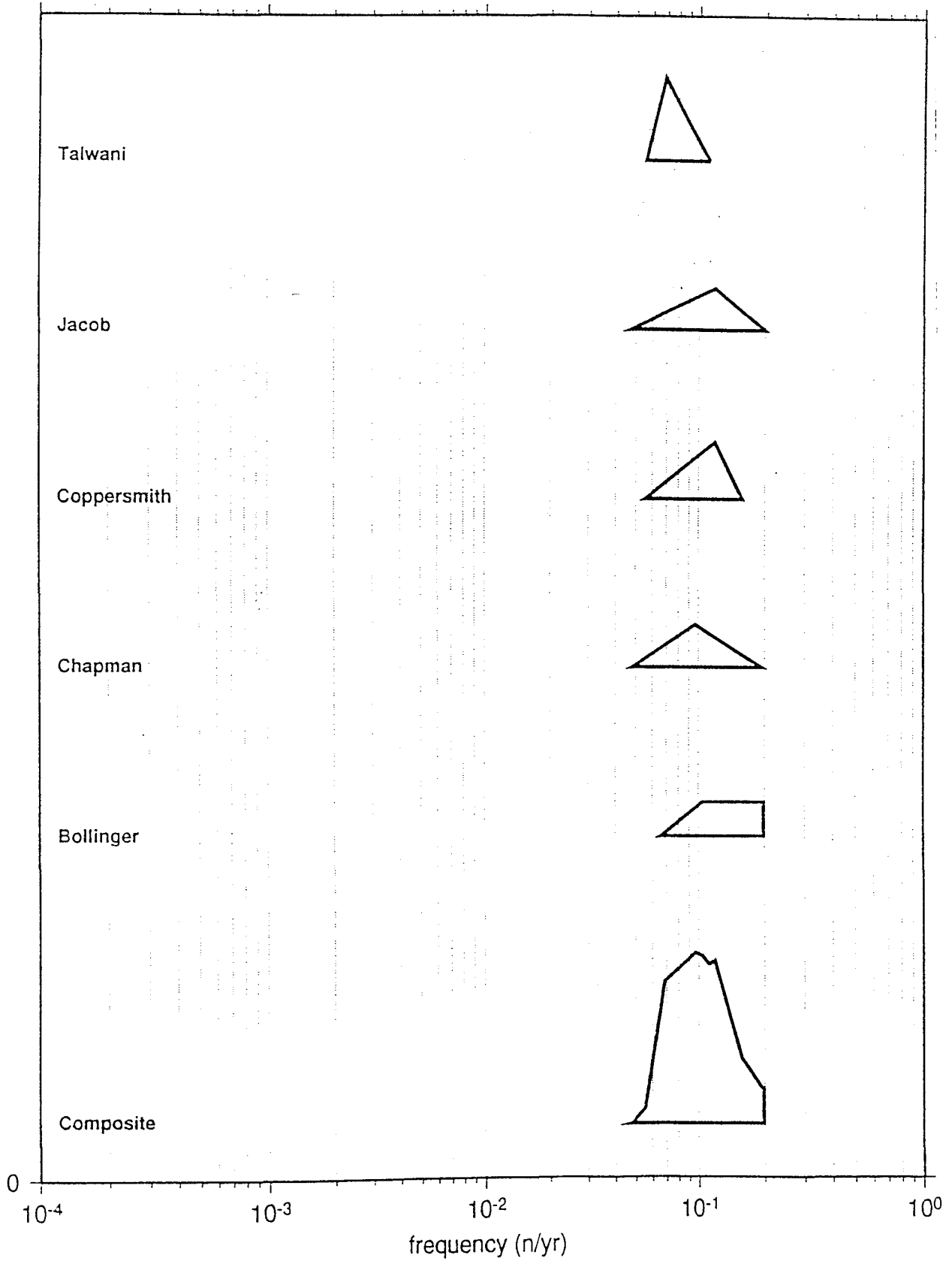
FREQUENCY at M4 ; ZONE 4c



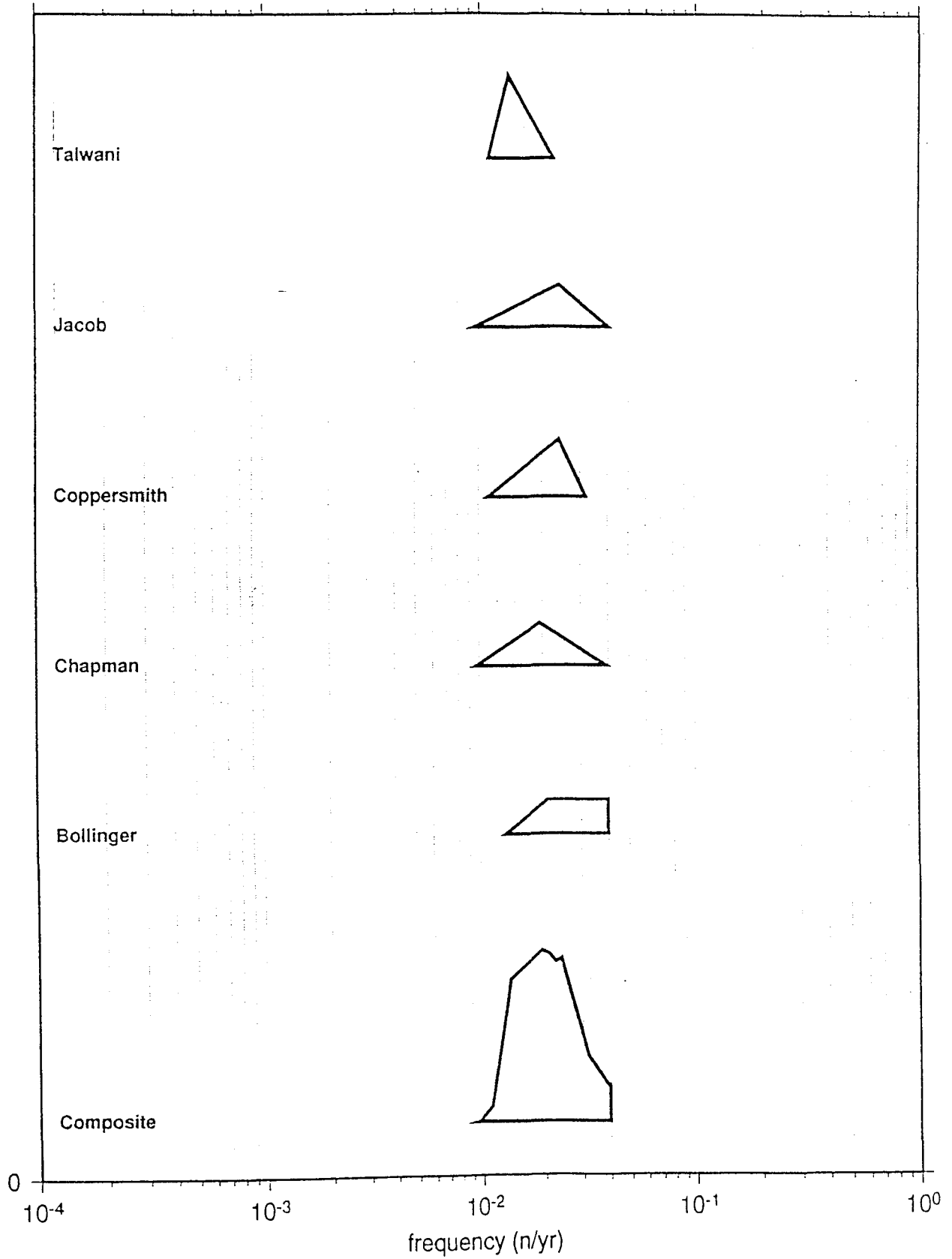
FREQUENCY at M4 ; ZONE 4d



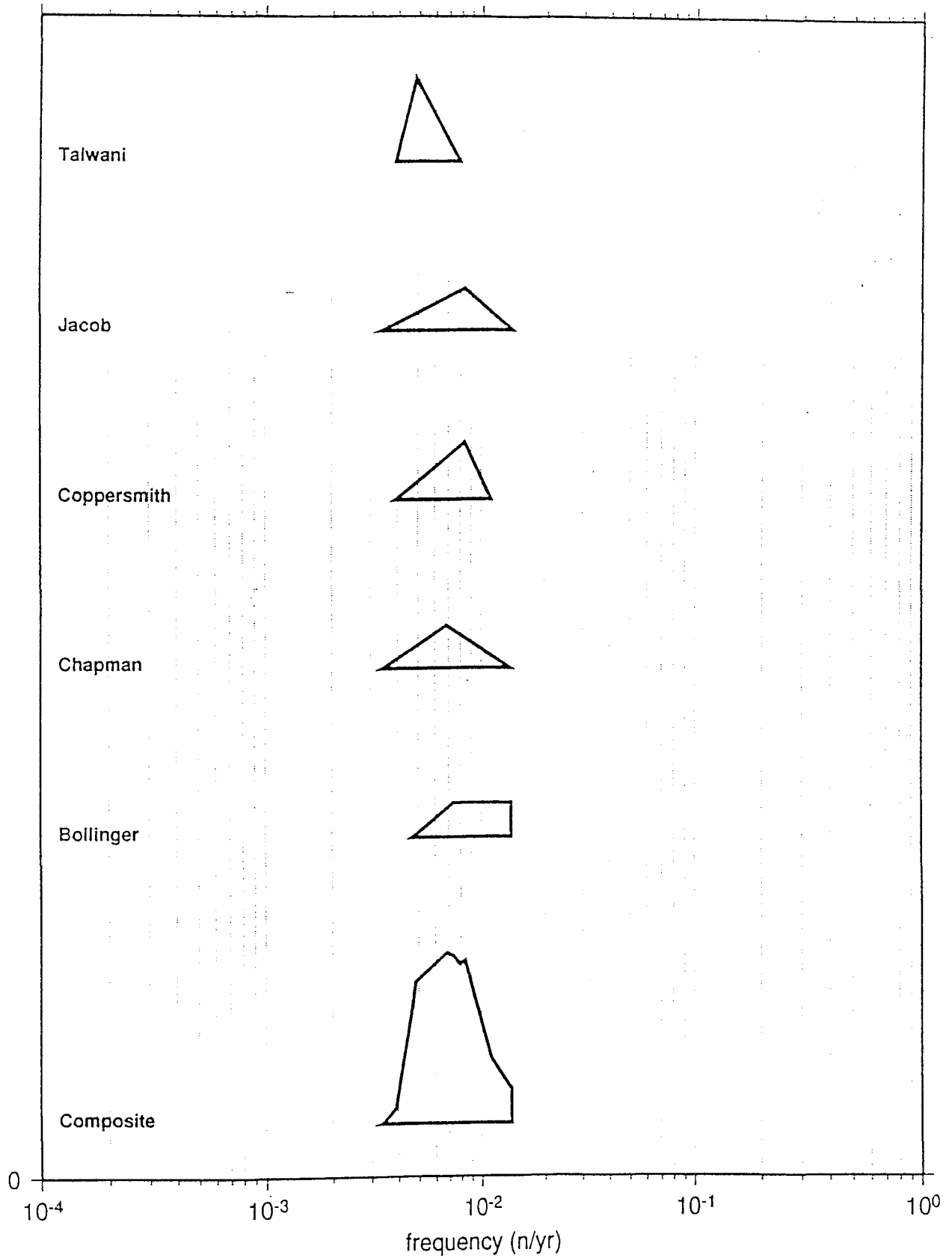
FREQUENCY at M4 ; ZONE 4e1



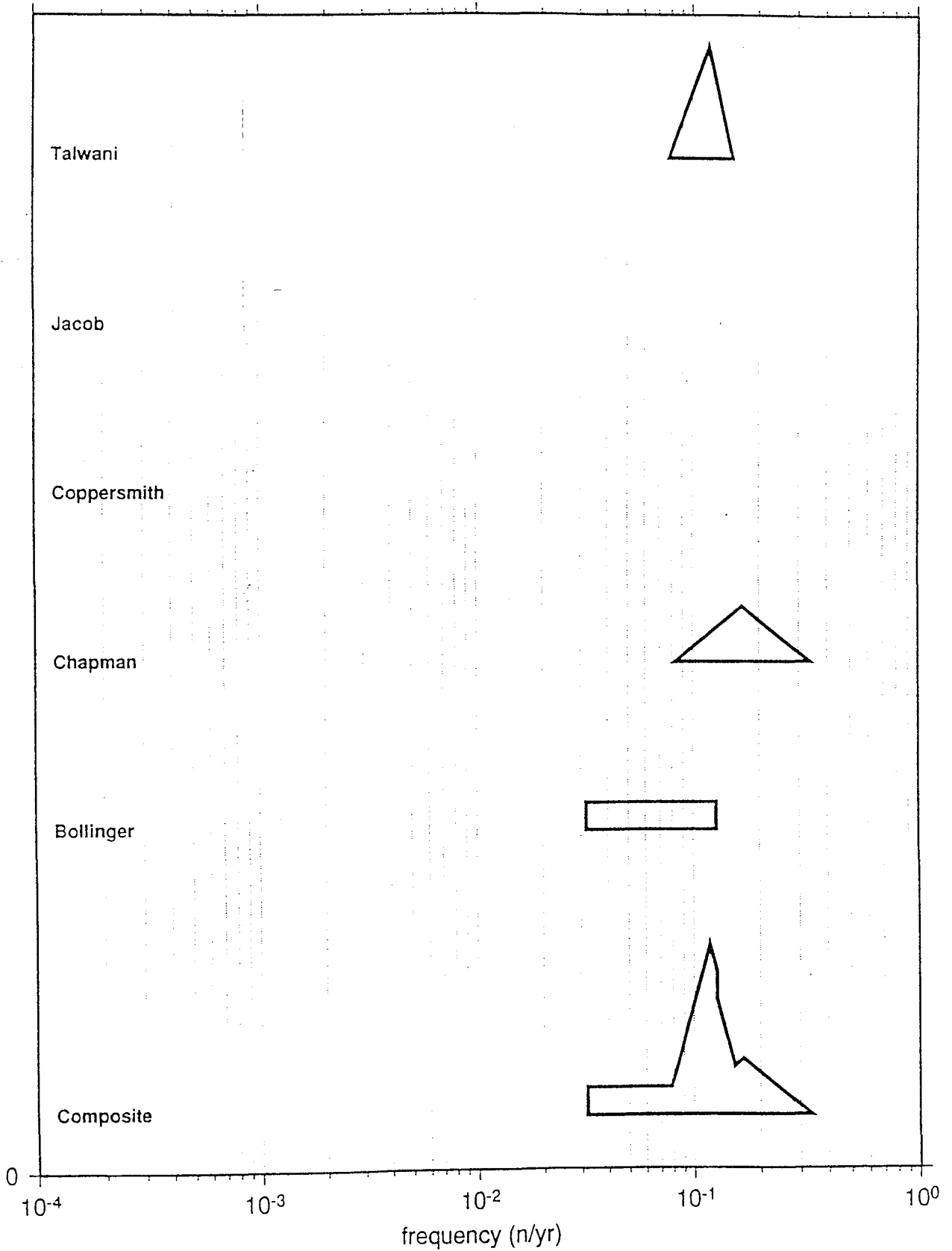
FREQUENCY at M4 ; ZONE 4e2



FREQUENCY at M4 ; ZONE 4e3

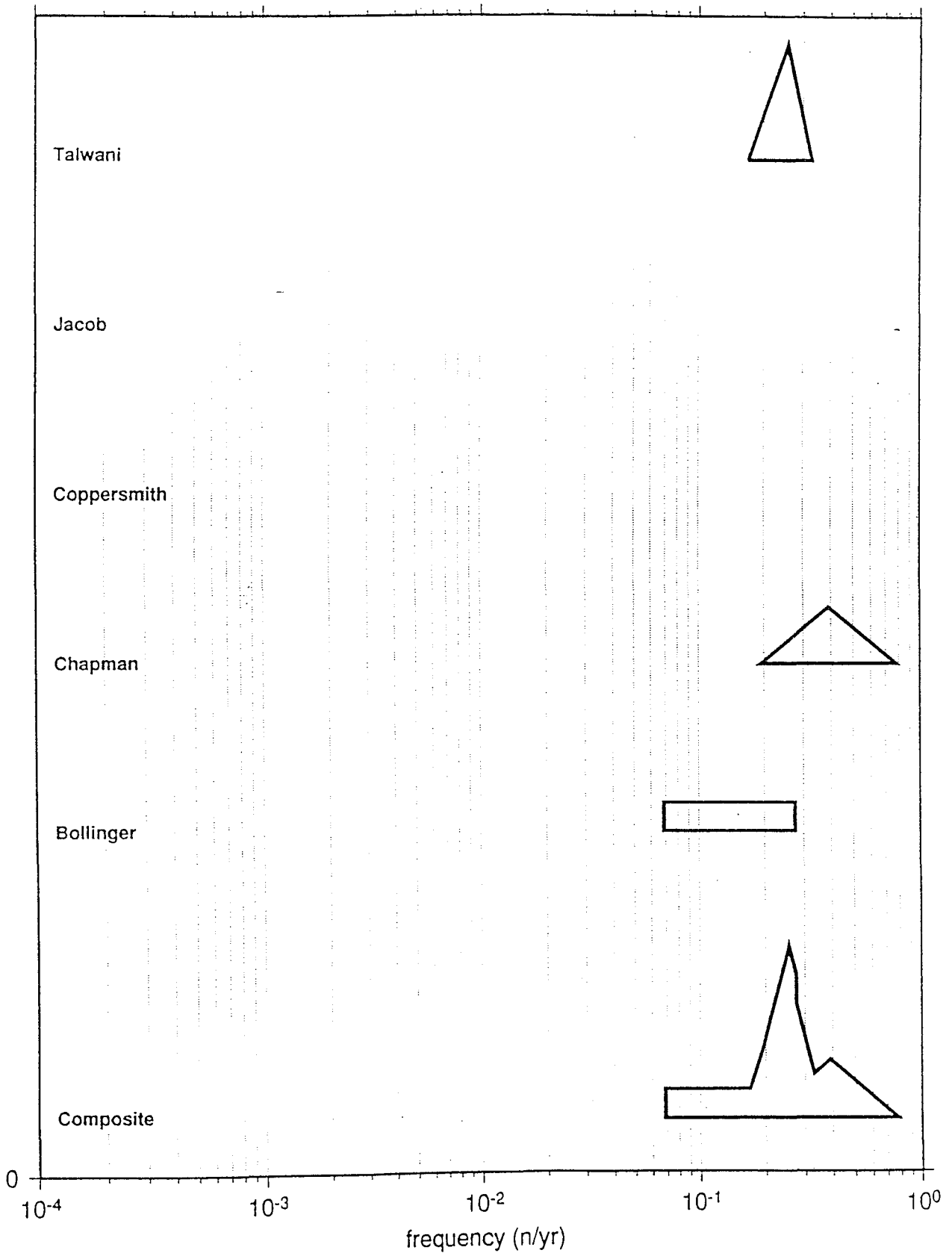


FREQUENCY at M4 ; ZONE 5-1

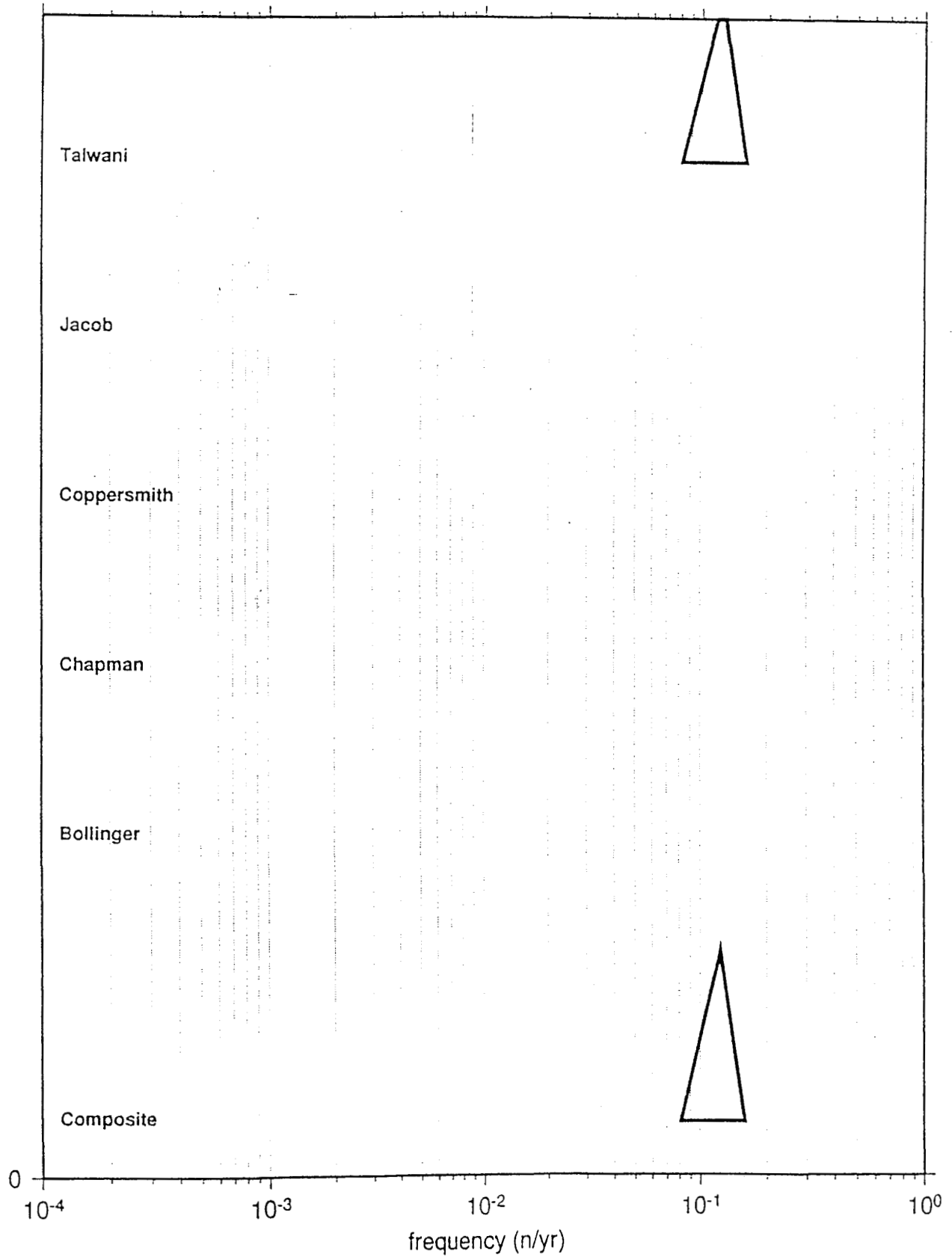


24

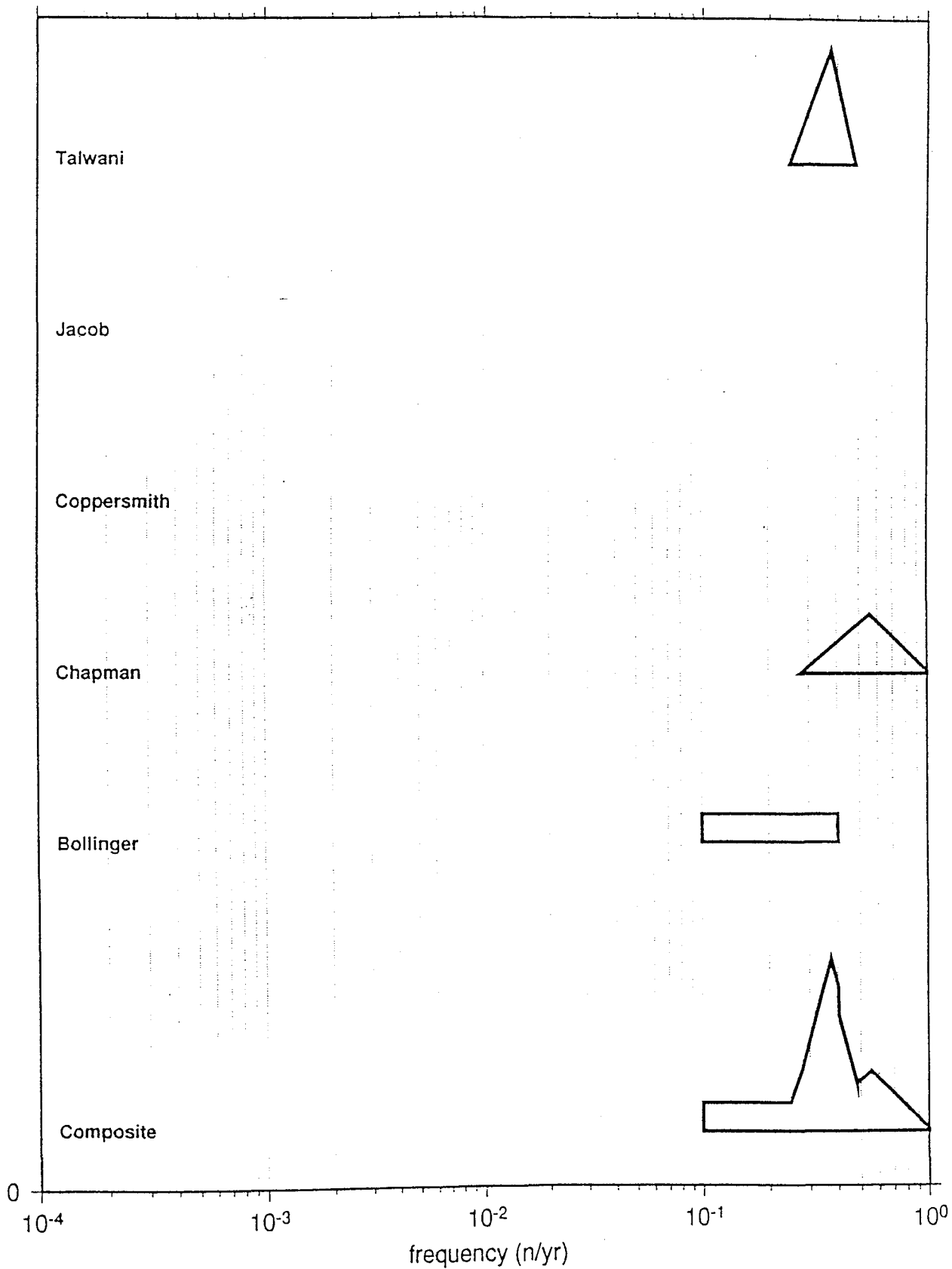
FREQUENCY at M4 ; ZONE 5-2



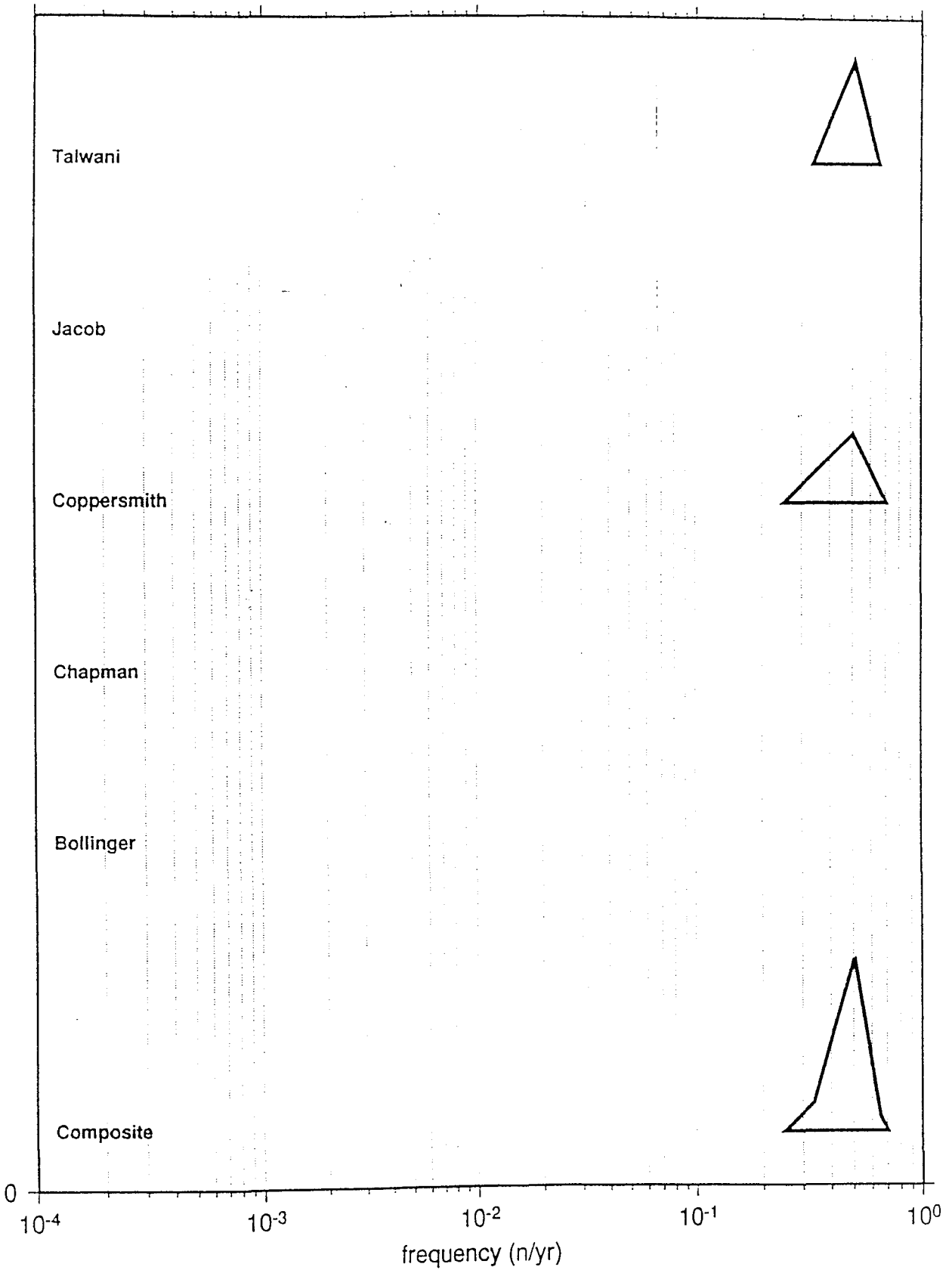
FREQUENCY at M4 ; ZONE 5-3



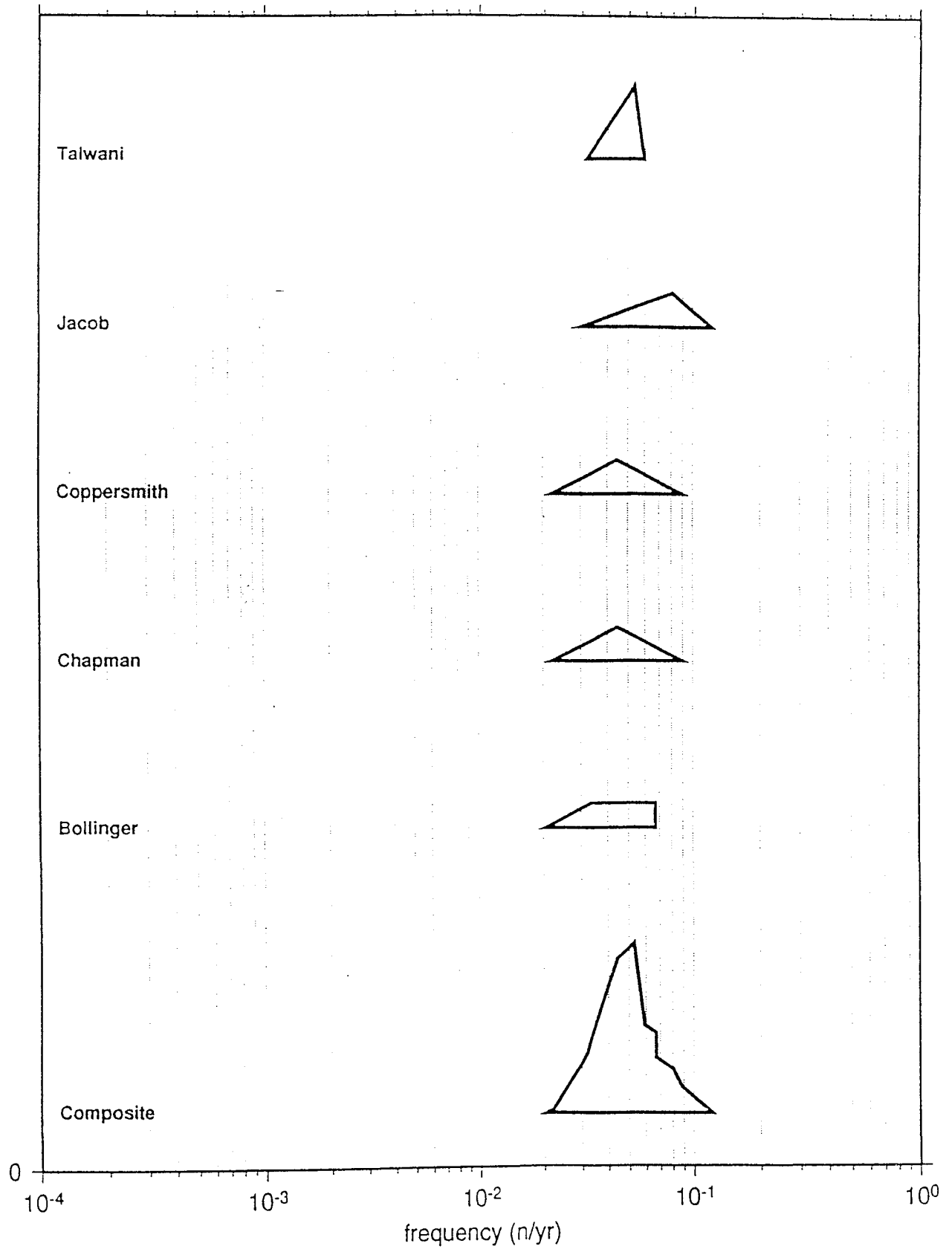
FREQUENCY at M4 ; ZONE 5-1+2



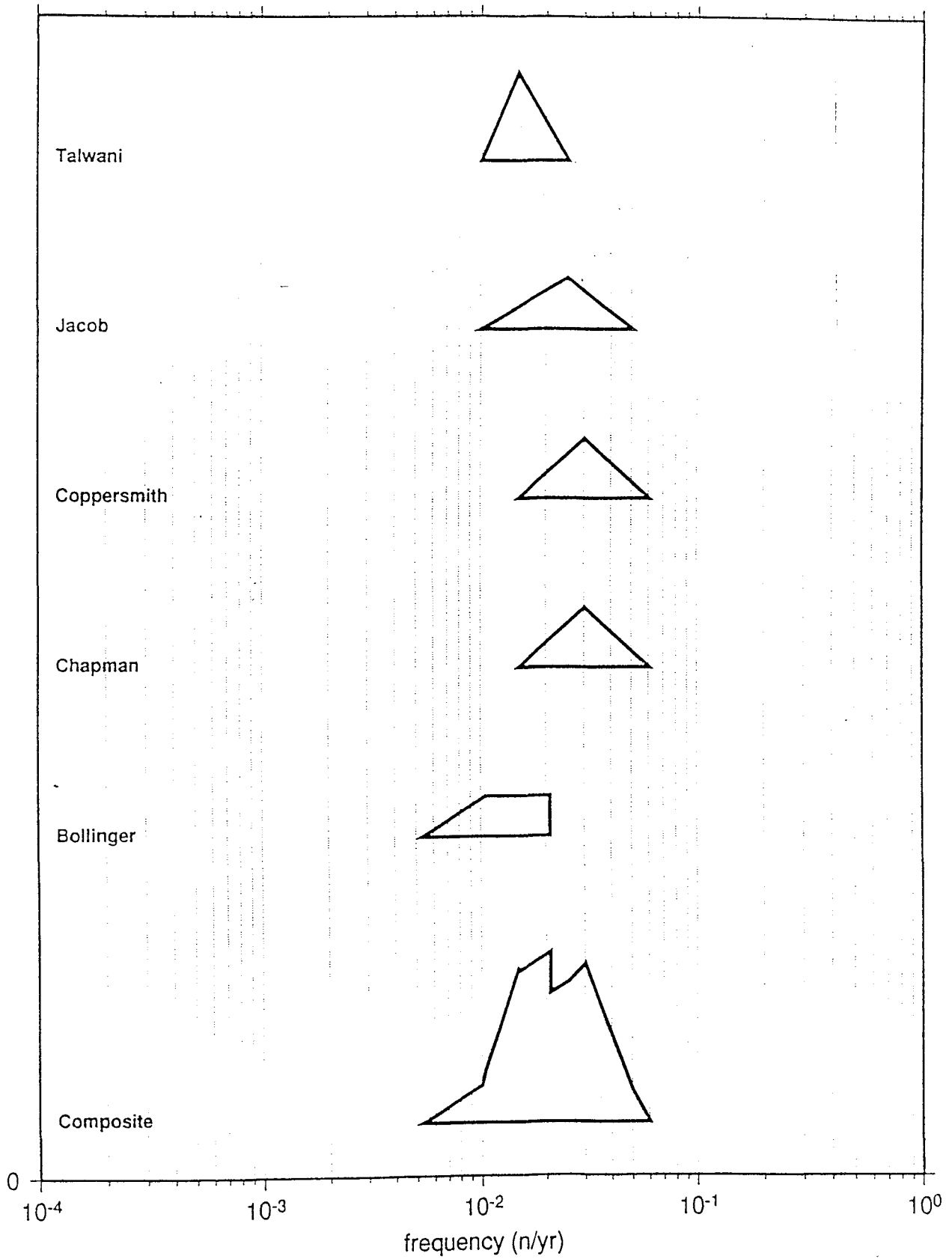
FREQUENCY at M4 ; ZONE 5-1+2+3



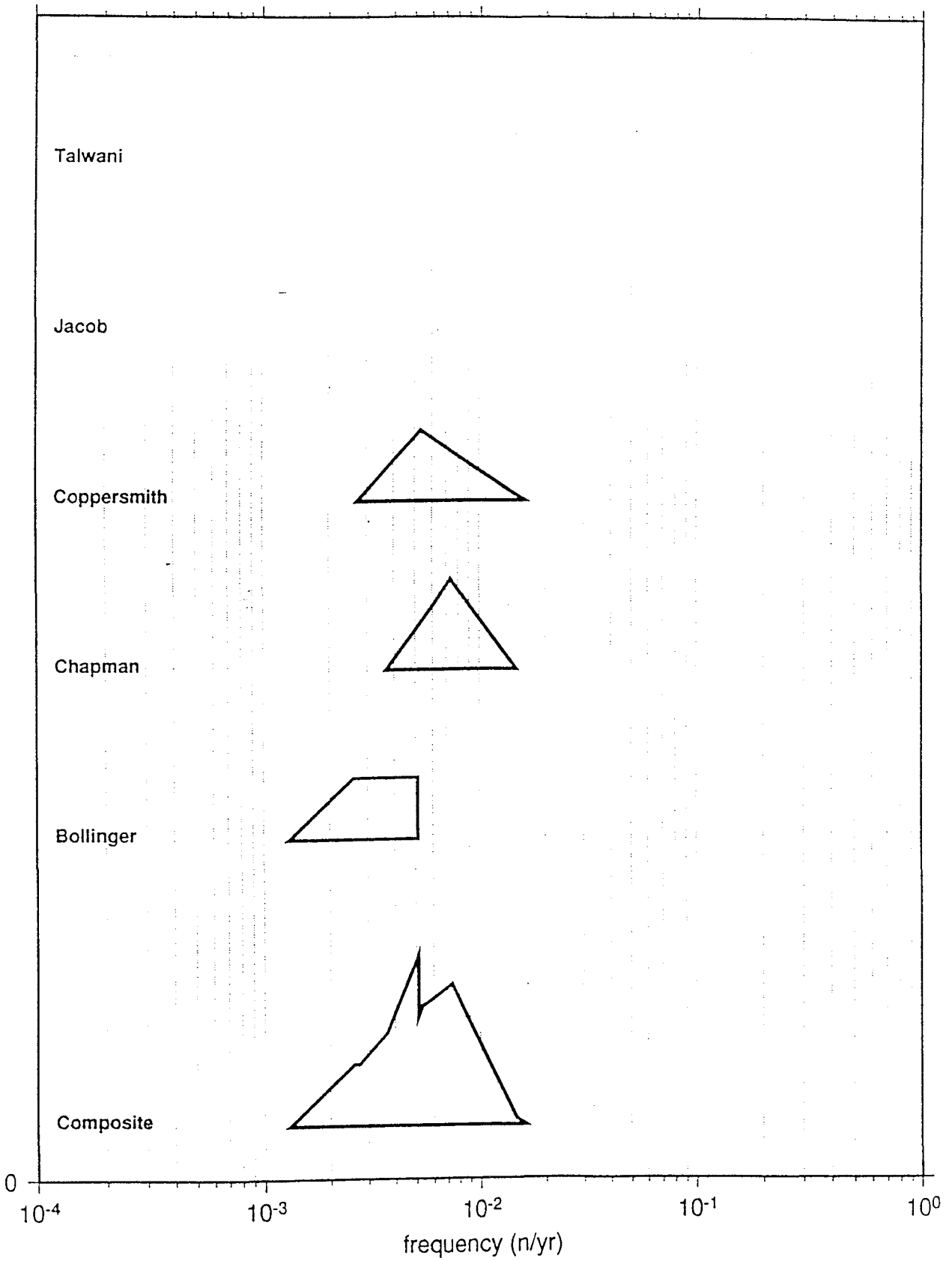
FREQUENCY at M4 ; ZONE 6



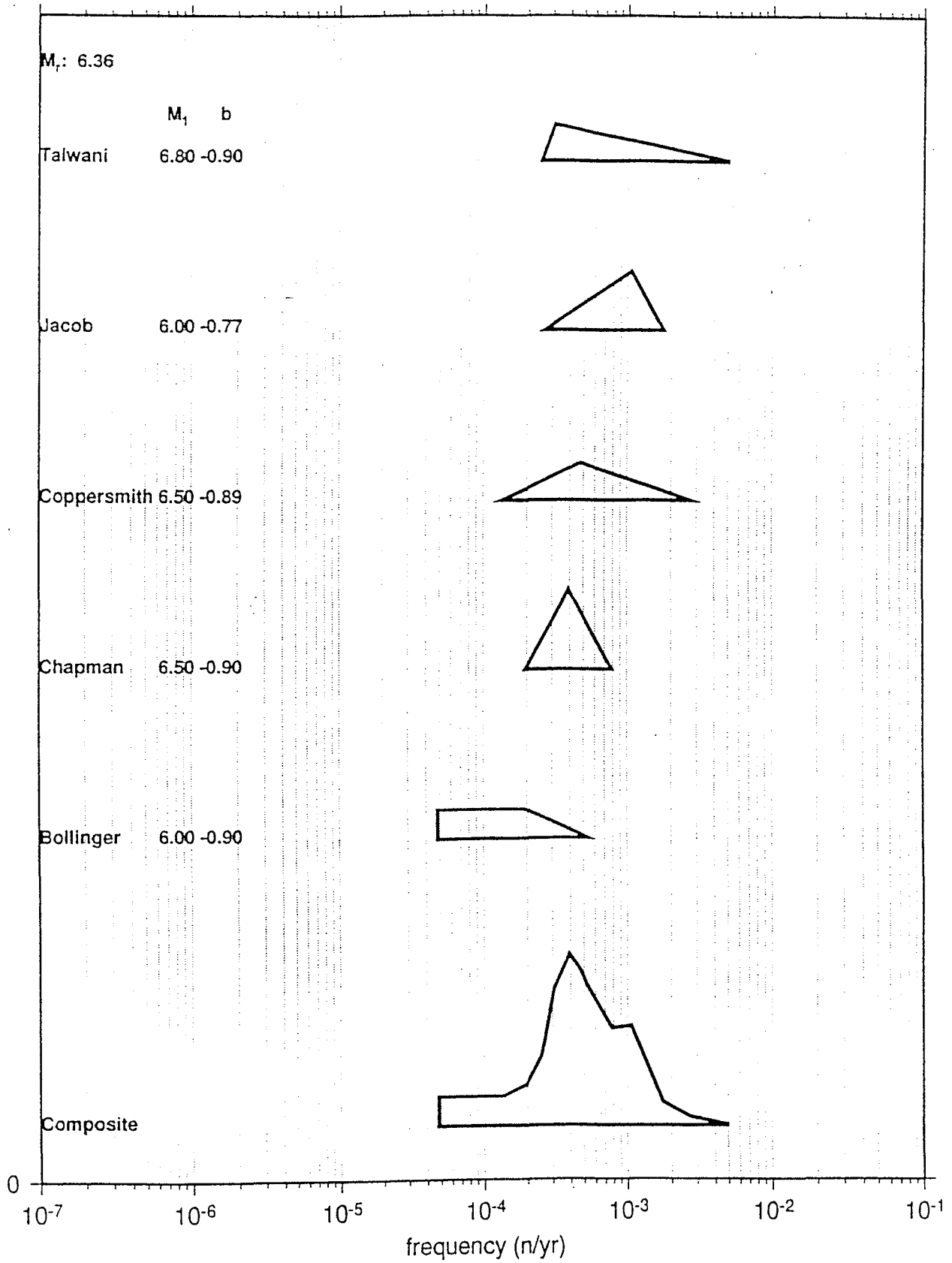
FREQUENCY at M4 ; ZONE 7



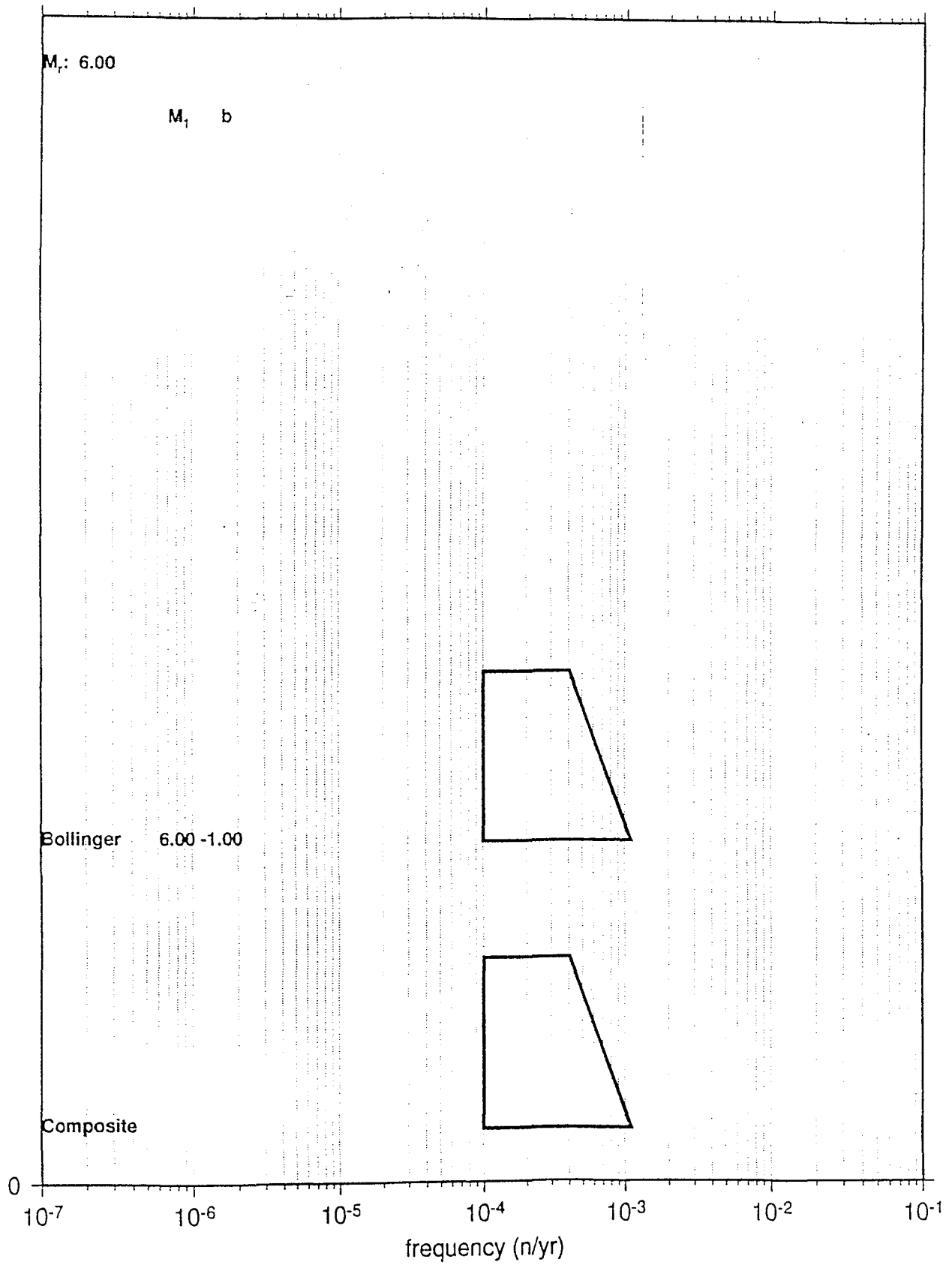
FREQUENCY at M4 ; ZONE 8



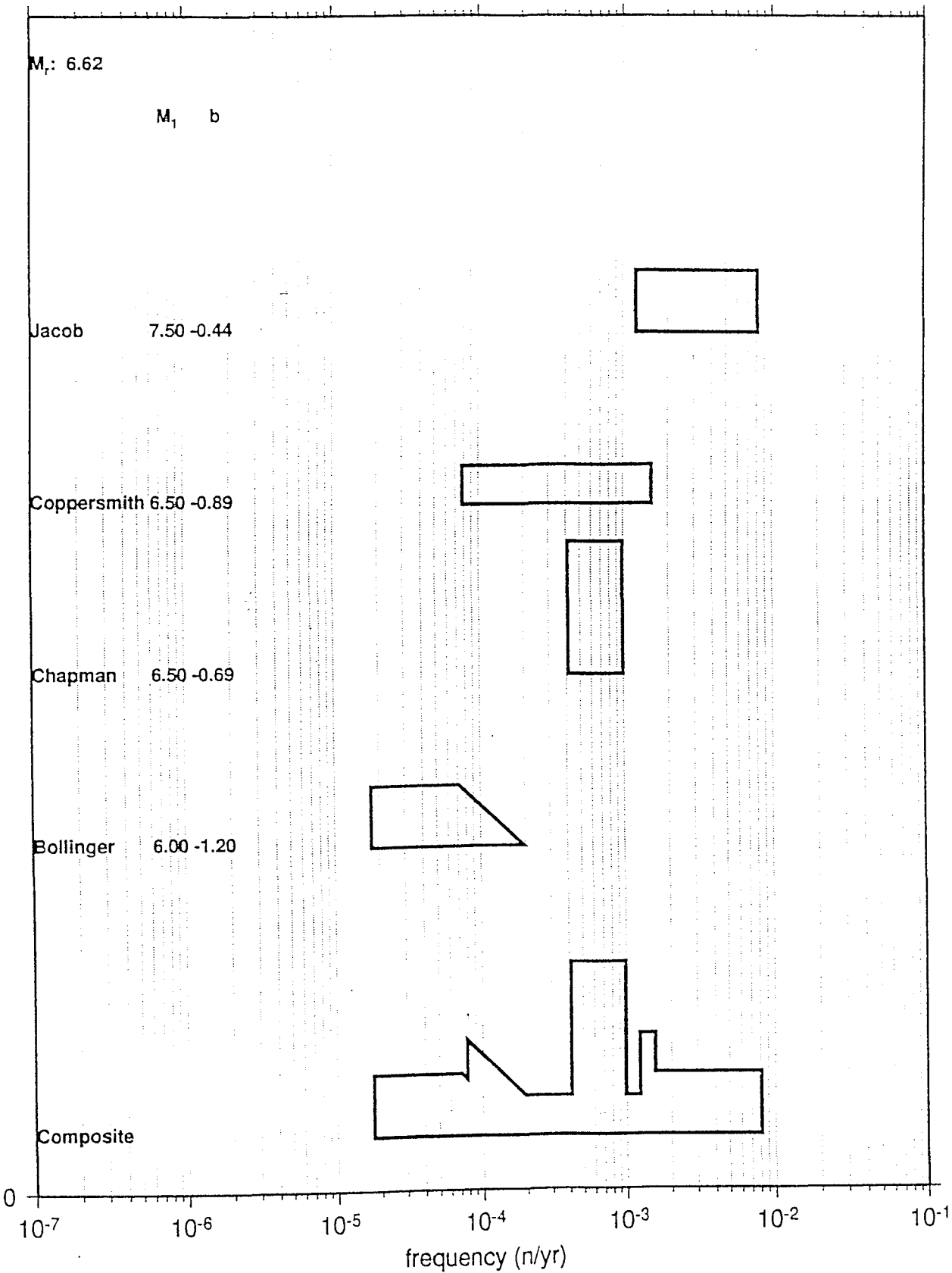
FREQUENCY at M_r ; ZONE 1a



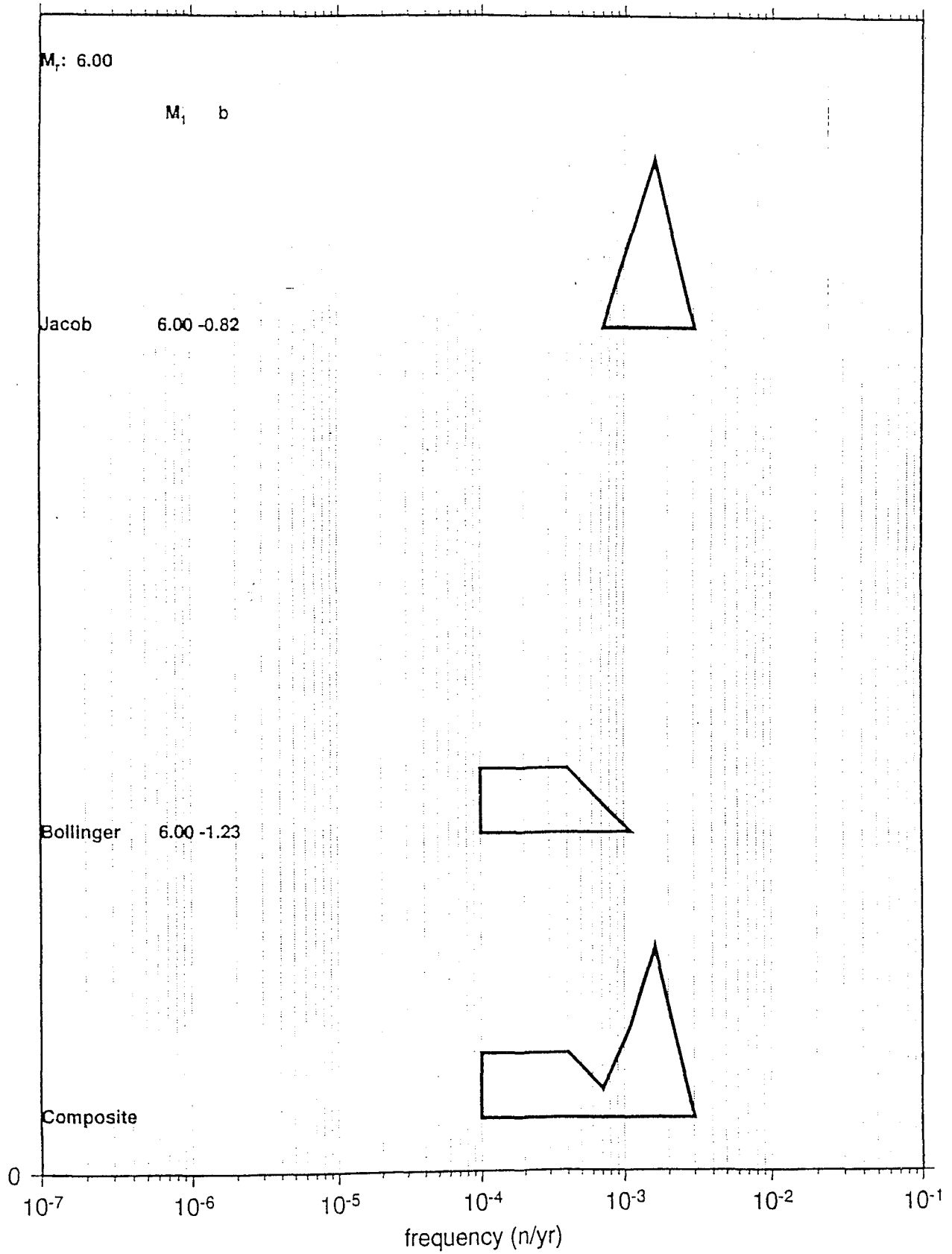
FREQUENCY at M_r ; ZONE 1b



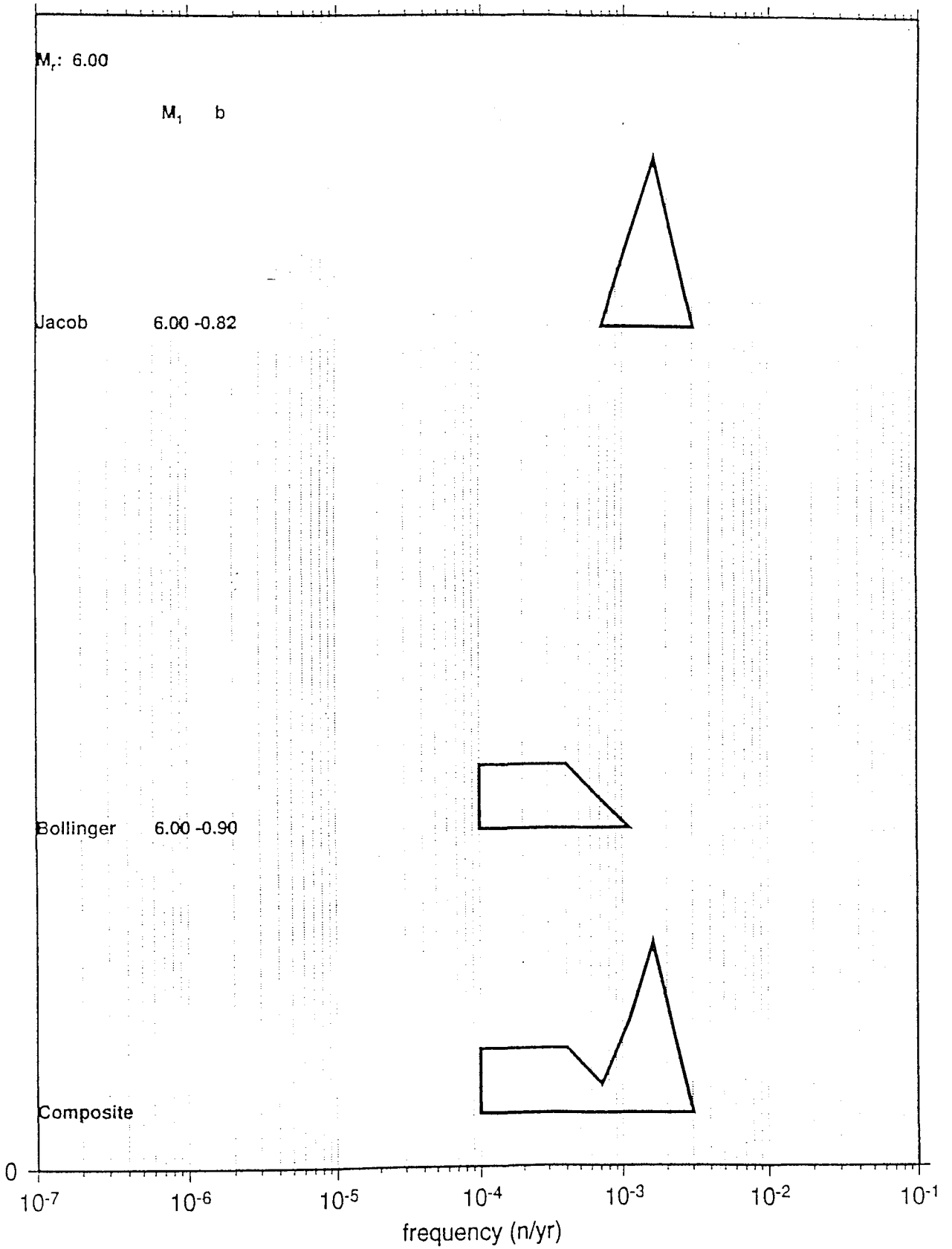
FREQUENCY at M_r ; ZONE 1c



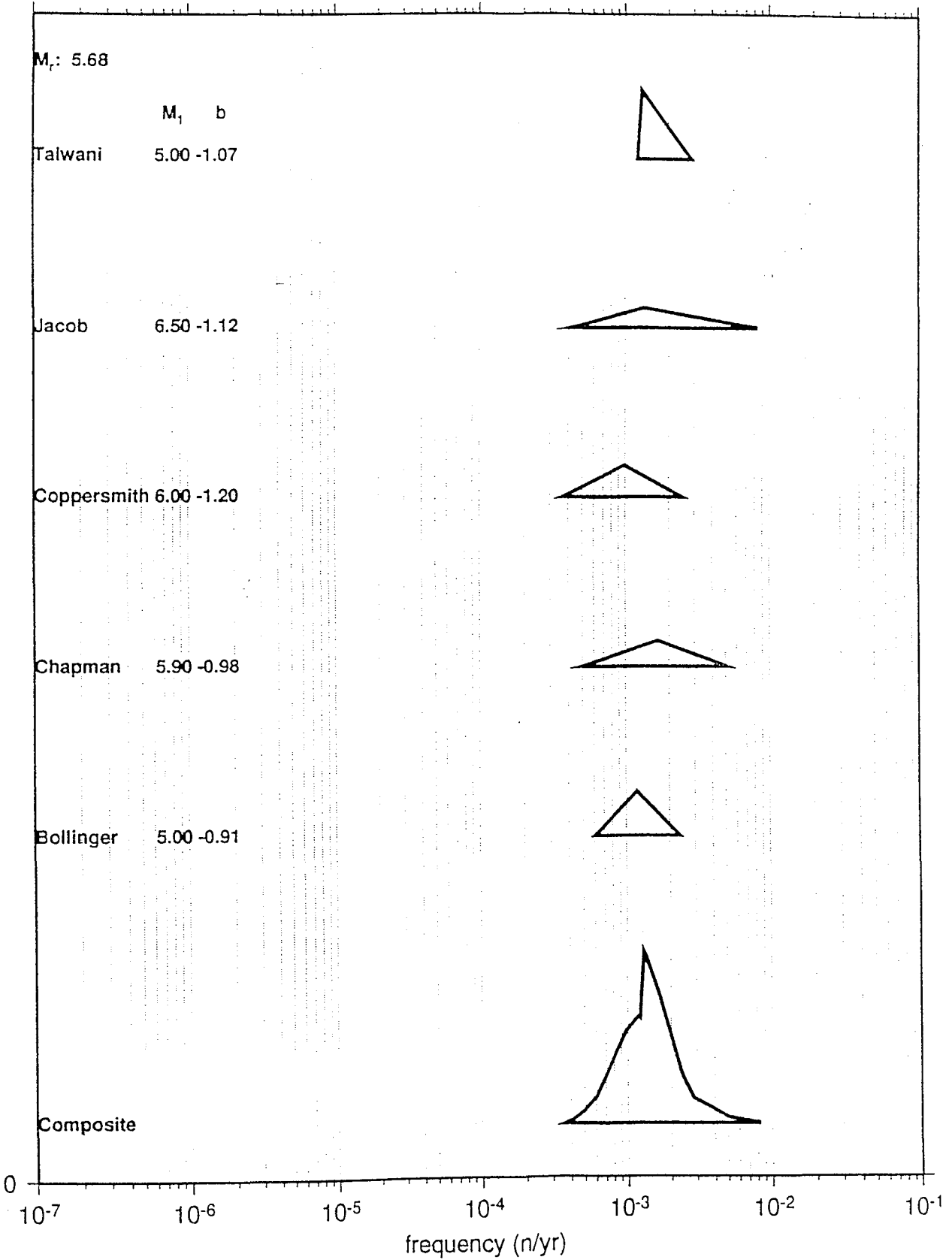
FREQUENCY at M_r ; ZONE 1d



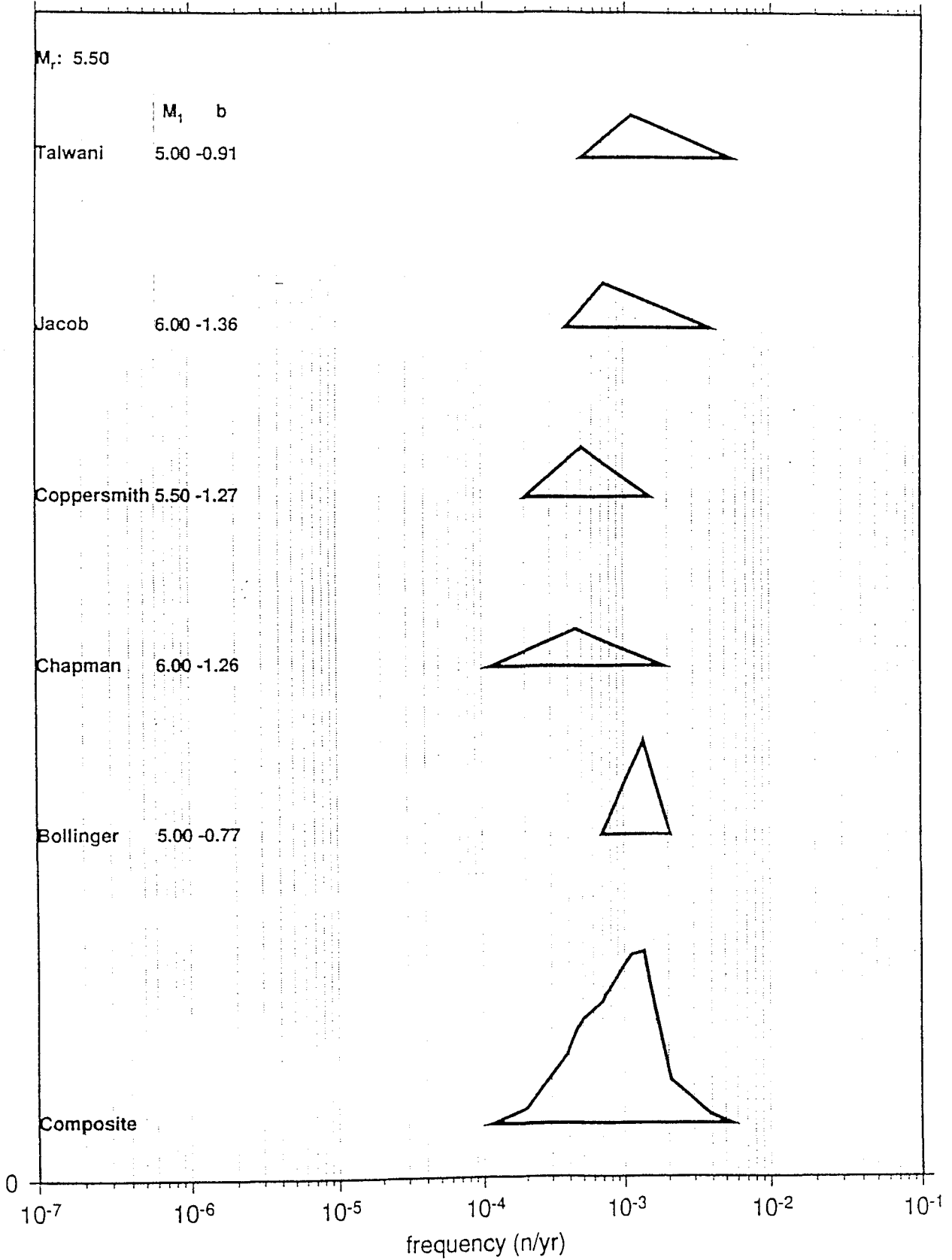
FREQUENCY at M_r ; ZONE 1e



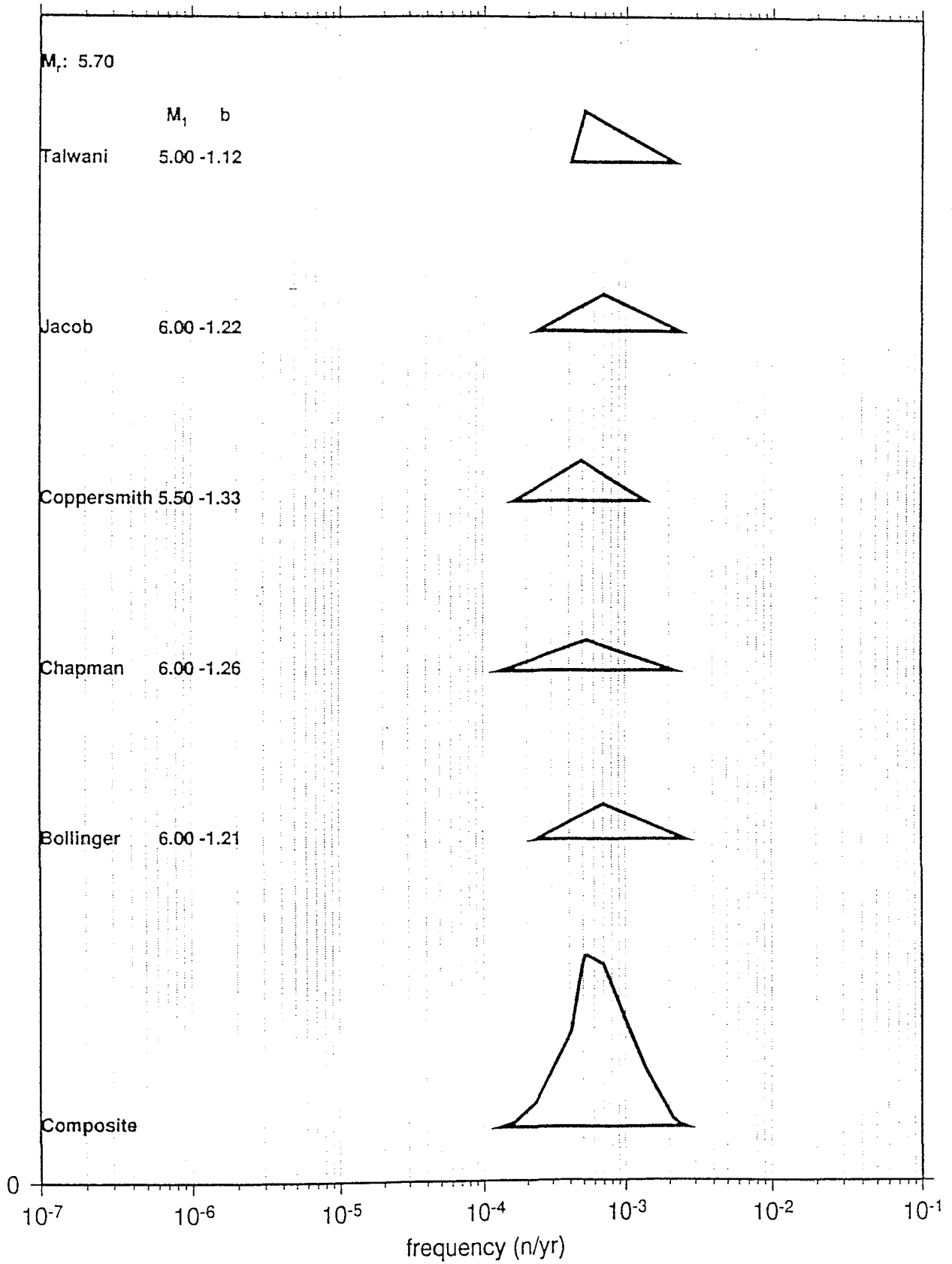
FREQUENCY at M_r ; ZONE 3a



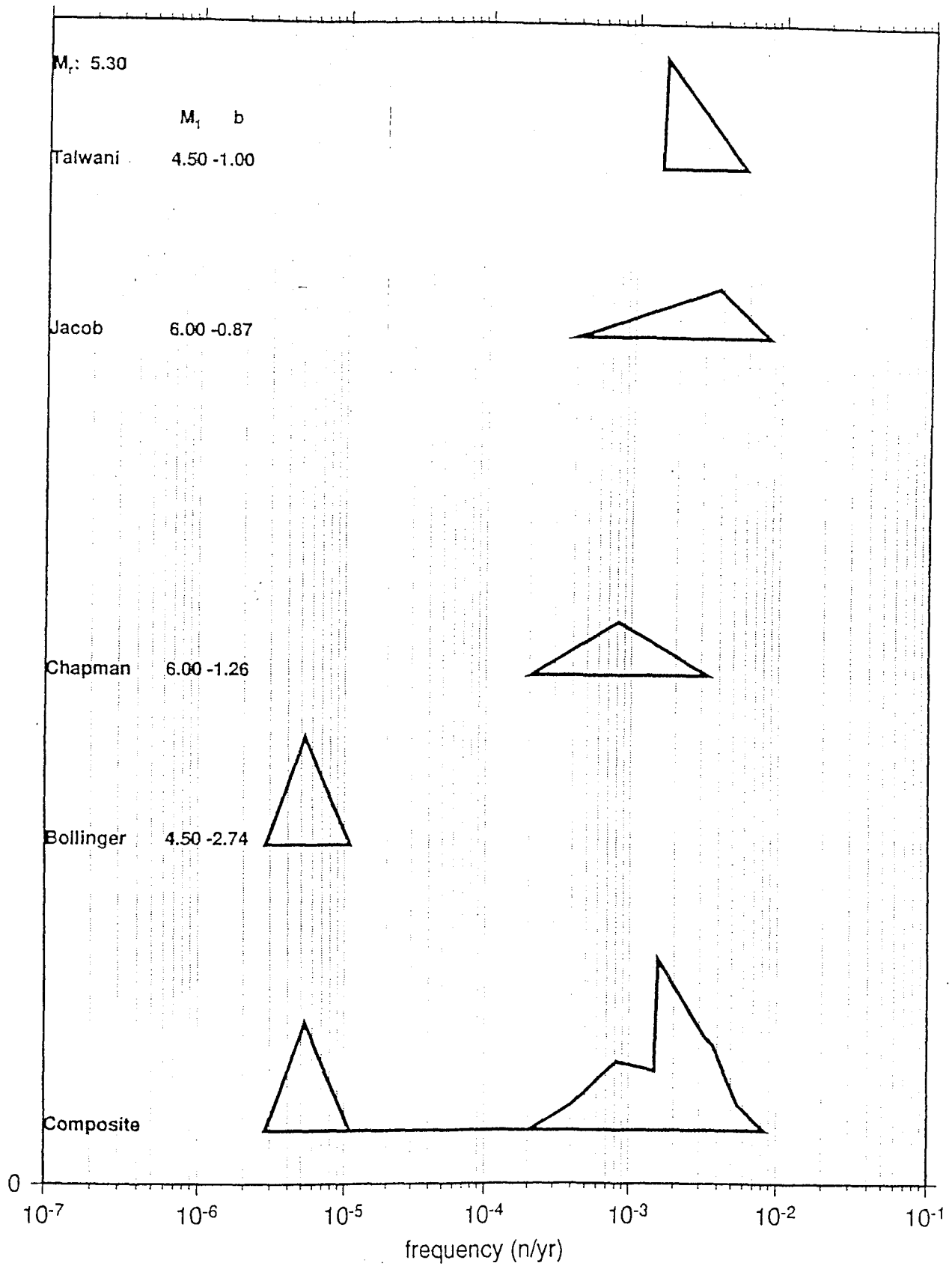
FREQUENCY at M_r ; ZONE 3b-3a



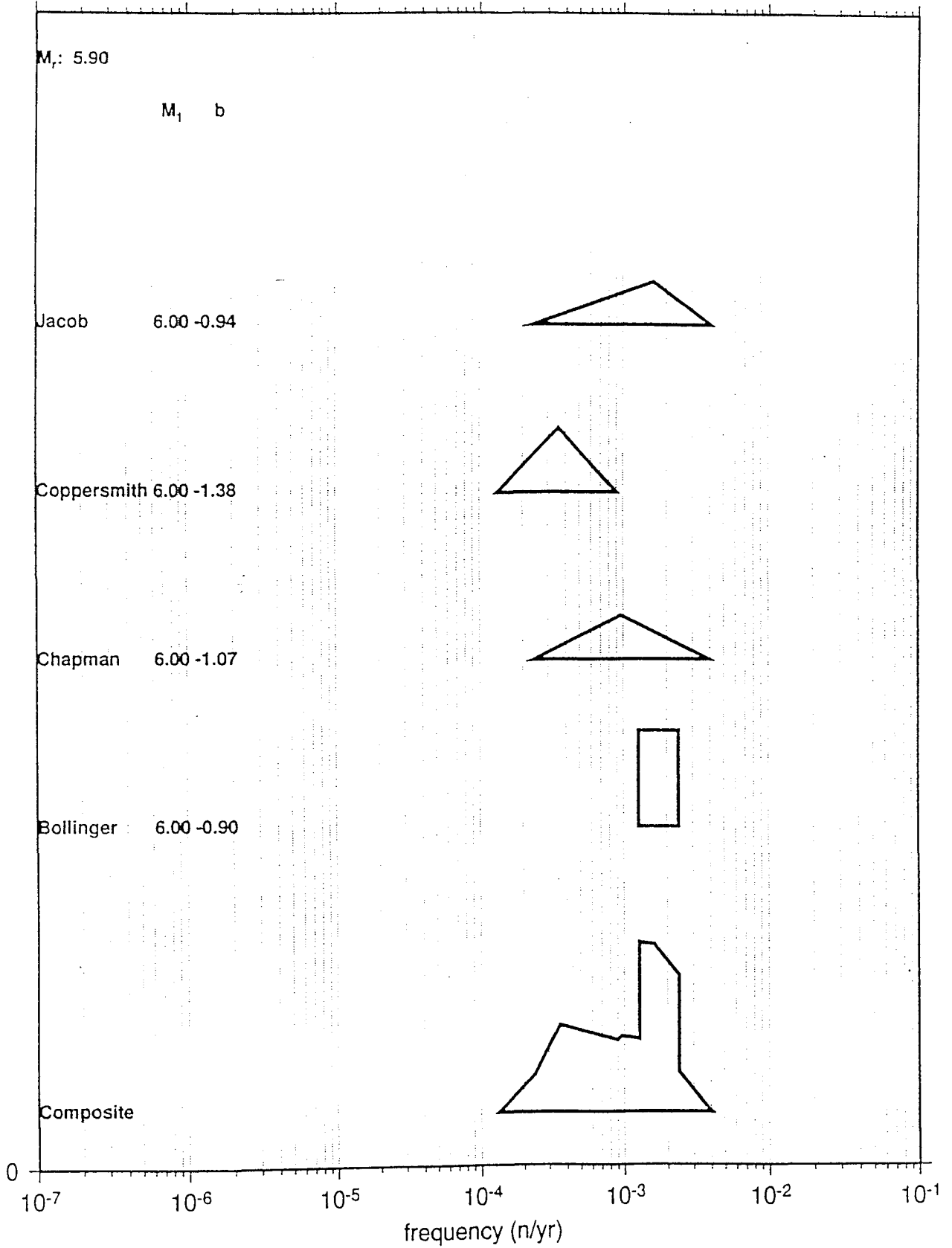
FREQUENCY at M_r ; ZONE 3c



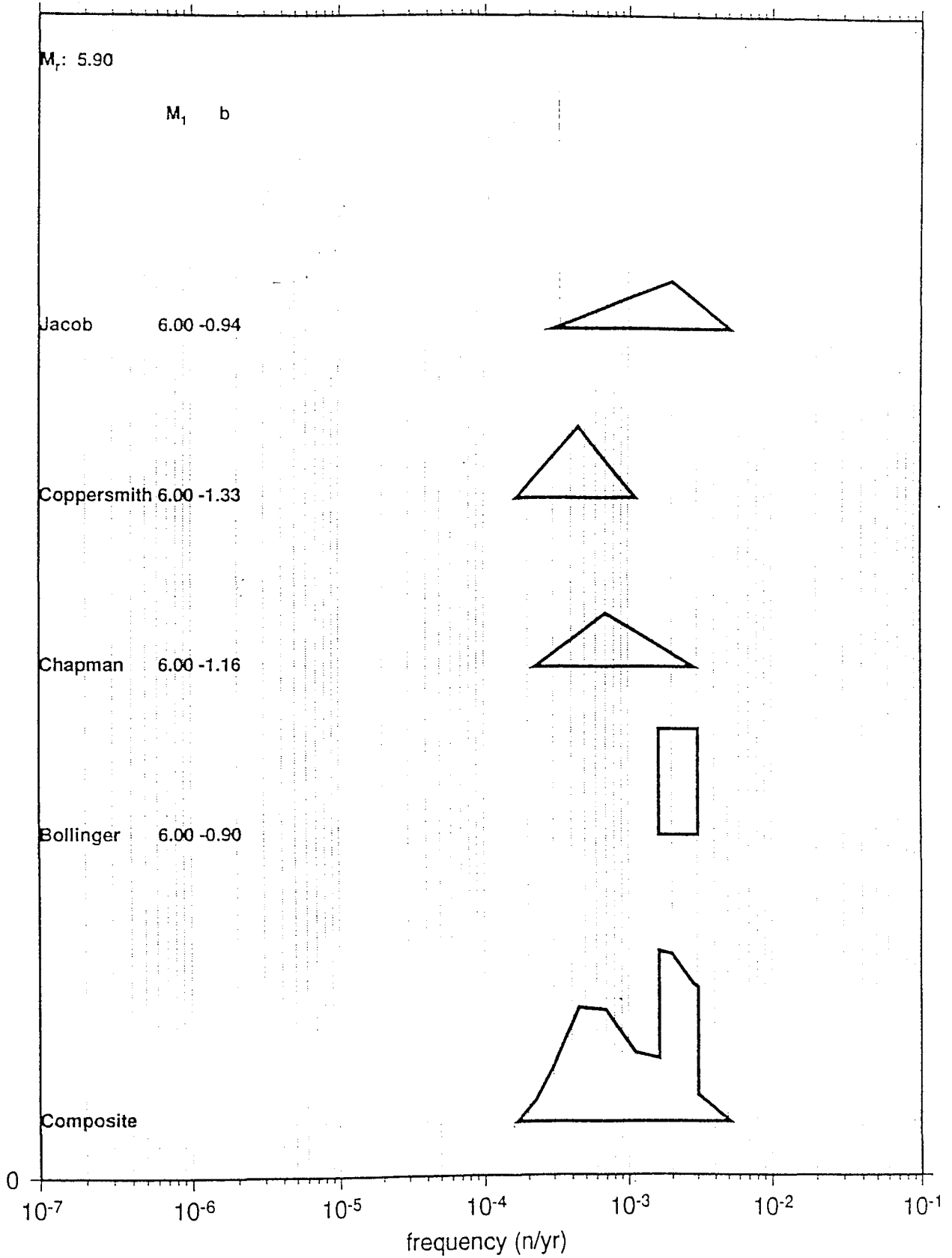
FREQUENCY at M_r ; ZONE 3b-3c



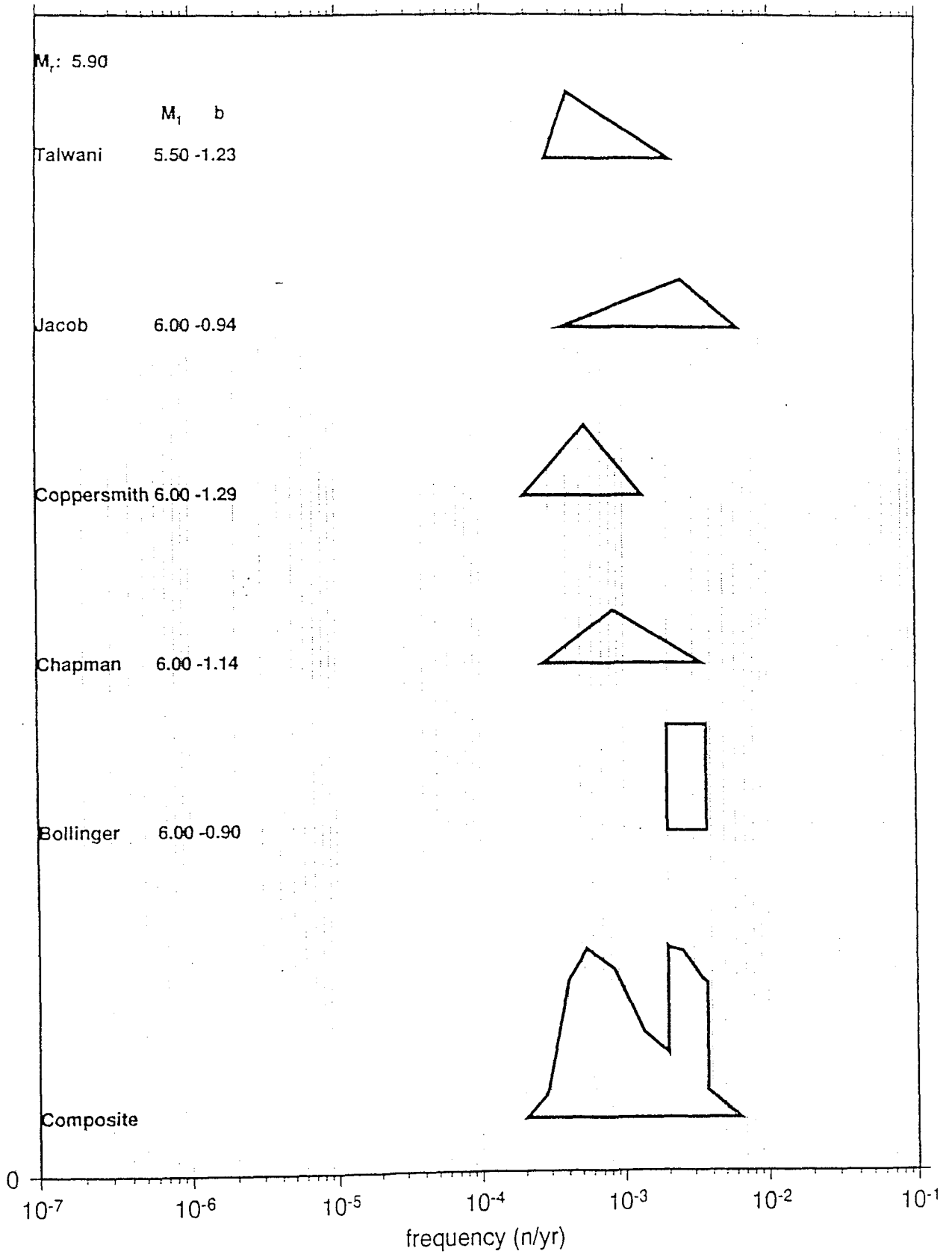
FREQUENCY at M_r ; ZONE 4a1



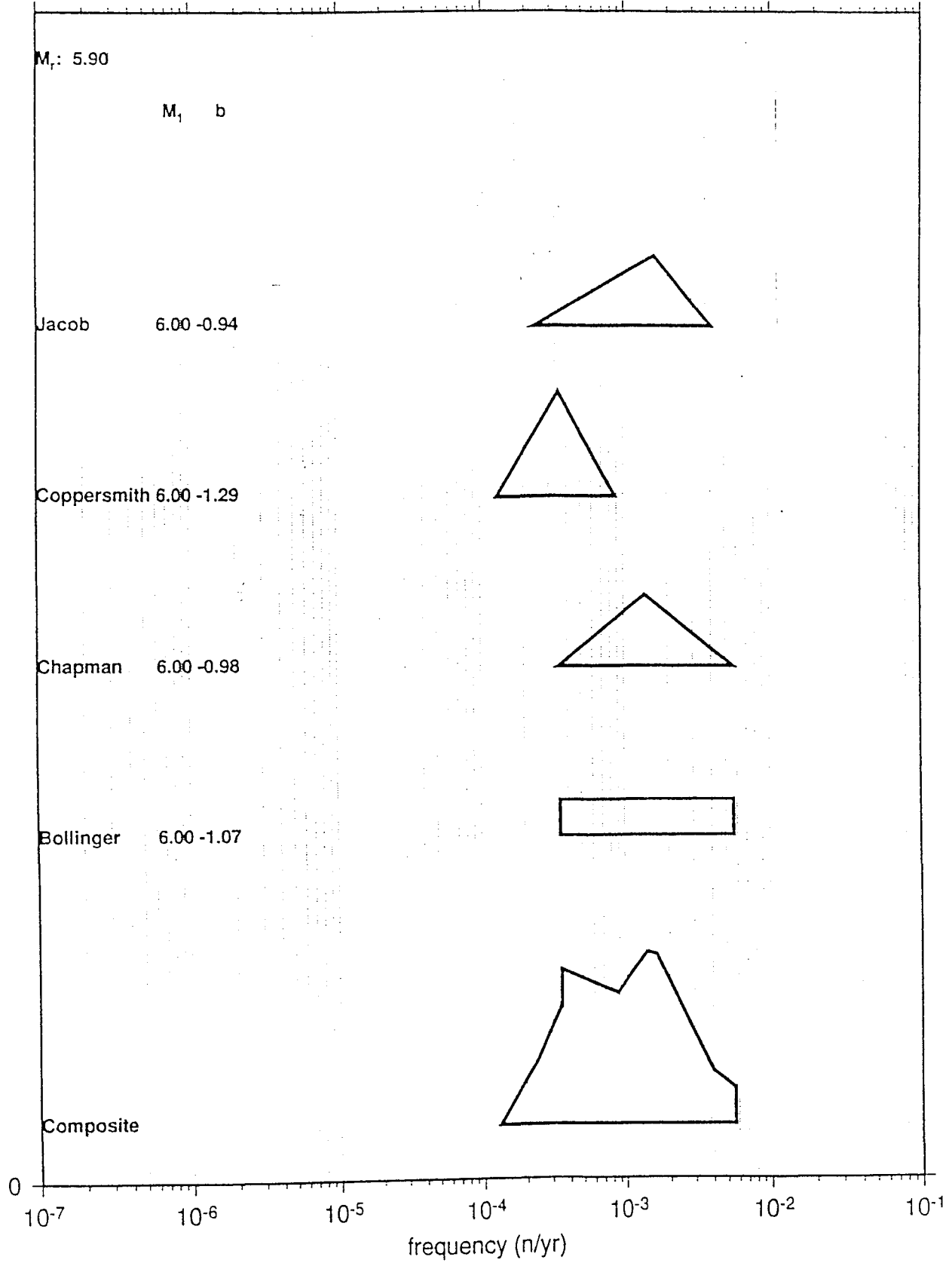
FREQUENCY at M_r ; ZONE 4a1+2



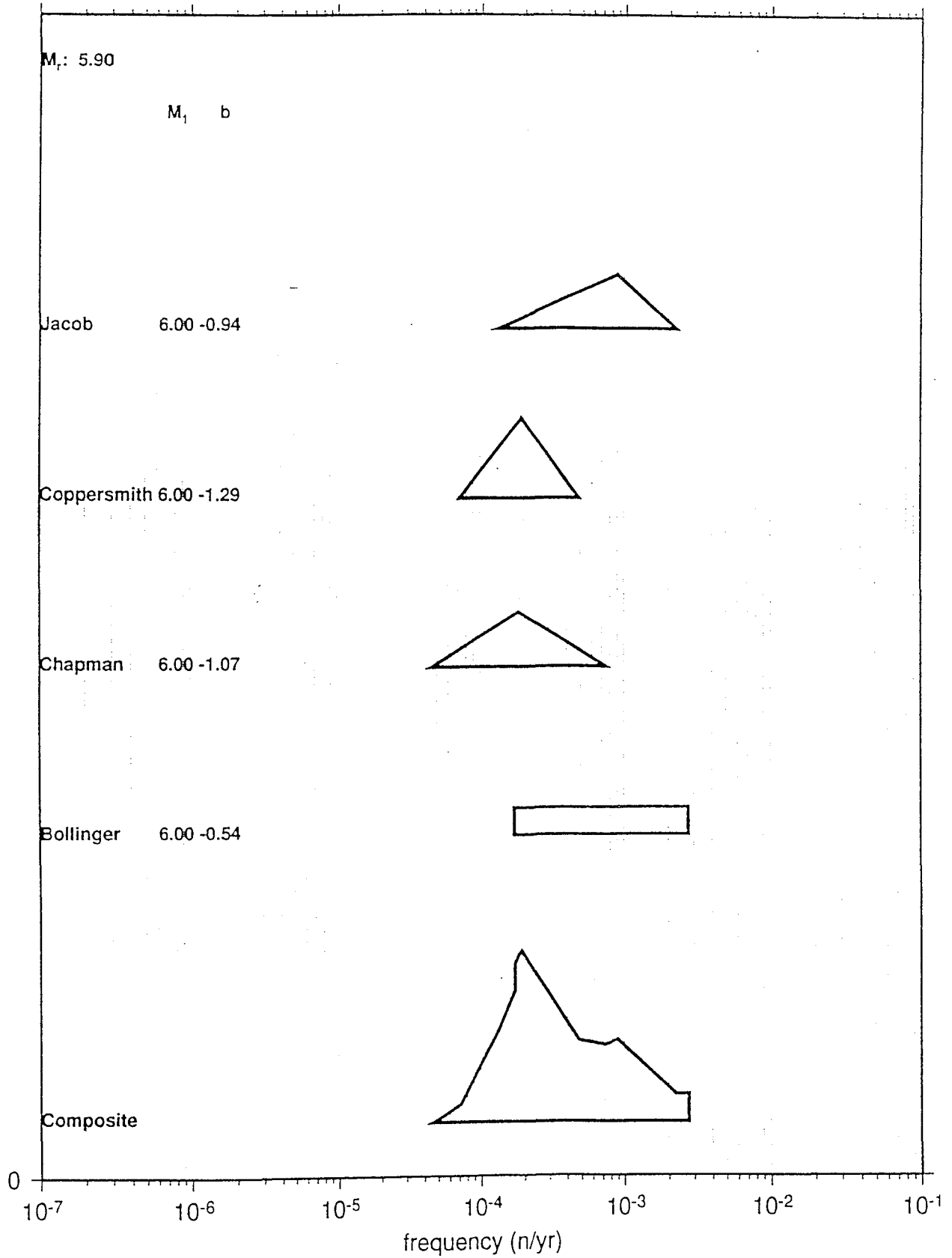
FREQUENCY at M_r ; ZONE 4a1+2+3



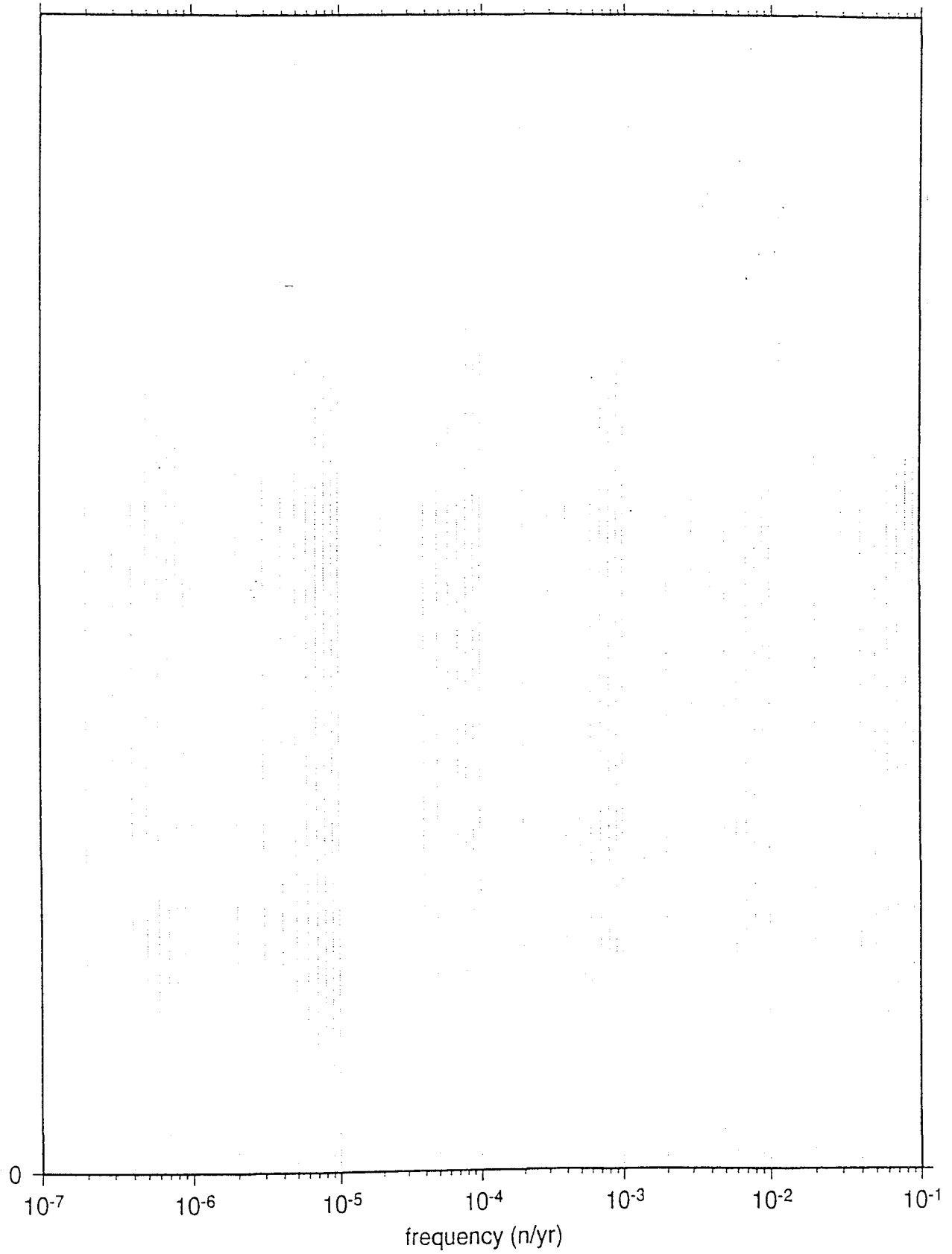
FREQUENCY at M_r ; ZONE 4b1



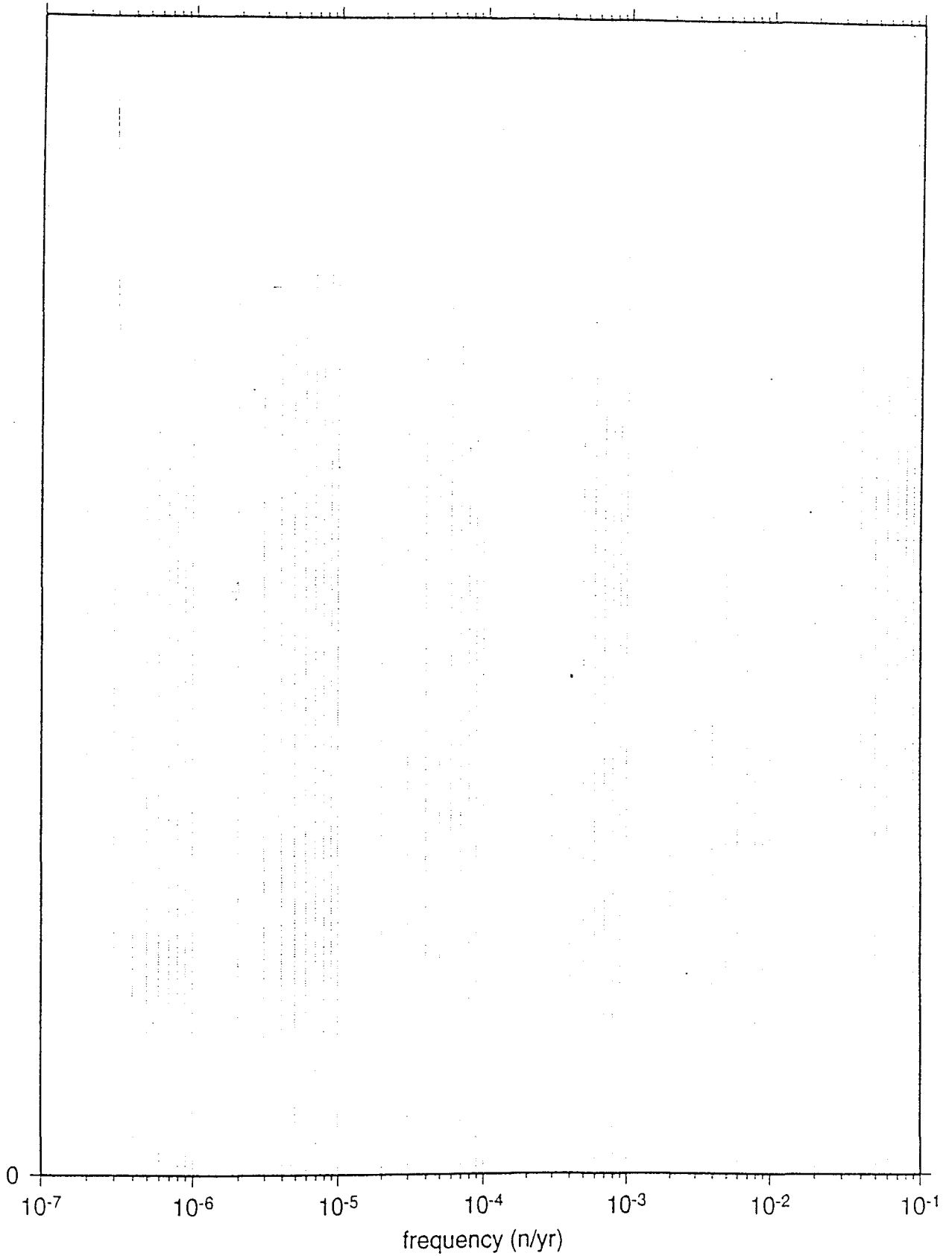
FREQUENCY at M_r ; ZONE 4b2



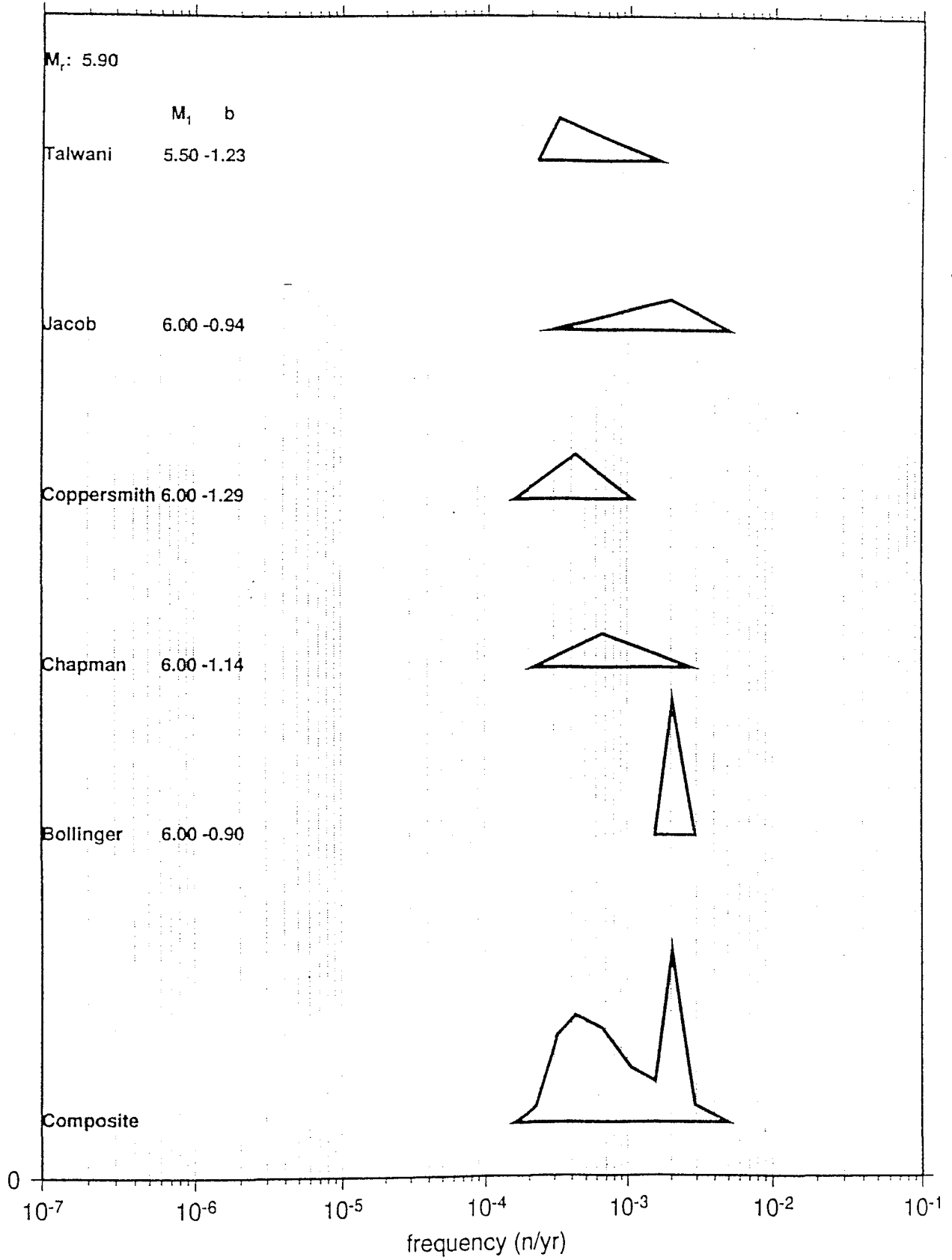
FREQUENCY at M_r ; ZONE 4c



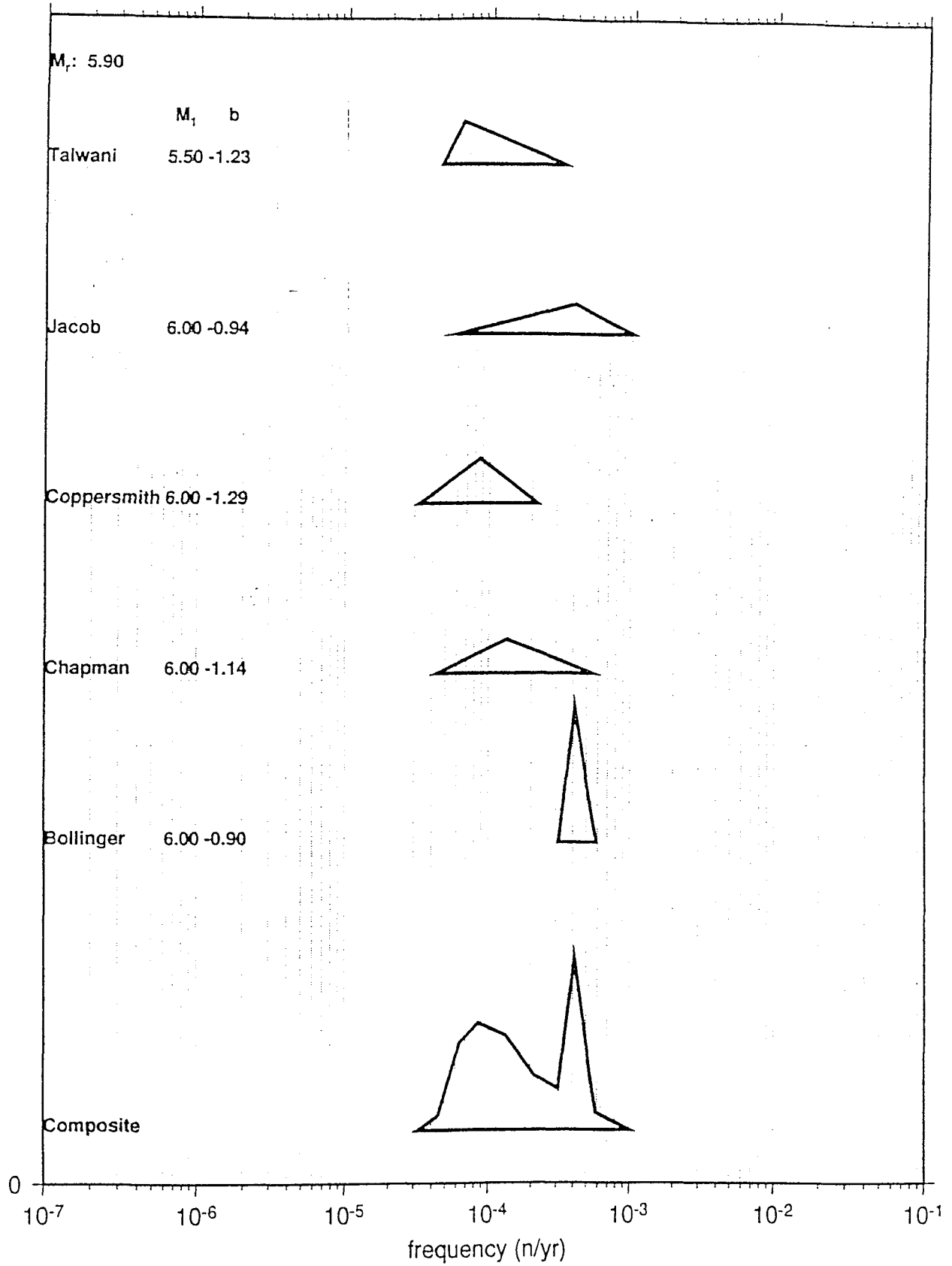
FREQUENCY at M_r ; ZONE 4d



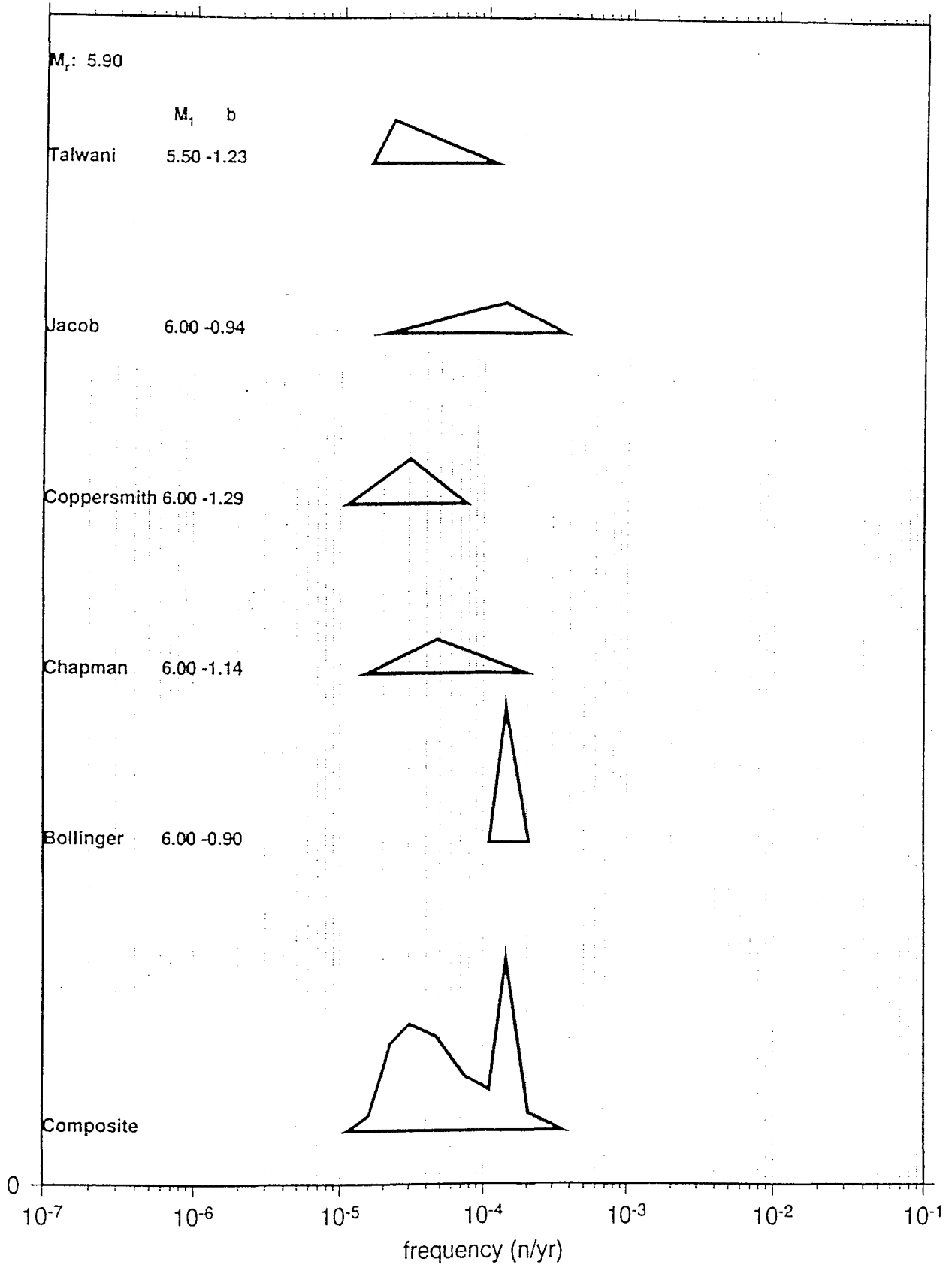
FREQUENCY at M_r ; ZONE 4e1



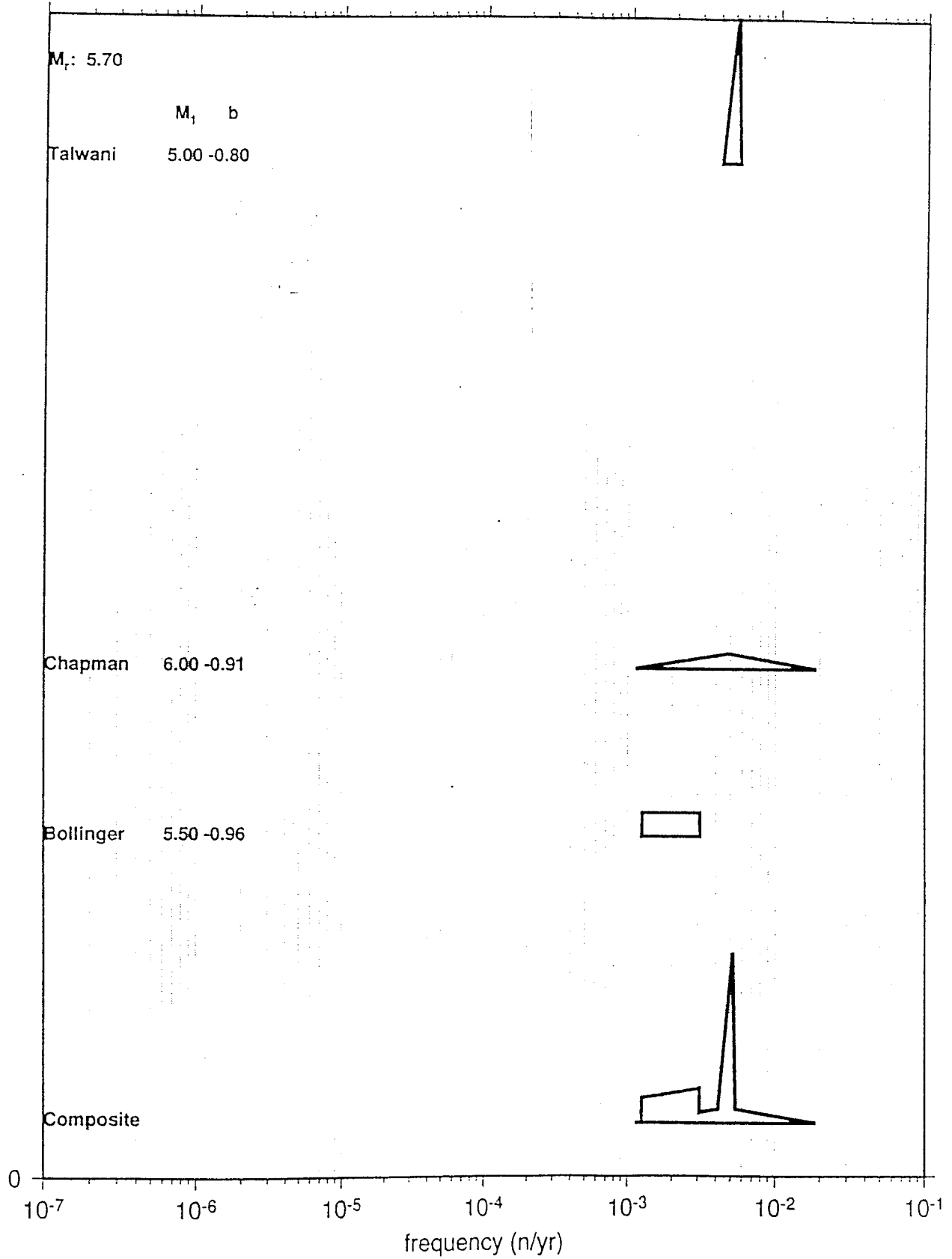
FREQUENCY at M_r ; ZONE 4e2



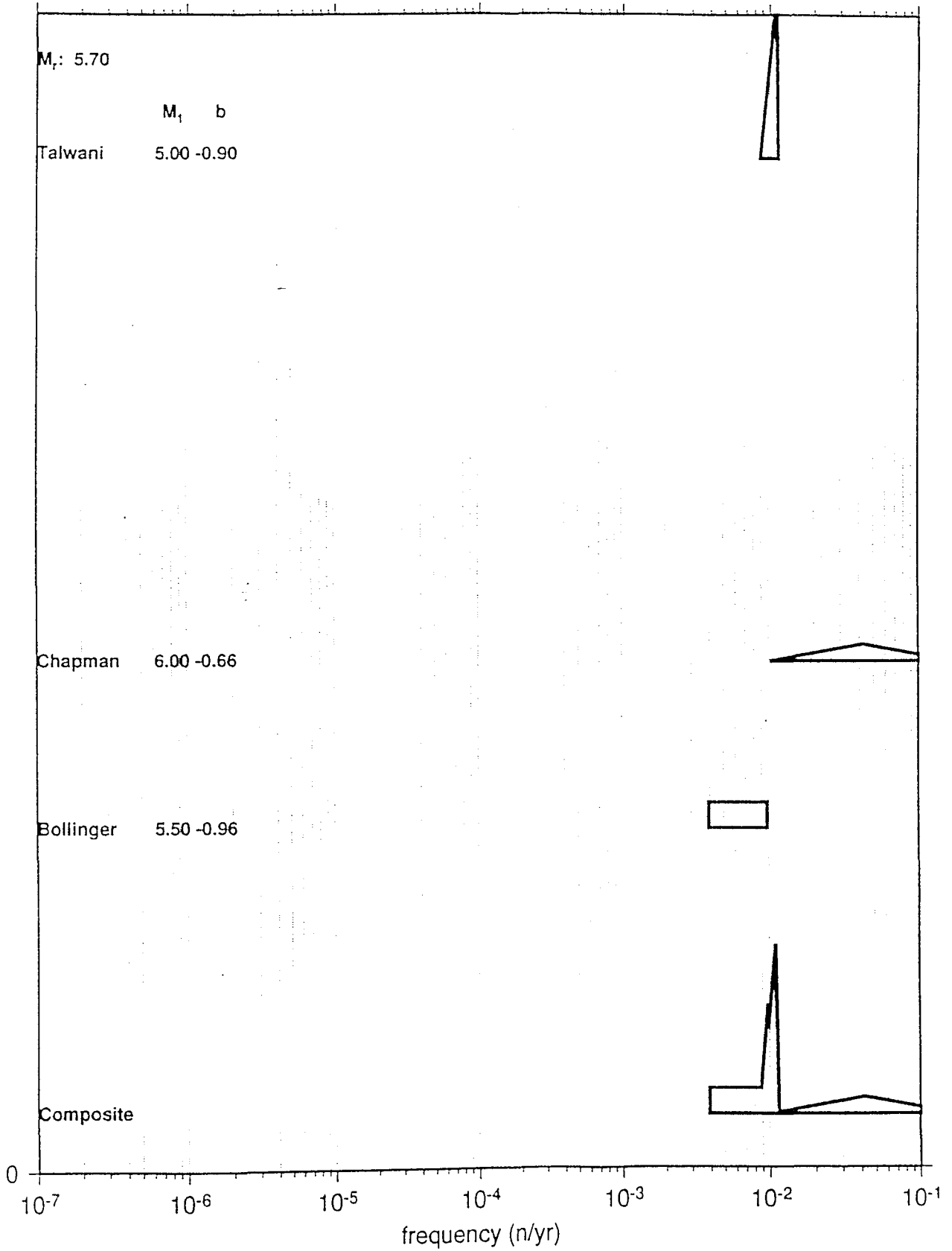
FREQUENCY at M_r ; ZONE 4e3



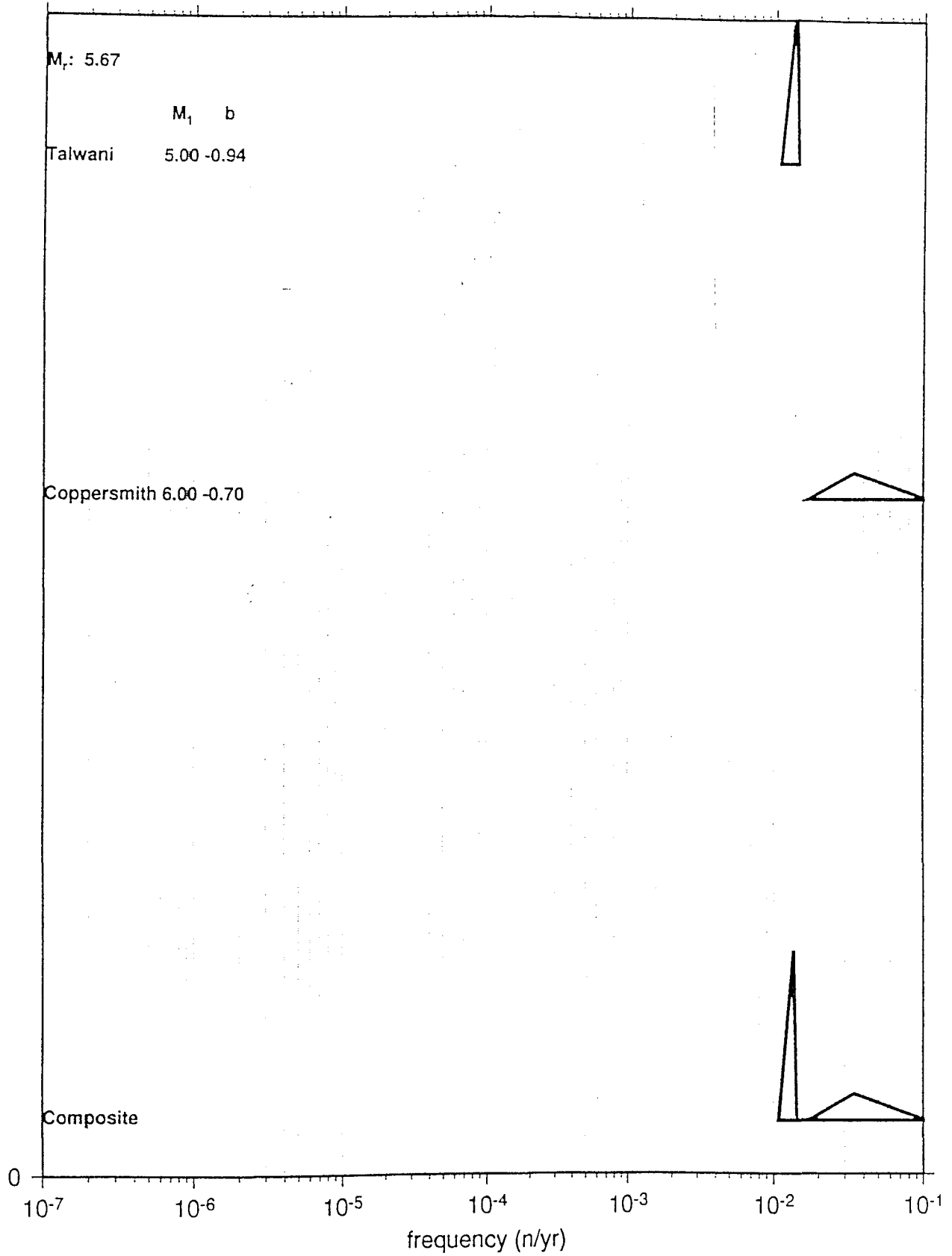
FREQUENCY at M_r ; ZONE 5-1



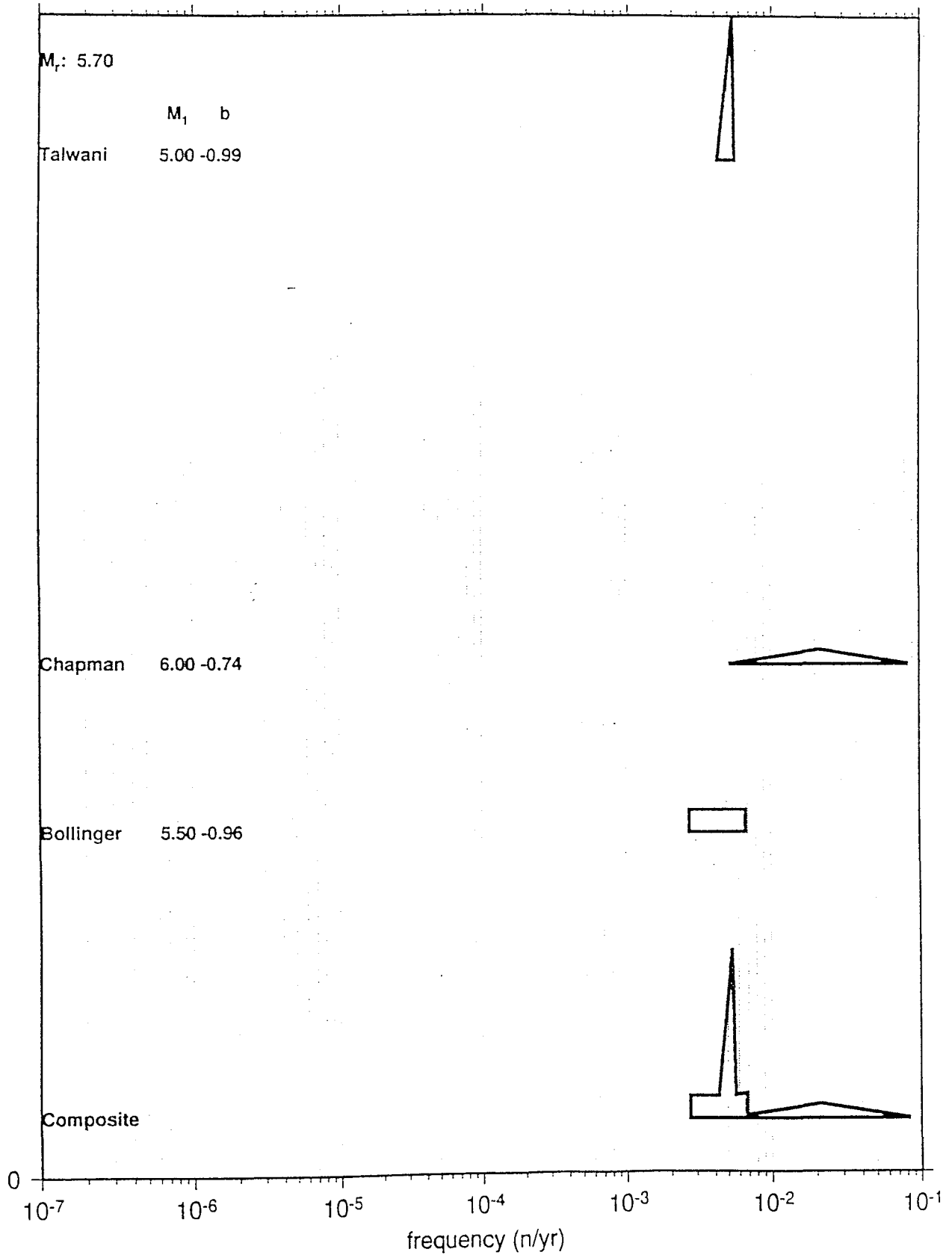
FREQUENCY at M_r ; ZONE 5-1+2



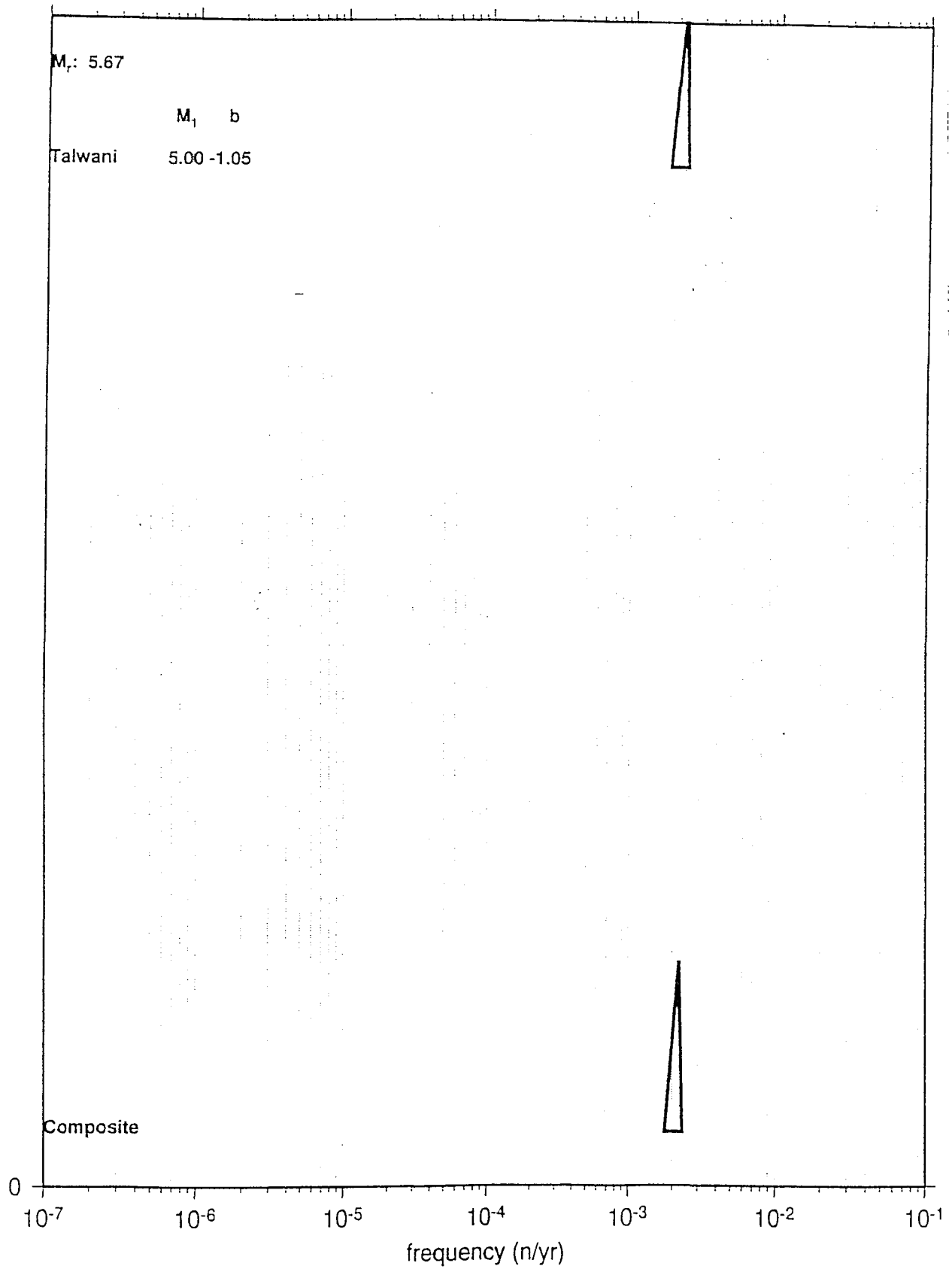
FREQUENCY at M_r ; ZONE 5-1+2+3



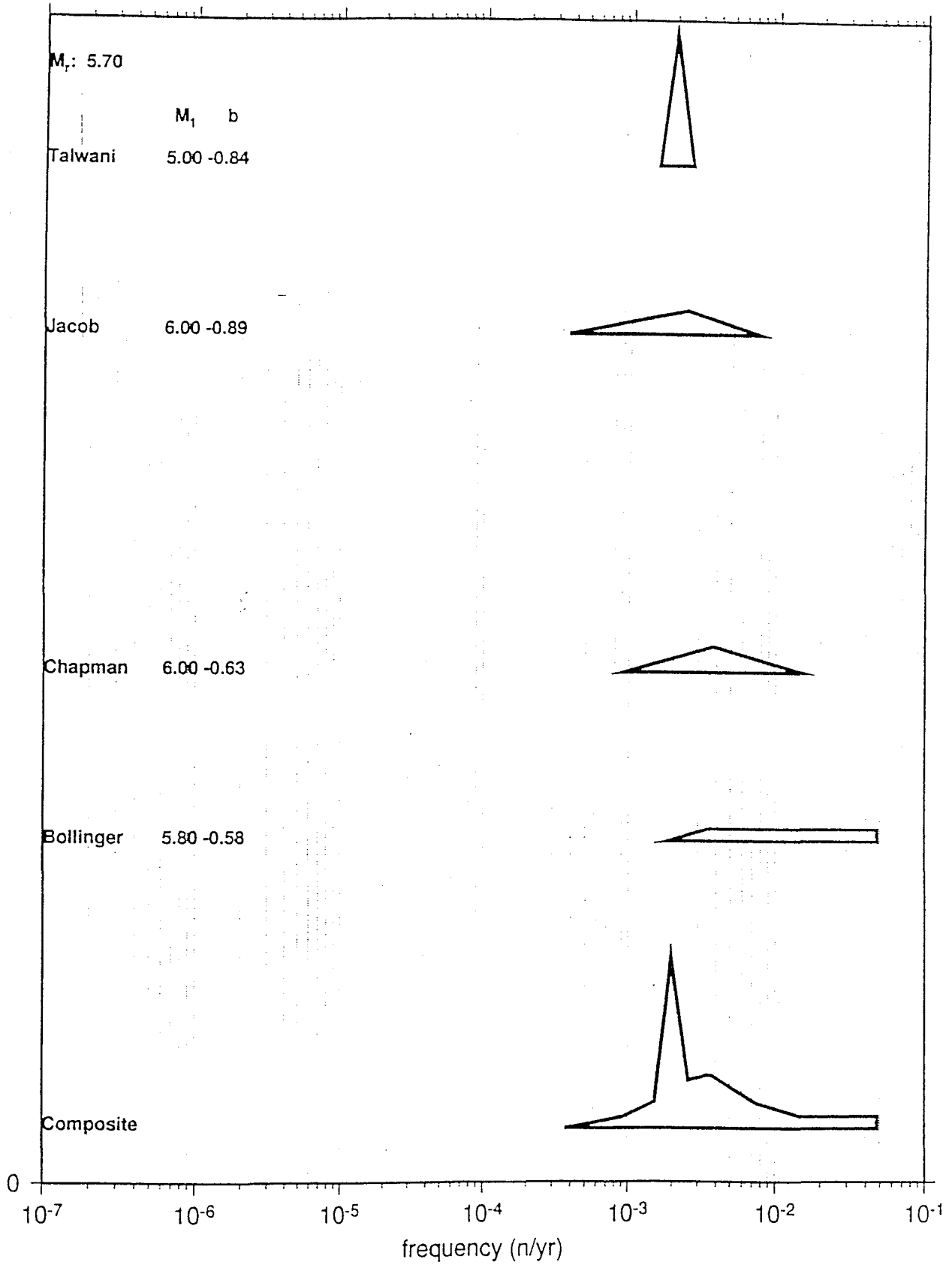
FREQUENCY at M_r ; ZONE 5-2



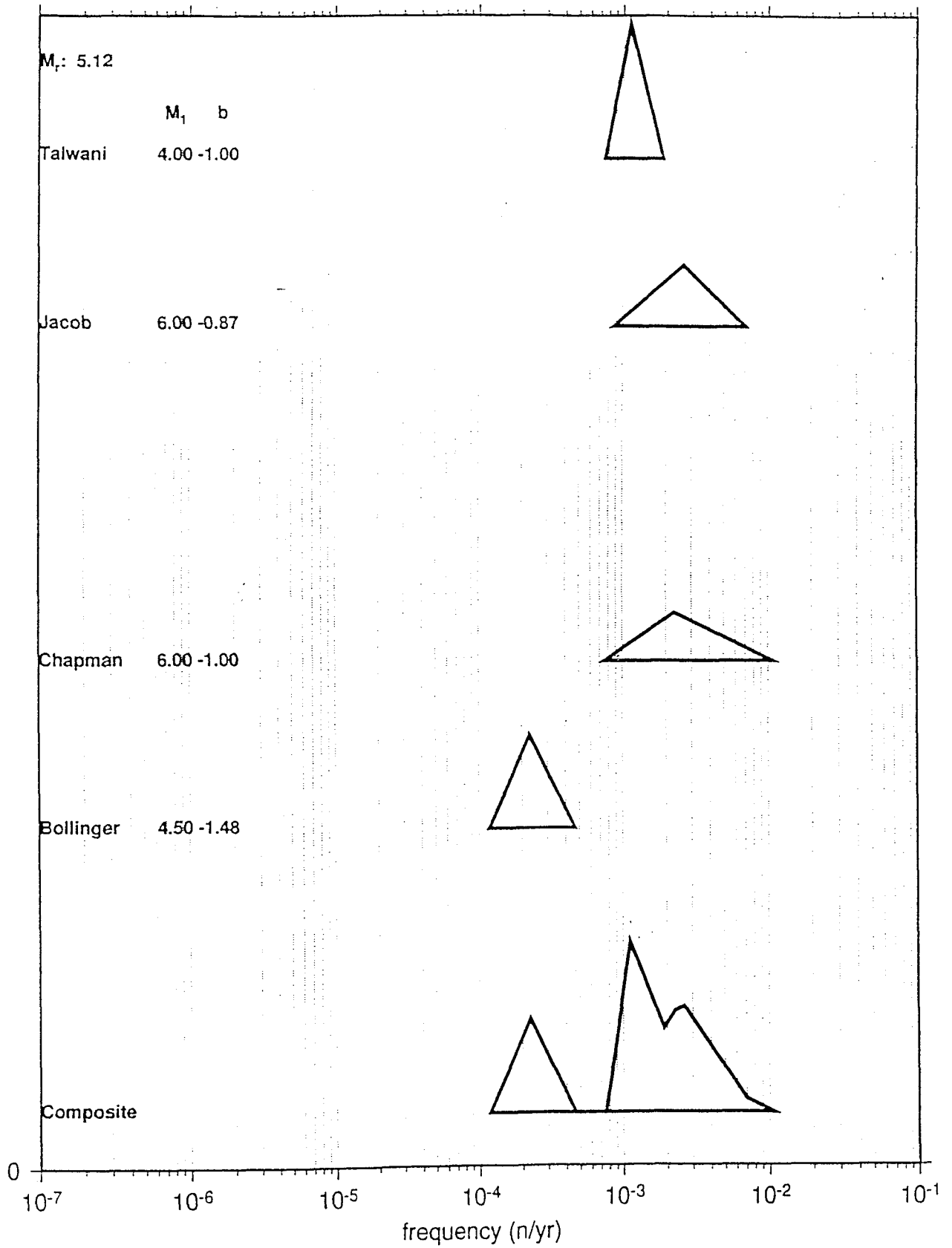
FREQUENCY at M_r ; ZONE 5-3



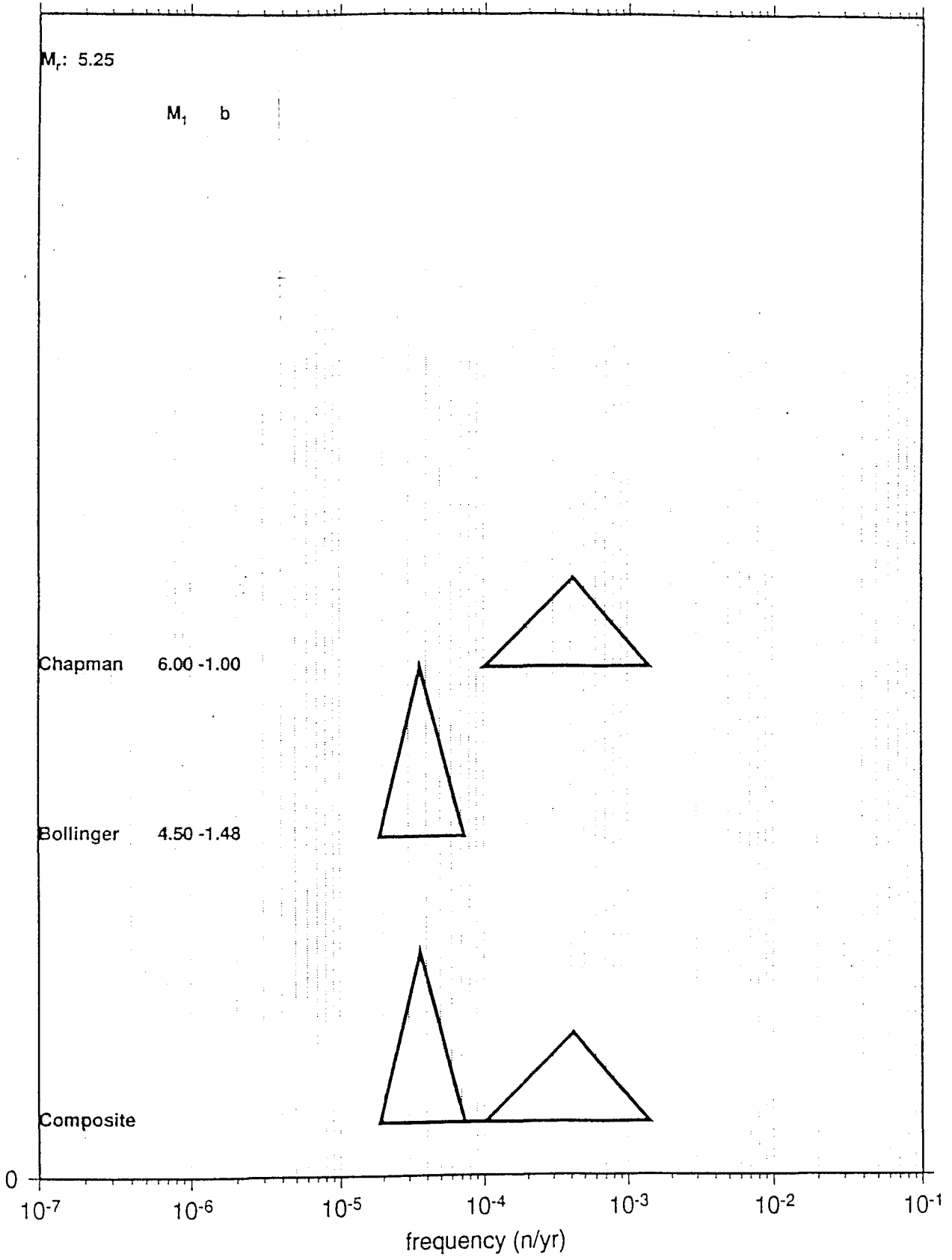
FREQUENCY at M_r ; ZONE 6



FREQUENCY at M_r ; ZONE 7



FREQUENCY at M_r ; ZONE 8



**APPENDIX G: COMPARISON OF PROBABILISTIC SEISMIC
HAZARD ANALYSIS RESULTS OF 1993 EASTERN U.S. UPDATE
AND 1998 TRIAL IMPLEMENTATION PROJECT STUDIES
FOR WATTS BAR**

Comparison of Probabilistic Seismic Hazard Analysis Results of 1993 Eastern U.S. Update and 1998 Trial Implementation Project Studies for Watts Bar

Manuscript Completed: March 2002

Prepared by
J. B. Savy, D. Bernreuter

Lawrence Livermore National Laboratory
Livermore, CA 94550

E. Zurflueh, S. Pullani, NRC Project Managers

**Prepared for
Division of Engineering
Office of Nuclear Regulatory Research
U.S. Nuclear Regulatory Commission
Washington, DC 20555-0001
NRC Job Code Y6245**

ABSTRACT

From 1981 to 1989, Lawrence Livermore National Laboratory (LLNL) developed for the Nuclear Regulatory Commission a method for performing Probabilistic Seismic Hazard Analysis (PSHA) for the eastern United States; results were documented in NUREG/CR-5250. Improvements in the handling of the uncertainties led to updated results, documented in the 1993-EUS-Update study (NUREG-1488.) These results were substantially different from those of the utilities-sponsored study performed by the Electric Power Research Institute (EPRI, 1989.)

In order to understand the differences between the two studies, the NRC and the Department of Energy with EPRI co-sponsored a study led by the Senior Seismic Hazard Analysis Committee (SSHAC), whose task was to explain the differences and provide guidance on how to perform a state-of-the-art PSHA. The work and conclusions of the SSHAC are documented in NUREG/CR-6372 (1997).

As a follow-up to the 1997 SSHAC study, the Trial Implementation Project (TIP) (UCRL-ID-133494, 1998, NUREG/CR-6607) made use of the SSHAC recommendations and developed a set of more detailed guidance for performing PSHA. The TIP project tested the more complicated issue of development of the seismic zonation and seismicity models on two sites: Watts Bar and Vogtle. It was found that the uncertainty generated by artificial disagreements among experts could be considerably reduced

through interaction and discussion of the available data and by identifying the elements common to all experts' interpretation. By concentrating on those elements, it was possible to develop a consensus and eliminate large unnecessary differences.

The present study compares the results of the 1993-EUS-Update and the 1998-TIP studies and identifies the reasons for the differences, which were found to be:

1. Differences in the ground motion (GM) attenuation models.
2. The introduction of the Eastern Tennessee Seismic Zone (ETSZ) in the TIP study.

We found that these two factors accounted for a factor of 6 difference in mean estimates of peak ground acceleration (PGA) hazard at high GM levels. The agreement between the two studies improved at lower PGA values. The results were in better agreement and differed only by about a factor of 2 at high ground motion levels when the same GM model was used with each seismicity model. Finally, it was found that the composite rate of earthquakes around the Watts Bar site was about a factor of 2 higher for the TIP composite seismicity model than for the composite 1993-EUS-Update seismicity model.

We identified some of the root causes for the differences in results and formulated several criteria that will help in determining whether a new evaluation using the latest available data is necessary.

Contents

Abstract.....	5
EXECUTIVE SUMMARY	13
ACKNOWLEDGMENTS	15
ABBREVIATIONS.....	15
1. INTRODUCTION	17
1.1 Background	17
1.2 Purpose of the Study, Scope.....	18
2. DIFFERENCES IN HAZARD ESTIMATES	19
3. IMPACT OF THE GROUND MOTION MODELS.....	23
3.1 Direct Comparison of the Ground Motion Models Used in the Two Studies.....	23
3.2 Comparison of the Hazard Estimates.....	24
3.3 Sensitivity to the Ground Motion Models	24
3.4 Sensitivity to the Seismic Zonation and Seismicity Models.....	24
4. IMPACT OF THE SEISMICITY MODELS.....	35
4.1 Methodological Differences	35
4.2 Differences of Interpretation of the Data by the Experts	35
4.3 Case of the Local Zones	36
5. UNCERTAINTIES AND SENSITIVITY STUDIES	47
5.1 Parameters of Interest	47
5.2 Sensitivity to the Formulation of the Zonation Maps.....	47
5.3 Sensitivity to the Parameters of the Monte-Carlo Simulation.....	47
5.4 Site-Specific versus Regional Studies.....	47
5.5 ETSZ versus Local Faults.....	48

5.6 Ground Motion Saturation.....	48
5.7 Uncertainty in the Ground Motion Models Estimates.....	48
6. CASES OF THE 2.5- AND 25.0-HZ RESPONSE SPECTRAL VELOCITIES.....	55
7. DISCUSSION.....	63
7.1 General Findings.....	63
7.2 Causes for the Differences in Hazards Estimates.....	63
7.2.1 Ground Motion Models.....	63
7.2.2 Source Zones and Seismicity Models.....	63
7.2.3 Regional Versus Site-Specific Window: Impact on Uncertainty.....	64
7.2.4 Comparison with the Vogtle Site.....	64
7.3 Criteria for Formulating Conclusions at Other Sites.....	64
8. CONCLUSIONS.....	67
REFERENCES.....	69

Figures

Exec-1: Comparison of the Mean Estimates of the Seismic Hazard for the Watts Bar Site.....	14
2.1: Mean PGA hazard estimates for Watts Bar.....	20
2.2: Median PGA Hazard Estimates for Watts Bar.....	21
2.3: “Best Estimate” PGA Hazard for Watts Bar.....	21
3.1a: Comparison of the Median Ground Motion Attenuation Models for the 1993-EUS-Update and 1998-TIP Studies for Magnitudes 5, 6, and 7.....	25
3.1b: Ratios of the Median PGA Estimates from the 1998-TIP Study, Divided by the 1993-EUS-Update Median Estimates, as a Function of Distance.....	25
3.2a: Comparison Between the 1-sigma 1998-TIP and the 85% 1993-EUS Updated Ground Motion Attenuation Models.....	26
3.2b: Ratios of the 1-Sigma PGA Estimates from the 1998-TIP Study, Divided by the 1993-EUS-Update Median Estimates, as a Function of Distance.....	26
3.3: Cumulative Contribution of the Distance Bins to Hazard in the 1998-TIP Study. Seismic Source Zones within 40 km of Watts Bar Contribute Approximately 80% of the Total Hazard.....	27

3.4:	Cumulative Contribution of the Magnitude Bins to the Hazard in the 1998-TIP Study. Magnitude Events Smaller Than 6 Contribute Approximately 80% of the Total Hazard.....	27
3.5:	Contribution of the Magnitude–Distance Bins to the Total Hazard for a 10,000-Year Return Period.....	28
3.6:	Estimates of the Mean Hazard Using the 1998-TIP Seismic Zonation. Comparison between the 1993-EUS-Update and 1998-TIP Ground Motion Attenuation Models.....	28
3.7:	Estimates of the Median Hazard Using the 1998-TIP Seismic Zonation. Comparison between the 1993-EUS-Update and 1998-TIP Ground Motion Attenuation Models.....	29
3.8:	Estimates of the Mean Hazard Using the 1993-EUS-Update Zonation. Comparison between the 1993-EUS-Update and 1998-TIP Ground Motion Attenuation Models.....	29
3.9:	Estimates of the Median Hazard using the 1993-EUS-Update Seismic Zonation. Comparison between the 1993-EUS-Update and 1998-TIP Ground Motion Attenuation Models.	30
3.10:	Contribution of Magnitude Bins to the Total Hazard in the 1998-TIP Study for Two Peak Ground Acceleration Levels.....	30
3.11:	Results of the 1993-EUS-Update Study. Comparison of the Mean Estimates of the Hazard between the 11 Experts (comb) and Expert 3 (X3).....	31
3.12a:	Contribution of Magnitude Bins in the 1993-EUS-Update Study for Two Peak Ground Acceleration Levels for the Case of Expert 3.....	32
3.12b:	Comparison of the Magnitude Contributions for a 1G PGA Using the 1998-TIP Ground Motion Model. The Seismicity of Expert 3 (X3) Leads to a Strong Mode at M5.6 and the 1998-TIP Composite Seismicity Leads to a Monotonically Decreasing Contribution.....	32
3.13:	Sensitivity to the Seismicity and Zonation Model. The Two Curves Represent the Mean Hazard Estimated with the 1998-TIP and with the 1993-EUS-Update Seismicity-Zonation Models. Both Are with the Same 1998-TIP Ground Motion Attenuation Model.	33
3.14:	Comparing the Median Hazard Curves between the Cases of 1998-TIP Seismicity to the Case of 1993-EUS-Update Seismicity, Both with the Same 1998-TIP Ground Motion Model.	33
4.1:	First-Order Regional Seismic Sources Zonation Map for the Study of the Watts Bar Site in the 1998-TIP Study.....	39
4.2:	Detail of the Geometry of the Local Seismic Source Zones Considered in the 1998-TIP Study.	39
4.3:	One of the Seismic Source Zone Maps Submitted by Seismicity Expert 3 in the 1993-EUS-Update Study. The Site Location is Shown by the Circle on the Map.....	40
4.4:	One of the Seismic Zone Maps Submitted by Seismicity Expert 1 in the 1993-EUS-Update Study. The Location of the Site is Indicated by a Circle on the Map.....	40
4.5:	Expected Budget of Earthquakes within 35 km of Watts Bar from the Zonation and Seismicity Models of the 11 Seismicity Experts of the 1993-EUS-Update Study.....	41

4.6:	Comparison of the Earthquake Seismicity Budget within 35 km of Watts Bar for the 1993-EUS-Update and the 1998-TIP Seismic Zonation and Seismicity Models. The 1993-EUS-Update Curve is an Average Over the 11 Seismicity Experts; the 1998-TIP Curve is from the Composite Zonation and Seismicity Model.....	41
4.7:	Comparison of the Best Estimate Seismicity Budget for a Region within 35 km of Watts Bar, Provided by Expert 3 (X3 1993-EUS-Update) in the 1993-EUS-Update Study and by G. Bollinger in the 1998-TIP Study (1998-TIP-BOL).....	42
4.8:	Historical Seismicity in Zone 35 of 1998-TIP.....	42
4.9:	Comparison of the Budget of Historical Earthquakes with the Expected Estimates in Zone 35 of 1998-TIP. The Composite Seismicity Model Including All Experts' Input is Labeled "1998-TIP" and "1998-TIP-BOL" for Bollinger's Input Only.....	43
4.10:	Comparison of the Budget of Historical Earthquakes with the Expected Estimates in Zone B1 of 1998-TIP. The Composite Seismicity Model Including All Experts' Input Is Labeled "1998-TIP" and "1998-TIP-BOL" for Bollinger's Input Only.....	43
4.11:	Budget of Historical Earthquakes and Modeling for Zone B2 in 1998-TIP.....	44
4.12:	Yearly Rates in Zone 5 for Expert 3 of the 1993-EUS-Update Study. "X3 Model" Refers to Expert 3's Estimates. The Other Curves are for Historical Earthquakes.	44
4.13:	Mean Estimates of the Seismic Hazard at Watts Bar Using the 1998-TIP Composite Seismicity Model (1998-TIP composite) and Bollinger's Model (1998-TIP-BOL). The Ground Motion Model is the 1998-TIP Model.	45
5.1:	Comparison of the Annual Rates of Occurrence of Earthquakes within 33 km of Watts Bar, for the 5 Highest-Weighted Zonation Maps of the 1998-TIP Study. The Relative Weights of the Maps Are Given in Table 4.1.	49
5.2:	Comparison of the Mean Estimates of the Hazard for Each of the Five Highest-Weighted Maps with the Overall Mean Hazard.....	49
5.3:	Sensitivity of the Mean Estimates to the Seed of the Monte-Carlo Simulation.	50
5.4:	Historical Seismicity in Expert 3's Zone 5 of the 1993-EUS-Update Study.....	50
5.5:	Location of the Faults Relative to the Site and the Eastern Tennessee Seismic Zone (ETSZ).....	51
5.6:	1998-TIP Study. Comparison of the Best Estimate Hazard Curves Obtained Using the Highest Weighted Map (Map 1) to that of a Typical Fault Map.....	51
5.7:	Effect of the Ground Motion Saturation at 10 km in the Ground Motion Model. Comparison of Best Estimate Hazard Estimates with and without Saturation.....	52
5.8a:	1998-TIP Study. Contribution of the Bins of Distance to the Total Hazard at the Watts Bar Site with the Non-Truncated Ground Motion Model.....	53
5.8b:	1998-TIP Study. Contribution of the Bins of Distance to the Total Hazard at the Watts Bar Site with the Ground Motion Model Truncated at Distances below 10 km.	53
5.9:	Range of Earthquake Magnitudes that Contribute to the Hazard for the 1998-TIP Seismicity Model Combined with the 1993-EUS-Update Ground Motion Model.....	54

6.1:	Comparison of the Mean Uniform Hazard Spectra for Return Periods of 100,000 and 10,000 Years Between the 1998-TIP Seismicity Model and Expert 3 of the 1993-EUS-Update Study Both Using the TIP Ground Motion Model.....	56
6.2:	Mean Spectral Hazard Curves for 2.5 Hz and 25 Hz using the 1998-TIP Ground Motion Model and both the 1998-TIP and 1993-EUS-Update Expert 3 Seismicity Models.....	57
6.3:	Cumulative Contribution of the Magnitude Bins to the Total Hazard for a 100,000-yr Return Period at 2.5 Hz.....	57
6.4:	Cumulative Contribution of the Distance Bins to the Total Hazard for a 100,000-yr Return Period at 2.5 Hz.....	58
6.5:	Comparison of the Yearly Rate of Earthquakes Occurrence within 75 km of the Watts Bar Site between the Best estimate 1998-TIP Seismicity Model (Map 1) , the Median Best Estimate 1993-EUS-Update Seismicity Model, and Expert 3's Seismicity Model.....	58
6.6:	Rate of Earthquakes Versus Magnitude around the Site Using the 1998-TIP Seismicity Model for Distances of 33 km, 81 km, and 156 km All Normalized to 35 km.....	59
6.7:	Rate of Earthquakes around the Site Using the 1993-EUS-Update Expert 3's Seismicity Model (X3), for Distances of 35 km, 75 km, and 150 km, All Normalized to 35 km.....	60
6.8:	Enlarged view of Expert 3's Seismic Source Map Showing Zone 1 as a Large Background Zone with Low Rate of Seismicity.....	61
7.1:	Comparison of Results for Vogtle.....	65

Tables

4.1	Best Estimate Earthquake Budgets of Earthquakes with Magnitudes Greater than 3.5 within 33 km of Watts Bar in the 1998-TIP Study, for Bollinger Alone and for the 1998-TIP Composite Seismicity Model.....	38
4.2	Contribution of Selected Seismic Zones to the Budget of Earthquakes Greater Than Magnitude 3.5 within 33 km of Watts Bar, in the 1998-TIP Study.....	38

EXECUTIVE SUMMARY

Probabilistic Seismic Hazard Analysis (PSHA) is a methodology that estimates the likelihood that various levels of earthquake-caused ground motion will be exceeded at a given location in a given future time period. Due to large uncertainties in all the geosciences data and in their modeling, multiple model interpretations are often possible. This leads to disagreement among experts, which in the past has led to drastically different estimates of the seismic hazard at a site and can lead to disagreement on the selection of ground motion for design at a given site.

From 1981 to 1989, Lawrence Livermore National Laboratory (LLNL) developed for the U.S. Nuclear Regulatory Commission (NRC) a method for performing PSHA in the Eastern US; results were documented in NUREG/CR-5250. Improvements in the handling of the uncertainties led to updated results, documented in the 1993-EUS-Update study (NRC, 1993, NUREG-1488). These results were substantially different from those of the utilities-sponsored study by the Electric Power Research Institute (EPRI.)

To improve on the overall stability of the PSHA process, the NRC and the Department of Energy with EPRI co-sponsored a project to provide methodological guidance on how to perform a PSHA; the goal was to narrow the spectrum of possible estimates of hazard at a given site.

The project was carried out by a seven-member Senior Seismic Hazard Analysis Committee (SSHAC) supported by a large number of other experts, who examined ways to improve on the state-of-the-art, the results of which are documented in NUREG/CR-6372 (1997).

As a follow-up to the SSHAC study, the Trial Implementation Project (TIP) used the SSHAC recommendations and developed a set of more detailed guidance for performing PSHA. The TIP project tested the more complicated issue of development of the seismic zonation and seismicity models. It was found that the uncertainty generated by artificial disagreements among experts could be considerably reduced through interaction and discussion of the

available data and by identifying the elements common to all experts' interpretations. By concentrating on those elements, it was possible to develop a consensus of the group on the way to characterize them and eliminate large unnecessary differences. The TIP study considered two sites with different seismic environment in the Southeast US: Vogtle, in South Carolina, which is affected by the issue of the Charleston earthquake, and Watts Bar, close to the Eastern Tennessee Seismic Zone (ETSZ), which is a theater of small-to-medium-magnitude seismic events. The results of the TIP study (this report) were found to be different from those of the 1993-EUS-Update study for the Watts Bar site.

This study compares the results of the 1993-EUS-Update and the 1998-TIP studies and identifies the reasons for the differences as:

1. Differences in the ground motion (GM) attenuation models.
2. Introduction of the ETSZ in the TIP study.

It was found that these two factors accounted for a factor of 5 difference in mean estimates of peak ground acceleration (PGA) hazard at high GM levels as shown in Figure Exec-1 below. The agreement between the two studies improved at lower PGA values. The results were in better agreement and differed only by about a factor of 2 at high GM levels when the same GM model was used with each seismicity model. Finally, it was found that the composite rate of earthquakes around the Watts Bar site was about a factor of 2 higher for the TIP composite seismicity model than for the composite 1993-EUS-Update seismicity model.

The root causes for the differences were found to be a combination of characteristics proper to the Watts Bar site, such as the site-specific source zones characterization, and more generic ones such as the modified GM model. Studies of other sites, depending on whether and what new information is available, could have similar conclusions (or not, such as in the case of Vogtle, for which the mean estimates of the hazard decreased between the EUS 1993 and the TIP 1998 studies).

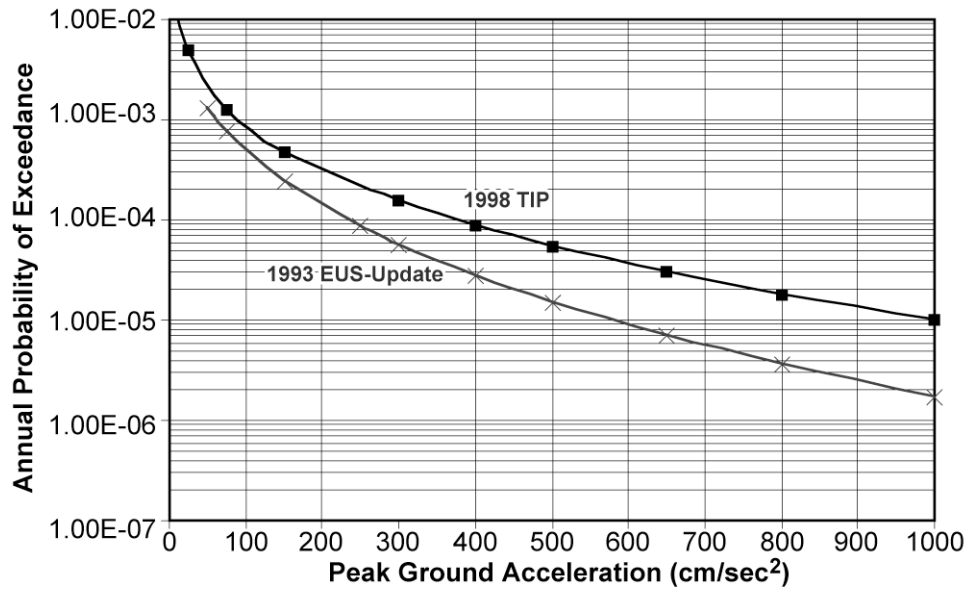


Figure Exec-1: Comparison of the Mean Estimates of the Seismic Hazard for the Watts Bar Site. The Curve with the Square Markers is for the Estimates of the 1998-TIP Study. The Curve with the Crosses is for the Estimates of the 1993-EUS-Update Study.

ACKNOWLEDGMENTS

This project was sponsored by the U.S. Nuclear Regulatory Commission (NRC). The project manager for the NRC was Ernst Zurflueh, and Jean Savy led the project for Lawrence Livermore National Laboratory. Don Bernreuter, who has been working on these methodologies and specifically on the NRC projects at LLNL since 1994, did all the calculations and sleuthing for sections 2 to 7.

ABBREVIATIONS

APE	Annual Probability of Exceedance
BE	Best Estimate
CEUS	Central and Eastern United States
DOE	Department of Energy
EPRI	Electric Power Research Institute
ETSZ	Eastern Tennessee Seismic Zone
EUS	Eastern United States
GM	Ground Motion
LLNL	Lawrence Livermore National Laboratory
NRC	Nuclear Regulatory Commission
PGA	Peak Ground Acceleration
PGV	Peak Ground Velocity
PSHA	Probabilistic Seismic Hazard Analysis
PSV	Peak Seismic Velocity
RP	Return Period (Inverse of Annual Probability of Exceedance)
SRS	Savannah River Site
SSHAC	Senior Seismic Hazard Analysis Committee
TIP	Trial Implementation Project

1. INTRODUCTION

1.1 Background

Probabilistic Seismic Hazard Analysis (PSHA) is a methodology that estimates the likelihood that various levels of earthquake-caused ground motion will be exceeded at a given location in a given future time period. Due to large uncertainties in all the geosciences data and in their modeling, multiple model interpretations are often possible. This leads to disagreement among experts, which in the past has led to disagreement on the selection of ground motion for design at a given site.

From 1981 to 1989, Lawrence Livermore National Laboratory (LLNL) developed for the Nuclear Regulatory Commission a method for performing PSHA in the eastern United States; results were documented in NUREG/CR-5250. Improvements in the handling of the uncertainties led to updated results, documented in the 1993-EUS-Update study (NUREG-1488.) These results were substantially different from those of the utilities-sponsored study performed by the Electric Power Research Institute (EPRI.)

In 1994, in order to review the present state-of-the-art and improve on the overall stability of the PSHA process, the U.S. Nuclear Regulatory Commission (NRC) and the U.S. Department of Energy (DOE) with the Electric Power Research Institute (EPRI) co-sponsored a project to provide methodological guidance on how to perform a PSHA.

The project was carried out by a seven-member Senior Seismic Hazard Analysis Committee (SSHAC) supported by a large number of other experts.

The SSHAC reviewed past studies, including the Lawrence Livermore National Laboratory and EPRI landmark PSHA studies of the 1980s, and examined ways to improve on the present state-of-the-art.

The Committee's most important conclusion was that differences in PSHA results are due to procedural rather than technical differences. Thus, in addition to providing a detailed documentation on state-of-the-art elements of PSHA, the SSHAC report (NRC, 1997) provided

a series of procedural recommendations. As part of the SSHAC effort, the recommendations of the SSHAC were partially tested in the development of a ground motion attenuation model for North America. That test had been selected because of the relative simplicity of formulation of the ground motion attenuation models. The issues to be discussed and the input to be generated are limited to the characterization of a few well-defined single parameters. In contrast to the case of the development of ground motion attenuation models, the development of seismic zonation maps involves the evaluation of multidimensional data sets. Descriptions of future seismicity by seismic zonation maps and occurrence models are multi-parameter models with very complex formulation and correlation structure.

Although the SSHAC did not test its recommendations on the development of zonation and seismicity models, it was understood that the recommendations provided were general enough to apply to any problems in which it is important to characterize epistemic uncertainty through the use of multiple experts' inputs, including the case of seismic source zonation modeling.

Under the TIP project (W6496, Testing and Implementation of SSHAC Guidelines), new expert elicitations and seismic hazard calculations were performed by Lawrence Livermore National Laboratory (LLNL) for the southeastern United States using the SSHAC guidelines. Included in the study were site-specific hazard evaluations for the Savannah River and Eastern Tennessee areas. It was found that, for the Eastern Tennessee area, the hazard in terms of annual probability of exceedance was several times larger than that of the previous regional LLNL hazard estimates for the central and eastern United States (CEUS) (1993-EUS-Update study).

This observation emphasizes the importance of conducting site-specific hazard assessments, for instance, for plant site investigations. Because a part of the Eastern Tennessee Seismic Zone (ETSZ) was included in the specific location for which a hazard value was derived, the question of using an exclusion zone arises.

1.2 Purpose of the Study, Scope

This study investigates the causes of differences in probabilistic hazard estimate between the 1998-TIP and the 1993-CEUS-Update studies:

1. It evaluates the validity of the new results, which may be affected by the replacement of the ETSZ boundaries, the seismicity rates in the subunits of the ETSZ, and the choice

of the ground motion attenuation parameters.

2. It compares the two studies and identifies the reasons for the differences.
3. It performs sensitivity studies to isolate the parameters responsible for the differences

2. DIFFERENCES IN HAZARD ESTIMATES

The 1993-EUS Update Study was actually an update of the 1989 study performed by LLNL for the NRC (Bernreuter et al., 1989). The seismic zonation models were developed by sampling the interpretations of 11 experts and the ground motion attenuations were developed by sampling a set of 8 ground motion experts. In 1992, LLNL performed a new PSHA for the Savannah River Site (SRS), located at the boundary between South Carolina and Georgia. The concept of a composite ground motion model was developed for SRS and applied to the entire EUS. These results are summarized in Figure 2.1.

The development of the composite ground motion model was based on sampling the interpretation of the GM experts and generating an artificial database of estimates of ground motion for many pairs of distances and magnitudes. Including the full distributions of possible models for each expert included the epistemic uncertainty, and the physical correlation was modeled by preserving the correlation observed in the original models in the final composite model. The elicitation of the experts' interpretation was performed according to a process, which in large part became the process adopted by SSHAC. It had all the essential elements that constitute the SSHAC recommendations. This composite model was very different from the GM models used in the previous NRC study (Bernreuter et al. 1989) and warranted a re-estimation of the seismic hazard at the 69 EUS sites. The 1993-EUS-Update then essentially used the same seismic zonations as the 1989 study, but it used the newly developed SRS/EUS composite GM model, and in addition all of the seismicity experts' estimates of the seismicity rates were re-evaluated, with new elicitation of the experts' interpretations, to eliminate the unrealistic seismicity interpretations which had been identified for some of the zones of the 1989 study. The TIP study was performed later, to demonstrate that SSHAC principles could also be applied to the seismic zonation and seismicity modeling.

Figure 2.1 shows the final estimates of the mean annual probability of exceedance (APE) of the Peak Ground Acceleration (PGA) for the 1993-EUS-Update and 1998 TIP studies.

At higher PGA values (1000 cm/sec^2) the APE from the 1998-TIP study is about a factor of 5 higher than for the 1993-EUS-Update study. However, at low PGA values (100 cm/sec^2) the results from the two studies are in better agreement (a factor of 1.6).

Similarly, Figure 2.2 gives a comparison between the median in the APE. In this case, there is over a factor of 10 differences between the two studies at high PGA values and a factor of 2.5 at 100 cm/sec^2 . Comparisons between other hazard estimators show similar differences. Figure 2.3 shows the comparison between the best estimate (BE) hazard curves from the two studies. The BE estimator is not a true statistical estimator. The so termed BE hazard curve is based on using only the mode of the probability distribution of each of the seismicity continuous parameters (such as rate, upper bound magnitude) and the highest weighted zonation map.

Figures 2.1 to 2.3 show consistently that there is a significant difference in the estimation of the seismic hazard between the two studies at long return periods. Since the Hazard calculation algorithms were common to the two studies, the reasons for these differences lie in the actual inputs to the calculations. The possible causes of differences in the APE estimates are listed below:

- Differences in ground models including uncertainty modeling.
- Differences in seismic zones.
- Differences in the estimation of the rates of occurrence of earthquakes (a and b values) and independent estimates for discrete magnitudes.
- Differences in the estimation of the upper bound magnitudes.
- Differences in the uncertainty modeling.

In the following sections, we examine these issues and their impact on the estimation of the seismic hazard at the Watts Bar site and draw conclusions on the causes of differences.

It is interesting to note the hazard estimates from the two studies are in reasonable agreement at

return periods of less than 1000 years (PGA levels less than 0.1G) where estimates are primarily controlled by the data rather than by predictive models, which inherently include greater uncertainties for lack of sufficient data.

At long return periods (PGA levels greater than 0.5G), the estimates are controlled as much by the uncertainty models as by the historical seismicity data

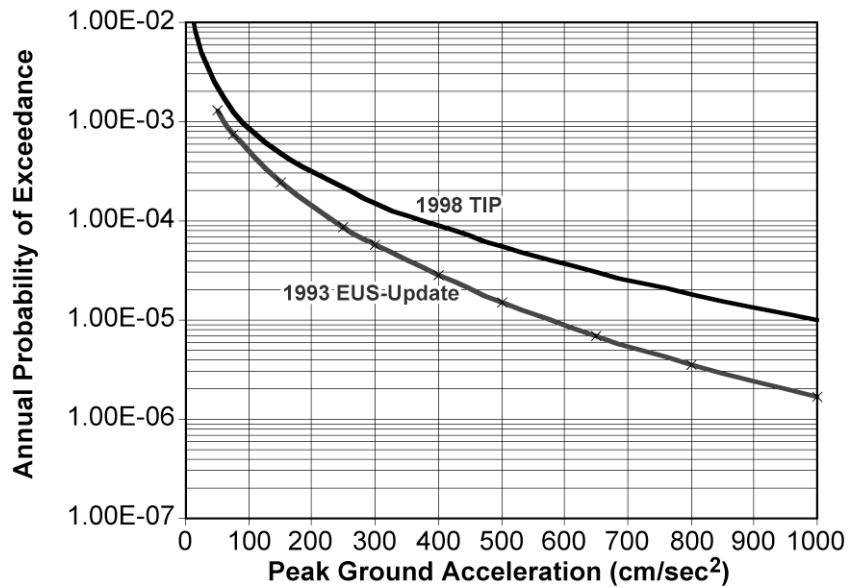


Figure 2.1: Mean PGA hazard estimates for Watts Bar.

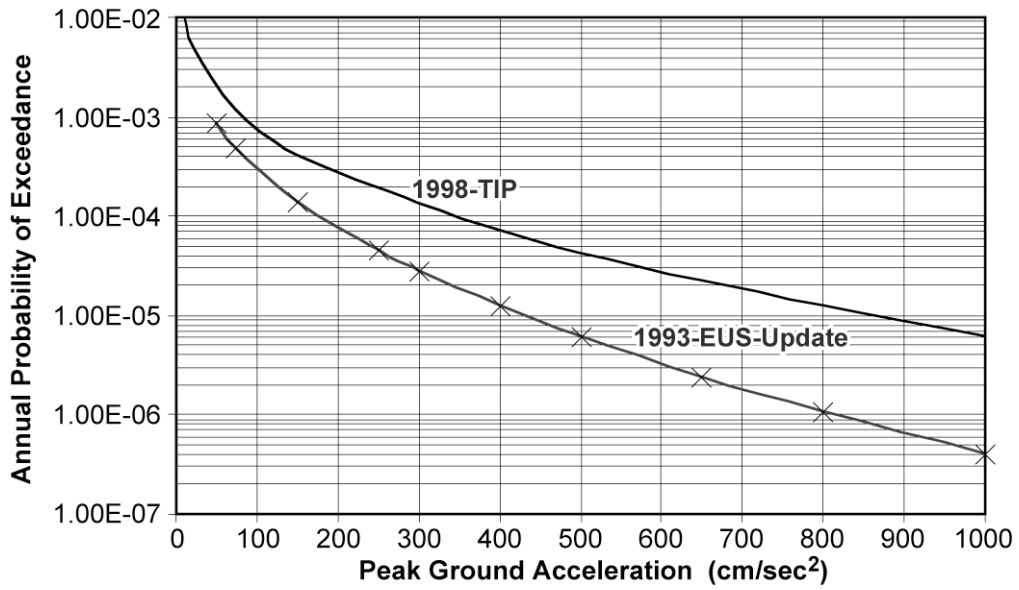


Figure 2.2: Median PGA Hazard Estimates for Watts Bar.

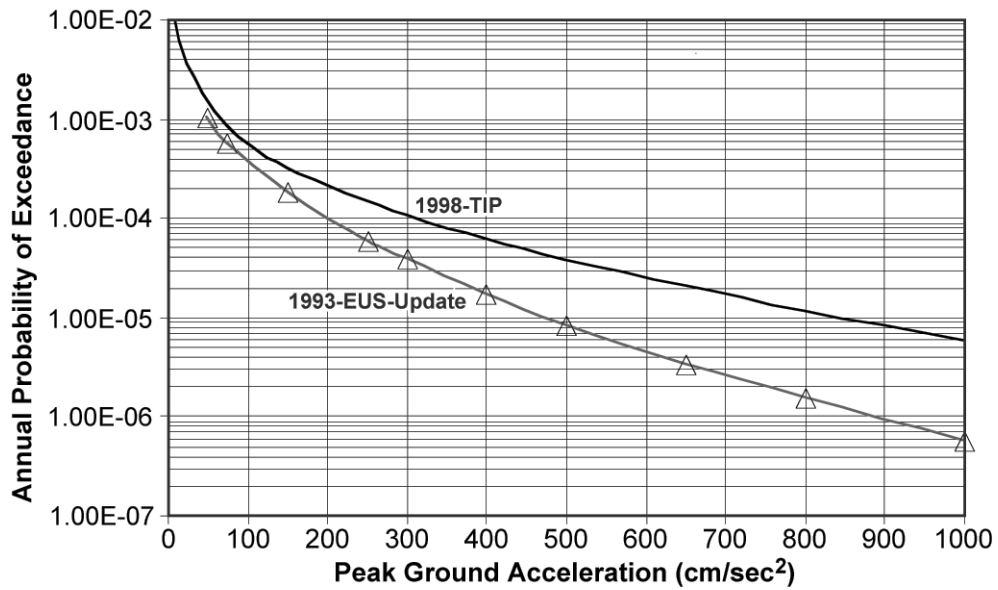


Figure 2.3: "Best Estimate" PGA Hazard for Watts Bar.

3. IMPACT OF THE GROUND MOTION MODELS

3.1 Direct Comparison of the Ground Motion Models Used in the Two Studies

Two different composite GM models were used in the two studies. For ease of reference, the GM model in the TIP study is referred to as the 1998-TIP GM model, and the model in the 1993 study as the 1993-EUS-Update GM model. Let us first examine the two GM models in terms of estimates of PGA for given pairs of magnitudes and distances. Figure 3.1a shows a comparison between the median estimates of ground motion for three magnitudes and a range of distances between 5 and 100 km. The 1993-EUS-Update model had a built-in saturation at 10 km, meaning that the median estimate of the PGA ground motion for distances less than 10 km is equal to its value for 10 km.

These estimates are shown to be in reasonable agreement for distances between 10 km and 100 km, which is the range of distance in which most of the available data fell at the time of the two studies. For distances smaller than 10 km, the saturation imposed on the 1993-EUS-Update model makes it lower than the other model. That area immediately around the site generally does not contribute enough seismicity to have an impact on the total hazard.

The epistemic uncertainty in the 1998-TIP study was included by providing a probability distribution function on the standard deviation on the natural logarithm (σ), with a minimum bound of 0.36, a mode of 0.63 (also labeled BE, for “Best Estimate”), and an upper bound of 0.94.

Combining the inputs of eight GM Experts and using a simulation process to include their complete uncertainty developed the 93-EUS-Update GM model. The experts’ input was in the form of estimates of the probability distribution function of the ground motion (PGA or peak seismic velocity, PSV) at the sites for a selection of distances and magnitudes. The resulting model was obtained as an empirical distribution of several of the percentiles (a different empirical model for each percentile.)

By contrast, the 1998-TIP model used a similar approach with the inputs from five GM experts.

It assumed that the probability distribution function of GM for a given magnitude and distance is lognormal, with a given median and σ , the standard deviation of the log (GM). Thus, when comparing the two models, it is important to refer to the appropriate percentiles. For example, in this study, at times, the medians are compared, i.e., the 50% percentile model for the 1993-EUS-Update and the “mean attenuation” for 1998-TIP. Similarly, in other instances the 85th percentile 1993-EUS-Update and the (mean + 1σ) values are computed.

To directly compare the 1998-TIP model to the 1993-EUS-Update model would have required us to run a simulation over the range of sigma, then develop the percentiles. We did not attempt to carry out this simulation. The effect of the relative difference between the two models is shown in Figure 3.2a where we compare the 1-sigma value of the 1998-TIP GM model using the BE estimate for sigma (0.63) to the 85 percentile estimate for PGA from the 1993-EUS-Update GM model.

Figure 3.2b shows clearly the relative impact of the two models for the range of conservatism frequently used in seismic design parameters. It shows the ratio of GM estimates (1998-TIP/1993-EUS-Update) at the 85th percentile level, between 10 and 100 km of distance and for magnitudes between M5 and M7.

In the magnitude range of 5-6 and distance ranges 0-30 km Figure 3.1b shows that the 1998-TIP GM model gives higher PGA estimates than the 1993-EUS-Update GM model. A strict comparison of the two simulated distributions could probably have led to slightly different observations. This would have made the differences between the two models even larger in the most important range of magnitudes between 5 and 6.

Comparing Figure 3.1b with 3.2b shows that the total uncertainty is larger for the 1998-TIP than for the 1993-EUS-Update GM model. Since the aleatory uncertainty was in the same order of magnitude, the observation shows that the epistemic uncertainty was higher in the 1998-TIP than in the 1993-EUS-Update study.

3.2 Comparison of the Hazard Estimates

In order to understand better how the GM model affects the results, it is necessary to determine the magnitude and distance range that contribute most to the estimates of the hazard as shown in Figures 3.3, 3.4, and 3.5 for the 1998-TIP study.

These figures show that 80 percent of the hazard comes from the distance range 0-40 km and a magnitude range 5-6, which was shown in Figure 3.2 to be the region where the two GM models significantly differ. In addition, the uncertainty in sigma for the 1998 TIP GM model would also increase the differences between the two GM models. Thus, everything else being equal, it is expected that the two GM models would lead to potentially different hazard results, with higher estimates for the 1998-TIP GM model.

3.3 Sensitivity to the Ground Motion Models

Using a common zonation and seismicity model, namely the 1998-TIP model, the hazards estimates are compared directly in terms of the mean hazard curves in Figure 3.6, and the median hazard curves in Figure 3.7, for both 1998-TIP and 1993-EUS-Update GM models.

Similarly, Figures 3.8 and 3.9 compare the mean and median hazard curves using the 1993-EUS-Update zonation and seismicity, and alternatively the TIP and 1993-EUS-Update GM models.

Figures 3.6 to 3.9 show that, as expected, changing GM models has an impact on the hazard. It is interesting to note that the difference in the hazard estimates is larger for the median hazard estimate than for the mean hazard estimate. The impact of the GM model is less for smaller PGA values than larger PGA values. Lastly, it is observed that the effect of changing GM models is larger for the 1993-EUS-Update seismicity model than for the 1998-TIP seismicity model. This last observation is consistent with the fact that the 1993-EUS-Update study had larger area source zones including the Watts Bar site, whereas the 1998-TIP study had smaller zones and local faults, farther from the site. In the latter, the seismicity appeared to be restrained to be more distant from the site.

Figure 3.10 shows the contribution of magnitudes to the mean and median hazard curves at PGA levels of 150 and 1000 cm/sec² for the Watts Bar site using 1998-TIP seismicity and the 1998-TIP GM model.

A similar comparison using the 1993-EUS-Update is difficult because there are 11 seismic zonation and seismicity models and some sort of averaging would be required. However, it was found that expert 3's (Bollinger) results were a good proxy representation of the combined 1993-EUS-Update results as shown in Figure 3.11. Based on this figure, we conclude that for the needs of this study, expert 3's seismicity model is a reasonable proxy model for the 11 1993-EUS-Update experts. Figure 3.12a shows results similar to those shown in Figure 3.10 but based on expert 3's seismicity model. Figure 3.12b compares the contribution to the hazard for 1G PGA, from Figures 3.10 and 3.12a.

Figure 3.12a is similar to Figure 3.10 but shows that earthquakes in the magnitude 5.5 ranges contribute more to the hazard. This is also apparent in Figure 3.12b. Thus, we might expect that the change in the GM model would have more effect for the 1993-EUS-Update seismicity case than for the 1998-TIP case, as seen in Figures 3.8 and 3.9.

3.4 Sensitivity to the Seismic Zonation and Seismicity Models

Figure 3.13 compares the mean hazard curves for the case of 1998-TIP seismicity and GM model to the case of the 1993-EUS-Update seismicity and the 1998-TIP GM model. This figure shows the 1998-TIP results to be a factor of 2 greater than with the 1993-EUS-Update seismicity, as compared to a factor of 6 observed from Figure 2.1 when different GM models were used.

Figure 3.14 compares the median hazard curves between the case of 1998-TIP seismicity and 1998-TIP GM model to the case of the 1993-EUS-Update seismicity and the TIP GM model. We see from this figure that the difference between the two hazard curves is about a factor of 2.3 as compared to a factor of 10 observed in Figure 2.2. When the same GM model is used for the two sets of seismicity models, the difference between the two studies is greatly reduced.

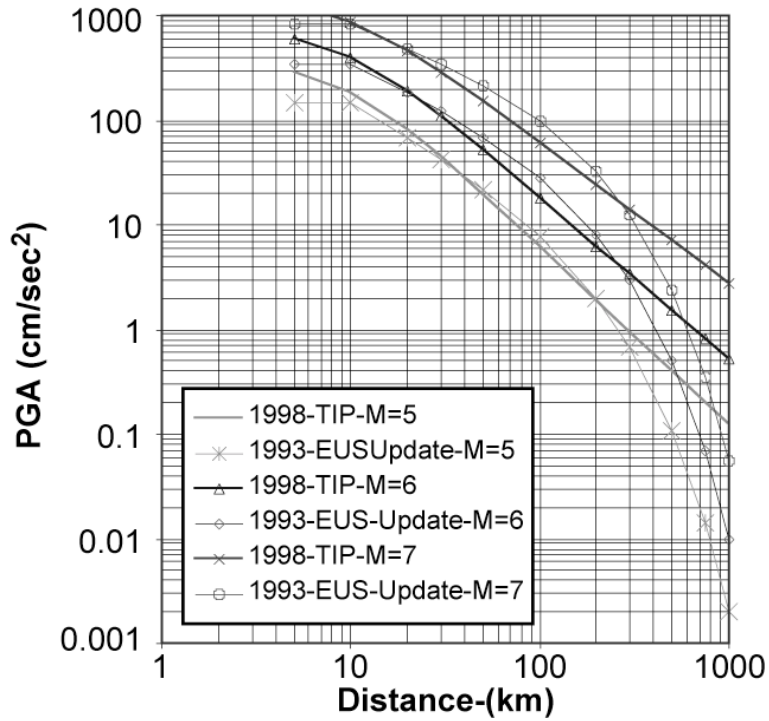


Figure 3.1a: Comparison of the Median Ground Motion Attenuation Models for the 1993-EUS-Update and 1998-TIP Studies for Magnitudes 5, 6, and 7.

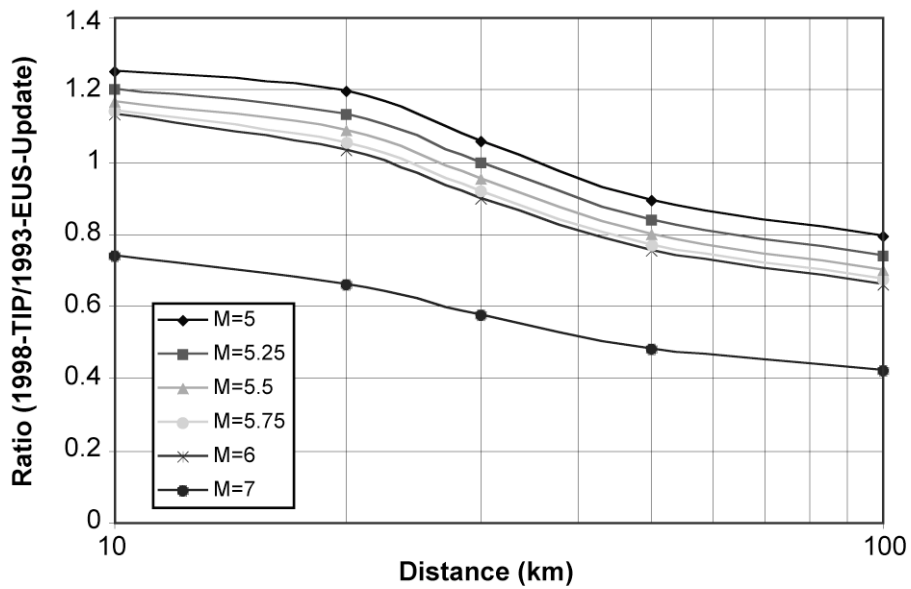


Figure 3.1b: Ratios of the Median PGA Estimates from the 1998-TIP Study, Divided by the 1993-EUS-Update Median Estimates, as a Function of Distance.

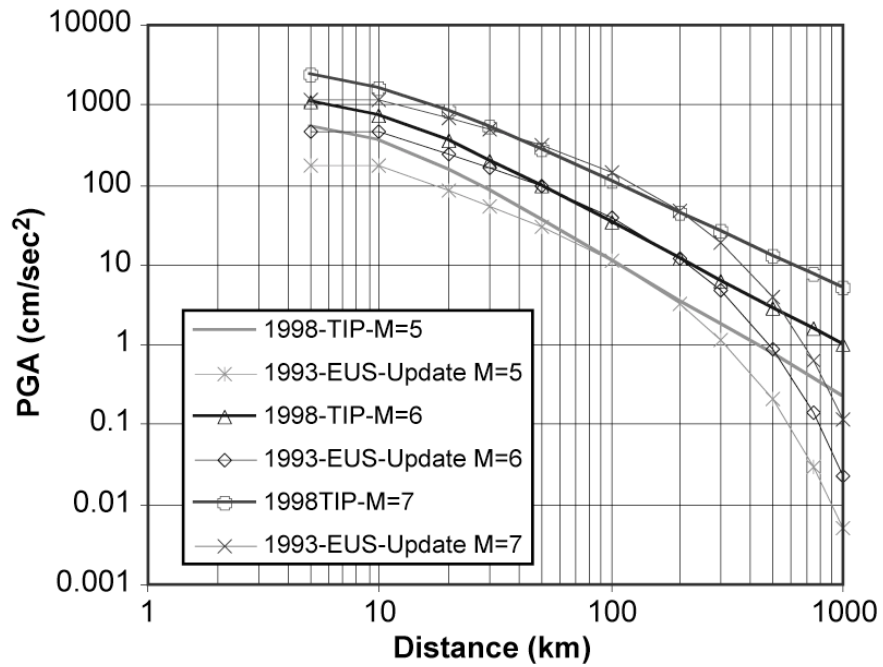


Figure 3.2a: Comparison Between the 1-sigma 1998-TIP and the 85% 1993-EUS Updated Ground Motion Attenuation Models.

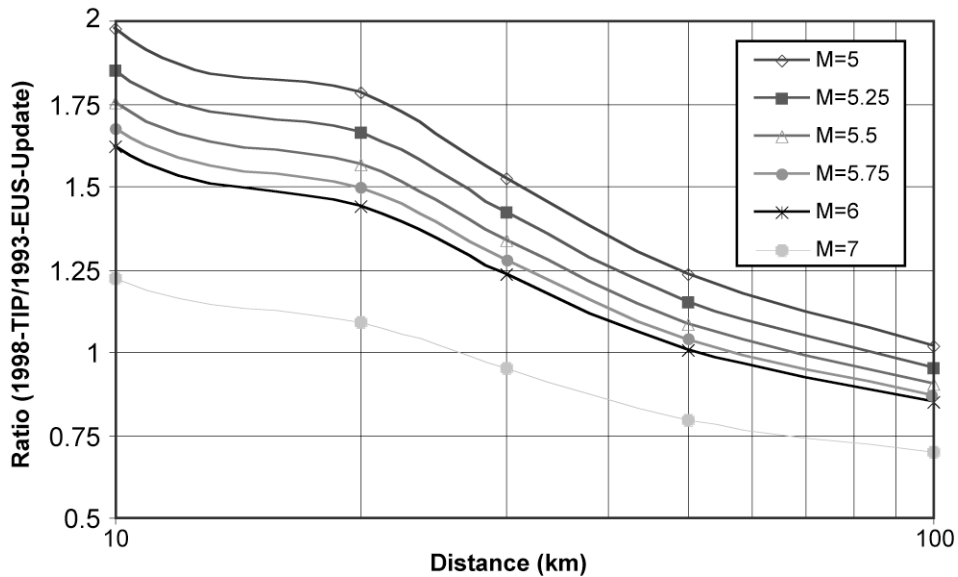


Figure 3.2b: Ratios of the 1-Sigma PGA Estimates from the 1998-TIP Study, Divided by the 1993-EUS-Update Median Estimates, as a Function of Distance.

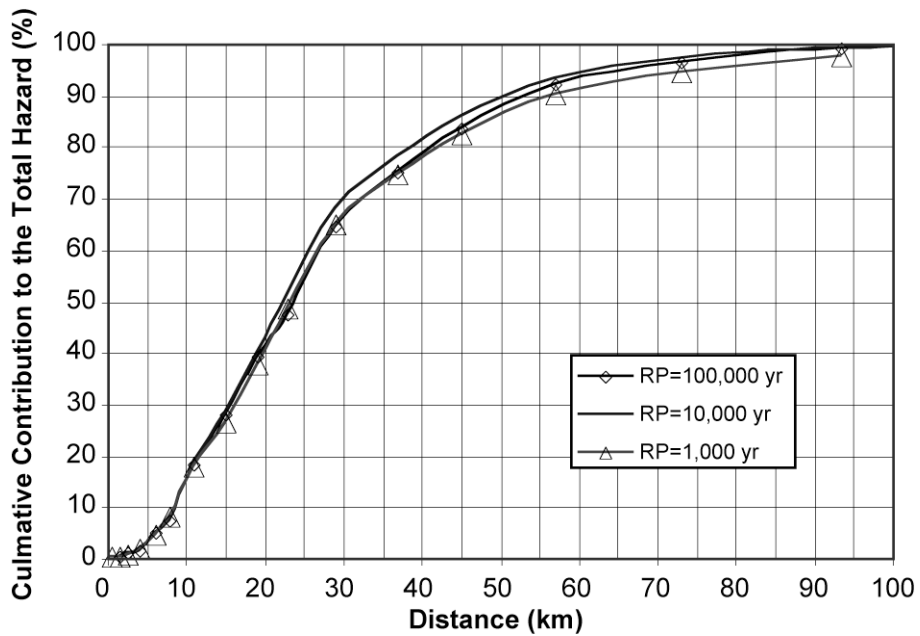


Figure 3.3: Cumulative Contribution of the Distance Bins to Hazard in the 1998-TIP Study. Seismic Source Zones within 40 km of Watts Bar Contribute Approximately 80% of the Total Hazard.

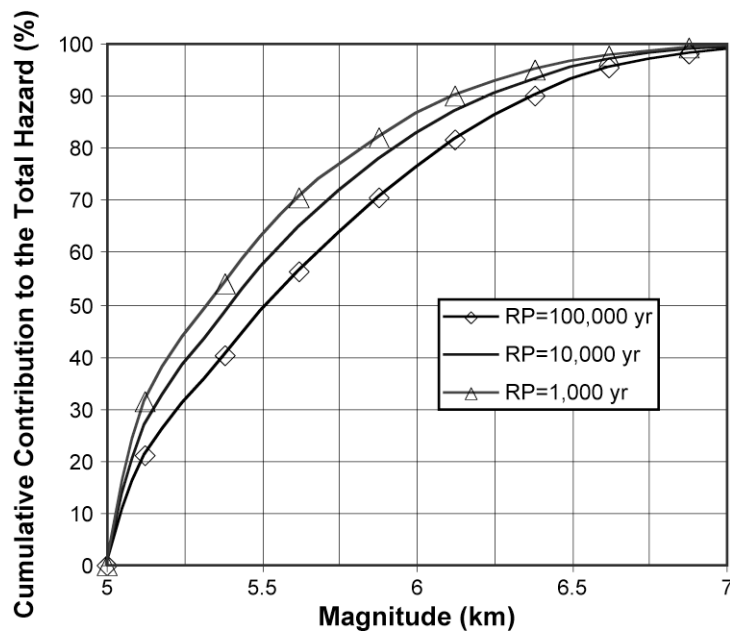


Figure 3.4: Cumulative Contribution of the Magnitude Bins to the Hazard in the 1998-TIP Study. Magnitude Events Smaller Than 6 Contribute Approximately 80% of the Total Hazard.

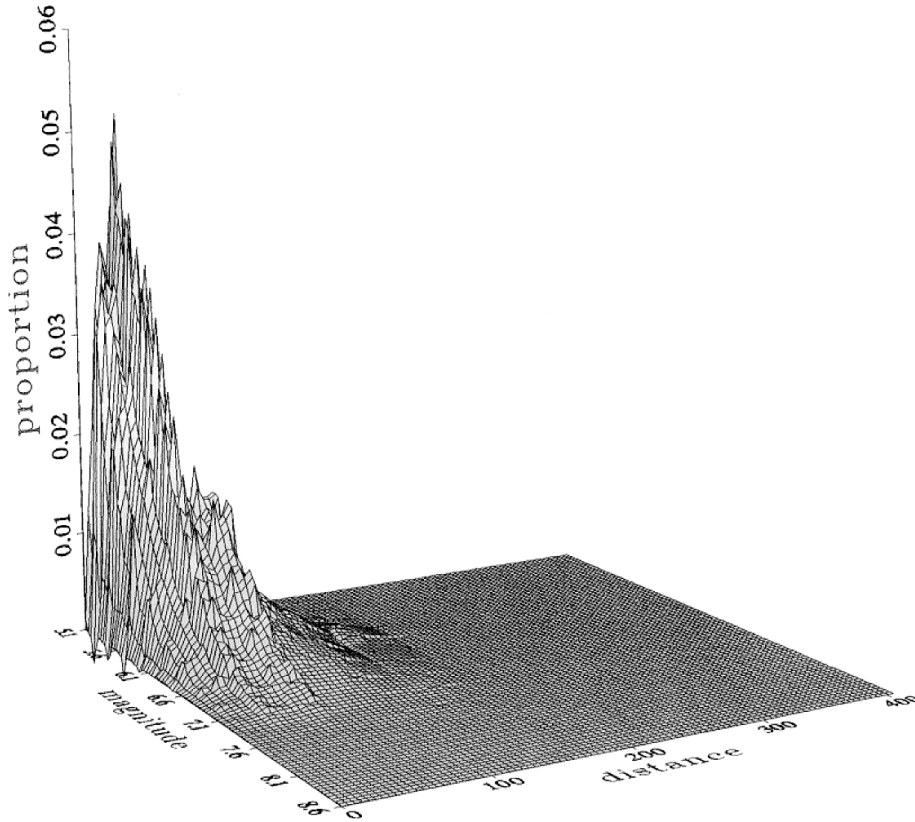


Figure 3.5: Contribution of the Magnitude–Distance Bins to the Total Hazard for a 10,000-Year Return Period.

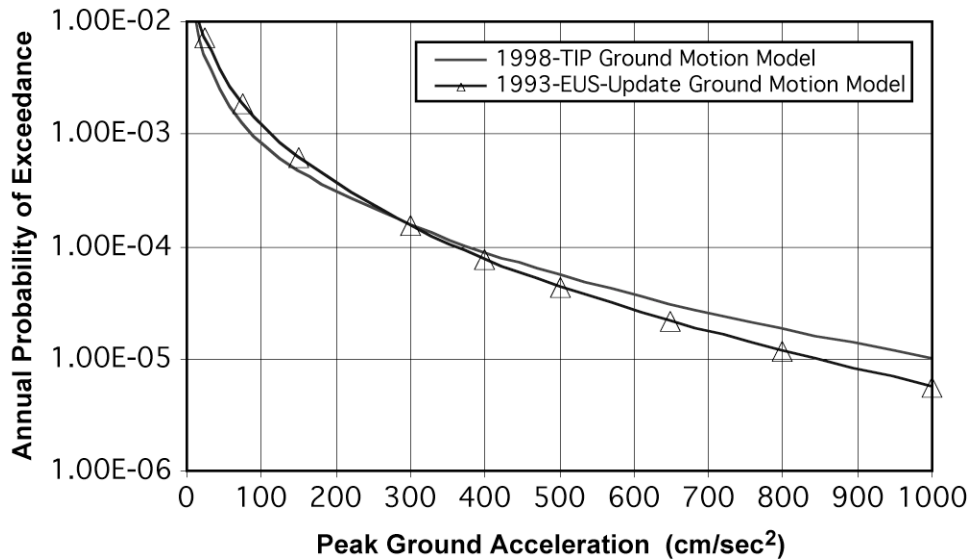


Figure 3.6: Estimates of the Mean Hazard Using the 1998-TIP Seismic Zonation. Comparison between the 1993-EUS-Update and 1998-TIP Ground Motion Attenuation Models.

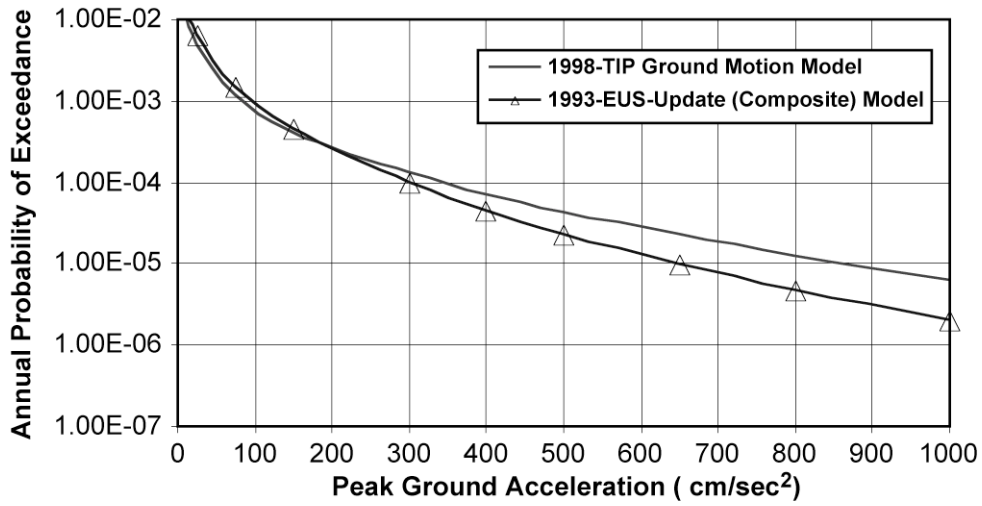


Figure 3.7: Estimates of the Median Hazard Using the 1998-TIP Seismic Zonation. Comparison between the 1993-EUS-Update and 1998-TIP Ground Motion Attenuation Models.

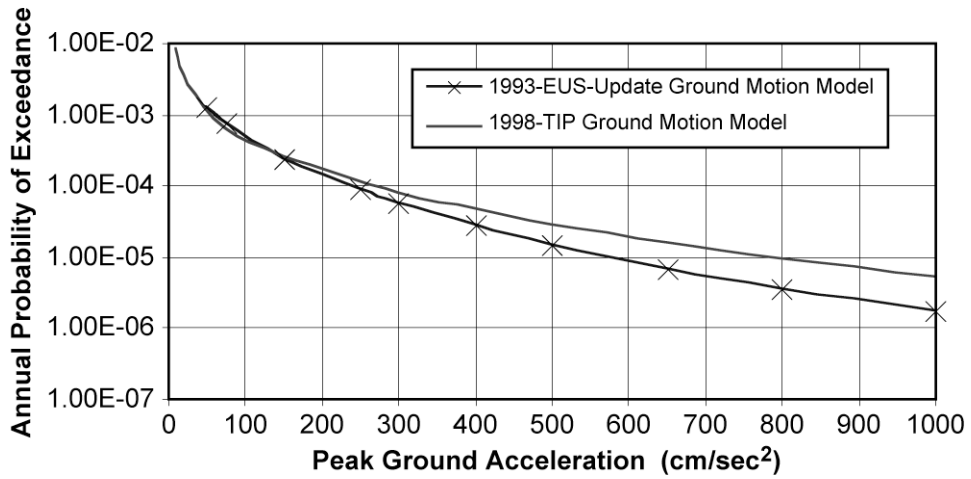


Figure 3.8: Estimates of the Mean Hazard Using the 1993-EUS-Update Zonation. Comparison between the 1993-EUS-Update and 1998-TIP Ground Motion Attenuation Models.

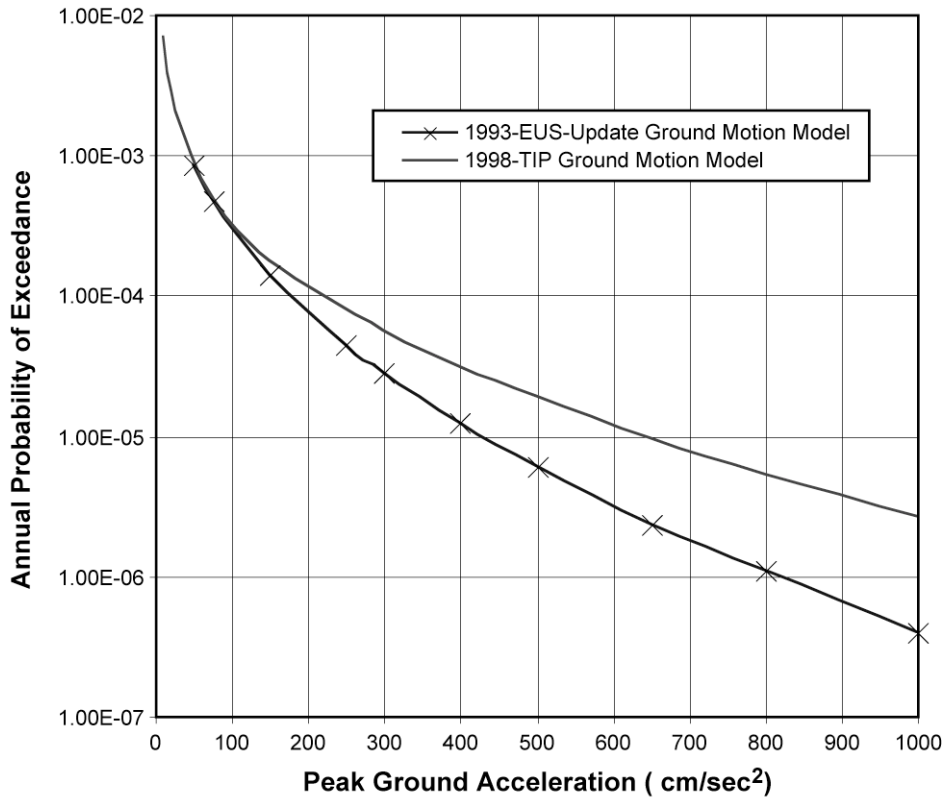


Figure 3.9: Estimates of the Median Hazard using the 1993-EUS-Update Seismic Zonation. Comparison between the 1993-EUS-Update and 1998-TIP Ground Motion Attenuation Models.

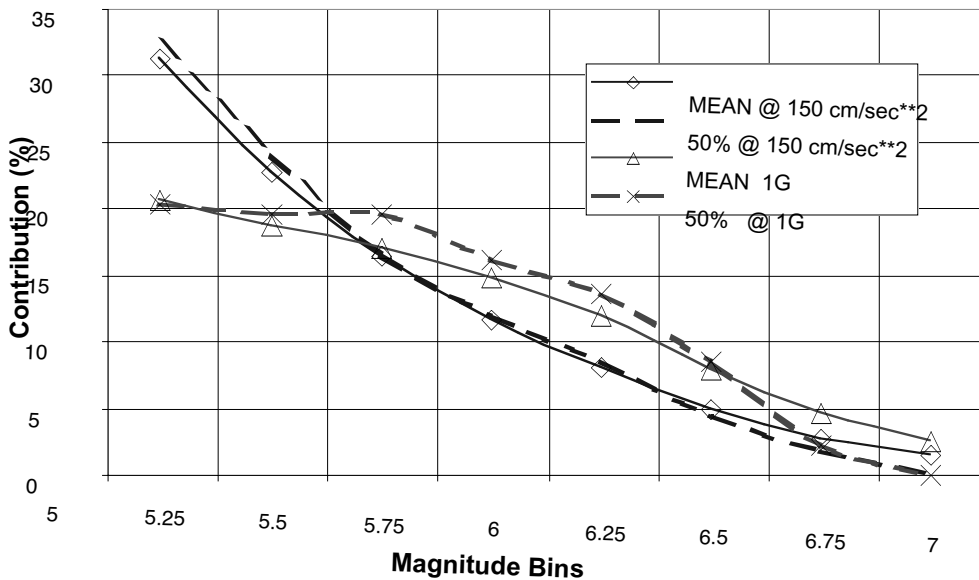


Figure 3.10: Contribution of Magnitude Bins to the Total Hazard in the 1998-TIP Study for Two Peak Ground Acceleration Levels.

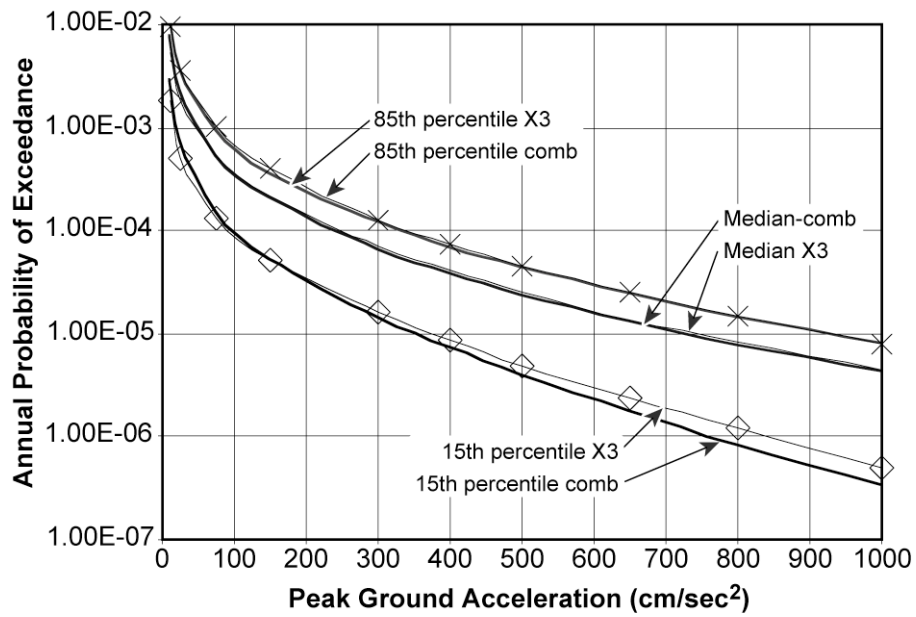


Figure 3.11: Results of the 1993-EUS-Update Study. Comparison of the Mean Estimates of the Hazard between the 11 Experts (comb) and Expert 3 (X3).

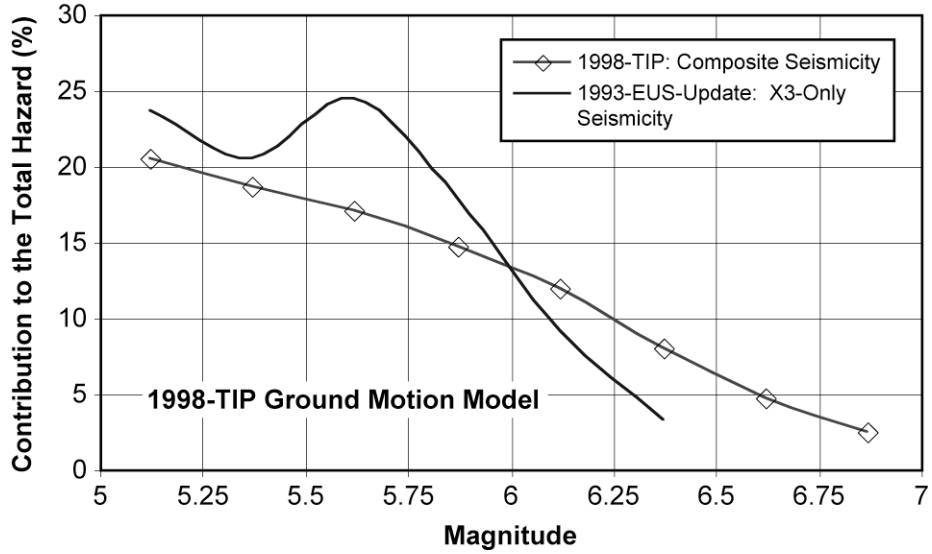


Figure 3.12a: Contribution of Magnitude Bins in the 1993-EUS-Update Study for Two Peak Ground Acceleration Levels for the Case of Expert 3.

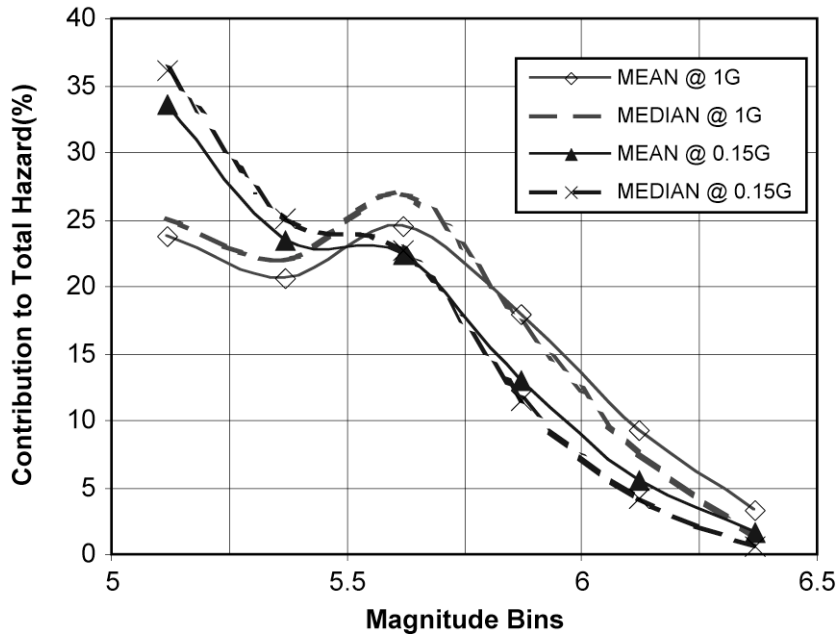


Figure 3.12b: Comparison of the Magnitude Contributions for a 1G PGA Using the 1998-TIP Ground Motion Model. The Seismicity of Expert 3 (X3) Leads to a Strong Mode at M5.6 and the 1998-TIP Composite Seismicity Leads to a Monotonically Decreasing Contribution.

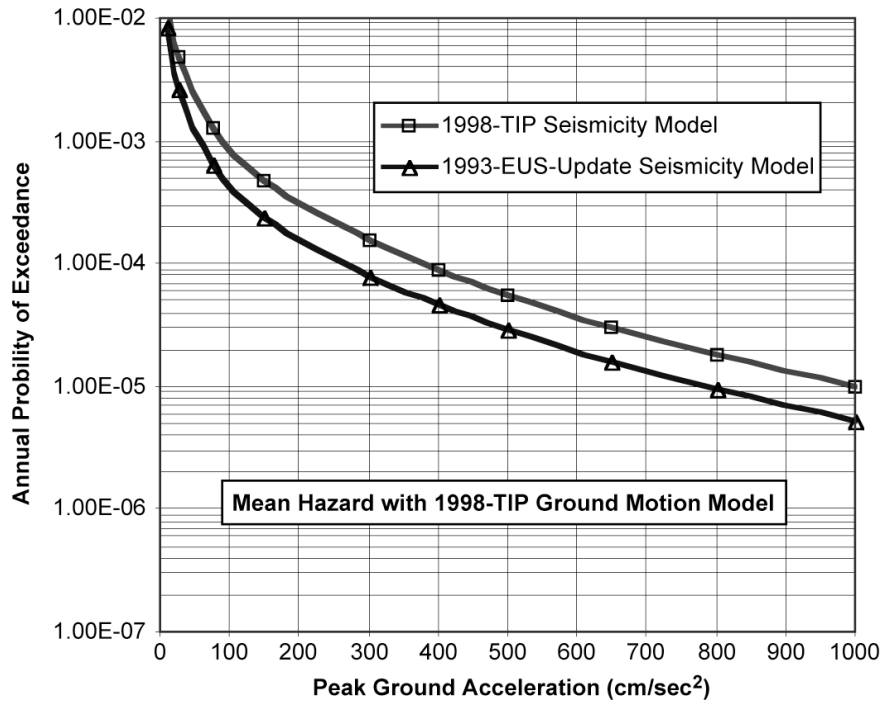


Figure 3.13: Sensitivity to the Seismicity and Zonation Model. The Two Curves Represent the Mean Hazard Estimated with the 1998-TIP and with the 1993-EUS-Update Seismicity-Zonation Models. Both Are with the Same 1998-TIP Ground Motion Attenuation Model.

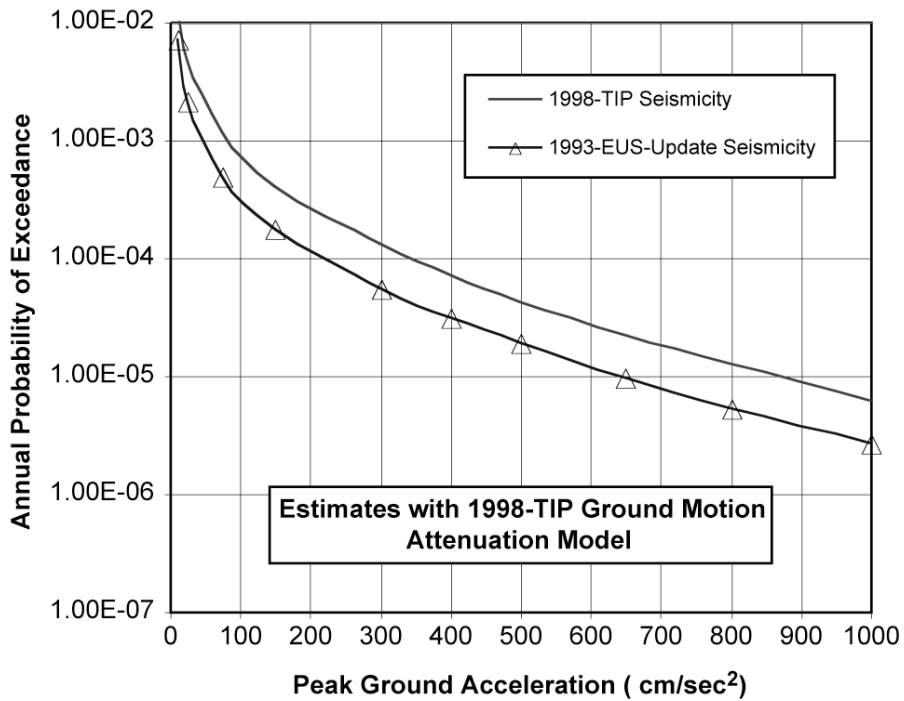


Figure 3.14: Comparing the Median Hazard Curves between the Cases of 1998-TIP Seismicity to the Case of 1993-EUS-Update Seismicity, Both with the Same 1998-TIP Ground Motion Model.

4. IMPACT OF THE SEISMICITY MODELS

4.1 Methodological Differences

This section examines the differences in the zonation and seismicity models between the two studies. The 1993-EUS-Update study used 11 seismicity experts, each giving his own characterization of the seismic zones and their seismicity parameters. In the 1998-TIP study, five experts were used. One expert was common to both studies—Dr. Bollinger. Dr. Bollinger was labeled expert 3 in the 1993-EUS-Update study. In the rest of this study, Dr. Bollinger is referred to as expert 3 when referring to his contributions to the 1993-EUS-Update study.

The 1993-EUS-Update study used the inputs from the eleven seismicity experts as independent inputs. Each represented the interpretation of one expert. It fully described the seismic environment with the uncertainty that each expert independently perceived. The probabilistic hazard was performed for each pair of seismicity and attenuation experts and the final estimates were a weighted average of all the (paired) hazard curves. The 1998-TIP study used a different approach, similar to that of the approach used in the development of the GM models in the 1993-EUS-Update study and following the recommendations of the SSHAC (NRC, 1997). The basic principle was to decompose each of the seismicity experts' interpretations into an exhaustive set of elemental zones, feature, or physical processes that globally could be used as a "LEGO" to build any of the interpretation of the experts. Consequently, every single part of this "LEGO" no longer belonged to a single expert's interpretation but several, and often all of them. Thus every single one of these elemental parts could be the object of a reflexion, analyses, review discussions, challenges, comparison with data, by all of the experts, thereby automatically including the epistemic uncertainty, by assuming that the sample of experts represented an unbiased sample of the community at large.

In the 1998-TIP study, nine maps were introduced. Figure 4.1, taken from Savy et al. (1998), gives a typical map of the seismic zones near the Watts Bar site.

The region of most interest around the Watts Bar site is shown in Figure 4.2 as an enlarged view of the region.

4.2 Differences of Interpretation of the Data by the Experts

Figure 3.3 showed that 95 percent of the total hazard comes from the zones within 70 km of the site. Figure 4.2 shows that the corresponding important zones within this distance are zones 4A-3, 4A-2, 4A-1, 5-2 and 5-1. The 4A zone is labeled "The Eastern Tennessee Seismic Zone" (ETSZ). The nine alternative maps contain interpretation of the data and different models of the ETSZ. See Savy et al. (1998) for details.

A great deal of research on the seismicity was performed in the late 1980s and early 1990s due to the observation of enhanced seismicity of small events in the eastern Tennessee area, leading to an evolution of the experts' thinking on the zonation of seismicity modeling of that area. In particular, this led to significant differences between the models of the early 1980s and those of the early 1990s.

For the 1993-EUS-Update study, each of the eleven seismicity experts had a number of maps. These maps were first developed during the 1980s; see Savy et al. (1993), and Bernreuter et al. (1989). None of these maps recognized the ETSZ. The details of each expert's map differ considerably. For example, Figure 4.3 shows seismicity expert 3's zones that impact the Watts Bar Site. Figure 4.4 shows seismicity expert 1's zones that impact the Watts Bar Site.

The seismic hazard is directly influenced, in the first order, by the seismicity rate in the zones around the site. Since the hazard at Watts Bar is contributed mostly by the areas within 35-40 km from the site, a budget of events predicted by the models of zonation and seismicity of each of the experts in the 1993-EUS-Update study is calculated and shown in Figure 4.5.

Figure 4.5 shows the BE rate of earthquakes within 35 km of the site for each of the eleven seismicity experts' inputs. In this case, the mode (BE) of the distribution of seismic rates is used.

For some experts, more than one seismic zone may be within 35 km of the site.

Figure 4.5 shows the diversity between the eleven experts. It also shows the relative agreements for the magnitudes below 5.5. The experts had to evaluate the data to determine the maximum ever possible magnitude event for each of their postulated seismic source zones. Each came up with specific probability distribution functions, which globally represent the epistemic uncertainty on this parameter. In Figure 4.5, this translates into a range of maximum magnitudes between 6 and 7.25.

In Figure 4.6, we compare the median of the distribution of rate curves shown in Figure 4.5 to the similarly constructed BE rate curve based on the composite 1998-TIP seismicity model. It can be seen that the BE 1998-TIP rate is about a factor of 2 higher than the BE rate for the 1993-EUS-Update study which is about the difference we observed in Figures 3.13 and 3.14 between the hazard curves based on the two seismicity models using the same 1998-TIP GM model.

It is instructive to see how Dr. Bollinger's seismicity model has changed between the two studies. Figure 4.3 shows expert 3's seismicity zones used in the 1993-EUS-Update study and Figure 4.1 shows his seismicity zones for the 1998-TIP study. Comparing these two figures shows that the major change in seismic zones is the introduction of the ETSZ in the 1998-TIP study. The real test is not so much in how the zone boundaries have changed but how these changes impact the seismicity models. Figure 4.7 compares the BE seismicity models for the region within 35 km of the Watts Bar Site for Dr. Bollinger's inputs to the two studies.

4.3 Case of the Local Zones

Figure 4.7 shows that the rates in the new ETSZ are much higher than that of the zones in the 1993-EUS-Update study where the Watts Bar Site is located in the large zone 5. Comparing Figure 4.7 to Figure 4.6 shows that the experts' rates are about a factor of 2 higher than the composite 1998-TIP seismicity model.

The BE rate of earthquakes of $M \geq 3.5$, shown in Table 4.1, are calculated for the 1998-TIP composite model and Bollinger's model for the

region within 33 km of the Watts Bar site for the five highest-weighted maps. Table 4.1 shows that Bollinger's rates are significantly higher than the rates of the composite 1998-TIP model for the two highest-weighted maps (maps 1 and 2) within 33 km of the site.

Table 4.2 gives the rate of earthquakes of $M \geq 3.5$ for the zones within 33 km of the Watts Bar site that are incorporated in Maps 1 to 5. The rates are each zone's contribution to the total rate; i.e. the rates for each zone listed in Table 4.2 are equal to:

$$\left(\text{total zone rate} \right) \times \left(\text{area of the zone within 33 km of the site} \right) / \left(\text{total area of the zone} \right)$$

The rates in Table 4.1 are for the same surface area but may be for more than one zone.

The zone number is an arbitrary labeling system used in the computations. The zone name refers to the names in Figures 4.1 and 4.2. (Additional details can be found in Savy et al., 1998). Bender Cylinder refers to a type of zone with uncertain (fuzzy) boundaries modeled by a series of cylinders of constant seismicity rates.

Tables 4.1 and 4.2 show that the most important zones are zones B1, B2, and zone 35 with respect to the hazard at Watts Bar. In Figure 4.2, zone B2 is zone 4A-3 and zone 4A-2 combined into a single zone. Zone B1 is zone 4A-3 as an independent zone. Zone 35 is made up of zones 4A-1 and 4A-2. Figure 4.8 shows this zone and the historical seismicity in this zone. (See also Figure 4.1.)

Let us examine the recurrence model in zone 35. It is a zone with significant seismicity, and the recurrence model should be reasonably well defined by the earthquake data. Figure 4.9 compares the raw counts of earthquakes in zone 35 for three time frames (normalized to a yearly rate) to both the 1998-TIP composite and Bollinger's recurrence models.

Figure 4.9 shows that there is sufficient data in Zone 35 to define the recurrence model. Both Bollinger's and the composite 1998-TIP's models agree reasonably well with each other and with the "budget" of historical earthquakes in the zone.

A similar comparison is shown in Figure 4.9 for Zone B1 (using data from only two time frames this time). There is much less data in Zone B1 than in Zone 35 to estimate a recurrence model; however, there is sufficient data to make a reasonable estimate of the recurrence model for the zone. Figure 4.10 shows that both Bollinger's and the composite 1998-TIP's models agree reasonably well with each other and the data.

Finally, Figure 4.11 gives the data in Zone B2 showing that there are too few earthquakes for completeness, for any of the three time frames, probably due to the relatively small size of the zone. Because there is so little data in Zone B2, it is not meaningful to talk about a "budget" of earthquakes. To develop a recurrence model for this zone the experts must bring other factors into their estimates for the recurrence model. This leads to a considerable difference between Bollinger's model and the composite 1998-TIP recurrence models as was discussed in Savy et al. (1998) in Section 4.2.6.3.

In Figure 4.12, the recurrence model for expert 3 in the 1993-EUS-Update study is compared to the "budget" of earthquakes in zone 5 (see Figure 4.3), showing that the recurrence model reasonably fits the "budget" of earthquakes in this zone.

Figures 4.9 to 4.12 show that for the zones where there is sufficient data to establish a budget of earthquakes, the recurrence models developed by the experts are in reasonable agreement amongst themselves and with the data. However, in a site-specific study, small seismic zones can be defined on the basis of geological or geophysical data that are not necessarily associated with sufficient seismicity in the historical record to adequately define the recurrence model. This has been the case in previous studies (e.g., Savannah River Site hazard study, 1992), and was extensively discussed at the SSHAC interactive working meetings (NRC, 1997). The lack of knowledge in the characteristics of Zone B2 leads to a single expert's higher uncertainty and consequently higher mean hazard estimate than in the composite. Zone B2 is such a zone. The experts highly weighted this zone so it appeared in the most important maps and thus has a significant impact on the estimation of the seismic hazard. This point is illustrated in Figure 4.13, where the mean estimates of the seismic hazard at the Watts Bar site based on the 1998-TIP composite model are compared with Bollinger's model that appear to be the highest, simply due to the impact of Zone B2.

Table 4.1: Best Estimate Earthquake Budgets of Earthquakes with Magnitudes Greater than 3.5 within 33 km of Watts Bar in the 1998-TIP Study, for Bollinger Alone and for the 1998-TIP Composite Seismicity Model			
Maps Ranked by Relative Weight	Relative Weight of the Maps	1998-TIP Bollinger	1998-TIP Composite
1	1.0	0.071	0.034
2	0.89	0.072	0.036
3	0.57	0.032	0.038
4	0.51	0.044	0.044
5	0.27	0.054	0.065

Table 4.2: Contribution of Selected Seismic Zones to the Budget of Earthquakes Greater Than Magnitude 3.5 within 33 km of Watts Bar, in the 1998-TIP Study. "Tip Rate" Refers to the Rates from the 1998-TIP Composite Seismicity Model and "Bol Rate" Refers to the Seismicity Rates from Bollinger Only, in the 1998-TIP Study									
Zone #	Bol Rate	Tip Rate	Map1	Map2	Map3	Map4	Map5	Zone	Name
28	0.006	0.0096		Yes		Yes		{5-1} +	{5-2}
29	0.012	0.0094	Yes	Yes				B1	
30	0.054	0.017	Yes	Yes				B2	
32	0.014	0.017					Yes	4A-1 Bender	Cylinder
33	0.026	0.03					Yes	4A-2 Bender	Cylinder
34	0.0084	0.01					Yes	4A-3 Bender	Cylinder
35	0.023	0.027			Yes	Yes		4A-1 +	4A-2
46	0.03	0.03						Fault6	

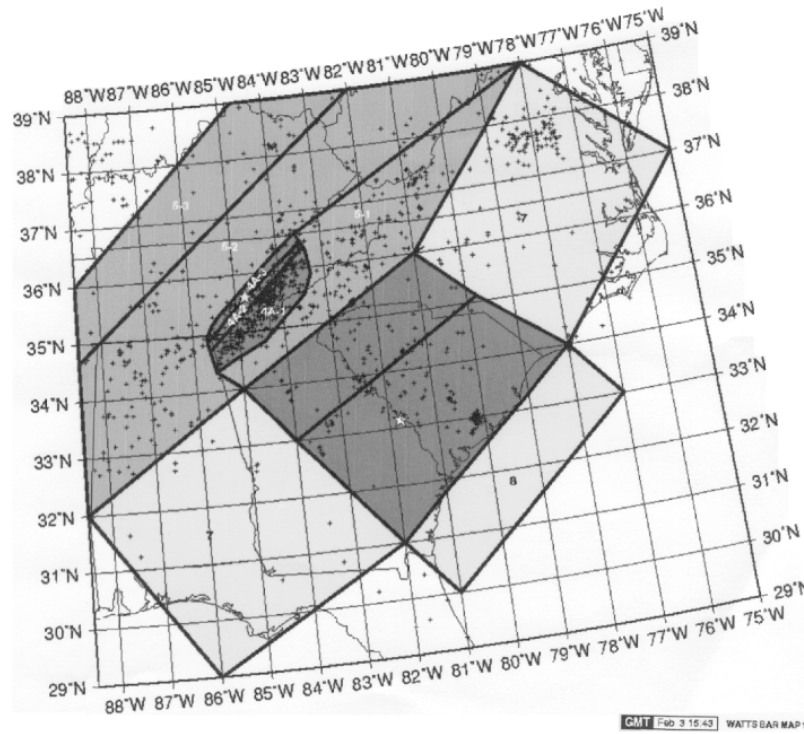


Figure 4.1: First-Order Regional Seismic Sources Zonation Map for the Study of the Watts Bar Site in the 1998-TIP Study.

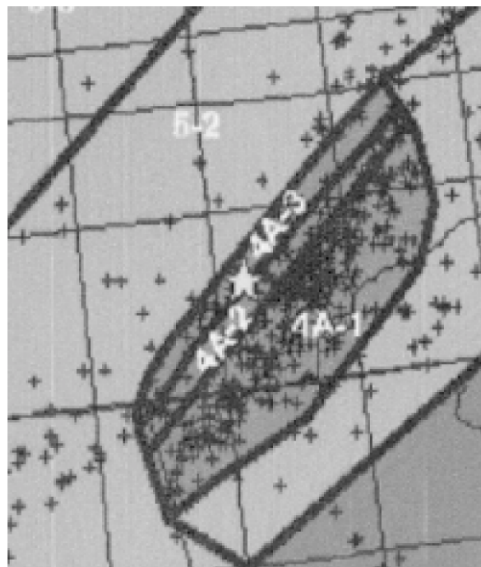


Figure 4.2: Detail of the Geometry of the Local Seismic Source Zones Considered in the 1998-TIP Study.

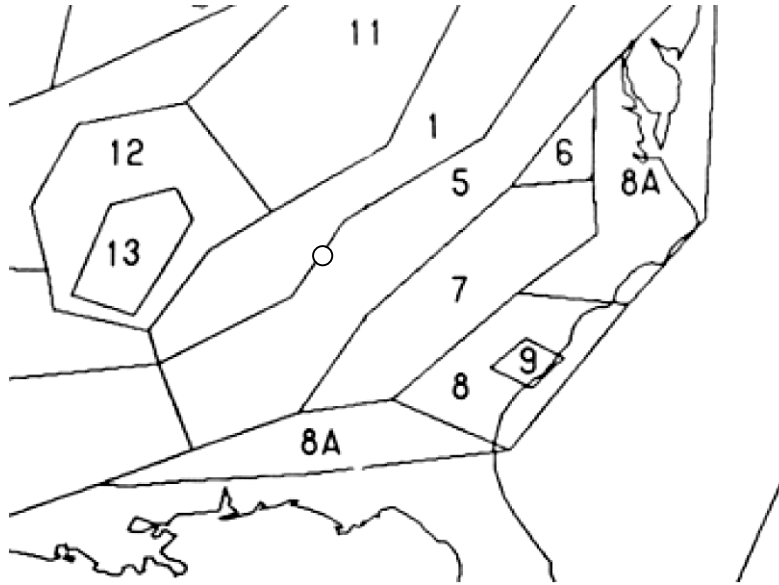


Figure 4.3: One of the Seismic Source Zone Maps Submitted by Seismicity Expert 3 in the 1993-EUS-Update Study. The Site Location is Shown by the Circle on the Map.

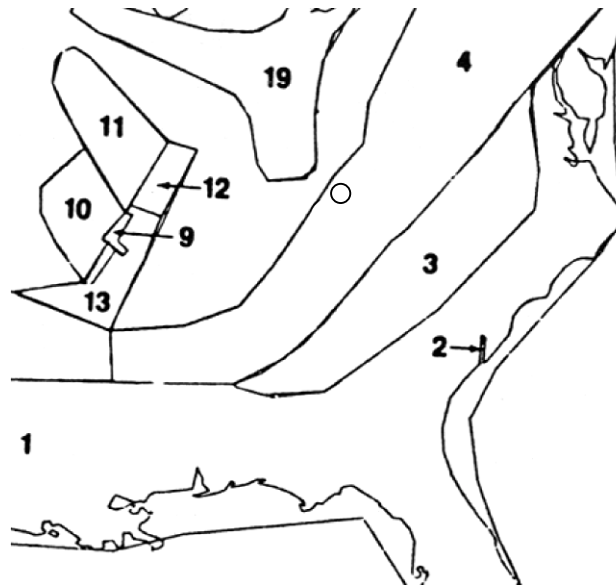


Figure 4.4: One of the Seismic Zone Maps Submitted by Seismicity Expert 1 in the 1993-EUS-Update Study. The Location of the Site is Indicated by a Circle on the Map.

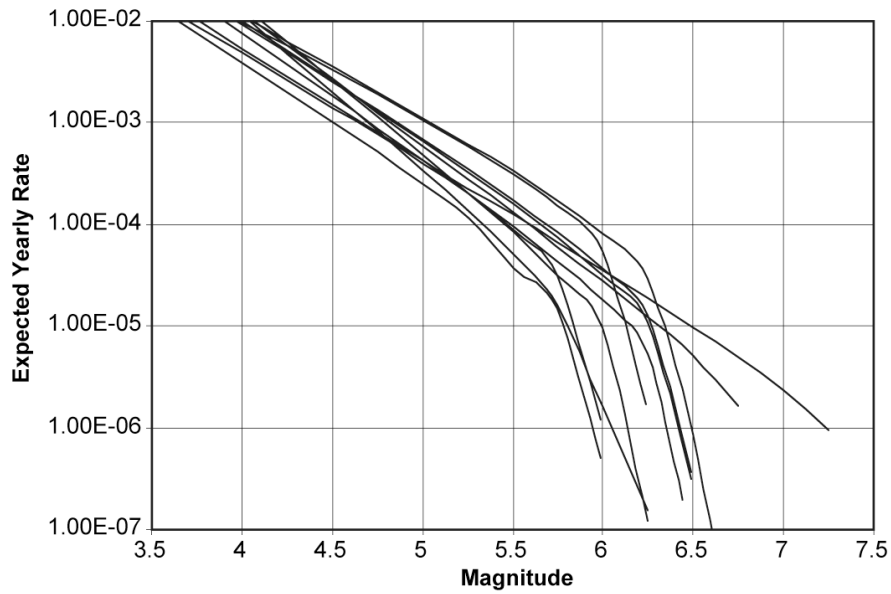


Figure 4.5: Expected Budget of Earthquakes within 35 km of Watts Bar from the Zonation and Seismicity Models of the 11 Seismicity Experts of the 1993-EUS-Update Study.

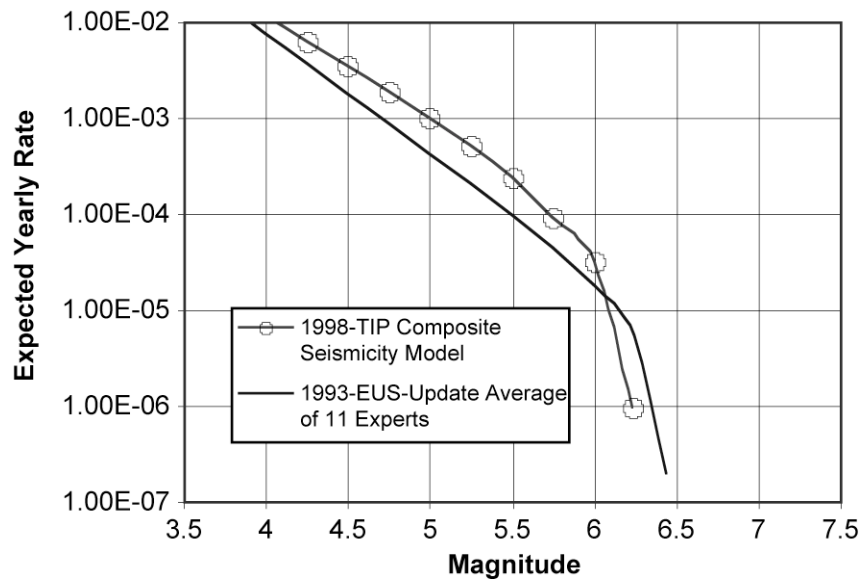


Figure 4.6: Comparison of the Earthquake Seismicity Budget within 35 km of Watts Bar for the 1993-EUS-Update and the 1998-TIP Seismic Zonation and Seismicity Models. The 1993-EUS- Update Curve is an Average Over the 11 Seismicity Experts; the 1998-TIP Curve is from the Composite Zonation and Seismicity Model.

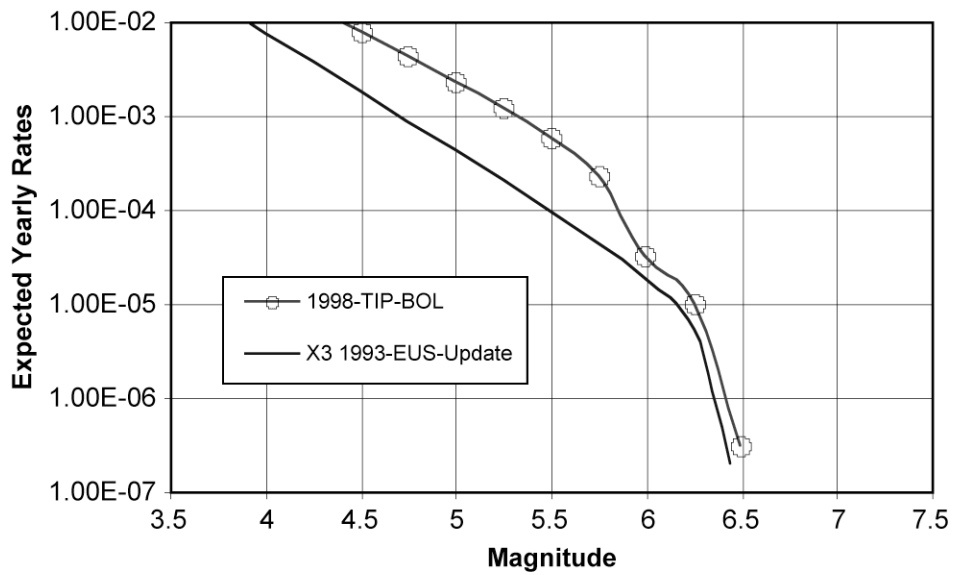


Figure 4.7: Comparison of the Best Estimate Seismicity Budget for a Region within 35 km of Watts Bar, Provided by Expert 3 (X3 1993-EUS-Update) in the 1993-EUS-Update Study and by G. Bollinger in the 1998-TIP Study (1998-TIP-BOL).

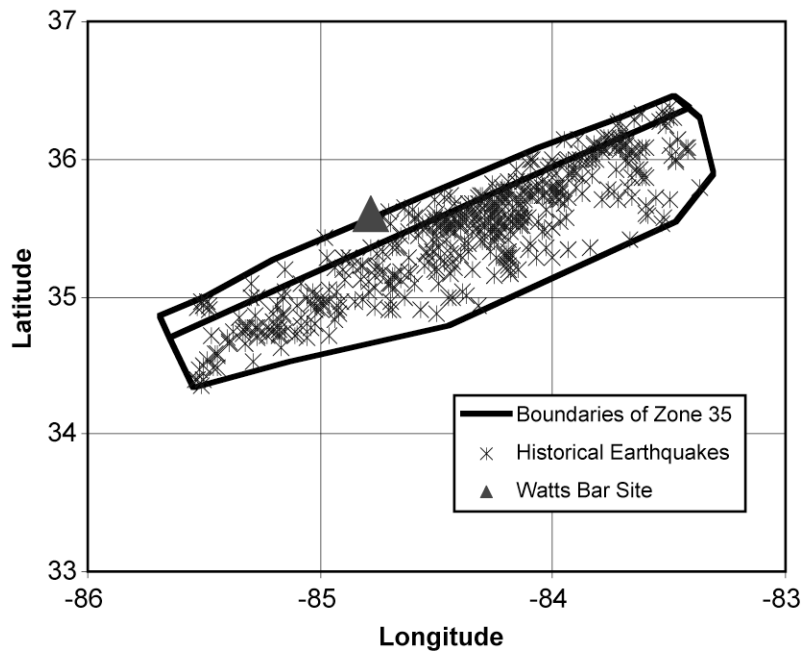


Figure 4.8: Historical Seismicity in Zone 35 of 1998-TIP.

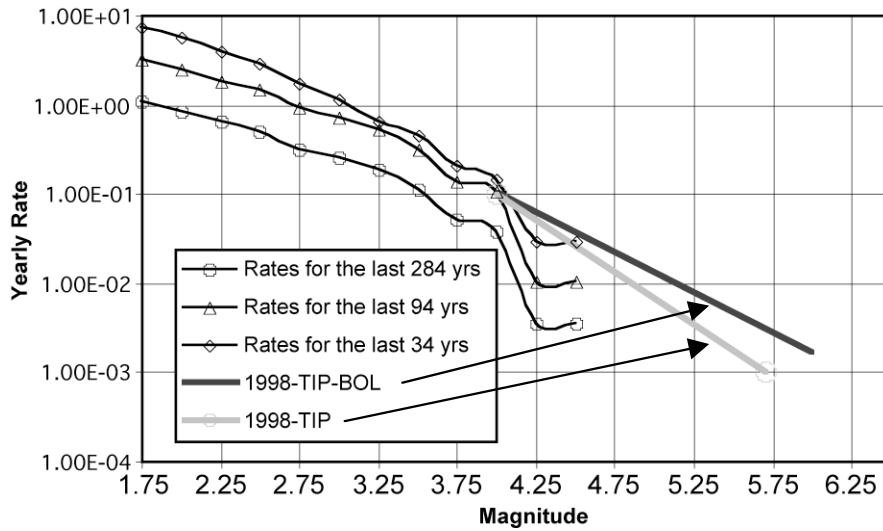


Figure 4.9: Comparison of the Budget of Historical Earthquakes with the Expected Estimates in Zone 35 of 1998-TIP. The Composite Seismicity Model Including All Experts' Input is Labeled "1998-TIP" and "1998-TIP-BOL" for Bollinger's Input Only.

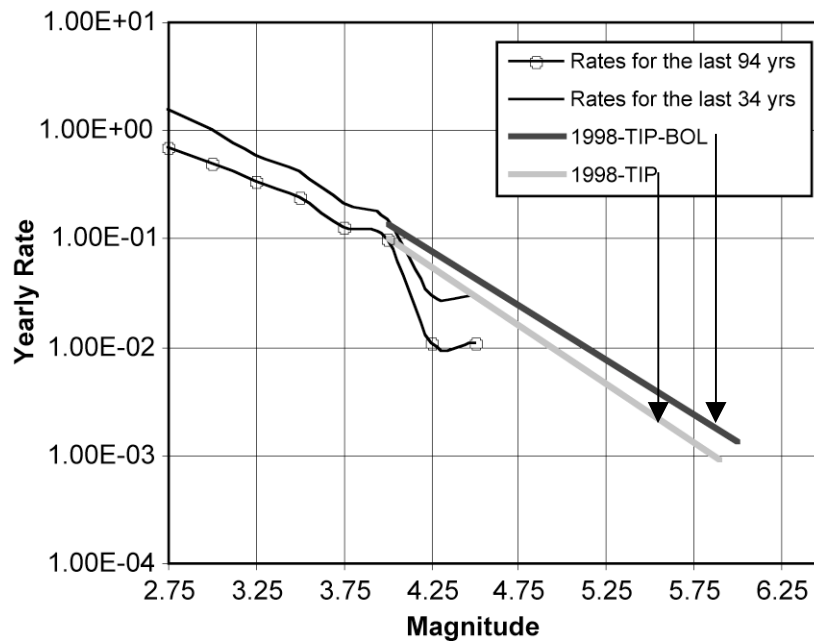


Figure 4.10: Comparison of the Budget of Historical Earthquakes with the Expected Estimates in Zone B1 of 1998-TIP. The Composite Seismicity Model Including All Experts' Input is Labeled "1998-TIP" and "1998-TIP-BOL" for Bollinger's Input Only.

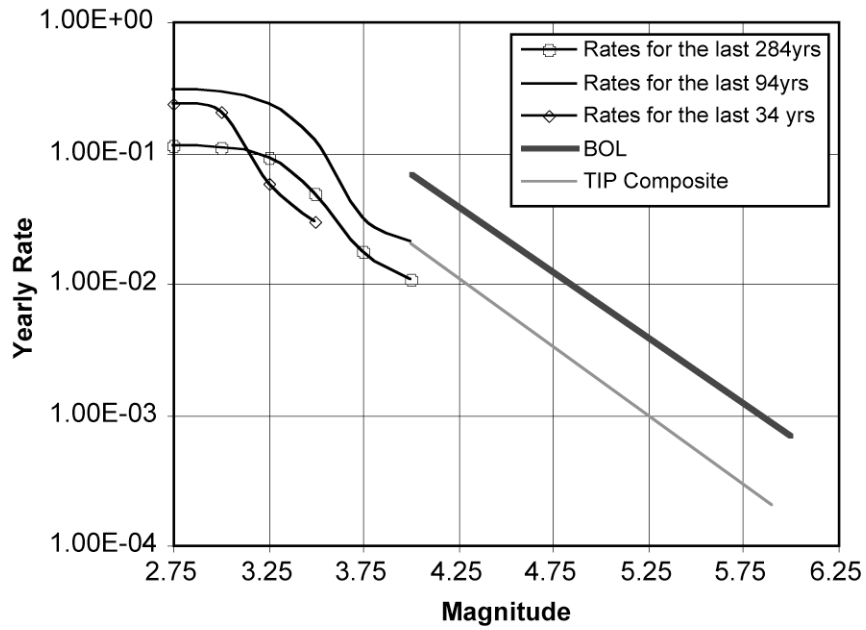


Figure 4.11: Budget of Historical Earthquakes and Modeling for Zone B2 in 1998-TIP.

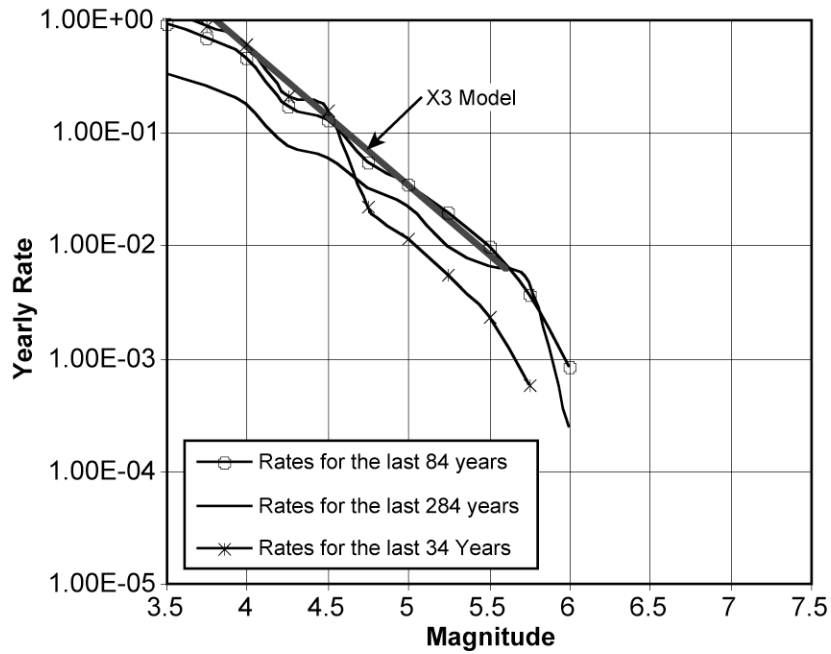


Figure 4.12: Yearly Rates in Zone 5 for Expert 3 of the 1993-EUS-Update Study. “X3 Model” Refers to Expert 3’s Estimates. The Other Curves are for Historical Earthquakes.

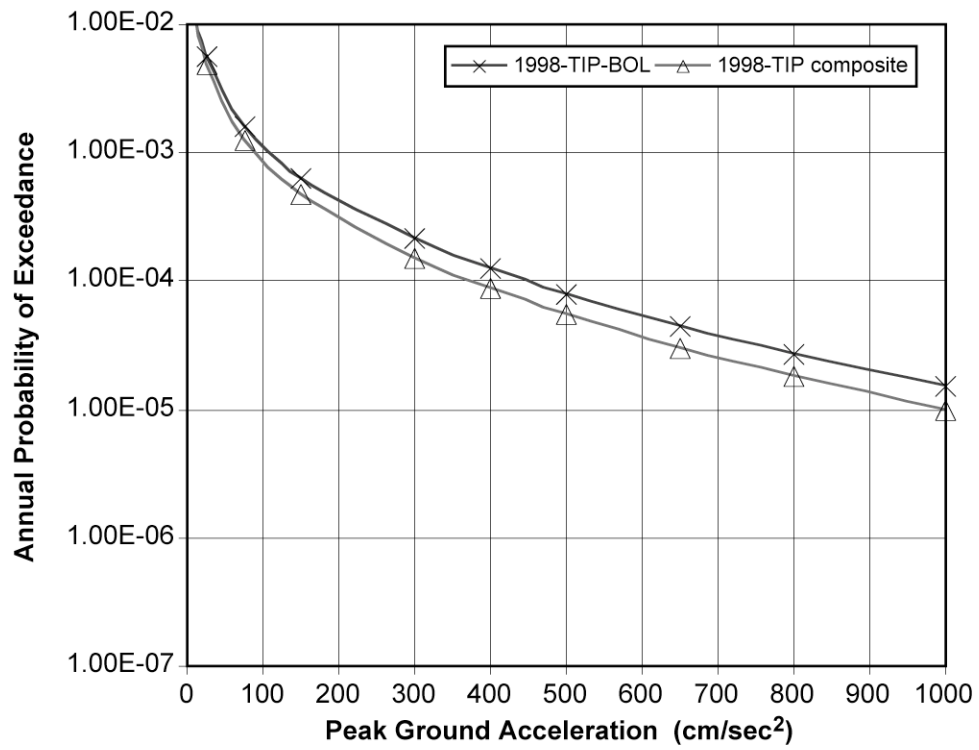


Figure 4.13: Mean Estimates of the Seismic Hazard at Watts Bar Using the 1998-TIP Composite Seismicity Model (1998-TIP composite) and Bollinger's Model (1998-TIP-BOL). The Ground Motion Model is the 1998-TIP Model.

5. UNCERTAINTIES AND SENSITIVITY STUDIES

5.1 Parameters of Interest

The methodological differences between the two studies lead to differences in the modeling of the epistemic uncertainty in the formulation of the zonation maps. In this section, the impacts of those differences are analyzed as well as other causes of differences such as whether an analysis is regional or local. The level of refinement of the seismicity and zonation model is examined by evaluating the impact of considering faults, rather than area zones, for modeling the seismicity in the ETSZ. Finally, the issue of saturation in the GM models is evaluated.

Figure 5.1 shows the predicted mean annual rate of occurrence within a 33-km radius of Watts Bar, for the five highest-weight zonation maps of the 1998-TIP study (see relative weights in Table 4.1). This figure shows that the difference between the lowest curve (Map 1) and the highest (Map 4) in the magnitude range of 4.5 to 6 is a factor of 2 to 3, which is reasonably small, and not likely to generate a large uncertainty in the hazard estimates.

5.2 Sensitivity to the Formulation of the Zonation Maps

The general approach to model the epistemic uncertainty in the estimation of the seismicity is to use a range of zonation maps with the seismicity rates probability distributions corresponding to each seismic zone, or fault. Table 4.1 gives an example of five such maps used in the 1998-TIP study. The set of maps, with the associated weights, constitutes the discrete probability distribution of maps and thus quantifies the uncertainty in the zonation. The total seismic hazard is a weighted average of the hazard calculated for each map.

It is seen that although Map 5 has the highest rate at $M \geq 3.5$, Map 4 has the highest rate in the range of interest of $M5$ to $H6.25$. Figure 5.2 compares the mean estimate of the hazard for each of the five highest-weighted maps as well as the total mean hazard curve. When the weights are applied to each of the maps, actual impact on the hazard is smaller than shown in Figure 5.2. Hence, the various alternative maps

do not introduce significant uncertainty in the final hazard estimates.

The actual uncertainty introduced by the different maps might even be less than the amount implied by Figure 5.2, as some of it is actually introduced by the simulation process itself (see the discussion in section 5.3 below).

5.3 Sensitivity to the Parameters of the Monte-Carlo Simulation

In performing the simulations, the size of the samples was determined by the limits of the computation capabilities in 1993. Given this limited number of simulations, the choice of the seed introduced some variability in the estimates of the hazard. At the time this number of simulations was selected after a careful consideration of that variability, with sensitivity analyses showing that the selected seeds were adequate for the purpose (see Bernreuter et al., 1989). The order of magnitude of this uncertainty is shown in Figure 5.3 in the comparison of the mean hazard curves for four different random seeds. It shows that this variability in the mean hazard curve is small but must be considered before drawing conclusions, such as in section 5.2 above.

5.4 Site-Specific versus Regional Studies

One important difference between the 1993-EUS-Update study and the 1998-TIP study was the introduction of the ETSZ in the 1998-TIP study.

Would the experts of the 1993-EUS-Update study have introduced an ETSZ if it had been a site-specific study that focused on the Watts Bar site?

To answer that question, the issue of modeling the seismicity of the region around the site is examined. Figure 5.4 shows the earthquake locations in zone 5 of expert 3 of the 1993-EUS-Update study. The figure shows that there is a high density of earthquakes in the region assigned to the ETSZ. This points out one of the possible differences between a site-specific study and a broad regional study—namely, a broad

regional study might miss a small zone of increased seismicity near a specific site. On the other hand, as discussed above, site-specific studies can introduce problems by defining zones too small to have sufficient data to adequately develop a recurrence model, and other less reliable methods might have to be used to develop the recurrence model.

5.5 ETSZ versus Local Faults

One interesting feature of the 1998-TIP seismicity model was the introduction of faults to replace the ETSZ (see Figure 5.5). The estimate of the hazard at the site could possibly be increased by the fact that Fault 6 is very near to the site. Little is known about these possible faults and the experts had no additional data to use to model the recurrence model for Fault 6, other than distribute the seismicity of the zone among the faults. Because of this, introduction of the faults into the seismicity model did not have a significant impact on the estimate of the hazard at the Watts Bar site. Figure 5.6 compares the BE estimate of the hazard based on the highest-weighted map to the BE estimate of the hazard based on a typical fault map.

It is seen from Figure 5.6 that the hazard estimate is lower for the fault model than for the zone model. This is in part an artifact of the way the recurrence model was assigned to the fault. If there had been sufficient information about Fault 6 to make an independent assessment of the recurrence model for the fault, then the fault model might have supplied a better estimate of the hazard than the zone model.

5.6 Ground Motion Saturation

Figure 3.1 shows one major difference between the GM models. The 1993-EUS-Update GM model saturates at 10 km and the 1998-TIP GM model does not. To see what impact this has we ran a sensitivity study modifying the 1998-TIP GM model so that it saturated at 10 km. Figure 5.7 shows a comparison of the BE hazard estimates between the 1998-TIP GM model and the modified (saturation of PGA at 10 km) 1998-TIP GM model. This figure shows that saturation of the GM at 10 km has little effect on the estimated hazard.

At first, it may seem surprising that there is so little impact on the hazard between the saturated version of the 1998-TIP GM model and the unsaturated version. However, referring to Figure 3.3 shows that only approximately 15 percent of the hazard comes from the distance range 0-10 km. In addition, in this same distance range the saturated 1998-TIP GM model also contributes almost a similar amount to the hazard. Figure 5.8a gives a plot of the percent contribution to the hazard as a function of the distance to the site, using the 1998-TIP GM model, for a range of return periods. Figure 5.8b gives the same information for the saturated 1998-TIP GM model. These two figures show that the shapes of the percent contribution curves are similar. The net effect is that the resultant hazard curves are very similar, with the hazard for the saturated GM model being slightly lower.

5.7 Uncertainty in the Ground Motion Models Estimates

Figure 3.1 showed a significant difference in the rate of attenuation of PGA for distances greater than 200 km. However, Figure 3.3 also showed that over 99 percent of the hazard comes from the earthquakes within 100 km of the site. Thus, the difference in attenuation has little impact on the hazard at the Watts Bar site.

In Section 3, it was noted that the uncertainty in the 1998-TIP GM model is greater than that of the 1993-EUS-Update GM model. This difference in uncertainty models can impact the identification of those factors that contribute most to the hazard.

For example, Figure 5.9 shows the range of earthquake magnitudes that contribute to the hazard for the 1998-TIP seismicity model combined with the 1993-EUS-Update GM model. This should be compared to Figure 3.10 where the 1998-TIP seismicity model was combined with the 1998-TIP GM model.

It is seen that at longer return periods (higher PGA levels) the range of magnitudes that contribute most to the hazard changes depending on which uncertainty model is used for the GM model.

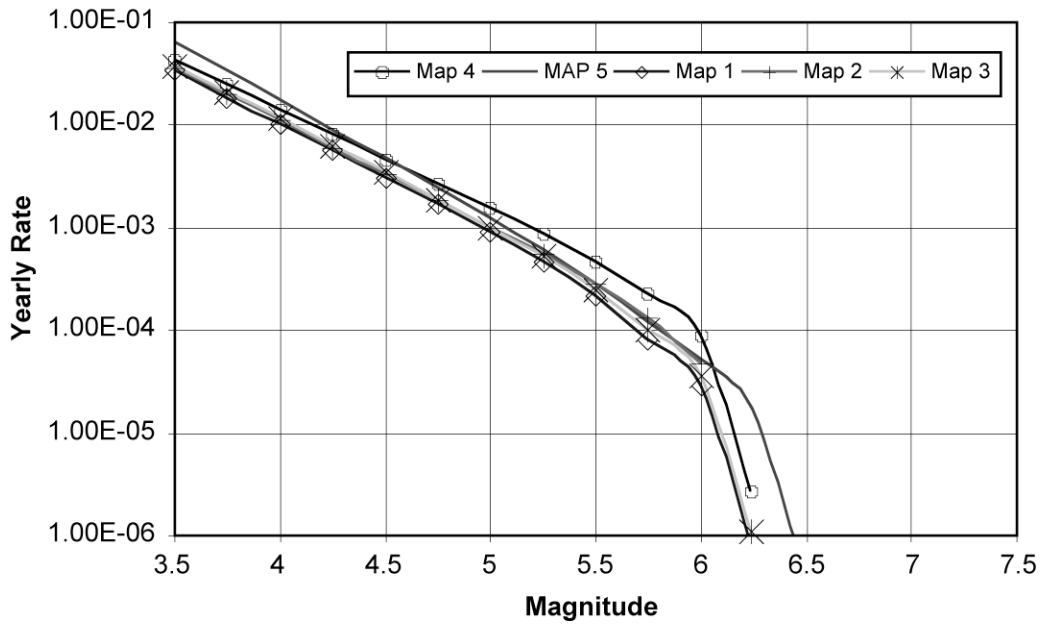


Figure 5.1: Comparison of the Annual Rates of Occurrence of Earthquakes within 33 km of Watts Bar, for the 5 Highest-Weighted Zonation Maps of the 1998-TIP Study. The Relative Weights of the Maps Are Given in Table 4.1.

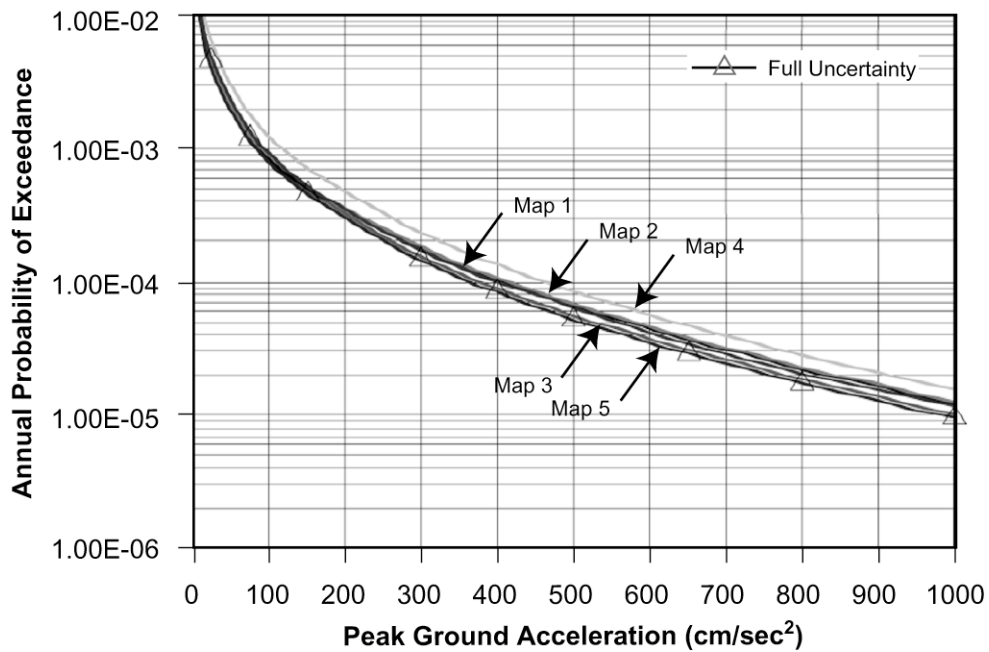


Figure 5.2: Comparison of the Mean Estimates of the Hazard for Each of the Five Highest-Weighted Maps with the Overall Mean Hazard.

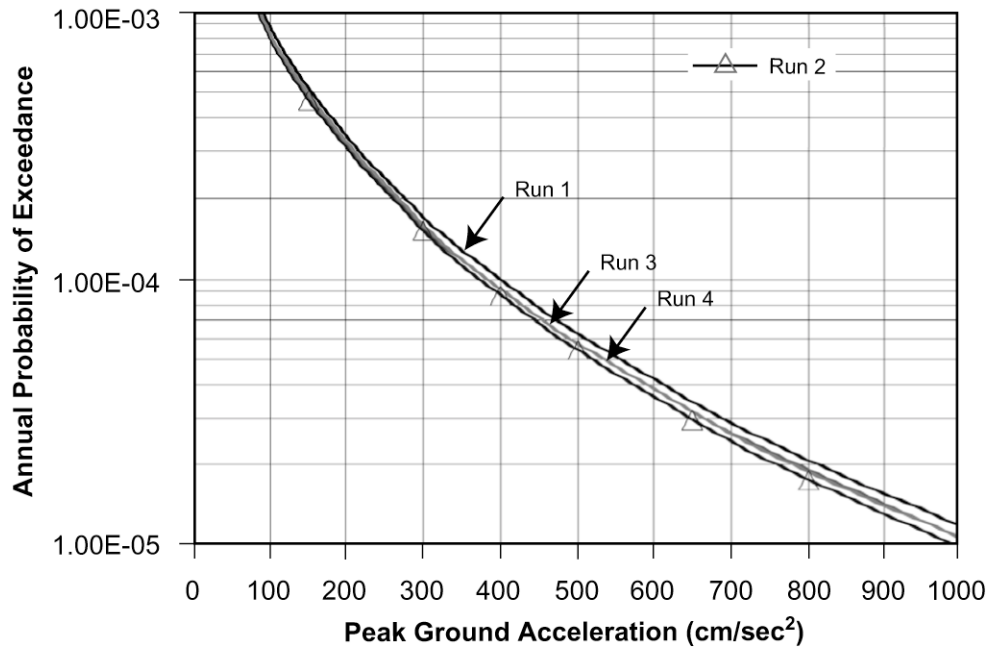


Figure 5.3: Sensitivity of the Mean Estimates to the Seed of the Monte-Carlo Simulation.

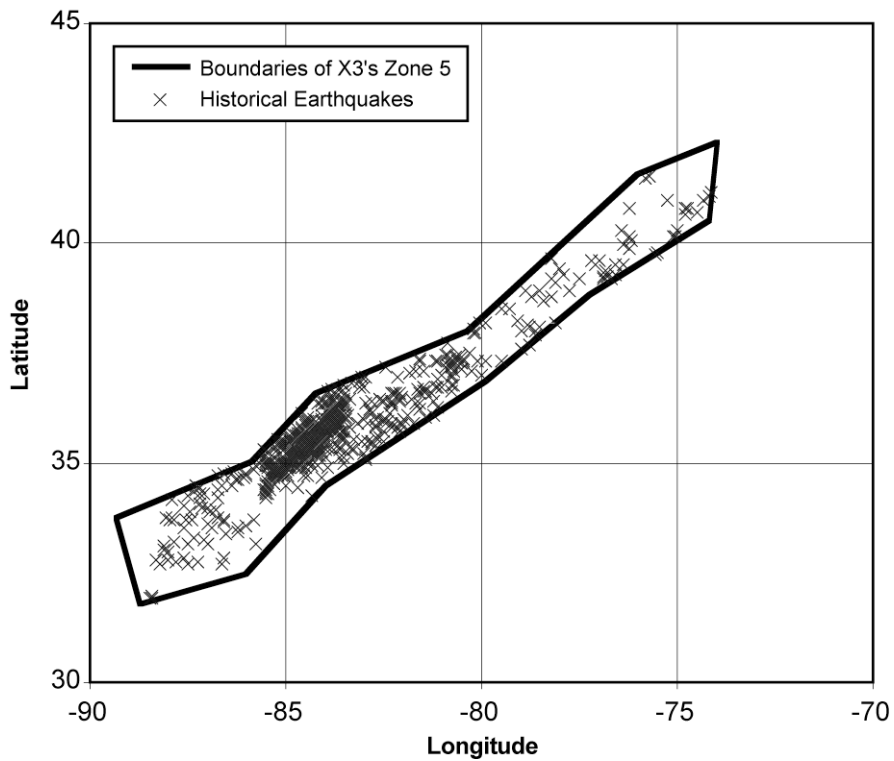


Figure 5.4: Historical Seismicity in Expert 3's Zone 5 of the 1993-EUS-Update Study.

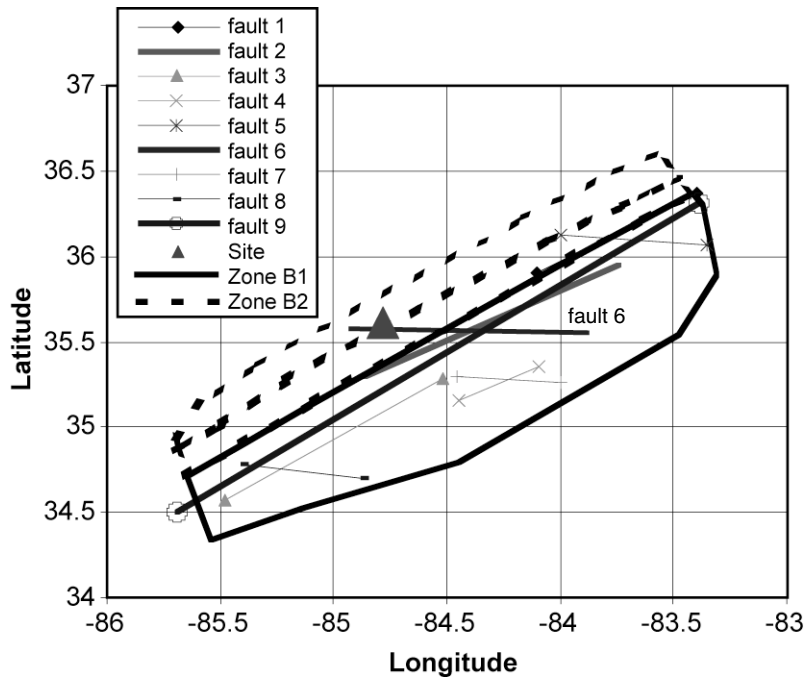


Figure 5.5: Location of the Faults Relative to the Site and the Eastern Tennessee Seismic Zone (ETSZ).

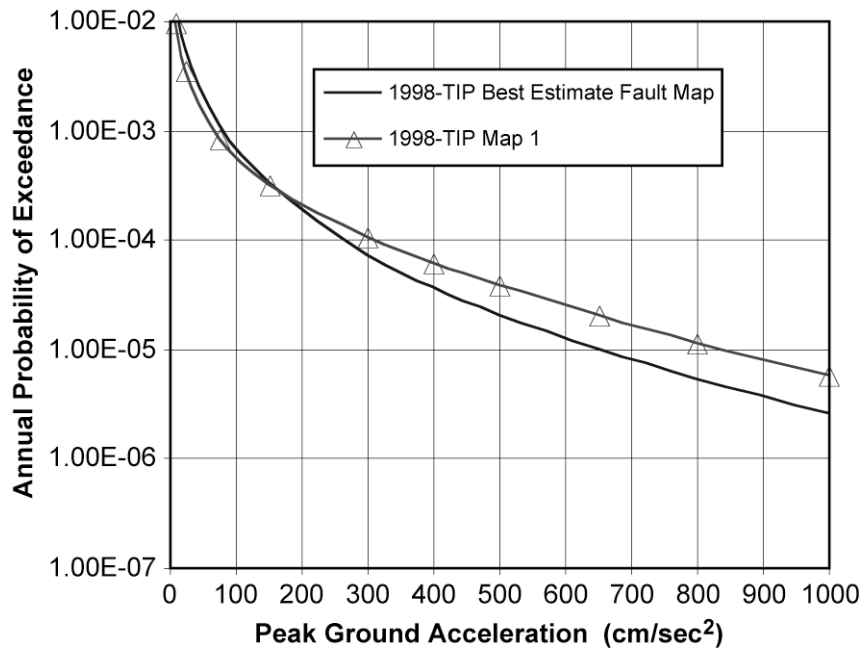


Figure 5.6: 1998-TIP Study. Comparison of the Best Estimate Hazard Curves Obtained Using the Highest Weighted Map (Map 1) to that of a Typical Fault Map.

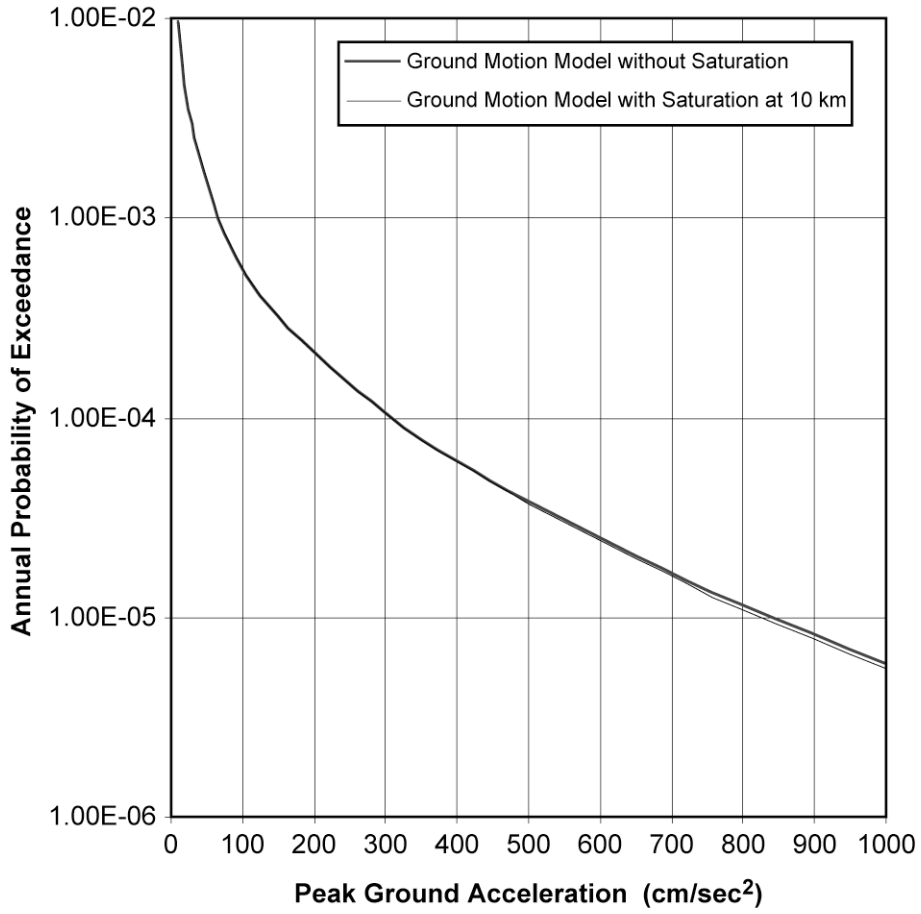


Figure 5.7: Effect of the Ground Motion Saturation at 10 km in the Ground Motion Model. Comparison of Best Estimate Hazard Estimates with and without Saturation.

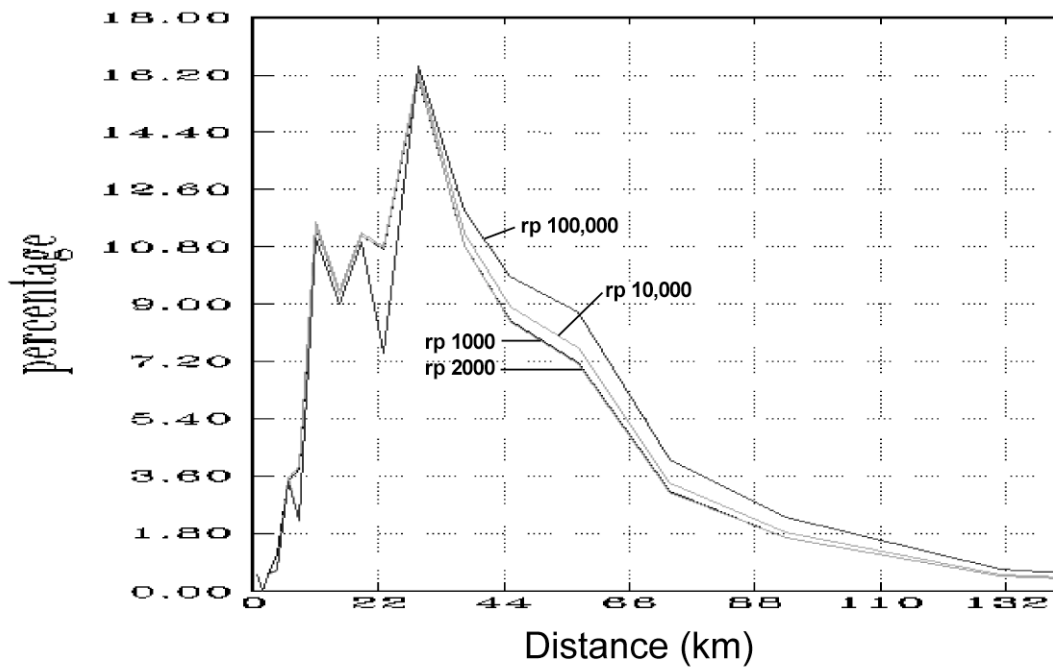


Figure 5.8a: 1998-TIP Study. Contribution of the Bins of Distance to the Total Hazard at the Watts Bar Site with the Non-Truncated Ground Motion Model.

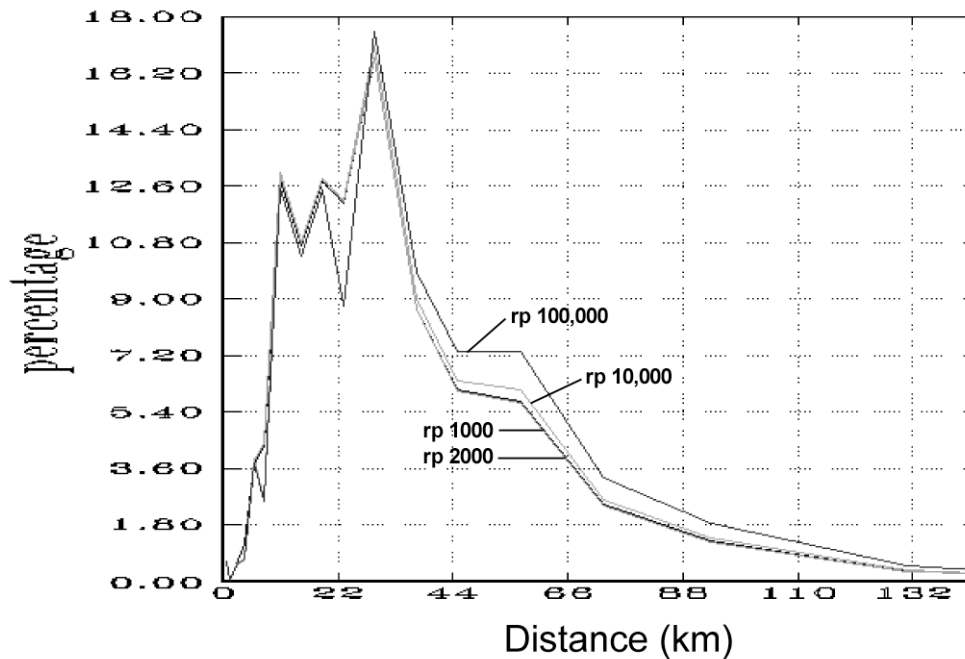


Figure 5.8b: 1998-TIP Study. Contribution of the Bins of Distance to the Total Hazard at the Watts Bar Site with the Ground Motion Model Truncated at Distances below 10 km.

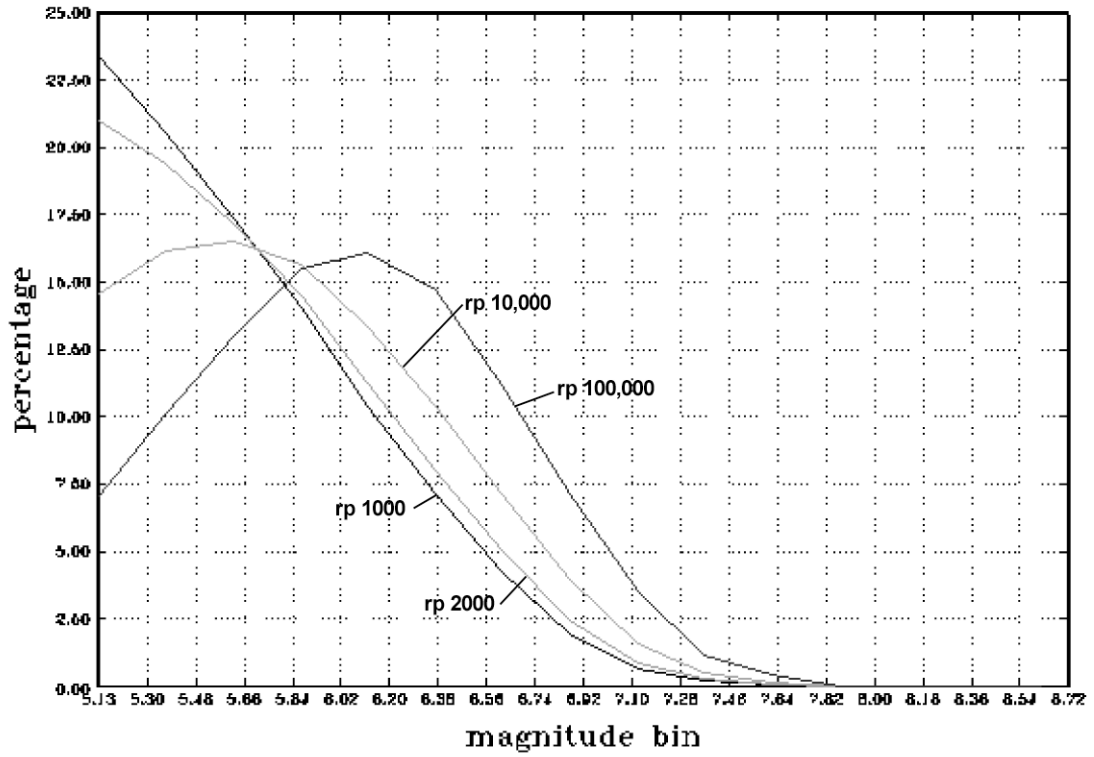


Figure 5.9: Range of Earthquake Magnitudes that Contribute to the Hazard for the 1998-TIP Seismicity Model Combined with the 1993-EUS-Update Ground Motion Model.

6. CASES OF THE 2.5- AND 25.0-HZ RESPONSE SPECTRAL VELOCITIES

Up to this point, the two studies were evaluated on the basis of comparisons of the hazard of the ground motion at high frequency, namely the PGA. This section examines the case of lower-frequency ground motion, for 2.5 Hz and 25 Hz. Certainly it is expected that more distant larger-magnitude earthquakes will be more important because smaller-magnitude earthquakes do not generate as much long-period ground motion as larger earthquakes.

The uniform hazard spectra for return periods of 100,000 and 10,000 years between the 1998-TIP seismicity model and expert 3 of the 1993-EUS-Update study, both using the 1998-TIP GM model, are shown in Figure 6.1.

The spectral velocities of the 1998-TIP study are a factor of 2 higher than those of the 1993-EUS-Update study at 1 Hz. They are only a factor of 1.5 at 25 Hz, and approximately 1.8 at 2.5 Hz.

Figure 6.2 gives the mean spectral hazard curves for 2.5 Hz and 25 Hz using the 1998-TIP GM model and both the 1998-TIP and expert 3 seismicity models.

For a spectral velocity of 21 cm/s at 2.5Hz, the 1998-TIP hazard curve is about a factor of 3.4 times larger than expert 3's hazard curve. At 41cm/s, it is a factor of about 3.8 larger. To understand why the 2.5-Hz hazard curves are so different we need to examine both the distance ranges and the magnitude ranges that contribute to the hazard at this frequency. The distance and magnitude ranges that contribute to the 2.5-Hz hazard curve are similar to the PGA shown in Figures 3.3 and 3.4. Figure 6.3 shows cumulative distribution of the contribution of magnitude to the 2.5-Hz hazard curve for the 1998-TIP seismicity model and Figure 6.4 shows the cumulative distribution of distance to the 2.5-Hz hazard curve.

Figures 6.3 and 6.4 show that larger distant earthquakes contribute much more significantly to the 2.5-Hz hazard curve than to the PGA and 25-Hz hazard curves. Thus, in order to understand why there is such a large difference between expert 3's and the 1998-TIP 2.5-hz hazard curves, there is a need to examine the rate

of earthquakes in regions around the site larger than the 35-km radius region used in Section 3. Figure 6.5 shows a comparison between the yearly rate of earthquakes within 75 km around the Watts Bar site for the BE 1998-TIP seismicity model, the median BE 1993-EUS-Update seismicity model, and the expert 3's seismicity model.

Figure 6.5 shows that expert 3's rate of earthquakes is lower in the 75-km region around the site than the median rate of earthquakes based on the 1993-EUS-Update seismicity model. Referring to Section 3, the region within 35 km of the site, expert 3's rates were about the same as the combined 1993-EUS-Update seismicity model. This is illustrated in Figures 6.6 and 6.7. In Figure 6.6, the rate of earthquakes around the site using the TIP seismicity model for distance of 33 km, 81 km, and 156 km all normalized to 35 km. This is compared to Figure 6.7, for a similar plot using expert 3's seismicity model for distances of 35 km, 75 km, and 150 km.

Note the differences in radius of the areas considered: 33 and 35 km, 75 and 81 km, and finally 150 and 156 km. Due to some selection of parameters when performing the calculations of the 1993-EUS-Update study, it was not possible to have a perfect match of these radii. In each case, the closest radius was selected. Therefore, being tied by the 1993 values of 35, 75, and 150 km, the closest 1998-TIP values were 33, 81, and 156 km radii. Although the comparison is therefore not perfect, analyzing the differences in yearly rates, normalized, is still meaningful, due to the relatively minute error introduced by this approximation.

Figure 6.6 shows that, for the TIP seismicity model, the rate of earthquake activity around the Watts Bar site stays relatively constant with increasing distance. On the other hand, Figure 6.7 shows that the rate of activity around the site based on expert 3's seismicity model decreases with increasing distance. For example, at magnitude 5.5 there is a factor of 3.5 difference between the rates using the largest distance. Thus the difference between expert 3's 2.5-hz

hazard curve and the 1998-TIP 2.5-hz hazard curve is primarily due to the difference in the rate of activity between the two seismicity models around the Watts Bar site. Why expert 3's seismicity model shows such a strong dependence on the radius of the region around the Watts Bar site is an issue needing special examination. This is done by examining expert 3's complete seismic zone map shown in Figure 6.8, where zone 1 is a very large background zone. Because of this, the activity rate in this zone is very low compared to zone 5. Thus, as

the radius of the region used to evaluate the rate of activity is increased for expert 3, more and more of zone 1 is included. By contrast, Figures 4.1 and 4.2 show that the 1998-TIP seismicity model introduced a zone 5-2 which has a much higher seismicity rate than expert 3's zone 1.

Examining Figures 6.3 and 6.5 shows that the uncertainty in the maximum magnitude is important, as Figure 6.5 indicates that the BE for the maximum magnitude is about 6. However, Figure 6.3 shows that larger-magnitude earthquakes contribute to the hazard.

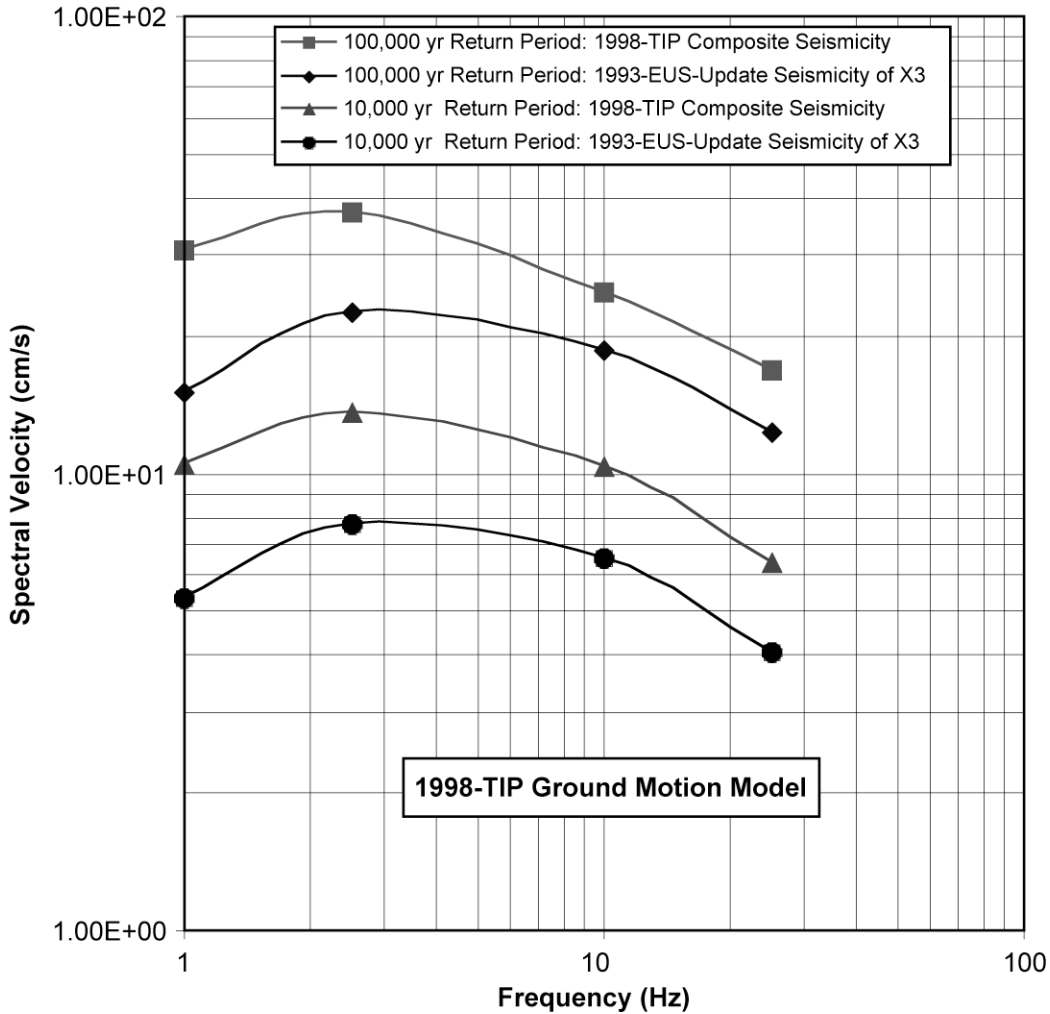


Figure 6.1: Comparison of the Mean Uniform Hazard Spectra for Return Periods of 100,000 and 10,000 Years Between the 1998-TIP Seismicity Model and Expert 3 of the 1993-EUS-Update Study Both Using the TIP Ground Motion Model.

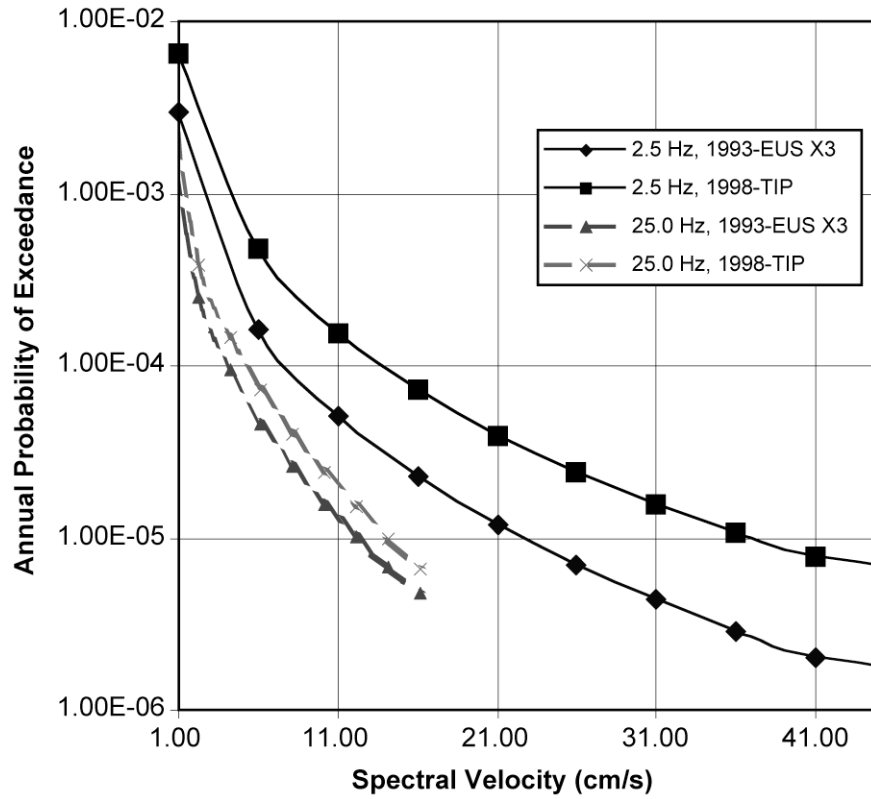


Figure 6.2: Mean Spectral Hazard Curves for 2.5 Hz and 25 Hz using the 1998-TIP Ground Motion Model and both the 1998-TIP and 1993-EUS-Update Expert 3 Seismicity Models.

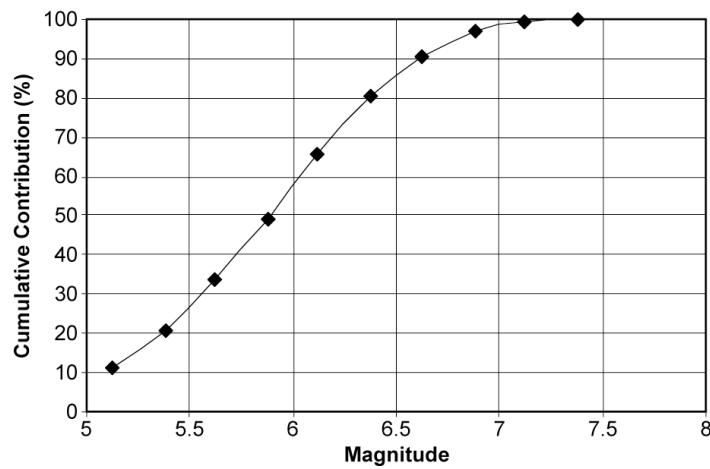


Figure 6.3: Cumulative Contribution of the Magnitude Bins to the Total Hazard for a 100,000-yr Return Period at 2.5 Hz.

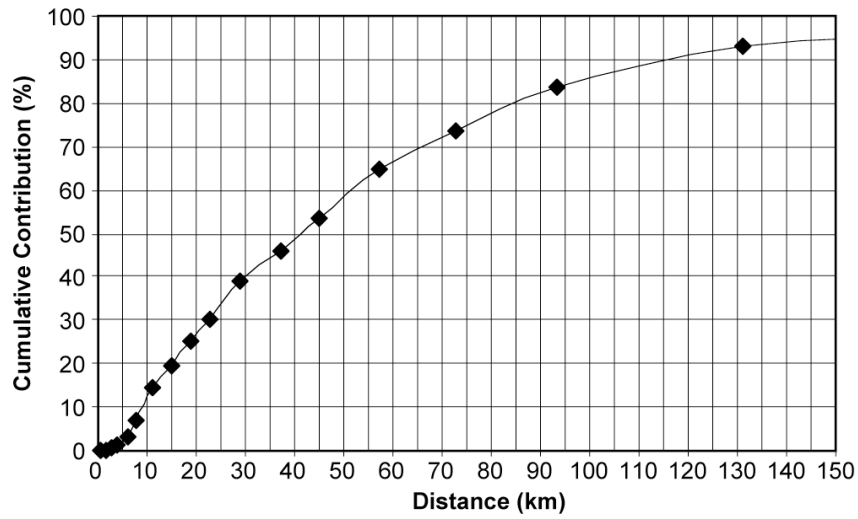


Figure 6.4: Cumulative Contribution of the Distance Bins to the Total Hazard for a 100,000-yr Return Period at 2.5 Hz.

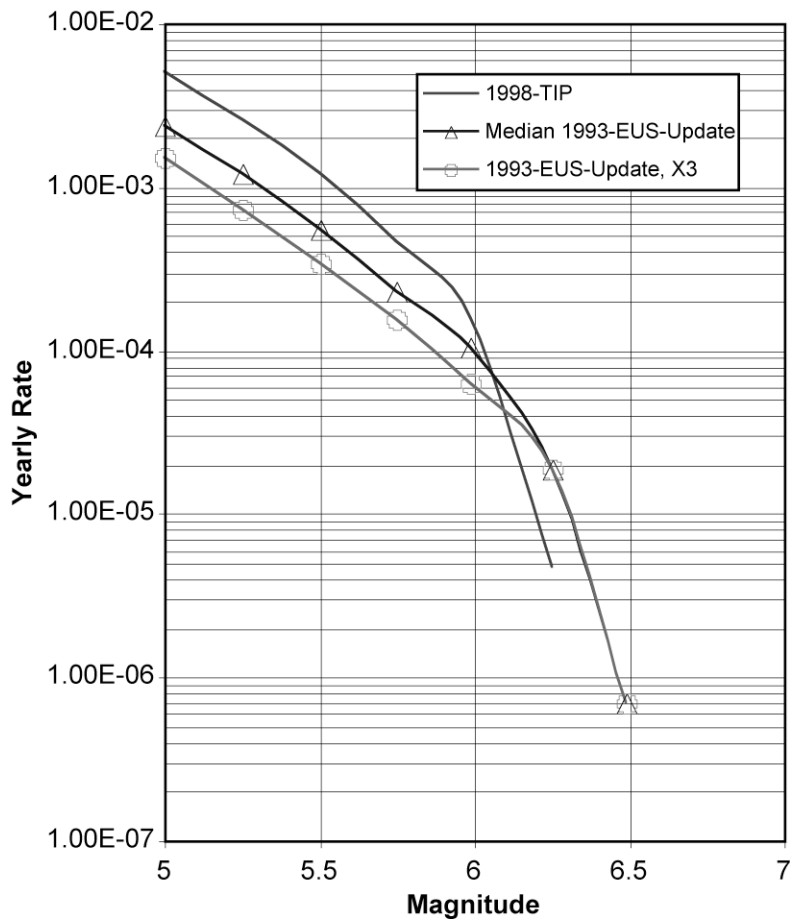


Figure 6.5: Comparison of the Yearly Rate of Earthquakes Occurrence within 75 km of the Watts Bar Site between the Best Estimate 1998-TIP Seismicity Model (Map 1), the Median Best Estimate 1993-EUS-Update Seismicity Model, and Expert 3's Seismicity Model.

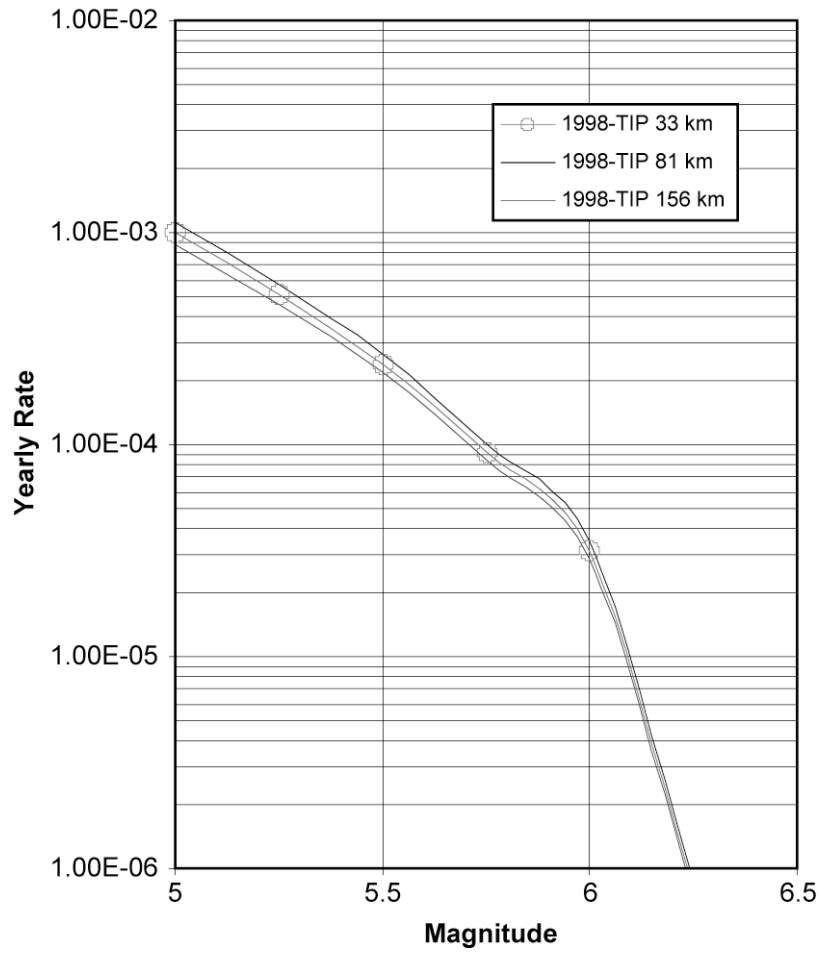


Figure 6.6: Rate of Earthquakes Versus Magnitude around the Site Using the 1998-TIP Seismicity Model for Distances of 33 km, 81 km, and 156 km All Normalized to 35 km.

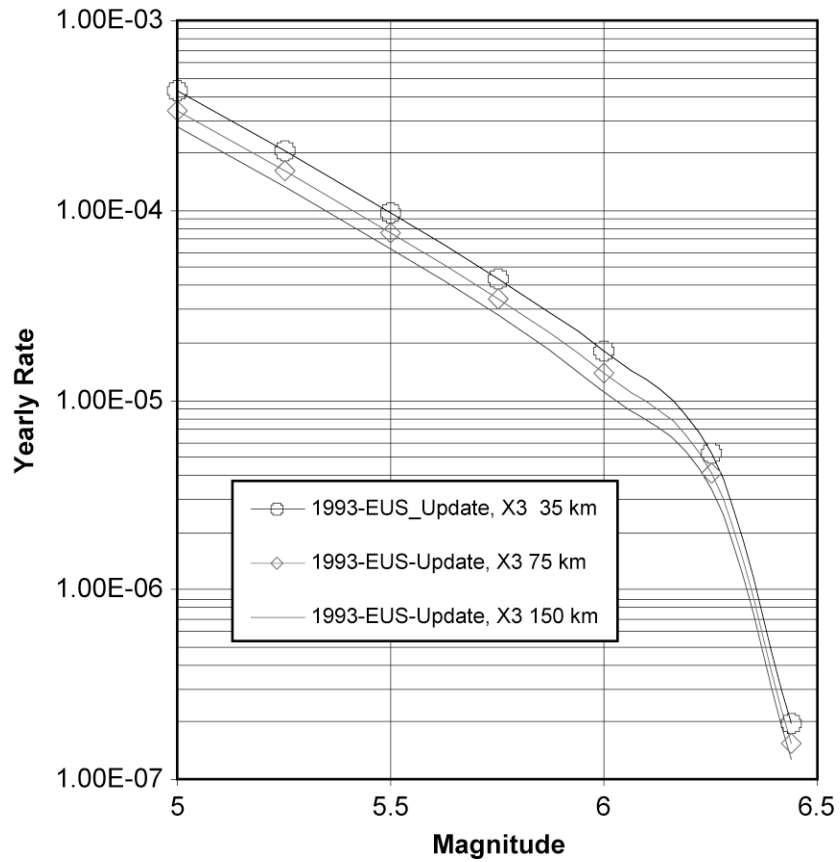


Figure 6.7: Rate of Earthquakes around the Site Using the 1993-EUS-Update Expert 3's Seismicity Model (X3), for Distances of 35 km, 75 km, and 150 km, All Normalized to 35 km.

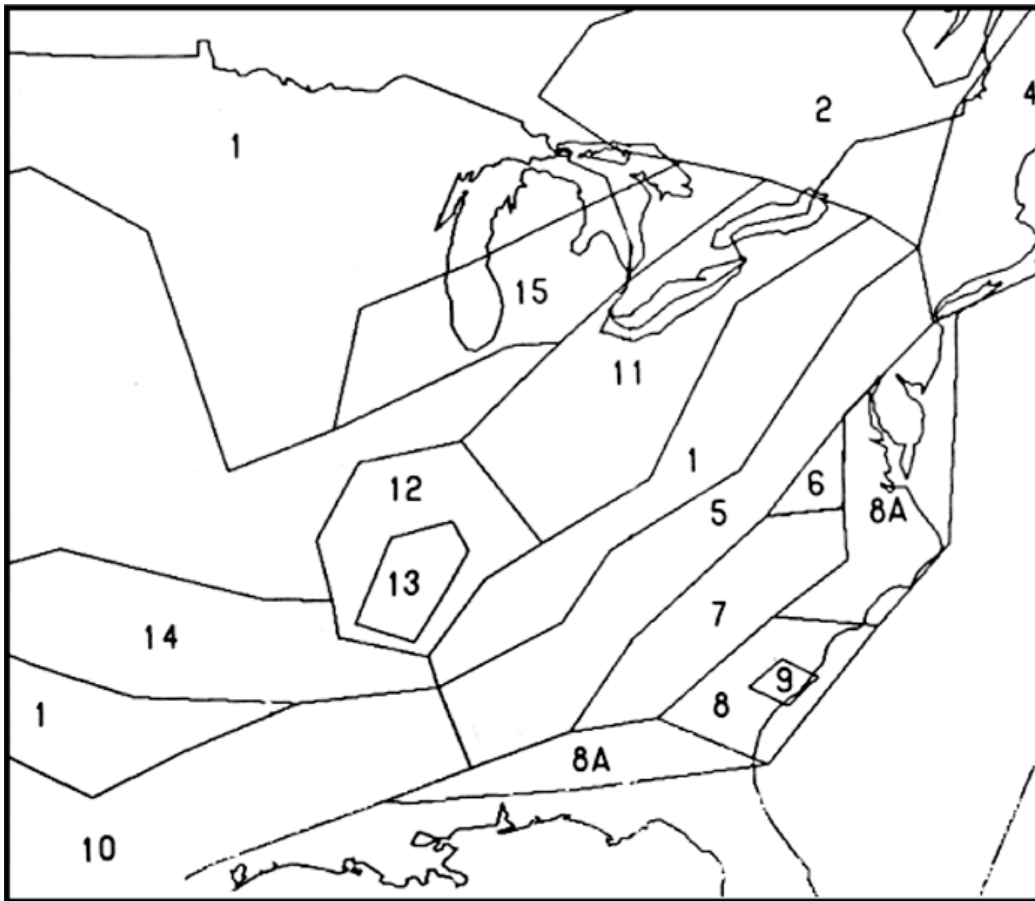


Figure 6.8: Enlarged view of Expert 3's Seismic Source Map Showing Zone 1 as a Large Background Zone with Low Rate of Seismicity.

7. DISCUSSION

7.1 General Findings

The differences over the 11 experts' seismicity model estimates of the seismic hazard at the Watts Bar site between the 1993-EUS-Update and the 1998-TIP studies are due to two main factors:

1. Differences between the GM models used in the two studies.
2. The introduction of the ETSZ in the 1998-TIP study.

We found that these two factors lead to about a factor of 5 difference between the two studies for the mean estimate of the PGA hazard at high GM levels. At 100 cm/sec² the agreement between the two studies was much better (about 1.6). We also found that if the same GM model was used in each seismicity model the results were in better agreement and only differed by about a factor of 2 at high GM levels. The composite rate of earthquakes around the Watts Bar site was about a factor of 2 higher for the 1998-TIP composite seismicity model than the rates in the 1993-EUS-Update averaged over the 11 experts' seismicity model.

By comparing Figures 2.1, 2.2, and 2.3, it is also apparent that the median estimates follow approximately the same trend as the mean curves, and that the uncertainty in the estimates is greater in the 1993 study, increasing with increasing PGA values.

In this section, we attempt to uncover some of the possible root causes of these differences and formulate a set of criteria to determine in what cases such differences would be likely to be observed for other sites of the 1993 EUS study.

7.2 Causes for the Differences in Hazards Estimates

7.2.1 Ground Motion Models

The ground motion models were used in a generic fashion in both studies, independently of the type of source zones and of their position with respect to the sites. Both composite models were based on the same approach, but the 1998 model benefited from the most recent analyses of

strong motion data that were not available at the time of the 1993 calculations. This led to an elimination of the limitation of motion amplitude in the distances smaller than 10 km, a slight decrease for distances between 20 and 200 km, and large increases beyond 200 km. Therefore, aside from the uncertainty estimates, overall the ground motion models are not very different and their impact depends essentially on the location of the dominant source zones. In the case of Watts Bar, the dominant source zones are relatively close to the site, and the dominant magnitude is between M5 and M6, so that the net effect on the hazard is a slight increase, as shown by Figure 3.8. It is very likely that different conclusions would be reached for other sites. Sites dominated by close-by faults, within 10 to 15 km, would definitely see a large increase in the mean hazard estimates. Sites whose dominant sources are between 30 km and 200 km would actually see a decrease in the estimates, and sites dominated by distant sources, beyond 200 km, would see an increase from the ground motion model alone.

7.2.2 Source Zones and Seismicity Models

There were substantial differences between the source zonation in the two studies. The 1993 study, based on the zonation models of the 1989 study, was primarily a regional study that did not concentrate on the details of the geology and tectonics of each of the sites. On the contrary, the 1998 study deliberately emphasized the importance of local tectonics.

In addition, the community of seismology experts had begun formulating a number of new tectonic models for the Eastern Tennessee region. These studies, which were posterior to the date of formulation of the source zones in the 1993 study, were based on micro-seismicity studies. They led to the determination of the existence of active faults near the Watts Bar site. Because of the immediate importance of these new sources on the estimate of the hazard at Watts Bar, the TIP study spent much effort in characterizing them. The experts were first asked to write white papers explaining their understanding of the data. They were asked to present their models to the groups of experts, and debate the merits of each proponent model. In

the end, the group of experts formulated a number of alternative models that included previous models of the 1993 study, but that also included new models with faults located near the site. These new faults included the possibility of rare but large events.

To de-emphasize the impact of these new source zones near the site, the TIP study allowed for the boundaries of the ETSZ to be randomized, to express the uncertainty on their location because no firm evidence actually exists on their actual position.

These differences between the two studies, in themselves, do not necessarily mean that the estimates of the hazard would be different since the hazard also depends on the seismicity rates of each source. However, in this case, this “micro-zonation” had the effect of shifting the spatial distribution of the earthquakes, from a smooth uniform distribution over a large region, to a more localized peak of activity near the site, thereby increasing the hazard estimates.

7.2.3 Regional Versus Site-Specific Window: Impact on Uncertainty

One important difference between a regional vision and a local vision is in the considerations of uncertainty in the estimates of the seismicity rates of the sources.

In the regional vision, a small number of sources is fitted to a robust budget of events, and it is easy to ascertain whether a seismicity cluster belongs to one source or another.

In the local vision, smaller sources, to which are assigned small subsets of the catalogue of historical events, are used to estimate the uncertainty in the seismicity rates. It is common practice to analyze each source separately, as statistically independent items, when we evaluate the seismicity rate and their uncertainty. This practice, however, is not realistic since it does not account for the correlation between all the sources, resulting in estimates of the uncertainty that seem correct for each independent source, but that most likely overestimate the uncertainty for the entire map of source zones. To our knowledge, no general method exists to resolve this issue. One possible approach could be based on a Monte-Carlo simulation from the alternative source zonations, and feedback corrections based

on comparisons with the original set of catalogue data, as we are planning to develop in the next generation of methodology.

The impact of this overestimation of the uncertainty for the smaller zones and faults is to increase the mean estimate of the hazard, but not the median. To some extent, this effect is shown in the next section for the Vogtle site.

7.2.4 Comparison with the Vogtle Site

Contrary to the Watts Bar site, the Vogtle site did not have any new zones or faults in its vicinity. Although the source zonation is different from that of the 1993 study, it is made mostly of large source zones, with the exception of the Charleston area (that does not dominate the estimate of the hazard). Contrary to the models in the Watts Bar site analysis, the Vogtle models appear to be more of a regional nature than local. The uncertainty in each of the contributing sources is therefore still well constrained, like it was in the regional study that was the EUS 1993 study, and consequently the median estimates of the hazard are comparable in the two studies, as shown in Figure 7.1. Furthermore, because the rigorous SHHAC method was applied to identify the alternative models and root out the unrealistic alternatives or unnecessary differences between experts, the overall uncertainty in the source zonation and seismicity rates models was reduced, by comparison to the EUS 1993 study. This resulted in a lower mean estimate of the hazard in the 1998 results, as shown in Figure 7.1.

7.3 Criteria for Formulating Conclusions at Other Sites

The main parameters that determine whether a new site-specific study is likely to result in different estimates the EUS 1993 study are the following:

- Existence of local sources or faults. Newly discovered clusters of activity will lead to more localized near seismicity and will tend to increase the estimates of the hazard.
- Refining the definition of a large dominant source into a number of smaller independent dominant sources will likely lead to an increase in the hazard mean estimate without necessarily increasing the median estimate.

- Non-existence of new local sources will tend to lead to unchanged results.
- Distance of the site to the dominant sources, depending on the shape of the ground motion model, will lead to either higher or lower estimates. A comparison of the ground motion model will be necessary before making a conclusion.

The above generic observations can be used to evaluate the possible consequences of re-doing the PSHA for a site for which estimates by the EUS 1993 study are available. In all likelihood, a cursory first evaluation of the present available data would be done to determine which of the above elements apply.

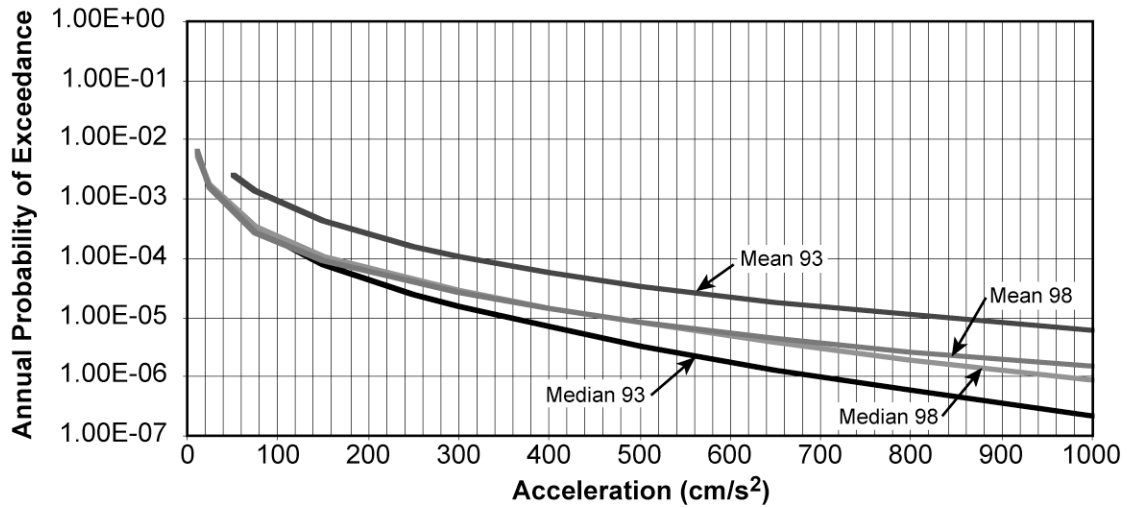


Figure 7.1: Comparison of Results for Vogtle.

8. CONCLUSIONS

In the 1998-TIP study, we found that the ETSZ enhanced the activity rate around the Watts Bar site as compared to the 1993-EUS-Update study by about a factor of 2. If the 1993-EUS-Update study had been a site-specific study like the 1998-TIP study, it is very likely that most, if not all, of the 1993-EUS-Update seismicity experts would have included a more detailed model representing the ETSZ. This would have brought the composite seismicity models between the studies into even better agreement because, as was shown in Figure 5.2, the various models for the ETSZ did not result in significant changes for the estimated hazard.

Although there are significant differences in the two studies' hazard estimates for the Watts Bar site, there are also areas of stability. We found that the largest contributor to the difference in the GM models was resting in the uncertainty models. The estimate of the hazard at a site is very sensitive to the uncertainty in the GM model. There is little hope of reducing or stabilizing the uncertainty in the GM model because very little GM data exists from EUS earthquakes. It is unlikely that this will improve in the near future because of the relatively low

rate of activity in the EUS and the low density of strong ground motion data recorders.

Considering the actual length of time between the time when the seismic zones were identified (mid 1980s) for the 1993-EUS-Update study and the time when the 1998-TIP study was performed, the seismicity models between the two studies were in good agreement. It appears that one possible cause of the differences between the two studies was the difference in scale between the two studies. Namely, the 1993-EUS-Update study was a large regional study covering the entire region east of the Rocky Mountains, whereas the 1998-TIP study was site-specific.

The last point was also demonstrated to be associated with a possible overestimation of the uncertainty in site-specific analyses due to the possible creation of myriads of poorly defined zones with large uncertainties in their characteristics. One possible remedy to such a situation is to impose criteria on the budget of earthquakes and its uncertainties for a small region around the site (say, 15 km) in these studies.

REFERENCES

- Bernreuter, D.L., Savy, J.B., Mensing, R.W. and Chen, J.C (1989). "Seismic Hazard Characterization of 69 Nuclear Plant Sites East of the Rocky Mountains," NUREG/CR-5250; Lawrence Livermore National Laboratory, Livermore, CA, UCID-21517; Vol. 1 to 8.
- EPRI (1989). "Seismic Hazard Methodology," NP-4726, Vol. 1 to 10.
- EPRI (1993). "Guidelines for Site Specific Ground Motions," Palo Alto, California, Electric Power Research Institute, November 1993. TR-102293.
- Frankel, A., Burnhard, C., Perkins, D., Leyendecker, E.V., Dickman, N., Hanson, S. and Hopper, M. (1996). "National Seismic Hazard Maps: Documentation," June 1996, U.S. Geological Survey Open-File Report 96-532, 110 p.
- National Research Council, NAS/NRC (1997). "Review of: Recommendations for Seismic Hazard Analysis: Guidance on Uncertainty and Use of Experts," National Academy Press.
- NRC (1993). "Revised Livermore Seismic Hazard Estimates for 69 Nuclear Power Plant Sites East of the Rocky Mountains," NUREG-1488, October 1993.
- NRC (1996). "Branch Technical Position on the Use of Expert Elicitation in the High Level Radioactive Waste Program," NUREG-1563.
- NRC (1997). "Recommendations for Probabilistic Seismic Hazard Analysis: Guidance on Uncertainty and Use of Experts," NUREG/CR-6372.
- Savy, J., Boissonnade, A., Mensing, R. and Short, S. (1993). "Eastern U.S. Seismic Characterization Update," Lawrence Livermore National Laboratory, Livermore, CA, UCRL-ID-115111.
- Savy, J., Foxall, W. and Abrahamson, N.(1998)."Guidance for Performing Probabilistic Seismic Hazard Analysis for a Nuclear Plant Site: Example Application to the Southern United States," NUREG/CR-6607; Lawrence Livermore National Laboratory, Livermore, CA, UCRL-ID-133494.